AD-A148 470 INTERNATIONAL CONFERENCE ON LUMINESCENCE HELD AT MADISON WISCONSIN ON 13-17 AUGUST 1984(U) WISCONSIN UNIV-MADISON W M YEN OCT 84 N00014-84-G-0053 1/1

UNCLASSIFIED F/G 20/6 NL

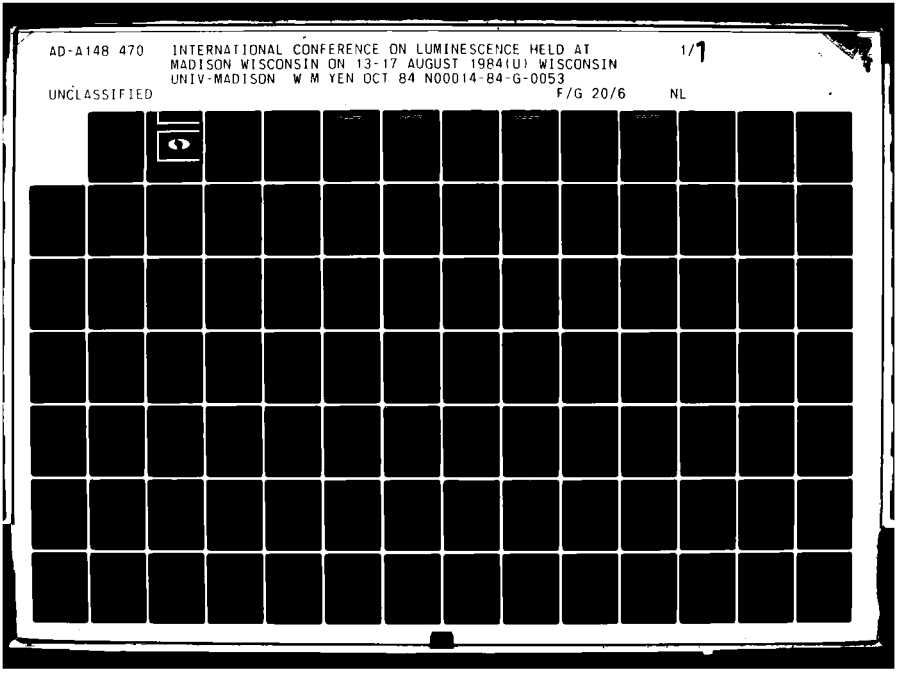

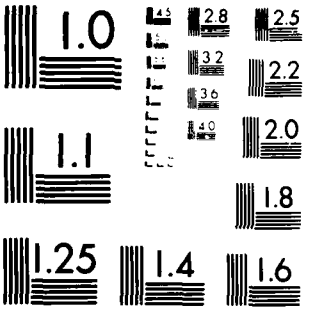

INTERNATIONAL CONFERENCE
ON LUMINESCENCE 1984

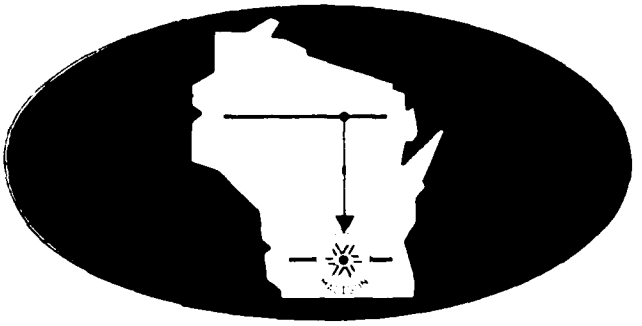

TECHNICAL DIGEST

AUGUST 13-17, 1984
UNIVERSITY OF WISCONSIN
MADISON, WISCONSIN

ICL '84 TECHNICAL PROGRAM COMMITTEE

William M. Yen, *General Chairman*
Department of Physics
University of Wisconsin-Madison

John C. Wright, *Program Chairman*
Department of Chemistry
University of Wisconsin-Madison

A. Z. Genack
Exxon Research and Engineering

Michael J. Heller
Standard Oil Company of Indiana

R. W. Hellwarth
Department of Physics
University of Southern California

David L. Huber
Department of Physics
University of Wisconsin-Madison

R. Kopelman
Department of Chemistry
University of Michigan

Roger M. Macfarlane
IBM Research Laboratory

Richard S. Meltzer
Department of Physics
University of Georgia

R. Orbach
Department of Physics
University of California-Los Angeles

Michael D. Sturge
AT&T Bell Laboratories

Willes H. Weber
Ford Motor Company

Philip E. Wigens
Ohio State University

Addenda to Program

Papers Withdrawn

Monday poster session - MB

MB19 Dosimetry by Thermoluminescence: Dating of Peruvian Pottery

E. F. Quinones and El Lopez Carranza

MB46 Time Behavior of Nonradiative Multiphonon Relaxation Processes

V. Denner and M. Wagner

Tuesday poster session - TuG

TuG4 Phase Coherence in the ^2E State of Cr^{3+} Ions in MgO Detected by oDMR

B. Henderson

Thursday invited paper - session ThE

ThE2 Secondary-Emission Spectra and Energy Relaxation of Polaritons in Layer Polar Semiconductors

M. S. Brodin and I. V. Blonskii

Friday poster sessions - FB and FE

FB5 Emission from Photoproducts of Benzene

A. N. Dharamsi and V. Shakmirian

FE1 Is the Barrier Height of Exciton Self-Trapping Evaluated So Far Correct?

H. Sumi

Title Changes

Monday Plenary Session

MA2 Luminescence Studies of Energy Transfer and Restricted Molecular Motion in Molecular and Biological Systems

R. Hochstrasser

Other Corrections

The invited paper on Tuesday - TuH2 entitled "Exciton Transfer and Quenching in Solid Solutions" by A. I. Burshstein will be presented instead by D. L. Huber.

The authors on paper TuE11 should read Y. Kotera, T. Higashi, M. Sugai, and A. Ueno.

INTERNATIONAL CONFERENCE ON LUMINESCENCE - 1984

AUGUST 13-17, 1984
UNIVERSITY OF WISCONSIN - MADISON

WORKSHOPS

Tuesday, August 14, 1984
3:30 - 6:30 PM

I. SYNCHROTRON RADIATION TECHNIQUES

Location: Sterling Hall (Physics) Rm 1300

Organizers: D.W. Lynch, Iowa State University
G. Margaritondo, University of Wisconsin

Participants: F. Bassani, Chair, Scoula Normale Superior, Pisa
M.A. Green, SRC, University of Wisconsin
G. Zimmerer, Hasylab, Hamburg
H. Kanzaki, ISSP, University of Tokyo
S. Sugano, ISSP, University of Tokyo

II. LASER INDUCED EMISSION OF CAROTENOIDS AND CHLOROPHYLLS

Location: Sterling Hall (Physics) Rm 1313

Organizer: J.A. Koningstein - Carleton University (Ottawa)

Participants: K.K. Rebane, Estonian Academy of Sciences
J.J. Katz, J.E. Hunt, J.C. Hindman, Argonne National Laboratories
G.R. Seely, Kettering Laboratories
A. de Wilton, L.V. Haley, N. Vinnie, Carleton University (Ottawa)
F.K. Fong, Purdue University

III. FRONTIERS IN CRYSTALLINE FIELD THEORY

Location: Daniels Hall (Chemistry) Rm B371

Organizer: H.W. Crosswhite, Argonne National Laboratories

Participants: J.P. Hessler, Chair, Argonne National Laboratories
D.S. McClure, Princeton University
C.J. Ballhausen, University of Copenhagen
B. Edelstein, LBNL
K. Rajnak, Kalamazoo College

IV. LARGE CRYSTAL SYSTEMS

Location: Daniels Hall (Chemistry) Rm 1351

Organizer: W.F. Krupke, LLNL

Participants: H.P. Jenssen, Chair, MIT
L.J. Andrews, GTE
W.F. Krupke, LLNL
K. Petermann, G. Huber, University of Hamburg

INTERNATIONAL CONFERENCE ON LUMINESCENCE - 1984

AUGUST 13-17, 1984

UNIVERSITY OF WISCONSIN - MADISON

ICL'84 PRIZE

Monday, August 13, 1984, 11:30 A.M.

Memorial Union Theater

Presenter: W.M. Yen, University of Wisconsin-Madison

ICL'84 PRIZE LECTURE:

LUMINESCENCE AND ULTRAFAST SPECTROSCOPY

S. SHIONOYA, UNIVERSITY OF TOKYO (20 Min)

The Organizing committee of ICL'84 is pleased to announce that the ICL'84 Prize will be awarded to Prof. Shigeo Shionoya in recognition of his contributions to our understanding of physical processes which affect the luminescence properties of solids and for his continuing service to the luminescence community. Professor Shionoya is known for his work in elucidating the properties of zinc sulfide phosphors and for his discovery of cooperative luminescence in rare earth systems. More recently he has made contributions to our understanding of ultrafast relaxation phenomena as well as coherent effects in the picosecond regime.

Professor Shionoya is a graduate of the University of Tokyo, he served as an Associate Professor in the Faculty of Engineering at Yokohama National University before joining the Institute of Solid State Physics, The University of Tokyo in 1959. Other than short visits overseas including a stay at New York University, Professor Shionoya served continuously at Tokyo until his retirement this year. In the course of his 25 years there Professor Shionoya has trained numerous students who have contributed greatly to the advancement of luminescence research in Japan and internationally.

The ICL'84 Prize was financed from contributions from industrial concerns interested in the promotion of luminescence research. We are also thankful to North Holland Physics Publishing for providing a cash stipend of $1000.- for the award.

The Selection Committee consisted of W.M. Yen (Chair), the late F. Williams, S. Ibuki, J. Kircz, M.D. Fayer and F. Auzel. Selection was made from nominations received from the luminescence community at large.

ICL'84 PRIZE ADDRESS

Luminescence and Ultrafast Spectroscopy

Shigeo Shionoya

In luminescence research, that is, in research on dynamics of optically excited states of materials, ultrafast spectroscopy using pico- and femto-second laser pulses is very important, in the sense that it enables one to obtain firsthand information on dynamic aspects of various processes. The author's group started their luminescence research by means of picosecond spectroscopy more than ten years ago. The present talk reviews some results of their recent studies done for exciton systems in CuCl and CuBr crystals both typical direct-gap semiconductors. The topics will be (1) luminescence of excitonic molecules, (2) measurements of the group velocity of excitonic polaritons, and (3) dynamical relaxation processes of excitonic polaritons. Optical dephasing of excitonic polaritons will also be mentioned. It will be demonstrated how our understanding of ultrafast relaxation processes associated with luminescence is deepened by utilizing techniques of ultrafast spectroscopy.

INTERNATIONAL CONFERENCE ON LUMINESCENCE - 1984

AUGUST 13-17, 1984
UNIVERSITY OF WISCONSIN - MADISON

MISCELLANEA

CONFERENCE OFFICES; MESSAGES: During the period August 13-17, ICL'84 will maintain an office at the Browsing Library on the 2nd floor of the Memorial Union. The message board will be kept at this location. Participants are requested to check the board at periodic intervals. A number of minor services will be available through this office.

BANKING: The UW Credit Union, located in the basement of the Peterson Building, 750 University Avenue, has agreed to act as our financial agent. UWCU will cash Conference as well as travel cheques upon presentation of your ICL badges. A very modest fee is involved. Sorry no personal cheques.

TRAVEL: Assistance in travel arrangements may be obtained from Rhodes Travel, our officially designated travel agent. Rhodes has offices throughout Madison, the most convenient of which is on the 1st floor of Memorial Union (Phone 263-8810).

LOCAL TRANSPORT: Madison is serviced by an outstanding bus network. Schedules and information may be obtained at the Madison Metro Downtown Customer Service Center, 25 W. Main Street (Phone 266-4466).

Madison Metro also operates a 10¢ shuttle which runs every 15 minutes from the UW Memorial Union to the Capital Square. Additionally, buses operate on the UW campus until late evening at 35¢/ride.

Of course, taxi and limousine services are available. Please consult your yellow pages. (Taxi Companies: Badger - 256-5566, Union - 256-4400, Bender Airline Limo - 249-7444).

RECREATION: The University of Wisconsin Hoofers Sailing Club has agreed to provide Temporary Memberships to delegates who wish to use the University's extensive sailing fleet. Cost of this membership is $10 for the Conference period. Persons signing on are subject to the Club's rules which include the necessity of proving competency in handling a particular boat class. A Hoofers sign up desk will be available on Sunday. Sign-ups thereafter will be at the Hoofers headquarters in Memorial Union. This mechanism for unlimited sailing is being provided as a service, the Conference bears no responsibility nor liability in individual sailing activities.

Jogging paths are plentiful on campus and those interested in this activity are invited to explore the campus on their own. A particularly pleasant path runs from the Memorial Union, along the lake to Picnic Point on the far West side of the University. Please consult your campus maps.

As the Conference is a bona-fide University activity, the extensive swimming, gymnasium etc. are open to ICL delegates on request. There are also some half a dozen municipal golf courses available in Madison for your entertainment.

DINING ETC.: Though a lot of you have prepaid meals, the cost of these meals is so modest that you are urged to sample the extensive selection of restaurants and foods available in Madison. All restaurants in Madison are modestly priced and delegates can count on friendly service anywhere in the city. Madison also has innumerable places for libations and night entertainment, a great many of them concentrated in the University area. Madison is one of the safest cities in the nation as we have a friendly and efficient police force.

POSTER: The ICL'84 poster was designed and executed by Prof. Bill Weege of the University. Prof. Weege is an internationally known artist who has had some 50 individual exhibitions in the US. His paper constructions and poster art is held in collections throughout the world. The first run of 200 ICL'84 posters has been signed and numbered by Prof. Weege, these are available for $10 at the Conference office. Mailing tubes to preserve your poster are also available for purchase at the office.

You are cordially invited to visit Prof. Weege's Jones Road Print Shop and Stable in Barnaveld (which was recently in the news) which is just 20 miles west of Madison. The original paper construction despicted in the poster is available for purchase at $800.-.

T-SHIRTS: Official ICL'84 T-shirts in two designs and in your choice of size and color (red, blue, green) are being provided at $5/each at registration and at the Conference office.

We believe we have the proper environment for an exciting gathering. I hope that you will enjoy yourselves at our Conference. I wish above all to thank you for your particpation and assistance in making ICL'84 a memorable occasion.

W.M. YEN
Chairman ICL'84

INTERNATIONAL CONFERENCE ON LUMINESCENCE - 1984

AUGUST 13-17, 1984
UNIVERSITY OF WISCONSIN - MADISON

ACTIVITIES

Sunday, August 12, 1984 -

4:00 - 7:00 PM	Registration - Wisconsin Center Lobby	
5:30 - 7:00 PM	Get Acquainted Reception - Hors and refreshments compliments of EGG-PAR and Questek. Cash bar -	
		Alumni Lounge Wisconsin Center

Monday, August 13, 1984

10:00 - 11:00 AM	Coffee in honor of accomapnying persons. All invited.	
		Lee Lounge Wisconsin Center
12:30 - 1:30 PM	Luncheon Business meeting of the International Organizing Committee of ICL	
		Rm. 205 Wisconsin Center
6:30 - 8:00 PM	General Conference Reception. Refreshment and wine will be served. Ticket necessary for entry.	
		State Street Entrance Capitol Building

Tuesday, August 14, 1984

12:00 - 5:00 PM	Technical exhibits. Door prizes and light refreshments will be offered throughout the exhibition	
		Tripp Commons Memorial Union
6:30 - 7:30 PM	Reception honoring invited speakers By invitation	
		Alumni Lounge Wisconsin Center

Wednesday, August 15, 1984

9:00 AM - 5:00 PM	Technical exhibits continued

Thursday, August 16, 1984

1:30 - 5:00 PM	Wisconsin Dells excursion is gratis. Tickets are required, however, in order to maintain a count.
2:00 - 4:00 PM	Visit to Synchrotron Radiation Center, PSL Stoughton. Limited to 100 on first come first serve basis. Sign up sheets at Conference Office. Depart from Memorial Union. Visit is also gratis.
5:30 PM	Conference Banquet. Cash bar 5:30 - 7:00 PM. Price is $15.- After dinner entertainment will be provided by Professor C. Moser's New Hybernian Fox Trot Band

Concourse Hotel

Friday, August 17, 1984

5:30 - 7:00 PM	Farewell Reception honoring the Chair of ICL'87 By invitation

Van Vleck Lounge
Math Bldg.

TOURS

The following tours are being offered.

Monday, 8/13	1:30 - 3:30 PM	Madison City Tour
Tuesday, 8/14	9:00 AM - 4:00 PM	House on the Rock
Wednesday, 8/15	8:30 AM - 5:00 PM	Old World Wisconsin
	8:30 AM - 5:00 PM	Day in Milwaukee
Thursday, 8/16	10:00 AM - 1:00 PM	Luncheon and Shopping

One of the two tours on Wednesday is cetainly worth taking. Accompanying persons are urged to participate. Please sign up for these tours at the registration desk as soon as possible.

INTERNATIONAL CONFERENCE ON LUMINESCENCE - 1984

A digest of technical papers presented at the
International Conference on Luminescence
August 13-17, 1984, University of Wisconsin, Madison, Wis.

N00014-84-G-0053

Cosponsored by:

University of Wisconsin
Optical Society of America
IUPAP
International Commission for Optics
National Science Foundation
Office of Naval Research

In cooperation with:

American Physical Society
Electrochemical Society
International Center for Theoretical Physics
Lawrence Livermore National Laboratory

PROGRAM AT A GLANCE

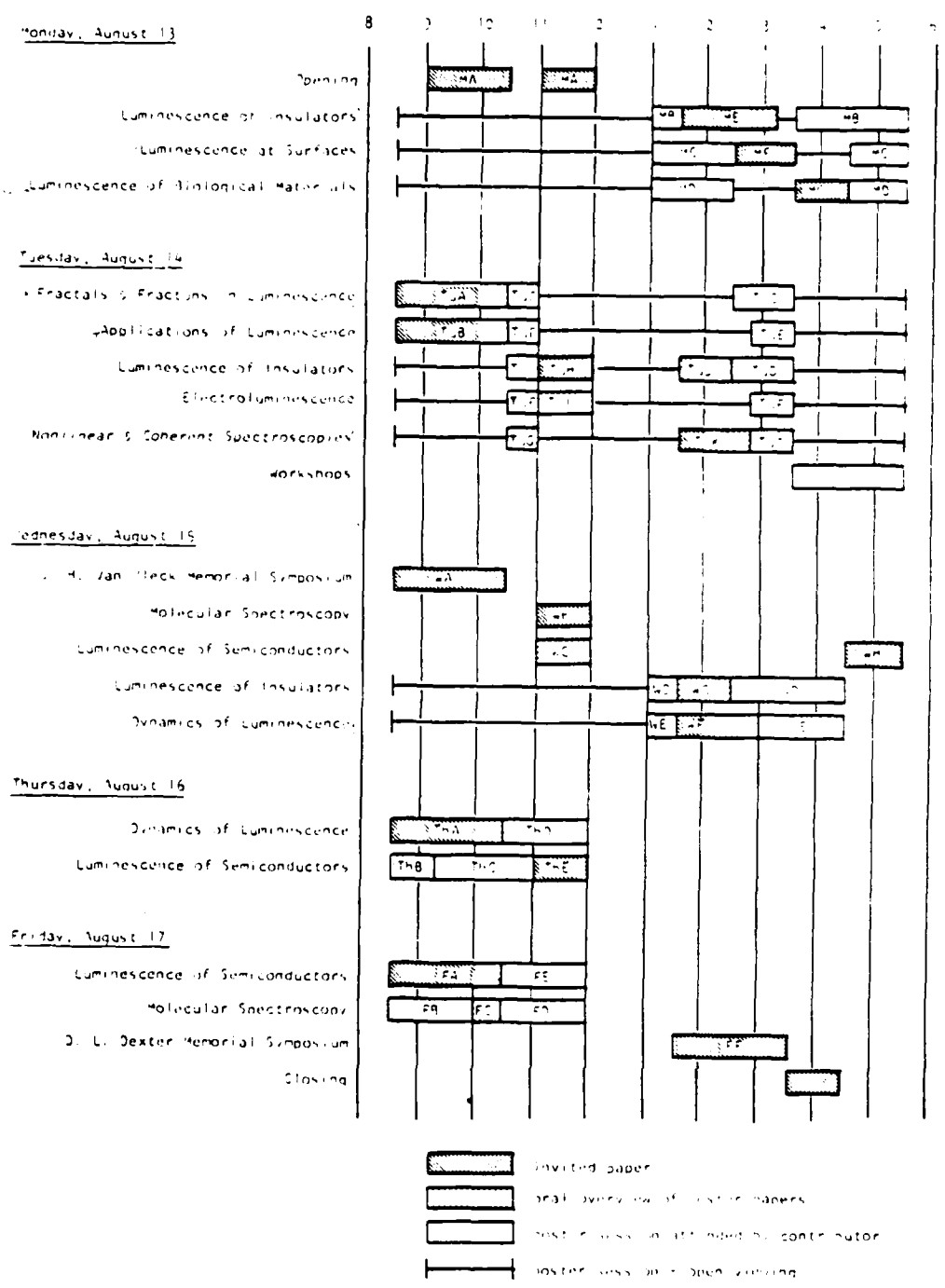

CONTRIBUTING SPONSORS

The following industrial concerns are providing ICL '84 with financial support:

Adolf Meller Co.
Allied Corp.
AMOCO
Coherent, Inc.
Cooper Laser-Sonics
Data Precision
Digital Equipment Co.
Dow Chemical Co.
Eastman Kodak Co.
EGG Princeton Applied Research
E. I. DuPont Co.
Exciton Chemical Co., Inc.
EXXON
Ford Motor Co.
General Electric
GTE
Hamamatsu Inc.
Hitachi Ltd.
Honeywell
Hoya Optics Inc.
Hughes Research Laboratories
Instruments S.A.
Karl Lambrecht Corporation
Kasei Optonix Corp.
Lumonics Inc.
3M Corp.
Matsushita Electronics Corp.
Matsushita Industrial Co.
Mitsubishi Electric Co.
Molectron Corp.
National Electrostatics Corp.
Newport Corp.
Nichia Chemical Industries
Optovac Inc.
Philips of North America
Photochemical Research Associates
Polaroid Corp.
Quanta-Ray Inc.
Questek Inc.
RCA
Schott Glass Technologies, Inc.
Sharp Corp.
SOHIO
Sony Corp.
Spectra Physics Inc.
Tektronix Inc.
Toshiba Corp.
Tracor Northern
Westinghouse
Xerox

Others
University of Wisconsin Credit Union
Sager-Wilson Travel

MA1 and MA2

MA1

Laser Spectroscopy of Atoms, Molecules, and Solids

Arthur L. Schawlow

Stanford University

California 94305

The powerful, directional and monochromatic light of tunable lasers makes it possible to resolve fine details in spectra and to distinguish spectroscopic centers within inhomogeneously broadened lines. Some particular examples of spectroscopic studies employing these laser techniques will be discussed.

MA2

Luminescence Studies of Restricted Molecular Motion in Liquids

R. M. Hochstrasser
University of Pennsylvania
Department of Chemistry
Philadelphia, PA 19104

Femtosecond Measurement of Configurational Relaxation with the Soliton Laser

L. F. Mollenauer
Rm 4C-306
AT&T Bell Laboratories
Holmdel, N.J. 07733

SUMMARY

There are many questions surrounding the configurational relaxation that follows optical excitation of luminescent systems. Fundamental to the resolution of these questions is a measurement of the configurational relaxation time. For systems involving an intimate coupling with phonons, such as organic dyes or color centers, relaxation times are expected to be on the picosecond or subpicosecond time scales, even at zero temperature. Thus, resolution to a very small fraction of a picosecond is required, if the (highly temperature-dependent) relaxation of such systems is to be measured over a significantly wide temperature range. Fortunately, recent developments[1,2] in ultrashort pulse lasers have opened up the possibility of such measurement. This talk concerns one such source, the "soliton laser"[2], and its use on systems with near-infrared absorption bands.

The soliton laser- a novel mode- locked color center laser that employs a length of single-mode optical fiber in its feedback loop- makes use of pulse compression and solitons in the fiber. (The solitons in this case are pulses whose shape changes periodically with propagation.) The fiber controls the laser's output pulse width, in accord with known soliton behavior: the pulse width scales as the square root of the fiber length. To date, pulse widths ranging from 2 to 0.2 psec have been produced, and widths <0.1 psec are expected soon. With compression in an additional, external fiber, it should be possible to produce pulse widths of just a few tens of femtoseconds.

Such ultrashort pulses should allow for the measurement of configurational relaxation time with a temporal resolution limited only by the uncertainty principle itself. (The band width of, say, a 20 fsec pulse is ~500 cm^{-1} - nearly the same as the homogeneous widths of most color center absorption bands.) Previous measurement[3] of configurational relaxation times- for the F_A(II) center in KCl:Li - employed a pump-probe technique requiring two lasers; temporal resolution was limited by poor signal-to-noise ratio as well as by the pump laser's pulse width of ~0.5 psec. In this talk, it will be shown how such measurements can be accomplished more simply, with just a single laser acting as both pump and probe on the center's absorption band. Signal-to-noise ratio will also be much improved.

As the soliton laser's output is wavelength tunable in the neighborhood of 1.5 microns, one likely candidate for study is a color center whose fundamental absorption band peaks at just about that wavelength, the F_2^+ color center in the host KBr. It should be possible to measure that center's configurational relaxation time over a wide temperature range, and from the temperature dependence to estimate the characteristic energies of the rate-controlling phonons.

References

1. C. V. Shank, R. L. Fork, R. Yen, R. H. Stolen, and W. J. Tomlinson, "Compression of femtosecond optical pulses", Appl. Phys. Lett. 40, 761 (1982)

2. L. F. Mollenauer and R. H. Stolen, "The Soliton Laser", Opt. Lett. 9, 13 (1984)

3. J. M. Wiesenfeld, L. F. Mollenauer, and E. P. Ippen, "Ultrafast Configurational Relaxation of Optically Excited Color Centers", Phys. Rev. Lett. 47, 1668 (1981)

4f-Electron-Phonon Interaction and Davydov-Splitting in PrF_3

M. Dahl, G. Schaack

Physikalisches Institut der Universitat, Röntgenring 8, D-8700 Würzburg, FRG

In the ionic Rare Earth compound PrF_3 we studied several interaction effects between the system of the low lying 4f-electron excitations and the optical phonons, which could be interpreted by a Jahn-Teller type interaction Hamiltonian between the two systems.

Both the E_g-phonon at ≈370 cm^{-1} and the E_u-phonon at ≈105 cm^{-1} show an anomalous temperature dependence of their frequencies compared with the corresponding modes in the isomorphic LaF_3. A theoretical interpretation is given by the phonon self-energy:

$$S_{ps}(w) = \sum_{\alpha MN} G_p^{\alpha} G_s^{\alpha} (n_M - n_N) \frac{{}^{\alpha}\langle\psi_N|O_p|\psi_M\rangle^{\alpha}\ {}^{\alpha}\langle\psi_M|O_s|\psi_N\rangle^{\alpha}}{w-(\varepsilon_M-\varepsilon_N)} \qquad (1)$$

which resulted from a Greensfunction treatment /1/ of the phonon system. (O_p: electronic tensorial operator; G_p: coupling constant; n_M: thermal occupation factor for the electronic states $|\psi_M\rangle$).

In an external magnetic field we could observe the splitting of an E_g-phonon at 78 cm^{-1}. In contrary to the phonon splittings reported earlier in Langevin paramagnets, e.g. CeF_3 /2/, the splitting observed for the Van Vleck paramagnet PrF_3 shows no saturation effects up to fields B = 8 T. The explanation could also be given on the basis of the self-energy (1) if we take into account the polarisation of the crystal-field eigenfunctions in the magnetic field.

The comparison between the diluted system Pr^{3+} in a LaF_3 host and the concentrated PrF_3 shows another interesting consequence of electron-phonon interaction: For several electronic levels lying close to optical phonon states, the single ion crystal-field model is no longer a suitable approximation, because interaction mechanisms, notably the virtual phonon ex-

change leads to a resonant energy transfer between the Pr^{3+} ions. In Fig. 1 we show the observed energy levels (Davydov splitting) for the two lowest excited crystal-field states. For the microscopic description we treated the 4f-system and the optical phonon system simultaneously by a Greensfunction formalism in an RPA approximation, which contains the above given phonon self-energy as a limit for the case where phonons and 4f-excitations are not in resonance. In the same limit we obtained an electronic self-energy of the form:

$$S_{\alpha NM,\beta RS}(w) = \sum_p G_p^{\alpha} G_p^{\beta} \frac{{}^{\alpha}\langle\psi_N|O_p|\psi_M\rangle^{\alpha}\ {}^{\beta}\langle\psi_R|O_p|\psi_S\rangle^{\beta}}{w^2 - w_p^2} \quad (2)$$

which describes the Pr^{3+}-Pr^{3+} interaction by the exchange of phonons. Using this self-energy the Dyson equation leads to a temperature dependence of the Davydov splitting. In Fig. 2 we show the experimental and theoretical resuls for two Davydov components of the lowest crystal-field excitation.

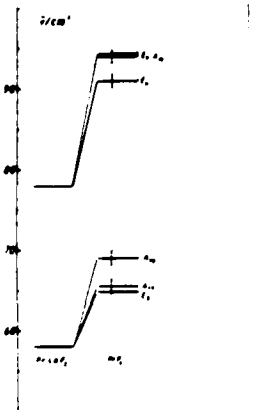

Fig.1: Energy states observed for Pr^{3+} in LaF_3 and PrF_3.

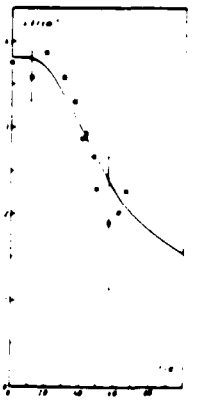

Fig.2: Temperature dependence of the splitting for the lowest crystal field excitation.

/1/ P. Thalmeier, P. Fulde: Z. Physik B26, 323 (1977)

/2/ K. Ahrens, G. Schaack: Phys. Rev. Lett. 42, 1488 (1979)

FLUORESCENCE IN THE ONE-DIMENSIONAL FERROMAGNET $CsNiF_3$

M. SOSCIA, J. CIBERT, M.C. TERRILE, Y. MERLE D'AUBIGNE

Laboratoire de Spectrométrie Physique, Université Grenoble 1,

B.P. 68, 38402 Saint Martin d'Hères-cédex, France

The nature of optical excitations in low dimensional stoechiometric compounds is of current interest. In one-dimensional antiferromagnets (TMMC, CMC)[1] the excitation is reported to be localized. However in rare-earth systems [2] a double-peaked lineshape has been attributed to the dispersion of the exciton.

From its structure $CsNiF_3$ is predicted to be fairly one-dimensional. This has been experimentally checked for the ground-state properties : short range ferromagnetic order develops along the chains for temperatures up to 40 K, and collective excitation (magnons) are observed. A magnetic field applied within the easy plane reduces the spin fluctuations, and so two independent external parameters allow to control the magnetic (dis)order. Their effect on a sharp zero-phonon absorption line observed in the near IR ($^3A_2 \rightarrow {}^3T_2$ transition) has been presented elsewhere. The corresponding electronic level usually fluoresces and studies of the zero phonon line should give interesting information on the nature and behaviour of the electronic excitations. A pulsed color center laser ($Tl^0(1)$ in KCl) built in the laboratory allows a direct excitation of the $^3T_2$ level. The intrinsic fluorescence is observed;with applied field it consists in a sharp (zero-phonon, zero-magnon) line and a broader(one-magnon)line,followed by the usual broad vibronic band. The two lines coincide in energy with the corresponding absorption lines. Without applied field the magnon gap

vanishes and both lines merge into one single asymmetric line. The decay time (approximately 60 μs at 4 K) is considerably shorter than the lifetime usually measured for Ni^{2+} impurities in diamagnetic crystals (∿ 10 ms).

When raising the temperature the lines broaden due to the increase of spin fluctuations. They can be followed up to temperatures (10-20 K) well above the Néel temperature for three dimensional ordering (T_N = 2.7 K). The decay time increases with temperature.

At lower temperatures (T < 4 K) a number of sharp lines develop corresponding to traps (with a very shallow trap at 12 cm^{-1}). Both the intensity and the decay time of these traps rapidly increase with decreasing temperatures. Application of a magnetic field results in a more efficient trapping. This is to be contrasted with TMMC where no trapping was observed at low temperature, and demonstrates the delocalized character of electronic excitation in $CsNiF_3$ at low temperature. Measurements of the variations of the lifetime of the free exciton with temperature and magnetic field (i.e. with magnetic disorder) are in progress.

(1) H. Yamamoto, D.S. Mc Clure, C. Marzzaco and M. Waldman, Chem. Phys. 22, 79 (1977) ; Weiyi Jia, E. Strauss and W.M. Yen, Phys. Rev. B 23, 6075 (1981)

(2) R.S. Meltzer, Solid State Commun. 20, 553 (1976)

(3) J. Ciber† and Y. Merle d'Aubigné, Phys. Rev. Lett. 46, 1428 (1981).

M.F. Joubert, C. Linarès, B. Jacquier and B. Wanklyn *
E.R.A. 1003 C.N.R.S.
Physico-Chimie des Matériaux Luminescents
Université Claude Bernard - Lyon I -
43 Bd du 11 Novembre 1918 - 69622 VILLEURBANNE CEDEX, FRANCE

* Department of Physics, Clarendon Laboratory
University of Oxford
OXFORD OX1 3PU ENGLAND

Summary

We report the results of an investigation of optical spectroscopy of two terbium concentrated materials : TbF_3 and $TbAlO_3$ at very low temperature. From magnetic measurements and neutron diffraction data, it is known that isomorphous TbF_3 and $TbAlO_3$ orders ferromagnetically below T_c=3.95 K and antiferromagnetically below T =3.8 K respectively.

At 4.4 K, the $^5D_4 \rightarrow {}^7F_J$ intense visible fluorescence of these materials originates mainly from impurity induced trap Tb^{3+} ions in agreement with a fast diffusion model. As a consequence, excitation spectra ($^7F_6 \rightarrow {}^5D_4$) from both intrinsic and trap fluorescences are identical but differ from lightly doped Tb^{3+} compounds (for example $LaF_3:Tb^{3+}$ or $EuAlO_3:Tb^{3+}$) by a broadening of the excitation lines. Consequently this broadening seems to be related to the ion-ion interactions in agreement with the exciton life time. (at 4.4 K, τ_{exc}=179 μs and 6,7 μs for TbF_3 and $TbAlO_3$ respectively).

At 1.6 K, where both materials order magnetically, the trap emission stays the more intense but the excitation spectra of the trap fluorescence exhibit new features which indicate the direct excitation of each trap center. Furthermore, at this temperature, excitation lines of the intrinsic fluorescence are now shifted and better resolved showing clearly two components for TbF_3 and shoulders for $TbAlO_3$ (see figure). These observations have to be related to the exciton decay which is now one order of magnitude longer than at 4.4 K. Moreover the application of an external magnetic field along

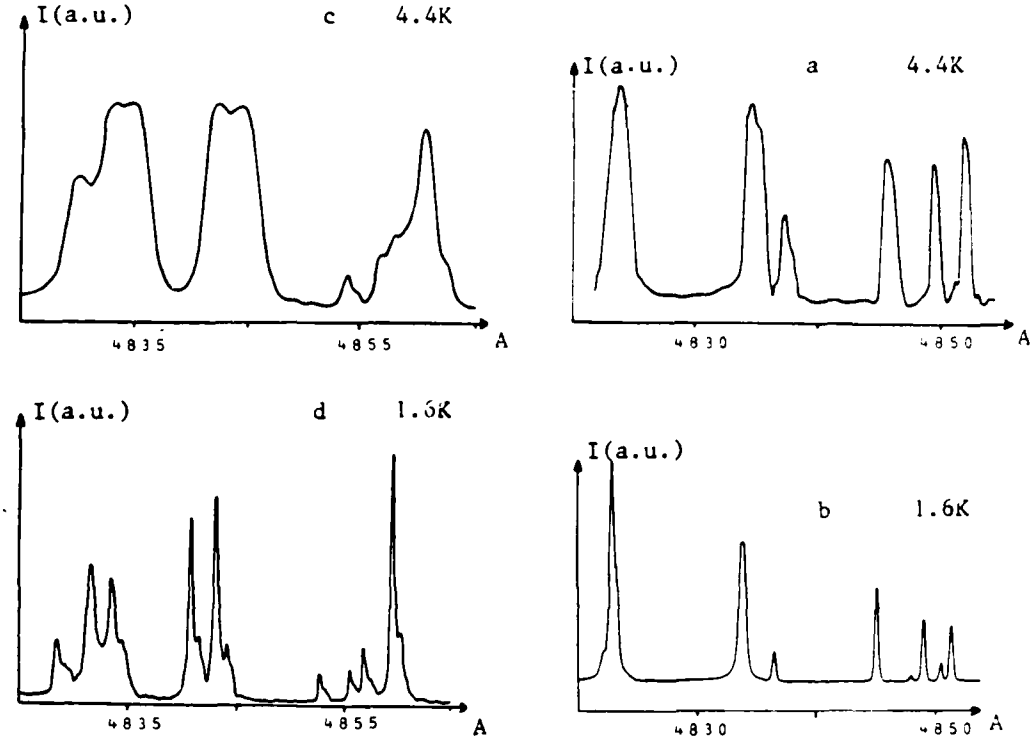

Figure I : Excitation spectra of the intrinsic fluorescence in TbF_3 (a,b) and $TbAlO_3$ (c,d).

different directions of the crystals shows a more complete localization of the excitation.

Two-Photon Excitation of the Luminescence in Bismuth Germanate.

M.Casalboni, R.Francini, U.M.Grassano, C.Musilli and R.Pizzoferrato.
Dipartimento di Fisica. Seconda Università di Roma,
Via Orazio Raimondo (La Romanina) - I 00173 ROMA, Italy.

Excitation of bismuth germanate ($Bi_4Ge_3O_{12}$) single crystals with ultraviolet or X-ray photons of wavelength shorter than 300 nm produces a broad emission band centered around 500 nm.

One photon excitation of this luminescence reveals at liquid nitrogen temperature a sharp edge at 280 nm followed by two broad maxima around 270 and 240 nm. These structures have been assigned to the $^1S_0 \rightarrow {}^3P_1$ and $^1S_0 \rightarrow {}^1P_1$ transitions of the trivalent mercury-like bismuth ion (1) or to transitions in molecular clusters (2). The luminescence excitation, due to the high absorption coefficient, mainly reflects the properties of a thin surface layer of the sample. In order to study bulk effects we have measured the emission excited by the simultaneous absorption of two photons from a flash lamp pumped dye laser tunable in the range 470-600 nm. The laser flux was kept of the order of 2 MW/cm^2 and particular care was taken to avoid dielectric breakdown of the crystal occurring at higher energy flux.

The two-photon excited emission has the same spectral distribution of the one-photon luminescence, but its excitation spectrum is very different. The two-photon excitation begins at higher energy. The first feature of the one-photon spectrum at 280 nm is almost completely disappeared and the edge is now found at 270 nm. The excitation spectrum rises slowly at first up to 250 nm and then more sharply, but no peaks are found in the investigated excitation range.

The room temperature data show a similar behaviour: the excitation begins at 288 nm, clearly above the one-photon threshold around 300 nm. The shift of the two-photon absorption edge and the disappearance of the

first one-photon excitation peak are similar to the results obtained in alkali-halides (3). Further experiments are in progress in order to determine the nature and the symmetry of the transitions.

References:

1) M.J.Weber, R.R.Monchamp, J.Appl.Phys. 44, 5495 (1973).

2) R.Moncorgè, B.Jacquier and G.Boulon, J.Luminescence 14, 337 (1976).

3) J.M.Worlock, Laser Handbook, eds.F.T.Arecchi and E.O. Sculz-Dubois (North-Holland, Amsterdam, 1972), p. 1323.

TWO-PHOTON LUMINESCENCE SPECTROSCOPY OF Hg_2Cl_2 SINGLE CRYSTALS

I.Pelant, M.Ambrož, J.Hála, V.Kohlová and K.Vacek
Charles University, Faculty of Mathematics and Physics, Ke Karlovu 3, 121 16 Prague 2, Czechoslovakia

Single crystals of Hg_2Cl_2 are known to be highly birefringent optical material of technical importance for polarizing prisms and other optical components in the visible region. However, some fundamental physical properties of Hg_2Cl_2, such as its energy band structure, are not known up to now. Absorption spectrum in the vicinity of absorption edge (~ 3.9 eV) was measured recently [1] showing a distinct structure, but unambiguous interpretation is difficult to be done due to the lack of any band structure calculation. Important complementary information can be obtained, however, from two-photon absorption experiments especially in systems possessing a center of inversion, what is the case of Hg_2Cl_2 crystals (D_{2h} point group for $T < 185$ K, D_{4h} for $T > 185$ K). Recently, we have reported for the first time observation of low-temperature two-photon absorption in Hg_2Cl_2 single crystals upon a pulsed dye-laser excitation and demonstrated the feasibility of its monitoring via a luminescence band at 396 nm (3.13 eV) /2/. In this contribution we wish to present and discuss two-photon exitation spectrum of the 396 nm emission band at $T \sim 10$ K in the region $4.16 \leq 2h\nu \leq 5.4$ eV. The excitation spectrum is characterized by a gradual smooth increase starting from the low-energy side, a shoulder at $2h\nu \sim 4.8$ eV and a dominating intense maximum at $2h\nu \sim 5.14$ eV. Compared to the one-photon absorption spectrum /1/, one finds "alternating" maxima which are observed or in one-photon or two-photon experiments, but which are not common for the both cases. Conclusions are made on the symmetry of related Brillouin-zone points and wavefunctions.

/1/ Z.Bryknar, W.Hersel and C.Barta: Crystal Res.&Technol. 17 (1982), 425

/2/ I.Pelant, M.Ambrož, J.Hála, V.Kohlová and Č.Bárta: Phys. Letters, to be published

Time-Resolved Photoluminescence in $SrTiO_3$

R. Leonelli and J. L. Brebner

Département de physique, Université de Montréal,
Montréal, Québec H3C 3J7, Canada

$SrTiO_3$ is an insulator with a band gap of 3,27 eV which shows evidence of strong electron-phonon interaction. Its luminescence spectra exhibits a broad band in the visible, apparently intrinsic in nature (1). Its transport properties reveal the existence of deep traps for holes (2) and small polaron behaviour has been observed for electrons in the conduction band (3).

We have illuminated nominally pure $SrTiO_3$ samples with intense 3 ns-long pulses from a nitrogen laser (excitation energy: 3,68 eV). The time evolution of the visible band luminescence intensity has been measured in the range 10^{-9} to 10^{-2} s. For temperatures between 4,2 and 35 K, the intensity follows first an exponential law with a time constant of $1,1 \times 10^{-6}$ s. Then, at times longer than 2×10^{-6} s, it assumes a t^{-m} form, where t is the elapsed time and $m \simeq 0,90$. This behaviour abruptly changes above 35 K. As the total luminescence intensity decreases, the behaviour at short times deviates from an ecponential law and the average time constant decreases. At longer times, the exponent m of the power law increases to reach 1,4 at 45 K.

These results indicate that there exists two parallel emission channels. One channel involves the recombination of delocalised excitations, either excitons or e-h pairs, and is responsible for the behaviour at small times. The other channel involves the recombination of trapped polarons, whose probability of recombining depends on the distance separating them. What happens as the temperature goes beyond 35 K is not well understood but could be partly explained by competition from other recombination processes. Finally, the deviation from a simple exponential law at small times as the the temperature is increased appears to indicate the presence of low energy potential fluctuations (4).

(1) L. Grabner, Phys. Rev. 177, 1315 (1969).

(2) T. Feng, Phys. Rev. B 25, 627 (1982).

(3) D. Kéroack, Y. Lépine and J. T. Brebner, J. Phys. C 16, 883 (1984).

(4) K. L. Ngai, Comm. Sol. St. Phys. 9, 127 (1979); 9, 141 (1980).

Mechanisms of Exciton Trapping in Oxides

W. Hayes

Clarendon Laboratory, Oxford OX1 3PU, U.K.

The localisation energy required for intrinsic self-trapping of excitons increases with increasing bandwidth and calculation suggests that oxides are marginal cases for self-trapping. We have used ODMR of recombination radiation of oxides to study exciton trapping mechanisms. Work carried out in the past has shown that in oxides such as YAG[1] and $YAlO_3$[2] excitons are trapped near defect sites. More recently we have studied the well-known blue emission of quartz at 4K[3]. Our results show that part of this emission arises from a triplet state of a trapped exciton and we have determined the principal magnetic axes of the centre. Comparison with other work[4] suggests that the exciton is trapped in an efficient intrinsic radiolytic process involving the transient production of an oxygen Frenkel pair. The fine-structure splitting of the triplet state is unusually large (D = 22.6 GHz), consistent with an oxygen molecular configuration involving an interstitial oxygen. The model for this centre requires the interstitial oxygen and vacancy to be close together and to recombine in the process of radiative decay.

Recently we have also carried out ODMR studies of recombination radiation in Y_2O_3 and Sc_2O_3[5]. Y_2O_3 has a band edge at $\sim$ 6.5 eV and a strong luminescence emission at 3.4 eV at 4K with $\tau \sim 1$ μs. Detailed optical studies[6] give results consistent with barrierless self-trapping of excitons. Our ODMR studies show that the 3.4 eV luminescence arises from a triplet state of a trapped exciton and suggest a self-trapping mechanism involving a lattice anion, an interstitial anion and an anion vacancy. The proposed structure is reminiscent of that found for the self-trapped exciton in fluorites[7] (Y_2O_3 and Sc_2O_3 have the bixbyite structure, closely related to the fluorite structure) and has some resemblance to the trapping mechanism we have proposed for

crystal quartz[3].

Sc_2O_3 has a bandgap of $\sim$ 5.9 eV and a luminescence emission at 3.6 eV at 4K. Although the ODMR properties are similar to those of Y_2O_3[5] there are interesting differences in the luminescence properties of the two materials.

Finally, we shall make comparisons between the trapping mechanisms proposed above for oxides and trapping mechanisms for halides; in the latter, hole-lattice interaction is the dominant factor.

References

1. W. Hayes, M. Yamaga, D.J. Robbins and B. Cockayne, 1981, J. Phys. C. 13 L1085.

2. R.L. Wood and W. Hayes, 1982, J. Phys. C. 15, 7209.

3. W. Hayes, M.J. Kane, O. Salminen and R.L. Wood, 1984, to be published.

4. K. Tanimura, T. Tanaka and N. Itoh, 1983, Phys. Rev. Lett. 51, 423.

5. W. Hayes, M.J. Kane, O. Salminen and A.I. Kuznetsov, 1984, to be published.

6. A.I. Kuznetsov, V.N. Abromov, V.V. Mürk, B.R. Namozov and T.U. Mibo, 1981, Proc. Int. Conf. on Lasers, p. 793.

7. R.T. Williams, M.N. Kabler, W. Hayes and J.P. Stott, 1976, Phys. Rev. B14, 725.

Spontaneous and Stimulated Emission by Self-Trapped Excitons in Cadmium Iodide.

A.Cingolani, M.Ferrara, M.Lugarà.
Dipartimento di Fisica dell'Università di Bari - Via Amendola 173
70126 Bari (Italy).

The spontaneous and the stimulated emission of CdI_2 have been studied in the temperature range from 10 to 200°K, under low and high intensity of excitation by means of a nitrogen laser (I_{max} = 10 MW/cm^2, τ= 5 nsec), whose photon energy was 3.68 eV, i.e. larger than the energy gap of the ionic crystals of CdI_2. Our samples showed a 4H-polytypism as confirmed by the spontaneous Raman spectroscopy measurements performed by means of a 500 mW Argon ion laser excitation. Our crystals appeared unintentionally dooed with Pb^{++}, as confirmed by the spontaneous emission spectra at T=20°K obtained under dye laser ($h\nu$ =3.25 eV) excitation in resonance with Pb levels. The absorption due to these impurity levels strongly appears even at RT in the photoacustic spectra we have carried out. The spontaneus emission spectra at low excitation show a worth evolution with the sample temperature of the competitive broad bands in the near ultraviolet and visible optical regions. The line shape of these bands,extracted from the total spectrum generated from their superimposing, results to be gaussian. The energy scheme to assign the nature of these bands could be that of self-trapped excitons typical of ionic crystals like CdI_2. At high intensity the spectrum consist only in a very broad band, whose halfwidth of about 100 nm is independent of the sample temperature. The emission comes out from the whole sample surface even if the excitation is localized in a small spot. The stimulated emission shows the same feature of the spontaneous spectra obtained under high excitation. On the contrary the optical gain spectra show several main peaks that at 80°K are localized at 2.81, 2.53, 2.37 and 2 eV respecti-

vely. These gain peaks are well consistent with the maxima of the deconvolved bands observed in spontaneous spectra under low excitation. The values of the optical gain coefficient are surprisingly high ($g \geq 10^4$ cm^{-1}) for all the peaks at 80°K whereas at temperatures either lower or higher than LNT the optical gain shows a sharp drop. The integrated external efficiency of the stimulated emission from CdI_2 at 80°K excited by N_2 laser results of about 0.1%. The very high value of the optical gain coefficient of CdI_2 at 80°K can be explained by taking into account that the self-trapped excitons levels diagram looks like the typical four levels laser scheme. Anyway the population inversion threshold up to-day can be overcome only by means of high intensity optical pumping[1].

(1) - R.W. Boyd, M.S. Malcuit, K.J. Teegarden; IEEE J. Quantum Electr. QE 18, 1202 (1982).

SELF-TRAPPING OF EXCITONS IN RARE GAS SOLIDS : MEASUREMENT OF SELF-TRAPPING RATES AND INFLUENCE OF DIMENSIONALITY

by

E. Roick, R. Gaethke, P. Gürtler* and G. Zimmerer

II. Institut für Experimentalphysik der Universität Hamburg,
Luruper Chausee 149, 2000 Hamburg 50, Fed. Rep. Germany
*Hamburger Synchrotronstrahlungslabor HASYLAB bei DESY,
Notkestrasse 85, 2000 Hamburg 52, Fed. Rep. Germany

The wavelike exciton states (free excitons, FE) in rare gas solids (RGS) are not stable. Exciton-phonon interaction induces a lattice deformation at which the excitons are self-trapped (STE). The FE and STE states are separated by a potential barrier. Therefore, in the luminescence spectra of (the heavier) RGS, FE and STE emission coexist[1,2]. This paper presents new experimental results concerning (i) the self-trapping rate and (ii) the influence of dimensionality on self-trapping.

Self-trapping rate of free excitons (Xe and Kr)

For the first time, decay curves of FE luminescence of Xe (8.3 eV) and Kr (10.2 eV) were measured under primary excitation of n = 2 FE with synchrotron radiation, the pulsed nature of which -in connection with fast channel plate detectors- enables measurements of decay rates Γ up to $2 \cdot 10^{10}$ s^{-1} in the VUV. The self-trapping rate Γ_{ST} was deduced via $\Gamma_{ST} = \Gamma - \Gamma_{rad}$ (Γ_{rad} : radiative rate). The temperature dependence of Γ_{ST} (fig. 1) is well described by

$$\Gamma_{ST} = \Gamma_0 \{1 - (T/\theta_D)^{\alpha}\}^{-1}$$

which was proposed by Rashba[3] for

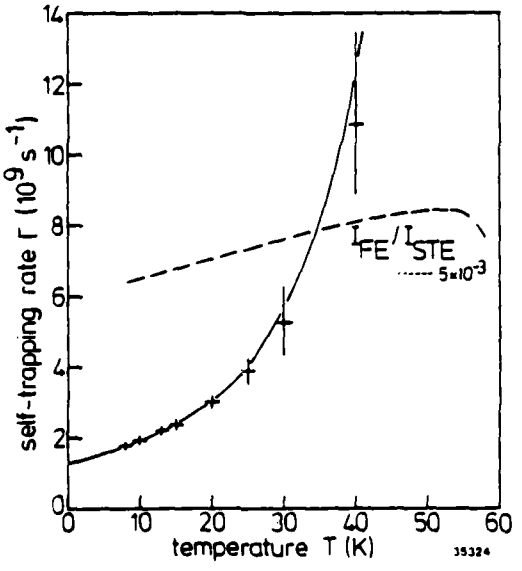

Fig. 1 Self-trapping rate of free excitons in Xe as a function of temperature

thermal assisted tunneling through the barrier separating FE and STE states (Γ_o : tunneling rate at T = 0 , θ_D : Debye temperature). From Γ_o we extracted the height of the barrier following the theory of Nasu and Toyozawa[4] (Kr : 42 meV, Xe : 30 meV). The lower value in Xe is explained by self-trapping at vacancies.

Influence of dimensionality (Ar)

In the special case of Ar, it was possible for the first time to distinguish between self-trapping in the bulk and at the surface by an appropriate choice of excitation energy in experiments with and without surface coverage by Ne. The branching between different trapping geometries is dramatically different in the bulk and at the surface. The results clearly show that exciton-phonon interaction at the surface of the three-dimensional sample behaves like in a two-dimensional system and is of the marginal type, whereas it is of the stiff type in the bulk[1,5].

At the surface, the coupling of the local oscillator of the molecular type STE to lattice vibrations is considerably weaker than in the bulk. This leads to a drastic enhancement of hot luminescence of surface-STEs. The effect will be discussed for Ar and Ne.

References :

[1]E.I. Rashba, in "Excitons", ed. by E.I. Rashba and M.D. Sturge, North-Holland Publishing Company (1982), p. 505.

[2]G. Zimmerer, J. Lumin. 18/19, 875 (1979).

[3]E.I. Rashba, in "Defects in Insulating Crystals", ed. by V.M. Tuchkevich and K.U. Shvarts, Zinatne Publishing House, Riga, and Springer Verlag, Berlin (1981), p. 255.

[4]K. Nasu and Y. Toyozawa, J. Phys. Soc. Japan 50, 235 (1981).

[5]Y. Shinozuka and Y. Toyozawa, J. Phys. Soc. Japan 48, 472 (1980).

Measurement of Exciton Absorption Spectrum in KI Using New Method

H. Nishimura
Department of Appl. Phys., Osaka City Univ.,
Sumiyoshi-ku, Osaka 558, JAPAN

Detailed information about optical absorption is very important in understanding the optical processes such as luminescence, excitation, reflectance and absorption itself. However, the information for alkali halides is poor compared with the detailed information about other processes which have been reported recently.[1,2] For alkali halides the measurement of optical absorption in crystal is impossible on account of the very high absorption coefficient and as a consequence one has to use other (substitutional) methods. The spectrum of thin film, however, is very broad and shifts to low energy, and the imaginary part of the dielectric constant derived from reflectance spectrum also deviates from the real spectrum of absorption because of the difficulty in measuring the reflectance over the whole spectral region. Besides, in general the imaginary part often does not show structures which are observed but weakly in absorption and excitation spectra. Therefore, we have to find new method to know real information about absorption.

In this study we have measured an improved absorption spectrum in KI in a new technique. First we shall show a measurement of the quantum yield (η_{tot} in Fig. 1) of total luminescence bands emitted under free exciton creation as a function of incident photon energy. This result is understandable in terms of free exciton diffusion length and penetration depth where the optical

conversion from incident photon to free exciton occurs. The free excitons created inside the crystal are not damped nonradiatively inside the crystal but damped at crystal surface after migration. The nonradiative damping rate of free excitons accordingly becomes large when the rate of free excitons to reach the crystal surface is large, namely, when the exciton diffusion length is large and the penetration depth is small. Analysing the result of η_{tot} by an exciton diffusion equation we obtained an absorption spectrum (Fig. 2). Very sharp absorption peaks exist in 1s and 2s exciton resonance regions where the 1s and 2s free exciton resonance lumines cence lines are observed respectively. We will discuss the absorption spectrum in comparison with the reflectance spectrum observed simultaneously, and also discuss the phonon structures in the absorption and reflectance spectra in terms of phonon assisted transition and exciton LO phonon bound state.

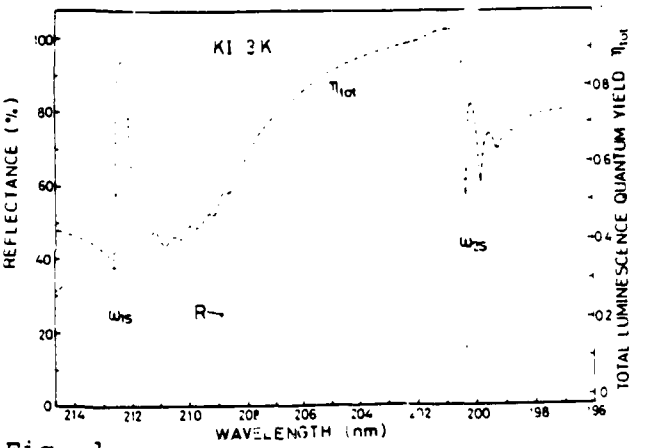

Fig. 1

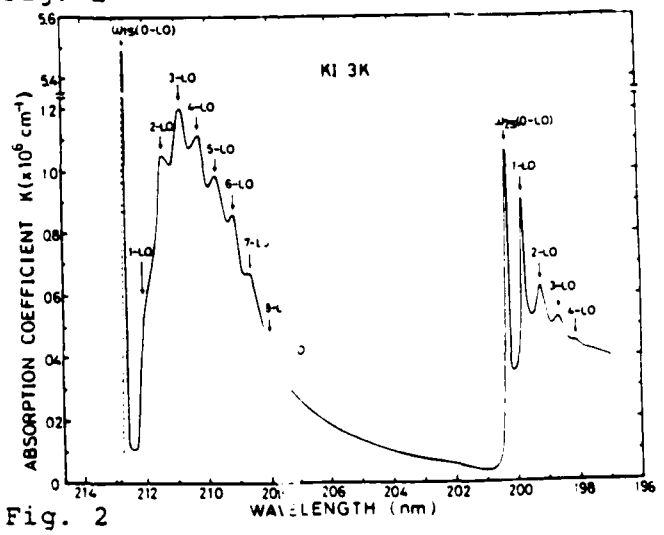

Fig. 2

1) H. Nishimura: Semiconductors and Insulators 5 (1983) 263.

2) H. Nishimura: J. Phys. Soc. Jpn. 52(1983) 3233.

INTRINSIC LUMINESCENCE IN CdF_2 CRYSTALS

F.Fermi, C.Paracchini
Dipartimento di Fisica - Università di Parma - Parma - Italy

CdF_2 crystals have the fluorite structure and a gap 7.6eV wide. Under X rays excitation pure crystals show, at temperatures lower than 100 K, an intense blue luminescence. The emission spectrum evidences a large band between 300 and 500 nm with a maximum at about 380 nm[1]. In doped samples one observes the same luminescence besides that of the intentional impurity. The same blue emission is obtained also in the electroluminescence of pure and doped CdF_2 crystals[2].

The presence of such emission independently on the intentional doping and on the excitation process suggests the intrinsic nature of the luminescence. The same indication is obtained by the analogy of the emission range and the efficiency dependence on the temperature with those observed in the electron-hole radiative recombination of other ionic compounds. A more precise indication of the nature of the luminescence is however obtainable from the comparison of the excitation spectrum of the luminescence with that of absorption and reflectivity in the excitonic region.

Nominally pure CdF_2 single crystals are illuminated at 80 K with u.v. light from a Deuterium lamp or with v.u.v. light from sinchrotron radiation (PULS Facility - Frascati) and the dependence of the emission spectrum on the excitation wavelenght is studied. Good agreement between the absorption and the excitation spectra for the emission at 380 nm are obtained.

The results indicate that, at least in part, the emission band observed between 300 and 500 nm is correlated with a radiative relaxation process excited in the band gap region.

The observed luminescence is then obtained with the formation of electron-hole pairs by pulling the electrons from the valence band up to the bottom of the conduction band. The energy required for this process is approximately that of the gap, while the emission, on the contrary, is around 3.3 eV. A large part of the energy acquired in the excitation process is then released non radiati vely.

The large Stokes shift indicates that a strong electron lattice coupling is involved in the relaxation process. This is in agreement with the highly ionic nature of this compound. The formation of self trapped hole centres may be responsible for the large phonon dissipation.

1) A.Tzalmona, J.Phys.Soc.Japan 34, 1108 (1973).
S.Benci, G.Schianchi, J.Luminescence, 11, 349 (1976).

2) C.Paracchini, G.Schianchi, Phys.Status Solidi (a), 52, K49(1979).
C.Paracchini, G.Schianchi, Solid State Commun. 21, 1107 (1977).
C.Paracchini, Phil.Mag. B 46, 391 (1982).

Emission Spectra of Thallium Bromide Solutions

U.Giorgianni, V.Grasso and G.Saitta
Istituto di Struttura della Materia, Università di Messina, and GNSM-CNR, Messina, Italy
U.M.Grassano
Dipartimento di Fisica, Seconda Università di Roma, Italy

Alkali-halide crystals when doped with heavy-metal ions with the s^2 configuration show absorption and emission bands which are characteristic of the impurity[2,3]. A close resemblance was observed by us between the absorption spectra of thallium bromide solutions and the spectra of thallium-doped potassium bromide single crystals[3] as shown in fig.1.Furthermore, the same similarity between doped crystals and solutions was also observed in the luminescence spectra on excitation in the UV absorption bands.Fig.2 reports the emission spectra at room temperature of an alcoholic TlBr solution of polycrystalline powder, for two different excitation wavelengths.The spectra consist almost entirely of two overlapping bands with an energy separation of about 0.5 eV and of several shoulders.The spectral positions of the two main structures are the same as in the solid as one can observe in the figure.

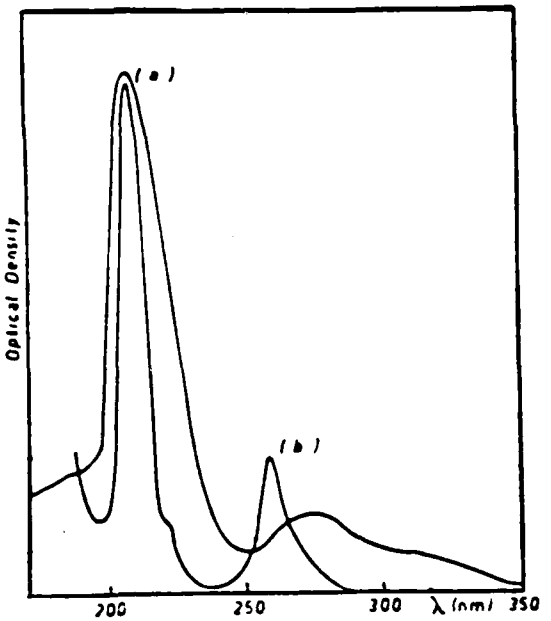

Fig. 1. Absorption spectra of an alcoholic solution of TlBr (a) and of KBr:Tl single crystal (b).

For A excitation (255 nm), however, the relative heights of the two main structures of solutions are reversed with respect to the solid.

The emission spectrum is dependent upon the excitation wavelength

and its shape drastically changes, showing a marked sensitivity for excitation in the B band region (235nm). On increasing the energy of the excitation, the structure centered at 365 nm for the curve (b), sensibly grows showing also a blue shift, while the intensity of the high energy component (320 nm) of the spectrum (b) seems to remain almost unchanged.

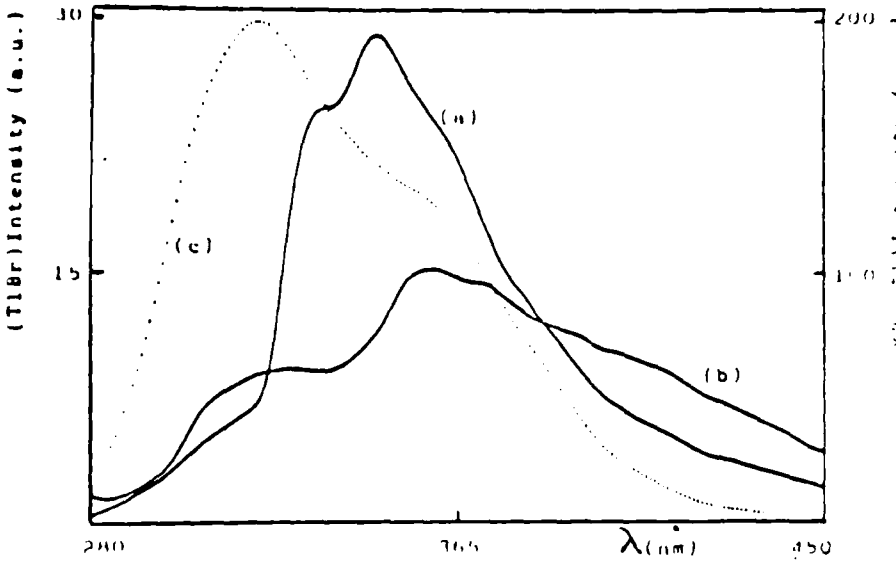

a)Emission of TlBr solution for excitation at 235 nm;
b)Emission of TlBr solution for excitation at 365 nm;
c)Emission of KBr:Tl single crystal for excitation at 255 nm.

The similarity of the emission and absorption spectra of the phosphors and of the liquid solutions would be explained by the fact that the involved chromophores are the same in both cases, suggesting, therefore, the existence in the solutions of a quasi-crystalline octahedral assembly of ions containing $(TlBr_6)^{5-}$ clusters[4]. As a consequence, thallous ions are embedded in an environment which is analogous to that of the solid, where the thallous ion can be thought belonging to the $(TlBr_6)^{5-}$ complex.

1)-A.Fukuda, Sci. Light (Tokyo) 13, 64 (1964)

2)-P.W.M.Jacobs and S.A.Thorsley, Journal of Luminescence 8, 391 (1974)

3)-U.Giorgianni, V.Grasso and G.Saitta, Solid State Commun. 40, 591 (1981)

4)-M.Bacci, A.Ranfagni and G.Viliani, J. Phys. Chem. Solids 42, 1021 (1981)

Steady-state and time-dependent luminescence of UO_2MoO_4

W.M.A. Smit,
Physical Laboratory, University of Utrecht,
P.O. Box 80.000, 3508 TA Utrecht,
The Netherlands

The crystal structure of UO_2MoO_4 is monoclinic with four molecules in the unit cell. The space-group is $P2_1/c\text{-}C_{2h}^5$ [1] and the uranium ions occupy sites with C_1 symmetry revealing that the uranyl groups have lost their $D_{\infty h}$ symmetry.

Adopting the energy level scheme developed by Denning et al. [2] for the symmetric uranyl group the lowest excited state has Π_g symmetry. In UO_2MoO_4 the degeneracy of this state will be removed resulting in two A-type levels. Taking into account the four molecules in the unit cell, correlation field splitting of these levels may be expected. With C_{2h} cell symmetry the original Π_g level may split into eight levels: $2A_g + 2B_g + 2A_u + 2B_u$.

The above expectations were investigated by studying the emission and excitation spectra of powdered samples of UO_2MoO_4 in the temperature range from 1.2 to 100 K. The steady-state emission spectrum is dominated by emission from traps. The vibrational structure shows the traps to be distorted uranyl groups. The vibronic satelites were identified by their temperature dependence in the range from 4.2 to 60 K. One after another the traps become depopulated at increasing temperature.

The intrinsic emission spectrum was obtained by time-resolved spectroscopy. At 50 ns after the excitation pulse only intrinsic emission is observed. The vibronic structure shows progressions in the A_g correlation field components of the symmetric and asymmetric UO_2 stretching modes, in agreement with the vibra-

tional frequencies obtained from the infrared and Raman spectra.

The intrinsic zero-phonon line was studied both in emission and excitation. The lineshape in the excitation spectrum at 4.2 K and the emission spectra at 4.2, 21 and 30 K could be interpreted in terms of four component lines, representing transitions between the ground state and the $2A_u + 2B_u$ excited levels. At 1.2 K the emission maximum shifts to lower wavelength due to emission from the lowest A_g component of the excited level.

By taking emission spectra at several times after the pulse energy migration from intrinsic to trap centres is demonstrated.

Decay-time measurements at 4.2 K for the trap lines resulted in τ values from 75 to 90 μs. Trap depths obtained from τ vs. T curves for the two more intensive trap lines are in agreement with trap depths obtained from the emission spectrum.

No single decay time was found for the intrinsic centres at 4.2 K. The decay time varied from 0.1 to 2 μs, probably emerging in a weak emission with a decay time of about 70 μs. The fast decay time of the intrinsic emission ($\approx$ 1 μs) corresponds to the building-up time of the trap emission revealing again energy migration from intrinsic to trap centres.

References

[1] V.N. Serezhkin, V.K. Trunov, and L.G. Makarevich, Sov. Phys. Crystallogr., 25 (1980) 492.

[2] R.G. Denning, T.R. Snellgrove, and D.R. Woodwark, Mol. Phys., 37 (1979) 1109.

Luminescence of Cs_2ZrCl_6 and Cs_2HfCl_6

Philip S. Bryan and Steven A. Ferranti, Research Laboratories, Eastman Kodak Company, Rochester NY 14650

The hexachlorometallates Cs_2ZrCl_6 and Cs_2HfCl_6, formed by the treatment of CsCl in concentrated HCl with either zirconium or hafnium oxychloride, fluoresce efficiently when excited by x-rays or radiation at 254 nm. The excitation and emission spectra obtained from powder samples of the two compounds are nearly identical. For the Zr complex, the maxima for excitation (narrow band) and the emission (broad band) are at 258 and 451 nm, respectively. The corresponding values for the Hf complex are at 254 and 449 nm. The quantum yields with excitation at 254 nm are near unity. The $t_{1/2}$ value for the fluorescence decay is about 10 μsec for both compounds when excited with a 40 nsec pulse from a filtered 110 kVp x-ray source.

Analytical results show that the major source of impurity is cross contamination by the metal ions in the zirconium and hafnium oxychloride starting materials. The samples that we studied have the following compositions: Cs_2HfCl_6:0.058 Zr and Cs_2ZrCl_6:0.002 Hf.

Addition of uranyl ion during the synthesis of Cs_2HfCl_6 gave samples in which the distinctive fluorescence spectrum of the uranyl ion was observed. Other ions added during

synthesis, such as Mn(II), Cu(II), or Eu(III), were not detected in the products.

The properties and the spectral characteristics of these materials will be presented.

Excitons in CuCl microcrystals embedded in NaCl

Tadashi ITOH and Toshio KIRIHARA
Department of Physics, Faculty of Science
Tohoku University, Sendai 980, Japan

In heavily Cu^+-doped alkali halides, microcrystals of Cu= halides having the size less than 0.1 μm are known to be formed due to the coagulation of Cu^+[1-3]. The present paper reports the optical properties of CuCl microcrystals (1 mol% in NaCl) in order to study the crystal size effect upon their exciton states. Figure 1 shows two exciton absorption bands, Z_3 and $Z_{1,2}$, which are located at the higher energy side with more broadened band= width compared with those in the bulk CuCl on account of the size effect: the smaller the size of the microcrystal, the larger the exciton energy [3]. Under the band-to-band excitation a broad emission band appears with the Stokes shift of ~30 meV from the Z_3-absorption band.

Figure 2 shows the emission spectra taken at 2 K under the selective excitation by a pulsed dye laser. The energy positions of excitation (a~f) are also shown in Fig.1 for the comparison. When the excitation energy Ω is tuned around the $Z_{1,2}$= exciton region, two narrow peaks O and Δ, separated by ~25 meV appears, superimposed on the broad emission band as shown in the curve a. Their positions and intensities depend on Ω. The energy separation between Ω and the peak Δ, ~66 meV, nearly coincides with that between the bulk Z_3 and $Z_{1,2}$ exciton bands (~70 meV). As Ω is tuned into the Z_3-exciton region, these peaks disappear and instead, another emission peak ● appears

with the Stokes shift of ~25 meV from Ω as shown in the curve b. Since an emission ▲ without Stokes shift is also observed at 77 K at the foot of the excitation light, the emission, ▲ and Δ, are assigned as the resonance emission of the Z_3 exciton: the emission Δ is caused through the inter-valence-band scattering of the hole. The energy correlation of these emission peaks upon Ω is the clear evidence of inhomogeneous broadening both in the absorption and emission, which is brought about by the fluctuation of the crystal size over a wide range. The emission peaks, ● and O, may be ascribed to a bound exciton. However, in the curves from b to f, the Stokes shift of the emission ● from Ω gradually decreases to zero as Ω approaches the energy of the Z_3-bulk exciton. The exciton is considered to be bound with the aid of a certain kind of size effect because the binding energy is essential only for the small crystal size.

(1)M. UETA et al.: J. Phys. Soc. Jpn. 20, 1724 (1965).
(2)H. KISHISHITA: Phys. Status Solidi (b)55 399 (1973).
(3)T.TSUBOI: J. Chem. Phys. 72 5343 (1980).

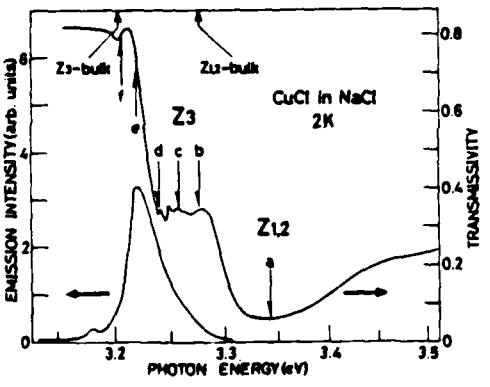

Fig.1

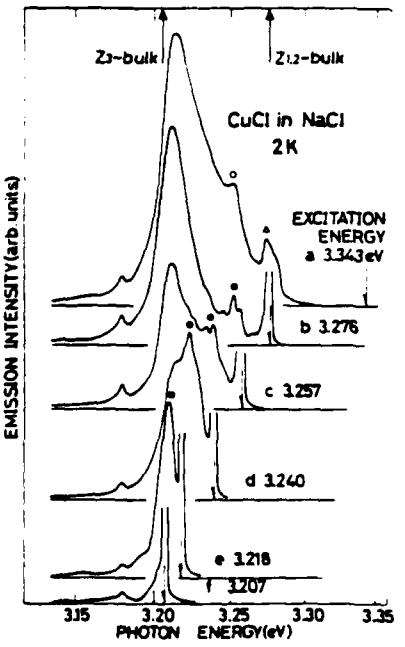

Fig.2

Characterization of the luminescent triplet state of the $K_2Cr_2O_7$ crystal at 1.2 K via EPR and optical spectroscopy

J.H. van der Waals and W.A.J.A. van der Poel
(Huygens Laboratory, P.O. Box 9504, Leiden)

We are currently investigating the luminescent state of crystals in which the anion is a transition metal complex with the metal formally in a d^0 configuration, tetrahedrally surrounded by oxygen. Examples under study are VO_4^{3-}, MoO_4^{2-}, and also the $Cr_2O_7^{2-}$ ion in which two tetrahedra share a common oxygen. First we established the triplet character (S=1) of the emitting state of this type of ion - which had been proposed [1] but never proven [2] - in some qualitative ESR experiments with optical detection on YVO_4 and $K_2Cr_2O_7$ crystals. We then initiated a systematic study of the latter system, the results of which are here reported, by three experimental techniques [3]:

1. Excitation and fluorescence spectroscopy with simultaneous (variable frequency) microwave irradiation to induce ESR transitions between the sublevels of a spin triplet in zero field.
2. ESR with optical detection in an external field.
3. Optical Zeeman spectroscopy.

The first type of experiment has enabled us to provide an assignment for the spectra previously observed by Freiberg and Rebane [4]. The complexity of these spectra proves to be caused by the marked inequivalence of the two types of site (A and B) in the triclinic $K_2Cr_2O_7$ crystal, see figure. The spin-

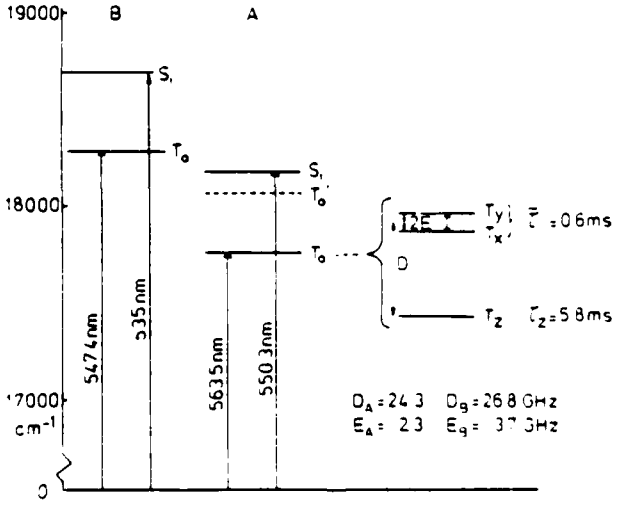

allowed transitions from the ground state S_0 to the first excited singlet state S_1 are some 10^2 times stronger than those to the lowest triplet state T_0. The triplet character (S=1) of T_0, from which the luminescence originates, follows from the observation that the phosphorescence intensity is affected by irradiation with microwaves at ν_A = 4.628 and ν_B = 7.367 GHz. The resonances correspond to transitions between the upper two spin components (T_x, T_y) for the two sites. The splitting of 0.7 cm^{-1} between the lower spin state T_z and the upper two (which exceeds the frequency of our microwave equipment) has been resolved optically in luminescence excitation experiments on the T_0 - S_0 0-0 bands. Upon laser flash excitation the luminescence from T_x, T_y predominates at short times ($\bar{\tau}$ = 0.6 ms), whereas the emission from T_z becomes predominant at later times (τ = 5.8 ms). The zero-field splitting and decay characteristics of the triplet state derived from the optical and ESR experiments are summarized at the right in the figure.

The ESR experiments in an external field also yield information on the spatial character of the triplet state wave function. We find that in each of the two sites the z principal axis related to the bottom spin sublevel lies along the bond from one of the Cr atoms in the $Cr_2O_7^{2-}$ complex to the bridge oxygen. Apparently the excitation is localized on one side of the anion, as previously suggested by Ballhausen *et al.* for the singlet state S_1 [5]. By considering the excited fragment as a perturbed CrO_4^{2-} ion with approximate C_{3v} symmetry (the bridge oxygen to be compared with Cl in $CrClO_3^{2-}$ [5]), the experimental finding that the decay of the T_x, T_y sublevels is much faster than that of T_z follows from an analysis of the spin-orbit coupling between the singlet and triplet states arising from the ($t_1 \rightarrow 2e$) electron excitation in the trigonally perturbed CrO_4^{2-} ion [3]. At present Zeeman experiments are in progress from which preliminary evidence has been obtained for the location of the second triplet state, in which the excitation presumably resides on the other half of the anion, see the dotted line in the figure.

[1] H. Ronde and G. Blasse, J. inorg. nucl. chem. 40 (1978), 215; G. Blasse, Structure and Bonding 42 (1980), 1.

[2] S.L. Holt and C.J. Ballhausen, Theor. Chim. Acta 7 (1967), 313.

[3] W.A.J.A. van der Poel et al. Chem. Phys. Lett., 103 (1984), 245, 253.

[4] A. Freiberg and L.A. Rebane, J. Luminescence, 18/19 (1979), 702.

[5] V. Miskowski, H.B. Gray and C.J. Ballhausen, Mol. Phys. 28 (1974), 729; C.J. Ballhausen, J.H. Høg and E.I. Solomon, Colloques Internationaux du C.N.R.S. no. 255, Paris.

Low Temperature Luminescence Studies of Two Polymorphs of Bis(Urea)Dioxouranium(VI) Sulfate

Harry G. Brittain*

Department of Chemistry, Seton Hall University, South Orange, NJ 07079

and Dale L. Perry

Earth Sciences Division, Lawrence Berkeley Laboratory, University of California, Berkeley, CA 94720

Abstract

Recently, Toivonen and Niinisto reported that $UO_2SO_4 \cdot (urea)_2$ is capable of existing in two crystalline forms. The structures of these are very similar, with the uranium atom lying at the center of a pentagonal bipyramid formed by oxygen atoms. Of the five equatorial oxygens, three belong to sulfate groups and two to urea molecules:

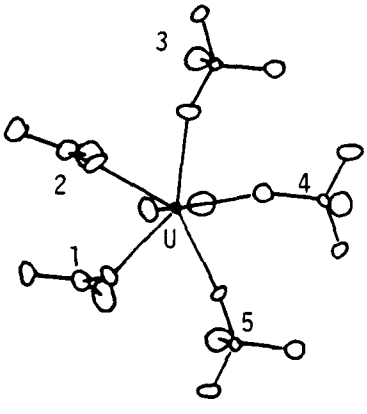

α-form

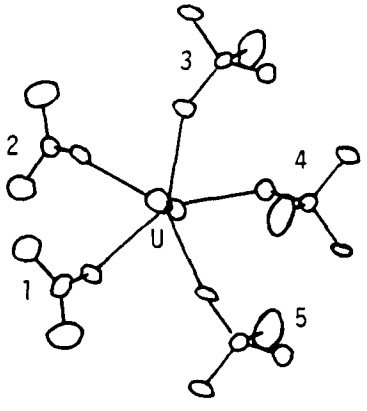

β-form

The bridging tridentate sulfate groups (labeled as 3,4,5) join the bipyramids into infinite double chains, and the α and β polymorphs

differ in how these chains are packed.

Samples of the α and β polymorphs were obtained from Toivonen and Niinisto, and the UV-excited luminescence was obtained at 9.0 ^{o}K at 1 cm^{-1} resolution. Although the coordination polyhedron of the uranyl ion is quite similar in the two crystal forms, the luminescence spectra obtained from each system were found to differ significantly. The electronic origin for the α-form was located at 20,205 cm^{-1}, while the origin for the β-form was located at 20,349 cm^{-1}.

The remainder of the luminescence spectra was found to result from the coupling of the totally symmetric uranyl stretching vibration to these electronic origins. For the α-form the frequency of this mode was found to be 845 cm^{-1}, while the frequency associated with the β-form was determined to be 850 cm^{-1}. Each vibronic origin observed for the β-form was located approximately 150 cm^{-1} lower in energy relative to the corresponding vibronic origin associated with the α-form. The coupling to the antisymmetric uranyl stretching mode was found to be very weak, and these vibronic origins were found to be of uniformly low intensity. The antisymmetric stretching frequency of the α-form was found to be 932 cm^{-1}, while the frequency associated with the β-form was measured as 928 cm^{-1}.

Reference

J. Toivonen and L. Niinisto, Inorg. Chem., 22, 1557 (1983).

Dependence of emission properties on the counter-ion in crystalline $[Ru(bpy)_3]X_2$

H. Yersin[a], E. Gallhuber[a], G. Hensler[a], L. O. Schwan[b], W. Rettig[c]
a. Inst. für Phys. und Theor. Chemie, Univ., 8400 Regensburg, FRG; b. IV. Phys. Inst., Univ., 4000 Düsseldorf; c. I. Stranski-Inst., TU Berlin, 1000 Berlin 12

During the past decade $[Ru(bpy)_3]^{2+}$ complexes have been investigated intensively.[1-4] From measurements with dissolved complexes it has been concluded that the second coordination sphere (solvent sphere) strongly influences the spectroscopic behavior. Thus, it is near at hand to analyze crystalline compounds with different counter-ions, leading to a more defined variation of the second coordination spheres. Such investigations are presented here for the first time. Fig. 1 reproduces

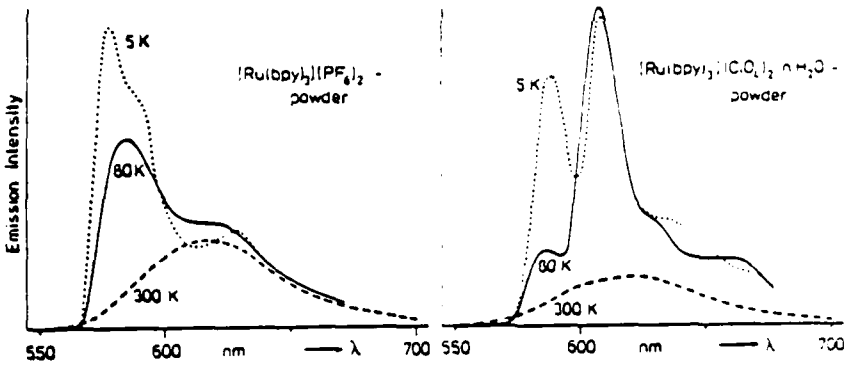

Fig. 1. Emission spectra of $[Ru(bpy)_3]X_2$ powders. The intensities between different powders are not comparable, but see Table 1. The origin of the emitting states is discussed in [3].

the emission spectra of two compounds and Table I summarizes spectroscopic data for different counter-ions and crystal water contents. These results show that counter-ions and/or crystal water strongly influence the emission spectra and their temperature behavior, the decay properties, and the emission intensities and their temperature dependence. For instance, the in-

$[Ru(bpy)_3]X_2$ Compounds	λ_{max}[nm] 300 K	80 K	τ[μs] at λ_{max} [a]	I(X)/I(PF_6) [b] 300 K	80 K
[ ]$(PF_6)_2$	612	576	2.8 (300 K) 5.8 (50 K) 60;4.4;≤1 (5 K) 140 (1.7 K)[d]	1	1.1
[ ]$(ClO_4)_2 \cdot nH_2O$[c]	617	578	0.9 (300 K)	0.25	0.9
[ ]$(SCN)_2 \cdot nH_2O$[c]	604	579	1.2 (300 K)	0.34	0.8
[ ]$Cl_2 \cdot 6H_2O$[e]	612	573	1.0 (300 K)[d] 5.5 (50 K)[d] 25 (10 K)[d]	0.1	1.1
[ ]$Br_2 \cdot nH_2O$[c,e]	613	603	1.1 (300 K)	0.4	1.0
[ ]$J_2 \cdot nH_2O$[c,e]	608	585	1 (300 K) 5 (90 K) 90;20;3;1 (5 K)	0.2	0.9
[ ]$J_2 \cdot \approx 0\ H_2O$	610	599		0.02	0.6
[ ]Cl_2 dissolved in water	612	578	0.4 (300 K) 5 (80 K) 20 (5 K)	-	-

Table I.
Emission data of crystalline $[Ru(bpy)_3]X_2$ powders.
a. The decay components depend on the wavelength of emission.
b. Intensity ratio compared to $[Ru(bpy)_3](PF_6)_2$ at 300 K.
c. Crystal water content unknown.
d. Only the longest component has been measured.
e. Photoactivity at T = 300 K, λ_{ex} = 280 nm.

tensity of the PF_6-salt is at 300 K appreciably larger than that for other salts. However, with temperature reduction all compounds seem to come to a comparable value. This can be understood on the basis of an electronic state strongly coupled to lattice vibrations, only accessible over an activation barrier. An equivalent behavior has also been found for dissolved complexes.[4] The corresponding quenching state has been assigned in [4] to a charge-transfer-to-solvent state and in [2] to a Ru 4d state. Our results indicate the significance of the counter-ion redox potential. This suggests - in analogy to [4] - that a charge-transfer state coupled to the second coordination sphere (counter-ion) is responsible for the quenching properties.

1. R.J.Watts; J. Chem. Educ. 60, 834 (1983)
2. J.V.Caspar, T.J.Meyer; J. Am. Chem. Soc. 105, 5583 (1983)
3. H.Yersin, E.Gallhuber, A.Vogler, H.Kunkely; J. Am. Chem. Soc. 105, 4155 (1983)
4. J.Van Houten, R.J.Watts; J. Am. Chem. Soc. 97, 3843 (1975)

DOSIMETRY BY THERMOLUMINESCENCE: DATATION OF PERUVIAN POTTERY

E. F. Quiñones, E. López Carranza
Departamento de Física, Universidad Nacional de Ingeniería,
Casilla 1301, Lima, Peru

C. Rozenberg and E. Bonnier
Institut Francais d'Etudes Andines, Casilla 278, Lima 1°, Peru

Natural radioactivity can produce measurable quantities of radiation damage in rocks and buried pottery and its gradual accumulation in time gives us a "clock" which can be used for datation in Geology and Archaeology. Thermoluminescence (TL) is used to estimate the accumulation of radiation damage in pottery. In this paper we present first results in the datation of some of the sherds coming from the archaeological site Piruro, Tantamayo, Huánuco, situated at 3900 m of altitude in the Peruvian Andes, excavated by Rozenberg and Bonnier. Two of the sherds, the 3063 and the 3071, come from the same layer and have the ages 910±140 and 840±100 respectively which give for the context the age 870 (±30, ±90) A.D. 1110. Other two sherds, the 3131 and the 3162 have the ages 520±60 (A.D. 1460) and 590±80 (A.D. 1400) respectively. All ages are in years refered to 1950.

The fine-grains technique was used in the preparation of the samples and a ^{90}Sr-^{90}Y source (40 mCi, nominal) to calibrate the natural TL signals coming from the sherds. First - and second - glow growth curves were used to obtain the equivalent dose and the supralinearity. On the other hand the intrinsic radioactivity was determined by measuring the gross alpha particle emission rate (U and Th) with an alpha counter and using flame photometry (K). The extrinsic dose-rate coming from the soil and stones was estimated in the same way, and that coming from the cosmic rays assumed equal to 15 mrad/yr. Moisture content of the ceramic and the soil was taked in account to correct the total dose-rate.

X-Ray Transferred Thermoluminescence (XTTL) In Quartz Crystals.

A.Halperin and S.Katz
The Racah Institute of Physics, The Hebrew University of Jerusalem,
Jerusalem 91904 Israel.

Summary

The measurements in the present work were carried out on unswept synthetic electronic grade quartz crystals. Samples were cut out of a Y-grown bar into separate plates belonging to each of the different growth sectors of a Y-plate (namely, +X, -X, +Z, -Z). Each sample was about 2x3x1mm^3 with the main faces perpendicular to the Y-direction. Crystals were normally X-rayed (55Kv, 18 ma) for a few minutes at about 10K. The glow curve obtained then on warming the crystal exhibited a variety of peaks and differed in the +X samples compared to the +Z ones.[1] The XTTL was observed when the X-irradiated +X-growth sample was warmed up to about 220K, cooled down and X-irradiated again at 10K. During the warm-up after the re-irradiation the glow curve exhibited an extremely strong peak near 190K (at a heating rate of 1K per minute). The 190K peak did not appear in the Z-growth samples. A necessary condition for the appearance of the 190K peak was the pre-population of the traps associated with the regular thermoluminescence peaks appearing in the 200 - 300K temperature range.

It was unnecessary to warm up the sample after the first X-irradiation to precisely 220K; pre-warming to about 150K also produced the 190K, though its intensity rose sharply with the temperature of the pre-warming to a maximum near 240K. At higher pre-heating temperatures the 190K peak turned weaker with the exhaustion of the carrier in the traps associated with the glow peaks in the 200 - 300K range.

The 190K peak could also be produced by X-irradiation at temperatures above 10K and up to about 170K. At still higher temperatures the trapping level associated with the 190K peak became unstable thermally when carriers were released during the X-irradiation.

The emission spectrum of the 190K peak has its maximum at 3.2eV (390 nm and its spectral half-width was about 0.77eV. Its thermal activation energy was about 0.6eV.

The 190K peak has been observed previously. Malik et al[2] have reported the appearance of a very strong peak at 180 - 210K. They considered it "a

most intriguing and unexpected effect'. They have observed the effect after a double irradiation, first at temperatures between 145 and 300K and then at 95K. They were unable to explain it. Schlesinger[3] has observed the peak at 190K in Ge-doped quartz after X-irradiation at room-temperature followed by cooling to 77K and illumination by 280 nm light at this temperature. He claimed that the peak was associated with electron traps.

We suggest tentatively that X-irradiation at low temperatures of the pre-excited crystal produces a re-arrangement of the carriers in the trapping levels in such a way that many of them are now located in the vicinity of the recombination centers. This results in a very high probability for recombination on the release of the carriers during warming, and hence the extremely high intensity of the emission. The effect might be connected with the Al-M^+ centers present in the X-growth sectors (M^+ stands for an alkali ion). It is known that the aluminum impurity in unswept crystals appears primarily in the form of Al-M^+ centers. Irradiation above 200K is known to remove the alkali ions from their sites at the Al and makes possible their migration in the channels along the optical axis of the crystals, when they may re-arrange as suggested above.

References.

1) S.Katz, A.Halperin and M.Ronen, Proc. of the 37th Symposium on Freq. Control, 181 (1983).

2) D.Malik, E.E.Kohnke and W.A.Sibley, J.Appl.Phys. 52, 3600 (1981).

3) M.Schlesinger, J. Phys. Chem. Solids 26, 176 (1965).

THERMOLUMINESCENCE KINETICS IN SYSTEMS MORE GENERAL THAN THOSE DESCRIBED BY THE USUAL 1st AND 2nd ORDER KINETICS*

Paul W. Levy, Brookhaven National Laboratory, Upton, New York 11973

In an effort to explain anomalous thermoluminescence (TL) measurements, that cannot be described by the well-known 1st and 2nd order kinetics, more general TL kinetics have been developed. The anomalous results include glow peak shapes that cannot be described by the usual kinetics, the appearance of physically unrealistic parameters that are unusual functions of the premeasurement dose, etc. As is well known, the usual 1st order TL kinetics is obtained from an expression, called here the general one-trap kinetic equation, by assuming that thermally released trapped charges undergo light emitting recombination without being retrapped. The usual 2nd order kinetics is obtained, from the same equation, by assuming that retrapping occurs and, first, that the retrapping and recombination cross sections are equal, and, second, the trapped electron and hole concentrations are equal. The general one-trap kinetic equation has been investigated by numerically computing glow curves using physically reasonable parameters. In turn, these curves are regarded as "data" and analyzed by fitting them to the usual 1st and 2nd order expressions. A number of anomalous results are reproduced. The computed glow peaks depend strongly on the dose, the retrapping-recombination cross section ratio, etc. They are approximated, but not in the wings, by the usual 1st and 2nd order kinetics. However the kinetic parameters obtained usually differ appreciably from those used to compute the glow peaks.

Most importantly, in glow curves with more than one peak, the use of the usual 1st and 2nd order kinetics requires the implicit assumption, usually unstated, that charges released from one type of trap do not interact with other types of traps. TL systems in which these interactions do occur can be described by an equation set that is a straight forward generalization of the one-trap equation. Numerical solutions of these "interactive kinetic equations" demonstrate many of the anomalous results. Furthermore, when regarded as "data" and fitted to the 1st and 2nd order equations, kinetic parameters are obtained that are similar to those obtained by analyzing measured TL data. Lastly, curves of glow peak height vs. dose, constructed from the computed glow curves, often exhibit supralinearity. Consequently, this often observed and not understood phenomena appears to be a natural characteristic of TL systems in which "interactive" retrapping occurs between different types of traps.

*Research supported by the U.S. Dept. of Energy under contract DE-AC02-76CH00016.

ON THE MECHANISMS OF NON-ISOTHERMAL RELAXATION THROUGH THERMALLY STIMULATED LUMINESCENCE PROCESSES.

V.V. Ratnam and Jairam Manam
Physics Department, Indian Institute of Technology, Kharagpur-721302, INDIA.

Non-isothermal relaxation techniques in the form of thermally stimulated luminescence phenomena and processes have been utilised to understand the mechanisms involved in the occurrence of luminescence emission during the formation and subsequent destabilisation (by thermal annealing) of the radiation induced and stabilised defects in pure and doped alkali halide crystals. Techniques like thermally stimulated luminescence (TSL) spectra, monochromatic thermoluminescence (MTL) glow curves, photo-stimulated thermoluminescence (PSTL) glow curves have been successfully utilised in this study. Effects of pre-and post-deformation on the X-irradiated crystals on the above luminescence manifested properties have also been studied.

Results of experiments on a typical alkali halide, KCl doped with Na will be reported here. Whether it is X-ray fluorescence or TSL emission of the X-irradiated crystal, the emissions occur always in the same region and in KCl they occur at 400, 435 and 545 nm regions. The mechanisms and processes for their occurrence are controversial ; they are regarding (i) the charge species responsible for TSL glow peaks (ii) the initiating step in the luminescence emission process in TSL and (iii) the site of recombination. PSTL and TSL spectral emission experiments before and after mechanical

deformation have been undertaken. It is found that in the X-irradiated KCl : Na, one of the three glow peaks (413°K peak) is F-stimulable both after (i) thermal clean upto 433°K and (ii) RT, deformation of the irradiated crystal. Further, deformation prior to the X-irradiation enhances the TSL spectral emissions in the above regions.

From the intensity changes of the different emissions in the TSL spectra of the crystal irradiated at different temperatures between LNT and RT, with the information on the thermal stability of the radiation induced optical absorption bands, the charge species responsible for the three TTL glow peaks occurring around 387, 415 and 503°K are identified to be V_3, early stage and late stage F-centres respectively. The breakaway products of V_3 (Cl_3^-) centers (as well as higher aggregate hole centers) namely Cl_2^- and Cl^0 get involved in the above indicated emissions. And the intensities of the emissions occurring due to the recombination of these charged species with their counterparts are shown to be governed by their concentration at the sites of recombination (which are modifed by the treatments given after irradiation) and the temperature of X-irradiation. From all these experiments it is concluded that the emissions occurring at 400, 435 and 545 nm are identified to be those due to the radiative decay of the STEs at the site of Na impurity, cation vacancy and unperturbed regions of the lattice. The mechanisms for the occurrence of these emissions are also indicated.

KINETICS OF RADIATION INDUCED THERMOLUMINESCENCE

By

* D.M.Kulkarni, Willingdon College, SANGLI(INDIA) 416 415

A.V.Narlikar, National Physical Laboratory, New Delhi (INDIA) 110 012

SUMMARY

Gamma-ray induced thermoluminescence of strontium chloro phosphate $Sr_{10}(PO_4)_6Cl_2$ is studied from the glow curves, the activation energy, escape frequency factor are determined and the values are given in Table 1.1.

The present theory is developed on the similar lines in chemical kinetics (1) The observed intensity in current is expressed as electrons/sec. and following equations are used

$$I = \left(\frac{KTm}{h}\right) e^{\Delta s/K} . e^{-E/KTm} \quad .... \quad (1)$$

or

$$I = P\ S\ e^{-E/KTm} \quad .... \quad (2)$$

Where P = Probability factor , $P = \frac{KTm}{sh} e^{\Delta S/K}$ ... (3)

K = Boltzmann constant

h = plank's constant

A = Pre-exponential constant

$\frac{KTm}{h}$ = Universal frequency factor.

S = escape freqnency factor

$$I = A\ e^{-E/KTm} \quad .... \quad (4)$$

$$A = \frac{KT}{h} e^{\Delta S/K} \quad .... \quad (5)$$

$$A = IS \simeq PS \quad ... \quad (6)$$

The values of $e^{\Delta S/K}$ were found by

$\Delta F = KTm \ln I$ ... (7 a)

$\Delta F = E - T\Delta S$ ... (7b)

Where ΔE = Energy of activation

ΔF = free energy of activation.

ΔS = entropy of activation .

In some cases above formulae are not applicable to give constant results and therefore, modified as

$$I = S \left(\frac{KTm}{h} \right) e^{\Delta S/K} e^{-E/KTm} \quad \ldots \quad (8)$$

$$A = S \left(\frac{KTm}{h} \right) e^{\Delta S/K} \quad \ldots \quad (9)$$

The values of A, ΔF ΔS are given in Table 1.2

In both the cases, however, pre-exponential constant

$A = IS \simeq PS$

The above relations are true in kinetics of radiation induced thermoluminescence of $Sr_{10}(PO_4)Cl_2$. It was also observed that pre-exponential constant is related exponentially to escape frequency factor and activation energy.

REFERENCE

Glasstone et al. "Theory of Rate Process" 1941

Table 1.1.

Material	Glow peak Temperature Tm°K	Activation Energy Chen's method E eV	Escape frequency factor S	Universal frequency factor $S' = \frac{KTm}{h}$	Symmetry factor $\mu = o/w$
1)SAP I peak	358	0.525	1.9×10^{6}	7.4×10^{12}	0.4255
2)SAP III peak	523	1.05	9.67×10^{8}	1.8×10^{13}	0.4259
3)SAP-Nd 1% I^{I} peak	428	0.540	3.14×10^{5}	8.9×10^{12}	0.5909
4)SAP-Dy 2% Mn 1% I peak	378	0.512	4.6×10^{5}	7.87×10^{12}	0.4000
5)SAP-Dy 1% II peak	423	1.428	1.5×10^{16}	8.8×10^{12}	0.6666

SAP = $Sr_{10}(PO_4)_6Cl_2$

Table 1.2

Material	Observed Intensity el/s I	Intensity from (1) I*	Pre-expon. Constant From(4) A El/c	Pre-expon. Constant from (5) A*	Spec. Expon. Constant from(6) A' = IS	Free Energy of Act. ^{n} FeV	Entropy of Act. ^{n} T S eV	Probability factor P
SAP-I peak	1.01×10^{11}	1.36×10^{9}	2.47×10^{18}	3.34×10^{16}	1.9×10^{17}	0.7854	0.259	1.7×10^{10}
SAP-III peak*	1.06×10^{11}	1.5×10^{13}	1.38×10^{22}	9.66×10^{19}	1.01×10^{22}	1.1500	0.100	1.8×10^{23}
SAP-Nd 1% II peak	1.12×10^{11}	7.9×10^{9}	6.21×10^{17}	4.4×10^{16}	3.5×10^{16}	0.8540	0.314	1.4×10^{11}
SAP-Dy 2% Mn 1% Peak	1.59×10^{11}	2.86×10^{10}	1.07×10^{18}	1.9×10^{16}	7.5×10^{16}	0.8400	0.329	4.1×10^{11}
SAP-Dy 1% II peak	7.5×10^{11}	2.92×10^{12}	7.63×10^{28}	2.82×10^{29}	1.28×10^{28}	1.3960	0.028	2.9×10^{29}

SAP = $Sr_{10}(PO_4)_6Cl_2$

* Values calculated by using equations (8) and (9) .

MB23-4

Deformation Induced Thermoluminescence in NaCl:Ca(T).

R.V. Joshi, K.P. Dhake and T.R. Joshi
Applied Physics Department, Faculty of Technology and Engineering
M.S.University of Baroda, BARODA-390 001, INDIA.

The polycrystalline specimens of NaCl:Ca. (10^{-3} m.f.) obtained by recrystallization from aqueous solution followed by annealing and rapid quenching from 750°C, designated as NaCl:Ca(T), exhibited well defined glow peak at 147°C. This has been found useful in determining the dose of ionizing radiations in radiation applications[1]. The present paper includes the study of effect of mechanical deformation on the nature of glow curves of NaCl:Ca(T) material. About 5×10^3 Kg/cm^2 uniform pressure is applied for preparing tablets of 0.1 cm thick and 1 cm diameter. TL glow curve reader used for recording the glow curves, after a test dose of 700 R, is described earlier[1].

Figure indicates that the mechanical compression induces (i) enhancement in the intensity of the glow curve (curves 1 and 2) (ii) shift in the position of main glow peak from 147 to 235°C in the first heating run itself (curves 1 and 2) (iii) annihilation of the compression induced 235°C glow peak with production of 113 and 190°C peaks in the second and subsequent cycles (curves 3 and 4).

Besides atomic dispersion and solution of precipitated impurity, plastic deformation creates dislocation debris in the form of vacancy clusters and dislocation dipoles due to dislocation motions. It is also reported[2,3] that Ca^{+2} ions, together with

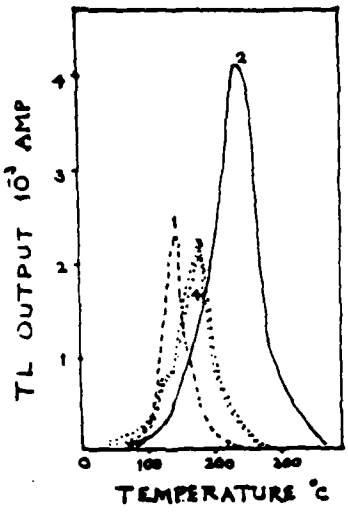

the +ve ion vacancies form metastable plate-like aggregates on 310 stable blow 100°C and 111 stable above 150°C. It is suggested that such metastable aggregates may be associated with the deformation induced peak at 235°C. Their break - up during heating upto 400°C in the first cycle leads to the formation of free dipoles in the dislocation region. These are presumed to be used up in the generation of the TL-centres associated with peaks at 113 and 190°C in subsequent cycles. It is quite reasonable to believe that the major fraction of Ca^{++} ions precipitates out as a separate phase at the end of the first cycle to bring about the equilibrium solubility at room temperature. This precipitation is responsible for the observed reduction in intensity of glow curves subsequently.

References :

1. R.V.Joshi, T.R.Joshi, K.P.Dhake and S.P.Kathuria, Health Physics 44, 29 (1983).
2. Miyake S. and Suzuki K. J. Phys. Soc. Japan 10, 794 (1955).
3. Suzuki K. J. Phys. Soc. Japan 13, 179 (1958) ; 16, 67(1961).

Point Defects in BaS:Cu Phosphors

R.P.Rao and D.R.Rao
Materials Science Centre
Indian Institute of Technology
KHARAGPUR-721 302.

The role of defects (intrinsic / extrinsic) is well known in the general understanding of different electronic processes involved in the various structure-sensitive properties. Impurities present as traces or doped intentionally in the luminescent materials (activators/ or co-activators) may act as trapping or recombination centres depending on their nature. Conventational measurements on TL, TSC, dielectric constant (k'), conductivity (σ_{ac}) and EPR are being used to obtain information on the trapping and recombination mechanisms related to such impurity centres.

Polycrystalline BaS prepared by reducing pure $BaSO_4$ and doped with different concentrations of Cu was studied under UV and X-irradiation (1). In all the cases, TL and TSC peaks are observed in the same temperature region. The dielectric constant (k') and dielectric conductivity (σ_{ac}) increase with temperature. The results on dielectric measurements have clearly indicated the formation (during preparation of the phosphors) of neutral complexes like $\left[Cu_{Ba}\text{-}V_S\text{-}Cu_{Ba}\right]^0$ possessing an effective dipole moment. The breaking of such neautral complexes during irradiation by ionising radiations like UV and X-rays, give rise to native defects and their complexes such as $\left[V_S\right]$ and $\left[Cu_{Ba}\text{-}V_S\right]$ which act as sites for trapping electrons / or holes. It is further concluded that the creation and distruction of these neutral complexes are responsible for the energy storage properties of the system and for the increase of k' and σ_{ac} with the increase of temperature.

1. R.P.Rao and D.R.Rao, Mat.Chem. and Phys. 9 (1983) 501.

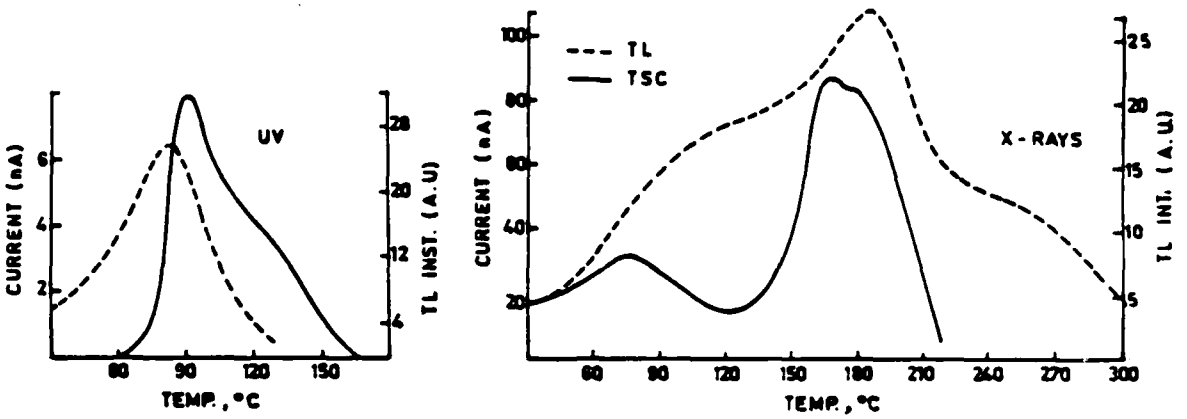

FIG.1 TL AND TSC OF BaS: Cu (0.012 % by wt)

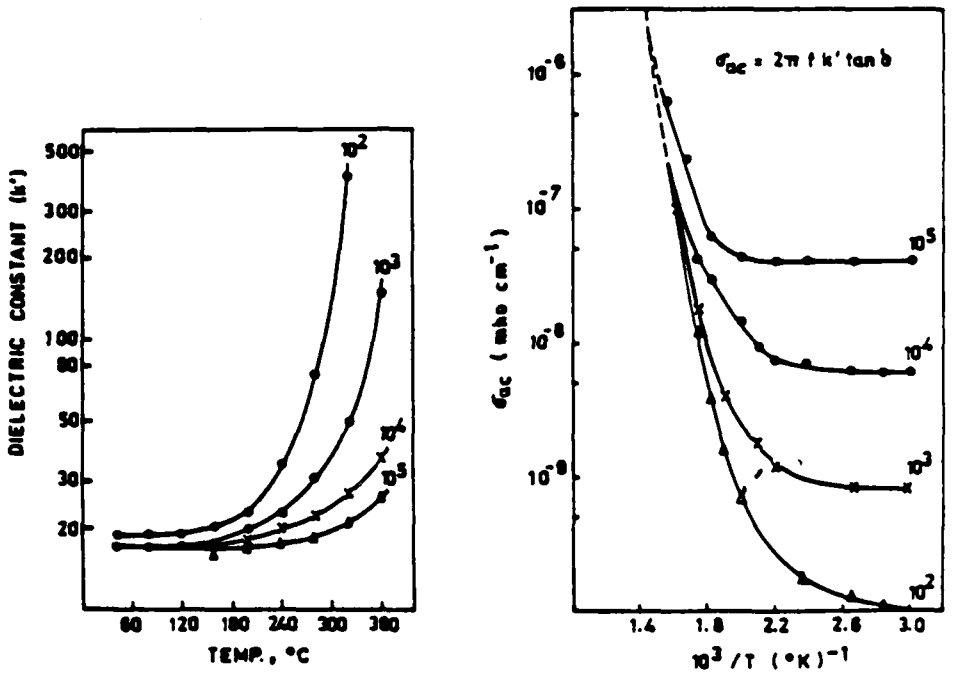

FIG.2 k' AND σ_{ac} OF BaS : Cu (0.012 % by wt)

Effect of Ba^{+2} Cation Impurity Concentration on the Thermally Stimulated Luminescence of Sodium Chloride.

O. H. Mahajan, T. R. Joshi, S. P. Kathuria* and R. V. Joshi

Applied Physics Department, Faculty of Technology and Engineering

M. S. University of Baroda, Baroda-390001, INDIA.

* Health Physics Division, B.A.R.C., Bombay-85, India.

ROLE OF DISLOCATIONS IN THE MECHANOLUMINESCENCE EXCITATION OF IRRADIATED AND NON-IRRADIATED ALKALI HALIDE CRYSTALS

B. P. Chandra

Department of Physics, Government Science College, Raipur

492002, India

SUMMARY

Mechanoluminescence (ML) or triboluminescence is a type of luminescence produced during mechanical deformation of solids. The present paper reports the role of dislocations in the ML excitation of irradiated and non-irradiated alkali halide crystals.

The ML in γ-irradiated alkali halide crystals was excited by applying or releasing a statical uniaxial pressure along their [100] direction of the crystallographic axis. The ML in non-irradiated alkali halide crystals was excited impulsively by a piston moving with a velocity of 390 cm/sec. The ML intensity was monitored in terms of the deflection of a ballistic galvanometer, using an RCA IP21 photomultiplier tube coupled to a DC amplifier [1,2].

All the X or γ-irradiated alkali halide crystals exhibit ML during the application or release of a uniaxial pressure. The ML intensity increases with the irradiation dose and applied pressure. The ML intensity of γ-irradiated KCl, KBr, NaCl and LiF crystals increases with temperature (from RT to 110°C), however, the ML intensity of γ-irradiated KI crystals decreases with increasing temperature.

The ML intensity increases with the impact velocity of the piston on to the crystals, and then it attains a saturation value for the higher values of the impact velocity. The ML efficiency of non-irradiated alkali halide crystals decreases with increasing values of the nearest neighbour distance and with increasing temperature. The temperature at which ML disappears also decreases with increasing value of the nearest neighbour distance.

Four models are proposed for the ML excitation in X or γ-irradiated alkali halide crystals. These models are : (i) dislocation defect-stripping model, (ii) dislocation unpinning model, (iii) dislocation-interaction model, and (iv) dislocation-annihilation model. The dislocation annihilation model is found to be the major process for the ML excitation, where the thermal energy release may give rise to thermoluminescence in the crystals.

The ML excitation in non-irradiated alkali halide crystals may be due to the cleavage-electrification, where the newly created surfaces may contain some percentage of the charged surfaces and the electric field produced may give rise to ML. The non-irradiated crystals of KCl, KBr, and KI do not show ML because the mobile charged dislocations in these crystals may decrease the surface charge density and may thus decrease the strength of the electric field.

References

1. Chandra B.P. and Elyas M., Indian J.Pure & Appl.15(1977);744.
2. Chandra B.P. and Zink J.I., Phys. Rev.B21 (1980); 816.

DEFORMATION-INDUCED TUNNELING IN II-VI SEMICONDUCTORS AND THEIR MECHANOLUMINESCENCE

B. P. Chandra and B. Majumdar

Department of Physics, Government Science College Raipur, 492002

India

SUMMARY

Luminescence produced during mechanical deformation of solids is known as mechanoluminescence (ML) or triboluminescence. A large variety of organic and inorganic compounds exhibit the phenomenon of ML [1-3]. The present paper reports the mechanism of ML excitation in II-VI semiconductors.

The ML and photoluminescence (PL) spectra were recorded by a monochromator-based spectrometer. The ML and PL intensity at different impact velocities and temperatures was measured in terms of the deflection of a ballistic galvanometer, using an IP21 photomultiplier tube coupled to a DC amplifier.

A survey of ML was made in nearly 100 phosphors and it was found that ZnS:Mn, (Zn,Cd)S:Cu, ZnS:Cu and ZnS:Ag exhibit intense ML. The ML spectra of ZnS:Cu, ZnS:Mn and ZnS:Ag phosphors are similar to their PL spectra. A considerable shift towards shorter wavelength is found in the ML spectra of (Zn,Cd)S:Cu phosphors as compared to the PL spectra. The shift between the ML and PL spectra increases with the increasing concentration of Cd in (Zn,Cd)S:Cu phosphors. Certain phosphors like ZnS:Ag, CdS:10^{-3}Te and ZnS:Cl exhibit ML but they do not show electroluminescence.

The ML intensity initially increases and then it attains a saturation value for the higher values of the deformation rate. The ML intensity decreases faster with temperature as compared to the decrease in the PL intensity. If the mechanical pulse used for the ML excitation is of shorter duration than the PL decay time, then the delayed luminescence from the trapping levels responsible for phosphorescence can clearly be seen after the deformation of the phosphors.

Several mechanisms may be speculated for the ML excitation in phosphors. They are : (i) thermal population due to the high stress near the tip of the mobile crack, (ii) triboelectrification, (iii) piezoelectrification, (iv) cleavage-electrification and (v) movement of the charged dislocations. The earlier four processes can be ruled out on the basis of the experimental results: It seems that the ML excitation takes place due to the movement of charged dislocations. The electric field near the core of charged dislocation is calculated and it is found to be sufficient for giving rise to the tunneling of electrons from the impurity levels and trapping centres.

References

[1] Zink, J.I., Acc. Chem. Res., 11 (1978); 289.

[2] Walton, A.J., Adv. Phys., 26 (1977); 887.

[3] Hardy, G.E., Kaska, W.C., Chandra, B.P. and Zink, J.I. J. Am. Chem. Soc., 103 (1981); 1075.

..

Polarized Luminescence from Divalent s^2-ion/cation Vacancy Complexes in Potassium Halide Single Crystals

A. Scacco
Instituto de Fisica, Universita di Roma, Roma, Italy

P. W. M. Jacobs
University of Western Ontario, London, Ontario, Canada

T. F. Belliveau, J.-G. Kang, D. J. Simkin
McGill University, 801 Sherbrooke St. W., Montreal, Quebec, Canada

Polarized emission has been used to establish the excited state symmetry of s^2-ion doped alkali halide single crystals. The polarization from univalent s^2-ions (Ga^+, In^+, Tl^+) has been attributed to vibronic coupling (dynamical Jahn-Teller effect) causing a tetragonal distortion of the center[1]. Some authors have attributed the polarization from divalent s^2-ions to the Jahn-Teller effect[1], while others have attributed it to a center with lower than cubic symmetry due to the associated charge-compensating vacancy[2]. In this paper, we show that either of the above models can be valid for divalent ions, depending on the relative magnitudes of the spin-orbit (SO) and Jahn-Teller (JT) interactions.

The azimuthal dependence of the polarization of the A_1 and A_2 emission bands from $KBr:Sn^{2+}$ and $KI:Sn^{2+}$ show maxima at 0°, 90° and 180°; and minima close to 0% at 45° and 135°. This behavior is consistent with a tetragonal JT distortion like the univalent s^2-ions. The A_1 emission shows very little temperature dependence of polarization, while the A_2 emission polarization is markedly temperature dependent at low temperatures. Decay kinetics measurements show that JT > SO for Sn^{2+} systems[3]. Using the same model and the decay parameters obtained in the above work, the observed temperature depen-

dence can be fit quantitatively for both KBr:Sn^{2+} and KI:Sn^{2+} if the cation vacancies are assumed to be in the next-nearest-neighbor positions. This model applied to KBr:Sn^{2+} also predicts the observed negative polarization at low temperatures.

The polarization diagrams of the single A-band emission in KCl:Pb^{2+} and KBr:Pb^{2+} show maxima at 0° and 180°, and negative minima at 90°. In KI:Pb^{2+}, the azimuthal dependence exhibits maxima at 0° and 180°, negative minima at 45° and 135°, and a smaller maximum at 90°. These results are consistent with a linear dipole oriented along a C_4 axis arising from the Pb^{2+} center/nnn cation vacancy. This is reasonable when one considers that in the Pb^{2+} systems SO > JT (from decay time measurements[4]), and large SO quenches the JT effect. The KI:Pb^{2+} system has the smallest SO coupling of the three, so the slightly different polarization arises from an incomplete quenching of the JT effect. The absence of any temperature dependence of the polarization is consistent with this interpretation. Further evidence for this model is provided by the residual polarization in the divalent systems at high temperatures. In contrast, the univalent systems, where the polarization arises only from the JT effect, show no such high temperature polarization.

References:

1. A. Fukuda, S. Makishima, T. Mabuchi and R. Onaka, J. Phys. Chem. Solids 28 (1967), 1763.

2. S.G. Zazubovich, N. E. Lushchik and Ch. B. Lushchik, Optics and Spectrosc. 15 (1963), 203.

3. Y. Kamishina, P. W. M. Jacobs, D. J. Simkin, J.-P. Martin, K. Oyama-Gannon and D. Le Si Dang, Phys. Rev. B 22 (1980), 3010.

4. J. G. Kang, Ph.D. Thesis, unpublished, McGill University (1984).

MB30-1

Laser Spectroscopy of Point Defects in CdF_2 on the Transition to a Semiconductor

Sun-Il Mho and John C. Wright

Department of Chemistry

University of Wisconsin

Madison, WI 53706

Defect equilibria in fluorite materials have been extensively studied. The behavior does not agree with that expected from simple mass action relationships. Competing equilibria caused by extensive defect clustering are found to be very important such as scavenging of interstitial fluoride (F_i') by the clusters to make negatively charged clusters (1). CdF_2 is the only one of the fluorites that can be converted to a semiconductor by heating. It is also a system where scavenging equilibria might be particularly important because the higher electron affinity of Cd^{2+} would result in stabilization of the scavenged clusters by delocalization of the excess negative charge.

Site selective laser spectroscopy has enabled the identification of the individual sites and the monitoring of their behavior in $CdF_2:Er^{3+}$ when it is changed from the insulator to the semiconductor state. Dissociated cubic sites, clusters and minor sites of single associated pair are observed. The site distribution is controlled by clustering. The single pair sites never become important in contrast with other fluorites. The relative importance of different sites strongly depends on the dopant concentration. The cubic sites increased and the relative concentrations of different types of clusters changed after the conversion. The changes are the

same as in the $CdF_2:Eu^{3+}$ system which does not become a semiconductor (2). No new sites appear that can be assigned to the presence of an electron associated with the conversion. However, most of the fluorescence was quenched and the lifetime shortened. The quenching is particularly strong for the clusters.

Inconsistent with the generally accepted model of the conversion (3), the fluoride interstitials that are used in the conversion are not the free F_i' but F_i' that are associated with local compensation of the clusters. The extra F_i' in a scavenged site would be more susceptible to oxidation than the other F_i' ions in the cluster. This explanation suggests that the conversion process should be highly dependent on the site distribution. The site distribution changes markedly as the ionic radius of the dopant is changed (4). This fact accounts for the inability of some dopants such as La, Ce and Pr to produce the semiconducting state. The observation of the dominance of clustering in CdF_2 supports previous interpretations of the activation energies for electron transport.

References:

(1). D.S.Moore and J.C.Wright, Chem. Phys. Lett. 66, 173 (1979).

(2). S.I. Mho and J.C. Wright, J. Chem. Phys. 77, 1183 (1982).

(3). J.S. Prener and J.D. Kingsley, J. Chem. Phys. 38, 667(1963).

(4). C. Andeen, D. Link and J. Fontanella, Phys. Rev. B 16, 3762 (1977).

Nucleation of Defects in Alkali Halides

Albert J. Ramponi and John C. Wright

Department of Chemistry, University of Wisconsin

Madison, Wisconsin 53706

Single crystals of KCl:Sm^{2+} have been investigated using selective laser excitation into the $^5D_0$ and $^5D_1$ levels of the $4f^6$ electron configuration for Sm^{2+} as a model system for the study of point defects in the alkali halides. Fluorescence occurs in the red and near ir via relaxation from the $^5D_0$ excited state down to the various components of the ^7F_J ground state multiplet.

Considerable controversy surrounds the site distribution associated with KCl:Sm^{2+}. The aliovalent ion enters the cubic lattice substitutionally for a potassium ion while overall charge neutrality is maintained through the creation of potassium ion vacancies (V_{K^+}). This work resolves the question as to whether the prevailing sharp line emission originates from a single Sm^{2+}-V_{K^+} pair possessing C_{2v}(110) symmetry[1,2] or from a distribution of pairs based on a statistical mechanical treatment of ion-defect interactions.[3] The local site symmetry depends on the location of the charge compensation vacancy relative to the rare earth defect. Our results indicate that the dominant fluorescence spectrum is not comprised of a distribution of Sm^{2+}-V_{K^+} symmetries but rather arises from a single C_{2v} center.

At 12K a total of nine different crystallographic sites are clearly distinguishable. All the dominant sharp line emission corresponds to the C_{2v}(110) site. The other centers can be considered minor by comparison. The distribution of sites can be broadly classified into two groups depending on their fluorescence decay rate. Four sites including the dominant C_{2v} site possess lifetimes $>$ 1 ms while the lifetimes for the remaining five sites

are $<$ 15 μs. The short-lived sites are difficult to characterize due to broad background emission which effectively interferes with fluorescence from these sites. The sites with long lifetimes share similar emission spectra which most likely represent differences in the location of the charge compensation vacancy relative to the rare earth ion.

Cooling the crystal to approximately 2.2K produces marked changes in the site distribution. Although the C_{2v} center still remains the dominant site, an additional long-lived site that is not present at 12K is observed. This low temperature site is characterized by an extremely strong thermal dependence since at 4.2K the fluorescence intensity is reduced by about 60%.

The predominance of the C_{2v} center relative to the other sites was further enhanced for crystals that were rapidly quenched from elevated temperatures. This behavior of the site distribution is predicted from simple defect equilibria models and should be contrasted with the lack of success in describing site populations in the fluorites.[4]

[1] W. E. Bron and W. R. Heller, Phys. Rev. 136, A1433 (1964).

[2] R. E. Bradbury and E. Y. Wong, Phys. Rev. B4, 690, 694, 702 (1971).

[3] R. H. Heist, C. R. Chilver, and F. K. Fong, Phys. Rev. B5, 4237 (1972).

[4] D. S. Moore and J. C. Wright, J. Chem. Phys. 74, 1626 (1981).

KINETICS OF RELAXATION PROCESSES IN X-IRRADIATED ALKALI HALIDE CRYSTALS BY THE ISOTHERMAL MONOCHROMATIC LUMINESCENCE DECAY METHOD.

Jairam Manam and V.V. Ratnam,
Physics Department, Indian Institute of Technology, Kharagpur-721302, INDIA.

The isothermal luminescence decay method, one of the two basic types of relaxation methods, can be used to study the electron hole reaction kinetics in solids. The kinetic theories developed, pertaining to the electron - hole recombination reactions based on the theories of simple mono-and bi-molecular reactions and statistical thermodynamic theory of absolute reaction rates could not satisfactorily fit in nor explain the experimentally observed decays. The lack of correlation between theory and experiment is to be traced back to the need of an 'apriori' assumption of the order of kinetics parameter. Even the second type of relaxation, namely the non-isothermal relaxation in the form of thermally stimulated luminescence and thermally stimulated conductivity, can at best give estimates of the thermal activation energies or the trap depths, only when the order of kinetics parameter is obtained from other measurements.

Since a good deal of information regarding the nature of the traps and their energy levels can be obtained from after glow characteristics, a new method called the isothermal monochromatic luminescence decay method, developed recently by us is utilised to experimentally determine all the three trapping parameters, namely trap depth, frequency factor as well as the order of kinetics parameter. The method which was first meant

for the experimental evaluation of the Ist and 2nd order kinetics, was extended to general order kinetics also, thereby removing the drawback of the earlier decay methods. The isothermal monochromatic luminescence decay method (I.LD) consists of recording the monochromatic isothermal decay of luminescence with the monochromater set at the emission wavelengths known from the X-ray fluorescence and thermally stimulated luminescence spectra, at a few (at least three) temperatures on the rising side of the glow peak temperatures. The straight line nature of the plots ln I Vs time and $(I_o/I)^{\frac{1}{2}} - 1$ Vs time establishes first and second order kinetics respectively. This has been successfully applied to pure and doped KCl and KBr systems. The uniqueness of this method lies in its applicability even to intermediate order of kinetics (between 1 and 2). And thus, this has been profitably applied to the system LiF. For such cases $(I_o/I)^{\frac{b-1}{b}} - 1$ Vs time plots are drawn for the test values of'b'(order of kinetics) between 1 and 2. The particular value of 'b' for which the plot is a straight line is the order of kinetics. The credit of this method is that even the changes in the order of kinetics during the decay process can be detected. And with the unique establishment of the order of kinetics, the other two trapping parameters, E and s could be obtained. F-centre associated glow peaks in KCl and KBr obey first order kinetics. But in LiF order of kinetics decreases from 1.3 to 1.0 with increasing X-ray dose. These results highlight the success of this method.

Pulsed luminescence from non-equilibrium distribution of F_A(II) centers in KCl:Li^+.

G. Baldacchini[(a)], U.M. Grassano[(b)], M. Meucci[(c)], A. Scacco[(b)], F. Somma[(b)] and M. Tonelli[(c)]

(a) ENEA, TIB-FIS, Centro Ricerche Energia, 00044 Frascati, Italy

(b) Dipartimento di Fisica, Università La Sapienza, P.le A. Moro 2, 00185 Roma, Italy

(c) Dipartimento di Fisica, Università di Pisa, P. Torricelli 2, 56100 Pisa, Italy

After their first appearance and the following developments in the connected technology during the last few years, color center lasers proved to be a powerful tool for a widespread range of applications, such as high resolution molecular spectroscopy, laser chemistry, pollution detection and studies of propagation in optical fibers. Although several types of color centers in different alkali halide crystals have been investigated in order to obtain laser action, the F_A(II) center still appears the most suitable for operation in the 2-3 μm range.

The behavior of the F_A(II) center under irradiation with polarized light is of remarkable relevance to the development of the color center lasers using these defects. As it is well known, optical pumping within the F_{A1} band with monochromatic light polarized along one of the <100> directions leads in general to a reorientation of the F_A(II) centers along directions where they can no longer be excited, causing the bleaching of their absorption bands and consequently the quenching of their luminescence. To avoid this effect, the orientation of the crystal axes with respect to the direction of polarization of the pumping beam has to be chosen so that all centers laying along the three equivalent <100>

directions can be excited. Nevertheless, various experiments showed that appreciable emission can be observed even in the case of F_A(II) centers in KCl:Li^+ crystals pumped with light polarized along one of the crystal axes. These results can be interpreted as the effects of the off-center position of the Li^+ ions, which causes a tilt of the F_A(II) dipoles out of the <100> direction thus preventing their complete alignment. The kinetics of the F_A(II) centers optical reorientation process under sudden rotation of the pumping beam polarization has been investigated by monitoring the intensity of the F_A(II) centers emission, peaking at 2.7 μm, with both lamp and laser excitation sources. The minimum value of the emission intensity, after the steady state has been reached, is about 10% of the maximum luminescence intensity. The reorientation time is strongly dependent on the pump incident power, the average value being about 1 ms for a pump of 1 W/cm^2.

Similar experiments, presently in progress, are concerning other kinds of color centers which could exhibit analogous off-axis characteristics.

Spin Mixing Processes of the Optically Pumped F Centers via the Study of Magnetic Circular Polarization of Luminescence

H.Ohkura, *) S.Muramatsu, N.Akiyama, K.Kawano, and Y.Mori

Department of Applied Physics, Osaka City University, Sumiyoshi-ku, Osaka Japan 558, and *) Department of Electronic Engineering, Utunomiya University, Utsunomiya Japan 321

Summary

The spin mixing processes of optically pumped F center are specified by the spin mixing parameters ε's which represent the probability for the spin to be flipped in the optical cycle. One of the main aim of this talk is to estimate the mixing parameter ε_{rl} in the non-radiative transition (NRT) process as a function of pumping photon energy E_{ph}. The spin mixing is caused by the spin orbit interaction in the optical cycle.[1] The mixing parameter in the unrelaxed excited state (URES) denoted as ε_+ and ε_- are dependent on the spin quantum number of $\pm(1/2)$ of the ground state.[2] $\varepsilon_0=(1/2)(\varepsilon_+ + \varepsilon_-)$ and $\delta\varepsilon=(\varepsilon_- - \varepsilon_+)$ are used for convenience. Now, the spin-orbit interaction constant λ in the relaxed excited state (RES) was found to be small of less than one hundredth of λ value in the URES.[3] The calculated mixing parameter in the RES was also found to be negligibly small.[4] This evidence implies that, during the NRT process from the URES to the RES, the pumped F electron should pass down many sorts of multi-phonon levels characterized by λ values decreased gradually. Thus, the spin mixing parameter ε_{rl} cannot be neglected in the argument of the spin mixing processes in the cycle.

From the analysis of magnetic circular polarization of F center emission observed, the amount of ε_t, that is the net spin mixing parameter in the cycle derived as $(1/2)[1-(1-2\varepsilon_0)(1-2\varepsilon_{rl})]$, and $\delta\varepsilon(1-2\varepsilon_{rl})$ are determined for KI as a function of E_{ph}, as shown in Figs. 1 and 2 by white circles. Dotted lines in the figures are the F band. Dot-dashed lines are theoretically calculated curves of ε_0 and $\delta\varepsilon$ by the Monte Carlo method on the same basis as

in ref.2, except that the Γ_5^+-mode Jahn-Teller interaction is newly included. With adjusting the E_{ph}-dependence of ε_{rl} shown by broken lines in Fig.1, the E_{ph}-dependence of ε_t and $\delta\varepsilon(1-2\varepsilon_{rl})$ calculated are plotted by solid lines. The coincidence of these lines and experimental points is fairly good. This may show the validity of the present treatment. The fact that ε_{rl} is large at the higher energy side of the F band in comparison with that at the lower side is reasonably understood by an idea that more spin mixing occurs in the NRT process when the F electron is excited into higher energy levels.

References:

1) A.Winnacker and L.F.Mollenauer: Phys.Rev. B6 787 (1972).

2) K.E.Mauser et al. : Z.Phys. B26 107 (1977).

3) H.Ohkura et al.: J.Phys.Soc.Jpn. 51 3615 (1982).

4) K.Imanaka et al.: Solid State Commun. 27 1009 (1978).

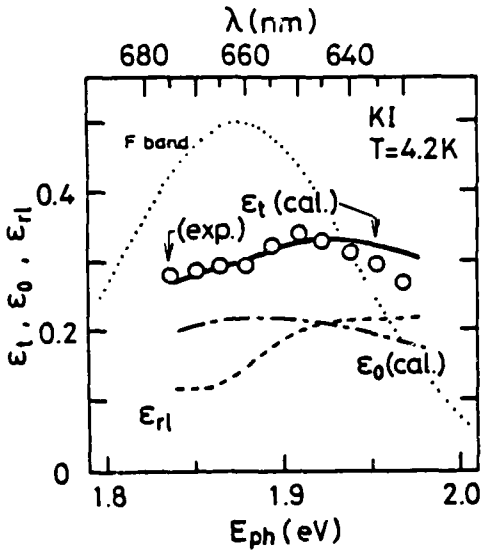

Fig.1

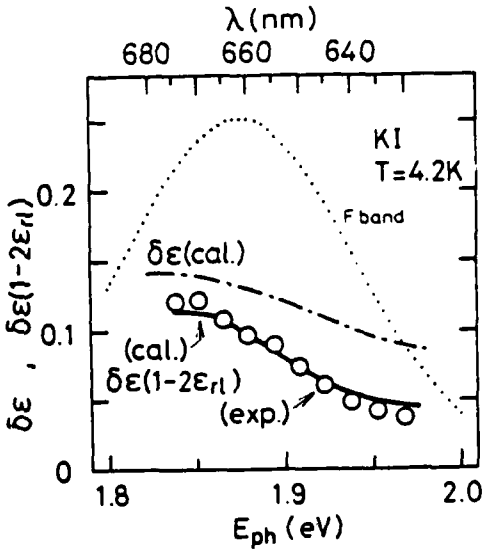

Fig.2

Simple Semicontinuum Vibronic Model of the F Center

M. Georgiev

Departamento de Materia Condensada, Instituto de Física, Universidad Nacional Autónoma de México, Apartado Postal 20-364, Delegación Alvaro Obregón, 01000 México, D. F., México.

This is an extension of our earlier work on the F center[1]. We had calculated the thermal ionization rates of excited F centers (F^*) in KCl using experimental data on the F center photoionization efficiency and luminescent lifetime. When plotting them versus the respective reciprocal temperatures, considerable deviations from the Arrhenius temperature behavior were found to occur below 100 K leading to a nonvanishing residual ionizability at low temperature. These were suspected to result from a strong lattice tunneling at the lower temperatures. A reaction-rate theory was applied for a quantitative analysis which expresses the rate constant in terms of four adjustable parameters: vibrational frequency ω, lattice-reorganizational energy E_r, reaction heat Q at 0 K, and electron-exchange integral V_{12}.[2] The ionization transition was regarded as the one in which the F^* electron transferred to a polaron state by virtue of the strong interaction with a promoting mode. Very reasonable values were obtained for the fitting parameters, as the theory was compared numerically with the experiment. V_{12} was also estimated independently within the BWK approximation resulting in a remarkable agreement between fitted and computed values.

In an attempt to pre-calculate all the free parameters of the theoretical rate constant, a simple vibronic model of the F center was now constructed by coupling a breathing-mode A_{1g}- type vibration to the semicontinuum electronic potential. This coupling was effected by allowing the vibration to mo-

dulate both the depth and width of the spherical well, while leaving the Coulomb tail essentially unchanged. The electronic eigenstates were found by a self-consistent procedure following Krumhansl & Schwartz's prescription for calculating the effective dielectric constant[3]. Such calculations were made for the 1s- and 2p- like states of the F center, and for the 2p-like bound polaron state. Further, a configurational-coordinate diagram of the NaI F center was computed within the frameworks of the adiabatic approximation by assuming harmonicity of the lattice vibration and linear electron-phonon coupling. The diagram predicts two radiative deexcitation channels following optical absorption which start from the relaxed excited F state and bound polaron state, respectively. The F^* polaron transition occurs via a nonradiative process involving lattice tunneling at low temperature. The positions of all optical bands agree reasonably well with those found in recent experiments[4]. So does the height of the computed crossover barrier between the F^* and polaron parabolae, as compared with the observed activiation energy of the F-F' conversion in NaI,[4] now assumed to occur via translational motion of the polaron to another F center.

1. M. Georgiev et al., Phys. Rev. B 26, 6936 (1982).
2. S. G. Christov, Phys. Rev. B 26,6918 (1982).
3. W. B. Fowler, Phys. Rev. 135, A1725 (1964).
4. G. Baldacchini et al., Phys. Rev. B 24,2174 (1981).

The Calculation of the Formation Energies of Point Defects

W.A. Runciman, B. Srinivasan*

Department of Solid State Physics
Research School of Physical Sciences
Australian National University
Canberra ACT 2601 Australia

and

D.D. Richardson†

Department of Theoretical Physics
Research School of Physical Sciences
Australian National University
Canberra ACT 2601 Australia

*Present Address
D1-119 Bonn Avenue
IIT Madras 600 036
India

†Present Address
Materials Research Laboratories
PO Box 50
ASCOT VALE VIC 3032

Summary

There are many different centres formed when uranium is incorporated into LiF or NaF in an oxidizing atmosphere.[1] Some of these centres are due to the presence of additional impurity ions, such as magnesium. It is also possible that lattice vacancies may be present. It was decided to calculate the formation energies of different models for centres in order to find the most likely candidate for the observed centres. In general, we require to calculate the interaction energies due to the presence of the defect and the lattice relaxations around the defects. It is assumed that changes in the electronic band structure due to the defect are negligible. This appears reasonable since screening and electronic relaxation will be negligible in an electronic insulator such as LiF . However the remaining calculations are still formidable as there are non-Coulomb short range interaction potentials as well as the Coulomb potentials. In order to make a preliminary survey of a large number of types of centre calculations were made using the Coulomb potential only and without lattice relaxation. Ions are assumed to substitute for lattice ions and are assigned the conventional ionic charges. Using the Madelung constant for the alkali halide lattice the calculations can be reduced

to simple hand calculations. In practice we used a programme which could also cope with non-Coulomb potentials.[2] There is a problem in finding suitable short-range potentials and this more than complexity of calculation was the reason for their initial neglect. Calculations were made for 57 varieties of uranium centres in lithium fluoride which showed local charge compensation.

As an example consider two possible configurations of UO_6M centres, where M is a divalent ion.

(a) UO_5 + OM = -292.43eV

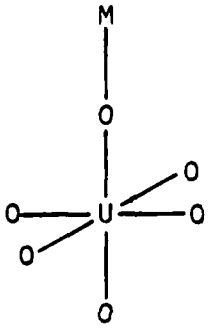

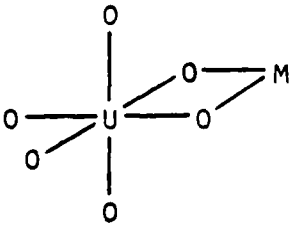

(b) -301.82eV (c) -301.03eV

The formation energies of the complexes (b) and (c) are compared in energy with the sum (a) of the formation energies of UO_5 and OM centres and are found to have lower energies. Note that most nearest-neighbour interactions if included would be common to both models and hence would not affect the relative energies. There is only one extra O-M interaction in (c) in place of an O-Li interaction in (b). The tetragonal centre (b) with the U-M axis along a crystal axis is calculated to have a lower formation energy than the more compact orthorhombic centre (c). A similar tendency was found in other uranium -oxygen-aliovalent ion complexes. Complexes with positive ion vacancies were shown to be energetically unfavourable, but this did not apply to complexes with negative ion vacancies.

References

1. Runciman, W.A. and Wong, E.Y. J.Chem.Phys. 71, 1838 (1979).

2. Richardson, D.D. Computer Phys.Commun. 28, 75 (1982).

LASING FROM A VIBRATIONAL TRANSITION OF A MOLECULAR DEFECT

T. R. Gosnell, R. W. Tkach and A. J. Sievers
Laboratory of Atomic and Solid State Physics
and Materials Science Center
Cornell University
Ithaca, New York 14853

Infrared fluorescence from CN^- defects in alkali halides was first observed by Yang and Luty[1]. Recently, we have observed lasing in the KBr:CN^- system. This is the first report of a laser operating between pure vibrational levels of a defect in a solid. While CN^- will fluoresce at high temperatures, (up to 500 K), lasing is only observed at temperatures below 4 K. This is due to the nature of the pumping.

The lasing in this system is on the v=2 to v=1 vibrational transition (2054 cm^{-1}), but the system is optically pumped on the 0->1 transition (2079 cm^{-1}) by the second harmonic of a TEA CO_2 laser operating on the 9P28 line. Population of the v=2 state occurs through the vibrational energy exchange reaction

$$CN^-(1) + CN^-(1) \rightarrow CN^-(2) + CN^-(0) + 25\ cm^{-1} . \qquad (1)$$

When the temperature is sufficiently low, the reverse reaction is inhibited, and an "up the ladder" cascade results. This has been observed[2] and calculated[3] for CO in solid rare gas matrices. In the CN^- system, it is experimentally observed that the v=2 state is populated and the v=1 depopulated on a time scale of roughly 100 microseconds. The population inversion thus established has been measured with a tunable diode laser, and persists for several milliseconds. Gain coefficients as high as .7 cm^{-1} have been measured. Figure 1 shows an example of laser emission obtained at 1.7 K from a KBr + .5% KCN crystal fabricated as a laser cavity. The crystal was cleaved to a 1x1x14 mm prism and coated with an evaporated gold film on all surfaces, except for a 4mm region on one side left open for pumping. Output coupling was provided by a .2mm hole in the coating on one face. Approximately 200 microjoules of pump energy was found to be the threshold for oscillation in this cavity. When the temperature is raised, phonons can provide the necessary energy for the reverse of the reaction (1) to occur, and inversion disappears. Figure 1b shows the effect of raising the temperature to 4 K. The gain is observed to completely vanish at roughly 6 K.

In these samples, made with naturally occurring KCN, an additional energy exchange process can take place:

$$^{12}C^{14}N^{-}(1) + {}^{13}C^{14}N^{-}(0) \rightarrow {}^{12}C^{14}N^{-}(0) + {}^{13}C^{14}N^{-}(1) + 44\ cm^{-1}\ , \quad (2)$$

and similarly for $^{12}C^{15}N$. These processes absorb as much as 50% of the input pump energy. Results will be presented on samples prepared with isotopically pure $K^{12}C^{14}N$. This should result in considerably improved laser performance.

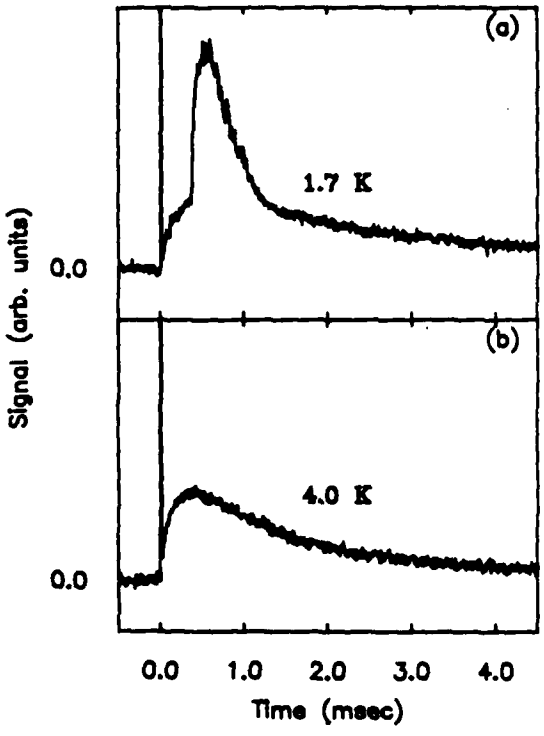

Figure 1. a) Single shot example of laser output at 2054 cm^{-1} for a sample at 1.7 K. The spikes at t=0 are electrical noise and scattered light. b) Only the fluorescence background remains when the temperature is raised to 4 K.

This work has been supported by USARO Grant DAAG-29-83-k-0044, USARO Grant DAAG-29-83-c-0035, and NSF Grant DMR-79-24008. T. R. Gosnell is a USARO Predoctoral Fellow, and R. W. Tkach is a General Motors Postdoctoral Fellow.

1. Y. Yang and F. Luty, Phys. Rev. Lett. 51, 419 (1983)
2. H. Dubost and R. Charneau, Chem. Phys. 12, 407 (1976)
3. J. Manz, Chem Phys. 24, 51 (1977); Chem. Phys. Lett. 51, 477 (1977)

TWO-COLOR SUPERFLUORESCENCE OF O_2^- CENTERS IN KCl

R.Florian, L.O.Schwan and D.Schmid (Physikalisches Institut IV,
Universität Düsseldorf, D 4000 Düsseldorf, Germany)

If O_2^- centers in KCl are excited in their fundamental absorption band (at about 250 nm), they yield a fluorescnece spectrum which at low temperatures is dominated by a progression of very narrow zero-phonon lines ($\Delta\nu_{1/2} \approx 1 cm^{-1}$) with a large Stokes shift (roughly 23000 cm^{-1} or 2.9 eV). At very high excitation intensities ($\gtrsim 20$ GW/cm²) with single pulses of the fourth harmonic of a modelocked Nd-YAG laser (λ = 266 nm, pulse duration 30 ps, pulse energy ~ 100 μJ) and at low temepratures (T < 30 K) one observes a simultaneous coherent emission at the wavelength of two of the zero-phonon lines (0-10 and 0-11 transition at 594.77 and 629.14 nm, respectively) /1/, which can be identified as two-color superfluorescence from a three-level system /2,3/.

Some of the observed features will be discussed:

(1) If the sample is excited in a thin "pencil-shaped" volume (length 1 cm, diameter 0.1 nm, Fresnel number $\sim$ 1), one observes superfluorescence pulses in forward and backward direction, which originate at the same time within the limits of error (± 100 ps) and which are phaselocked with respect to each other. Evidence for the last statement is given by the interference pattern in a Michelson-like arrangement. The observed coherence time is more than 100 ps, the spectral width of the pulse is about 0.5 cm^{-1}. The red and the yellow contribution in the superfluorescence pulse also originate simultaneously within the limits of error.

(2) The delay times of the superfluorescence pulses with respect to the excitation pulse vary statistically between 500 ps and 10 ns. The peak in-

tensities and pulse widths also fluctuate statistically within about the same limits. Roughly 10% of the excited O_2^- centers in the active volume contribute to the superfluorescence.

(3) By feeding back a small fraction of the superfluorescence pulse into the active volume after an appropriate delaytime a second superfluorescence event can be triggered yielding a lower bound for the reorientation time of the centers in the excited state (> 10 ns).

(4) If the excitation takes place in a "thin sheet" instead of a "pencil a two-dimensional coherent emission is observed.

(5) Limits for the vibrational relaxation times in the excited state (τ_R^*) and in the ground state (τ_R) of the O_2^- centers can be estimated on the basis of these observations: $\tau_R^* < 20$ ps /4/ and $\tau_R \gtrsim 50$ ps. The minimum delay time of 500 ps observed for the superfluorescence pulses may be explained tentatively as the time required for the excited O_2^- to transfer the relaxation energy to the lattice phonon bath.

References

/1/ R.Florian, L.O.Schwan and D.Schmid, Phys.Rev. A29 (3), in press.

/2/ F.Haake and R.Reibold, submitted to Phys.Rev.A.

/3/ P.Schwendimann, submitted to Optica Acta.

/4/ L.O.Schwan, R.Florian, D.Schmid, E.Betz, W. Schrof, B.Walker and H.Port, submitted to Phys.stat.sol. b.

ON THE NATURE OF Gd^{3+} LUMINESCENCE CENTERS IN THE CRYSTALS OF THE ALKALINE EARTH FLUORIDES

Ju.N.Orlov, V.I.Aleshin, V.E.Bozhevolnov, L.N.Ivanov, V.V.Karelin, G.V.Saparin
Moscow State University, Moscow II9899, USSR

Unlike other rare-earth ions the ions of Gd^{3+} have intense luminescence in all solid solutions with fluorite structure as MF_2-GdF_3 where M is Ca, Sr, Ba [I]. The ESR, scanning electron microscopy, optical spectroscopy have been used for the study of MF_2- GdF_3 structures which included GdF_3 with concentration in the range of 0,00I - 40,000 %. As the results of experiments the three intervals of Gd^{3+} concentration were discovered in CaF_2- GdF_3 system (below I%, I - I5% and over I5%) characterized by different sets of Gd^{3+} luminescence centers. The peculiarities of the Gd^{3+} luminescence centers are: presence of cubic centers for all concentration intervals of impurity and high concentration of superfluous anion vacancies F_v^- in CaF_2- GdF_3 and SrF_2- GdF_3 systems. The latter stabilizes a complex claster of Gd^{3+} centers including also interstitial ions of fluorine F_i wich are prevalent type of Gd^{3+} luminescence centers for second and third concentration intervals.

Experimental results explain some peculiarties of Gd^{3+} luminescence in the crystals of the alkaline earth fluorides and allow to offer a new model of Gd^{3+} thermoluminescence (TL) for above systems.

The data of TL and thermal bleaching show that in the concentration region of less than I% Gd^{3+}, photochromic centers serve as electron centers of Gd^{3+} thermoluminescence but not divalent ions that is right for others rare-earth elements in similar systems. For larger concentration F-centers play a analogous role. As hole centers act interstitial F-ions in the structure of different types of centers including optical centers. In according to the new model the TL process of Gd^{3+} is explained by the recombination of delocalized holes F_i^0 and F-centers which can take place in the vicinity of Gd^{3+} ion or in claster centers. A recombination energy transfered to Gd^{3+} and irradiated by this ion.

Thus the peaks of TL curves are determined by interaction energy between Gd^{3+} and F_i^- for optical centers. Such conclusion is confirmed by comparison of the co-

nsideration of formation energy of impurity centers with TL experimental data of deep traps location and also by the absence of the visible TL Gd^{3+} in BaF_2-GF_3 crystals where the presence of the anion vacancies is not discovered.

TL investigations of some rare-earth elements in the crystals of the alkaline earth fluorides confirmed that new model is correct for the interpretation of the concentration dependences of luminescence using TL curves. This approach can be useful for studies of impurity defects in the crystals.

I. V.E.Bozhevolnov, L.N.Ivanov, V.K.Koslov, Yu.V.Voronov, Yu.P.Timofeev and V.V.Karelin. Phys.Stat.Solidi (b), 78, 483, I976 .

LASER INDUCED MULTISITE EMISSION OF Pr^{3+} IN CaF_2 AT LOW AND ROOM TEMPERATURES

John Chrysochoos

Department of Chemistry, University of Toledo,
Toledo, Ohio 43606

Summary

Direct excitation of the $^3P_0$-state of Pr^{3+} in CaF_2 using 4765 Å (Ar-ion laser) at low temperatures leads to emission attributed to at least three distinct Pr^{3+}-sites (1,2). The present paper deals with multisite emission of Pr^{3+} in CaF_2 under excitation conditions leading to indirect population of the $^3P_0$-state.

Low temperature excitation of Pr^{3+} in CaF_2 with 4579 Å ($^3P_1$, $^1I_6 \leftarrow {}^3H_4$), led to emission originating primarily from the $^3P_0$-state at low $[Pr^{3+}]$ and from both the $^3P_0$ and the $^1D_2$-states at higher $[Pr^{3+}]$. Emission lines arising from the $^3P_0$-state were classified mainly as group (II) and (III) lines, in agreement with earlier results (1,2). A few, very weak, lines were classified as group (I). The ratios $(I_F)_{II}/(I'_F)_{II}$ and $(I_F)_{III}/(I'_F)_{III}$ are independent of $[Pr^{3+}]$, whereas the $(I_F)_{II}/(I_F)_{III}$-ratio increases at higher $[Pr^{3+}]$. Emission arising from the $^3P_1$-state, at low temperatures, was virtually nonexistent, indicating a very effective electronic relaxation of the $^3P_1$-state, $^3P_1 \rightsquigarrow {}^3P_0$, via host lattice vibrations. The efficiency of the $^3P_1 \rightsquigarrow {}^3P_0$-transition decreases at room temperature giving rise to emission from the upper excited state.

Low temperature emission arising from the $^1D_2$-state was observed under 4579 Å excitation at higher $[Pr^{3+}]$, but not under 4765 or 4880 Å. Therefore,

the $^3P_0$-state of Pr^{3+} in CaF_2 does not appear to be a precursor of the $^1D_2$-state. The most likely process leading to the population of the $^1D_2$-state at low temperatures appears to be

$$^3P_1 + {}^3H_4 \rightarrow {}^1D_2 + {}^3H_6 + \Delta E \qquad (1)$$

which involves a very small energy mismatch (about 150 cm^{-1}).

The evolution of the emission from the $^1D_2$-state, monitored at 16650 cm^{-1} ($^1D_2 \rightarrow {}^3H_4$), 14240-14260 cm^{-1} ($^1D_2 \rightarrow {}^3H_5$) and 12520-12560 cm^{-1} ($^1D_2 \rightarrow {}^3H_6$), is accompanied by a reduction of the emission arising from the $^3P_1$-state, under the conditions used, indicating that process (1) is very fast and comparable with the radiationless relaxation of the $^3P_1$-state. Such a rapid energy transfer process is rather unlikely at the concentrations used assuming a statistical distribution of Pr^{3+}-sites. It indicates that Pr^{3+}-ion pairs and clustering play a significant role.

The nature of Pr^{3+}-sites and the significance of ion clustering in radiative and radiationless processes of Pr^{3+} in CaF_2 will be discussed. A mechanism leading to the formation of both trigonal Pr^{3+}-sites and ion-clustering will be considered.

---

1. J. Chrysochoos, M. J. Stillman and P. W. M. Jacobs "The Rare Earths in Modern Science and Technology" Vol. 3 (Plennum Press, New York 1982) p. 161.

2. J. Chrysochoos, P. W. M. Jacobs, M. J. Stillman and A. V. Chadwick, J. Luminesc. 28 (1983) 177.

Luminescence and Defects in Ca^{2+} Doped Thoria Crystals

N. Kristianpoller and A. Rehavi

Department of Physics and Astronomy, Tel Aviv University

Tel Aviv 69978, Israel.

SUMMARY

The luminescence emitted during X-irradiated (XL) as well as the thermoluminescence (TL) of single ThO_2:Ca crystals were studied. Results were compared to those obtained for pure Thoria crystals.[1] The TL was excited at 80 K by X or monochromatic vacuum-ultraviolet (vuv) radiation and excitation spectra were measured between 130 and 250 nm. Measured were also the spectral composition of the emission and the temperature dependence of the main XL emission bands. Results show that after uv irradiation TL peaks appeared at the same temperatures and with the same activation energies as after X-irradiation and after self excitation of the radioactive material, indicating that they are due to the same defects. The absorption edge of ThO_2 is at about 213 nm. The excitation spectrum of ThO_2:Ca showed maxima at 146, 163, 170 and 183 nm. Essentially the same maxima were recorded for pure ThO_2.

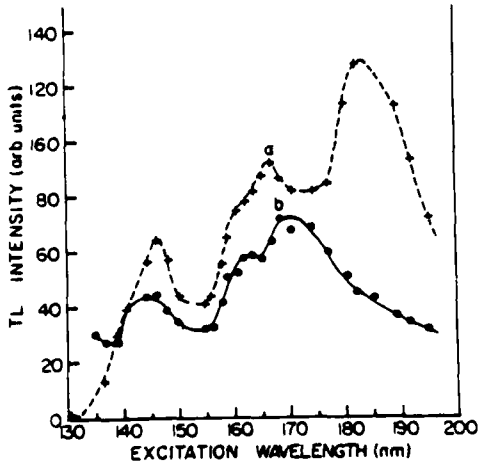

Fig. 1. Excitation Spectra of the TSL peaks at (a) 142 K, (b) 215 K.

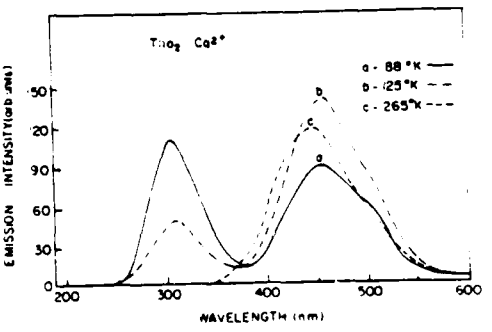

Fig. 2. Emission Spectra recorded at (a) 88 K, (b) 125 K, (c) 265 K.

AD-A148 470 INTERNATIONAL CONFERENCE ON LUMINESCENCE HELD AT MADISON WISCONSIN ON 13-17 AUGUST 1984(U) WISCONSIN UNIV-MADISON W M YEN OCT 84 N00014-84-G-0053 2/1

UNCLASSIFIED F/G 20/6 NL

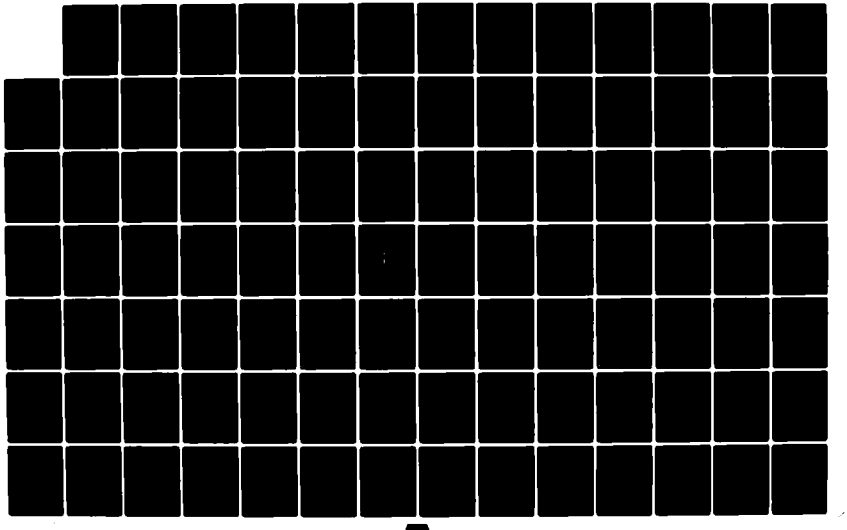

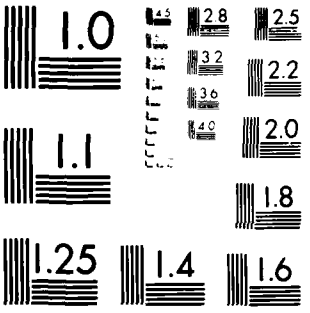

MICROCOPY RESOLUTION TEST CHART

Emission bands were measured for the various TL peaks at 350, 420, 450 and 500 nm; the same bands appeared also in the XL, indicating that also the same luminescence centers are responsible for the emission in these cases. At low temperature an additional band at 305 nm appeared in the XL of the pure and doped crystals, which decreased sharply with increasing temperature. This band is attributed to the radiative decay of self trapped excitons. The 450 nm band reaches its maximal intensity near 200 K and at higher temperatures a shoulder near 500 nm becomes dominant. The 450 nm band is ascribed to the recombination of free holes with F centers. This assumption is in accordance with the previous findings that this band is dominant at temperatures where hole centers become unstable;[2,3] and is also supported by the fact that this band is strongly enhanced in the Ca^{2+} doped samples, which contain larger concentrations of charge compensating anion vacancies.

References

[1] N. Kristianpoller and A. Rehavi, Rad. Effects 72, 209 (1983).

[2] E. T. Rodine and P. L. Land, Phys. Rev. B4, 2701 (1971).

[3] P. J. Harvey and J. B. Hallett, J. Electrochem. Soc. 123, 398 (1976).

Slow Transitions in Diamond: the Photoluminescing S_1 Centre

M. Estela Pereira, M. Isabel B. Jorge, M.F. Thomaz

Departamento de Física
Universidade de Aveiro
3800 Aveiro Portugal

The luminescing S_1 centre in diamond has some characteristic features, eg, its lifetime in the milisecond region and two zero-phonon lines 34 meV apart with temperature dependent intensities and different vibronic structure. Although some preliminary studies on it have been carried out (1) a detailed study of this interesting centre has not yet been reported. We found this centre present in the wide class of the so called brown diamonds whose characteristic centres began to be studied recently (2, 3) and studied it under steady state conditions and by time resolved spectroscopy.

Fig 1.a. shows the luminescence spectrum at 20 K, when only the low energy state (α) luminesces. The spectrum was reconstructed using the linear electron-phonon coupling model (4), the best agreement being achieved with a Huang-Rhys factor of 7.0 ± 0.1 and a phonon of 57 meV replicated at 114 meV (insert fig 1.a.) with characteristics of a nearly localized phonon.

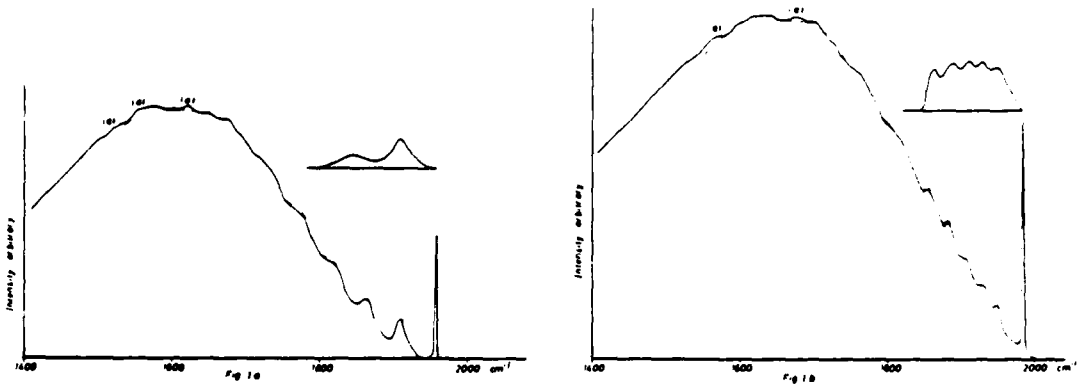

Fig 1 — Luminescence of S_1 centre. 1.a. — from state α. 1.b. — from state β. — experimental — reconstructed. (a) independent features. Insert — calculated 1st phonon band.

Fig 1.b. shows the luminescence of the high energy state (β), obtained at 77 K after subtracting the α part of the spectrum; this band can be reconstructed in a similar way with a Huang-Rhys factor of 5.9 ± 0.2 and several dominant phonons (insert fig 1.b.).

The excitation spectrum is no mirror image of α or β luminescen-

ce and starts only at least 220 meV above the energy of the β zero-phonon line. Between 40 K and 110 K the relative intensities of the bands (I_β/I_α) show an exponential dependence on 1/kT (fig 2). Below 40 K, I_β drops to less than 10^{-4} of I_α. Time resolved spectroscopy shows a fairly exponential decay between 0.6 and 20 ms, in that temperature range, the same for the two bands.

These results fit in a model for the S_1 centre in which upon excitation into a higher electronic state by a fully allowed transition, a very fast non-radiative decay leaves the centre in the α state. Thermal equilibrium between α and β states is at least 10^5 times faster than the radiative decay from the α - state. From the plot of fig 2, an activation energy Ea of 37 ± 3 meV for the $\alpha \rightarrow \beta$ transition indicating that the non-radiative conversion between α and β falls in the strong coupling case (5), and a ratio of radiative rate constants k_β/k_α of 2×10^2 can be derived. Above 110 K an overall decrease of luminescence points to the onset of a non-radiative process, and a corresponding departure from the exponential dependence.

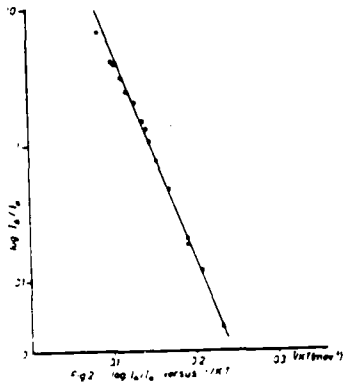

According to this model the decay times τ will be given by $\tau = \tau_\alpha \left[1 + \exp(-Ea/kT)\right] \cdot \left[k_\alpha + k_\beta \exp(-Ea/kT)\right]^{-1} \cdot k_\alpha$ that agree with experimental values, being $\tau_\alpha = 8.5 \pm 0.2$ ms.

A possible explanation for the long lifetime, that needs further confirmation (eg. by Zeeman effect and EPR studies), is that different multiplicity states are involved in the luminescing transitions, as the presence of strong zero-phonon lines excludes the hypothesis of bands due to vibronic mixing.

1 - D.S. Nedzvetskii, V.A. Gaisin - Sov. Phys. Solid State 15 427 (1973)

2 - A.T. Collins, K. Mohammed - J. Phys. C Solid State Physics 15 147 (1982)

3 - M.I.B. Jorge, M. Estela Pereira, M.F. Thomaz, G. Davies, A.T. Collins - Portugaliae Physica 14 135 (1983)

4 - G. Davies - Rep. Prog. Phys. 44 787 (1981)

5 - A.M. Stoneham - Rep. Prog. Phys. 44 1251 (1981)

Resonant Light Scattering and Hot Luminescence at the Indirect Gap in BiI_3

T. KARASAWA, T. KOMATSU and Y.KAIFU

Department of Physics, Osaka City University, Sumiyoshi-ku, Osaka 558, JAPAN

Layered BiI_3 crystals exhibit allowed indirect exciton absorptions with unusually large transition probabilities assisted by LO-phonons. This makes us possible to observe clearly the secondary emission (SE) resonant to the exciton state.[1] The SE spectra give deep informations on the dynamical relaxation processes of exciton. The spectra under resonance excitation by a tunable dye laser consist of one-phonon Raman lines, two- and multi-phonon resonant Raman lines (RRL) associated with hot-luminescence (HL) bands. The typical spectra observed in three samples are shown in Fig.1. The R_{A+C} line is the two-phonon RRL due to the zone edge LO-phonons A and C. As shown in Fig.2, the Raman intensity of R_{A+C} shows resonant enhancement at the indirect edge (E^i_{gx}+ A(Z)) and changes sensitively depending on excitation energy ω_ℓ, lattice temperature and samples. The results can be interpreted by three kinds of damping processes; the sample dependent nonradiative decay σ_o, the scattering by LA- and LO-phonons which depends on temperature and ω_ℓ. These three parameters can be estimated quantitatively from the Raman intensity in Fig.2.[2] The HL part L_C due to recombination of the exciton assisted by the LO-phonon C has rather broad and structured lineshape reflecting directly the non-thermal equilibrium distribution which is constructed through the above three relaxation processes. The structures shift with ω_ℓ. The strong and relatively structureless L_C band is observed in sample a (small σ_o), in which multiple LA-phonon scattering is dominant (Fig.1(a)).

As going from sample a to b and c, since the nonradiative decay is getting to be significant, the HL band becomes weak, and the Raman-like structures coming from lower order LA-phonon scattering appear clearly (Fig.1(b) and (c)). These results give new informations on interpretation of the resonant Raman and hot-luminescence spectra observed in the secondary emission accompanied by phonons.

References

1) T.karasawa et al, J. Phys. Soc. Japan 52 (1983) 2592.

2) T.Iida et al, J. Phys. C 16 (1983) 4719.

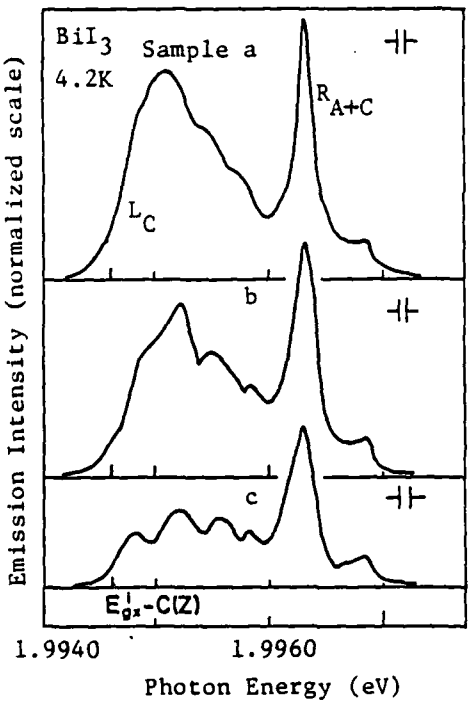

Fig. 1
Secondary emission spectra in samples a(σ_o= 0.08), b(0.18) and c(0.50).

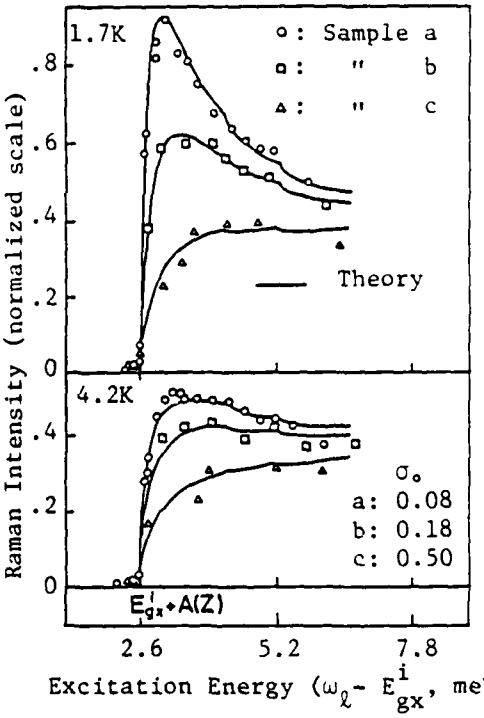

Fig. 2
Raman cross sections of the R_{A+C} line in samples a, b and c at 1.7K and 4.2K.

Spectral Structure of Secondary Emission in Indirect Exciton-Phonon System

T. Iida and M. Sakai

Department of Physics, Osaka City University,
Sumiyoshi-ku, Osaka 558, Japan

We study the secondary emission due to recombination of excitons near the indirect band bottom, where the relaxation is governed by the multiple scattering by acoustic phonons and a nonradiative decay process. In this case, the secondary emission can be separated exactly into the Raman scattering (S_R) and the hot luminescence (S_L) parts.[1,2] General expressions of the excitation spectrum (I_R) of S_R and the lineshape of S_L are presented. The nonradiative decay is attributed to the scattering by imperfections, and therefore the decay rate σ represents the sample dependence. Near the band bottom, the scattering by acoustic phonons is quite sensitive to temperature and the kinetic energy of exciton (E_{ac}) moving with the sound velocity. From the temperature dependence of I_R, we can determine σ and E_{ac} uniquely. It should be emphasized that in our theory, only σ and E_{ac} values are necessary for the calculation of S_L.

The spectral structure of S_L reflects the non-thermal equilibrium exciton distribution, which is determined by the Chapmann-Kolmogorov type integral equation with the source term due to the phonon assisted photoexcitation (Ω_1). We solve the integral equation by two methods; the iteration method and approximation with the Fokker-Planck (FP) equation.[2] We fined that (1) in the iteration method, the sharp spectral structure is obtained associated with successive steps of multiple scattering by acoustic phonons, (2) in the FP approximation, the sharp structure is

smeared out but the result can be compared with spectra observed with not so high resolution, (3) our theory can gives consistent interpretation to the spectral structure of S_L and I_R observed in AgBr and BiI_3. We show typical examples of S_L computed by the iteration method in AgBr (Fig.1) and by the FP approximation in BiI_3 (Fig.2) together with observed ones.[3,4]

References

1) H. Kurita et al, J. Phys. Soc. Japan 49 (1980) 1920.

2) T. Iida et al, J. Phys. C 16 (1983) 4719.

3) J. Windscheif et al, J. Phys. C 13 (1980) 6299.

4) T. Karasawa et al, to be submitted to J. Phys. C.

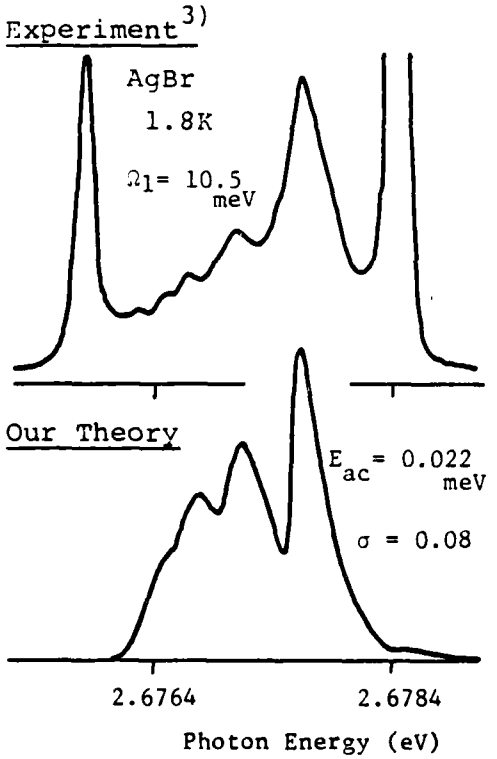

Fig.1 Luminescence part S_L in AgBr

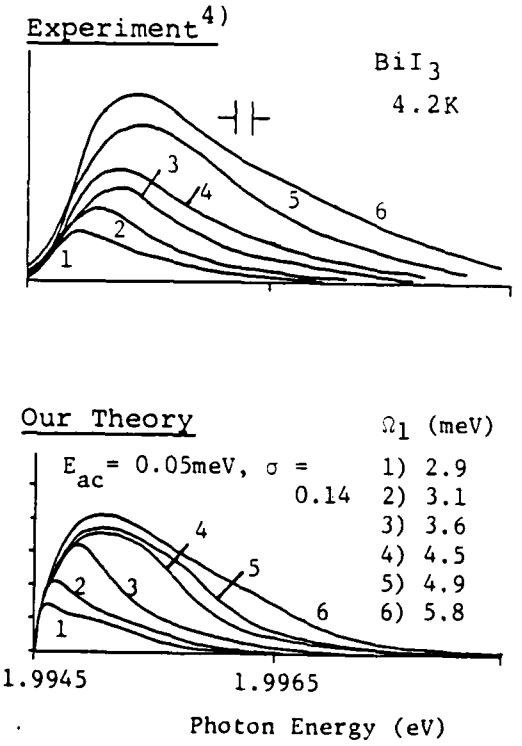

Fig.2 Luminescence part S_L in BiI_3

COLLECTIVELY DESACTIVATING EXCITED CONFIGURATIONS IN IMPURITY SYSTEMS

Alexander A. BEREZIN

Department of Engineering Physics, McMaster University
Hamilton, Ontario, Canada , L8S 4M1

Consider a system of several spatially separated potential wells (trapping sites) in impure crystal or in a large molecule. Let *few* (*but not all!*) of these traps to be filled with electrons, which we call "outer" or "extra" electrons. As a practical realization of this situation one can think of a crystalline or a molecular complex with impurity centers in various charge states [1-3]. Consider, e.g., a 2-site impurity subsystem AB with an extra electron initially residing on site B. Due to the random fields of other crystalline defects the (filled) energy level of an electron on site B may be slightly raised relatively to the corresponding (vacant) level of the site A. As a result, the outer electron can make a spontaneous tunnel transition (TT) from the site B to the site A. An excess of energy can be emitted as either phonon(s) or a low energy photon (infrared or microwave). Therefore, the initial configuration of the impurity pair is, in fact, a configurationally excited state which can decay to a lower lying (ground) state configuration through the exponentially slow spontaneous TT $B \rightarrow A$ of an extra electron [2, 3].

There is a considerable literature on 2-site 1-electron radiative TTs (see, e.g., [1-5] and references therein). Here we consider some more involved forms of the excited state configurations in impurity systems. Namely, we give an example of the collective (polycenter) excited state which can spontaneously undergo to the ground state by the way of the collective TT of not just one but several electrons which jump in a correlated manner (simultaneously) between various pairs of lattice sites.

Consider the square 4-site plane configuration ABCD with a side a. Two negatively charged centers are located in corners A and C while corners B and D are occupied by neutral centers. Let us shift the site D along the line AD by a small distance d ($d \ll a$). It is easy to verify that for this modified geometry (when $|AD| > a$) all four one-electron TTs ($A \rightarrow B$; $A \rightarrow D$; $C \rightarrow B$; $C \rightarrow D$) would increase the total energy of the Coulombic repultion because any of them would lead to a configuration in which two uncompensated negative charges become closer to each other than before such TT have occured. Consequently, all four mentioned one-electron TTs are energetically prohibited (strictly!).

However, one can verify that the energy of the configuration $A\bar{B}C\bar{D}$ (extra electrons reside on sites B and D) is lower than the energy of the initial configuration $\bar{A}BC\bar{D}$ (the distance between both negative charges in the configuration

$A\bar{B}C\bar{D}$ is greater than in $\bar{A}\bar{B}CD$!). In other words, the initial configuration $\bar{A}\bar{B}CD$ has a certain degree of excitation over the genuine ground state $A\bar{B}C\bar{D}$. Consequently, our 4-site system can, at least in principle, to decay spontaneously into the state $A\bar{B}C\bar{D}$. Such spontaneous double TT (simultaneous correlated TT of both electrons) can be accompanied by the emission of phonon(s) and/or by the radiation of one (or more) low-energy photons. The energy gain of this double TT, i.e. the total energy emitted as phonons or photons is (in atomic units; $q_0 = 1$)

$$\Delta E = 1/AC - 1/BD \simeq d/(2\sqrt{2}\cdot a^2) \quad .$$

So, we constructed an example of the 4-site 2-electron excited state in which *all* (geometrically conceivable) one-electron TTs are strictly prohibited by the energy conservation law and, consequently, the *only* channel available for the spontaneuos decay of this excited state to the ground state configuration is the simultaneous (correlated) TT of both participating electrons. Note, that if the initial configuration of the impurity array is unstable against one-electron TTs (e.g., in the above example the site B is also a negatively charged center), then the detachement (photo or thermal) of the corresponding extra electron (from the site B) will "lock" the remaining one-electron decay channels and turn the collective TT into the only channel of the spontaneous desactivation.

In the same manner, one can consider an exited state configuration with an arbitrary number of electrons (N) distributed over 2N sites. It is possible to construct such spatial arrangement of this 2N-electron N-site system that the only channel open for the energy transition onto a ground state level will be a simultaneous (correlated) TT of all N electrons [e.g., a regular 2N-polygone with alternately populated vertices in which one (empty) vertex is slightly shifted radially outwards].

Therefore, we demonstrated the principle existence of the specific polyelectron excited states which can decay to the ground-state configuration *exclusively* through the collective TTs of all participating electrons jumping simultaneously between different pairs of sites.

REFERENCES

1. A.A. Berezin, Solid State Communs., 49, 87 - 89 (1984).
2. A.A. Berezin, Phys. Letters, 95 A, 266 - 268 (1983).
3. A.A. Berezin, Zf. Naturforsch., 38 A, 959 - 962 (1983).
4. E.A. Kotomin and A.L. Shluger, Phys.Stat. Solidi(b), 109, 75 - 81 (1982)
5. G.B. Inglis and F. Williams. J. Luminescence, 12/13, 525 - 530 (1976).

TIME BEHAVIOR OF NON-RADIATIVE MULTIPHONON RELAXATION PROCESSES

V. Denner and M. Wagner
Institut für Theoretische Physik, Universität Stuttgart,
Pfaffenwaldring 57, 7000 Stuttgart 80, Germany

Non-radiative multiphonon transitions are investigated on the basis of a widely used model consisting of an electronic two-level system interacting with a set of accepting and promoting phonon modes. It is assumed that both types of modes have different parity.

The relaxation behavior of an initially prepared non-equilibrium state is studied by means of the canonical autocorrelation function $\langle\sigma_z(0)\sigma_z(t)\rangle$ in the framework of the Kubo-Mori formalism. For short times a moment expansion is employed. Due to the complexities arising from the diagonal electron-phonon interaction (accepting modes) an analytical expression for these moments cannot be given. But it is shown that there exists an upper and lower limit for the second moment of the autocorrelation function. This consideration leads to the interesting conclusion that for the short-time decay the accepting modes only play a minor role.

The long-time behavior is studied in a twofold way. First the conventional Markovian approximation is considered, leading to exponential decay in a Golden Rule like fashion. Alternatively a more sophisticated treatment is proposed. The integro-differential equation for equilibrium correlation functions originally derived by Mori is studied for a Gaussian memory function. This form of the

memory function which is obtained from the information-theoretical approach of Berne and Harp leads to an autocorrelation function whose first four moments are exact. The corresponding Mori equation for the autocorrelation function has only been solved numerically so far. Adopting this Gaussian memory we derive an asymptotic expansion for the long-time behavior of the relaxation process. Comparison with the corresponding numerical solution shows that the long-time expansion together with the known short-time expansion yields an excellent overall representation of the autocorrelation function in this Gaussian memory approach. It turns out that there exists a critical moment's ratio $\tau_c = 2\mu_2/(\mu_0^2\sqrt{\pi}) = 3{,}83$ which separates the regime of oscillatory from that of non-oscillatory decay of the autocorrelation function. The analytical equation determining τ_c is derived and solved numerically.

Finally we point out how the present theory, whose validity is restricted to systems near thermal equilibrium may be generalized to situations far from equilibrium. This gives rise to interesting implications with respect to the statistical mechanics of the radiationless decay problem.

Photocaloric reevaluation of the nonradiative relaxation of Cr^{3+} in crystalline and amorphous hosts.

E. Strauss, W. Seelert
Fachbereich Physik, Universität, P.O.Box 2503
2900 Oldenburg, FR Germany

We report on an investigation of the nonradiative relaxation of photoexcited Cr^{3+} employing photocaloric spectroscopy. It is shown, that this method supplements fluorescence lifetime and photoacoustic measurements[1] to completely determine the branching into different relaxation channels.
In photocaloric experiments one measures quantitatively that part of the absorbed photon energy that is converted into heat. Precise heat measurements are performed using a caloric compensation scheme. Suitable tests proved that all energy absorbed from a laser beam is detected to within ±2 %, in the range 5 mW to 200 mW. A higher sensitivity can be achieved with more sophisticated control circuitry.[2]

The heat detected was exactly corrected for fluorescence absorbed in the calorimeter. The error bars in fig. 1 are mainly due to the uncertainty in the measurements of the absorbed light power. The fluorescence quantum efficiency QE (number of photons emitted per photon absorbed) is calculated from the fraction of energy converted to heat using the pump wavelength and the first moment of the corrected fluorescence spectrum.
We investigated Cr^{3+} in various crystalline hosts and in lithium lime silica glasses. The data for the least complicated case of Ruby are presented here. The characteristic spectroscopic features of Cr^{3+} are sharp, red transitions (^2E) and broad phonon-assisted yellow ($^4T_2$) and blue ($^4T_1$) bands. The ^2E to $^4A_2$ fluorescence is known as R-lines.

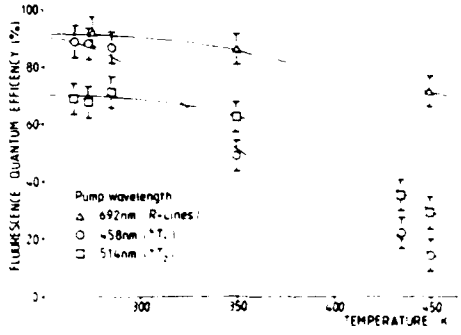

The data are summarized in fig. 1. The values are all independent of the power absorbed and of the focus size. At ambient temperatures the QE is 90 % when pumping the R-lines directly, and slightly lower when pumping the $^4T_1$ band at 458 nm. However, when the $^4T_2$ band at 514 nm is excited, the QE is considerably lower. This gives clear evidence, together with the ratio of "slow" and "fast" heat release obtained from photoacoustic measurements[1], that the $^4T_2$ to ^2E relaxation is less effective than that from $^4T_1$ to ^2E. At 300 K, 20 % of the excited $^4T_2$ population relaxes directly and nonradiatively to the $^4A_2$ ground state. Neither this behaviour nor the observed temperature dependence can be satisfactorily explained within the generalized configuration coordinate model[3] or by thermal activation[4].

1) M. Gallmaier, E. Strauss, W. Schubert, R.T. Brundage, W.M. Yen J de Phys. C 6,401 (1983)
2) E. Stark, private communication
3) B. Barnett, R. Englman J of Lumin. 3,55 (1970)
4) P. Kisliuk, C.A. Moore Phys Rev 160,307 (1967)

Phonon-coherent States and Response of Molecules and Crystals to Short Time Processes

N. Terzi, Dipartimento di Fisica, Università di Milano,
Via Celoria 16, I.-20133 Milano, Italy

The coherent (or quasiclassical or Glauber) quantum states give in author's opinion a very concise and physical way to describe transient vibrational dynamics of molecules and solids, either when these systems are excited (mainly by processes which are short on the vibrational time scale) or when they, afterwards, relax under the action of internal forces. At such length that it seems possible to say that matter is much more coherent than so far assumed.

Here, the generation of phonon coherent states (PCS) is studied, and three different phenomena, deeply involving PCS are presented:

i) Scattering of elementary probes, like neutrons, interacting with the crystal or molecular ions via an interaction local in space and time.[1] While each scattered probe is shown to generate a PCS, the whole beam generates heat in the shined volume.[2] It is shown, in particular, that the ubiquitous Debye-Waller factor is nothing but the squared normalizing constant of the PCS generated by scattering.

ii) Absorption of short pulses of coherent i.r. light by molecules.[3] A rather amazing result is found: while the absorption coefficient shows a peak at the harmonic molecular frequency, the excited state is a molecular PCS. The intrinsic non linear character of such a state may then contain the dissociative

channel, experimentally found in unimolecular reactions. One can say that multiphoton state of the coherent light generates a multiphonon coherent state of the molecule!

iii) Radiative and non radiative electronic transitions.[4] Both the absorption/emission coefficients and the rate coefficient of the non radiative decay are easily written in terms of PCS. In particular, the Huang-Rhys factor e^{-S} has the identical meaning of the Debye-Waller factor, i.e. is the squared normalizing constant of the PCS, where S is the average number of excited phonons, contained in the PCS.

References

1) G.M. Mazzucchelli and N. Terzi, Solid State Comm. 48, 679 (1983).

2) N. Terzi, Proc. of the 4th European Condensed Matter Division (The Haag, March 1984), to be published in Physica B (1984).

3) G.M. Cicchese and N. Terzi, Lett. Nuovo Cim. 38, 151 (1983).

4) A. Giorgetti and N. Terzi, Solid State Comm. 39, 635 (1981).

SELF TRAPPING OF EXCITONS AT THE SURFACE OF RARE GAS SOLIDS AND ITS MANIFESTATION IN LUMINESCENCE AND DESORPTION

by

F. Coletti and J.M. Debever

Groupe de Physique des Etats Condensés ERA 070373

Faculté des Sciences de Luminy, Case 901

70 route Léon Lachamp - 13288 Marseille Cedex 9, France

This paper presents the first results on a correlation between the luminescence of excitons self-trapped at the surface of solid argon and desorption. Recently, Jennison and Emin showed that localisation of electronic excitation at the surface of the crystal is an essential condition, and that especially self-trapping of excitons can lead to desorption of neutral atoms[1]. In the case of solid argon, self-trapping of excitons at the surface has been proved to exist[2]. It leads to characteristic luminescence bands which were also measured with electron excitation techniques[3]. Two of them exactly coincide with the $^3P_1$ and $^1P_1$ emission of isolated argon atoms and were not understood up to now. In the course of this work it turned out that they are emitted by desorbing neutral atoms.

We investigated luminescence and desorption of rare gas solids (mainly argon) under low energy electron excitation (a few eV to 100 eV). The experimental set up was described in ref. 4. Figure 1 shows the luminescence yield (number of photons per number of incident electrons) of the argon-W-band of excitons self-trapped at the surface[2] as a function of the energy E of the electrons. It has a pronounced threshold at E_1 = 14 eV which corresponds to a creation of a free exciton by scattering the incident electron to the bottom of the conduction band. If the free exciton reaches the surface (via diffusion), it is self-trapped there.

Figure 2 shows the luminescence intensity I_L of the W band as a function of sample thickness for fixed $E > E_1$. Desorption manifests itself in a decrease of luminescence as a function of time (electron current and E fixed). Desorption can be balanced by condensation if an appropriate partial pressure, P, of argon is introduced. Then I_L is constant, P is proportional to the desorption rate. The broken line in fig. 1 shows P as a function of E. It has the same threshold than luminescence. Moreover, the

Fig. 1

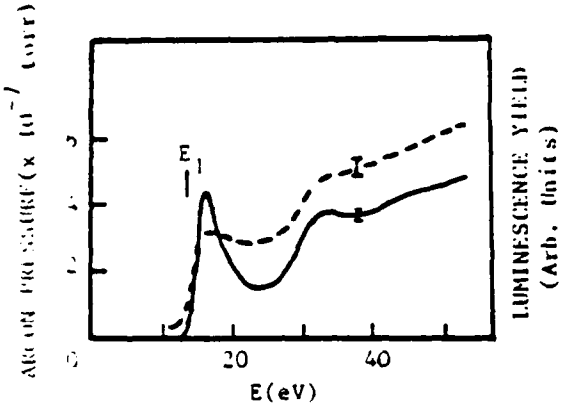

Fig. 2

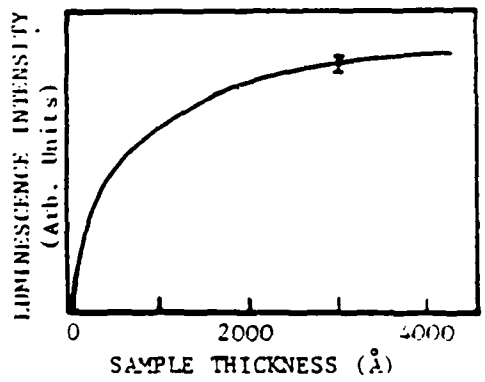

ratio P/I_L is independent from the thickness of the sample. Therefore, the desorption rate is proportional to the concentration of excitons self-trapped at the surface. Similar effects were also observed in solid neon. In solid krypton, desorption is weak. No desorption was found in solid xenon.

The mechanism of desorption corresponds to the mechanism of cavity formation around a self-trapped exciton in solid neon and solid argon. Recently, the energy of self-trapped excitons was calculated as a function of cavity radius[5]. Elastic deformation of the lattice and surface energy of the cavity were treated separately. At the crystal surface, both energies are minimised, if the self-trapped exciton (excited atom) is ejected.

In general, our results show that luminescence spectroscopy can serve as a probe to investigate desorption of neutral atoms.

References :

1. D.R. Jennison and D. Emin, Phys. Rev. Lett. 51, 1390 (1983)
2. E. Roick, G. Gaethke, G. Zimmerer, P. Gürtler and T.O. Woodruff, J. Phys. C : Solid State Phys. 17, 945 (1984)
3. F. Coletti and A.M. Bonnot, Chem. Phys. Lett. 55, 92 (1978)
4. F. Coletti and J.M. Debever, Solid State Commun. 47, 47 (1983)
5. F.V. Kusmartsev and E.E. Rashba, Czech. J. Phys. B32, 54 (1982)

Luminescent and Photochemical Properties of Molecules Near Rough Metal Surfaces

S. Garoff, D. A. Weitz, and M. S. Alvarez
Exxon Research and Engineering Company
Route 22 East - Clinton Township
Annandale, New Jersey 08801 U.S.A.

The luminescent properties of molecules near rough surfaces of some metals are radically different than these properties near flat surfaces of the same metal. In both cases, the luminescence is an excellent probe of the electrodynamic interaction among the optical fields, the adsorbate, and the electronic excitations in the metal surface. It is the differences between these electronic excitations in the rough and smooth surfaces which give rise to the new properties found on the rough surfaces. These new excitations also give rise to other unusual inelastic light scattering processes at rough metal surfaces such as surfaced-enhanced Raman scattering (SERS). Thus, our studies of the luminescent processes on rough metal surfaces not only provides information on the electrodynamics at these surfaces but also the origins of their many unusual optical properties.

In this paper, we describe detailed measurements of the photochemical and photophysical properties of an adsorbate on discontinuous metal island films. We focus on "delayed" processes, those occurring after dephasing and thermalization of the excited state of the adsorbate. Our goal is to present a comprehensive and unified analysis of all our observations. We measure the temporal decay, the fluorescent emission, and rate of the photochemically induced degradation of the adsorbate, as well as the shape of the fluorescent emission (a) on different types of island films, (b) before and after photochemical degradation, and (c) as a function of time after pulsed excitation. We use the same adsorbate in all our measurements,

Ruthenium tris-bipyridine (RuTBP). Our surfaces are island films which are optically well characterized. The discontinuous structure of these films create an inherent variation in distances between adsorbates and roughness features of the surface. We exploit this structure to probe the distance dependence of the electrodynamic interactions on this rough surface. Our measurements show that molecules nearest islands on the film have emission properties most severely altered compared to their properties in an electromagnetically inert environment. Their emission rate is dramatically increased; and their spectra are significantly shifted. The observed changes probe the spatial dependence of the electrodynamic couplings and thus the inhomogeneities in the environment inherent in the discontinuous structure of the island films. The temporal and spectral behavior compliment each other in probing the spatial dependence. All these results are interpreted in a consistent fashion within the framework of the electrodynamic couplings at the surface with the details of the molecular resonance and the relaxed emission process included, thus providing a detailed picture of the consequences of the electrodynamic interactions on the delayed emission and photochemistry of the adsorbates. Particularly intriguing are the spectral shifts of the emission from molecules most strongly coupled to islands. We believe that these shifts originate from the strong interaction between the island and the vibronic structure of the electronic state manifolds of the adsorbed molecules.

Fluorescence of Molecules on Metal Island Films

Timothy D. Harris
AT&T Bell Laboratories
Room 1A-317
Murray Hill, NJ 07974

Summary

The same substrates used to produce surface enhanced Raman scattering can also induce large changes in the fluorescence of nearby molecules. Unlike Raman scattering the rate of emission and the intensity are considered separately. The increase in emission rate has been shown to exceed 10^3 on silver island films (1,2) with a simultaneous enhancement of intensity. Such a large change in emission rate with no loss of intensity provides an avenue for exploitation in emission spectroscopy.

The possibilities for exploitation include, the observation of luminescence from, species with fundamentally low emission rates (spin and parity forbidden transitions), species which normally undergo photochemistry, and emission in the presence of large quencher concentrations. All these applications are potentially significant to improved fluorescence determinations but the tolerance of quenchers has the broadest potential.

An initial report of the quenching tolerance of near metal surface molecules has been made (3). We will report a systematic study of the effect of quenchers on the luminescence yield of molecules on both silver and gold island films. The effect of gold islands on luminescence is made for the first time. Several important variables are studied. Included are wavelength of excitation, island size, coverage, dye absorption and emission wavelength, quencher concentration, atmospheric quenching effects, and studies of both dry and immersed films. Among several surprising results is the complete suppression of emission from gold films below 600 nm. The prediction of the enhancement of emission with increased refractive index is tested for the first time and a comparison of the effects on normally ns, μs, and ms luminescence lifetimes is made. The extent of quenching tolerance is assessed.

The breadth of this data enables a more complete assessment of the accuracy of the currently available models. Especially important are the immersed film measurement which allows a much more accurate knowledge of quencher concentrations and local molecular environments.

References

(1) D. A. Weitz et. al., Opt. Lett. 7, 1982, p 89-91.

(2) D. A. Weitz, et. al., J. Luminescence 24/25, 1981, 83-86.

(3) T. D. Harris, A. M. Glass, and D. H. Olson, Proceedings of the 25th Annual Conference on Analytical Chemistry in Energy Technology, Elsevier, Amsterdam 1984, in press.

Optical-Environment-Dependent Lifetimes and Radiation Patterns of Luminescent Centers in Very Thin Films

Ch. Fattinger and W. Lukosz

Swiss Federal Institute of Technology, Professur für Optik, 8093 Zürich, Switzerland

The emission from luminescent centers located in a thin film (C) of thickness $d_o << \lambda$ (where λ is the emission wavelength) is optical-environment-dependent: The raditive lifetimes depend not only on the refractive index n_o of the film but also on the indices n_1 and n_2 of the adjacent media 1 and 2. The angular distributions of the emitted light differ drastically from the well-known multipole radiation patterns. From these electrodynamical effects informations about the emitting centers can be obtained (determination of quantum efficiencies, multipolarity assignments, orientation of the emission dipoles).[1,2]

We report on measurements of time and angle resolved polarized spectra of laser induced luminescence of thin films. The films were deposited on a glass prism P. Medium (2) was either air (n_2=1), or a glass (n_2>1). The sample was excited with s or p polarized light of wavelength λ_e from a pulsed dye laser (Lambda Physik FL2002, pulse duration ≈ 15 ns), incident at angle of incidence α_e. The intensity $I^{(s,p)}(t,\alpha,\lambda)$ of the luminescent light emitted in direction α passed through a polarization analyser and a double prism monochromator and was detected

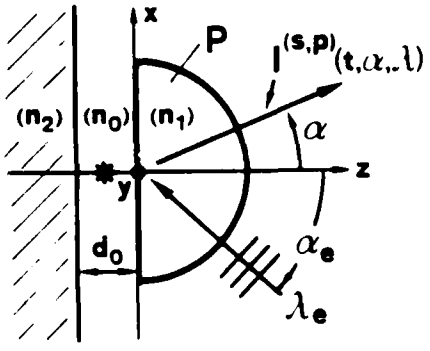

by photon counting. Time decays were measured with the multi-channel scaling method (MCS module in LeCroy system 3500 with 1 μs/channel minimum dwell time).

The theory[1,2] predicts different radiative lifetimes for electric dipoles oriented parallel and perpendicular to the film. Choice of the angles α_e and α and of the polarizations (s or p) for λ_e and λ, permits us to excite and to observe, respectively, the x, y, and z components of the absorption (and emission) dipole moments selectively.

Results are presented, for example, for evaporated 8-80 nm thick films and acetonitrile solutions of europium benzoyl trifluroacetone chelate (EuBTF). Their luminescence was excited with λ=365 nm (ligand absorption) and λ=395, 465, 525 and 580 nm (ion absorption lines). For many of the Eu^{3+} emission lines both radiation patterns and time decays have been measured. Multipolarity assignments: e.g., the line λ=594 nm ($^5D_0 \rightarrow {}^7F_1$) is emitted in a magnetic dipole transition. For λ_e=365 nm, we found: the decay times are practically independent of the polarization and of the angles α_e and α (their dependance on the refractive indices n_1 and n_2 will be compared with the theory); the luminescence starting from $^5D_0$ level is time-delayed, its maximum appearing 5-6 μs after the laser shot; and a small polarization memory effect in the main emission line $^5D_0 \rightarrow {}^7F_2$.

[1] W. Lukosz, Phys. Rev. B 22, 3030 (1980).

[2] R.E. Kunz and W. Lukosz, Phys. Rev. B 21, 4814 (1980), and Opt. Commun. 31, 251 (1979).

Luminescence from Adsorbates

Kazumasa Shinjo and Satoru Sugano

The Institute for Solid State Physics, The University of Tokyo
7-22-1 Roppongi, Minato-ku, Tokyo 106, Japan

Theory[1] of multivalency of adsorbates on metal surfaces, taking into account the effect of the image-force stabilization measured by η^2 in addition to those of the electron-transfer between the adsorbate and the substrate measured by Γ and Coulomb interaction between the adsorbate electrons, has revealed that the critical lines exist in a parameter space, across which the valence charge of the adsorbate ground state changes discontinuously. Dynamical calculations[2] have been made on the line shapes of optical absorption and photoelectron emission spectra of a similar system. It has been found that the lines are broadened when the energy, $\varepsilon_a - U_a$, of the core-hole-stabilized valence level of the adsorbate goes up across the critical line at $-\eta^2/2$: the broadening may be considered to be due to a short life-time of the excited neutral configuration from which an electron escapes into the substrate. The broadening of the absorption lines has been discussed in connection with the experiment of Cunningham et al[3] concerning persistence or non-persistence of exciton lines in the reflection spectra of rare-gas-atoms on metal surfaces.

The purpose of the present paper is to perform a dynamical calculation on the line shapes of luminescence spectra of the same adsorbates. We assume that the radiative life-time is much

longer than the electronic relaxation time of the excited state. The calculated spectra given in the figure shows an abrupt change of the line shape when $\varepsilon_a - U_a$ goes up across the critical line at $-\eta^2/2 = -0.20$. A satellite due to the excitation of a surface plasmon, whose energy is assumed to be 0.0, appears when $\varepsilon_a - U_a > -\eta^2/2$. We are studying the case where the radiative life-time is comparable or shorter than the electronic relaxation time of the excited state.

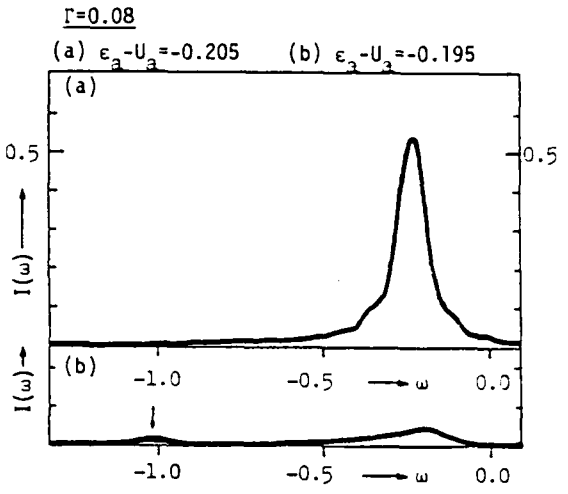

Fig. The calculated luminescence line shape with $\eta^2 = 0.4$ and parameter values indicated in the figure. The intensities are given in an arbitrary unit.

1) K. Shinjo, S. Sugano and T. Sasada, Phys. Rev. B 28, 5570 (1983).

2) K. Shinjo and S. Sugano, to be published.

3) J. A. Cunningham, D. K. Greenlaw and C. P. Flynn, Phys. Rev. B 22, 717 (1980).

Quantum statistical theory of Laser/surface-catalyzed migration

Jui-teng Lin

U.S. Naval Research Laboratory, code 6540, Washington, DC 20375 USA

The possibility of laser-controlled heterogeneous catalysis is theoretically investigated in terms of the laser/phonon-enhanced migration of species adsorbed on a catalytic surface. The migration rate, influenced by both the thermal phonon energy and the coherent laser excitation, is studied by a quantum statistical theory.

The dynamics of laser/surface-stimulated migration, or lattice-site hopping, of an adspecies is governed by a microscopic Hamiltonian:

$$H(t) = H_A + H_B + H_C + H_C' + H_M + H_{AF}(t) ,$$

where H_A, H_B and H_C are the unperturbed Hamiltonians of the active (A) mode, bath (B) modes and the unperturbed site-energy of the adspecies, respectively; H_C' describes the perturbed site-energy caused by the excitations of the A and B modes; H_M represents the lattice-site hopping (migration) Hamiltonian associated with both the coherent laser excitation and the incoherent thermal fluctuation of the substrate; and $H_{AF}(t)$ is the time-dependent interaction Hamiltonian between the active mode and laser field.

The above described Hamiltonian is transformed to a phonon-dressed new Hamiltonian by a canonical transformation. By employing the steepest descent method,[1] the migration rate of the adspecies subjected to IR radiation is calculated for the strongly chemisorbed case without utilizing a perturbation method. It is shown that a novel non-Arrhenius form of the migration rate arises from the anharmonic mode-mode coupling among the phonon modes. It is characterized by various system parameters such as the energy barrier of surface migration, bond strength of the adspecies, the initial and transient final temperature of

the substrate, the frequency spectrum of the system (based on the "energy-gap-law"), and laser intensity and fluence for different laser pulse shapes.[2-4]

Using the above calculated migration rate, the root-mean-square migration distance, which plays an essential role in diffusion-limited surface rate processes, is evaluated by a master equation. It is also shown that, by a two-dimensional master equation defined both in the lattice-site and the photon energy space, the adspecies may migrate in a preferential direction which has a small energy barrier for migration. Furthermore, by absorbing photon energy, the adspecies may change its states from a strongly chemisorbed state to a highly mobile physisorbed state.

Applications of laser-induced surface phenomena including adsorption desorption, migration/diffusion, decomposition and recombination in the areas of heterogeneous catalysis and microelectronic processing will be discussed based on the present theory .

1. T. Hostein, Ann. Phys. (N.Y.) 8, 343 (1959).
2. J. Lin and T. F. George, Chem. Phys. Lett. 66, 5 (1979); J. Phys. Chem. 84, 2957 (1980); J. Chem. Phys. 72, 2554 (1980); 78, 5197 (1983).
3. J. Lin, Technical Digest, CLEO'83(May 17-20, Baltimore, MD), paper ThD2.
4. J. Lin and T. F. George, Phys. Rev. B 28, 76 (1983).
5. J. Lin, M. Hutchinson and T. F. George, in Advances in Multi-Photon Processes and Spectroscopy, ed. by S. H. Lin (World Scientific Pub. Co., Singapore, 1984), in press.

Differential Equations for Delayed Fluorescence-Kinetics in Living Plants

H. Krause, G. Kretsch, and V. Gerhardt

Institut Physik II - Festkörperphysik, Universitat Regensburg

8400 Regensburg, Universitätsstr. 31, West Germany

The decay of the long-living delayed fluorescence (DF) of plants seems to have a complicated kinetic (1). The decay-curves of chlorella algae as a function of temperature are given in Fig. 1. The kinetic also depends on the excitation-wavelength.

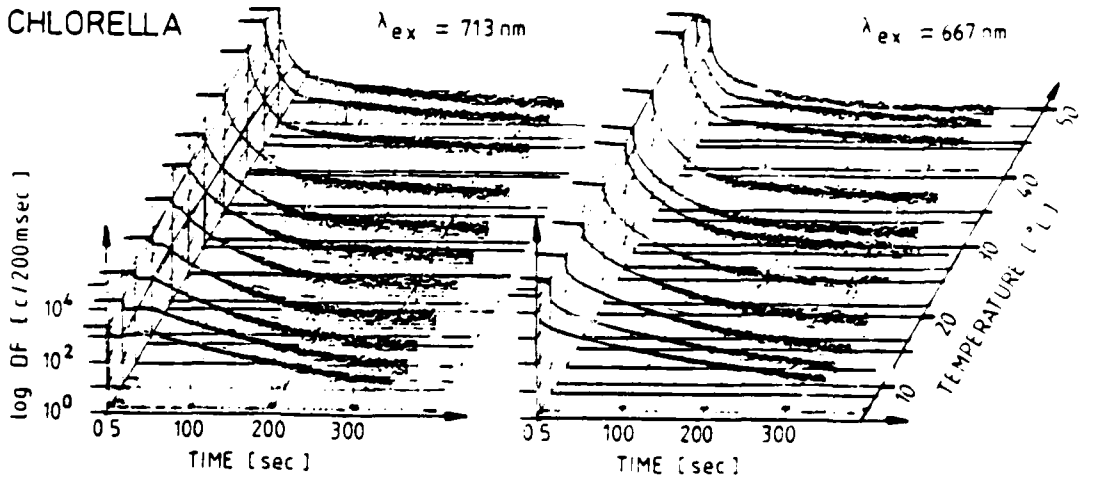

We have tried to describe the behavior of DF by a system of differential equations which take into account that DF is produced by the $S_1 \rightarrow S_0$-transition at the reaction-center of Photosystem II. DF occurs after P_{680}^+ has accepted an electron from the charged pools of the electron-transport-chain. The main characteristic of the model is - according to the Z-scheme - that the electron-pools of Photosystem I and II are coupled in series via the plastoquinon-pool.

We get the solutions of the system of differential equations by numerical integration. The pathway of electrons within the Z-scheme can be derived by varying the differential equations and comparing their solutions to the experimental DF-curves.

The most simple solution-curve for the DF-decay runs as follows:

$$I_{DF}(t) = I_{PSII} \cdot e^{-t/\tau_1} + I_{PSI} \cdot [1 - e^{-t/\tau_2}] \cdot e^{-t/\tau_3}$$

Using this equation the experimental decay-curves can well be fitted up to 30 seconds. The model can be verified, if Photosystem I and II are decoupled by using the electron-blocker DCMU.

(1) BERTSCH, W.F. and AZZI, J.R.: BBA 490, 15 (1965)

BJORN, L.O.: Physiol. Plant. 25, 316 (1971)

Application of Delayed Fluorescence of Phytoplankton in Limnology and Oceanography

H. Krause and V. Gerhardt

Institut Physik II - Festkorperphysik, Universitat Regensburg

8400 Regensburg, Universitatsstrasse 31, West Germany

The phytoplankton synthesizes higher organic substances from anorganic matter and sunlight and normally drives the limnic and maritim ecosystems. The scientists use classical methodes (Draw Water, Cell-counting, Extraction of Chl a, ^{14}C-Method, O_2 Productionrate) to monitor the concentration, the population and the primary production, and recently more physical methodes become usual.

We use the delayed fluorescence (DF) (emission at 685 nm) to measure three different parameters of biomass (1):

A) Chl a Concentration, B) Population Analysis, C) Primary Production.

The DF has some advantages compared to the normal fluorecence:

- DF is emitted only by living cells.
- Products of decomposition of the phytoplankton (Chlorophylls, phaeopigments) do not influence the measurements.
- There is no influence by other optical excited substances with fast emitting components, e.g. yellow substances, because DF is measured with delaytimes > 100 ms.
- Light scattering by suspended matter is unimportant, because we use the full solid angle for collecting the emission and the location of excitation and emission are separated.
- Self-absorption of DF by Chlorophyll is observed only at concentrations greater than 300 mg Chl a / m^3.

A) Measurement of concentration of Chl a with DF (2) :

The signal is proportional to the concentration of Chl a over 4 1/2 decades and the lowest detectable concentration is 0.01 mg Chl a / m^3.

B) Analysis of population of phytoplankton: The variation of pigments within one colour-class of algae is small, but very drastic between different classes. We record excitation spectra with DF at 685 nm (delaytime .5sec, sampling time 1.5 sec) from different classes of algae. The spectra of a mixed sample is a superposition of the spectra of clean samples. Fig. 1 gives the result of the deconvolution. With this method it should be possible to monitor the population-dynamik of phytoplankton.

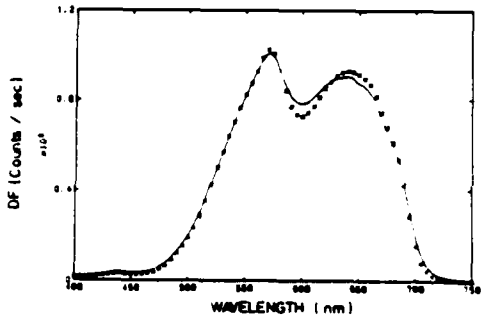

Fig.1) Excitation spectra

Algae	green	red	diat.	blue
- measured	0%	69%	31%	0%
* calculated	0.4%	49%	38%	3%

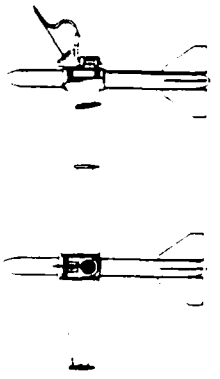

Fig.2) DF-sensor head length 0.9 m, span 0.85 m towing velocity 15 km/h

C) Primary production of phytoplankton: Fig. 2 shows the submarin sensor head, which measures the DF from daylight excited phytoplankton.The DF gives a snapshot of the condition of the electron-transport-chain and therefore of the rate of photosynthesis. The correlation between DF and ^{14}C - fixation measurement is linear.

(1) Krause H. 1980, German Patent Nr. P 30 27 317

(2) Krause H.et.al.1982,Arch.Hydrobiol.Beih.Ergebn.Limnol.16,pp47-54

Interactions and Energy transfer in Chlorophyll a aggregates studied by picosecond fluorescence spectroscopy

W.W.A. Keller, B.A. Albers, E. Strauss, K. Maier-Schwartz
Department of Physics, University of Oldenburg, P.O.Box 2503
D-2900 Oldenburg, FR Germany

Chlorophyll a (Chl a) in pure non-polar solvents (e.g. dodecane) interacts via its polar groups and forms dimers[1]. These aggregates are considered model systems for the study of the primary processes in the photosystem II (P 680)[1]. Minute nucleophilic traces change the kinetic balance towards solvated monomers. The dimer absorption consists of two redshifted peaks, that of the (nucleophilic) acceptor molecule at 663 nm and that of the donor molecule at 678 nm. This indicates, that the π electron systems of the two molecules are not coupled.

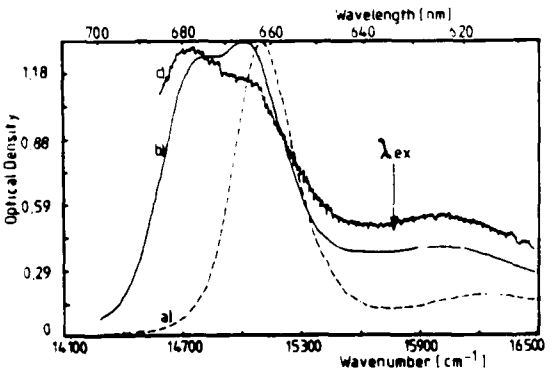

Fig. 1:

Absorption of Chl a in pure dodecane
a) monomer
b) dimer
c) Excitation of 685 nm fluorescence

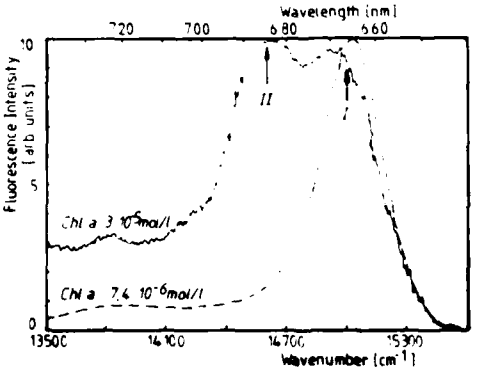

Fig. 2:

Fluorescence of Chl a monomers (dashed), intensity x 10, and of dimers (full line) excited at 633 nm

The monomer fluorescence has been long known[1] (fig. 2). The dimer was considered to be nonfluorescent[2]. Evidence for dimer fluorescence when pumping the Soret band was claimed recently[3]. We observed pronounced dimer fluorescence in carefully prepared solutions, even in highly deluted samples (fig. 2). The identification is supported by excitation spectra (fig. 1) and by the concentration dependence. The fluorescence quantum yield is about 40 times lower than that of the monomer. The peak of the dimer fluorescence is at 685 nm, the maximum at 664 nm is due to the superimposed fluorescence of trace monomers.

Time resolved fluorescence spectra were obtained using a Nd:YAG synch-pumped dye laser. At ambient temperatures the monomer fluorescence and a second, shorter component are observed (fig. 3). Its time constant varies between 650 ps and 950 ps depending on the fluorescence wavelength. The fast component constitutes a time resolved spectrum identical to the dimer fluorescence. However, an additional contribution of the slow component is observed in the region of the dimer fluorescence near 685 nm. This is attributed to monomer to dimer energy transfer. Different models will be discussed for the monomer to dimer energy transfer and for the transfer within the dimer.

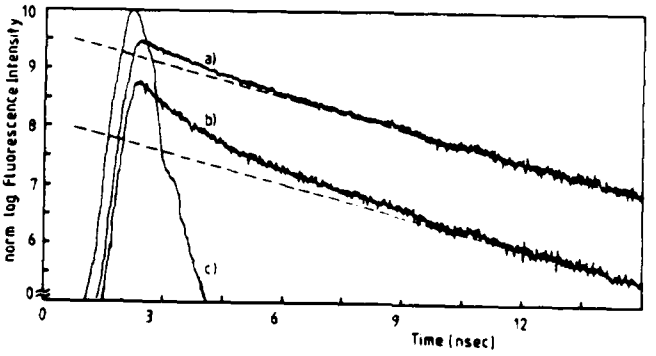

Fig. 3: Fluorescence decay a) 666nm, b) 685 nm
c) Excitation Pulse

1) Livingston, R. et al.; J. Am. Chem. Soc. (1949) 1542-50
2) Katz, J.J. et al.; in Alfano, R.R.: Biological Events... Academic Press, 1982, N.Y., Chapter 5
3) Wilton, A.C. et al.; Journ. Phys. Chem. (1983),87(2), 185-8

Delayed Fluorescence of Algae

V. Gerhardt and H. Krause

Institut Physik II - Festkörperphysik, Universität Regensburg

8400 Regensburg, Universitätsstr. 31, West Germany

The absorption of photons by the antenna pigment-molecules of plants is the first step of the photosynthesis. This absorption leads to the excitation of the two reaction-centers P_{700} and P_{680} of Photosystem I and II and, furthermore, to a charge-separation at both reaction-centers. By means of this charge-separation the energy of photons is transfered to electrons which have a high chemical potential within the electron-transport-chain. The charge-separation process is very efficient: Only about 1 % of the excited reaction-centers re-emit the absorbed photon-energy by prompt fluorescence (allowed $S_1 \rightarrow S_0$-transition). The main part of the excitation-energy feeds the photosynthesis by pumping electrons from water-molecules to NADP-molecules. If the flow of electrons is suppressed all at once by switching off the photon-flux to the antenna pigments, the system will tend to an equilibrium: At physiological temperatures the trapped electrons with high chemical potential within the electron-transport-chain have a probability to go back to the primary acceptor Q of Photosystem II (see Fig. 1). If P_{680} is oxidized, a delayed fluorescence (DF) $S_1 \rightarrow S_0$ at 685 nm will occur by elctron-hole

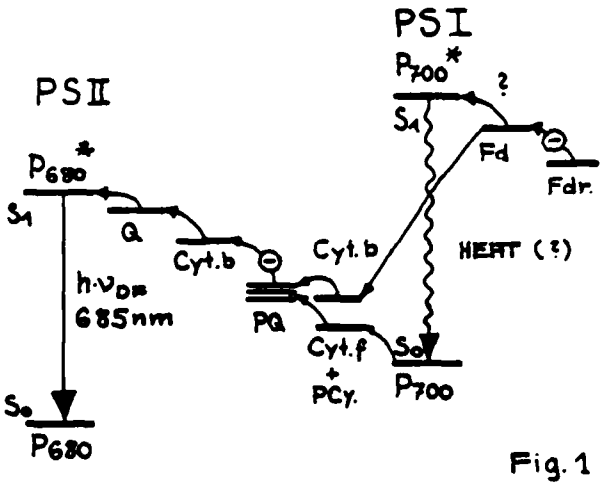

Fig. 1

recombination at P_{680}.

The decay-kinetic of this DF is temperature-dependent. The different decay-times directly can be correlated to the position of the electron-storage molecules within the Z-scheme. Those electrons which are trapped near Photosystem I, e.g. at the plastocyanin- (PCy) or the ferredoxin- (Fd) molecule, contribute to the intensity of the DF after longer times (1).

Therefore, we can get for living plants the following information by time-resolved measurements of the DF:

1. The spectra of the antenna pigments of Photosystem I and II can be separated by taking time-resolved excitation-spectra.
2. The intensity of the Chlorophyll a-band directly gives the concentration of active Chlorophyll a which is important for limnology and oceanography.
3. The intensity of the DF under natural excitation-conditions is a measure for the primary-production.

The decay-kinetic of the DF will change drastically, if the electron-transport-chain is disturbed, e.g. by electron-blockers. Already concentrations of 1 nmol DCMU effects the kinetic which points to the possible importance of this method investigating influences of environmental poisons on photosynthesis.

(1) GERHARDT, V., KRAUSE, H., RABA, G., and GEBHARDT, W.: J. Lumin. 23/24, 799 (1981)

SITE-SELECTION SPECTROSCOPY OF PHEOPHORBIDE-POLYPEPTIDE MODEL PHOTOSYNTHETIC SYSTEM

J.Hála, M. Ambrož, I. Pelant, P. Pančoška, K. Bláha* and K. Vacek

Department of Chemical Physics, Faculty of Mathematics and Physics, Charles University, Ke Karlovu 3, 121 16 Prague 2, Czechoslovakia

*Institute of Organic Chemistry and Biochemistry, Czechoslovak Academy of Sciences, 166 10 Prague 6, Czechoslovakia

Site-selection spectroscopy has been found as a powerful technique for studying large organic molecules (e.g. porphyrins) as well as more complex systems (e.g. chlorophyll in membranes). In the last decade an extraordinary attention has been dedicated to spectral investigations of photosynthetic systems. In vivo photosynthetic systems are very large and complex objects containing chlorophylls, proteins, membranes,... in some since now not completely known functional and structural organization. Therefore it seems to be very fruitful to start a study on some well defined model photosynthetic systems (e.g. chlorophyll-like molecule bonded to a synthetic sequential polypeptide).

The aim of this paper is in a spectral characterization of both the isolated pheophorbide a molecules and the model photosynthetic system pheophorbide a covalently bonded to the synthetic poly(L-Lys-L-Ala-L-Ala) peptide at the same conditions (concentration = 2 μM, solvent dimethylformamide, temperature = 10 K). A pulsed dye laser excitation tuned in the region from 600 to 650 nm provides a set of fluorescence spectra with well resolved vibrational structure on a broad band background from 650 to 690 nm. The wavenumbers of particular vibrational lines change as the dye laser is tuned, however the energy differences between laser excitation lines and fluorescence ones remain constant within an experimental accuracy. Also a very similar displacement of fluorescence excitation vibrational lines and relevant fluorescence lines has been observed. The vibrational analysis has been performed for spectra of both isolated and bonded pheophorbide. The obtained frequencies of normal vibrations in the first excited singlet state have been compared to characterize the interaction of pheophorbide and polypeptide.

A New Luminous State of Bacteriorhodopsin

Masamitsu HIRAI, Yoshiro SUZUKI and Tomonori NAKAYAMA

Department of Applied Physics
Faculty of Engineering
Tohoku University, Sendai 980,
Japan

In spite of change of the luminescence spectra during the illumination of light for the spectral measurement of the bacteriorhodopsin, most reports failed to notice this change. We have made the change clear and propose a new model for the luminescence species. Trans-bacteriorhodopsin is refered as T-bR.

Curve 1 in Fig.1 shows the emission spectrum of T-bR at 36 K immediately after the illumination by lights at 530nm (band width of ~60nm) absorbed by T-bR. During observation of the spectrum, equilibrium between T-bR and Batho-bR (B-bR) has finished. B-bR is not luminous.[1] The intensity of the luminescence at 780nm increased during further prolonged illumination as shown in Fig.2, and reached a constant intensity. The emission spectrum at a time indicated by the arrow 2 is shown by curve 2 in Fig.1. Most references[2] report only this state of luminescence. Curve 2 is clearly different from curve 1', which is obtained from curve 1 by normalizing its peak height to that of curve 2. Curve 2-1 presents the difference between curves 2 and 1. This spectrum presents a newly developed part, and differes again from curve 1.

Intensity increase I(t) shown in Fig.2 can be decomposed into four components as follows,

$$I(t) = I_{const} + I_1 \left(1 - e^{-\frac{t}{\tau_1}}\right) + I_2 \left(1 - e^{-\frac{t}{\tau_2}}\right) + I_3 \left(1 - e^{-\frac{t}{\tau_3}}\right). \quad (1)$$

I_{const} is a component corresponding to curve 1 in Fig.1. The rest three components stand for newly growing species corresponding to the part of curve 2-1 in Fig.1. New species are named as fluorescent-bR (F-bR), hereinafter. Growth time-constants, τ_1, τ_2 and τ_3 become shorter at high temperature.

Results suggest formation of three kinds of the trimer consisting of T-bR, F-bR and B-bR as shown in Fig.3. During observ-

ation of curve 1 in Fig.1, the 1st conversions are finished within less than 1 min. T-bR in TTT, TTB and TBB are responsible for curve 1. During the prolonged illumination, the 2nd conversions proceed. F-bR in TFF, TFB and FBB are responsible for curve 2-1 in Fig.1. The reverse conversion of these processes are also observed. Possible conversion kinetics will be discussed with quantitative data such as activation energy for conversions.

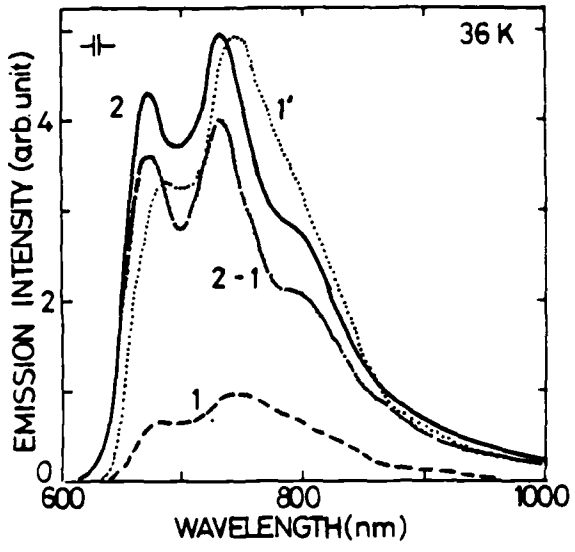

Fig. 1

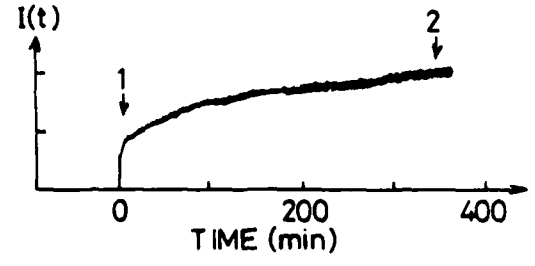

Fig. 2

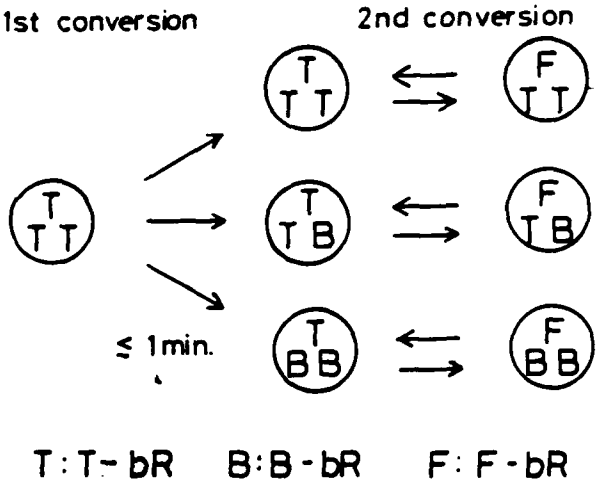

Fig. 3

References
1) R. Govindjee, B. Becker and T.G. Ebrey : Biophys. J. 22 (1978) 67.
2) A. Lewis, J.P. Spoonhower and G.J. Perreault : Nature 260 (1976) 675.

Fluorescence Depolarization of Fluorescein in Living Lymphocytes

Shuichi Kinoshita, Tatsuya Fukami, Akiya Saito,
Kuniko Hirata, and Takashi Kushida
Department of Physics, Osaka University,
Toyanaka, Osaka 560, Japan

Yoshihiro Kinoshita and Shuhei Kimura
Department of Physiology, Osaka City University,
Osaka 545, Japan

The degree of polarization of fluorescence from fluorescein, introduced into living lymphocytes, changes according to physiological conditions of the cells and also with antigenic stimulations on lymphocytes. This property can be used for a sensitive detection of malignant diseases. However, the physical mechanism of this fluorescence depolarization is not yet known.

To clarify this, we have measured time dependence of the fluorescence depolarization of fluorescein in rat thymus lymphocytes, using a time-correlated single-photon counting technique. The degree of polarization has been found to decrease very quickly first with a time constant of $\sim$ 360 ps, and to remain nearly constant after then. This time behavior is interpreted in terms that at least two types of dye molecules are present inside the lymphocytes, i.e., one having larger degree of polarization (bound) and the other having smaller one (free).

We have determined the emission spectrum of only the bound dye molecules, from the difference of time-resolved spectra of fluorescence with two polarization directions at a sufficiently late time after the excitation, when the polarization memories of the free dye molecules in a cytoplasmic solution are lost. The obtained spectrum is very similar but about 7 nm red-shifted, compared with that of fluorescein in a solution. We have further found that close correlations are present among the degrees of polarization, the fluorescence intensities, and the intensity ratios of fluorescence under the excitation of two different wavelengths or with two different emission-wavelengths. If we assume that there exist only two types of dye molecules, free and bound ones, inside the lymphocytes, these correlations can be readily verified theoretically. From these correlations, it is possible to determine the degree of polarization and the fluorescence excitation and emission spectra of only the bound dye molecules. The emission spectra of the bound dye molecules, obtained in this way, are in very good agreement with those obtained from the time-resolved spectra.

The above results clearly indicate that the spectroscopic properties of fluorescein inside the lymphocytes are expressed as a simple superposition of two types of dye molecules. Therefore, the degree of polarization is concluded to be determined mainly by three factors, i.e., their molar ratio, the ratio of their emission efficiencies, and the degree of polarization especially of bound molecules. The biological implication of the change of these factors will also be discussed.

Site Selective High Resolution Laser Spectroscopy of Europium in Calcium Binding Proteins

Mark A. Valentini and John C. Wright
University of Wisconsin
Department of Chemistry
1101 University Avenue
Madison, WI 53706

Lanthanide ions are generally known to possess narrow $4f^n$ to $4f^n$ transitions in both excitation and fluorescence that are sensitive to the coordination environment surrounding the ion. Selective excitation with a narrowband laser can spectrally discriminate one lanthanide ion environment from another based upon differences in the crystal fields associated with the unique lanthanide ion sites. This paper describes site selective laser spectroscopic experiments where europium ions have been coordinated to proteins in sites normally occuppied by calcium ions.

The position of the $^7F_0 \longleftrightarrow {}^5D_0$ transition, as well as other europium transitions, are shown to provide the spectral purity necessary for substantial spectral deconvolution of the excitation and fluorescence spectra associated with unique europium sites in the proteins thermolysin and calmodulin. Spectral studies of europium doped proteins at low temperatures are shown to provide useful information about individual rare earth ion sites for both thermolysin and calmodulin.

Fluorescence line narrowing in europium doped thermolysin is observed to a limited extent at low temperatures. Increasing the resolution between europium ion sites in thermolysin by fluorescence line narrowing methods is observed to be limited by severe accidental degeneracies (1).

Europium titrations of calmodulin in solution at room temperature were obtained to identify the ordering in the filling of calmodulin calcium ion sites. Increasing the acidity of the titrated calmodulin solution is shown to prevent europium from filling two calmodulin calcium ion sites thus preventing europium induced precipitation of the concentrated calmodulin solution. The

europium induced precipitation of concentrated calmodulin solutions in the physiologic pH range is shown to be stoichiometric and relevant to questions regarding the mode of action of calmodulin in vivo. Liquid phase titrations of calmodulin with europium indicate two metal ion sites are filling simultaneously. One or both of the first calmodulin sites filled by europium is shown to be a tyrosine containing site.

1. M.A. Valentini and J.C. Wright, Chem. Phys. Letts., 100 (2), 133, 1983.

Food Oxidation as Measured by Chemiluminescence

Jürg Löliger, Françoise Saucy, Nestlé Research Department
P.O.Box 88, 1814 La Tour-de-Peilz
Switzerland

The deterioration of dietary lipids by oxidation reactions is an important topic of food science and nutrition. A large number of scientific approaches have been chosen to deal with this problem. The analytical assessment of the state of oxidation of foods is an important aspect for better understanding lipid autoxidation.

It is not yet generally recognized that all organic materials react with oxygen at ambiant temperature already and that this oxidation is normally accompagnied by light emission phenomena (Mendenhall, 1977). It has been shown that hydrocarbons (Vassil'ev, 1967) and lipids (Goldenberg et al., 1978) while being oxidized emit light. This chemiluminescence could be attributed to different possible steps of the radical chain lipid autoxidation: chain braking reactions forming *electronically excited aldehydes*, decomposition of peroxide adducts leading to singulet oxygen and reactions which involve the superoxide ion.

Ultraweak chemiluminescence has been used by many authors for the investigation of oxidation reactions of foods containing polyunsaturated lipids (Usuki et al., Timms and Roupas). These reports show a good correlation between photon emission rates and several autoxidation related parameters like hydroperoxydes, anisidin values, conjugated unsaturated fatty acid concentration and an organoleptic evaluation for rather highly oxidized foods or fats.

We were measuring ultraweak chemiluminescence in homogenized meats, precooked infant cereals, spray dried milks, dried potato flakes and many other foods, all containing various amounts of fat (0.1% potato flakes and up to 26% for full milk powder).

Most of the analytical results correlated reasonably well with the standard methods for the evaluation of the state of oxidation and with taste testing results.

These foods show very different levels of chemiluminescence according to their lipid composition and according to the lipid distribution in the animal/vegetable tissues.

***

REFERENCES :

V.I. Goldenberg, N.I, Yurchenko, V.G. Shulovich, Khim. Farm. Zh., 12, 135 (1978).

G.P. Mendenhall, Angens. Chem.,89, 220 (1977)

R.E. Timms, P. Roupas, Lebensm.- Wiss. u. - Technol., 15, 372 (1982)

R. Usuki, T. Kaneda, A. Yamagishi, C. Takyu, H. Inaba, J. Food Sci., 44, 1573 (1979)

R.F. Vassil'ev, Prog. React. Kinet., 4, 305 (1967)

Extra-Weak Spontaneous Chemiluminescence of Human Blood Detected by Ultra-High Sensitive Photon Counting System Developed for Biomedical Applications

H. Inaba, C. Takyu, B. Yoda*, and Y. Goto*

Research Institute of Electrical Communication, Tohoku University

Katahira 2-1-1, Sendai 980, Japan

*The Third Department of Internal Medicine, Tohoku University School of Medicine, Seiryo-cho 1-1, Sendai 980, Japan

With the development of optical electronics and a variety of its applications, the challenge of measuring ultraweak intensities of light from various types of faint source which releases merely a small number of photons is of considerable interest and attractive. With this aim, the photon counting technique has been developed and is now customarily utilized to detect very weak light intensities less than about 10^{-12}W in the visible and near infrared regions in conjunction with the high-sensitive photomultiplier. As a fascinating and interesting application of this technique to photobiology and photochemistry, we have detected extremely weak bioluminescence[1] and chemiluminescence[2,3] from various biological and chemical systems, such as living tissues like tumors and organs, and enzymatic reactions, and also analyzed their exceedingly weak spectra using a specially designed spectral analyzer system[4].

As a further extension, extra-weak spontaneous chemiluminescence, generated without any external excitation, from human blood was detected for the first time with the ultra-high sensitive photon counting system that was developed recently using a selected photomultiplier operated under optimum conditions[5]. In this paper, we describe and discuss the measured results which revealed the significant difference of the intensity between cigarette smokers and non-smokers as well as healthy and diseased people.

Figure 1 shows the comparison of average intensities of ultraweak chemiluminescence from plasma samples taken from non-smokers (26 males; average age 46.3 years) and smokers (47 males; average age 47.5 years), both seemed quite healthy on clinical examinations. Whole-blood 2-ml samples from non-smokers exhibited a low count rate of single photoelectrons, 470 counts/300 sec on an average, which is of the order of 10^{-18} W. A plasma sample usually gives a higher count level than a whole-blood sample. It is quite evident that the non-smokers have approximately half of the intensity of the smokers. In Fig. 2, the relation between measured extra-weak light intensity from plasma samples of male smokers and the product of the number of smoked cigarette in a day with their smoking duration in years is depicted. This product is considered to be a factor indicating some influences of smoking on living body in long terms. In fact, the positive correlation betweem them was found with the statistical meaning.

Also it is to be noted that the ultraweak chemiluminescence intensity of the blood of healthy subjects is 3 to 4 times lower than that of subjects having liver diseases and diabetes mellitus on an average.

Although the clinical and biological significance of these novel findings need to be investigated fully, they are likely related to the presence of chemically active oxygens and free radicals in the blood.

References

1. Y. Shimizu, H. Inaba, K. Kumaki, K. Mizuno, S. Hata, and S. Tomioka, IEEE Trans. Instrum. Meas. IM-22, 153 (1973).
2. M. Nakano, K. Takayama, Y. Shimizu, Y. Tsuji, H. Inaba, and T. Migita, J. Amer. Chem. Soc. 98, 1974 (1976).
3. T. Yoshimoto, S. Yamamoto, K. Sugioka, M. Nakano, C. Takyu, A. Yamagishi, and H. Inaba, J. Biolog. Chem. 255, 10199 (1980).
4. H. Inaba, Y. Shimizu, Y. Tsuji, and A. Yamagishi, Photochem. Photobiol. 30, 169 (1979).
5. H. Inaba, A. Yamagishi, C. Takyu, B. Yoda, Y. Goto, T. Miyazawa, T. Kaneda, and A. Saeki, Opt. Lasers Eng. 3, 125 (1982).

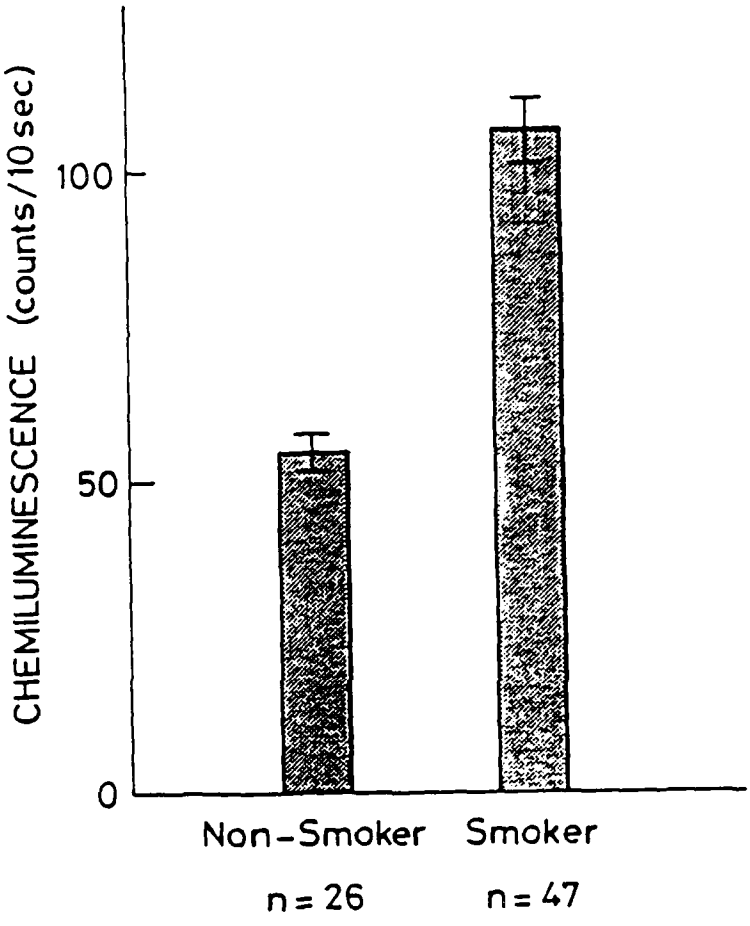

Fig. 1 Measured result of average intensities of ultraweak chemiluminescence from blood plasma samples taken from cigarette smokers and non-smokers (n is the number of samples)

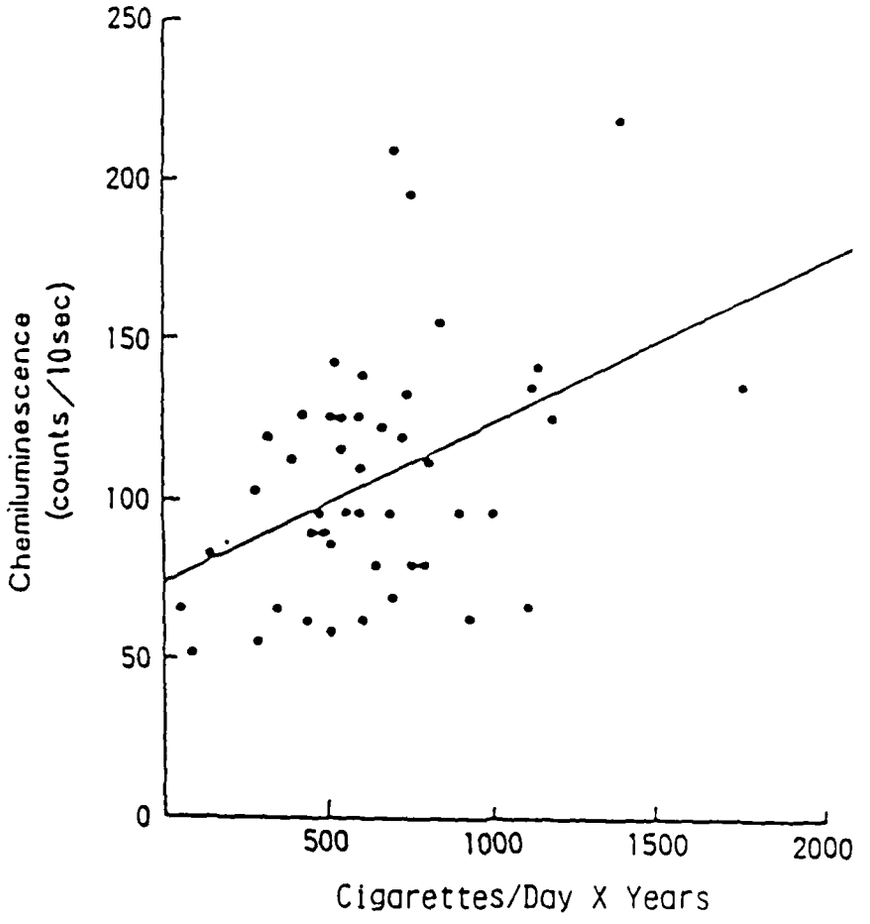

Fig. 2 Measured relation between ultraweak chemiluminescence intensity from blood plasma samples of male smokers and product of number of smoked cigarette in a day with their smoking duration in years (cigarettes/day x years)

VIBRATIONAL EXCITATION DYNAMICS OF SMALL MOLECULAR IMPURITIES IN CRYSTALS.

H. DUBOST

Laboratoire de Photophysique Moléculaire CNRS
Bâtiment 213 - Université de Paris-Sud
91405 - ORSAY CEDEX France.

In this paper time resolved infrared spectroscopy of small impurities in crystals is presented. Optical pumping into the fundamental or overtone absorption results in vibrational emission of several molecular species in solid hosts, Van der Waals-type or ionic crystals. Vibrational relaxation in solids is also probed by infrared double resonance which is a more appropriate technique for short lived systems. Line narrowing techniques involving site selection by a narrow band laser are employed in both molecular and ionic systems. IR time resolved hole burning experiments very similar to those performed in optical spectroscopy of luminescent ions in insulators have become feasible. Coherent transient spectroscopy is also very promising.

A few examples of energy transfer and relaxation phenomena taking place in these systems are described. For instance, localisation and accumulation of vibrational excitation on isotopic traps resulting from phonon assisted processes is a spectacular phenomenon which has no equivalent in other areas of energy transfer. Spectral transfer also behaves quite differently in Van der Waals crystals compared to ionic crystals. Homogeneous broadening of vibrational transitions in the guest molecules results from their orientational motion. The possible mechanisms leading to vibrational relaxation, dephasing, interline and intraline energy transfer are discussed. Emphasis is placed on the important role played by the localized phonons in the dynamics of vibrational excitation in diluted solids.

LUMINESCENCE OF TETRAVALENT URANIUM IN THE INCOMMENSURATE PHASE OF $ThBr_4$ AND $ThCl_4$

M. Genet, P. Delamoye, J.C. Krupa, C. Khan Malek
Laboratoire de Radiochimie, Institut de Physique Nucléaire
B.P. N° 1, 91406 Orsay Cedex (France)

The incommensurate phase of $ThBr_4$ [1] and $ThCl_4$ have been found recently. The complete study of the crystal structure by neutron diffraction leads to the following results :

- $ThBr_4$ shows a phase transition at 95 K and, down to 4 K, the observed phase is incommensurate all over this temperature range (without any lock-in). A similar behaviour is exhibited by $ThCl_4$ with a temperature transition at 70 K.

- The new structure could be represented by a modulation of the atom positions whose wave vector is directed along c axis with : $q_s = \frac{2\pi}{\lambda} = \frac{2\pi}{c} \cdot \frac{1}{3}(1-\delta) = 0.310\ c^* \pm 0.05$.

- The dynamics shows that the Th^{4+} positions are not affected by the modulation, while Br^- positions are modified leading to two types of symmetry of the tetravalent ion site : D_{2d} and D_2. The most important consequence being that the D_2 symmetry affects continuously all the M^{4+} ion sites while D_{2d} must be considered as a unic symmetry case.

There are two main spectroscopical consequences upon U^{4+} when this ion is placed in a such structure. First, the lineshape observed in some absorption and in some emission as well, are very unusual. Instead of the classical shape corresponding to a mixture of a gaussian and a lorentzian character, some peaks exhibit a continuous absorption domain (or emission) limited by two edge singularities. The widths of the peak depend on the polarization, but are broader than what we observed for the other lines of the spectrum. Some σ line spread over 70 cm^{-1} and present sometimes a third peak between the two singularities while the π line lies only over 15 cm^{-1}. In all cases, the intensity of the singularities are higher than those of the continuum.

The complete interpretation of the lineshape and the intensity of the peak in connection with the modulated structure have been given by

Delamoye [2].

Secondly, it has been proved by selective excitation into these "special" absorption peaks that the emission took place over a single line whose width is related to those of the dye laser line used, and, as we scan into the absorption peak, the corresponding emission line is varying in energy over two limits which are directly connected to the site symmetry of the excited ion.

Finally we measured the lifetime for each kind of site symmetry (the D_2 continuum and the D_{2d} single case). The experimental values at 4 K for $ThBr_4 : U^{4+}$ [3] and $ThCl_4 : U^{4+}$ are reported on the figure 1.

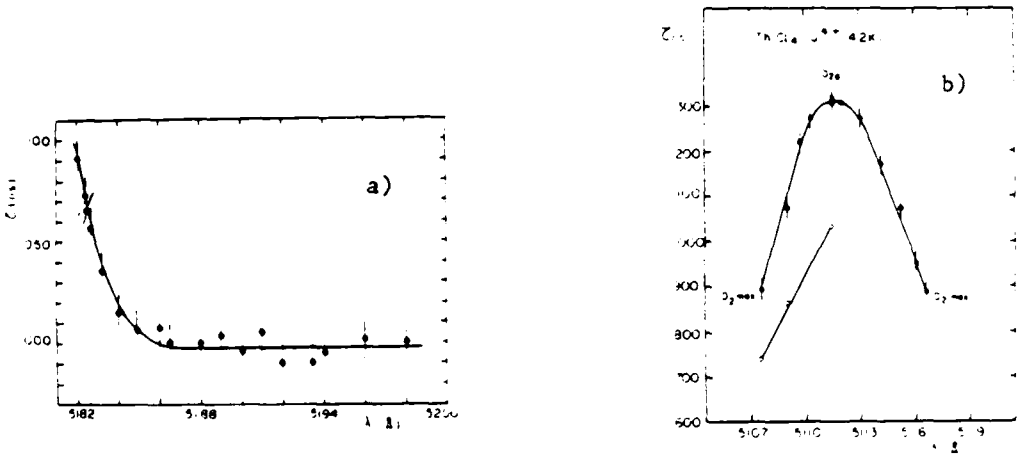

Fig. 1 - Lifetime values versus wavelength emission : a) for $ThBr_4 : U^{4+}$; b) for $ThCl_4 : U^{4+}$.

The interpretation of the lifetime "modulation" is not yet found.

References

[1] L. Bernard, R. Currat, P. Delamoye, C.M.E. Zeyen, S. Hubert, R. de Kouchkovsky, J. Phys. C ; Solid State Phys. 16 (1983) 433.

[2] P. Delamoye, R. Currat, J. Phys. Lettres 43 (1982) L-655.

[3] M. Genet, P. Delamoye, R. Guillaumont, C. R. Ac. Sc. Paris (to be published).

ME3 Two-Color Superfluorescence of O_2^- Centers in KCl, R. Florian, L. O. Schwan, and D. Schmid, Universität Düsseldorf, FRG. See MB38 for summary.

ME4 Lasing from a Vibrational Transition of a Molecular Defect, T. R. Gosnell, R. J. Tkach, and A. J. Sievers, Cornell University. See MB37 for summary.

ME5 Spectral Band Assignments for Cu^+ and Ag^+ in Alkali Halides via Two-Photon Spectroscopy, Donal S. McClure, Princeton University, and Christian Pedrini, Universite de Lyon, France. See WD25 for summary.

Characterization of Optical Techniques of Particles Emitted from Surfaces

N. H. Tolk
Bell Communications Research
Murray Hill, NJ 07974

I will discuss recent measurements of (a) laser-induced fluroescence of neutral atoms electronically desorbed from surfaces, and (b) coherence in excited states of hydrogen formed near surfaces.

Inverse Photoemission in the Ultraviolet

F. J. Himpsel, Th. Fauster, and J. Straub

IBM T. J. Watson Research Center

P. O. Box 218

Yorktown Heights, New York 10598

Inverse photoemission (or bremsstrahlung spectroscopy) is the time-reversed photoemission process. Electronic states are probed via radiative transitions of an incoming electron into unoccupied states. X-ray bremsstrahlung spectroscopy is a well-established technique but its extension to the ultraviolet (with electrons incident at about 4-30 eV energy) has only begun recently. With lower electron energies the surface sensitivity increases such that monolayers can be probed. Also, the momentum of electrons in a solid can be determined by angle-resolved inverse photoemission, i.e., energy band dispersions can be mapped. Unoccupied electronic states play an important role, e.g., in ferromagnetism (minority spin states), in chemisorption (electron acceptor states of adsorbates), and for semiconductors (conduction by electrons). A status report is given and illustrated by examples in band mapping, the identification of adsorbate orbitals and the observation of surface states.

FLUORESCENCE PROBES FOR BIOLOGICAL SYSTEMS: STRUCTURAL AND DYNAMICAL STUDIES OF RED CELL MEMBRANES

Josef Eisinger
AT&T Bell Laboratories
Murray Hill, NJ 07974

Fluorescence probes which are sensitive to their environment, to the proximity of other chromophores and other structural or dynamic parameters have many applications in the investigation of biological systems on the molecular level. Their use in complex biological assemblies has been hampered by artifacts resulting from the absorption and scattering of excitation and emitted light within the sample. We have demonstrated that by measuring fluorescence intensity (I) or anisotropy (r) at a series of concentrations (h), the limiting values of these parameters at vanishing concentration ($h \to 0$) are given by the intercepts of the straight lines obtained by plotting log (I/h) or log r *versus* h. The slope of the line is a function of the absorption and scattering characteristics of the particles (e.g., cells) at the excitation and emission wavelengths and of the configuration of the fluorometer.

Applications of this and similar techniques to biological systems include the use of hemoglobin proximity probes embedded in the outer leaflet of the erythrocyte membrane. By measuring the probes' lifetime (or intensity) in intact cells and in ghosts, one determines the rate of resonance energy transfer to the hemes in the cytoplasm. From this, the location and concentration of hemoglobin in the cytosol boundary layer was determined for normal and pathological cells under various conditions (e.g., oxygenation state). These experiments provide new understanding of the structure of the membrane and its cytoskeleton.

By measuring the relative quantum yields of monomeric and excimeric emission from pyrene containing fatty acids or phospholipids one may determine their lateral mobility in the membranes of intact cells. The lateral diffusion constants (D) are obtained with the aid of a random walk model and may be compared to values of D measured by the fluorescence photobleaching recovery method (FPR). Results obtained with 1-pyrene hexadecanoic acids show that the lateral fluidity of erythrocyte ghosts is 50 percent greater than that of intact cells. When measured by the excimerization method one obtains a considerably smaller value for the activation energy of D ($\sim$3.5 kcal M^{-1}) than by FPR, presumably because the latter method sample diffusion over large distances ($\sim$500 nm) on the cell surface, which include many membrane proteins. On the other hand, the typical diffusion distances for PHD in membranes is of the order of 5 nm which is comparable to inter-membrane spacings.

Total Internal Reflection Fluorescence in Biological Systems

Daniel Axelrod
University of Michigan
Ann Arbor, Michigan

Fluorescence of labeled proteins near a solid/liquid interface can be excited by the evanescent field of total internal reflection to study reversible adsorption kinetics and surface diffusion.

Fractal Structures in Condensed Matter

T. A. Witten

Exxon Research and Engineering Company

Corporate Research-Science Laboratories

Clinton Township - Route 22 East

Annandale, New Jersey 08801

Polymers in solution and colloidal aggregates form complex structures which are statistically invariant under spatial dilation. We survey the special properties of these "fractal" structures.

Energy Transfer and Trapping of Excitons

Joseph Klafter

Exxon Research and Engineering Company

Corporate Research-Science Laboratories

Clinton Township - Route 22 East

Annandale, New Jersey 08801

Direct Electronic Energy Transfer on Fractals

U. Even, K. Rademann and J. Jortner

Department of Chemistry, Tel Aviv University, 69978 Tel Aviv Israel

and

N. Manor and R. Reisfeld

Department of Inorganic and Analytical Chemistry, The Hebrew University, Jerusalem, Israel

The site distribution of a fractal structure was characterized by the interrogation of electronic energy transfer in a porous glass, resulting in the fractal dimension of $\tilde{d} = 1.74 \pm 0.12$ for this irregular structure.

TuA4 and TuA5

TuA4 Continuous-Time Random Walks and Luminescence Decay in Disordered Systems, A. Blumen, Technische Universitat Munchen, FRG, and G. Zumofen, ETH-Zentrum, Switzerland. See TuC2 for summary.

TuA5 Photophysical Studies of SA_2 on Silica and Aluminum Oxide -- A Molecular Probe of Surface Heterogeneity, J. M. Drake, Exxon Research and Engineering Company. See TuC4 for summary.

Physical Processes in High-Field Electroluminescence

J W Allen, Department of Physics, University of St Andrews, North Haugh, St Andrews KY16 9SS, Fife, UK.

High-field electroluminescence offers the promise of large area solid-state displays with a wide range of applications. It also presents a challenge to our understanding, requiring a synthesis of atomic and solid-state physics. Early work was on copper-doped ZnS AC powder panels which were spatially heterogeneous, amenable to precise measurement of only macroscopic properties, and unreliable. Recent devices use thin films of ZnS:Mn which are better defined physically. In addition, Schottky diodes on n-type ZnS:Mn have been used to study particular physical mechanisms.

The processes involved are initial electron production, acceleration, possibly avalanche multiplication, excitation of the luminescent centre and light emission. A simple phenomenlogical model shows that the number of photons emitted in unit time in a unit volume is

$$q^{-1} J \sigma N_L \eta_{rad}$$

where q is the electronic charge, J the current density, σ the excitation cross-section averaged over the hot electron distribution, N_L the concentration of luminescent centres and η_{rad} their radiation quantum efficiency. The light output varies with applied voltage through a combination of field or voltage dependent factors, such as the electron generation rate. These processes, together with the luminescence efficiency, may be dependent on the concentration and nature of other impurities. It is therefore important to isolate each step as far as possible if one is to progress in physical understanding, and in particular if one is to relate experimental data to microscopic theory.

Going back through the mechanisms listed above, we know a grest deal about light emission in ZnS:Mn although unsolved problems arise at high concentrations or high excitation densities. (There are other luminescent centres, such as those involving rare earths, where even the atomic identities are in doubt). Experimental data is available on the distribution-averaged excitation cross-section and its inverse, the Auger recombination coefficient, but our knowledge of the cross-section as a function of the incident electron energy and crystal momentum is rudimentary. The process of acceleration in high fields is well understood in principle although detailed calculations appear not to have been made for ZnS. The mechanism of initial electron production is not understood.

We are still a long way from having enough physical knowledge to be able to design a high-field electroluminescent device as distinct from optimising an empirical device. Advances are being made experimentally as better defined structures are made. Some theoretical problems are far from being solved as they involve, for example, field ionization or impact excitation which require advanced theoretical techniques for solution in the case of isolated atoms. Modification of these techniques to an impurity in a solid in not easy. The challenge to the experimental and theoretical physicist is great: knowledge gained can be of interest in its own right but can also be of use to the device engineer.

Luminescence of Amorphous Si_xC_{1-x}:H and Its Applications

Hiroshi Kukimoto

Imaging Science and Engineering Laboratory, Tokyo Institute of Technology, Nagatsuda, Midori-ku, Yokohama 227, Japan

Hydrogenated amorphous silicon-carbon alloy(a-Si_xC_{1-x}:H) prepared by glow-discharge deposition is a new luminescent material; the spectrum of photoluminescence and its decay time can be changed widely with composition.[1,2] The emission mechanism is discussed based on the observations of the Stokes shift,[2] decay time and polarization memory[3] of luminescence.

One of the applications of this amorphous alloy is the light-emitting devices with fast response time which could be made on suitable Si integrated circuits or large area arrays of a-Si thin film transistors. The ac-driven electroluminescent devices which show white emission at room temperature can be made using wide-gap materials of a-Si_xC_{1-x}:H($x = 0.2$-0.3).[4]

Optical properties of the heterostructure which consists of an ultrathin(<50Å) a-Si:H layer sandwiched between two wider-gap a-$Si_{0.2}C_{0.8}$:H layers show a quantum size effect; The optical absorption spectrum for the a-Si:H well layer shifts toward higher photon energies with decreasing the well width, while the emission spectrum due to the band tail states of a-Si:H remains unchanged.[5] This is the first observation in amorphous materials. In relation to this effect, new applications for light-emitting devices utilizing amorphous multiple quantum wells or superlattice structures are discussed.

1) H. Munekata, S. Murasato, and H. Kukimoto, Appl. Phys. Lett. 37, 536 (1980); Erratum, Appl. Phys. Lett. 38, 188 (1981).

2) H. Munekata, A. Shiozaki, and H. Kukimoto, J. Luminescence 24/25, 43 (1981).

3) Y. Masumoto, H. Kunitomo, S. Shionoya, H. Munekata, and H. Kukimoto, J. Non-Cryst. Solids 59/60, 345 (1983).

4) H. Munekata and H. Kukimoto, Appl. Phys. Lett. 42, 432 (1983).

5) H. Munekata and H. Kukimoto, Jpn. J. Appl. Phys. 22, L544 (1983).

TuB3-1

Fluorescence Technology Biopolymer Binding Studies

J. Michael O'Donnell

Luminescence Technology, Inc.

Suite 605

3221 Camino Capistrano

San Juan Capistrano, California 92675

A review of fluorescence technology in immunochemical procedure will be presented. The extension of this technology into the area of DNA probes will be discussed along with additional future opportunities for research.

TuB4 and TuB5

TuB4 Ambipolar Carrier Drift in Silicon by an Optical Time-of-Flight Method, J. Laurich, A. Forchel, and T.K. Hoai,* Universitat Stuttgart, F.R.G. See TuB10 for summary.

*Permanent address: Academy of Sciences of Vietnam, Vietnam

TuB5 Nonlinearity of the Cathodoluminescence Intensity of [illegible] Phosphors, D. A. de Leeuw, Philips Research Laboratories, The Netherlands, and Systematic Analysis of Phosphor Degradation under Cathode-Ray Excitation, D. B. M. Klaasen and D. A. de Leeuw, Philips Research Laboratories, The Netherlands, and J. Volker, Philips Research Laboratories, F.R.G. See TuB2 and TuB3 for summaries.

Fluorescence Line Narrowing in Dilute Systems with Nearest-Neighbor Transfer

D. L. Huber

Department of Physics, University of Wisconsin, Madison, Wi 53706

Summary

We outline the results of an analysis of fluorescence line narrowing[1] in dilute systems. We assume that a fraction, p, of the sites on a d-dimensional lattice are occupied at random by optically active ions and that the transfer of optical excitation can only take place between ions occupying nearest-neighbor sites. The normalized intensity of the sharp line fluorescence following excitation of an inhomogeneously broadened line by a monochromatic source is equal to $\exp[-\gamma_R t]\langle P(t)\rangle$, where γ_R is the radiative decay rate and $\langle P(t)\rangle$ is the probability that an ion excited at t=0 is also excited at time t.[2]

If W denotes the nearest-neighbor transfer rate, then for $t \ll W^{-1}$ we have

$$\langle P(t)\rangle \gtrsim 1-pzWt \qquad (1)$$

where z is the number of nearest-neighbor sites. The asymptotic behavior of $\langle P(t)\rangle$ depends on the number and size of the clusters of optically active ions [A cluster is defined as a set of ions connected by non-zero transfer rates; transfer can not take place between ions belonging to different clusters]. We calculate $\langle P(\infty)\rangle$ for the square and simple cubic lattices using cluster data given by Flammang.[3] $\langle P(\infty)\rangle$ decreases from the value 1 at p=0+ to 0 at p=1. At the percolation concentration ($p_c \gtrsim 0.59$ for d=2, $p_c \gtrsim 0.31$ for d=3) we obtain $\langle P(\infty)\rangle \gtrsim 0.049$ (d=2) and $\langle P(\infty)\rangle \gtrsim 0.170$ (d=3).

In analyzing the behavior between the short and long-time regimes we focus on the critical percolation concentration. Using scaling arguments[4,5] we find

$$\langle P(t) \rangle \sim t^{z_1 - 1}$$

where $z_1 \gtrsim 0.3$ (d=2) and $z_1 \gtrsim 0.2$ (d=3).

References

1. P. M. Selzer, Laser Spectroscopy of Solids, Topics in Applied Physics, Vol. 49, W. M. Yen and P. M. Selzer, eds. (Springer, Berlin, 1981) Chap. 4.
2. D. L. Huber, D. S. Hamilton, and B. Barnett, Phys. Rev. B 16, 4642 (1977).
3. A. Flammang, Z. Physik B28, 47 (1977).
4. E. F. Shender, Zh. Eksp. Teor. Fiz. 70, 2251 (1976) [Sov. Phys. JETP 43, 1174 (1975)].
5. S. Alexander, C. Laermans, R. Orbach, and H. M. Rosenberg, Phys. Rev. B 28, 4615 (1983).

Continuous-Time Random Walks and the Luminescence Decay in Disordered Systems

A. Blumen
Lehrstuhl für Theoretische Chemie
Technische Universität München
Lichtenbergstr. 4
D-8046 Garching, West Germany

and

G. Zumofen
Laboratorium für Physikalische Chemie
ETH-Zentrum
Universitätsstr. 16
CH-8092 Zürich, Switzerland

Many dynamical problems in solid-state physics and chemistry are related to random-walks on periodic structures. In the last years processes of energy transfer and decay in disordered media have attracted considerable attention. One way to account for the disorder is the continuous-time random walk (CTRW), as used for electron migration in amorphous solids[1]. The standard CTRW involves a spatial regularization, in that the walk takes place on a periodic lattice and the disorder is mirrored in waiting-time distributions $\psi(t)$[2,3]. Another way to mimic the disorder consists in letting the walk take place on fractals, geometrical structures which are not translationally invariant but which display the dilatational symmetry of the percolative cluster[4,5]. For fixed waiting-times this procedure is complementary to the CTRW, in that the disorder is included in the spatial aspect.

In this contribution we focus on the luminescence decay due to trapping and recombination in random media, such as substitutionally disordered crystals and molecular dye layers adsorbed on different substrates. For strongly disordered systems the luminescence decay $\Phi(t)$ is markedly nonexponential, and may even display algebraic time dependences at longer times[1],

$\Phi(t) \sim t^{-\gamma}$. Here we model the random dynamics by extending the CTRWs to fractal lattices. We use a deterministic family of fractals, the Sierpinski-gaskets, which, depending on the embedding d-Euclidean space, span different fractal ($\bar{d}=\ln(d+1)/\ln 2$) and spectral ($\tilde{d}=2\ln(d+1)/\ln(d+3)$) dimensions. For the $\psi(t)$ we use both Förster-type expressions, which follow from direct-transfer considerations[5], $\psi_F(t)=\alpha C t^{\alpha-1}\exp(-Ct^{\alpha})$ with $\alpha \sim \bar{d}$, and also broad waiting-time forms of Scher-Lax-Montroll type, $\psi_{SLM}(t) \sim t^{-\beta-1}$ $(0<\beta<1)$.

The waiting-time distributions and the fractal aspects of the model influence in different ways the diffusion coefficients, D(t), and the luminescence decays due to trapping, $\Phi(t)$. At longer times, for $\psi_F(t)$, D(t) is proportional to $t^{\tilde{d}/\bar{d}-1}$, a generalization of the $D(t) \sim D(\infty)$ behavior valid for regular lattices. For $\psi_{SLM}(t)$ the coefficient D(t) goes as $t^{\beta\tilde{d}/\bar{d}-1}$, a typical example for subordination, for which the exponents behave multiplicatively. On the other hand, the long time behavior of the luminescence parallels the slowest decay component; in general one finds for $\psi_F(t)$ $\Phi(t) \sim \exp(-Ct^{\alpha})$ and for $\psi_{SLM}(t)$ $\Phi(t) \sim t^{-\beta}$. Thus the distributions $\psi(t)$ override the asymptotics $\Phi(t) \sim \exp(-\tilde{C}t^{\delta})$ with $\delta=\tilde{d}/(\tilde{d}+2)$, which obtain for fixed waiting-times. Using numerical methods we present the full time-dependence of the decay laws and discuss the experimental relevance of the asymptotic expressions.

1. A.Blumen, J.Klafter and G.Zumofen, Phys.Rev.B2[illegible], 1429(1983)
2. A.Blumen and G.Zumofen, J.Chem.Phys.77,5127(1982)
3. G.Zumofen, J.Klafter and A.Blumen, J.Chem.Phys.79,5131(1983)
4. A.Blumen, J.Klafter and G.Zumofen, Phys.Rev.B28,6112(1983)
5. J.Klafter and A.Blumen, J.Chem.Phys.80,875(1984)

Luminescent Fractal Reactions: Exciton Annihilation on Percolation Clusters

L.W. Anacker and R. Kopelman, Dept. of Chemistry, The University of Michigan, Ann Arbor, Mi.48109 and P.W. Klymko, IBM, East Fishkill, Hopewell Junction, N.Y. 12533.

We report here the first complete study of fractal reaction kinetics.[1-3] This fractal reaction is a prototype of heterogeneous chemical kinetics and is of potential application to chemical catalysis and biological molecular energy transport. We note that for the binary reaction

$$2T \rightarrow S$$

the classical (Euclidean space) kinetic equation is:

$$dS/dt \propto T^2.$$

However, on fractal spaces, the equation is

$$dS/dt \propto T^2 t^{-h}, \qquad 0 < h < 1$$

where $h=1-d_s/2$ and d_s is the spectral dimension of the fractal space. As for the delayed fluorescence

$$F \propto dS/dt$$

and for the phosphorescence

$$P \propto T ,$$

$$\log(F/P^2) \propto (-h)\log(t) .$$

Guest-guest triplet-triplet annihilation in highly purified mixed crystals of naphthalene (guest) - naphthalene-d_8 (host) was studied at 1.8K via simultaneous spectrally and time-resolved phosphorescence and delayed-fluorescence over a large guest concentration range and for a number of excitation densities. Fig.1 shows a sample of results for samples well below the dynamic percolation concentration (about 8% naphthalene). (F/P^2) is normalized at early times (t=20 ms). The steady state excitation (via Xe arc) was shuttered off at t=0. Both P and F were signal averaged. The slope (h) is about 0.45, giving d_s of about 1.1. This is in good agreement with superuniversality (d_s=1.3), in even better agreement with long-range random walks on percolation clusters (d_s=1.1)[4], but in contradiction with the Euclidean (classical) result (d_s=2, h=0). However, at naphthalene concentrations well above criticality (e.g. 12% or 16%), the lines are horizontal (i.e. h=0, d_s=2), as expected classically, and in agreement with literature experiments on pure naphthalene crystals ($F \propto P^2$). Our results agree with the long-range exciton percolation mechanism (tunneling via superexchange), followed by fast, short-range fusion, but not with a direct long-range fusion model. The latter would

result in classical kinetics.

1. P.W. Klymko and R. Kopelman, J.Phys.Chem.87, 4565(1983).
2. P. Meakin and H.E. Stanley, J.Phys.A:Math.Gen. 17, L173(1984).
3. R. Kopelman, P.W. Klymko, J.S. Newhouse and L.W. Anacker, Phys.Rev. B (in press).
4. P. Argyrakis and R. Kopelman, Phys.Rev. B (submitted).

Supported by NIH Grant No. 2R01 NS80116-16.

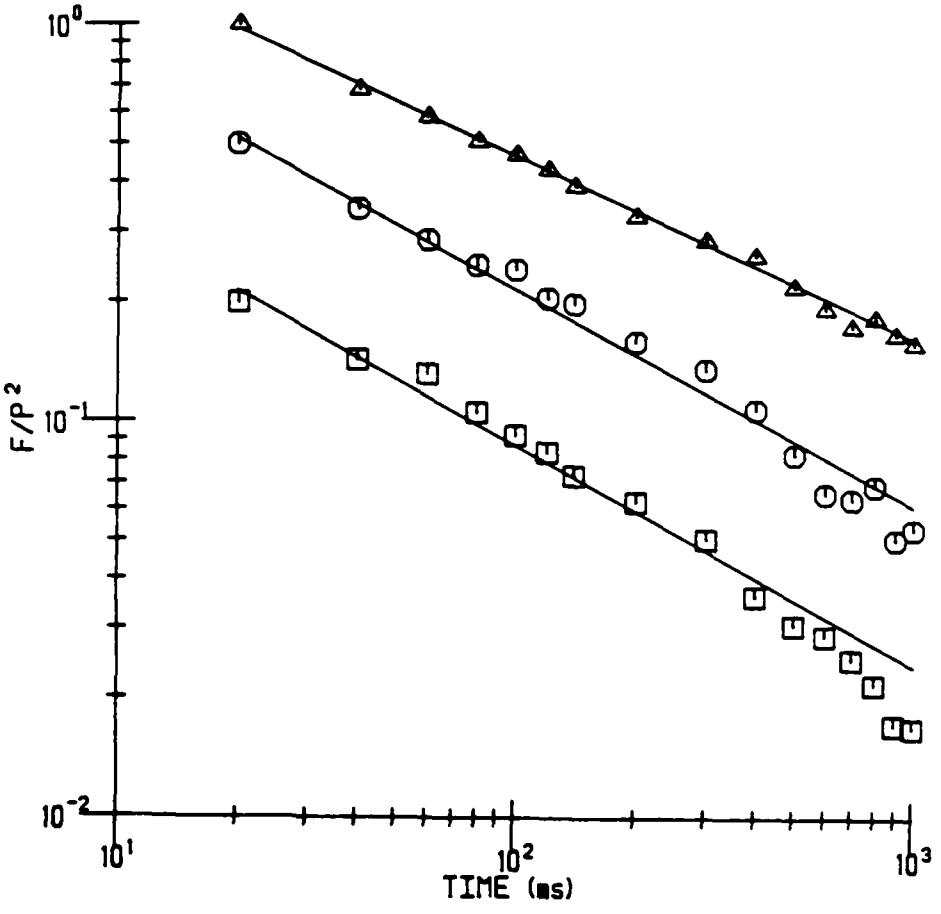

Fig.1: log F/P^2 vs. log t for 5.9%, 3.1% and 2% crystals of naphthalene-h_8 in naphthalene-d_8 (top to bottom, respectively). Both experimental data (symbols) and fitted curves are shown. The curves are essentially co-linear, but have been separated for purposes of illustration.

Photophysical Studies of DAQ on Silica and Aluminum Oxides. A Molecular Probe of Surface Heterogeneity

J. M. Drake

Exxon Research and Engineering Company
Corporate Research-Science Laboratories
Clinton Township - Route 22 East
Annandale, New Jersey 08801

The optical features of organic molecules adsorbed to the surface of oxides, such as silica and alumina, can be strongly perturbed by the chemical properties of the surface adsorption sites. The topography of the surface as it relates to the fractal dimension and its relation to the nature and distribution of surface sites is important information if we are to be able to understand the photophysics and photochemistry of surface bound molecules. The work we report here is for the molecule 1,4 dihydroxyanthraquinone (DAQ, Quinizarin). This molecule provides striking evidence of how the surface of silica gel modifies the optical features of DAQ in different ways depending on the nature of the surface adsorption site.

The direction of our work with DAQ is to develop an understanding of the relationship between the spectroscopic changes (compared to homogeneous solution) observed for the surface bound molecule and the chemical and physical nature of surface adsorption sites. We chose DAQ because of the range of chemical behavior it exhibits. As a site specific molecular probe of surfaces, DAQ interacts with the surface through: hydrogen bonding, charge transfer and proton transfer. The features of the hydrogen bonding between the surface and DAQ are studied by the technique of photochemical hole burning (PHB). This is a very unique form of site selective surface photochemistry, which for DAQ is based on a phototautomerization reaction. We have been successful in doing PHB of DAQ on selected silica surfaces.

The charge transfer and proton transfer interactions, both the intramolecular and intermolecular processes, are studied using optical techniques. We use the absorption, fluorescence and fluorescence lifetime features of surface bound DAQ to interrogate the polarizable nature of the local surface site environment. The broad structureless inhomogeneously broadened absorption feature of the total ensemble of surface bound molecules is separated into two subsets, those DAQ molecules which are chemisorbed to sites which result in quenched fluorescence and those adsorbed to sites which allow the molecule to continue to fluoresce. Those which fluoresce, can be subdivided further into those which are weakly adsorbed and therefore exhibit fluorescence features similar to homogeneous solution and those which are adsorbed forming a strong complex with the surface. The DAQ molecules which form a surface complex exhibit strongly perturbed fluorescence features.

The dynamics of the excited state proton transfer reaction are modeled using fluorescence lifetime data obtained for each of the surface bound forms of DAQ. Time resolved fluorescence spectra are taken to understand the apparent shifts in the fluorescence spectra of DAQ in different surface environments. The resulting spectroscopic and dynamic data demonstrate the usefulness of optical techniques in probing the chemical nature of heterogeneous oxide surfaces.

PROGRESS IN UNDERSTANDING OF MECHANISMS OF RE^{3+} EXCITED STATES NONRADIATIVE RELAXATION IN CRYSTALS

V.P.Gapontsev, M.R.Sirtlanov
Institute of Radioengineering & Electronics AS USSR,
103907, Moscow, Marx 1?
W.M.Yen
Department of Physics, Univ. of Wisconsin, Madison,
Wisconsin 53706

It was shown earlier [1-3], that the regularities of nonradiative relaxation (NR) of RE^{3+} excited states in oxide glass hosts are quantitatively described in the frames of model of dipole-dipole energy transfer to those high-frequency molecular oscillators of impurities or host, which overtones have the resonance with electronic transition. However the attempts [2,4] to apply this model to NR description in crystals gave contradictory results. It was pointed the satisfactory agreement of theory and experiment for $Y_3Al_5O_{12}$, $YAlO_3$ crystals [2], but for Y_2O_3 crystal situation was less consolatory [4].

In this paper we describe the results of systematic investigations of NR processes regularities for different RE^{3+} excited states in a variety of oxide ($Y_3Al_5O_{12}$, $NaLa(MoO_4)_2$, LaP_5O_{14}, $YAlO_3$, $Gd_3Ga_5O_{12}$, and so on) and some fluoride ($LiYF_4$, LaF_3) single crystals, which were carried out with the use of modern techniques of selective laser excitation and photon counting. As it was established, in the most of investigated crystals there was observed a good correlation between the intensity $k(\nu)$ of infrared absorption of crystal in multiphonon region and the dependence $W^x(\nu)$, where W^x is the probability of NR process, normalized to the value of electrodipole part of radiative transition rate, and ν^{-4}. Moreover, in spite of big structure variety of investigated crystals, the measured values of the coefficient

$\alpha = \frac{W^X(\nu)}{k(\nu)}$ proved to be close each other ($\alpha = 10^{20} cm^{-3}$) and exceeded the beforefounded data for oxide glasses [2] not more than 2 - 3 times. These data showed on the decisive contribution of dipole-dipole resonant mechanism of NR process in discussed systems. The same conclusion was made by us for $LiYF_4$ crystals. Another situation was observed for crystals of LaF_3, Y_2O_3, and, as it was defined more precisely, $YAlO_3$, where the spectral dependences of $W^X(\nu)$ and $k(\nu)$ are essentially different , and the estimations of W values made within limits of the resonant model proved to be much less of the measured values.

Analysis of obtained data allows us to draw an important conclusion that there are two principally different situation with NR processes of RE^{3+} in crystalline hosts in dependence whether the highest- frequency modes are localized outside RE center or directly coupled with it. In the first case the dominant contribution in the NR efficiency is connected with the dipole-dipole resonant energy transfer from the electronic transition to vibrational modes of crystal. The mechanism of NR process in the hosts of second type demands additional investigations. One of possible models may be the model, discussed in [5].

1. V.P.Gapontsev, In: Laser Phosphate Glasses (Nauka Press, Moscow, 1980), Ch.3.
2. V.P.Gapontsev et al., In: Proceedings of the Int. Conference LASERS'81 (STS Press, McLEAN, VA, 1981), p.763.
3. E.B.Sveshnikova et al., Izv. AS USSR, s.Physics, v.44,722(1980).
4. E.B.Sveshnikova et al., Optics and Spectroscopy, v.54, 259(1983).
5. K.K.Pukhov, V.P.Sakun, Pys. Stat. Sol.(b), v.95, 391, (1979).

The Effect of the J-mixing on the Intensities of the f-f Transitions of Rare-earth Ions

Hsia Shang-ta, Chen Yi-min
Department of Physics
University of Science and Technology of China
China

SUMMARY

Taking the effect of the J-mixing into account in the consideration of luminescense of rare-earth ions on low symmetry positions in solids, we derive the following line strength formula for electric-diople transition from term $\Psi_i J_i$ to term $\Psi_f J_f$ (modified Judd's three parameter band intensity formula [1])

$$S_{if}^{ed} = e^2 \sum_{k=2,4,6} \Omega_k \sum_{\Psi_i J_i'} \sum_{\Psi_f J_f'} \frac{|Q(\Psi_i J_i, \Psi_i' J_i')|^2}{2J_i'+1} \frac{|Q(\Psi_f J_f, \Psi_f' J_f')|^2}{2J_f'+1} |\langle \Psi_f' J_f' \| U^{(k)} \| \Psi_i' J_i' \rangle|^2 \qquad (1)$$

where ΨJ is the same thing as $^{2S+1}L_J$, the term label; $|Q(\Psi J, \Psi' J')|^2/(2J'+1)$ is defined as the j-mixing coefficient between term ΨJ and term $\Psi' J'$. The j-mixing coefficients are introduced to describe approximately the degrees of the j-mixing between terms. One can easely obtain them from crystal field spliting data of a few terms with the use of the equations

$$|Q(\Psi J, \Psi' J')|^2 = \sum_{k=2,4,6} \bar{S}_k^2 \langle \Psi' J' \| U^{(k)} \| \Psi J \rangle^2 / [\bar{E}(\Psi J) - \bar{E}(\Psi' J')]^2 \qquad (2)$$

and

$$\sum_n [E(\Psi Jn) - \bar{E}(\Psi J)]^2 = \sum_{k=2,4,6} \bar{S}_k^2 \langle \Psi J \| U^{(k)} \| \Psi J \rangle^2 \qquad (3)$$

where $E(\Psi Jn)$ is the energy level of the nth component of the term ΨJ and $\bar{E}(\Psi J)$ $(=\sum_n E(\Psi Jn)/(2J+1))$ is the centre of gravity of the stark levels belonging to the term ΨJ. The sum $\sum_n$ is taken over all of the $2J+1$ components of the term ΨJ. The defination of the parameter $\bar{S}_k$ is given by

$$\bar{S}_k = \left| \sum_q |B_{kq}|^2 \langle f \| C^{(k)} \| f \rangle^2 / (2k+1) \right|^{1/2} \qquad (4)$$

where B_{kq}'s are the crystal field parameters.

If some crystal spliting data of a few terms are known, Eq's. (3) can be used to determine $\bar{s}_k$'s. Then the j-mixing coefficients can be obtained from Eq.(2). Thus intensity formula Eq.(1) can be used without difficulty and the j-mixing effect is taken into account. Examples are taken to be the applications to the the emision spectrum of EuP_5O_{14} and the absorption spectrum of $Er^{3+}:Y_2O_3$. Eq.(1), with Ω_2, Ω_4 and Ω_6 as fitting parameters, gaves a good fit with the experiment data of branching ratio of $^5D_0$ of Eu^{3+} and oscillator stengths between ground and excited terms of Er^{3+}. Especially, the results show that the intensities of the $^5D_0 - {}^7F_0$ and $^5D_0 - {}^7F_3$ transitions of Eu^{3+} in EuP_5O_{14} can be attributed to the J-mixing effect (see Table.1). But these transitions are forbidden by the Judd's three parameter formula where not taking into account the j-mixing effect.

Table.1 The observed and calculated branching ratio of $^5D_0$ of Eu^{3+} in EuP_5O_{14}.

	β_{obs} [2]	β_{calc}
$^5D_0 - {}^7F_0$	.003	.0023
$^7F_1$	.429	.4500
$^7F_2$	.443	.4441
$^7F_3$	.014	.0120
$^7F_4$	.108	.1090
$^7F_5$	.002	.0018
$^7F_6$	.000	.0010

References

1. B.R.Judd, Phys. Rev. 127, 750(1962).
2. I.Laulicht & S. Peled, J.Lumin. 24/25, 87(1981).

f-f Electric Dipole Intensity Mechanisms for Rare Earth Ions

Michael F. Reid and F. S. Richardson

Department of Chemistry

University of Virginia

Charlottesville, VA 22901 USA

Transitions within the f^N configurations of rare-earth ions are parity forbidden and only became allowed by virtue of external perturbations. A general parametrization of the intensities of transitions between crystal-field levels requires a set of parameters $\{A^{\lambda}_{tp}\}(\lambda=2,4,6;\ t=\lambda-1,\ \lambda,\ \lambda+1;$ p determined by symmetry).[1] However, if the 'superposition' approximation, that the rare-earth-ligand interactions are cylindrically symmetric and independent, is valid, the $t=\lambda$ parameters are unnecessary and the parametrization reduces to the usual Judd-Ofelt parameter set $\{A_{tp}\Xi(t,\lambda)\}$.

These parameters contain a considerable amount of information. For example, the signs of the parameters reported in the literature cannot be rationalized in terms of the crystal-field configuration-mixing model. The addition of the 'ligand polarization' (or 'dynamic coupling') mechanism provides a possible explanation.[2] The latter mechanism involves excited ligand states, whereas in the former all excited states are on the rare-earth ion. Clearly, any refinements to the models for f-f transitions must be able to account for these signs.

In systems where the ligands are not spherical ions, but complex molecules, the superposition approximation breaks down, and the full set of A^{λ}_{tp} parameters is needed. We find that ligand polarization calculations which take into account the polarizability anistropy of the ligands give

qualitative agreement with experiment.

1. D. J. Newman and G. Balasubramanian, J. Phys. C 8, 37 (1975).

2. M. F. Reid, J. J. Dallara, and F. S. Richardson, J. Chem. Phys. 79, 5743 (1983).

Supported by NSF Grant CHE-82-15815.

Electronic Structure and Energy Levels of the Phosphor ZnS:Tm^{3+} Using Nonrelativistic and Relativistic Cluster Calculations

Changxin Guo* and D.E. Ellis
Physics Department, Northwestern University,
Evanston, Illinois 60201, U.S.A.

Luminescence properties of rare earth doped ZnS were extensively studied recently. The main purpose of these works was to optimize the synthesis methods for phosphors, to study the properties of luminous centers and energy transfer from ZnS → Ln^{3+}, and by using the rare earth ion as a local structural probe, to study the crystal field properties of the environment. The studies of trivalent thulium Tm^{3+} doped in crystalline ZnS was reported by several authors[1,2,3]. The experimental results of emission properties and crystal field parameters of ZnS:Tm^{3+} were mentioned.

In this paper, we report first principles calculations on ZnS:Tm^{3+}. This work is done in the framework of (1) the nonrelativistic Hartree-Fock-Slater self-consistent one-electron local density discrete variational method (HFS-Xα-DVM)[4], and (2) the relativistic Dirac-Slater model (DS-Xα -DVM)[5,6]. In these calculations, spin polarization was considered. The finite clusters calculated include Tm-S_4 and Tm-S_4-Zn_{12} clusters for cubic ZnS, which were embedded in the crystal environment. Matrix elements of the secular equation were obtained by the discrete variational method as a weighted sum over a set of sample points, and diagonalized by standard methods. The cluster wavefunctions were represented by an expansion in numerical atomic wavefunctions. In order to calculate luminescence of ZnS:Tm^{3+}, the so-called transition state (TS) procedure was used[7] directly to estimate the total energy difference between initial and final states.

For rare earth ions, spin-orbit coupling energy in the 4f shell is larger than the crystal field splitting energy; this means that relativistic effects on the electronic structure and energy levels cannot be negligible. We used both relativistic

---

*Permanent Address: Department of Physics, University of Science and Technology of China, Hefei, Anhui, The People's Republic of China.

DS-Xα -DVM and nonrelativistic HFS-Xα-DVM methods to calculate levels of the ZnS:Tm^{3+} cluster, in order to explore consequences of relativistic level shifts and spin-orbit splittings. The resulting one-electron scheme does not compare directly with traditional |LSJ> many-electron models of the Tm^{3+} ion. We compare TS energies with experimental luminescence data, and discuss their relation to multiplet energies.

The following table shows Mulliken atomic orbital populations (atomic configuration) of Tm^{3+} in ZnS; results of self-consistent ground state calculation:

	nonrelativistic				relativistic	
	$Tm-S_4-Zn_{12}$ (free cluster)		$Tm-S_4-Zn_{12}$ (embedded in crystal)		$Tm-S_4$ (embedded in Zn_{12})	
	charge	spin	charge	spin	charge	spin
4f	12.13	1.85	12.15	1.81	11.98	1.98
5d	0.61	0.02	0.45	0.02	0.62	0.03
6s	0.02	0.01	0.07	0.00	0.03	0.00
effective charge	+2.24		+2.33		+2.37	

References:

[1] Yves Charreire and Pierre Porcher, J. Electrochem. Soc., 130 , 175 (1983).

[2] L. Jastrabik, J. Mares and S. Pacesova, J. Lumines., 24/25 , 293-296 (1981).

[3] S. Ibuki and D. Langer, J. Chem. Phys. 40 , 796-808 (1964); Appl. Phys. Lett., 2 , 95 (1963).

[4] E.J. Baerends, D.E. Ellis, and P. Ros, Chem. Phys., 2 , 41 (1973); E.J. Baerends and P. Ros, Chem. Phys. 2 , 52 (1973).

[5] D.E. Ellis, Actinides in Perspective (Edited by N.M. Edelstein, Pergamon Press, New York, 1982).

[6] A. Rosen and D.E. Ellis, J. Chem. Phys. 62 , 3039 (1975).

[7] J. C. Slater and K.H. Johnson, Phys. Rev. B 5 , 844 (1972).

Optically Stimulated Luminescence of MgS:Eu Phosphors

R.P.Rao, J.Gasiot* and J.P.Fillard*
Materials Science Centre
Indian Institute of Technology
KHARAGPUR-721 302.

The phenomena of optically stimulated luminescence (OSL) has been known since long time (1). Antonov-Romanovski (2) first suggested that IR sensitive phosphors like SrS:Eu,Sm for the dosimetry of ionising radiation. On these lines quite a number of publications appeared discussing OSL dosimetry over TL dosimetry (3) and also X-ray iamging. To understand the OSL phenomena, one needs excitation (UV), emission (visible) and stimulation (IR) spectra. OSL is identical to TL evaluation, which is also known as 'Cold Method' where stored energy in the material after excitation is obtained optically and thermally in case of thermoluminescence.

Polycrystalline MgS has been prepared by reducing $MgSO_4$ with CS_2 in presence of argon at 900°C and doped with different concentrations of Eu. Thin films are prepared by depositing fine powders on cleaned glass substrates by sedimentation. The samples are then protected from atmosphere moisture by coating with a polymer binder Dow Corning 805. The UV excitation (in the range 200 to 400 nm), emission (in the range 500 to 700 nm) and IR stmulation (in the range 0.9 to 1.3 μm) spectra of all the samples have been recorded at room temperature (300°K). Some results on a typical concentration of MgS:Eu (0.1 % by wt.) are shown in Fig.1. By considering all the results obtained in this investigation, the different transistions involved in the process of excitation, emission etc. are discussed. The advantages of this method over TL in dosimetry particularly in neutron dosimetry

are explained.

1. S.P.Keller, J.E.Mapes and G.Cheroff, Phys. Rev. 108 (1957) 663.
2. V.V.Antonov-Romanovski, et al, Conf.Acad.Sci.Sessions Div. Phys.Maths.Scinece USAEC Report AEC tr 2435 (1956) 239.
3. J.Henniger et al Nucl.Instruments and Methods 204 (1982) 209.

* C. E. M., U. S. T. L., 34060 Montpellier Cedex, France.

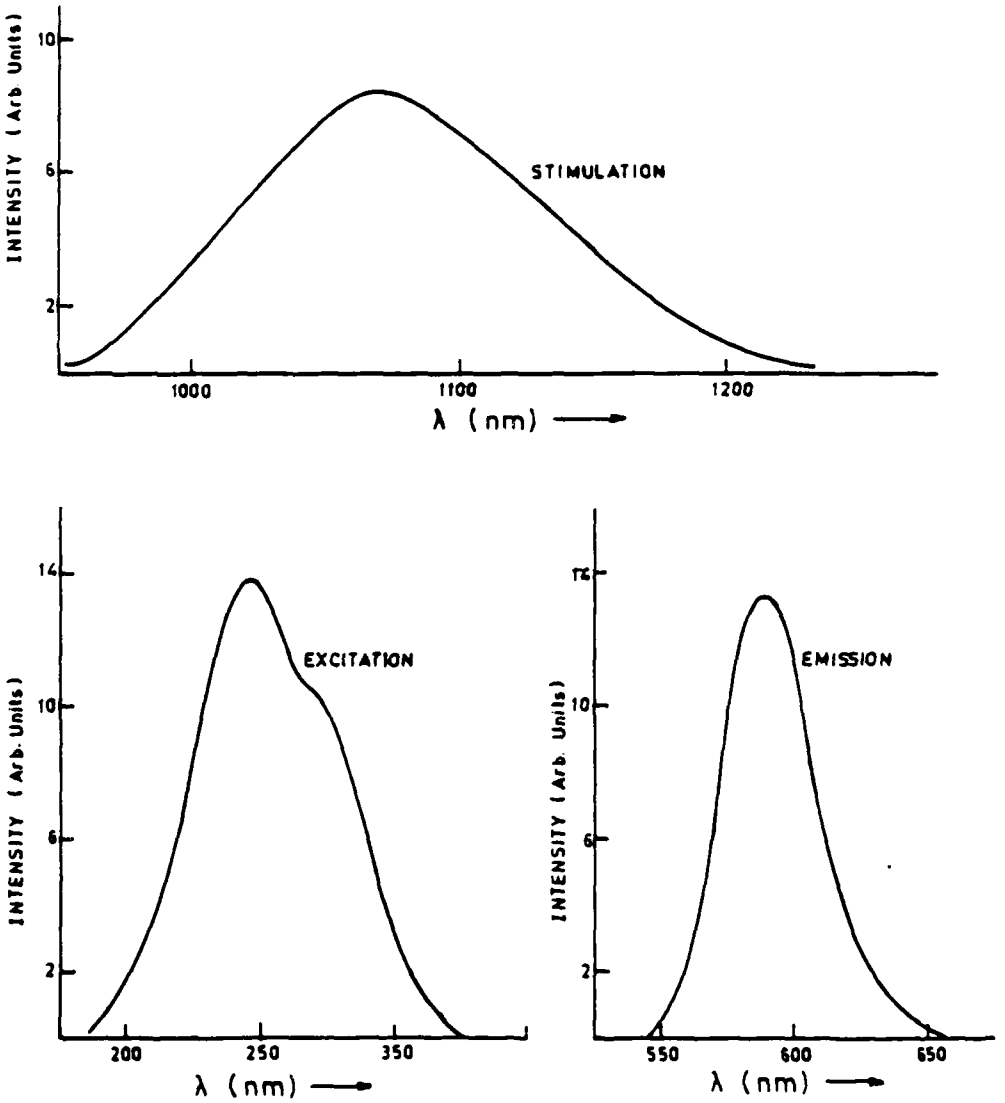

FIG.1 EXCITATION, EMISSION AND STIMULATION SPECTRA OF MgS : Eu (0.1 % by wt) PHOSPHORS

LUMINESCENCE OF CERIUM IN THE SYSTEM $Ba_{1-x}Ce_xMgF_{4+x}$

by

E. Banks, Liu Xing-ren and A. M. Srivastava

Department of Chemistry
Polytechnic Institute of New York
333 Jay Street
Brooklyn, New York 11201

Summary

Samples of composition $Ba_{1-x}Ce_xMgF_{4+x}$ were prepared by heating in dry nitrogen. At Ce concentrations below 10 mole %, X-rays showed the $BaMgF_4$ structure[1]. Above that composition a new structure appears. Excitation spectra of samples containing 0.3, 3 and 10 mole % Ce are shown in Figure 1. The excitation peaks shift to longer wavelength as the Ce concentration increases.

The emission spectra, excited at the excitation peaks, are shown in Figure 2, which shows two overlapping bands peaking at 334 nm and 342 nm. The splitting of the bands is due to the splitting of the ^2F ground state, the excited state being in the 5d' configuration. The fluorescence intensity increases linearly with Ce^{3+} concentration and a maximum is observed near 10 mole %, where the new structure is formed. At 20 mole % Ce, the intensity decreases due to concentration quenching.

Reference

1. E. T. Keve, S. C. Abrahams and J. L. Bernstein, J. Chem. Phys., 51, 4928(1969).

LUMINESCENCE OF $Ba_{1-x}Ce_xMgF_{4+x}$

Fig.1 EXCITATION SPECTRA

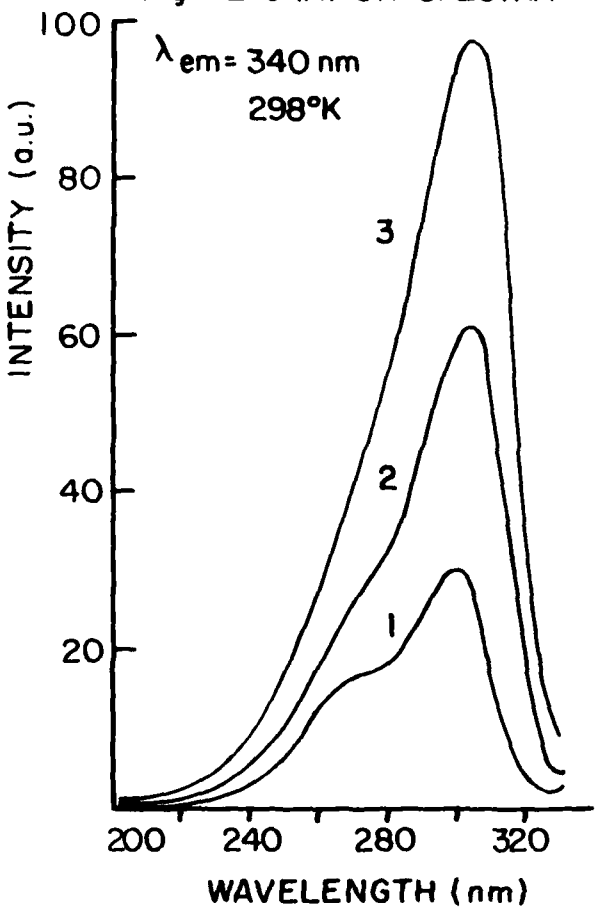

Fig.2 EMISSION SPECTRA

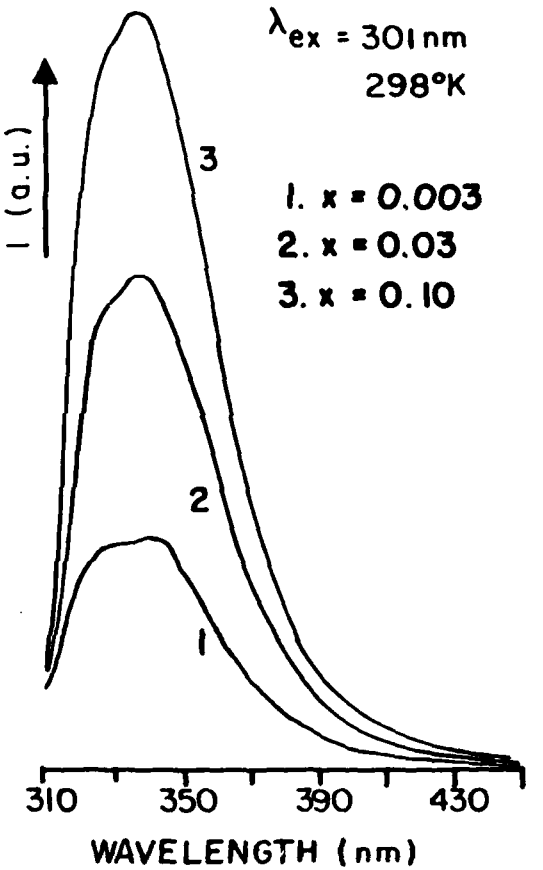

Up conversion of U^{4+} in $ThBr_4$

S. HUBERT, Chong Li SONG, M. GENET
Laboratoire de Radiochimie, Institut de Physique Nucléaire
B.P. N° 1, 91406 Orsay Cedex (France)

F. AUZEL
C.N.E.T., 196 rue de Paris, 92260 Bagneux (France)

Up to now, most of the experimental examples involving the anti-Stokes fluorescence called up-conversion were dealing with rare earth ions [1]. For the first time we have found that tetravalent uranium as a doping ion in single crystal as well as in microcrystalline powder form of thorium tetrahalides acts as an up-converter. In the case of $ThBr_4 : U^{4+}$, infrared excitation with $\lambda > 0.82$ μ at room temperature gives an emission band in the red between 0.67 and 0.72 μm [2]. The power law of the red emission with respect to the infrared excitation is found to be quadratic ; this is the evidence that excitation is obtained by a two-photon process. Furthermore, we found that the 0.69 μm emission follows a linear law with the U^{4+} concentration for a concentration range from 0.006 % up to 0.05 % in weight. From this result, we can conclude that the up-conversion process takes place in one uranium ion. For higher concentration a quenching effect is observed. We found that the efficiency was optimized using microcrystalline powder with grain size of about 0.2-0.3 μm and a concentration of 0.05 %. In this case the efficiency is multiplied by a factor of 20 in comparison with the same sample single crystal. This is believed to be due to photon trapping as demonstrated by life time variations with sample shapes. The red emission from $^3P_0$ is obtained by the absorption of photons at 0.95 μm $^3H_4 \rightarrow {}^3H_6$ and 1.17 μm $^3H_4 \rightarrow {}^3F_3$ as shown by the double beam [1] excitation spectra of figure 1. The level diagram (fig. 2) of U^{4+} shows that the $^3P_0$ fluorescence can be obtained by different ways such as summation of two photons (0.95 μm plus 1.17 μm or 2 × 0.95 μm or 2 × 1.17 μm) with phonon assistance, followed by a multiphonon relaxation. A simple rate equation obtained from the variation of population of implicated levels yields to

$$n_3 = \sigma_2 + {}^2\sigma_1 \, n_1 \, \tau_3 \, \tau_2$$

The large value for the absorption oscillator strength at 0.95 μm for the

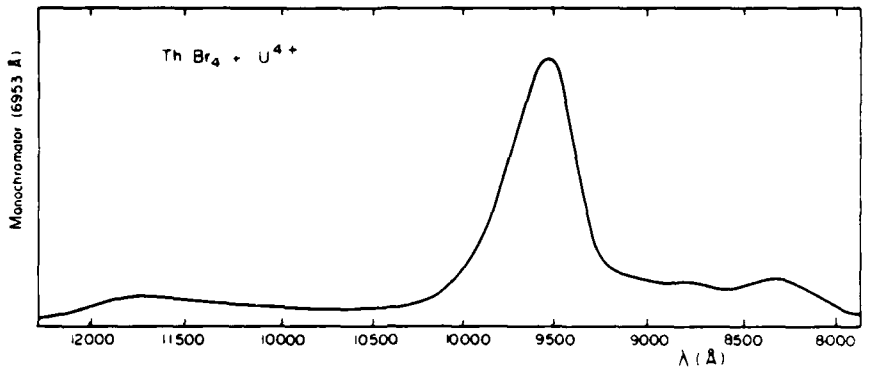

Fig. 1 - Double beam excitation spectra.

$^3H_3 \rightarrow {}^3H_6$ transition which is about 10^{-4} (10^2 times more than the rare earth ones) [3] and for τ_3 = 4.5 µs can explain the existence of the successive absorption which is also observable with a pure $ThBr_4$ crystal containing uranium as unwanted impurity (a few ppm).

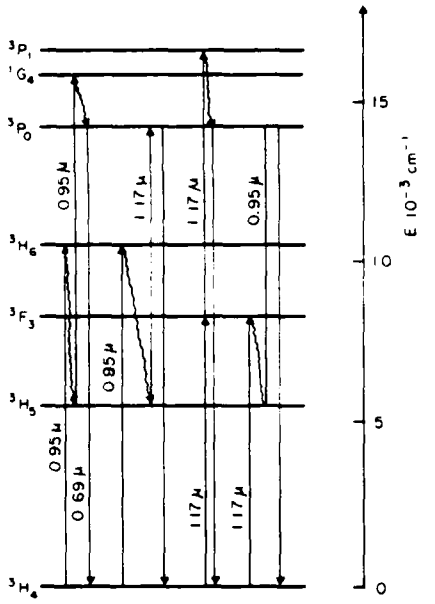

Fig. 2 - Level diagram of U^{4+} :
. level 1 ($^3H_4$) ; . level 2 (intermediate level) ; . level 3 ($^3P_0$)

The same red fluorescence is readily observed using a classical ultraviolet excitation. Whatever the excitation ultraviolet or infrared, an extra green emission (weak) is observed at 77 K (∿ 0.52 µm) probably connected with the phase transition of the matrix which is incommensurate below 95 K [4].

[1] F. Auzel, Proceedings of the IEEE 61 (1973) 758.

[2] M. Genet, S. Hubert, F. Auzel, C. R. Ac. Sc. Paris t. 293 (1981) 267.

[3] F. Auzel, S. Hubert, P. Delamoye, J. of Luminescence 26 (1982) 251.

[4] S. Hubert, P. Delamoye, S. Lefrant, M. Lepostollec, M. Hussonnois, J. Solid State Chem. 36 (1981) 36.

6 d - 5 f transitions of Pa^{4+} in $ThBr_4$

R.C. Naik and J.C. Krupa
Laboratoire de Radiochimie, Institut de Physique Nucléaire
B.P. N° 1, 91406 Orsay Cedex (France)

I.R. emission and absorption of Pa^{4+} in thorium tetrahalide crystals due to transitions between $^2F_{7/2} \rightleftarrows {}^2F_{5/2}$ of 5 f^1 configuration have earlier been reported . In this paper, the visible and near U.V. spectra of Pa^{4+} in $ThBr_4$ are discussed. From the low temperature luminescence, absorption and excitation spectra it is concluded that 6d - 5f transitions are responsible for the observed spectra. Table I summarizes the spectral data recorded on a Jobin-Yvon HR 1000 spectrometer. Oriel-7240 monochromator in conjunction with a tungsten halogen continuum source was used to record the excitation spectra. The visible and near U.V. excitation bands were assigned

Table I - Pa^{4+} in $ThBr_4$.

Sample temperature	Emission peaks Å	Excitation peaks of the emission bands Å	Absorption peaks and their (half-widths) Å	Decay time of emission ns
	7395	-	-	
4.2 K	6848	-	-	
	5931	4195, 4032, 3818 broad band 2500-3000	-	
	5304	4815, 4627, 4195, 4032, 3818 broad band 2500-3000	4688 (325)	41
	5008	4815, 4627, 4195, 4032, 3818 broad band 2500-3000		40
	4318	4195, 4032, 3818 broad band 2500-3000	4063 (225)	38
	3915	-	3750 (200)	-
200 K	5215	4854, 4671, 4349, 4015, 3800	4700 (350)	
			4187 (375)	-
			3688 (225)	

to 6d-5f transitions in Pa^{4+}. It is seen that 5304 and 5008 Å emissions have five excitation bands corresponding to five energy levels into which the $6d^1$ configuration of Pa^{4+} in $ThBr_4$ can split under the combined influence of the spin-orbit and the crystal field interactions (of D_2 and D_{2d} symmetry). Fig. 1 shows the tentative energy level scheme derived from the spectra. Energy level positions in cm^{-1} derived from emission (shown in brackets in fig. 1) and from excitation spectra differ considerably because of Stokes shifts

between absorption and emission. Intensity distribution among fluorescence lines originating from different levels changes substantially depending upon whether the fluorescence is excited through lattice absorption using U.V. radiation or through excitation into the absorption bands of Pa^{4+}.

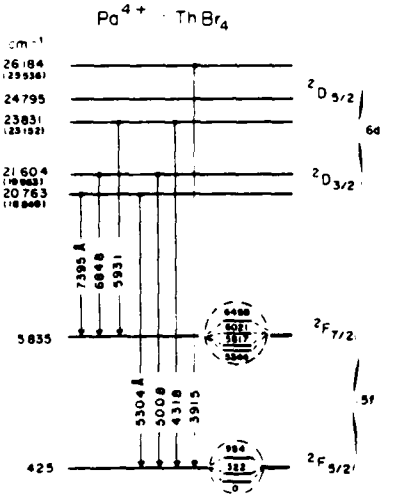

Fig. 1 - 6d-5f transitions in Pa^{4+} : $ThBr_4$.

The radioluminescence which occurs in this crystal resembles in its intensity distribution among its spectral lines to that observed in U.V. excitation, suggesting that the primary excitation in radioluminescence takes place in the lattice.

By using laser excitation and tuning the laser wavelength to pump into the strong band of Pa^{4+} at 4688 Å, anti-Stokes luminescence at 3915 Å and 4318 Å could be excited in addition to the Stokes luminescence. Presumably lattice absorption taking place via a two step process involving the intermediate Pa^{4+} level and the subsequent transfer of energy to Pa^{4+} by the lattice leads to the observed anti-Stokes fluorescence, from the higher levels of Pa^{4+}

Selective excitation into 4688 Å absorption band leads also to I.R. emission at 5022 cm^{-1} which corresponds to the known transition from Γ_6 level of $^2F_{7/2}$ to Γ_7 level of $^2F_{5/2}$. Radiative transition from 6d, populating the $^2F_{7/2}$ level is considered responsible for this emission.

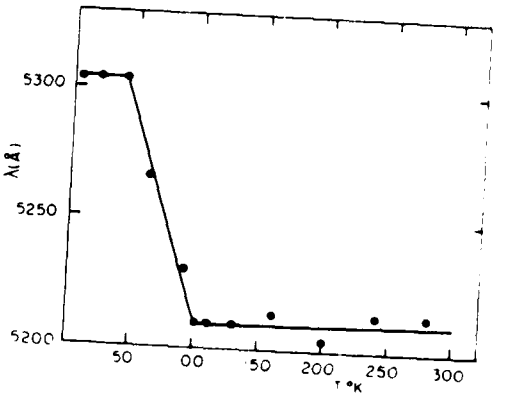

Fig. 2 - Peak position of 5304 Å fluorescence as a function of temperature.

Luminescence as well as excitation peaks show large wavelength shifts between 4.2 K and 300 K. A study of the luminescence and their excitation spectra at different temperatures ranging from 4.2 K to 300 K leads to the conclusion that the wavelength shifts in peak positions are associated with the structural phase change taking place in $ThBr_4$ at 95 K (fig. 2).

"A THEORETICAL SCHEME FOR 4f↔4f INTENSITY CALCULATIONS. OPTICAL ABSORPTION INTENSITIES IN $YAlO_3:Pr^{3+}$."

O.L. Malta, E.A. Gouveia[†] and G.F. de Sá
Departamento de Química Fundamental and
Departamento de Física da UFPE
Cidade Universitária - Recife - PE - 50000 - BRASIL

The Judd-Ofelt theory [1] has been successfully used in the interpretation of rare-earth 4f↔4f intensities. It is a common practice in this theory to express the oscillator between two J-manifolds, belonging to the ground $4f^N$ configuration, as a function of three intensity parameters Ω_λ (λ= 2, 4, 6). If these parameters are treated phenomenologicaly, besides the eletric-dipole mechanism other contributions are automaticaly absorved making it impossible to distinguish between them. Among these contributions, the Pseudo-Multipolar Field has been shown to be of particular importance [2,3]. Vibronic as weel as correlation effects may also be of relevance. It is, therefore, of interest to perform theoretical calculations in order to assesss the relative contribution of each of these mechanisms.

These theoretical calculations turn out be complicated mainly by two reasons among others. Firstly, since perturbation theory is in general used, one is involved with a summation over as infinit set of intermediate excited configurations. Secondly, a satisfactory representation, in terms of spherical tensor operators, of the crystal field hamiltonian, which is responsible for the configuration mixing, has shown to be a difficult task.

Recently, we have developed a theoretical scheme in an atempt to overcome these difficulties [4,5]. In this sheme the single energy denominator method is used to allow the summation over the complete set of intermediate configurations and a simple overlap model is introduced to represent the perturbing crystal field hamiltonian.

In the presente work we discuss this sheme and carry out an application to the study of the optical absorption spectrum of $YA\ell O_3$ doped with Pr^{3+}. This system is particularly interesting to raise discussions about the application of the theory due to the fact that the Pr^{3+} ion is a special case from the point of view of crystal-field and standart $4f \leftrightarrow 4f$ intensity theories.

REFERENCES

[1] B.R. Judd, Phys. Rev., 127, 750 (1962)

[2] C.K. Jørgensen and B.R. Judd, Mol. Phys., 8, 281 (1964)

[3] O.L.Malta, Mol. Phys., 42, 65 (1981)

[4] O.L.Malta, Chem Phys. Lett., 88, 353 (1982)

[5] O.L.Malta and E.A.Gouveia, Phys. Lett., 97A, 333 (1983)

TERBIUM ACTIVATED RARE EARTH OXYORTHOSILICATES

Markku Leskelä[a] and Juha Suikkanen[b]

Department of Chemistry, Helsinki University of Technology, SF-02150 Espoo 15, Finland. Present address: [a] Department of Chemistry, University of Oulu, SF-90570 Oulu 57, Finland. [b] Noiro Ltd, Lasihytti 9, SF-02780 Espoo 78, Finland.

Two different monoclinic structures have been found in rare earth oxyorthosilicates: the first (La...Tb) has the space group $P2_1/c$ and contains 9 and 7 coordinated cations, the second (Dy...Lu) has the space group $B2/c$ and also has two different cation sites with coordination numbers 6 and 7 (1). The literature concerning $La_2(SiO_4)O$ is contradictory and it seems that lanthanum does not belong to the first structure group but has an unknown structure of its own (2). The literature of rare earth silicate phosphors is limited and is mostly patented.

Rare earth oxyorthosilicates can be prepared from RE_2O_3 and SiO_2 but flux material should be used to accelerate the reaction and to lower the reaction temperature. With alkali fluoride fluxes it is possible to prepare pure oxyorthosilicate already at 1000°C.

The excitation spectrum of Tb^{3+} in $RE_2(SiO_4)O$ matrices contains strong $4f$-$5d$ band at about 240 nm and weaker $4f$-$4f$ peaks between 290 and 380 nm (Fig. 1). The position of the band shifts from 230 nm in $La_2(SiO_4)O$ to 240 and 245 nm in $Gd_2(SiO_4)O$ and $Y_2(SiO_4)O$, respectively. In $Gd_2(SiO_4)O$: Tb^{3+}, the excitation spectrum contains a peak at 275 nm indicating energy transfer from Gd^{3+} to Tb^{3+}.

The emission spectrum of Tb^{3+} reveals typical strong lines at the

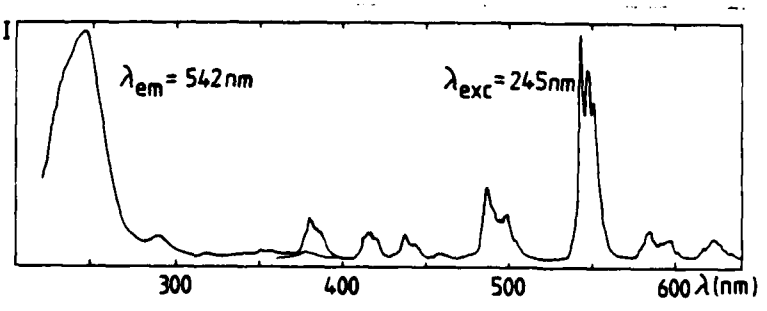

Fig. 1.

The excitation and emission spectra of Tb^{3+} activated (1 %) $Y_2(SiO)O$.

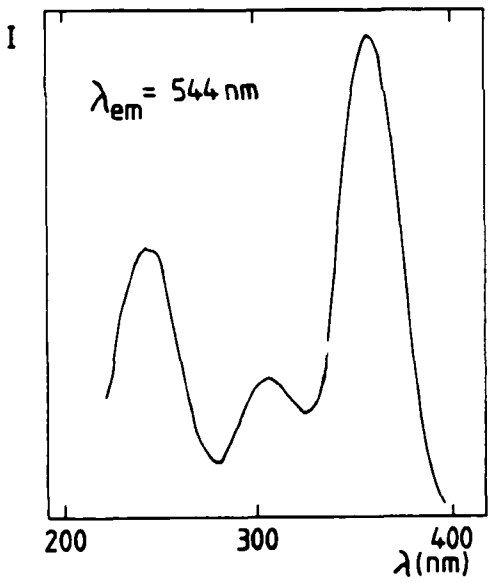

Fig. 2. The excitation spectrum of Ce^{3+} (2 %) and Tb^{3+} (9 %) co-doped $Y_2(SiO_4)O$.

green region (540-560 nm), originating from the $^5D_4$ level (Fig. 1). The highest emission intensity in $Y_2(SiO_4)O$ was obtained with a Tb^{3+} concentration of 20-mole-%. The transitions from the $^5D_3$ level are lacking in $Y_2(SiO_4)O$ when the Tb^{3+} concentration exceeds 5 %. Below that level their intensity increases so that the visible colour of a sample with 0.5 % of Tb^{3+} is blue. In $La_2(SiO_4)O$ and $Gd_2(SiO_4)O$, however, the emission is green at lower activator concentrations than in $Y_2(SiO_4)O$.

The splitting of the emission lines in all oxyorthosilicate matrices is complicated because of the two crystallographic sites with a low symmetry of the rare earth ions. The splitting of the $^5D_4$-$^7F_5$ transition is, however, similar for all matrices.

The terbium emission can be sensitized with Ce^{3+}. The emission band of cerium lies at the near-uv and blue region, overlapping with the $4f$-$4f$ transitions of Tb^{3+} at 360-380 nm. The excitation spectrum of $Y_2(SiO_4)O:Ce^{3+}$, Tb^{3+} codoped sample shows three bands: 240, 300 and 350 nm (Fig. 2). The first band is the $4f$-$5d$ absorption of Tb^{3+} and the others are caused by cerium. The emission spectrum of the codoped sample contains both Ce^{3+} and Tb^{3+} emissions when excited upto the strongest absorption band at 360 nm.

Yttrium turned out to be the best matrix cation among rare earth oxyorthosilicates for terbium. The brightness of the samples prepared was good and $Y_2(SiO_4)O:Tb^{3+}$ is a possible material for a low-pressure fluorescent lamp, whereas $Y_2(SiO_4)O:Ce^{3+}$, Tb^{3+} absorbs at 360 nm.

References

1. J. Felsche, *Struct. Bonding (Berlin)* 13 (1973) 99.
2. G.V. Ananeva, A.M. Korovkin, T.I. Merkulyeva, A.M. Morozova, M.V. Petrov, I.R. Savinova, V.R. Startsev, P.P. Feofilov, *Inorg. Mater.* 17 (1981) 754.

FLUORESCENCE AND LIFETIMES OF EXCITED STATES OF Pr^{3+} IN $LiLa_{1-x}Pr_xP_4O_{12}$ CRYSTALS

Z.Mazurak, E.Łukowiak, R.Cywiński, E.Mugeński, B.Jeżowska-Trzebiatowska

Institute of Low Temperature and Structure Research, Polish Academy of Sciences, P.O.Box 937, 50-950 Wrocław, Poland,

and

D.Schultze, Ch.Waligora

Zentralinstitut für Optik and Spektroskopie, Akademie der Wissenschaften der DDR, 1199 Berlin-Adlershof, DDR.

The spectroscopic properties of praseodymium ions in inorganic matrices are certainly less investigated then other rare earth ions. This is mainly to difficulties which arrise in the interpretation of the experimental data. In our previous papers [1,2] the intensity analysis of f-f transitions of the Pr^{3+} ion in $LiPrP_4O_{12}$ as well as the crystallographic data, are presented. A laser action in this crystal was observed by Szafrański et al. [3].

This paper reports the results of measurements of the fluorescence spectra and the fluorescence lifetimes of excited levels of the Pr^{3+} ions in $LiLa_{1-x}Pr_xP_4O_{12}$ crystals (where x = 0.005 to 1). The $LiLa_{1-x}Pr_xP_4O_{12}$ crystals were grown by a method described by us in Reference [4]. The crystallographic data shows that the crystal belongs to the space group $I_{2/c}$ with the C_2 local site symmetry of Pr^{3+}. The fluorescence of the metastable $^3P_0$ and $^1D_2$ levels in $LiLa_{1-x}Pr_xP_4O_{12}$ was excited from the 457.9 nm line by argon laser, and selected by double monochromator. The spectrum of the Pr^{3+} ions in the lithium

tetraphosphate crystals is complex. At 77 K, for all except the $LiPrP_4O_{12}$ compound a simultaneous emission from the $^3P_0$ and $^1D_2$ levels was observed. The contributions of these levels to the fluorescence strongly depend on the concentration of Pr^{3+} ions. A similar behaviour was observed for $La_{1-x}Pr_xP_5O_{14}$ crystals [5].

The fluorescence decay times were measured using the Boxcar BCI 280 and a nitrogen pulse laser with an excitation source of 10 [ns]. The calculated radiative lifetime for the excited state $^3P_0$ of Pr^{3+} in $LiPrP_4O_{12}$ amount 43 [μs]. The $^3P_0$ level is spaced from the next $^1D_2$ level by about 3800 [cm^{-1}], whereas the highest energy of P-O stretching vibrations is equal 1300 [cm^{-1}]. Consequently the nonradiative relaxation should play a predominant role in the depopulation of the $^3P_0$ state. The rate of the multiphonon relaxation in the phosphates crystals for energy gap of 3800 [cm^{-1}] reaches values of 10^6 [s^{-1}]. In conclusion we did not observed any kind of dependence of fluorescence decay time of the $^3P_0$ level from the Pr^{3+} concentration.

REFERENCES

[1] Z.Mazurak, E.Łukowiak, B.Jeżowska-Trzebiatowska, D.Schultze, Ch.Waligora, J. Phys. Chem. Solids, in press.

[2] Z.Mazurak, E.Łukowiak, Z.Ciunik, B.Jeżowska-Trzebiatowska, D.Schultze, Ch. Waligora, J. Molec. Struct., in press.

[3] C.Szafrański, W.Stręk, B.Jeżowska-Trzebiatowska, Optics Commun. 47, 268 (1983).

[4] W.Ryba-Romanowski, Z.Mazurak, B.Jeżowska-Trzebiatowska, D.Schultze, Ch. Waligora, Phys. Stat. Sol.(a) 62, 75 (1980).

[5] M.Szymański, J. Luminescence 28, 87 (1983)

AD-A148 470 INTERNATIONAL CONFERENCE ON LUMINESCENCE HELD AT MADISON WISCONSIN ON 13-17 AUGUST 1984(U) WISCONSIN UNIV-MADISON W M YEN OCT 84 N00014-84-G-0053 3/1

UNCLASSIFIED F/G 20/6 NL

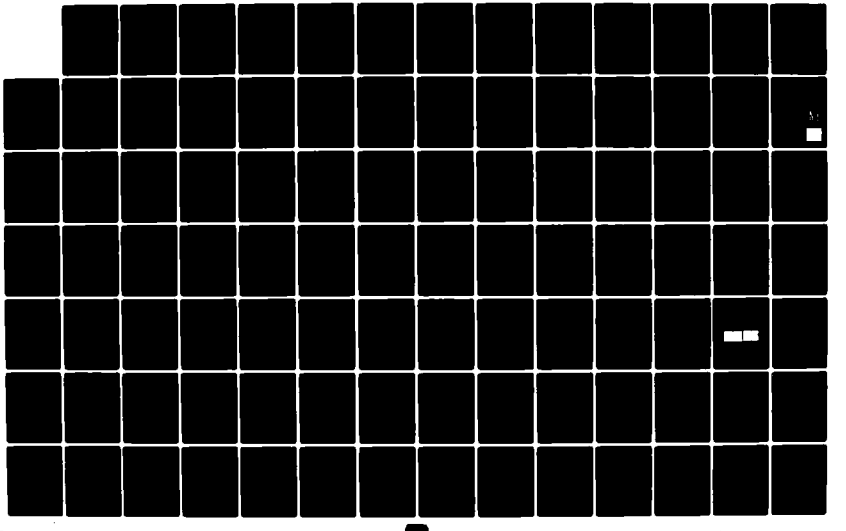

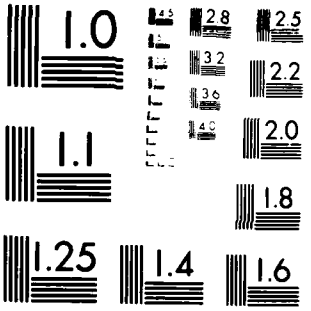

FLUORESCENCE PROPERTIES OF $(Ho,Ln)P_5O_{14}$ CRYSTALS

C. Szafrański, W. Stręk and B. Jeżowska-Trzebiatowska
Institute for Low Temperature and Strcuture Research, Polish Academy of Sciences, P.O.Box 937, 50-950 Wrocław, Poland

In last decade of years the class of stoichiometric lanthanide pentaphosphate (LnP_5O_{14}) crystals has been extensively investigated. This class of lanthanide crystals has attracted much attention because of their application to miniature lasers as well as because of their unusual fluorescence properties. Among of lanthanide pentaphosphates the spectroscopic properties have been reported for Ln = Pr, Nd, Eu, Tb, Er ions [1].

In this paper the absorption and fluorescence spectra of Ho^{+3} ion in LaP_5O_{14} crystal were reported.

The single monocrystals of $(Ho,La)P_5O_{14}$ were grown in the form of thin platelets by the hydrothermal technique. The space group of HoP_5O_{14} is Pnma [2]. The absorption spectra of HoP_5O_{14} were measured at room temperature and the Judd-Ofelt intensity analysis of f-f transition was performed. The empirical parameters Ω_λ were determined from the experimental oscillator strengths by means of the least squares method; $\Omega_2 = 0.45 \cdot 10^{20}$ cm^{-2} , $\Omega_4 = 1.70 \cdot 10^{-20}$ cm^{-2} and $\Omega_6 = 0.73 \cdot 10^{-20}$ cm^{-2}.

The fluorescence spectra of Ho^{+3} ion in LaP_5O_{14} were measured at room and liquid nitrogen temperatures using the argon and pulsed dye lasers as excitation sources. The assignment of fluorescence spectrum given. It was found that Ho^{+3} ions occupy the different crystallographic positions in this crystal.

On a basis of empirical Ω_λ parameters the emission rate constants from the $^5F_4$, $^5S_2$ and $^5F_5$ levels to all lower-lying terminal levels were calculated and the theoretical values of fluorescence branching ratios were determined. They were next compared to those measured from the emission spectra. Due to the calculated radiative rate constant the nonradiative rate constants

were determined which then were used for discussion of inter- and intraion quenching processes in the $(Ho,La)P_5O_{14}$ crystal.

REFERENCES

1. H.G. Danielmeyer, Stoichiometric Laser Materials, ed. H.J. Quiesser, Adv. in Solid State Physics, Vol. 15, Pergamon Press, 1975; H. Dornauft and J. Huber, J. Lumin. 20, 271, 1979; M. Szymański, J. Lumin. 28, 87, 1983; C. Brecher, J. Chem. Phys. 81, 2297, 1974; B. Blanzat, J.P. Denis and Reisfeld, Chem. Phys. Lett. 51, 403, 1977; Z. Mazurak, W. Ryba-Romanowski and B. Jeżowska-Trzebiatowska, J. Lumin. 17, 403, 1978.

2. D. Tranqui, M. Bagieu-Beucher and A. Durif, Bull. Soc. fr. Minerl. Cristallogr. 95, 437, 1972.

Electronic Structure of the Principal Uranium Centre in Sodium Fluoride

W.A. Runciman, B. Srinivasan*

Department of Solid State Physics
Research School of Physical Sciences
Australian National University
Canberra ACT 2601 Australia

and

S. Saebo†

Research School of Chemistry
Australian National University
Canberra ACT 2601 Australia

*Present Address

D1-119 Bonn Avenue
IIT Madras 600036
India

†Present Address

Chemistry Department
University of Arkansas
Fayetteville Arkansas 72701
USA

Summary

It has long been known[1] that uranium in sodium fluoride provides a complex fluorescence spectrum due to the presence of several centres. These centres are believed to be different uranium-oxygen complexes. The principal centres have C_{4v} symmetry and have been attributed to UO_5 groups[2]. Charge compensation is obtained if the hexavalent uranium ion substitutes for a sodium ion and the divalent oxygen ions substitute for five neighbouring fluorine ions. The fluorescence transition has a magnetic dipole character between non-degenerate states. Hence if the ground state has A_1 symmetry the lowest excited state has A_2 symmetry. The resonant fluorescent transition occurs at 563.6nm (17743cm^{-1}). A theoretical model has been constructed along the lines of the calculations for the uranyl ion[3]. In this model excitation consists of an electron in a 2p oxygen ligand orbital being transferred to a uranium 5f orbital. There are a number of possibilities to consider as the electron may come from either the axial oxygen or the equatorial oxygens and in either case it can come from a σ orbital

or a π orbital. Consider first the case of an electron coming from the axial oxygen ion. The determinantal wave functions for the excited states are of the form $|\sigma\ f|$ or $|\pi^3\ f|$. The Hamiltonian includes one-electron, crystal field, spin-orbit, Coulomb and exchange terms. The ω-ω coupling scheme was used throughout the calculation. Matrices were constructed for the different representations of C_{4v} symmetry. In the σf model there are $3A_1$, $3A_2$, $4B_1$, $4B_2$ and 7 pairs of E states. The spin-orbit coupling constant for the uranium 5f electron was taken to be $1950cm^{-1}$. Starting values for the exchange parameters were calculated from atomic basis functions using the computer program system MOLECULE. The crystal field, exchange and one-electron parameters were treated as variables. The matrices were diagonalized for different sets of parameters, and in the case of the E states g-values were calculated. Numerous calculations were made for different sets of parameters and a least squares fitting routine was used to get a fit between experimental and theoretical values of energy levels and g-values for the lowest seven excited states. It was not found possible to get a good fit on a σf model and the calculations were extended to the π^3 f axial model and the equatorial model. For the equatorial model linear combinations of the various σ orbitals are formed to provide orbitals transforming as representations of C_{4v}. A good fit has been obtained for the energy levels and g-values in the $b_2 f$ model. This solution will be assessed critically for applicability to uranium centres in sodium fluoride.

References

1. Runciman, W.A., Proc. Roy. Soc. A 237, 39 (1956).
2. Feofilov, P.P., Opt. i Spektr. 7, 842 (1959) [Opt. Spectr. 7, 493 (1959)].
3. Denning, R.G., Snellgrove, T.R. and Woodwark, D.R., Molec. Phys. 37, 1109 (1979).

Spectral Studies on Luminescence of Dy^{3+} in $CaSO_4$ Phosphors

M.R. Mulla, and S.H. Pawar

Department of Physics, Science College, Karad.

KARAD - 415 110, M.S., INDIA

The paper reports comparative study of electroluminescence emission spectra (EES) of $CaSO_4$:Dy with respect to EES of CaS:Dy, $CaSO_4$:Bi, and CaS:Bi. The details regarding phosphor preparation, electroluminescence (EL) cell, electroluminescence set-up etc. have been reported elsewhere[1,2].

(I) The EES of $CaSO_4$:Dy and CaS:Dy reveal the following features :

(i) The $CaSO_4$ phosphors doped with Dy^{3+} ions show the characteristic luminescence spectrum.

(ii) The wavelengths lying at around 4750 A°, 5671 A°, 6575 A°, and 7478 A° are the characteristic spectral emission of Dy^{3+} ion.

(iii) The characteristic spectral emission is attributed to the spectral transtitions from $^4F_{9/2} \longrightarrow {}^6H_{15/2}$, $^4F_{9/2} \longrightarrow {}^6H_{13/2}$, $^4F_{9/2} \longrightarrow {}^6H_{11/2}$, and $^4F_{9/2} \longrightarrow {}^6H_{9/2}$.

(iv) The EES of CaS:Dy is found to exhibit similar characteristic spectral emission to that of $CaSO_4$:Dy .

(II) The EES of $CaSO_4$:Bi and CaS:Bi reveal the following features :

(i) The doping of Bi^{3+} ions in $CaSO_4$ gives EL emission in red region at around 5850 A°.

(ii) This emission is different than the characteristic emission of Bi^{3+}, which lies in blue region with spectral transition $^3P_1 \longrightarrow {}^1S_0$, When doped in CaS[3,4].

The experimental results (I & II) indicate that the energy levels of Bi^{3+} are modified by the host, but in case of Dy^{3+} the energy levels remain unperturbed despite of change of host. The unperturbed energy levels of Dy^{3+} are attributed to the ^4F electrons, which are responsible for energy transitions.

References :

1) Mulla, M.R., and S.H. Pawar, Mat. Res.Bull.12,929,(1977).

2) Mulla, M.R., and S.H. Pawar, Indian J. of Pure and Applied Phys., 19,407-411,(1981).

3) Blasse G., and Brill, A., The J. of Chemical Phys., 50, No-7, 2974, (1969).

4) Pawar, S.H., and Narlikar, A.V., Mat.Res.Bull., 11, 821, (1976).

Hyperfine properties of Tb^{3+}: $LaCl_3$

N. Pelletier-Allard, R. Pelletier

Labo. A. Cotton, C.N.R.S.II, bâtiment 505, 91405 Orsay, France

Lanthanum chloride is a good crystal host to get highly resolved optical spectra of substituted lanthanides, as some lines exhibit very narow widths (1, 2, 3). Therefore we have used it to study the dipolar magnetic and quadrupolar electric effects of Tb IV.

All results have been obtained by the joint use of the techniques of laser-induced fluorescence line-narrowing and monochromatic excitation of the laser-induced fluorescence, as both homogeneous and inhomogeneous profiles are sharp. The studied transitions are those related to the visible range of the absorption spectrum, i.e. the transitions between the $^7F_6$ ground level, a doublet whose degeneracy is slightly removed at second order, and the four $^5D_4$ Stark levels of lowest energy (two orbital singlets and two doublets).

Knowing the symetry of the levels, their structures can be calculated as functions of the magnetic dipole and electric quadrupole hyperfine structure constants of the $^7F_6$ and $^5D_4$ states. All spectra are then calculated as functions of 5 parameters. Using second-order analysis, all experimental spectra have actually been perfectly interpreted, and the values of the parameters have been deduced by fitting the calculated spectra to the corresponding recorded spectra.

From these experimental parameters, the magnetic hyperfine constant and the electric quadrupole constant of the 4f electrons have been deduced. By introducing the perturbations due to the spin-polarisation and to the electronic Sternheimer shielding in further calculations, the value of the nuclear electric quadrupole moment of ^{159}Tb has been obtained.

Bibliography

(1) N. Pelletier-Allard, R. Pelletier, J. Phys. C 12, 4647 (1979)

(2) N. Pelletier-Allard, R. Pelletier, J. Physique 41, 855 (1980)

(3) N. Pelletier-Allard, R. Pelletier, J. Physique 43, 403 (1982)

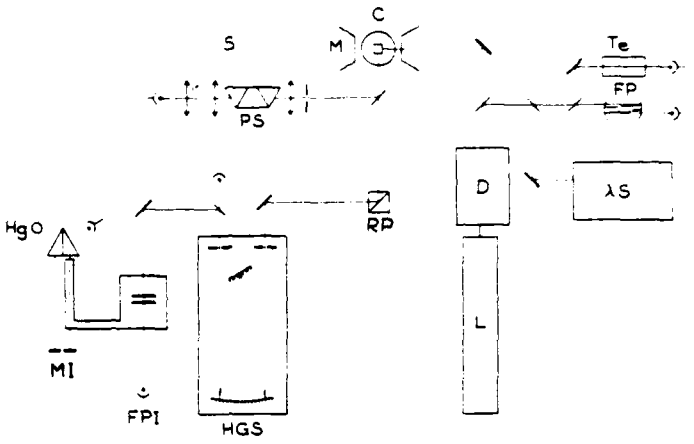

Fig. 1 Experimental set-up

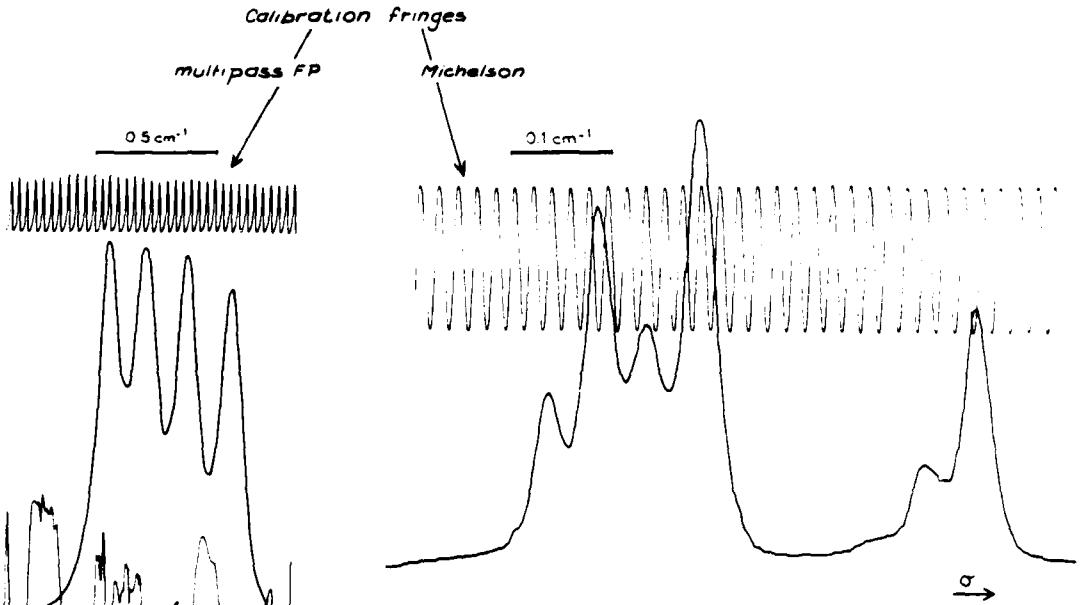

Fig. 2 A three level FLN spectrum

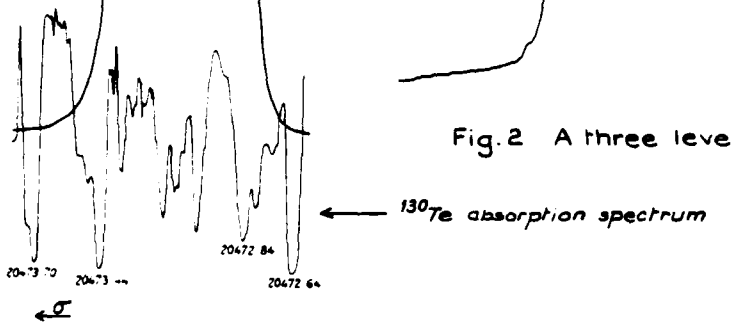

Fig. 3 Excitation spectrum of a Zeeman component

Excitation of the $^1S_0$ State of Pr^{3+} in Crystal Hosts

C. G. Levey, T. J. Glynn, and W. M. Yen

Department of Physics, University of Wisconsin-Madison, Madison, Wi. 53706

We excite the $(4f^2)\,^1S_0$ state directly through a two photon excited state absorption (from the $^1D_2$ level) and indirectly through excitation of the 4f5d band (using an ArF excimer laser). In Pr^{3+}:LaF_3 the $^1S_0$ state lies below the band, and only $^1S_0$ emission is observed. In most hosts examined, it is above the band, and only 4f5d emission is observed. In Pr^{3+}:CaF_2 there are sites with each of these properties, and both $^1S_0$ and 4f5d emission are observed, with a relative strength that is concentration dependent.

The uv fluorescence spectra for Pr^{3+}:LaF_3 are consistent with the $^1S_0$ energy of $46965\pm2cm^{-1}$, which we measured in the 2 photon absorption experiment. The lifetime is concentration dependent, rising from 520 ns in PrF_3 to over 800 ns for concentrations less than 1%. Using intensity data from transitions involving only lower levels, standard Judd-Offelt theory predicts a 3.6 μs lifetime for the $^1S_0$ state[1]. A modified theory which considers the close proximity of the 4f5d band (making other approximations) predicts a lifetime of 525 ns, in closer agreement to the experimental value, and weakly allows two transitions which are forbidden in the standard theory. We have not been able to obtain lasing of the $^1S_0$ transitions at room

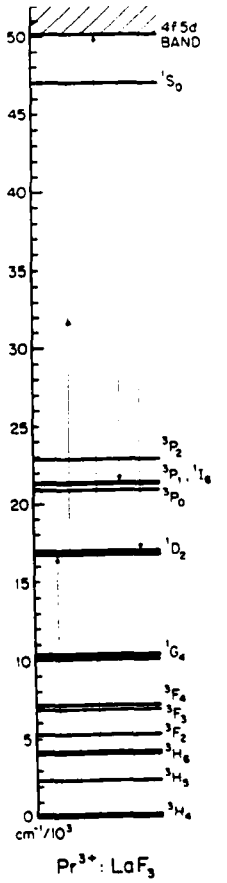

temperature or at 100K, and attribute this fact to an excited state absorption of the emitted radiation (from the $^1S_0$ state and into an absorption band observed by Elias[1] above the 4f5d band).

The uv fluorescence spectra of Pr^{3+}:CaF_2 consists of two components[2]. There is a set of sharp lines with a lifetime of about 700 ns which originate from $^1S_0$ fluorescence, and there is a set of fast (<50ns) broad bands which arise from emission directly from the Pr^{3+} 4f5d band (we also see Ce^{3+} impurity emission). The low concentration samples (<.05%) show primarily 4f5d emission, whereas the $^1S_0$ fluorescence dominates for higher concentrations. We attribute the $^1S_0$ fluorescence to particular sites where the $^1S_0$ level falls below the 4f5d band. We have observed only fast, broad band emission from samples of Pr^{3+} doped into YAG, $YLiF_4$, and in PrP_5O_{14}.

We have excited the $^1S_0$ state directly (via two photon excited state absorption) only in LaF_3, and have been unable to observe this absorption in hosts where the $^1S_0$ state lies in the 4f5d band, or even for those sites in CaF_2 where it is below the band. One might expect two photon spectra to show $4f^2$ to $4f^2$ transitions which are masked in the one photon spectra by the electric dipole allowed $4f^2$ to 4f5d band.

---

[1] L. R. Elias, Wm. S. Heaps, and W. M. Yen, Phys. Rev. B11, 4989 (1973)

[2] W. W. Piper, J. A. DeLuca, and F. S. Ham, J. Lumin. 8,3444 (1973)

Laser Selective Excitation of Fluorine and Hydrogenic Charge Compensated Sites in $SrF_2:Pr^{3+}$

R.W.G. Syme*, R.J. Reeves and G.D. Jones

Department of Physics

University of Canterbury

Christchurch

New Zealand

Laser selective excitation methods were used to identify C_{4v} and rhombic symmetry sites in hydrogenated crystals of $SrF_2:Pr^{3+}$. The hydrogenic sites also display local mode vibronic lines which correlate with those measured in the infrared by Edgar et al.[1]

The fluorescence lifetime of the transition from the lowest crystal field level of the $^1D_2$ multiplet varies from 2.3 msec for the fluoride ion C_{4v} site through 350 μsec for the deuterium C_{4v} site to 2.7 μsec for the hydrogenic C_{4v} site. These results support a model for non-radiative decay to the $^1G_4$ multiplet through the local mode phonons.

Analyses of the crystal field splittings for the $^3H_4$, $^1D_2$ and $^3P_1$ multiplets yield crystal field parameters for the fluoride, hydrogen and deuterium C_{4v} sites. These parameters may be compared with those found for the F^-C_{4v} sites of Ce^{3+}, Nd^{3+} and Er^{3+} by Freeth et al.[2] and for the H^- C_{4v} site of Er^{3+} by Edgar et al.[3]

The changes in crystal field parameters in going from the F^- C_{4v} to the H^- C_{4v} sites and along the rare-earth series in both CaF_2 and SrF_2 are accounted for by a superposition model of the crystal field. The small

* On leave: National Research Council, Division of Physics M36/150, Ottawa, Ontario, Canada KIA OR6.

difference in the parameters between the hydrogenic and deuterium C_{4v} sites is due to the electron-local mode phonon interaction and is explained on a point charge model, as was done for Er^{3+} by Edgar et al.[3]

Thompson[4] identified six distinct hydrogenic sites in $CaF_2:Er^{3+}$ by laser selective excitation methods. Similar measurements being done for $CaF_2:Nd^{3+}$ and $CaF_2:Pr^{3+}$ will be reported. The different equilibria found for hydrogenic sites for different rare-earth ions and for either CaF_2 or SrF_2 will be discussed.

The $SrF_2:Pr^{3+}$ system has two near coincidences of its transitions with argon laser lines. The application of these near coincidences for high resolution laser studies will also be discussed.

1 A. Edgar, C.A. Freeth and G.D. Jones, Phys Rev B15 5023-37 (1977)

2 C.A. Freeth and G.D. Jones, J Phys C 15, 6833-49 (1982)

3 A. Edgar, G.D. Jones and M.R. Presland, J Phys C 12, 1569-85 (1979)

4 D. Thompson, M.Sc. Thesis (University of Canterbury, 1983) unpublished.

Laser Induced Defect Centers in $Ce^{3+}:CaF_2$

G. J. Pogatshnik, S. K. Gayen, D. S. Hamilton
Department of Physics and Institute of Materials Science
University of Connecticut
Storrs, Connecticut 06268

Upon irradiation of a 1.3 mm thick sample of 0.05% $Ce^{3+}:CaF_2$ with the 308 nm emission of a XeCl excimer laser, we have observed coloration of the crystal by laser induced defect centers. The absorption spectrum of the induced centers is broad band and peaks at about 500 nm. The defect center has been associated with the excitation of cerium ions in the crystal. By irradiating with a 351 nm laser of comparable intensity, no coloration was produced. The centers are only created if one pumps into the 4f to 5d absorption band of the cerium ions in near resonance with 308 nm.

The coloration was found to be photo-reversible and can be bleached out by illumination into the broad absorption bands of the center. This bleaching has been observed with 532 nm and 633 nm laser emission as well as white light. The bleaching can also be induced by the 5d to 4f luminescence of the Ce^{3+} ions.

To measure the creation kinetics of the defect, we monitored the absorption coefficient at 633 nm as a function of the number of incident 308 nm laser pulses. The output power of the He-Ne laser was reduced to 10 nW to insure that the bleaching due to

the probe was negligible. By varying both the incident energy and the spot size of the 308 nm beam, we were able to determine that the creation rate depends linearly on the 308 nm intensity, as shown in the accompanying figure. Here we have plotted the defect center absorption after a single 5 nsec 308 nm pulse versus the intensity of the pulse. After subsequent irradiation, the defect center density continues to grow until it saturates at a steady state value. In the range of incident intensity from 15 to 55 MW/cm^2, the saturation absorption value depends very weakly on the intensity.

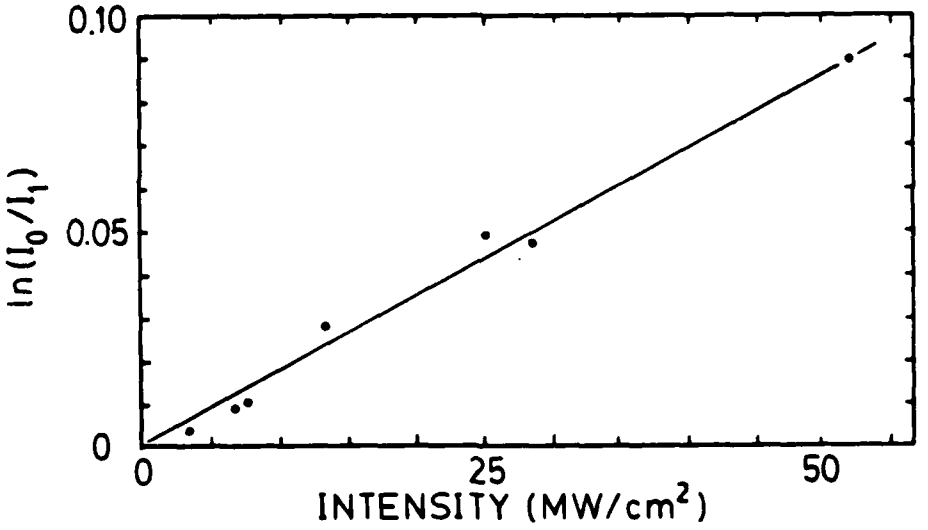

The measurements of the growth of the defect centers agree well with a creation mechanism involving the Ce^{3+} excited state. On absorption of a 308 nm photon, the cerium ion is promoted from its 4f ground state to the lowest 5d state. The creation of a defect center is an alternate relaxation mechanism to the 5d to 4f fluorescence.

R. J. Abbundi and V. K. Mathur

Naval Surface Weapons Center

White Oak, Silver Spring, MD 20910

The effects of radiation on rare earth doped calcium fluoride have been the subject of a number of investigations in the past two decades. Merz and Pershan[1,2] have shown that these materials undergo a charge conversion of $RE^{3+} \longrightarrow RE^{2+}$ when subjected to gamma or x-ray radiation at low temperature. The fluorescence spectra of Sm^{2+} in CaF_2 has been examined using optical excitation[3] and Sm^{3+} has been observed in x-irradiated CaF_2.[1,2]

In this work we report on an extensive investigation of the temperature dependence of the fluorescence spectra of x-ray excited CaF_2 doped with approximately 0.1% Sm. This work encompasses a larger spectral region (530-820 nm) and temperature range (15-666 K) than has previously been reported. The data was taken using a microcomputer based Si-diode array. This system allows for the simultaneous acquisition of the entire fluorescence spectrum of both Sm^{2+} and Sm^{3+} and thus permits a very rapid accumulation of data.

The experimental results show emission lines corresponding to both Sm^{2+} and Sm^{3+} existing at the same temperature. At 15 K, the Sm^{2+} emission[3] consists of a very narrow and intense line at 708 nm positioned on the edge of a broad band which extends to about 820 nm. Although the Sm^{2+} emission dominates the spectrum, there also exists three groups of lines centered near 568, 607 and 641 nm, corresponding to Sm^{3+} emission. As the temperature is raised, the 708 nm line decreases in intensity and by 115 K is indistinguishable from the broad band. The band itself is not detectable above 300 K. The Sm^{3+} emission lines remained fairly constant in intensity between 15-80 K but then increased by a factor of about 2, in the temperature region of 80-150 K which also contains a series of glow peaks for CaF_2:Sm.

Further increases in temperature caused a reduction in their intensity. The relative intensity of the emission lines depended upon the temperature and a broadening of the lines took place as the temperature was increased. These two effects result in a complex evolution of the spectra as the temperature changes between 15-666 K.

Finally, the crystal was subjected to a dose of 10^6 rad of gamma radiation from a ^{60}Co source in order to charge convert Sm^{3+} to Sm^{2+}. This dose changed the crystal from transparent to a green color, indicating that charge conversion had occurred. This is further supported by the appearance of additional absorption bands.[4] Then the experiment was repeated. In spite of this conversion, only small changes were noted in the temperature evolution of the fluorescence spectra.

1. J. L. Merz and P. S. Pershan, Phys. Rev. 162, 217 (1967).
2. J. L. Merz and P. S. Pershan, Phys. Rev. 162, 235 (1967).
3. D. L. Wood and W. Kaiser, Phys. Rev. 126, 2079 (1962).
4. G. A. Royce, V. K. Mathur, R. J. Abbundi, M. D. Brown, J. J. Fontanella and M. C. Wintersgill, J. of Luminescence, to be published.

Cooperative Optical Transitions in $CaF_2:Yb^{3+}$

H. Y. Zhang, R. T. Brundage, and W. M. Yen

Dept. of Physics, Univ. of Wisconsin-Madison, Madison, WI 53706

It has been shown that Yb^{3+} ions in crystalline hosts can exhibit optical transitions involving pairs of ions, either two Yb^{3+} ions[1] or Yb^{3+} paired with another rare earth, such as Gd^{3+},[2] or upconversion processes involving a number of Yb^{3+} ions.[3] We have studied such transitions in CaF_2:Yb using tunable laser spectroscopy.

Figure 1 is an energy level diagram showing the various excited states of Yb^{3+} in CaF_2. By tuning a narrow band pulsed dye laser through the spectral region corresponding to the sum of the energies of the different combinations of excited pair states, cooperative absorption was observed by monitoring the fluorescence of the resultant excited single ions, as shown in Figure 2.

Single ion absorption spectra indicate that the strongest transitions at this concentration are associated with the cluster sites, while in the pair excitation spectra the cubic-vibronic combination gives rise to the strongest transition. The excitation of single Yb^{3+} ions using a narrow band color center laser results in cooperative luminescence transitions. These cooperative processes will be discussed.

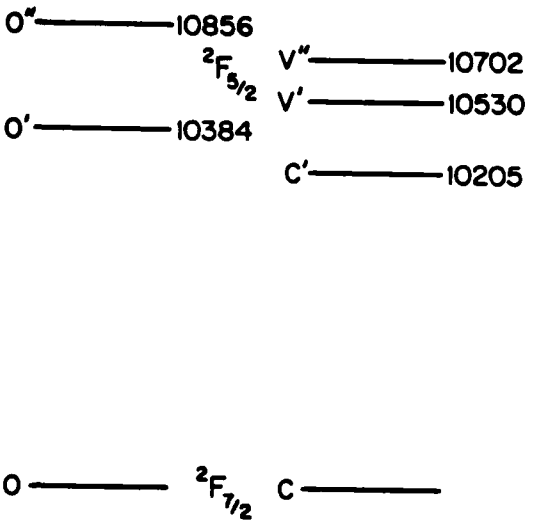

Figure 1. Energy level diagram of Yb^{3+} in CaF_2, with sites labeled O having cubic symmetry, C corresponding to ion cluster sites and V corresponding to vibronic sidebands of the cluster sites.

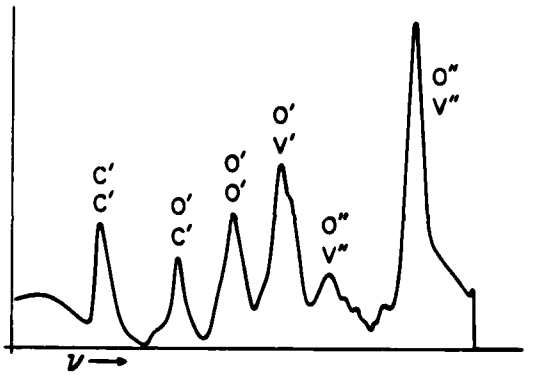

Figure 2. Excitation spectrum of 10 wt.% Yb^{3+} in CaF_2, with the site symmetry of the two excited states labeled as in figure 1. Energies corresponding to the cooperative absorptions are: $O''V^1 = 21,354cm^{-1}$, $O'V^1 = 20,935cm^{-1}$, $O'O^1 = 20,774cm^{-1}$, $O'C^1 = 20,630cm^{-1}$, and $C'C^1 = 20,407cm^{-1}$.

References

1. Eiichiro Nakazawa and Shigeo Shionoya, Phys. Rev. Lett. 25, 1710 (1970).

2. Eiichiro Nakazawa, J. Lumin. 12/13, 675 (1976).

3. F. Auzel, Compt. Rend. 263B, 819 (1966).

4. R. T. Brundage and W. M. Yen, Bull. Am. Phys. Soc. 29, 298 (1984).

Two-Photon Excitations of Higher 5d States in $Ce^{3+}:CaF_2$

S. K. Gayen, G. J. Pogatshnik and D. S. Hamilton
Department of Physics and Institute of Materials Science
University of Connecticut, Storrs, Connecticut 06268

The 4f-->5d near-ultraviolet transitions in $Ce^{3+}:CaF_2$ are dipole allowed in one-photon absorption (OPA) and first-order parity-forbidden for two-photon absorption (TPA). A relaxation of the parity selection rule due to odd crystal-field components has previously been observed[1] in the TPA from the 4f ground state to the lowest 5d state. In this paper the TPA measurements are extended to include transitions to the higher 5d states.

The two-photon excitation spectrum at 77 K from 590 to 398 nm for a 0.1% $Ce^{3+}:CaF_2$ sample is shown in the figure. The

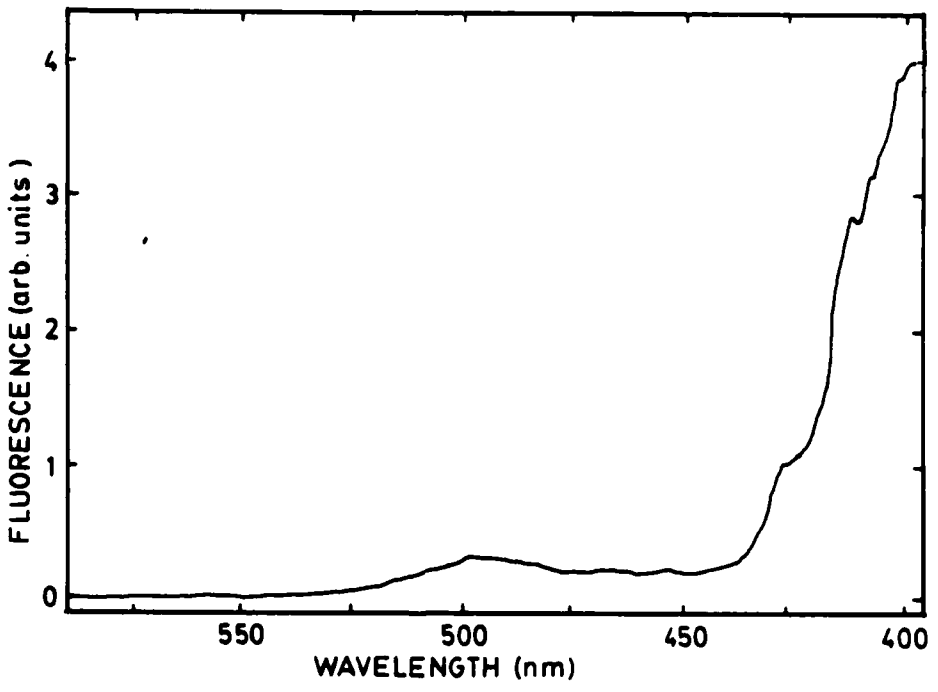

dye-laser light was incident along the (100) and polarized along

the (010) axes. The experimental apparatus is similar to that used before[1], except for additional narrow band UV interference filters used to minimize the elastically scattered light reaching the detector. However, a very significant amount of signal is also lost in the process.

The strong two-photon signal in the 410-400 nm range corresponds to the E and F bands in the OPA spectrum[2] and thus are due to TPA transitions from the ground state to these high-lying 5d states. This, in turn, implies strong crystal-field parity mixing of the 5d states. Of the five expected 5d bands, only four are observed in OPA with the fifth predicted[2] to peak around 280 nm. At the corresponding wavelengths for the TPA transition the predicted band is not observed either. However, a weak, broad band does appear at 500 nm, whose origin may be attributed to the 4f-->5d transition not observed in OPA. Of the two bands originating from cluster-ion cerium absorption in OPA, only the one at 210 nm is observed with comparable strengtn at the corresponding position in the TPA spectrum.

For a 0.003% concentration sample dominated by the C_{4V} center, similar spectra are observed for the electronic bands. However, a number of sharp resonance lines appear between 469 to 463 nm. The two-photon nature of these resonance lines, originating from other impurity centers, has been verified.

1. S. K. Gayen and D. S. Hamilton, Phys. Rev. B28, 3706 (1983).

2. W. J. Manthey, Phys. Rev. B 8, 4086 (1973).

Site Selective Laser Spectroscopy of Defects in $SrCl_2:Eu^{3+}$

John W. Wietfeldt and John C. Wright

Department of Chemistry, University of Wisconsin

1101 University Avenue, Madison, Wisconsin 53706

When fluorite crystals, such as CaF_2, are doped with trivalent rare earth ions, interstitial fluoride ions are known to provide charge compensation. The fluoride interstitial can exist either in association with a dopant ion, perturbing its electronic state, or in a distant position where the dopant site symmetry becomes cubic. Dimers, as well as higher order clusters, have also been observed.[1]

The distribution of defect sites has previously been measured as a function of dopant concentration and annealing temperature, and differs from the accepted simple model of defect equilibria.[2]

$SrCl_2$ is an interesting material to study because it crystallizes in the fluorite structure, but contains no fluoride ions. The small size and high electronegativity of the fluoride ion result in the anomalous behavior which often characterizes the chemistry of the fluoride materials, and might also result in the observed anomalous distribution of defects. Observation of the defect equilibria in doped $SrCl_2$ provides a test of the fluoride's role in the anomalous behavior.

Site selective spectroscopy is used to monitor the defect chemistry. The observed sites are classified into two categories on the basis of the Eu^{3+} $^5D_1$ manifold lifetimes. Cluster sites exhibit short $^5D_1$ fluorescence lifetimes due to rapid pair relaxation processes while single Eu^{3+} ions can only relax non-radiatively through multi-phonon processes.[3] Clusters are also distinguished in that they increase with dopant concentration relative to the other sites.

Section rules which forbid several transitions for the cubic site allow further separation of the single ion sites into cubic and associated ion sites.

Nine major sites have been classified in $SrCl_2$ Eu^{3+}; six clusters, a cubic, and two associated single ion sites. The concentration of cubic ions increases with dopant concentration relative to the associated single ions in the range, .01% to .3% Eu^{3+}.

These observations are consistent with those made previously on fluorite crystals containing fluoride, but cannot be explained by simple mass action equilibria relationships. They provide strong evidence that the size and electronegativity of the fluoride ion are not responsible for the anomalous defect chemistry of the fluorites.

[1]D. R. Tallant, D. S. Moore, J. C. Wright, J. Chem. Phys. 67, 2897 (1977).

[2]D. S. Moore, J. C. Wright, J. Chem. Phys. 74, 1626 (1981).

[3]D. R. Tallant, M. P. Miller, J. C. Wright, J. Chem. Phys. 65, 510 (1976).

New computed radiography utilizing photostimulated luminescence of $BaFX:Eu^{2+}$ (X=Cl,Br,I) phosphors

Junji Miyahara, Kenji Takahashi, Hisatoyo Kato
Fuji Photo Film Co.,Ltd., Technology Development Center,
Miyanodai,Kaiseimachi,Ashigarakamigun,Kanagawa,258 Japan

New computed radiography utilizing the phenomena of photostimulated luminescence (PSL) was developed to resolve the essential problems of the conventional radiography utilizing the intensifying screen-film combination. The basic constituents of the system are "Imaging Plate", in which photostimulable phosphors are used as the memory material for temporarily storing X-ray image; "Image Reader", which converts the latent image on the plate into digital time-series signals; "Image processor", which manipulates the image digitally with a high speed computer; "Image Recorder", which records the processed signals on a photographic film. The plate can be used repeatedly to store X-ray image simply by flooding it with light to erase the residual energy.

We made a search for the phosphor to realize the computed radiography, and found that $BaFX:Eu^{2+}$ (X=Cl,Br,I) phosphors have suitable properties. Fig.1 and Fig.2 show the stimulation and PSL spectra respectively.[1)] In the case of X=Br, the most favorable characteristics are obtained. The merits of this phosphor are as follows;

1)Stimulation spectrum peaks at around 590 nm to use He-Ne laser.

2)Emission spectrum peaks at 390 nm where photomultiplier tube has high quantum efficiency and the separation between stimulation and PSL spectrum is suitable for the system.

3)Response time of PSL is 0.8 μsec which permits the high speed reading of image on the plate by laser scanning.

4)Dynamic range of PSL is more than 10^5 to accommadate a wide range of radiographic exposures.

5)High X-ray absorption to decrease X-ray quantum noise.

6)High speed for erasing the residual energy in the phosphor.

7)High chemical stability in usual practical use.

The new system has been used in clinical research at several hospitals in Japan for more than three years. Many advantages compared to the screen-film system are revealed, that is,(1)Exposure dosage can be down about from 1/10 to 1/100. (2)Digital image processing techniques can improve the more diagnostic information.

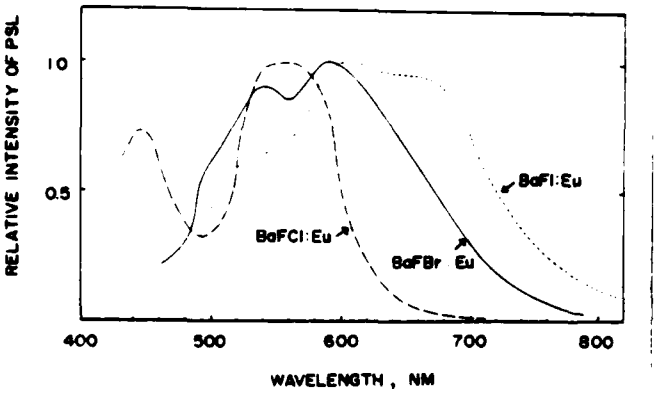

Fig.1 Stimulation spectra

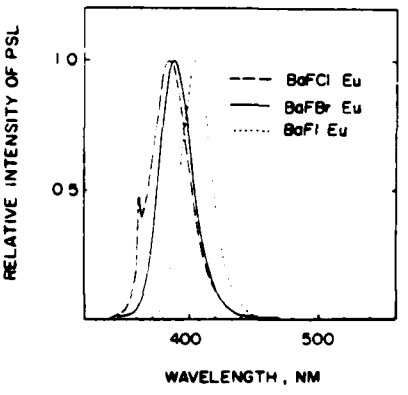

Fig.2 PSL spectra

1)M.Sonoda,M.Takano,J.Miyahara,H.Kato, Radiology 148(1983)833

CATHODOLUMINESCENT CONTRAST OF DIRECT WRITING PATTERNS MADE BY THE SCANNING ELECTRON MICROSCOPE

G.V.Saparin, S.K.Obyden, M.V.Chukichev, S.I.Popov

Moscow State University, Moscow 117234, USSR

An increase of quantum yield under action of electron beam on the i-layer of GaN:Zn structure and $KMgF_3$ crystals have been observed(1,2). By means of the SEM we have been studied the plastic scintillators, CdS, ZnO and GaN:Zn-layers on the sapphire. Long time kinetic of the CL for all above materials was taken by the SEM "Stereoscan MK IIA" equipped by luminescent attachments. The CL contrast of direct writing patterns made by e-beam in the SEM was also analized. The fig.1 shows normalized dependences of CL intensity on the e-beam irradiation time under room temperature. The CL kinetic for plastic scintillators and CdS are described by curve 1. A possible mechanism of CL decreasing is a degradation of materials under local temperature action and defects creation that increases the concentration of nonradiative centers. A CL intensity variation for ZnO crystal did not observed(curve2). The curve 3 shows GaN:Zn -kinetic function for CL. The evolution of the CL was studied when an e-beam is fixed on a point of specimen. The increase of quantum yield and a very long life time of nonequilibrium state induced by e-beam are specific for last material. Such peculiarity allows by the SEM in CL mode to separate activated and nonactivated regions with contrast factor in the range of 30-100%. Above noted phenomena as result of e-beam action on media are non reversible and therefore the CL patterns by means of the SEM are available. Comparing the contrast(K) for three above cases one can seen that $K=(I^{ir}-I^{nir})/I^{nir} \lesseqgtr 0$ (fig.2a,b), where I^{ir} is CL intensity of irradiated areas previousely, I^{nir} is CL intensity of nonirradiated areas previousely. The patterns on the plastic scintillators and CdS look like dark lines($K<0$) on the light field(fig.2a). The contrast patterns on ZnO crystals is absent($K=0$). In this case the e-beam action effect is reversible with relaxation time smaller than 10^{-6} s. For GaN:Zn layer $K>0$(fig.2b) and when I^{ir} attains a maximum the K-value can reach the factor of 100. Besides the previousely irradiation areas of GaN:Zn-layer

having $I^{ir} \gg I^{nir}$ keep the contrast under room temperature up to date more 24 month(for T=0-10°C over 10 year).Minimum sizes of luminescent patterns elements(lines,spots) are equal to 0,5-0,6 mkm. Patterns do not change own geometry in time. The limit of spatial resolution is determined by the volume occupied by scattered electrons of the primary beam.The direct writing and reading information by e-beam are available with digital and analogue modes.Writing density is over 10^8 bit/cm^2.No change in the luminescent spectrum of GaN:Zn before and after e-beam action on layers was detected. The CL intensity is only varied.We suggest that the luminescence changes vs the irradiation time are due to possible generation of new radiative recombination centers in the volume.

1.Saparin G.V. and oth.Bulletin of Moscow State Univ.ser.phys. astronomy,v.24,No.3,p.56-59(1983).

2.Saparin G.V. and oth.Preprint No.06/1983,Physical Faculty of Moscow State Univ.

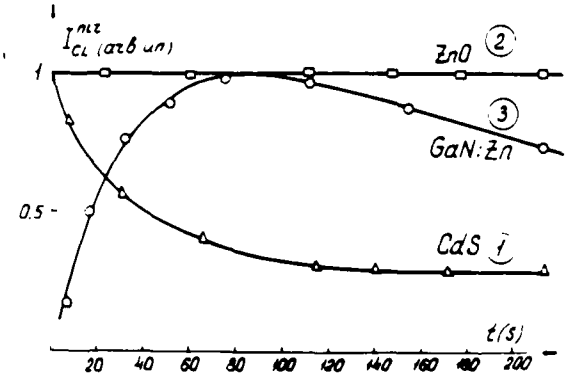

fig.1

fig.2a

fig.2b

Fig.1 Normalized dependences of CL intensities vs the electron beam irradiation time for nonirradiated areas previousely for CdS(1),ZnO(2) and GaN:Zn(3).E=20keV,i(e-beam)=1nA, Ø(e-beam)=0,08mkm.

Fig.2 Direct writing CL-patterns. Both recording and reading were made by means of the SEM in CL mode. Parameters of electron beam are above.

a. material is plastic scintillator. Width of dark line is equal to 5 mkm. (K < 0).

b. material is GaN:Zn layer. Width of light line is equal to 1mkm, (K > 0).

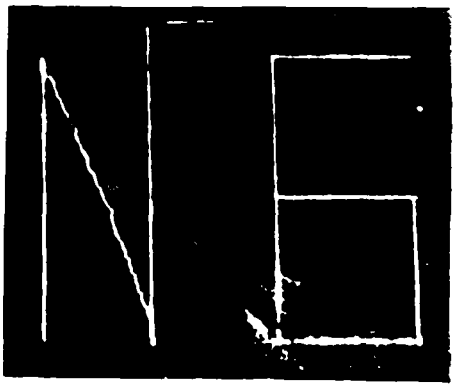

Nonlinearity of the cathodoluminescence intensity of ZnS-type phosphors.

D.M. de Leeuw
Philips Research Laboratories, 5600 AJ Eindhoven,
The Netherlands

Summary

The cathodoluminescence of ZnS-type phosphors shows a sublinear increase with increasing excitation density. The widespread use of these phosphors in cathode-ray (CR) tubes has led to many investigations on this so-called saturation behaviour (1,2). However, these studies have not resulted in a satisfactory understanding of the observed saturation phenomena for two reasons.

Firstly, all reported experiments were performed under pulsed excitation. The steady state was not reached. Interpretation of the measurements then requires a time-dependent solution of coupled rate equations describing in detail the energy flow in the phosphor.

Secondly, only saturation effects of ZnS:Cu,Al and ZnS:Ag have been reported. The decay of the luminescence of these phosphors depends strongly on both activator content and excitation density. However, a change in decay due to a change in excitation density cannot unambignously be assigned to the occurence of Auger type energy loss processes as proposed in ref (1,2), because the luminescence

mechanism is not sufficiently understood. To circumvent these problems the saturation of ZnS:Tm,Li phosphors was investigated under both pulsed and stationary CR excitation and analysed according to ref. (3). The decay of the main emission at 477 nm is exponential and independent of both Tm content and excitation density. Auger-type energy-loss processes related to excited Tm^{3+} ions therefore can be disregarded. From luminescence saturation measurements at various pulse durations it is concluded that Auger-type energy-loss processes in the ZnS host lattice can be disregarded too.

The measured saturation effects cannot be all explained by taking only ground-state depletion of one kind of luminescent Tm centres into account. At least two types of Tm^{3+} ions with different cross sections for capture of electron-hole pairs are involved. Taking two types of Tm^{3+} ions, and by adjusting the ratio of capture cross sections and concentrations both the ligth output under pulsed and stationary excitation as well as the risetimes as a function of excitation density can quantitatively be interpreted. The dependence of the saturation effects on Tm content can plausibly be explained by associating the two types of luminescent centres with close and distant Tm-Li pairs. This interpretation also explains our as well as reported (1,2) saturation data for ZnS-type phosphors like ZnS:Cu,Al and ZnS:Ag.

(1) S. Kuboniwa, H. Kawai and T. Hoshina, Jap. J. Appl. Phys. 19 (1980) 1647

(2) J. McColl, J. Electro Chem. Soc. 129 (1982) 1546

(3) D.M. de Leeuw and G.W. 't Hooft, J. Lum. 28 (1983) 275

Systematic analysis of phosphor degradation under cathode-ray excitation.

D.B.M. Klaassen, D.M. de Leeuw
Philips Research Laboratories, 5600 AJ Eindhoven,
The Netherlands
and T. Welker, Philips Research Laboratories, 51 Aachen, FRG

Summary

The external radiant efficiency of phosphors generally decreases under prolonged cathode-ray (CR) excitation. This so-called degradation effect is of great technological importance because it limits the lifetime of CR displays. The deterioration mostly increases with increasing excitation density. Thus, for applications at high density, such as projection television tubes, degradation is expected to be a major selection criterion for the phosphor.

The external radiant efficiency, η_{cr}, can be given by [1]:

$$\eta_{cr} = \frac{E}{\varepsilon} \eta_t \eta_{act} C_{extr} \qquad (1)$$

where E is the average energy of the emitted photons, ε is the average electron-hole pair creation energy, η_t, is the quantum efficiency for transfer of energy from electron-hole pairs to activators (the transfer efficiency), η_{act}, is the quantum efficiency of the luminescence process in the activators (the activator efficiency); C_{extr} accounts for

selfabsorption of the generated luminescence. Degradation effects are due to changes in physical properties which have impact on one or more of the parameters of eq. (1). For instance, formation of colour centres leads to an increased selfabsorption, formation of a non-luminescent surface layer and of bulk killers leads to a decreased transfer efficiency, and a disturbance of luminescence centres can lead to a decreased activator efficiency. These effects are known to be important from studies on phosphor depreciation in fluorescent lamps [2] and can be important for depreciation under CR excitation as well.

We show that by measuring and analysing the reflection at the emission wavelength, the decay of the luminescence, the efficiency as a function of the accelerating voltage, and the saturation of the luminescence of both the unexposed and deteriorated phosphor the contributions to the loss in efficiency of each of the parameters appearing in eq. (1) can be disentangled.

As an illustration deterioration of several phosphors is discussed. The degradation is shown to be dominated by the formation of a dead surface layer for monocrystalline Zn_2SiO_4:Mn at 77 K, by formation of colour centres for Eu^{2+} activated aluminates and by the formation of bulk killers in the host lattice for Y_2SiO_5:Ce.

(1). D.M. de Leeuw and G.W. 't Hooft, J. Lum. 28(1983)275.
(2). W. Lehman, J. Electro. Chem. Soc. 130(1983)426.

Soft X-ray Emission Excited by Electron Beams in a Superlattice

A. E. Kaplan and S. Datta
School of Electrical Engineering
Purdue University
West Lafayette, IN 47907

Fast moving electrons emit FM waves when passing through a spatially periodic medium (resonant transition radiation).[1,2] The wavelength λ of the radiation emitted at an angle θ with respect to the electron trajectory is determined by the formula $\bar{n}(\lambda)\cos\theta = \beta^{-1} - r\lambda/\ell$, where $\beta = v/c$ is dimensionless speed at the electron, $\bar{n}(\lambda)$ is averaged refractive index of the system, r is an integer, and ℓ is the period of spatial modulation. It is conventionally assumed that ultra-relativistic beams (e.g., up to 50 GeV[3]) are required to attain this kind of emission. We show[4] that if the period ℓ is much shorter than a "mean" plasma wavelength of the medium λ_p, (which can be done by using solid-state superlattices with the spatial period 50–200Å), the critical kinetic energy required to get a radiation, turns out to be extremely low. One can show that when parameter $Q = r\lambda_p/\ell \gg 1$, this energy is $(eU)_{cr} \simeq mc^2/2Q^2$, which is less than 10 KeV for all conventional materials if $\ell \simeq 100$ Å. One can get a significant radiation in the range 10Å–300Å using non-relativistic beams with energies 70–300 KeV. The spontaneous radiation from the system has a conical structure with the emission wavelength changing with angle. A single nonrelativistic electron traversing multilayer structure with N layers radiates energy I in a solid angle $d\Omega$ in the frequency interval between ω and $\omega + d\omega$,[1,2]

$$d^2I_o/d\Omega d\omega = e^2\beta^2[\Delta\epsilon(\omega))]^2\sin^2\theta\sin^2(\pi r\ell_1/\ell)\sin^2(\xi N/2)/\sin^2\xi\cdot\pi^2c \qquad (1)$$

where $\xi = (\beta^{-1} - \bar{n}\cos\theta)\pi\ell/\lambda$, ℓ_1 is the thickness of the first layer, and $\Delta\epsilon = \lambda^2(\lambda_1^{-2} - \lambda_2^{-2})$, λ_1 and λ_2 are the plasma frequencies of the respective layers. If the number N of layers is sufficiently large, $(N \gg |\bar{n}/\Delta\epsilon|)$, Eq(1) provides for very narrow spectral peaks of radiation for each particular angle θ [with central wavelength $\lambda \simeq \ell r^{-1}(\beta^{-1} - \cos\theta)$]. The total radiation power I in each order r per electron is

$$I \simeq 16e^2 L \ell^2 (\lambda_1^{-2} - \lambda_2^{-2})^2 \sin^2(\pi r \ell_1/\ell)/3\beta r^4 \pi \qquad (2)$$

the wavelengths of radiation being in the range $\ell r^{-1}(\beta^{-1}-1) < \lambda < \ell r^{-1}(\beta^{-1}+1)$. ($L = N\ell/2$ is the total thickness of the structure). If $\ell = 100$Å, $\ell_1 = \ell_2 = \ell/2$, $L = 1\mu$m, $eU = 75$KeV, $J = 1$mA where J is the total current, and $\lambda_1 \simeq 400$Å, $\lambda_2 \simeq 800$Å, the system can provide a radiation of first harmonic ($r = 1$) with a total power ~ 0.1 mW and a mean wavelength ~ 200 Å. If the total current density i is sufficiently large, the system can provide stimulated emission and amplification. The maximal EM wave amplification per pass is

$$\Gamma = 8\lambda^5 \ell^{-1}(\lambda_1^{-2} - \lambda_2^{-2})^2 (\cos\theta + r\lambda/\ell) ieRL^3 \sin^2(\pi r \ell_1/\ell) \sin^2\theta / mc^2 \ell \pi^4 \cos\theta, \qquad (3)$$

where $R = 377\ \Omega$ is the vacuum impedance. The required current density i is as high as $\sim 10^{10}$–10^{11} A/cm^2 in order to obtain a considerable gain (~5%), in the range ~ 100Å. With the mirrors situated outside the superlattice to form a Fabry-Perot resonator to provide feedback, the system becomes a short-wave laser. The amplifiers and lasers based on the proposed principle should work in the very short pulse regime of operation, with the duration of current pulse being determined by the heating, ionization, diffusion of absorbed electrons, etc. We consider also two-dimensional periodical structures (e.g., very thin dielectrical cylinders periodically located in vacuum) which provide an opportunity to get a much longer propagational path of electrons and at the same time to reduce absorption of radiation. This can drastically reduce a required current density of an electron beam and eliminate heating and other related problems.

1. V. L. Ginzburg and I. M. Frank, Zh. Eksp. Theor. Fiz., 16, 15 (1946) (in Russian).
2. M. L. Ter-Mikaelian, High Energy Electromagnetic Processes in Condensed Media, Wiley Interscience, New York, 1972.
3. M. A. Piestrup and P. F. Finman, IEEE J. of Quan. Elect., QE-19, 357 (1983).
4. A. E. Kaplan and S. Datta, Appl. Phys. Lett., 44, 1 April, 1984.

"1.5μm TO 0.65 m UP-CONVERSION BY "SUMMATION OF PHOTONS BY ENERGY TRANSFER" EFFECT IN DIODE PUMPED VITROCERAMICS".

G.F. de Sá, P.A. Santa Cruz, F. Auzel

Departamento de Química Fundamental e Departamento de Física - CCEN

UFPE, Cidade Universitária, 50000 - Recife - PE - BRASIL

APTE effect (Addition de Photons par Transferts d'Energie) in (Yb^{3+}, Er^{3+}) doped vitroceramics has been found to be a very efficient process to obtain up-conversion by summation of photons [1] [2] [3] [4].

Here we describe the obtention of an IRQC (Infra Red Quantum Counter) where APTE summation of 1.5μm photons (signal) with 0.95μm ones (pump) is obtained. The pump source is adequately a high efficiency GaAs: Si diode emitting 45mW at 0.95μm.

The signal source for the measurements is provided by a tungsten lamp and dieletric filter combination which gives optical concentration a power density of 10μW/cm² at 1.5μ. By analysing the different types of energy transfers which contribute respectively to signal, losses and noises, optimization of the Noise Equivalent Power (NEP) of the IRQC is obtained both with respect to pumping flux and composition. The pumping flux has to be carefully controled since signal is found to vary linearly with it, though losses and noises are found to vary quadratically. Due to the high efficienty of diffusions all processes involved, signal, losses and noises are APTE enhanced, contrary to previous systems where concentration where generally kept arround 1% [5],

which preduded difusion.

The best composition for the vitroceramics, the preparation of which has already been described [2], is found to be:

$$XPbF_2 + YGeO_2 + 10\% Yb_2O_3 + 5\% Er_2O_3$$

$$\text{with } (X+Y)/X = 1.46$$

For this composition a room temperature NEP of 10^{-11} $W/\sqrt{Hz}$ has been obtained for IRQC.

This figure can be favorably compared to the best figures published up to now for IRQC detection with lock-in detector: 3×10^{-9} x $W/\sqrt{Hz}$ in $BaY_2F_8:Er^{3+}$ at 1.5μ in which only sequential absorption is used without APTE enhancement.

REFERENCES

[1] F.Auzel, Proc. IEEE 61 758 (1973)

[2] F.Auzel, D.Pecile, D.Morin, J.Elect. Chem. Soc. 122, 101 (1975)

[3] Y.Mita, Appl. Phys. Lett. 39B 587 (1981)

[4] F.Auzel, W.de Azevedo, G.F.de Sã, "Proceeding International Conference on Lasers et Applications". Bucharest 10-15 Sept. 1982

[5] S.E. Stokowski, JAP 45, 2957 (1974).

A. Z. Genack, Exxon Research and Engineering Company, Clinton Township, Route 22 East, Annandale, NJ 08801

In this communication a method of electro-optic phase-sensitive detection is described. Phase-sensitive detection is exploited to suppress fluorescence which lags the modulated laser in phase while detecting Raman scattering, which is in phase with the excitation. In addition, ultra-fast phenomena may be studied using slow detectors by measuring the phase shift of the emission relative to the phase of the exciting laser light, which is modulated at high frequencies.

Phase resolution is achieved by passing the emission excited by an electro-optically modulated laser through a second electro-optic intensity modulator with adjustable phase relative to the first modulator. The light is then dispersed in a spectrometer and detected in an optical multichannel analyzer. Initial experiments were carried out with 30 MHz modulation. The laser modulator is a Lasermetrics 3030 ADP Pockels cell and polarization analyzer and the emission modulator is an SLM LM200 Sears-Debye acousto-optic modulator.

The phase lag of fluorescence, Φ, induced by light modulated at a radial frequency, ω, for a species with fluorescence decay time, τ, is given by $\tan \Phi = \omega\tau$ and the depth of modulation, m, is $m = (1 + \omega^2\tau^2)^{-1/2}$. For a single fluorescent species, for which τ is well defined, the fluorescence background is nulled by subtracting spectra detected $\pm 90°$ out of phase with the fluorescence. This corresponds approximately to being in and out of phase with Raman scattering. For multicomponent fluorescent decay, with decay times, τ_i, the phase lag may be forced to approach 90° by modulating at high frequencies, $\omega >> 1/\tau_i$ and the fluorescence may again be nulled. This makes

possible measurements of Raman scattering in cases where it is ordinarily swamped by fluorescence.

The method is demonstrated by suppressing fluorescence from 5 x 10^{-5} M fluorol 555, supplied by Exciton, while detecting Raman scattering from the toluene solvent. The results are shown in Fig. 1. The in phase spectrum taken with 35 mW of 4880 A light with an integration time of 100 sec is shown in Fig. 1a. The difference between the in and out of phase spectra for the CH stretching modes of toluene is shown in Fig. 1b and the spectrum of neat toluene is shown in Fig. 1c. Statistical noise associated with fluorescence is retained in the difference spectrum. The phase shift of fluorescence gives a lifetime of τ = 8.3 nsec for fluorol in toluene.

A microwave apparatus for phase-sensitive optical detection is presently under construction. Results with this device will be discussed.

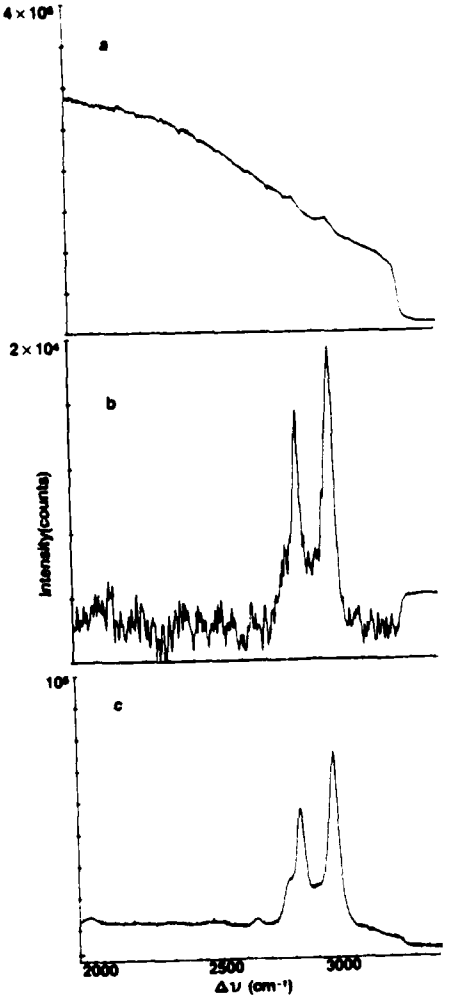

Figure 1

Spectra of 5 X 10^{-5} M fluorol in toluene excited with 35 mw of 4880 A light for 100 sec. a) in phase spectrum; b) difference between in and out of phase spectra displaying only Raman scattering; c) spectrum of neat toluene.

Frequency-Domain Phase-Modulation Fluorometry: Resolution of Complex Decays of Intensity and Anisotropy

Joseph R. Lakowicz[1], Enrico Gratton[2], Henryk Cherek[1] and Badri P. Maliwal[1]

1. University of Maryland School of Medicine, Department of Biological Chemistry, Baltimore, Maryland 21201, USA

2. University of Illionis, Department of Physics, Urbana, Illinois, 61801, USA.

We describe the use of frequency-domain phase-modulation fluorometry to determine time-resolved emission decay kinetics. Using newly constructed instruments (1,2) we measured the frequency-dependent phase angles and demodulation factors at frequencies ranging from 1 to 200 MHz. Such data were obtained for two and three-component mixtures of fluorophores. Two decay times were easily recovered if they differed by a factor of two, and a three-component mixture was resolved with decay times of 1.3, 4.4 and 12. nsec. Measurement at several emission wavelengths enhanced our ability to resolve closely spaced two and three-component decays.

We also used the frequency-domain measurements to construct time-resolved emission spectra of fluorophores in viscous solvents, and bound to proteins and lipid bilayers. We performed measurements on 2-p-toluidinyl napthalene sulfonic acid in propylene glycol and bound to apomyoglobin, and of 6-palmitoyl-2-[(2-trimethylamonium)ethyl] methylamino] naphthalene chloride bound to phospholipid vesicles. The frequency-domain data allowed these spectra to be calculated at times ranging from 0.1 to 120 nsec for a fluorophore with an average lifetime of 10 nsec. The data also allowed calculation of the time-resolved center-of-gravity and the time-resolved

spectral half-width. These results allowed us to distinguish continuous relaxation processes (3) from a stepwise process (4).

And finally, we measured the frequency-dependent phase angle differences between the parallel and perpendicular components of the polarized emission, and of the ratio of the polarized modulated amplitudes. These data were used to resolve the anisotropic depolarizing rotations of perylene in solvents and in lipids, as well as the hindered rotational motions of diphenylhexatriene in lipid bilayers.

In total, our results demonstrate that detailed time-resolved spectral data can be obtained by phase-modulation fluorometry, if a suitable wide range of modulation frequencies is available. In practice the measurements are simple and rapid, and the instruments appear to be remarkably free of systematic error. It appears likely that the future modifications will allow the upper frequency limit to be extended several-fold.

1. E. Gratton and M. Limkeman (1983), Biophysical J., 44, 315-324.

2. J.R. Lakowicz, unpublished observations.

3. N.G. Bakhshiev, Yu T. Mazurenko, and J.V. Piterskaya, (1966), Opt. Spectrosc., 21, 307-309.

4. J.R. Lakowicz and A. Balter (1982), Biophys. Chem., 16, 117-132.

Differential Lifetime Spectroscopy

D.J.S. Birch, R.E. Imhof and A. Dutch
Department of Applied Physics
University of Strathclyde
Glasgow, G4 ONG
Scotland.

The single photon correlation technique is now the most popular method of measuring fluorescence lifetimes.[1] Lifetime spectrometers traditionally use a single detection channel which necessitates consecutive measurement of the excitation pulse and fluorescence decay in separate experiments.[2] If the fluorescence decay is comparable to or less than the duration of the excitation pulse E(t) then the lifetime τ can be determined using reconvolution and a least-squares fit of F(t) to the decay using

$$F(t) = \int_0^t E(t') \exp - \frac{(t-t')}{\tau} \, dt'. \qquad (1)$$

Equation (1) is widely used but its validity depends passively on the stability of the excitation pulse profile. This stability cannot be guaranteed, even when using mode-locked lasers or the most stable flashlamps[3].

Differential techniques are widely used in spectroscopy to correct for variations in wavelength response and instabilities in the excitation source. However, they have so far been little used with the single photon method of measuring lifetimes.[4,5]

We have developed a differential spectrometer with dual detection channels for Simultaneous Acquisition of the Fluorescence and Excitation (SAFE).

If the excitation pulse profile changes during the experiment then the principle of linear superposition for j profiles can be applied to the matched detection channels 1 and 2, using equation (1).

$$\sum_j {}^2F_j(t) = \sum_j \int_0^t {}^2E_j(t') \exp - \frac{(t-t')}{\tau} \, dt' \qquad (2)$$

$$\sum_j {}^2F_j(t) = \int_0^t \sum_j {}^1E_j(t') \exp - \frac{(t-t')}{\tau} \, dt' \qquad (3)$$

Rather than relying passively on the stability of excitation equation 3 provides an automatic correction for changes in the excitation pulse profile.

Figures 1 and 2 illustrate the effects on fitting to the decay of PPO in ethanol caused by a sudden change in the excitation pulse when performing consecutive and simultaneous measurements.

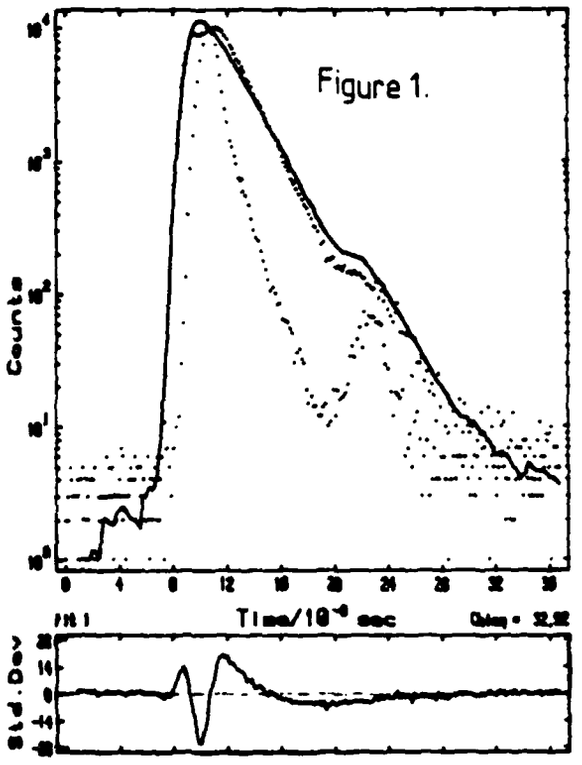

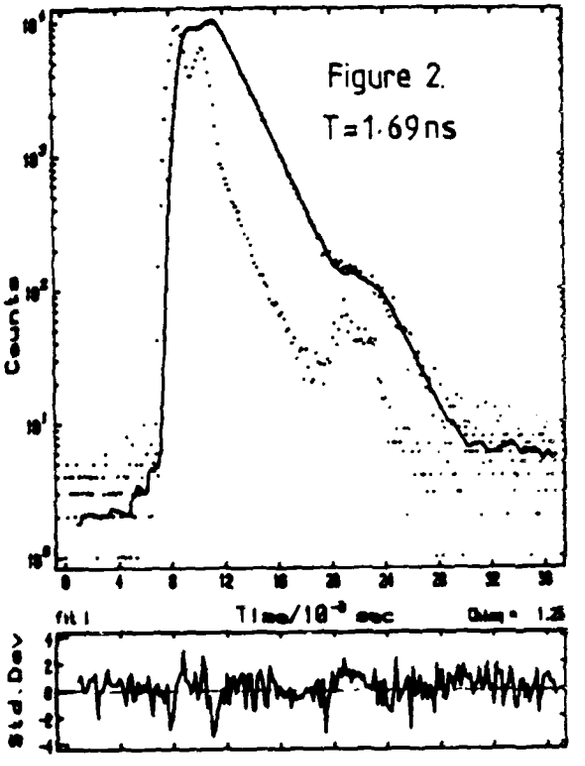

In figure 1 the convolution procedure is seen to be invalid whereas the simultaneous measurement of figure 2 gives a good fit.

SAFE techniques are potentially quicker, more precise and easier to use than conventional methods. Dual channel detection also has applications in the study of time-resolved emission anisotropy and wavelength dependent lifetimes. We will present data on the photophysics of scintillator systems which illustrate the advantages of these techniques.

1. D.J.S. Birch and R.E. Imhof, Euro. Spec. News. 48, 31 (1983).
2. W.R. Ware, in "Creation and Detection of the Excited State", ed. by A.A. Lamola (Dekker, New York, 1971). Vol. 1A.
3. D.J.S. Birch and R.E. Imhof, Rev. Sci. Instrum. 52, 1206 (1981).
4. R. Schuyler and I. Isenberg, Rev. Sci. Instrum. 42, 813 (1971).
5. R.W. Wijnaendts van Resandt, R.H. Vogel and S.W. Provencher, Rev. Sci. Instrum. 53, 1392 (1982).

H.G. Danielmeyer, Institute of Applied Physics, University of Hamburg,
Jungiusstr. 11, D-2000 Hamburg 36

E. Stark, Hochschule der Bundeswehr Hamburg,
Holstenhofweg 85, D-2000 Hamburg 70

Measurement of Quantum Efficiencies in Laser Crystals by Compensation Calorimetry

Nonradiative decay processes decrease the quantum efficiency and increase the pump threshold of lasers. We present a simple measurement method for quantum efficiencies adapted to the problem of small crystals of arbitrary shape and new results on sources of nonradiative decay.

Generally, quantum efficiencies can be measured by optical or calorimetric methods /1/. Optical spectroscopy entails solid angle and calibration problems, so that often comparisons with crystals of known quantum efficiency are preferred. The same must be said of photoacoustic measurements /2/. Knowledge of heat conductivity and heat capacity is essential for known calorimetric methods /3/. These parameters are not always available, especially for new crystals. Therefore, we developed a compensating calorimeter, which does not require knowledge of other parameters or spectral calibration.

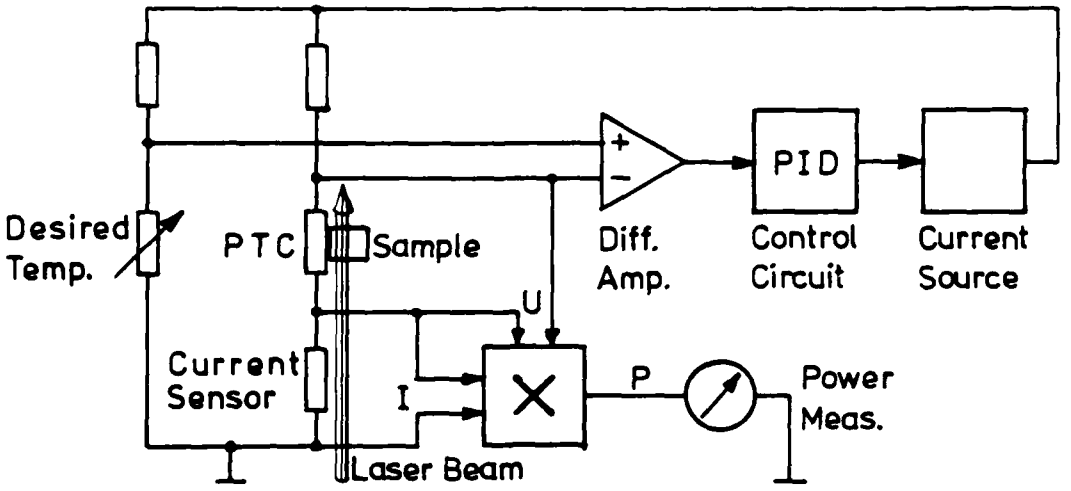

The sample is thermally connected with a resistor of positive temperature coefficient (PTC), forming one branch of a Wheatstone bridge. This bridge

is fed by a current capable of heating the PTC-resistor to about 50° C. The result is a constant heat flow from the resistor to its ambient. Bridge balance and PTC-temperature is kept constant by a PID control circuit. The electrical power dissipated in the PTC-resistor is measured by an integrated analog multiplier (P=U·I).

If now the crystal's active ions are excited by a laser beam heat is generated in the crystal and the temperature of crystal plus PTC-resistor rises. The control circuit restores bridge balance and PTC-temperature by diminishing the bridge current and the dissipated electrical power as well. The difference in electrical power equals the heat power generated in the crystal, i.e. the heat power is compensated in the calorimetric circuit by an electric power. For eliminating thermal drift problems the measurement can be repeated periodically by chopping the laser beam.

Measurement errors amount to $\pm$ 5 % ... $\pm$ 10 %, depending on the absorption coefficient of the crystal and on the geometry of the arrangement.

We present quantum efficiency measurements in $Nd_x Y_{1-x} P_5O_{14}$, $Nd_x La_{1-x} P_5 O_{14}$, Cr: $ZnWO_4$, Cr : GSGG, Ti : Al_2O_3 and in Nd-glass. In $YP_5 O_{14}$ we find considerable multiphonon decay ($1{,}5 \cdot 10^3 sec^{-1}$), which is lacking in LaP_5O_{14}. In both pentaphosphates the efficiency depends on the excitation intensity. A very strong temperature dependence is found in Ti : Al_2O_3. Concentration quenching is present in all systems. The different sources of decrease in quantum efficiency are separated by their concentration dependence.

Our first measurements have proved that our compensating calorimeter is a very reliable device. In spite of its simplicity it seems to be quite competitive with other much more complicated systems.

References

/1/ J.N. Demas et al. J. Phys. Chem. 75, 991 (1971)
/2/ A. Rosencwaig et al. Phys. Rev. B 23 3301 (1981)
/3/ G.A. Crosby et al. J. Res. Natl. Bur. Stand. 76 A 561 (1972)

Study of the Ambipolar Carrier Drift in Silicon by an Optical Time-of-Flight Method

B. Laurich, A. Forchel and T.X. Hoai[+]
Physikalisches Institut, Universität Stuttgart, Stuttgart, Germany
[+]Permanent address: Academy of Sciences of Vietnam, Hanoi, Vietnam

We present a new method to study the ambipolar expansion of surface excited plasma in Si, based on the time resolved detection of the luminescence of a doped layer opposed to the excitation area.

This novel time-of-flight technique is used to study directly the carrier transport below and above the critical temperature T_c=23K for electron-hole droplet (EHD) condensation. Previously studies of the movement of the EHD in Si have been limited by the lack of time resolution[1]. The same holds for the surface created plasma (EHP) above T_c for which a drift has been deduced indirectly by a line shape analysis of the EHP emission spectra[2].

Fig. 1 shows schematically the principle of our experiment. 200ps pulses of a mode-locked frequency-doubled Nd-YAG laser excite a high density plasma at the sample surface. The carriers pass through the sample and partially reach the doped layer where they are captured and recombine as bound excitons. The luminescence typical for the BE emission is recorded time resolved. From the known flight distance and the measured time delay to the excitation pulse the average velocity of the carriers is obtained.

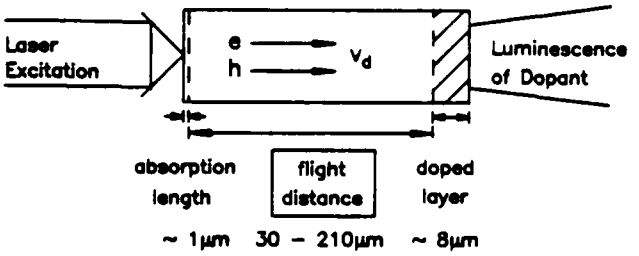

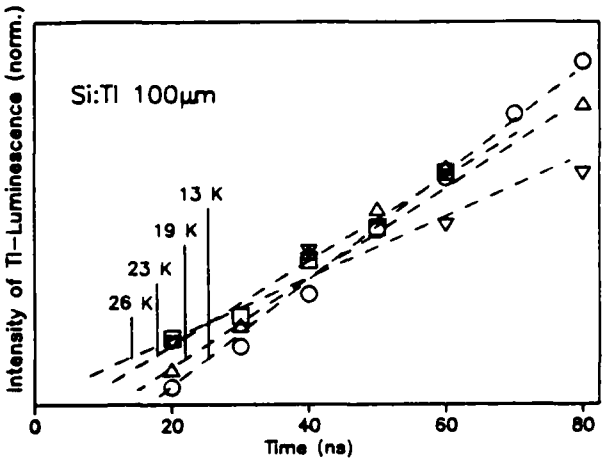

Fig. 2: Time dependent luminescence intensity of the Thallium bound exciton emission at different temperatures. The sample has a Thallium doped layer of 8µm thickness and a flight distance of 100µm.

We have studied the transport properties of the EHD and the EHP in Si as a function of temperature and excitation intensity.

In the temperature range below T_c and for thin samples (below 140µm) the maximum carrier velocities are $5.5 \cdot 10^5$ cm/s, i.e. very close to the speed of sound. With increasing sample thickness these velocities decrease corresponding to the increase of the phonon damping of the carrier motion. The velocities are consistent with the "phonon wind" propagation of the EHL.

For temperatures above T_c the carrier velocity obtained with this experiment is of the order of $1 \cdot 10^6$ cm/s, i.e. the carrier expansion is supersonic. Currently experiments with better spatial resolution (implanted layers of 0.3µm thickness) are under work.

The general advantages of our new time-of-flight method are:
- The intrinsic ambipolar expansion of the carriers is investigated without external perturbation such as strain or electric fields.
- No ad hoc assumptions or sophisticated theoretical model (such as a line shape analysis) are necessary to obtain the carrier velocity.
- Our method is not limited to Si. Rapid carrier expansion effects can be studied by this type of time-of-flight experiment in indirect gap and in direct gap semiconductors if appropriately thin spatial markers are prepared.

1. M.A. Tamor and J.P. Wolfe, Phys. Rev. B, 21, 739 (1980).
2. B. Laurich and A. Forchel, J. Physique, coll.C5, supp.10 (1983).

The effect of La substitution in Eu^{3+}-activated Y_2O_3 phosphors on their luminescent property.

Toyohashi University of Technology School of Materials Science
Tempaku-cho, Toyohashi, 440 Japan

The effect of impurity oxide on the luminescent property of yttrium oxide activated by Eu^{3+} was reported by Fuller[1]. In this report it was found that lanthanum oxide had no influence on the luminescent property of Eu^{3+}-activated yttrium oxide phosphor when 0.067m/o lanthanum oxide was added. Meanwhile the solid solution between Y_2O_3 and La_2O_3 is found to be stable till about 20 mol% of La_2O_3 between 700 and 1400°C.[2] We found that the addition of La_2O_3 to Eu^{3+}-activated Y_2O_3 made the intensity of luminescence under 2537Å stronger.

Starting materials were Y_2O_3, La_2O_3 and Eu_2O_3, and they were mixed in proper proportion, the mixture being fired at 1500°C for 3 hours. Emission intensity of phosphor was measured under 2537A excitation.

It was found that about 10 wt.% and more of La_2O_3 dissolved in the matrix of Y_2O_3 under exprimental condition cited above. The addition of La_2O_3 in the range of 15---20 wt% for Y_2O_3 resulted in the appearance of diffraction lines from La_2O_3 in X-ray diffraction patterns.

Figure shows the dependence of emission intensity of the phosphor on the Eu^{3+} concentration. In this experiment starting materials were prepared by alkoxide process, or coprecipitation process. They were dissolved in hydrochloric acid, then mixture of the methoxides was coprecipitated, or that

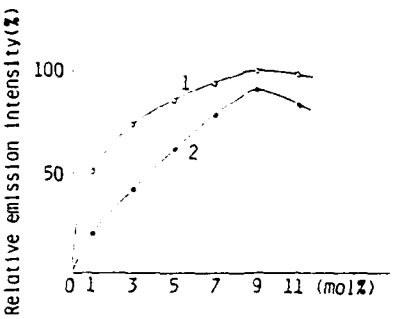

Fig.1 Dependence of emission intensity of Eu concentration.
1 : $(Y_{0.9}La_{0.1})_2O_3$:Eu
2 : Y_2O_3:Eu

of oxalate salts was precipitated by the addition of ammonium oxalate. In both cases $(Y_{0.9}\ La_{0.1})_2O_3$: Eu showed the stronger emission than Y_2O_3:Eu under 2537A excitation.

The dependence of emission intensity of $(Y_{1-x},\ La_x)_2O_3$ on x was found to have a maximum at x=0.1 when 9 mol% of Eu^{3+} was used as an activator. It is supposed that x would change with added amount of Eu^{3+}, as two oxides as well as Eu_2O_3 would form tertially the solid solutions. The lattice constant of $(Y_{1-x},\ La_x)_2O_3$ is found to increase with x till x=0.1, then to be constant. The particle size of the phosphor was 10μ or a little larger.

The emission intensity would be dependent upon the imperfection of the crystal lattice and in these phosphors the formation of solid solution would be preferable for the transition probability accompanying radiative transition.

Reterences

1) M.J.Fuller, J.Electrochem Soc., 128, 1381 (1981)

2) J.Cassedanne, H.Forestier, Compt.rend., 253, 2954 (1961)

ON SPECTRAL ENERGY DISTRIBUTION SHAPE OF FLUORESCENT LAMP PHOSPHORS

K.Narita

Toshiba R&D Center, 1 Komukai-Toshibacho,Kawasaki 210,Japan

Fluorescent lamp phosphors activated by complex ions(WO_4^{2-} etc.), s^2 configuration ions, Mn^{2+} or Eu^{2+} show broad band emissions. The spectral energy distribution(SED) shape for some selected phosphors has been discussed[1,2]. We report a more generalized observation on these phosphors to deduce the SED features inherent in each of the activators. Every observed SED was plotted in terms of $\sqrt{-\log(I/I_0)}$ vs. wavenumber to compare it with the Gauss error function(I:Energy,I_0:Maximum energy of SED). It is known that SEDs of tungstates match the Gauss curve extremely well[1]. Figure 1 shows that the SED plot for complex ion-activated phosphors gives straight lines with approximately the same slope, indicating the ions in this category have, in general, the Gaussian-shaped SEDs of similar halfwidth. In contrast, SEDs of s^2 ions deviates from the Gauss function at the high frequency side(Fig.2). This deviation tends to become smaller at lower temperatures. Further, by monitoring the high frequency side of the emission, a considerable difference in excitation spectrum is observed from that of the low frequency side. These results show that s^2 ions in the investigated phosphors have a common feature of yielding an emission with weak subband(s) on the high energy side of the main band. The most probable origin of these multiple emission bands is

the crystal field-split $^3P_1$ excited levels being in thermal equilibrium to each other.

Contrary to s^2 ions, both Mn^{2+} and Eu^{2+} exhibit SEDs with tailing into the low frequency region. This asymmetry may be due to the small Stokes shift in both of these activators.

References

(1)Brinkman,H. and Vlam,Chr.C., Physica 14,650(1949).

(2)Witzmann,H., Anderson,H.,Bajdala,H., Proc.Intern.Conf.Lum., 1342,1360,1365(Budapest 1966).

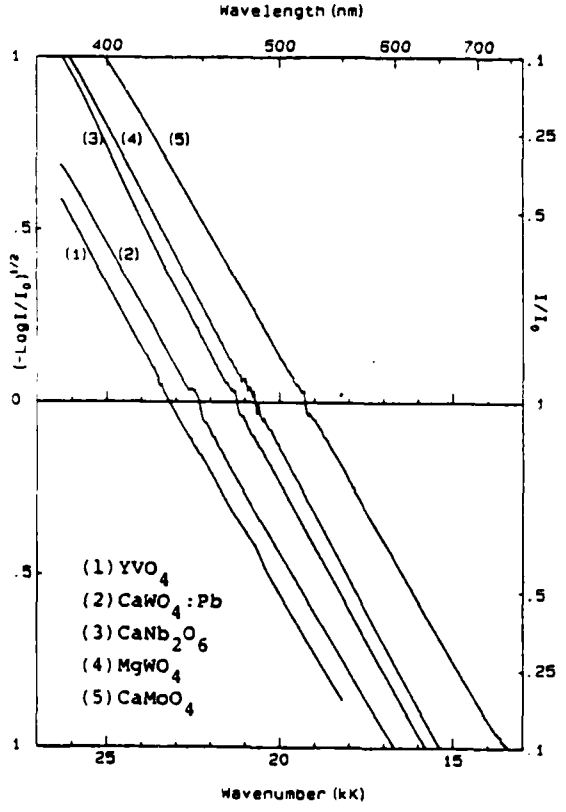

Fig.1 SEDs of complex ions

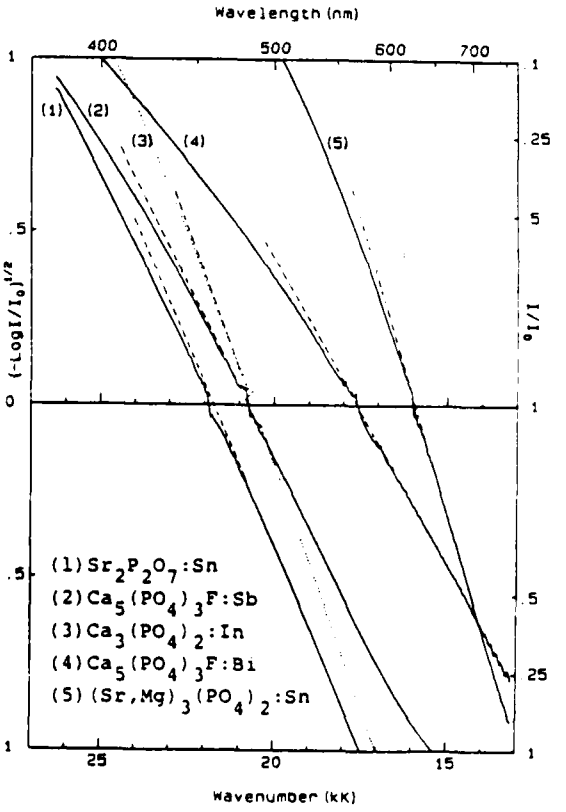

Fig.2 SEDs of s^2 ions

ENAMEL-TYPE ELECTROLUMINESCENT DISPLAY

Wu Chou-jen and Tan Hao-liang

Department of Physics
Shan-si Teachers' College
Lin-fen, Shan-si
People's Republic of Chnia

For more than ten years ago, electroluminescent display devices have been used primarily for lighting purposes, and have been largely confined to glass constrution. The simplest variable display device is a seven- or nine-segment numeric readout. by increasing the number of segments and changing rectangular to circular segments, more number and letter displays have been obtained. The familiar 35-dots-per-letter in 5×7 array is the best-known example

The present paper relates to the binary code and alphanumerical code, in which two columns consisting of ten dots, are used to express numbers and words.

DISPLAY IN NUMBER

In Figure 1, a front view of the display device is shown in enlarged scale. The surface size of the device is actually 20m.m.

Fig.1.

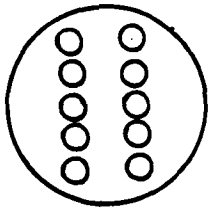

Fig.3.

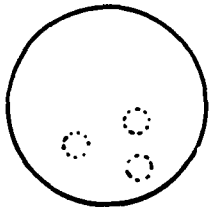

in diameter. As shown in Figure 2, for purposes of illustrution, the number 25 is displayed. To show this number, the mechanical or electrical switching component (SW) would excite the second dot in

Fig.2.

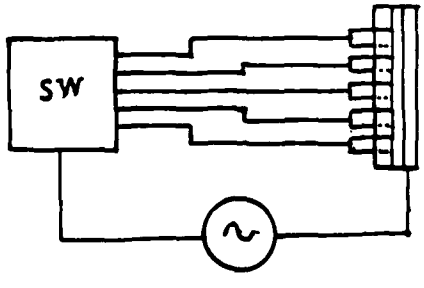

the left-hand column while exciting the first and the third dots in the right-hand column. In accordance with the well-known 1-2-4-8-16 weighted binary code, the illuminated dots would represent

the number 25, as can be seen in Figure 3. The unused dots can be also employed.

DISPLAY IN WORDS OR LANGUAGES

A farther object of this paper to express as a lighted-display means of expression would apply to words or languages, such as " ICL'84 ". In accordance with the familiar alphanumerical code

Table 1

	00	01	10	11
0000				
0001	1		J	A
0010	2	S	K	B
0011	3	T	L	C
0100	4	U	M	D
0101	5	V	N	E
0110	6	W	O	F
0111	7	X	P	G

	00	01	10	11
1000	8	Y	Q	H
1001	9	Z	R	I
1010	0			
1011		'		
1100				
1101				
1110				
1111				

is illustrated in Table 1, the illuminated dots representing the meaning " ICL'84 " can be expressed as follows:

I	C	L	'	8	4
111001	110011	100011	011011	001000	000100

The unused combinations in Table 1 can be assigned for other symbols the user may require.

ENAMEL MATERIALS

The display device may consist of the following composition:

SiO_2 - - - - - - - - 11.83 g.
ZnO - - - - - - - - 25.16 g.
BaO - - - - - - - - 17.25 g.
B_2O_3 - - - - - - - - 37.66 g.
Na_2O - - - - - - - - 8.10 g.

CONCLUSION

The potential efficiency and application scope of an enamel-type electroluminescent display device is greater than any other display device. The life expectance of an electroluminescent device is measured in years.

Fluorescence Spectroscopy through an Optical Fiber with a Time-Correlated Single-Photon Counting Method

Takashi Kushida, Junji Watanabe and Shuichi Kinoshita
Department of Physics, Osaka University,
Toyonaka, Osaka 560, Japan

It is possible to determine the spectrum of an optical pulse from the measurement of the photon time-of-flight distribution through a fiber, provided the time resolution of the system, including the original pulse duration and the time broadening of the monochromatic component (time dispersion) within the fiber, is sufficiently short.[1)]

We performed this type of fluorescence spectroscopy in several dye solutions such as hematoporphyrin dissolved in dioxane through a graded-index silica fiber, which has low time dispersion and good transmittance. The 150 ps duration pulses emitted from a cw mode-locked Ar laser were deflected at 5 MHz with an acousto-optic deflector and were used for the excitation of the sample. Fluorescence was focused into a fiber of 1 km length and the emitted light was detected using a time-correlated single-photon counting system of high time resolution.[2,3)]

The obtained photon time-of-flight distribution was transformed into the ordinary spectrum by the use of measured wavelength dependence of the attenuation and flight time. The

result was in good agreement with the fluorescence spectrum obtained by the conventional method.

The present method has the advantage that the sensitivity is high and the measurement can be completed within a short time. The spectrum is very reproducible because of the absence of the moving parts and also of simultaneous measurements of all the wavelengths. Furthermore, the fluorescence decay characteristics in the nanosecond and picosecond time ranges can be measured accurately by the same system using a short fiber. These features make this method very suitable to the applications in the field of endoscopy.

It is often necessary in this method to correct the blur due to the finite fluorescence decay time as well as to the time dispersion. These corrections by means of deconvolution will be discussed.

References

1) L.A.Franks, M.A.Nelson, T.J.Davies, P.Lyons and J.Golob: J. Appl. Phys. 48 (1977) 3639.

2) T.Kushida, S.Kinoshita, I.Tanaka, Y.Kinoshita and S.Kimura: J. Luminescence 24/25 (1981) 787.

3) S.Kinoshita and T.Kushida: Rev. Sci. Instrum. 53 (1982) 469.

Scintillating Glass Fiber-Optic Plates For The Detection of Ionizing Particles

R. Ruchti, B. Baumbaugh, J. Bishop, N. Biswas, N. Cason
R. Erichsen, V. Kenney, R. Mountain, and W. Shepard
Department of Physics, University of Notre Dame, Notre Dame, Indiana 46556

and

A. Kreymer
Firm: National Accelerator Laboratory, Batavia, Illinois 60510

and

A. Rogers
Synergistic Detector Designs, Mountain View, California 94043

and

R. Meade
Collimated Holes Inc., Campbell, California 95025

SUMMARY

We have developed and studied the performance of scintillating glass fiber-optic plates composed of: (1) Terbium activated cladded-glass cores in a matrix of 15 um spacing; and (2) Cerium activated cladded-glass cores in various matrices of 6-25 um spacing. The fluorescence properties of the base glasses and the fiber-optic plates have been studied extensively using Xe lamp and pulser laser spectrometers. The response of the fiber-optic devices to high energy charged particles was measured using 10 GeV/c particles at the SLAC test beam facility and 300 GeV/c particles at Fermilab. The plates were viewed with a three-stage, gateable image intensifier. Particle tracks and nuclear interactions were recorded on film. We observe 5 detected flourescence photons per millimeter for minimum ionizing particles for the Terbium glass and 3 detected photons per millimeter for the Cerium glass. The test results indicate that the scintillating glass fiber-optic plates can be used as high resolution tracking detectors for both fixed target and colliding-beam experiments in high energy and nuclear physics.

TuE16-1

Airborne Detection of Materials Stimulated to Luminesce by the Sun

by

William R. Hemphill and Arnold F. Theisen

U.S. Geological Survey, MS 591

Reston, Virginia 22092

The Fraunhofer line discriminator (FLD) is an airborne electro-optical instrument which permits daylight detection of materials on the Earth's surface which have been stimulated to luminesce by solar ultraviolet and visible light. This instrument uses glass spacer Fabry-Perot filters of narrow bandwidth (<0.1 nm) to isolate a Fraunhofer line of interest (Hemphill and others, 1983). To measure the luminescence of a material, the FLD computes from reflected light the ratio of the central intensity of a Fraunhofer line to the solar continuum a few tenths of a nanometer distant; it then compares this ratio with a conjugate measurement in skylight and direct sunlight. Luminescence is indicated where the ratio measured from the target material exceeds the ratio measured from skylight and direct sunlight.

To assess optimum wavelength and sensitivity requirements before conducting an airborne survey, the spectral luminescence intensity of a sample target material may be measured in the laboratory with the aid of a fluorescence spectrometer, such as the Perkin-Elmer/Hitachi MPF series. By comparing these measurements with the spectra of a luminescence standard, such as rhodamine WT dye, the luminescence of the material may be expressed in terms of rhodamine dye equivalency. The U.S. Geological Survey's FLD is sensitive to rhodamine WT concentration as low as 0.1 part per billion (ppb) in 0.5 m of distilled water at 20°C (Plascyk and Gabriel, 1975).

Figure 1 shows a geologic map of the Sespe Creek area, Ventura County, California, and an FLD image at the 486.1 nm Fraunhofer line. Black areas in both the image and the geologic map represent luminescence that exceeds 3.9 ppb rhodamine dye equivalency. Their position correlates well with the occurrence of the phosphatic Santa Margarita Formation (Tsm), and corroborates laboratory measurement of significant luminescence of samples of phosphate rock collected from that formation. Lower luminescence levels (2.2 to 3.8 ppb rhodamine dye equivalency, shown by enclosed white

areas) are believed to be luminescent detrius transported downslope from the Santa Margarita Formation, southward toward Sespe Creek. Luminescence values greater than 2.2 ppb rhodamine dye equivalency are rare south of Sespe Creek, where the Santa Margarita Formation is absent. Other materials imaged with the FLD include stressed vegetation, marine oil seeps, pollution effluents, and uranium bearing sandstone.

Hemphill, W. R., Theisen, A. F., and Watson, R. D., 1982, Use of the Fraunhofer line discriminator (FLD) for remote sensing of materials stimulated to luminesce by the Sun: in Killinger, D. K., and Mooradian, A., ed., Optical and Laser Remote Sensing, Springer-Verlag, Berlin Heidelberg New York, p. 213-222, 5 figs.

Plascyk, J. A., and Gabriel, F. C., 1975, The Fraunhofer line discriminator MKII --an airborne instrument for precise and standardized ecological luminescence measurement: Institute of Electrical and Electronic Engineers (IEEE), v. IM 24, no. 4.

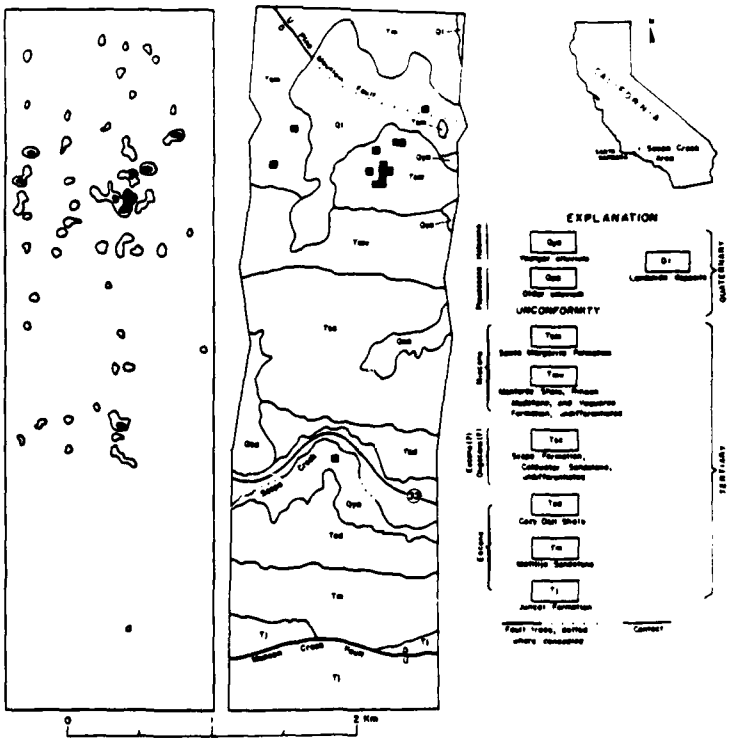

Figure 1. Luminescence image and geologic map.

Electroluminescence due to allowed 5d-4f transition of Ce^{3+} in a ZnS thin film

S. Tanaka, H. Kobayashi, M. Shiiki, T. Kunou, V. Shanker and H. Sasakura

Department of Electronics, Tottori University
Koyama, Tottori 680, Japan

Mn^{2+} ions and rare-earth ions (Ln^{3+}) such as Tb^{3+} ions are most commonly used as luminescent centers in ZnS thin film electroluminescence (EL) devices.[1] Luminescence of Mn^{2+} and that of Ln^{3+} ions are due to parity-forbidden (d-d) and (f-f) transitions, respectively. We report here, a greenish-white EL due to parity-allowed 5d-4f transition of Ce^{3+} ions in a double insulated ZnS:CeF_3 thin film device, for the first time.

Figure 1 shows typical EL spectra of the ZnS:CeF_3 devices under 1 kHz sinusoidal excitation. Cathodoluminescence (CL) spectrum of ZnS:Ce,Li phosphors, reported by Kawai and Hoshina,[2] is also reproduced in the same figure. The comparison of EL and CL spectra reveals that EL of Ce^{3+} ions in the ZnS thin films is caused by two parity-allowed transitions of $^2D(5d) - {}^2F_{5/2}(4f)$ and $^2D(5d) - {}^2F_{7/2}(4f)$. In the EL spectra, periodic oscillations due to interference effect

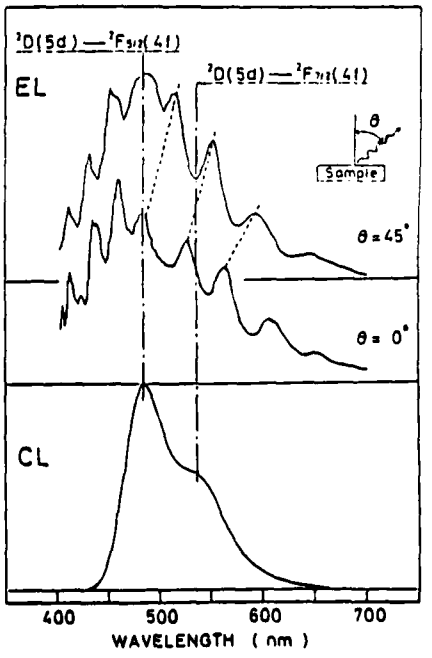

Fig. 1

caused by multiple internal reflections in the thin film are observed. As expected, wavelength of each peak depends on the viewing angle as shown in the figure.

Figure 2 shows the excitation voltage and EL waveforms under pulse voltage excitation with pulsewidth of 50 and 100 μs. When excitation voltage is turned off, EL output decreases immediately with time constant less than a few microsecond. This result is quite reasonable because EL of Ce^{3+} ions is due to allowed transition and emission lifetime of Ce^{3+} in ZnS lattice is of the order of 100 ns.[2] Since the lifetime is short, We may conclude that EL intensity follows conduction current and, therefore, observed rapid increase and gradual decrease in a period of voltage excitation may result from temporal variation of the conduction current.

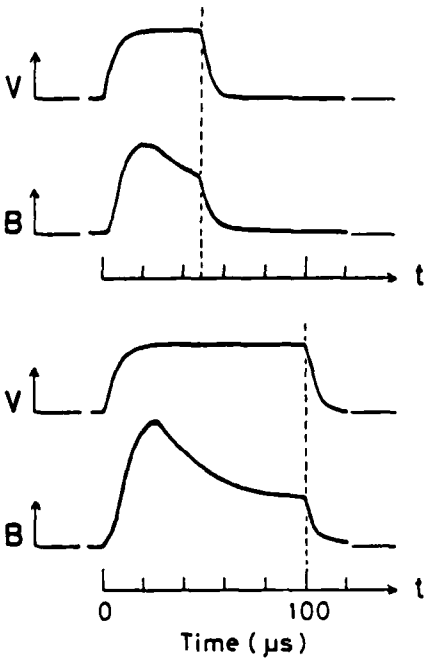

Fig. 2

Effect of allowed-transition on EL efficiency is also discussed.

1) H. Sasakura, H. Kobayashi, S. Tanaka, J. Mita, and T. Tanaka; J. Lumin. 24/25 (1981) 897.

2) H. Kawai and T. Hoshina; Jpn. J. Appl. Phys. 20 (1981) 1241.

Interband transitions and the electroluminescence of rare-earth implanted zinc chalcogenides.

F.J. Bryant, W.E. Hagston and A. Krier,
Department of Physics, University of Hull,
Hull, United Kingdom.

A comparison of the d.c. electroluminescence properties of reverse biased Schottky diodes in ZnS and ZnSe permits a valuable insight into the electronic processes responsible for the production of electroluminescence emission in rare-earth doped samples of these compounds. For unimplanted ZnS, application of an electric field does not result in any inter-conduction band transitions, whereas unimplanted ZnSe does exhibit transitions of this type even at room temperature. The ZnS and ZnSe Schottky diodes were prepared under similar conditions and would be expected to have similar diode properties, but these results indicate that a direct injection of the tunnelling electron into the upper conduction band is possible in ZnSe but not in ZnS.

If Er is implanted into ZnSe the broad inter-conduction band disappears and emission from Er^{3+} ions occurs, which suggests that the latter can Auger quench the inter-conduction band transitions. An alternative explanation could be that the lattice defects which accompany the implantation process are somehow responsible for quenching the inter-conduction band emission. Evidence against this being valid arises from observations of the electroluminescence emission from ZnSe containing implanted Tm^{3+} ions. In this case it is found that following the implant, which again produces lattice damage, the broad inter-conduction band emission is present at low temperature ($\lesssim$ 77 K) but that with increasing

temperature its intensity decreases considerably and the sharp line emission of the Tm^{3+} ions increases in intensity. These observations are consistent with the assumption that Tm^{3+} ions can Auger quench the inter-conduction band transitions. The difference between the effects of Er^{3+} and Tm^{3+} in this regard is consistent with the free-ion energy level structure of these two ions in that the energy mismatch between the broad inter-conduction band emission and the corresponding excited state of Tm^{3+} requires phonon-assistance in order to enable the transfer of energy to occur. Assumption that this phonon-assisted transfer rate depends exponentially on temperature shows why the Tm^{3+} line emission increases rapidly with increasing temperature. Such an energy mismatch does not occur for Er^{3+} ions.

These results demonstrate that the injection mechanism of electrons is not identical in these ZnS and ZnSe implanted diodes even though both materials have similar band structures. Furthermore, our observations indicate that the rare-earth ions can be involved with non-radiative Auger de-excitation of electrons in higher conduction bands. In turn, time reversal symmetry implies that the rare-earth ions can give rise to the inverse process, i.e. excited rare-earth ions can be Auger de-excited with a conduction electron making a transition from a lower to a higher band. The importance of such processes in limiting the electroluminescence efficiency could clearly be of major significance.

ELECTROMODULATION REFLECTION METHOD FOR STUDY OF THE FORMING PROCESS IN DC ELECTROLUMINESCENT ZnS:Mn,Cu [1]

Boxi Wu, Jianning Chen, Xiuxia Hong, Far Liu

Physics Department, Xiamen(Amoy) University

Xiamen, P.R.of CHINA

Summary

It is well known that the forming process is critical to the operation of DC electroluminescent ZnS:Mn,Cu powder panel.[1][2] However, the mechanisms of the forming process have not yet been completely known.

It is the first time that electromodulation reflection technique has been used to investigate the change resulting from the forming process. Because of the complexity of the powder sample system, to interpret the($\Delta R/R \sim \hbar\omega$)results clearly is almost impossible. But fortunately,we are only interested in whether there is any changing resulting from the forming process and not the exact energy band structure of the material used.Since the penetration depth of the light is of the order of that of the applied electric field,[4] the reflection modulation becomes possible.(Fig.1)

The results and tentative interpretations are as follows.

Without forming, all phosphor particles covered with thin conducting coating $Cu_xS(1.8 \leq x \leq 2)$,the whole sample being in a highly conducting state, no modulation signals are detected.

In the case of freshly formed sample, there are distinct electroreflectance signals detected.A $\Delta R/R$ minimum appears in the vicinity of $\hbar\omega_g$(energy gap of ZnS).These results confirm firmly the model proposed by other authors. [1]-[3] Under the influence of the applied forming field, the copper in the skin of the phosphor particles is made to migrate away from the anode(SnO_2), resulting in the creation of a thin copper-depleted insulating layer ZnS:Mn at the SnO_2-sample interface.

B.Hu et al/ electromodulation reflection

It was also found that a somewhat high temperature is necessary for the forming process. It is likely that a phase change occurs in the structure of Cu_2S above this temperature. In the forming process, this temperature condition may be offered by the surroundings and the Joule-heating. So, at lower ambient temperature, the forming voltages are higher than that at higher temperature.

Conclsions. In the forming process, with appropriate temperature condition, a phase change occurs in the copper-rich coating which is thereby turned into a state with significant ionic conduction. Under the applied field, copper ions migrate away from the anode interface resulting in a Cu-depleted layer, leading the rapid drop in current associated with the appearance of electroluminescence, which is found to be localized and confined close to the anode.

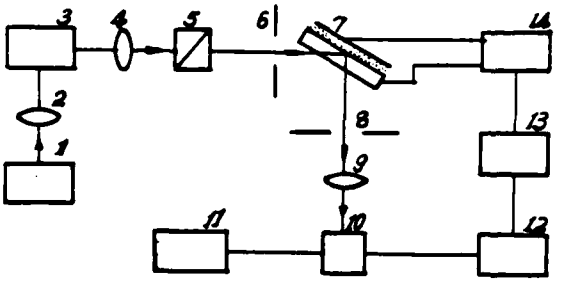

Fig.1.

1. light source
2,4,9 lenses
3. monochromator
5. polarizer
6,8 diaphram 7. sample
10,11 photomultiplier high voltage
12. phase lock amplifier
13. generator
14. DC bias source

References:

(1) A. Vecht, et al, J. Phys. D 2, p.953(1969)
(2) C.J.Alder, et al, Electronics lett. (GB), 16, p.571(1980)
(3) M.I. Abdalla, et al, J. Lum. 18/19, p. 743(1979)
(4) M.Cardona "Modulation Spectroscopy"

H. S. Reehal, C. B. Thomas and C. Cheung
Department of Applied Physics, University of Bradford
Bradford BD7 1DP, W. Yorkshire, England.

Summary

Thin film electroluminescence (TFEL), based on the ZnS:Mn system, is an active area of study for a flat-panel display technology. Although AC driven devices have been widely investigated and are currently in the market place, DC TFEL has many attractions from a commercial viewpoint. Unfortunately considerable difficulties exist in obtaining stable operation in DC structures and hence progress has been slow. The present authors have recently reported DC TFEL in a novel I.T.O./ZnS:Mn/p-n^+ Si diode structure capable of limiting the device current during luminescence[1]. In contrast with the very strong dependence of current (I) on voltage (V) observed during light emission in conventional structures, the new devices display a pronounced "knee" or reduction in the rate of growth of current with voltage at a voltage V_c corresponding to the onset of electroluminescence. A tentative model describing the I-V characteristics was proposed in reference 1.

In the present paper, in addition to further I-V and brightness-voltage data, we present capacitance (C) versus voltage characteristics for a variety of devices. The C-V data also exhibit a 'knee' or 'step' at V_c under forward bias conditions (ZnS electrode positive). The observations are consistent with the previous model in which the device current undergoes a transition from primarily ZnS-limited to semiconductor-limited in the vicinity of V_c. Below this voltage the ZnS layer is essentially insulating. An inversion layer of electrons thus builds up at the ZnS/Si interface with increasing forward bias. The voltage across the Si surface depletion region remains approximately constant whilst that across the ZnS increases. Eventually, at V_c, the latter becomes 'leaky' due to high field effects and further build-up of the inversion charge is prevented. A non-equilibrium mode ensues in which more and more of the applied voltage is dropped across the Si surface depletion region. The latter widens to satisfy current continuity

and the device capacitance therefore falls below its inversion value and displays the observed 'knee'. The device goes into deep-depletion and its behaviour becomes governed primarily by the supply of electrons from the depletion region. The I-V characteristics thus 'flatten-out' due to the current-limiting action of the depletion layer.

Data will be presented on the critical field for appreciable charge leakage through the ZnS films as a function of film thickness. Preliminary results on the behaviour of devices equipped with a third 'control' electrode to the p epi-layer region will also be presented.

Reference

1. J.M. Gallego, H.S. Reehal and C.B. Thomas, IEEE Trans. Electron Devices, ED-30, 475 (1983).

NONLINEARITIES IN THE Mn^{2+} SYSTEM SATURATING THE ELECTROLUMINESCENCE OF ZnS THIN FILM DEVICES

R. Mach, G. O. Müller
Zentralinstitut für Elektronenphysik, AdW der DDR, 1086 Berlin

The very high brightness, very good contrast and high efficiency of Inoguchi /1/ type electroluminescence devices (ELD) have boosted the interest in the mostly used emitter system - Mn^{2+} in ZnS. The highest brightness levels achieved - some 5000 ftL - are below the ones expected from crude estimates and several investigators found saturation of brightness upon drive /2,3/.

True saturation of EL brightness of thin film MISIM (Metal,Insulator,Semiconductor) structures at high applied a.c. voltages can always be traced to decreasing efficiency as in well-designed devices the transferred charge increases linearly with drive (well above threshold) /4/.

In a broad investigation of numerous test samples we found a rather confusing veriety of dependences of efficiency on amplitude and/or frequency of the drive voltage (as also published before by others), which collapse into one unique dependence of efficiency if plotted over brightness itself Fig. 1. As brightness monotonuously relates to the concentration of excited centres $[(Mn^{2+})^*] = N^*$ this of course must be interpreted as an efficiency - excitation dependence $\eta(N^*)$. Estimating N^* and N^*/N ($N=[Mn^{2+}]$) from well-known data, the decrease of efficiency by one order of magnitude can be located an an N^*/N scale to occur at about 0.1. This rules out the true activator saturation discussed by Smith /2/ and gives support to nonlinear nonradiative deexcitation processes which were mentioned recently by Törnqvist /3/. The most likely nonlinearity appears to be an excited state absorption or (more likely) transfer $^4T_1 \rightarrow {}^4A_2$ leading to a population of the second excited state of Mn^{2+} (about 5 eV above the groundstate). This process occurring with a much higher probability then the (usual) $^6A_1 \rightarrow {}^4T_1$ highly forbidden transition /5/ and its deexcitation, if radiative being absorbed by the host, qualitatively explain the observed facts but need for quantitative reasons the additional assumption of an (N-dependent) transfer of excitation energy via unexcited Mn^{2+} ions.

References

/1/ T. Inoguchi, S. Mito, Topics in Applied Physics (ed. Pankove), Springer, Heidelberg 1977, p.222

/2/ D. H. Smith, J. Lum. 23, 20 (1981)

/3/ R. Törngvist e.a., IEEE Trans. ED30.5, 468 (1983)

/4/ R. Mach, G. O. Müller, Efficiency and Saturation in ac thin film EL structures, phys.stat.sol. (a) 1984, in press.

/5/ T. Kushida, Y. Tanaka, Y. Oka, Solid State Com. 14, 617 (1974).

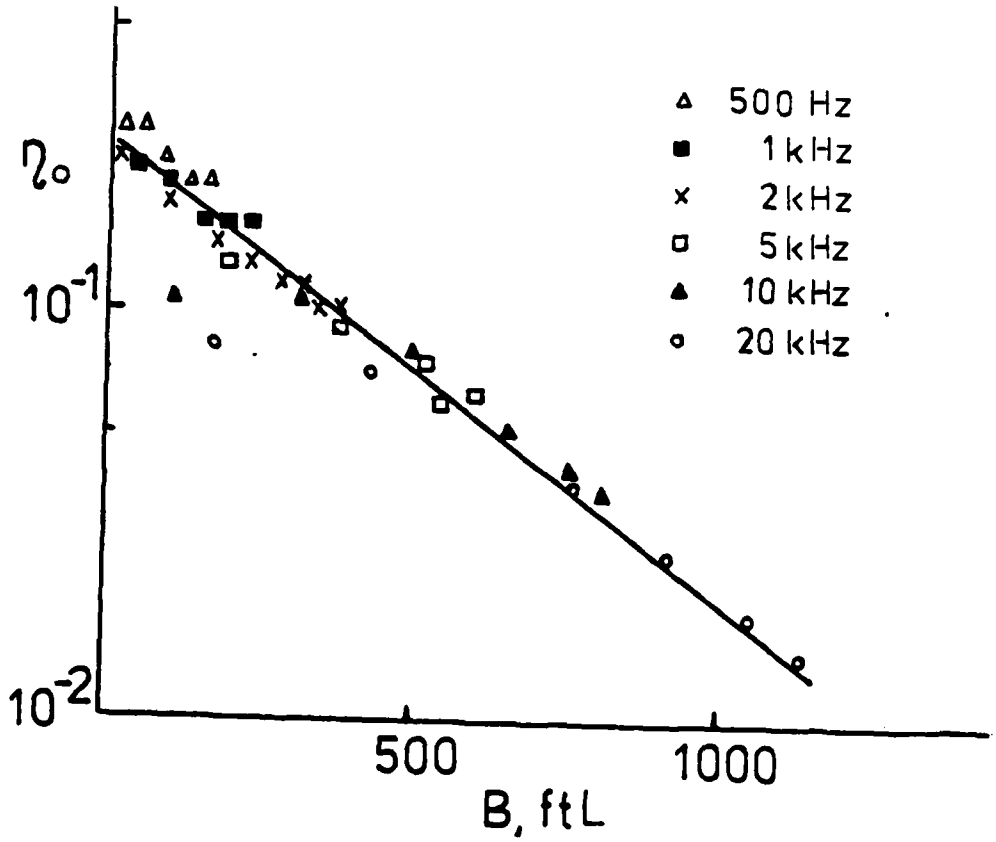

Spatial Distribution of Blue Electroluminescence in ZnSe MIS Diodes

Fan Xi-wu, Zhang Ji-ying, Zhang Zhi-shun, Wang Shou-yin,
Lu An-de, Li Wei-zhi, Jiang Jin-xiu, Sun Yao-wu

Changchun Institute of Physics
Chinese Academy of Sciences
Changchun, China

Spatial distribution of blue electroluminescence(EL) in ZnSe MIS diodes[1,2] using ZnS polycrystal film as an insulating layer has been studied. The diodes were fablicated by nominally undoped ZnSe crystals grown from the vapour phase in sealed capsules containing light excess of zinc[3].

With an optical microscope it was observed thet the blue EL in ZnSe MIS diodes appears as a few scattered bright spots dispersing on the crystal surface closed to the gold electrode. The number, size and luminance of the EL spots increase with the increase of the current density passing through the diode.

Scanning electron microscopy has been used to study the diodes. It was found that the electron beam-induced current image(EBICI) corresponded to the EL spots(ELS) observed with optical microscope for ZnSe MIS diodes, as shown in Fig.1. However, both the absorbed electronic current image of low-resistivity ZnSe dice and the EBICI of ZnSe MS diodes are homogeneous.

On the ground of the above results, it is concluded that the distribution of resistivity of ZnSe die along the crystal surface is homogeneous and the ZnSe crystal is flawless. The origin of nonuniformity of EBICI as well as of ELS must be attributed to the introduction of the insulating ZnS layer. Since in this case there is considerable mismatch of energy

band and more nonradiative recombination centers in the insulator-semiconductor interface of the ZnSe MIS diode.

It was expected that if a homo-insulating layer is used in fabricating the ZnSe MIS diode, the homogeneity of EL emission could be improved. A new ZnSe MIS diode was made in which a ZnSe polycrystal film instead of ZnS polycrystal film was used as an insulating layer. It was found that the EL becomes densely packed spots in the diode under an optical microscope as shown in Fig. 2, and appears homogeneous when observed with naked eyes.

We believe that perfectly uniform EL emission could be obtained for ZnSe MIS diode if a ZnSe epitaxial layer is used as the insulating layer.

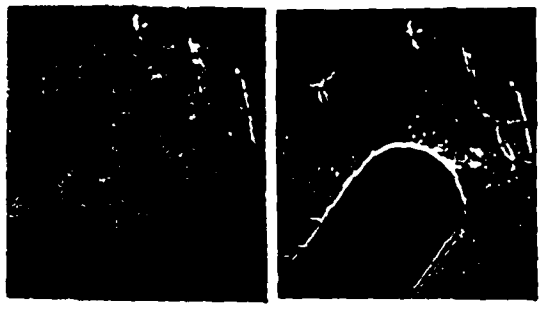

ELS (X40) EBICI (X40)
Fig. 1.

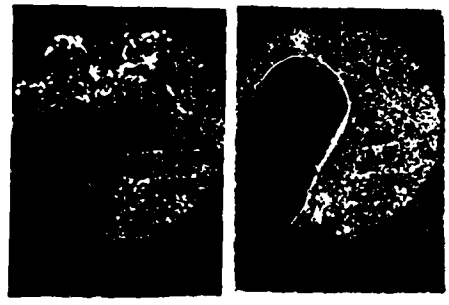

ELS(X30) EBICI (X30)
Fig. 2.

References:
(1) Fan X.W. and Woods J. IEEE Trans-ED ED-28, 428 (1981)
(2) Fan X.W. and Woods J.J. Phys. C. 14, 1863 (1981)
(3) Cutter J.R. and Woods J. J. Crystal Growth 47, 405 (1979)

Time-resolved blue luminescence and temperature-dependent characteristics in efficient forward-bias ZnS diode

Tsunemasa Taguchi

Department of Electrical Engineering, Faculty of Engineering, Osaka University, Suita, Osaka 565, JAPAN.

For the study of blue light-emitting diodes(LEDs) using ZnS, from a practical point as well as a physical point of view, it is desirable to find out the prerequistie for making reproducible and reliable metal-partially compensated semiinsulating layer-semiconductor (MπS) structure. Since oxygen gives rise to acceptor-like levels which can result in an accumulated layer or a compensated layer being formed at the crystal surface, the application of compensated high-resistive layers due to oxidation might be useful for making an interposed π-layer between the metal electrode and low-resistive n-ZnS to obtain an efficient blue LED. Most recently, we have shown that the chemically oxidised π-layer consists of ZnO and ZnS mixed alloys[1], and that the best diode records a room-temperature external quantum efficiency of about 8×10^{-4} photons/electron and the halfwidth of about 65 nm at a drive voltage of 6 V for 15-20 $mA.mm^{-2}$ current densities. It is worth noting that these characteristics are superior to those in GaN and SiC[2] blue LEDs.

We describe the detailed temperature-dependent characteristics of the forward-bias blue electroluminescence and discuss the nature of the injection-luminescent mechanisms involed in efficient LEDs prepared from n-ZnS doped with iodine, with the MπS structure. Time-resolved electroluminescent studies reveal that the 2.65 eV blue emission giving rise to the double peaks, at relatively low current densities, is related to the two types of donor-acceptor pairs, whilst the 2.76 eV (450 nm) band , appearing at higher current

densities, arises from an electronic transition between the conduction band and an acceptor level locating at about 0.85 eV above the valence band, as shown in Figs. 1 and 2. It is therefore suggested that the efficient blue 450 nm band is due to the free-to-acceptor transition.

On the other hand, the observed quantum efficiencies have a strong temperature dependence and exhibit a marked decrease for the π-layer thickness greater than about 500 Å. The first experimental results concerning the temperature-dependent characteristics of the blue diode, are shown in Fig. 2, where the minority-carrier injection (1), quantum (2) and radiative-recombination (3) efficiencies are separately measured. The injection blue luminescence as a function of temperature is quite similar to that of photoluminescence observed in bulk n-ZnS:I. It is concluded that the recombination properties of the blue emission observed in the forward-biased MπS blue LED can be completely explained in terms of the bulk photoluminescence characteristics (insert in Fig. 2), and the blue emission occurs in the bulk region, than at the interface. We believe that the forward-biased hole injection luminescence is mainly due to tunnelling process.

1) T.Taguchi and T.Yokogawa, J. Phys. D:Appl. Phys. 17 (1984) 563, 2) K.Hoffman, G.Jiegler, D.Theis and C.Weyrich, J. Appl. Phys. 55 (1982) 6962.

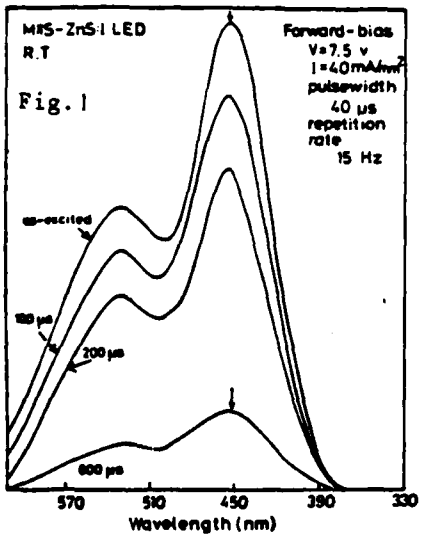

Fig. 1

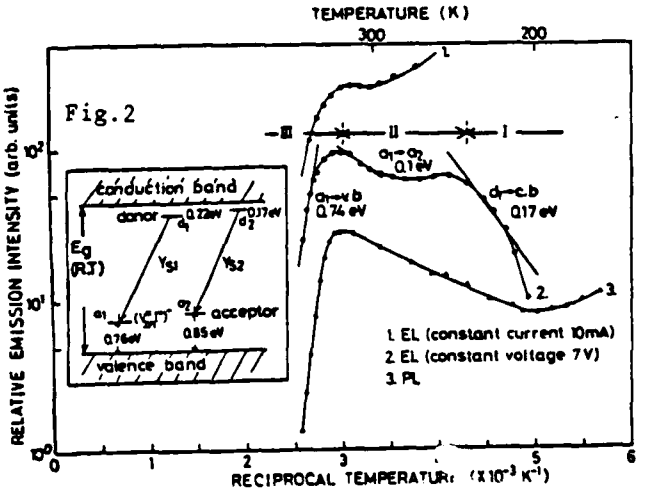

Fig.2

CAVITY AND DESTRIAU EFFECT

Wu Chou-jen and Tan Hao-liang

Department of Physics
Shan-si Teachers' College
Lin-fen, Shan-si
People's Republic of China

INTRODUCTION

Despite intensive research efforts, the theoretical situation about the Destriau effect is still in a state of confusion. The main reason for this is the deviation of observation. One of the most important electroluminescent finds has been made is that electroluminescent particles contain numerous voids at which the internal surfaces are deposited with thin, conducting, and transparent copper or copper sulfide layers. That such layers can indeed exist.

RESONANT CAVITY

It is obvious that the voids in electroluminescent particles are resonant cavities which contain not only numerous resonant frequencies, but also high quality factor (Q). The resonant frequencies, high or low, may be influenced directly by the partially rough internal surfaces with acicular conducting occlusions act as capacitance. The quality factor is defined as

$Q = 2\pi$energy stored / average power dissipated per cycle,

for the case of a round resonant cavity, the Q-value is rather high. If the quality factor of the electroluminescent condenser in a circuit is Q', and the voltage source is V'. The high voltage in the resonant cavity may be written, for a limited resonant frequency range, as

$$V = Q \cdot Q' \cdot V'.$$

ELECTROLUMINESCENT LIGHT EMISSION

Suppose the resonant cavity is energized in the applied voltage and may produce a high voltage adequate for direct ionization for

purpose of supplying the initial electrons, which are then accelerated to velocities sufficient to collision- ionize other illumination centers. And then, the electrons and the ionized illumination centers are responsible for the light emission by recombination.

OBSERVATION OF PHENOMENA

The spots of electroluminescent light emission, often in clusters of up to ten, occur in the cavities. The shape of the spots are isolated single round dots, if not, odd-shaped lines cannot be seen outside of the cavities.

It is obvious that any part of the cavity surface may be treated as a lens. Sometimes, as observed with a microscope from the outside of the cavity, odd-shaped lines can be seen with the typical double comets, zigzag or whip form which are vertual images, This can be easily accounted for because of the light refracting through the surface of the cavity.

ANALOGY OF PHENOMENA

For instances, if a round spot is situated far from the light axis of a lens, double comets form may be observed; if a group of round spots are situated on a straight line, a whip form may be observed.

Other phenomena of electroluminescent light emission may be also readily analogized by means of a lens.

This will be of importance for the theoretical interpretation of the Destriau effect.

References:

1. S. Larach, (ed.), " Photoelectronic Materials and Devices ", Van Nostrand, New Jersey (1965).
2. F. E. Terman, " Electronic and Radio Engineering ", Fourth edition, Mcgraw-Hill Book Company, Inc.
3. G. Destriau: New Phenomenon of Electrophotoluminescence, Philosophical Mag., Oct. 1947, Vol. P.700.
4. L. W. Strock, " Electronics World ", 1 (1965)
5. Wu Chou-jen, Hu Ju-ji and Wu En-curie: " Enamel Electroluminescence ", To be published.

Copper-Catalyzed Low-Voltage Cathodic Electroluminescence at Anodized Aluminium Electrode

K. Haapakka, J. Kankare and S. Kulmala

Department of Chemistry, University of Turku
SF-20500 Turku 50, Finland

Electroluminescence is observed at several semiconductor-electrolyte interfaces during the reduction of hydrogen peroxide, persulphate and oxygen.[1-3] This luminescence is presumably caused by the electron-hole recombination in a semiconductor.

In this work the effect of trace amounts of metal ions on the cathodic electroluminescence of anodized aluminium electrode is studied by using symmetric double step potential shown in Fig. 1a. The electroluminescence measurements could be made highly reproducible by rotating the electrode. Fig. 1b shows the electroluminescence generated from the reduction of hydrogen peroxide in 0.1 M sodium acetate solution. Fig. 1c reveals the catalytic effect of Cu(II) ($1x10^{-7}$ M) on the cathodic electroluminescence. In addition to Cu(II), the following metal ions Co(II), Cr(III), Fe(III), Hg(II), Ni(II), Pb(II) and Zn(II) were tested, and the catalytic effect was observed for Hg(II) and Pb(II). The anodic electrolumines-

Fig. 1. Electroluminescence at anodized aluminium electrode.

cence was independent on the changes in experimental variables.

The main purpose of the work is to study the feasibility of the cathodic electroluminescence on analytical applications of trace metals. Because of its strongest catalytic effect, copper(II) was selected for further measurements. The experimental variables were optimized and the dependence of the electroluminescent intensity on the Cu(II) concentration was determined under the optimized conditions as shown in Fig. 2. The relative standard deviation of the Cu(II) determination ($1x10^{-7}$ M) was 2 %.

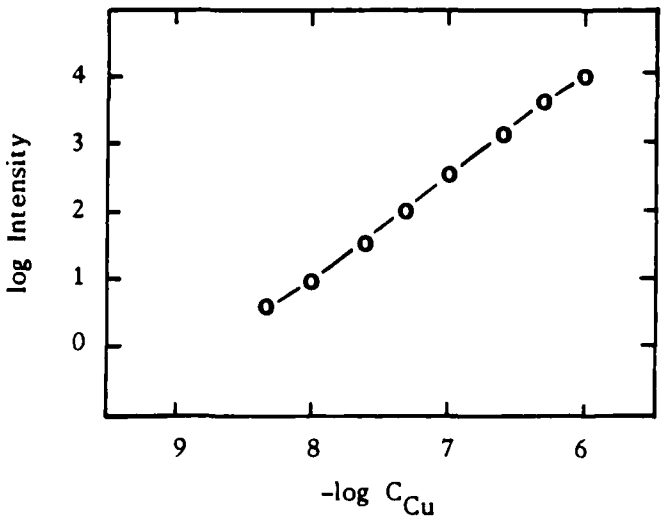

Fig. 2. Dependence of cathodic electroluminescence intensity on Cu(II) concentration.
Conditions: 0.1 M sodium acetate, pH 6.7, concentration of hydrogen peroxide $6.0x10^{-4}$ M, pulse amplitude 5.0 V, pulse width 17.0 ms, rotation rate 1500 rpm.

References

1. B. Pettinger, H. Schöppel and H. Gerischer, Ber. Bunsenges. Phys. Chem. 80 (1976) 849.

2. J. Kankare, D. Ryan and B. Fürst, Can. J. Chem. 55 (1977) 1193.

3. R. Noufi, P. Kohl, S. Frank and A. Bard, J. Electrochem. Soc. 125 (1978) 246.

Photoluminescent and Electroluminescent Properties of $Cd_{0.95}Mn_{0.05}Se$ Electrodes

A. A. Burk, Jr. and Arthur B. Ellis

Department of Chemistry, University of Wisconsin-Madison, Madison, Wisconsin 53706

Dana Ridgley and Aaron Wold

Department of Chemistry and Materials Research Laboratory, Brown University, Providence, Rhode Island 02912

Single-crystal samples of n-type $Cd_{0.95}Mn_{0.05}Se$, grown by a modified Bridgman method[1], have been used as electrodes in photoelectrochemical cells (PEC's) employing aqueous diselenide electrolyte. After etching with HCl/HNO_3 (1:1 v/v), the samples exhibit photoluminescence (PL) when excited with ultraband gap excitation (E_g ~1.75 eV[2]); the maximum of the PL band, ~690 nm, is near the band gap energy and blue shifts to ~680 nm at 77 K. In some samples, subband gap PL is also observed (uncorrected λ_{max} ~890 nm.) The radiative efficiency, ϕ_r, of the edge emission can be as large as $\sim 10^{-4}$ at 295 K and $\sim 10^{-2}$ at 77 K.

The intensity of PL from the electrodes can be quenched by the electric field present in the semiconductor during PEC operation, although the spectral distribution is unaffected. The extent of PL quenching has been studied as a function of carrier concentration ($n \sim 1\times10^{16}$-4×10^{18} cm^{-3}), excitation wavelength (457.9, 514.5, and 607 nm), and applied potential (-0.7 V to open circuit, ~-1.4 ±0.1 V vs. SCE).

The data are analyzed in terms of a dead-layer model previously used to describe PL quenching in semiconductor/metal[3] and PEC[4,5] Schottky barrier systems: electron-hole pairs formed within a distance on the order of the

depletion width do not contribute to PL. Since the model relates PL intensity to the electric field in the semiconductor, it may possibly serve to map the field and thus to probe how applied potential is partitioned across the semiconductor-electrolyte interface.

When used as a dark cathode in aqueous, alkaline peroxydisulfate electrolyte, samples of n-$Cd_{0.95}Mn_{0.05}Se$ exhibit red electroluminescence (EL). The EL spectrum at low resolution is similar to the PL spectrum. Measured EL efficiencies, $\sim 10^{-5}$ to 10^{-6}, are comparable to PL efficiencies and suggest that population of the emissive excited state can be very efficient in EL experiments. The influence of etching, including photoelectrochemical etching, on PL and EL properties will be discussed.

References

1. B. Khazai, R. Kershaw, K. Dwight, and A. Wold, Mat. Res. Bull. 18, 217 (1983).
2. H. Wiedemeier and A. G. Sigai, J. Electrochem. Soc. 117, 551 (1970).
3. R. E. Hollingsworth and J. R. Sites, J. Appl. Phys. 53, 5357 (1982) and references therein.
4. W. S. Hobson and A. B. Ellis, J. Appl. Phys. 54, 5956 (1983).
5. R. Garuthara, M. Tomkiewicz, and R. P. Silberstein, J. Appl. Phys. 54, 6787 (1983).

Inversion Layer Formation and Electroluminescence at p-GaAs/Persulfate Solution Interface

Kohei Uosaki and Hideaki Kita

Department of Chemistry, Faculty of Science,
Hokkaido University, Sapporo 060, JAPAN

When p-type semiconductor is cathodically biased very strongly, either deep depletion or inversion layer is formed. Inversion layer formation plays a significant role in the electron transfer kinetics at semiconductor/solution interface and it is of interest to probe the inversion layer formation. The measurements of surface conductance and impedance are most often used for this purpose. If the inversion layer is formed at p-type semiconductor surface and strong oxidant which can inject holes into the valence band exists, the electroluminescence (EL) should be observed. $SO_4^{\cdot -}$ which is generated *in situ* by one electron reduction of $S_2O_8^{--}$ is known to be a very strong oxidant and is often used to study EL of n-type semiconductors. When p-GaAs (Zn doped: 1.09×10^{19} cm^{-3}) in solutions containing 5 M NaOH and 0.15 M $S_2O_8^{--}$ is negatively biased, first the cathodic currents due to the reduction of $S_2O_8^{--}$ and $SO_4^{\cdot -}$ are observed between -0.5 V and ca. -2 V. When the potential becomes more negative than ca. -2 V, the cathodic current due to hydrogen evolution is observed. In this potential region, EL which has peak around 880 nm is observed. Since the peak

energy is in good agreement with the energy gap of GaAs, this EL seems to be due to band adge emission. Thus, when p-GaAs is biased more negative than ca. -2.0 V, the electrons are transferred from the valence band in the bulk to the conduction band in the surface bv turneling and some of them are consumed for hydrogen evolution and are recombined radiatively with holes, emitting band edge EL. The lower the carrier density, the more negative the critical potential at which the current due to hydrogen evolution started to flow and the weaker the intensity of EL. These results suggest that the electron concentration in the conduction band at the surface is lower at p-GaAs of lower carrier concentration. This is reasonable since the barrier width for the turneling is wider at p-GaAs of lower carrier concentration.

Transient Characteristic of Stimulated Raman Scattering in the Wave Guide of the Glass Fiber

Jin Deyun, Huang Guosong Chen Shizheng
Gan Fuxi
Shanghai Institute of Optics and Fine Mechanics,
Academia Sinica, Shanghai, China

Summary

In order to restrain the Brillouin scattering and increase the gain of the stimulated Raman scattering, the picosecond pulse train from the frequency doubled and mode-locked YAG laser with the repitition of 10-20 Hz was injected to a P_2O_5-GeO_2-SiO_2 glass fiber with the length of 20 meters. In the wave length region from 0.45μm to 1.00μm, the transient stimulated Raman scattering with the conservation effectivity higher than 50 petcent has been obtained.

In our experiment, the transient character of the stimulated Raman scattering in the wave guide of glass fiber has been researched by using the time-expander with the resolution of 10ps. The results show that the time-width of the Stokes pulse was narrowed obviously as the scattering order increasing. The mean time delay between the scattering and exciting light was 0.4ps/cm. We have also observed the frequency character of the Stokes light by injecting the scattering light into a GDM 1000 monochromator with the resolution $1cm^{-1}$. The Raman frequency shift is $430cm^{-1}$. Since the line width of the scattering light is much larger then that of the pumping light, all frequency compositions of the pumping light were contributed to the stimulated Raman scattering.

When the high power picosecond pulse at 0.53μm were injected to the fiber, the Stokes and anti-Stokes radiation were successfuly excited. The incident light excite the first order Raman light and the later excite the second order one and so on, and then the scattering spectra covers whole visible grequency region. With the increasing the scattering order, the Stokes frequency-width become broad. The product of the time-width and frequency-width of each Stokes pulse is a constant which is about 4.3ns/cm and is assignment with the indeterminaterelation.

Owing to the coupling and non-linear mixing frequency between each two Stokes lights and non-linear index effect caused by the second order Kerr effect, the spectra of both Stokes light over seventh order and the anti-Stokes light above third order become continunm. In the region from 0.83 to 0.93μm, the scattering light disappeared. This fact may be caused by the strong absorption of the glass fiber in this wave length region.

The theoretical calculation of the stable-state and transient-state gain of the low-order Stokes light and the time delay corresponding to the pumping light has been done. The experimental results were consistent with the theoretical values.

Holeburning and Optically Detected Nuclear Magnetic Resonance in $CaSO_4:Eu^{3+}$

Neil B. Manson and Ann J. Silversmith

Department of Solid State Physics
Research School of Physical Sciences
Australian National University
Canberra ACT 2601 Australia

Summary

We have studied two Eu^{3+} sites in $CaSO_4$ by selective excitation, emission, optical holeburning and optically detected nuclear magnetic resonance (ODNMR) techniques. Both centres (henceforth referred to as 1 and 2) have $^7F_0 \rightarrow {}^5D_0$ excitation signals at ~578.7nm; the two absorptions are 34GHz apart. The emission and excitation spectra of the two centres are very similar, and indicate that low symmetry sites are involved.

Hyperfine structure of Eu^{3+} has been studied in several hosts, the structure being determined primarily by an electric quadrupole term in the Hamiltonian[1]:

$$H = P\{I_z^2 - 1/3\ I(I+1) + \eta/3(I_x^2 - I_y^2)\}$$

P determines the overall size of the splitting and is proportional to the quadrupole moment of the nucleus. There are two naturally abundant isotopes of europium (^{153}Eu and ^{151}Eu) whose quadrupole moments are in the ratio of (2.5-2.6); this is reflected in the holeburning spectra. η indicates deviation from axial ($\eta = 0$) environment; for an $I = 5/2$ ion in an axial environment the ratio of the hyperfine splittings is 2:1.

In Eu^{3+}, as in other rare earth systems, holeburning is due to redistribution of the population among different hyperfine levels of the ground state. The main features in the holeburning spectra of both centres are side-holes at 50, 100, 130 and 260 MHz corresponding to excited state hyperfine splittings. No antiholes could be firmly assigned.

In the ODNMR measurements the laser frequency is kept fixed, maintaining saturation and rf radiation is applied. The frequency is swept; when the

rf is in resonance with a ground state splitting, transitions are stimulated. The saturation level becomes less and absorption of the laser increases. The holeburning rate is slow compared with the response of the system to rf and fast sweeps of the rf gave a sharp increase in absorption, followed by a long recovery to saturation. We have recorded the derivative of the spectrum to pick out only the sharp increases; these results are shown in the figure.

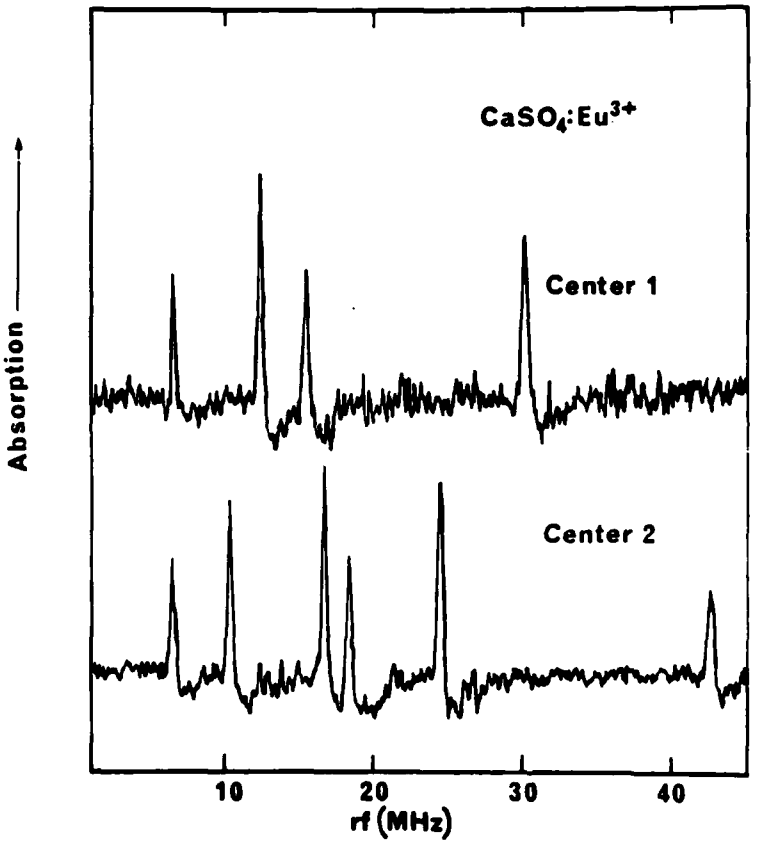

Table

^{151}Eu	^{153}Eu
Centre 1	
12.0	29.5
6.00	15.2
Centre 2	
16.6	42.6
10.2	24.4
6.30	18.3

ODNMR resonances (MHz) in the ground state of Eu^{3+}.

The ground state hyperfine structure is radically different for the two centres. Centre 1 shows an axial 2:1 ratio; also the ~2.5 ratio between quadrupole splittings in ^{153}Eu and ^{151}Eu is apparent. Centre 2 appears to be anomalous; the quadrupole Hamiltonian term cannot account satisfactorily for the observed splittings. Experiments using ODNMR with external magnetic field have been performed to characterize further the two centres.

Reference

1. R.J. Elliott, Proc. Phys. Soc. London, B70, 119 (1957).

LASER EXCITATION AND SPIN COHERENCE OF PHOSPHORESCENT F_2^{2+} CENTERS IN CaO.

M. Glasbeek, M. Casalboni and R. Vreeker
Laboratory for Physical Chemistry
University of Amsterdam
Nieuwe Achtergracht 127
1018 WS Amsterdam, the Netherlands

In recent years, extensive spectroscopic studies concerning F-type point defects in additively colored alkaline earth oxides have been reported. In particular, oxygen vacancies containing two electrons are of interest because they can be photo-excited into phosphorescent triplet states. Several experimental techniques have been applied for studying such triplet states including optical-microwave double resonance and spin coherence techniques [1]. In this paper, we report on a spin coherence study of the phosphorescent triplet state of the F_2^{2+} center in CaO, the triplet state being prepared by excitation with cw- and pulsed-dye laser light.

In CaO, the F_2^{2+} center consists of an oxygen divacancy (along a <110> direction of the fcc crystal) containing two electrons. Upon photo-excitation between 400 nm and 600 nm, the F_2^{2+} defects, which are randomly dispersed in the host lattice, become excited into the emissive $^3B_1$ state. Using a method of optical detection of spin echoes [2], irreversible spin dephasing was studied (at 1.2K and zero magnetic field) as a function of the wavelength of the

exciting cw dye-laser light. Data are presented showing that when for the F_2^{2+}-center defects the microscopic environment is changed (by choosing a different optical excitation energy) the spin dephasing dynamics changes as well. The interpretation of the observations involves other defects (F^+ centers) that surround the F_2^{2+} centers in random spatial configurations [2]. An inhomogeneous distribution in the mean density of the surrounding F^+ centers is discussed to induce (i) inhomogeneous broadening of the F_2^{2+}-center optical absorption band, and (ii) an inhomogeneity in the homogeneous broadening of the triplet spin transitions.

In addition, preliminary results obtained from laser-pulsed excitation of the F_2^{2+} defects in CaO are given. Upon pulsed-laser excitation near 500 nm, an enhanced spin dephasing of the $^3B_1$ state is observed. Results are presented that show the dependence of the enhanced spin coherence decay on the time delay between the laser flash and the microwave echo pulse sequence; the influence of the laser intensity is discussed as well. It is inferred that an additional feeding of the $^3B_1$ state takes place involving a hitherto unknown (dark) metastable excited level of the F_2^{2+} defect.

REFERENCES

[1]. M. Glasbeek, Radiation Effects 72, 13 (1983).

[2]. M. Glasbeek and R. Hond, Phys.Rev.B 23, 4220 (1981).

Phase Coherence in the ^2E state of Cr^{3+} ions in MgO detected via ODMR

by

Professor B. Henderson, Department of Physics, University of Strathclyde, Glasgow G4 ONG, Scotland, U.K.

The coupling between the Zeeman sublevels of an atom by a resonant microwave magnetic field also induces a phase coherence between the states. The effect is equivalent to the precession at the Zeeman frequency of a transverse magnetic moment about the static magnetic, and is manifest as a modulation of the circularly polarized emission at the Zeeman frequency. We have investigated such phase coherence in the ^2E excited state of Cr^{3+} ions occupying sites of both cubic and tetragonal symmetry in magnesium oxide, MgO. The experiments were carried out at 1.6K, in the X-band frequency range ($\nu \sim 9.5$ GHz) with the magnetic field parallel to the crystal [111] direction. In this orientation the optically detected magnetic resonance spectra from Cr^{3+} ions in cubic and tetragonal symmetry sites are well-separated in magnetic field. In addition all three resonances from the mutually orthogonal tetragonal species occur at the same magnetic field. The purpose of this geometry is to eliminate cross-relaxation between cubic and tetragonal sites.

The single crystal samples contained between 100 ppm and 1300 ppm of Cr^{3+} ions in MgO. Microwave-induced modulation of the light propagating perpendicular to the static field, B_o, was detected using a high frequency photoelectron multiplier, and a superheterodyne receiver with phase-sensitive detection. Optical excitation was by ca 500 mW of laser light in the 488 nm Ar^+ line. The observed signals at the appropriate resonance fields represent phase coherence between σ and π components of emission perpendicular to B_o, which leads to amplitude modulations of the $\sigma\pm$ components. At low concentrations the spectral dependences of these microwave modulated signals at the appropriate resonant fields clearly separate the zero-phonon line and vibronic sidebands from Cr^{3+} ions in cubic and tetragonal symmetry sites. However, in more concentrated samples, the resonances due to Cr^{3+} ions in cubic sites are observed even when detecting at the field value for resonance on the Cr^{3+} ions in tetragonal sites. In view of the experimental geometry used for these measurements, the origin of this effect appears to be incoherent energy transfer between Cr^3 ions in different symmetry sites.

Phase Coherent Laser Multiple Pulse Spectroscopy

W. S. Warren, M. Banash, F. Loiaza and F. Spano
Department of Chemistry
Princeton University, Princeton NJ 98544
(609) 452-3910

SUMMARY

Complex multiple pulse sequences have proven extremely valuable in NMR as probes of intermolecular and intramolecular interactions. Optical analogs of many of these sequences can be useful in elucidating the effects of collisional perturbations in gases, guest-guest and guest-host interactions in mixed molecular crystals, or any general perturbations which make the usual two-level approximations invalid.[1] But all of these sequences require phase coherence (the phase of each pulse must be specified relative to the first) which was more difficult to achieve in optical spectroscopy than at radiofrequencies.

We use a recently developed acousto-optic technique as the foundation for producing phase coherent laser pulse trains. In essence a radiofrequency version of the desired laser sequence is generated, with independently adjustable pulse shapes, frequencies, phases and delays. This sequence is then fed into an acousto-optic modulator along with the output of a single frequency ring dye laser. The diffracted beam is then a laser replica of the rf sequence, with peak powers of up to 1 watt and risetimes of 4 nsec.[1] Fluorescence measurements after such sequences can distinguish between different interaction mechanisms. These pulses can now be amplified when necessary to give ~100 kW peak power and ~100 psec risetimes, while still retaining phase coherence. Thus, a large number of systems with relaxation times down to the subnanosecond level can be studied by these phase coherent techniques.

We will be discussing two different sets of experiments. In the first case we use dual frequency pulse sequences to explore collisional energy transfer. Several research groups have probed atomic or gas-phase molecular

transitions with the optical analogs of simple NMR pulse sequences.[2] Several conflicting theoretical frameworks for translating observed T_1 and T_2 values into mean velocity changes per collision have been proposed. The fundamental limitation of previous single frequency experiments is that all these sequences probe how long population or coherence stays as it was prepared, but not where they go after collisions have occurred.

We can in principle surmount this limitation by exciting a single velocity component with one weak laser pulse, and then probing a different velocity component by a second frequency shifted pulse.[3] In fact the experiment is somewhat more complex, since the desired signal can only be extracted by comparing the observed decay with results from single frequency experiments. If the phases of the two pulses are random then only population transfer is measured; if they are fixed polarization transfer is measured as well. We can map out the complete time evolution of the initially excited molecules, and thus test different collisional theories. Results for I_2 and I_2+O_2 illustrate the effects of several different interaction mechanisms and clarify the meanings of T_1 and T_2.

We will also discuss sequences to remove pulse propagation artifacts in optically dense crystals. We pump and indirectly detect normally forbidden multiple-quantum transitions; since these transitions have no dipole moment, they do not couple back through Maxwell's equations. Applications in pure and mixed molecular crystals are presented.

References

1. W. S. Warren and A. H. Zewail, J. Chem. Phys. 75, 5956 (1981); W. S. Warren and A. H. Zewail, J. Chem. Phys. 78, 2279 (1983); W. S. Warren and A. H. Zewail, J. Chem. Phys. 78, 2298 (1983).
2. For a recent review see: M. Burns, W. Liu and A. H. Zewail, "Modern Problems in Solid State Physics" (North Holland, Amsterdam, 1982) vol. 20.
3. M. Banash and W. S. Warren, Proc. 5th Int. Conf. on Coherence and Quantum Optics (in press).

Four Wave Mixing Spectroscopy of Mixed Crystals Using Three Input Frequencies

Jack K. Steehler, Dinh C. Nguyen, and John C. Wright

Department of Chemistry, University of Wisconsin-Madison,
1101 University Avenue, Madison, Wisconsin 53706

Summary

Multiresonant four wave mixing provides information about each resonant level. Multiple resonances also provide sensitivity and selectivity. Specific methods for obtaining unambiguous information from two input frequency and three input frequency nonlinear experiments have been developed. Experimental data have been obtained for the single site pentacene in benzoic acid system, and for the four site pentacene in p-terphenyl system.

In the two input frequency case, a series of spectra, obtained at different frequencies of the unscanned laser distinguish between resonances at $\omega_1-\omega_2$ and $2\omega_1-\omega_2$, since the first is constant on an $\omega_1-\omega_2$ X-axis and the second shifts on this axis, for different spectra of the series, thus identifying both ground state and electronically excited state vibrational levels with one experimental method. Resonance intensities are determined by the overall resonance denominator, and can contain more than one doubly resonant position in a series of spectra. Relative intensities of double resonances have been related to measured resonant enhancements of single resonances.

In the case of three input frequencies, any two of the four frequency elements have been fixed to molecular resonances, providing high sensitivity, with the remaining two frequencies being scanned synchronously. Spectral peaks occurred for energy levels specifically in the region scanned, removing the ambiguity present in a two frequency experiment. Different choices of scanning frequencies allowed study of any of three possible

resonances (Figure 1). Use of three frequencies in CARS (Coherent Anti-Stokes Raman Spectroscopy) allowed selection of a particular ground electronic state vibration, followed by direct study of the intermode coupling of this state to electronically excited vibrational modes. For CSRS (Coherent Stokes Raman Spectroscopy), three independent frequencies allow experiments where the observed nonlinear signal has higher energy than the molecular fluorescence, a feature which frees CSRS from interfering fluorescence, promoting the use of the site selective capabilities of CSRS.

Resonant nonlinear spectroscopy is complicated by population changes induced by lasers resonant with allowed molecular transitions. Changing observed position shifts in a series of two frequency spectra, changing resonance shapes and changing relative intensities have all been predicted and observed at moderate laser powers. These effects markedly affect interpretation of spectra, including the situation at high power when observed spectra originate wholly from populated excited states.

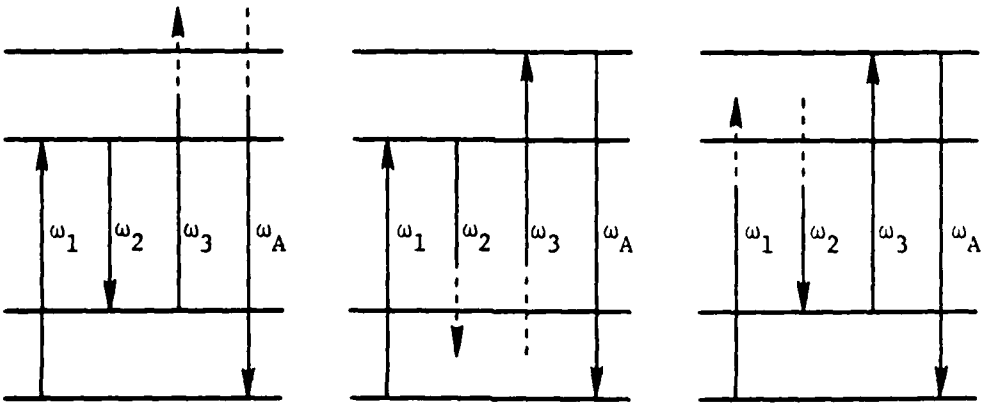

Figure 1. Three types of scans for three input frequency CARS.

Non-Degenerate Four-Wave Mixing in CuCl

R. Levy, F. Tomasini and J.B. Grun

Laboratoire de Spectroscopie et d'Optique du Corps Solide

Associé au C.N.R.S. n° 232 - Université Louis Pasteur

5, rue de l'Université - 67000 Strasbourg (France)

As it is well known from non-linear optics, the dielectric susceptibility χ of semiconductors is a function of the intensity of the impinging light. The non-linear part of the susceptibility gives rise to different light-mixing processes, the efficiency of which depends on the phase mismatch of the beams involved.

On the other hand, real and imaginary part of the dielectric susceptibility determine the polariton dispersion and the absorption coefficient, respectively. The non-linear part of the susceptibility thus gives rise to dispersion anomalies induced by light fields. They may be important when working near one- or two-photon resonances in semiconductors. When studying non-degenerate light-mixing processes, the question of whether or not the phase-matching condition is met, depends on the intensity of the light beams.

We have studied dispersion anomalies using non-collinear, non-degenerate four-wave mixing. The figure shows schematically our experimental configuration. A XeCl excimer laser pumps simultaneously two dye lasers : a pump beam (index "p") with photon energy $\hbar\omega_p$ and a maximum intensity of 50 MW/cm^2 and a test beam

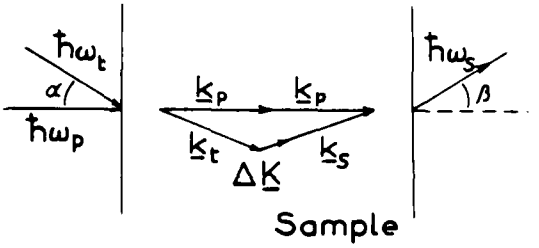

(index "t") with photon energy $\hbar\omega_t$ and a constant intensity of 200 KW/cm^2. The emitted light of both lasers is polarized linearly and focused onto CuCl crystals of about 10 to 40 μm thickness, cooled down to 1.6 K.

Inside the crystal, polaritons propagate with wave-vectors $\underset{\sim}{K}_p$ and $\underset{\sim}{K}_t$, respectively, and a four-wave mixing process may take place, giving rise to a signal beam (index "s") with photon energy $\hbar\omega_s$. The process obeys to energy conservation :

$$2\,\hbar\omega_p = \hbar\omega_t + \hbar\omega_s$$

Concerning wave-vector conservation,

$$\Delta\underset{\sim}{K} = 2\underset{\sim}{K}_p - \underset{\sim}{K}_t - \underset{\sim}{K}_s$$

phase-matching ($\Delta\underset{\sim}{K} = 0$) may be easily achieved if the angles of incidence $\alpha = \beta$ are kept small. The parametric signal $\hbar\omega_s$ is analysed by a spectrometer and an optical multichannel analyser.

When varying $\hbar\omega_t$, the signal intensity passes through a maximum if the phase-matching condition is fulfilled. The spectral position of this maximum depends on the intensity of the pump beam. Near two-photon resonances, a doublet structure of the maximum is observed if the laser beams have the same direction of polarization. In agreement with selection rules, a single maximum is observed for crossed polarizations. The intensity dependence of the shift and of the splitting of the excitation spectrum is explained by a theoretical calculation for the polariton dispersion, using the matrix density formalism applied to a four-level system. We, thus, obtain information on the real and imaginary part of the dielectric function which are of considerable interest for opto-electronics and especially for intrinsic optical bistability.

Laser Induced Gratings in CdS

H. Kalt, V.G. Lyssenko, K. Bohnert and C. Klingshirn
Physikalisches Institut der Universität
Robert-Mayer-Straße 2-4
D-6000 Frankfurt am Main, F.R. of Germany

The diffraction from laser induced gratings is investigated in CdS at low temperatures in the spectral region close to the absorption edge. The coherent, monochromatic laser beams of about 3 nsec temporal halfwidth coincide on the sample under an angle of $1{,}6^{\circ}$ forming a grating with a period of 17,4 µm. The sample thickness is about 7 µm, so we are dealing with a "thin" grating. The intensities of the beams are varied from about 50 W/cm^2 to 10^6 W/cm^2, either by simultaneously attenuating both beams (so keeping their ratio constant) or by changing only one intensity, while the other is fixed.

From the plots of diffracted intensity versus incident intensities (i.e. grating efficiency) at constant wavelength and of diffracted intensity versus wavelength at constant incident intensity (excitation spectra) we are able to deduce the optical nonlinearity producing the grating:

In the region from 50 W/cm^2 to 10^3 W/cm^2 the two laser beams create a mainly absorptive grating due to an excitation induced broadening of the free A-exciton resonance. At excitation intensities between $2 \cdot 10^3$ W/cm^2 and $5 \cdot 10^4$ W/cm^2 the nonlinearity yielding the grating is the appearance of additional resonances due to two photon- or two step transitions to the biexciton. In this region, the intensity dependences of both the absorption and refractive indices are

the reasons for the creation of a grating. The experimental findings may in this case equally well be explained in the wavepicture (see above) and in the particle picture as stimulated decay of a virtually excited intermediate biexciton level [1].

Above 10^5 W/cm^2 an electron-hole plasma is formed. The spectral dependence of the grating efficiency coincides with the variation of the indices of absorption and refraction determined in an independent experiment. The two exciting lasers produce an absorptive grating for laser photon energies above the chemical potential of the plasma and a dispersive one below, however with lower efficiency.

[1] A. Maruani and D.S. Chemla, Phys. Rev. B23, 841 (1981)

Study on the Renormalization Effects of Exciton Polaritons in CuCl by Non-Linear Ellipsometry

Makoto Kuwata and Nobukata Nagasawa

Department of Physics, Faculty of Science, University of Tokyo, Tokyo 113, Japan

Recently, the optical bistability associated with the formation of excitonic molecules (EM's) has been studied intensively. For the quantitative analysis of this effect the non-linear change in the refractive index should be measured. Here we present a new method to measure this accurately.

The Γ_1-EM can be created directly by the two-photon excitation with the combination of the circularly polarized photons of opposite senses. Here let us consider that the two monochromatic laser beams enter the sample holding the condition of the two-photon resonance; one is a circularly polarized excitation beam, say σ^- polarization, and the other is a linearly polarized probe beam which is the coherent superposition of the σ^+ and σ^- components. Since only the σ^+ component of the probe beam can couple with the excitation beam, optical anisotropy occurs for the probe beam to change its polarization elliptic reflecting the non-linear modulation induced in the complex refractive index for the σ^+ component of the probe beam. From the measurement of the orientation of the elliptical axis and the elliptical angle of the outgoing probe beam one can determine the real and imaginary part of the difference of the complex refractive index, $\Delta\tilde{n} \equiv \tilde{n}^+ - \tilde{n}^-$, where $\tilde{n}^\pm$ is the complex refractive index of the $\sigma^\pm$ component. Because $\tilde{n}^-$ is not subject to the non-linear modulation, $\Delta\tilde{n}$ represents the two-photon non-linear refractive index whose real and imaginary parts correspond to the induced renormalization of exciton-polariton (EP) dispersion and the two-photon absorption, respectively.

To measure $\Delta\tilde{n}$ we have developed a non-linear ellipsometer composed of a linear analyzer and a $\lambda/4$ plate which are able to rotate around the probe beam's optical axis in the control of a conventional micro-processor. Though

the pulsed dye lasers pumped by a N_2-laser are used as the beam sources, which have the fluctuation about 10 %, we can determine the elliptical parameters and the degree of polarization with sufficient accuracy.

Here we will report the principle of this method and the results obtained in CuCl. The intensity dependence of the two-photon dispersion, i.e. the induced renormalization of EP's and the relation between the spectrum of the real part and that of the imaginary part of $\Delta\tilde{n}$ will be discussed.

Two-Photon Polarization Spectroscopy in the Spatially Dispersive Region of Exciton Polaritons in CuCl

Makoto Kuwata and Nobukata Nagasawa

Department of Physics, Faculty of Science, University of Tokyo

Tokyo 113, Japan

Spatial dispersion effect has been one of the most important problems in exciton optics since Pekar pointed out the existence of the anomalous waves in 1957. Because this effect always appears in the highly absorbing region of exciton resonance, it is not easy to study this effect with the ordinary spectroscopy. Recently we have developed the two-photon polarization spectroscopy (TPPS), which is based on the photo-induced optical anisotropy coming from the renormalization of exciton polaritons (EP's) due to the two-photon formation of excitonic molecules (EM's). By this method we can monitor the number of EP's in the spatially dispersive region through the change in the polarization of the probe light with the energy in the transparent region. Here we will demonstrate how the TPPS displays its effectiveness to study the spatial dispersion effect of the EP's in CuCl and show the various features of EP's revealed by this method.

A CuCl single crystal is illuminated by two lasers: One is a linearly polarized probe beam of $\Omega_1(k_1)$ and the other is a circularly polarized excitation beam of $\Omega_2(k_2)$, where Ω_i and k_i are the photon energy and the wave vector of each beam in the crystal. If the energy sum $\Omega_1(k_1) + \Omega_2(k_2)$ and the momentum sum $\hbar(k_1 + k_2)$ are equal to $\Omega_M(k_M)$ and $\hbar k_M$, where Ω_M and k_M are the energy and the wave vector of the EM, the probe polarization becomes elliptic. Then we measure the intensity spectrum of the transmitted probe beam through a crossed analyzer, $I_{sig}(\Omega_1)$ with fixed Ω_2. As long as the excitation is not too high the shape of this spectrum is Lorentzian peaked at $\Omega_1 = \Omega_M(k_M) - \Omega_2(k_2)$. The peak intensity reflects the number of EP's of $\Omega_2(k_2)$ inside the crystal. Since the resultant EM energy depends on k_2 through the momentum conservation rule we can also know the wave vector

of Ω_2 polaritons from the peak position.

Here we set Ω_2 just above $\Omega_L(k=0)$, the longitudinal exciton energy; $I_{sig}(\Omega_1)$ shows two well resolved lines because in this energy region there exist two EP modes having the same energy but quite different wave vectors: One is the upper branch polariton (UBP) and the other is the lower branch polariton (LBP). From the intensity of these lines one can get the information about the additional boundary condition at the surface and the relaxation of EP's inside the crystal. In this case the production of LBP's from the UBP's at the rear boundary is also demonstrated clearly. Based on the above results we will discuss: 1) how the UBP's and the LBP's coexist in the crystal; 2) the dynamical behaviour of EP's and 3) further application of TPPS.

AD-A148 470 INTERNATIONAL CONFERENCE ON LUMINESCENCE HELD AT MADISON WISCONSIN ON 13-17 AUGUST 1984(U) WISCONSIN UNIV-MADISON W M YEN OCT 84 N00014-84-G-0053 4/9

UNCLASSIFIED F/G 20/6 NL

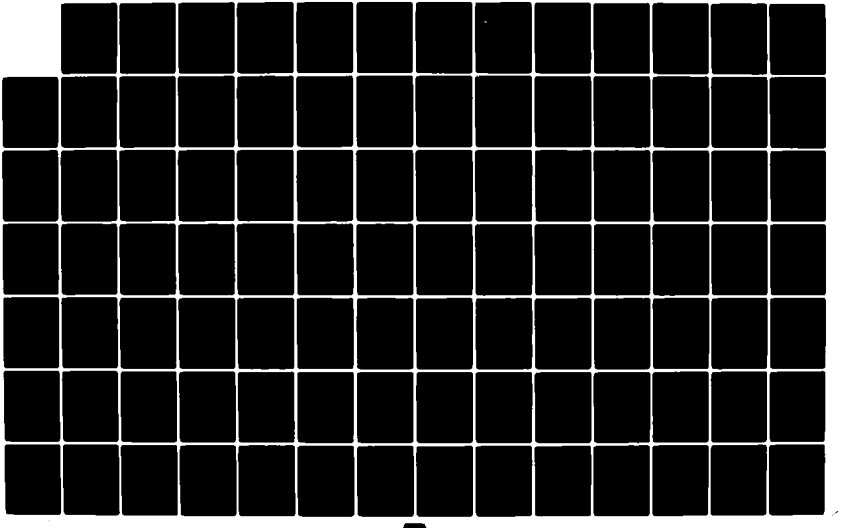

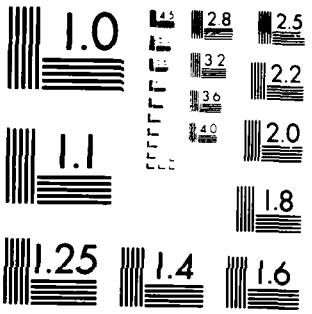

Optical studies of Rare Earth ion pairs : interaction and energy transfer - R. Buisson, Laboratoire de Spectrométrie Physique, Université de Grenoble 1, B.P. 68, 38402 Saint Martin d'Hères-cédex, France.

Rare earth ion pairs in isolators produce satellites for all optical transitions as a result of both the crystal field change induced at the site of each ion by its neighbour and the interaction between the two ions. The very narrow lines of diluted crystals make possible the selective excitation of these pairs and thus the direct study of the fundamental two ion mechanisms which are involved in transfer processes. Instead of measuring the average effect of transfer due to all classes of pairs, the rate can be measured for each class. The properties of concentrated crystals (a macroscopic result) can then be predicted from results obtained on pairs in a diluted sample (a microscopic measurement).

This new approach of the transfer problem has been used to study the quenching of the $^3P_0$ fluorescence in $LaF_3:Pr^{3+}$ and that of the $^4F_{3/2}$ fluorescence in $LaF_3:Nd^{3+}$. In the first case, the above prediction was well verified. In the same time, evidence for a short range interaction was reported [1]. For the second system, the method has also been fruitful since it has brought a complementary proof of the existence of the optical excitation diffusion at low temperature, a diffusion which curiously disappears at high temperature.

The selective excitation of pairs has also been used to study various processes by which a pair can be doubly excited. Since generally the pair produces then an anti-Stokes fluorescence, these processes are of importance, for instance in view of the U.V. lasers. Some indications on the possibility of a stimulated emission of an up converted fluorescence have

recently been reported [2]. Experiments on $LaF_3:Nd^{3+}$ have shown the existence of double quantum processes besides the two successive single quantum processes.

Two laser experiments, suggested by the absence of anti-Stokes fluorescence after selective excitation of some satellites have lead to a spectroscopy of pairs. The results have been well illustrated in the case of $LaF_3:Pr^{3+}$ [3] for which two lasers, whose pulses were slightly time shifted, were necessary to doubly excite some pairs. The difference between the photon energies gave an order of magnitude of the coupling. The same method, applied to $LaF_3:Nd^{3+}$, has also given informations on the coupling.

1 - J.C. Vial and R. Buisson, J. Physique Lett. 43, L 745 (1982)

2 - S.C. Rand, L.S. Lee and A.L. Schawlow, Opt. Com. 42, 179 (1982)

3 - J.C. Vial and R. Buisson, J. Physique Lett. 43, L 339 (1982).

Exciton Transfer and Quenching in Solid Solutions

A. I. Burshtein

Institute of Chemical Kinetics & Combustion

USSR

TuI1, TuI2, TuI3 and TuI4

TuI1 Self-Trapping of Excitons at the Surface of Rare-Gas Solids and its Manifestation in Luminescence and Desorption, P. Coletti and J. M. Debever, Faculte des Sciences de Luminy, France. See MC1 for summary.

TuI2 Luminescent and Photochemical Properties of Molecules near Rough Metal Surfaces, S. Garoff, D. A. Weitz, and T. S. Alvarez, Exxon Research and Engineering Company. See MC2 for summary.

TuI3 Photoluminescent and Electroluminescent Properties of $Cd_{0.95}Mn_{0.05}$ Electrodes, A. A. Burk , Jr., and Arthur B. Ellis, University of Wisconsin-Madison, and Dana Ridgley and Aaron Wold, Brown University. See TuF10 for summary.

TuI4 Optical-Environment-Dependent Lifetimes and Radiation Patterns of Luminescent Centers in Very Thin Films, Ch. Hattinger and J. Lukosz, Swiss Federal Institute of Technology, Switzerland. See MC4 for summary.

TuJ1, TuJ2, TuJ3 and TuJ4

TuJ1 Characterization of the Luminescent Triplet State of the $K_2Cr_2O_7$ Crystal at 1.2 K via Electron Paramagnetic Resonance and Optical Spectroscopy, J. H. van der Waals and M. A. J. A. van der Poel, University of Leiden, The Netherlands. See MB 16 for summary.

TuJ2 Self-trapping of Excitons in Rare-Gas Solids: Measurement of Self-Trapping Rates and Influence of Dimensionality, E. Poick and R. Gaethke, Universitat Hamburg, FRG, P. Gurtler, Hamburger Synchrotonstrahlungslabor HASYLAB bei DESY, FRG, and G. Zimmerer, Universitat Hamburg, FRG. See MB9 for summary.

TuJ3 4f-Electron-Phonon Interaction and Davydov Splitting in PrF_3, M. Dahl and G. Schaack, Universitat Wurzburg, FRG. See MB1 for summary.

TuJ4 Mechanisms of Exciton Trapping in Oxides, M. Hayes, Clarendon Laboratory, United Kingdom. See MB7 for summary.

Hyperfine Spectroscopy and Spin Dynamics by Optical and Sublevel Coherence

R.M. Shelby and R.M. Macfarlane

IBM Research Laboratory
5600 Cottle Rd., K32/281
San Jose, California 95193 U.S.A.

It has been well established that for many metastable electronic levels of impurity ions in insulators, optical coherence times at liquid helium temperatures are limited by magnetic interactions with host nuclear spins.[1] To understand coherence loss in detail, one needs measurements of optical and spin dephasing, magnetic properties and hyperfine structure of impurity ions, and spin dynamics of host nuclei. To this end techniques such as spectral hole burning,[2] coherent transients (e.g. photon echo),[1,3] and optical-rf double resonance[4] have been used. All of these are limited directly or indirectly by optical T_2, and have not directly probed the dynamics of host nuclei.

We have demonstrated a technique which is capable of extracting sublevel spectra which are limited in resolution by the sublevel T_2, and not by the optical T_2 or by the frequency jitter of the laser. The technique, called quantum beat free induction decay, is based on the excitation of sublevel coherence by a short optical pulse (impact excitation), and detection by coherent forward scattering[5] and Fourier transformation. The technique has the multiplex advantage inherent in Fourier spectroscopy, and because of the weak requirements on optical coherence, it may be applicable to a wide variety of materials. We have used this method to determine hyperfine splittings of the excited $^1D_2$ state of Pr^{3+} in YAG: *viz* 6.49 and 8.29 MHz. (See Fig. 1). The linewidths obtained are due to inhomogeneous broadening of the sublevels, but homogeneous dephasing can be measured

by using a second excitation pulse to produce a sublevel echo[5], or by fluorescence detection of spin echoes.

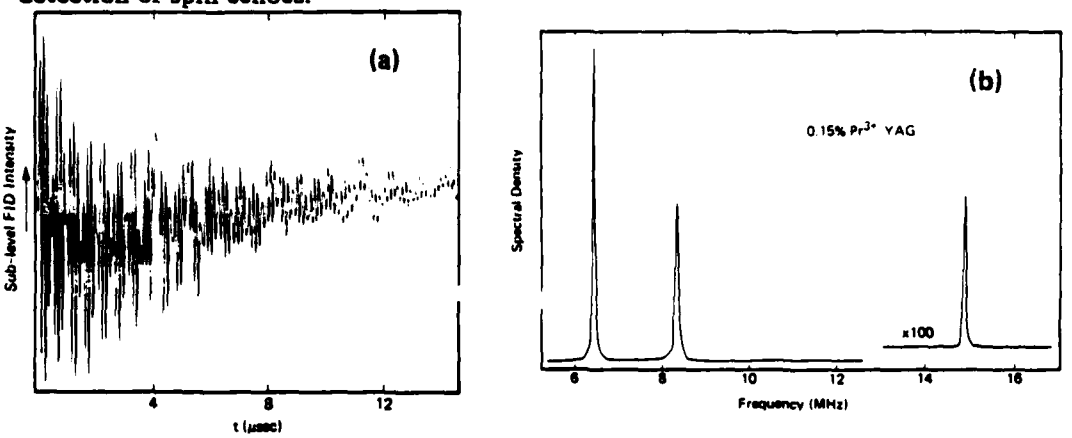

Figure 1. Quantum beat free decay signal, (a) and its Fourier transform, (b) for 0.2 Pr in YAG.

This kind of spectral information is useful in determining the magnetic response of the impurity ion to local fields. The dephasing of hyperfine sublevels or of optical transitions of these rare earth systems also depends on the dynamics of the host nuclear spins, which may be perturbed by the presence of the impurity. For example, in the tetragonal site of CaF_2:Pr^{3+} the ground state has a magnetic moment of $1.9\mu_B$. The result is a 'frozen core' of fluorine nuclei, the most important spins for optical dephasing being those on the fringe of the frozen core where the flip rates and strength of the ^{19}F -- Pr^{3+} interactions are comparable. These are just the spins that are difficult to probe with double resonance. We have used a delayed optical free induction decay technique to measure the time dependence of the width of a narrow hole burned in the optical absorption line, revealing the first direct indications of important frozen core dynamics on a timescale long compared to T_2 but shorter than the usual holeburning timescale (~ seconds).

REFERENCES

1. S.C. Rand, A. Wokaun, R.G. DeVoe, and R.G. Brewer, Phys.Rev.Lett. *43,* 1868 (1979); R.M. Macfarlane and R.M. Shelby, Opt.Comm. *39,* 169 (1981), and ref. therein.
2. L.E. Erickson, Phys.Rev. *B16,* 4731 (1977).
3. R.M. Macfarlane, R.M. Shelby, and R.L. Shoemaker, Phys.Rev.Lett. *43,* 1726 (1979).
4. L.E. Erickson, Opt.Comm. *15,* 246 (1975); K. Chiang, E.A. Whittaker, and S.R. Hartmann, Phys.Rev. *B23,* 6142 (1981).
5. J. Mlynek and W. Lange, Opt.Comm. *30,* 337 (1979); Y. Fukuda, K. Yamada, and T. Hashi, Opt.Comm. *44,* 297 (1983).

TuK2, TuK3 and TuK4

TuK2 Nondegenerate Four-Wave Mixing in CuCl, R. Levy, F. Tomasini, and J. B. Grun, Universite Louis Pasteur, France. See TuC7 for summary.

TuK3 Renormalization Effects of Exciton Polaritons in CuCl by Nonlinear Ellipsometry, Makoto Kuwata and Nobukata Nagasawa, University of Tokyo, Japan, and Two-Photon Polarization in the Spatially Dispersive Region of Exciton Polaritons in CuCl, Makoto Kuwata and Nobukata Nagasawa, University of Tokyo, Japan. See TuG9 and TuG10 for summaries.

TuK4 Laser Excitation and Spin Coherence of Phosphorescent F_2^{2+} Centers in CaO, M. Glasbeek, M. Casalboni, and R. Vreeker, University of Amsterdam, The Netherlands. See TuG3 for summary.

Excited States of Transition Metal Complexes

C. J. Ballhausen
Kobenhavns Universitet
H. C. Orsted Instituttet
Universitetsparken 5
2100 Kobenhavn O Denmark

The pure crystal field calculation by Finkelstein and Van Vleck "On the Energy Levels of Chrome Alum", published in 1940, marked the first quantitative calculation of the excited states of a large molecular entity. It succeeded also in identifying the emitting state in this $(3d)^3$ system as a ^2E_g state.

A detailed understanding of the behaviour of the excited states in transition metal complexes requires however, also the introduction of spin-orbit couplings and vibrational-electronic mixings. Furthermore, the "crystal field" is to be thought of as a "Pseudo-Potential". This lead to the orbital splittings being proportional upon the squares of the overlap integrals between the metal and ligand orbitals. The realization that many excited states have equilibrium conformations which differ widely from that of the electronic ground state complicates the analysis of the dynamical processes.

Two-Photon Absorption Spectroscopy of Rare Earth Ions

N. Bloembergen

Division of Applied Sciences, Harvard University

Pierce Hall, Cambridge, MA 02138

Observations on two-photon transitions in the $4f^7$ configuration of Gd^{3+} and Eu^{2+} reveal the importance of crystal field and spin-orbit interactions in the intermediate $4f^6$ 5d levels.

The Jahn-Teller Effect

R.J. Elliott

Department of Theoretical Physics, University of Oxford,
1 Keble Road, Oxford, OX1 3NP, UK.

Van Vleck developed the Jahn-Teller ideas to explain magnetic and optical properties of ions in crystal. The application to spectra will be reviewed.

Direct Optical Studies of Proton Tunneling in Hydrogen Bonded Mixed Molecular Crystals.

H.P. TROMMSDORFF, Laboratoire de Spectrométrie Physique associé au CNRS, Université Scientifique et Médicale de Grenoble, B.P. 68 - 38402 SAINT MARTIN D'HERES CEDEX, France.

Numerous carboxylic acids crystallize as cyclic dimers linked by two hydrogen bonds. The mobility of the acid protons is sufficiently high such that proton rearrangements, which can be induced thermally or by optical excitation, will anneal even at the lowest temperatures ($T < 1.5$ K). Dye molecules doped substitutionnally into carboxylic acid host crystals exhibit, at low temperatures, well resolved quasiline spectra as is commun for mixed crystal systems. These spectra are sensitive to changes in the environment of the dye molecule and can therefore be used to monitor the above mentionned proton rearrangement processes.

Tautomerisation of the dimers is the simplest such process, NMR studies of benzoic and p-toluic acid crystals have established an asymmetric double well for these systems (barrier heigh $V \sim 400$ cm^{-1}, energy difference 35 cm^{-1} and 85 cm^{-1} in the two crystals) and have determined the rate of tautomerisation as $\gamma_o e^{-V/kT}$, with $\gamma_o = 1\text{-}2 \times 10^{11}$ sec^{-1} (1). At temperatures below 120 K this double proton exchange was thought to be dominated by tunneling. For thioindigo doped crystals the energy difference of the tautomer forms of certain neighboring benzoic acid dimers is lowered to about 1-3 cm^{-1}, spectra of crystals at 2-4 K therefore reveal different sites. Site interconversion is observed to occur during the lifetime of the excited state of thioindigo and reflects the tautomerisation of the neighboring benzoic acid dimers. A measure of the fluorescence rise and decay following site selective excitation was thus used to make the first experimental determi-

nation of the proton tunneling rate leading to tautomerisation in a carboxylic acid crystal[2].

An other process involving the acid host protons was found in both, thioindigo and pentacene doped crystals. Reversible photoinduced hydrogen abstraction, giving rise to holeburning when the guest molecule is excited with a narrowband laser, can lead to the formation to metastable proton defects in the host[3]. In pentacene doped benzoic acid these defects anneal by proton tunneling on timescale of up to an hour. The lifetime (62,5 min.) of the most stable defect was found to be temperature independent up to $\sim$ 20 K and to decrease to $\sim$ 10 sec. around 100 K[4]. The (center symmetric) guest molecule acquires a crystal field induced dipole moment in the defect environment as established by optical Stark measurements : this can be used to gain information about the structure of the defect and therefore about the reversible photochemical process leading to its formation[5].

REFERENCES

(1) S. NAGAOKA et al. - Chem. Phys. Letters 80, 580 (1981)
B.H. MEIER, F. GRAF and R.R. ERNST - J. Chem. Phys. 76, 767 (1982)

(2) J.H. CLEMENS, R.M. HOCHSTRASSER and H.P. TROMMSDORFF - J. Chem. Phys. in press.

(3) R.W. OLSON et al. - J. Chem. Phys. 77, 2283 (1982).

(4) R. CASALEGNO and H.P. TROMMSDORFF, Photochemistry and Photobiology. Proc. of the Int. Conf. Jan. 1983, Alexandria, Egypt, Vol. 2, Ed. A.H. Zewail, (Haarwood Acad.) (to be published).

(5) R. CASALEGNO, R.J.D. MILLER and H.P. TROMMSDORFF, to be published.

Investigation of Excited State Dynamics in Condensed Phases Using Picosecond Nonlinear Techniques

Michael D. Fayer
Chemistry Department
Stanford University, Stanford, CA 94305

Excitation transport and excited state dynamics are investigated in ordered and disordered systems using picosecond nonlinear techniques and detailed statistical mechanical treatments. Transient holographic grating measurements on anthracene single crystals provide the first direct measurements of singlet exciton transport (1). The initial results measure the rate of transport and suggest transport is quasicoherent.

Picosecond photon echo experiments are then used to address the temperature dependence of the dephasing of delocalized states of molecular dimers (2). These experiments on tetracene and pentacene dimers in p-terphenyl host crystals conclusively demonstrate that scattering to dimer librational states rather than scattering between delocalized states dominate the temperature dependent dephasing.

Finally excitation transport among chromophores in disordered systems is described. Excitation transport among chromophores in solution is measured with fluorescence mixing experiments and accurately described by a diagrammatic, nonperturbative approximate solution to the systems Master Equation (3). Excitation transport among chromophores in a finite volume, such as dye molecules in micelles (4) and chromophores attached to the backbones of isolated polymer coils are examined experimentally and theoretically (5).

(1) Todd S. Rose, Roberto Righini, and M. D. Fayer, *Chem. Phys. Lett.*, **106**, 13 (1984).

(2) F. G. Patterson, William L. Wilson, H. W. H. Lee, and M. D. Fayer, *Chem. Phys. Lett.*, accepted (1984).

(3) C. R. Gochanour, Hans C. Andersen, and M. D. Fayer, *J. Chem. Phys.*, **70**, 4254 (1979); C. R. Gochanour and M. D. Fayer, *J. Phys. Chem.*, **85**, 1989 (1981).

(4) M. D. Ediger, R. P. Domingue, and M. D. Fayer, *J. Chem. Phys.*, **80**, 1246 (1984).

(5) M. D. Ediger and M. D. Fayer, *Macromolecules*, **16** 1839 (1983).

WC1, WC2, WC3 and WC4

WC1 Evidence for a Double Acceptor Bound Exciton in a II-VI Compound, P. J. Dean, M. Kane, and M. Skolnick, Royal Signals and Radar Research Establishment, United Kingdom, F. de Maigret, Le Si Dang, A. Nahmani, and R. Romestain, Universite Grenoble, France, and N. Magnea, Centre d'Etudes Nucleaires de Grenoble, France. See FE8 for summary.

WC2 Emission Properties of Quantized Excitonic Polaritons in a Thin GaGs Layer, L. Schultheis and K. Ploog, Max-Planck Institut fur Festkorperforschung, FRG. See FE4 for summary.

WC3 High-Density Excitation and Raman Spectroscopy of the Bound-Exciton Complex (A^0,X) in CdS, I. Broser and J. Gutowski, Institut fur Festkorperphysik II der Technischen Universitat Berlin, FRG. See FE10 for summary.

WC4 Excitons in CuCl Microcrystals Embedded in NaCl, Tadashi Itoh and Toshio Kirihara, Tohoku University, Japan. See MB15 for summary.

SELECTIVE EXCITATION OF EXCHANGE-COUPLED Cr^{3+} PAIRS

C M McDonagh and B Henderson

Department of Pure and Applied Physics
Trinity College
Dublin 2
Ireland

Selective excitation of $^2E \rightarrow {}^4A_2$ fluorescence from Cr^{3+} ions in MgO using a tunable CW dye laser has revealed optical transitions which are not observed in direct absorption or fluorescence measurements. These lines are assigned to a new centre involving an exchange-coupled pair of Cr^{3+} ions. Fluorescence measurements as a function of concentration show that the pair of lines at 698.9 nm and 703.5 nm arise from a tetragonally symmetric pair configuration. The assignment of these optical transitions to the system Cr^{3+} - VAC - Cr^{3+} has now been confirmed by an EPR study[1]. Selective laser excitation in this spectral region indicates the presence of another optical spectrum which almost overlaps that of the Cr^{3+} - VAC - Cr^{3+} system, and which also exhibits tetragonal symmetry. A number of lines are observed from 698.7 nm up to the region of the cubic R-line at 698.1 nm due to the higher ^2E_v orbital state of this new centre. The splitting due to the lower ^2E_v transition is not as readily observed partly because of the greater overlap with the Cr^{3+} - VAC - Cr^{3+} transitions. The data have been fitted to a configuration involving two Cr^{3+} ions in next nearest neighbour positions in a <100> crystal direction. The exchange coupling in the ground state is antiferromagnetic as is expected for Cr^{3+} ions. However, the energy intervals between the total spin states S = 0,2,1 and 3 do not follow the Lande interval rule predicted for simple linear

exchange coupling ($J\underline{S}_1\underline{S}_2$). The measured splittings are consistent with an exchange striction[2] model which results from the balance between elastic and exchange forces in the ground state and in consequence introduces a biquadratic exchange term of the form $j(\underline{S}_1.\underline{S}_2)^2$.

References

1. Carroll, J C G, McMurry, S, Corish J, Henderson B (to be published).

2. Harris, E A, 1972. J. Phys. C: Solid State Physics, 5, 338.

The Spectroscopy of Low-Ligand-Field Cr^{3+} in Germanium Garnets

W.J. Miniscalco, S.R. Desjardins, L.J. Andrews, and B.C. McCollum

GTE Laboratories Incorporated, 40 Sylvan Road, Waltham, MA 02254

The search for tunable solid state lasers has lead to a resurgence of interest in Cr^{3+}-doped materials. Crystals with an intermediate or low ligand field environment for the Cr^{3+} ion are of particular interest because of their potential as broadly tunable, 4-level, red and near-infrared lasers. These hosts are qualitatively different from high field materials such as ruby and luminesce in a broad band because the $^4T_2$ state is comparable or lower in energy than the ^2E state. We present the results of optical and electron paramagnetic resonance (EPR) spectroscopic investigations of a family of Cr^{3+}-doped germanium garnets with the formula $Ca_3M_2(GeO_4)_3$, where M = Al, Ga, or Sc. The Cr^{3+} ion substitutes for the M^{3+} and occupies a site of distorted octahedral symmetry. We have found significant variation among these three germanates with regard to ligand field strength and concentration quenching for Cr^{3+}. Moreover, the small ionic radii of Al^{3+} and Ga^{3+} enable these analogs to form high concentrations of a native defect believed to be a complex of the F^+ center. The presence of this color center makes it difficult to control the oxidation state of the Cr dopant. This defect does not form in the Sc germanate and Cr remains in the 3^+ oxidation state.

The color center complex was first detected using X-band powder EPR measurements which revealed unexpected Al and Ga hyperfine structure for both doped and undoped samples. These results are explained by a complex

of a F^+ center (one electron trapped at an oxygen vacancy) with an Al^{3+} or Ga^{3+} ion which alters the electron density at the Al or Ga nucleus. Accordingly, the unpaired spin revealed by the EPR measurements can be explained without resorting to Al or Ga in extremely rare oxidation states. Overall charge balance is preserved by an Al^{3+} or Ga^{3+} ion occupying the tetrahedral Ge site. The complex does not form for the Sc germanate because the ionic radius of Sc is too large for it to occupy the Ge site and provide charge compensation for the F^+.

The effect upon the oxidation state of Cr is apparent from absorption and luminescence measurements. The absorption spectrum of the Ga germanate shows three broad, Cr-related bands which, however, are not due to Cr^{3+} because they lie in the wrong spectral region. For all three germanates the room temperature emission spectrum is dominated by the phonon side band of the $^4T_2 \rightarrow {}^4A_2$ transition, indicating that some Cr^{3+} is present in the Al and Ga compounds. However, only for the Sc germanate is the luminescence decay exponential and wavelength-independent for all concentrations investigated. In addition, both the Al and Ga analogs are much more sensitive to Cr^{3+} concentration quenching. At low temperature the photoluminescence spectra of the Al and Ga germanates become more inhomogeneous and a broad band is resolved on the long-wavelength side of the $^4T_2 \rightarrow {}^4A_2$ transition. Low temperature emission spectra also reveal that for the Al and Ga analogs the ^2E is the lowest-lying excited state. The Sc germanate is a true low ligand field Cr^{3+} host with the $^4T_2$ state lowest in energy.

PRESSURE EFFECTS OF FLUORESCENT R-LINES OF CHRYSOBERYL $BeAl_2O_4:Cr^{3+}$

W.Jia,Y. Shang,R. Tang,and Zh. Yao
(Institute of Physics,Beijing,China)

The behavior of fluorescent R-lines of chrysoberyl $BeAl_2O_4:Cr^{3+}$(0.1%atm) has been investigated under hydrostatic pressures upto 68 kbar at room temperature. It was found that R_1 and R_2 lines were linearly shifted to the red, in contrast to the ruby system,with different rates of 0.62 and 0.71 cm^{-1}/kbar respectively, as a result,R_1 and R_2 lines gradually approach to each other with pressure. The line width s of R_1 and R_2 were narrowed,and the lifetimes were lengthened from 0.5 ms (R_1,R_2) at normal pressure to 3.5 ms (R_1) and 3.0 ms (R_2) at 68 kbar. Time resolution spectra of the fluorescent band have been measured. It was found that the background of fluorescent phonon band was blue shifted and was suppressed with pressure.

The red shift is analyzed by means of crystalline field theory[1] and lattice relaxation[2]. Hydrostatic pressure will modify π bond overlap integral between 3d orbital of Cr^{3+} ions and 2p orbital of O^{2-},and this will lead in part to decreasing of energy separation between ^2E and $^4A_2$ levels. High pressure will also modify frequencies of lattice vibration due to anharmonicity,and phonon state density and Huang-Rhys factor,as a consequence,the transition energy between ^2E and $^4A_2$ states will decrease somewhat.

The fluorescent phonon band background comes from $^4T_2$ level[3],which is thermally populated from the metastable states ^2E. $^4T_2$ energy level will shift to the blue due to increasing

of the crystalline field parameter Dq with pressure. Therefore the phonon band will be blue shifted at high pressure,and the intensity will decline because of decreased thermal population.

The lifetime lengthening and the line narrowing of R fluorescence have not been explained. At normal pressure,the fluorescence comes from Cr^{3+} ions on the mirror symmetry sites. At high pressure,however,the influence from Cr^{3+} ions on the inversion sites as trapping centers,which produce very weak,but long-lifetime emission,possibly plays a more and more important role.

Reference

1. J. Xu and M. Zhao,Scientia Sinica,24(1981), 1076.
2. K. Huang,Progress in Physics (in Chinese), 1(1981),31.
3. J. C. Walling et al., IEEE J. Quantum Electr. QE-16(1980),1302.

Interpretation of Hydrostatic Pressure Dependence of Ruby R-lines

D. E. Berry, Phys. Dept., University of Delaware, Newark, DE 19716, USA
D. Curie, Laboratoire de Luminescence, Université Paris, 75230 Paris, France
F. Williams, Phys. Dept.,University of Delaware, Newark, DE 19716, USA

The R-lines of ruby are red-shifted linearly with hydrostatic pressure, with no quadratic effect, to 200 kbars.[1] The shift has been attributed, from crystal field analyses, to delocalization of the d-orbitals resulting in changes in the Racah parameters B and C.[2,3] From the adiabatic potential theory of pressure effects the linear shift of the R-lines is attributed to differences between the effects of pressure on the zero point energies of the excited and ground electronic states, primarily due to difference in anharmonicities of the two states; a quadratic shift arises from differences in the change in equilibrium energies with pressure, due to differences in coupling and/or force constants for the two states.[4]

We have extended the adiabatic theory to include quadratic effects on the zero point energies and applied it to the R-lines of ruby. The transition energy at pressure P, $h\nu(P)$ is an analytic function of $\Delta A/A_g$, $\Delta K/K_g$ and $\Delta\beta/\beta_g$, where $\Delta\Gamma = \Gamma_e - \Gamma_g$, with linear and quadratic terms in P. Ground state parameters are obtained from experimental data: K_g from A_{1g} phonon energies, β_g from thermal expansion, and A_g from pressure dependence of the cation-anion distance for ruby. From values of $\Delta\Gamma$'s which make linear effects maximal but keep quadratic effects small we find that the main pressure effect is due to $\Delta\beta$ and that $\Delta\beta$ must be positive , i.e. the $^2E\ Cr^{3+}$ is softer then $^4A\ Cr^{3+}$. The pressure at which quadratic effects are appreciable is estimated as is in excess of 200 kbar.

In principle, the adiabatic potential and crystal field analyses can be inter-related. The crystal field energies are electronic energies, $E_j(R)$, and are related to the adiabatic potential, $V_j(R)$, as follows: $E_j(R) = V_j(R) - v_j(R)$, where $v_j(R)$ is the nuclear-nuclear interactions. In conventional crystal field analyses differences are calculated, i.e. $\Delta E(R) = E_e(R) - E_g(R)$, and only for unfilled shells, thus $\Delta v(R)$ is the difference in core-core interactions and is non-zero. This is evident from the existence of a linear dependence of $\Delta E(R)$ for ruby[3], its absence in each $V_j(R)$, and the equilibrium R for the ^2E and ^4A states being the same to a good approximation. We have expanded $v_j(R)$ in powers of $(R-R_o)$ and used the linear approximation for $\Delta E(R)$ and find that the parameters of crystal field theory for ruby are not simply related to those of the adiabatic potential theory.

New experiments are proposed to resolve the remaining ambiguities in the quantative interpretation of the pressure dependence of the ruby R-lines. Spectral shifts to megabar pressure will be predicted. We also include application of the theory to other Cr^{3+} doped oxides.

1. G. J. Piermarini, S. Block, J. D. Barnett and R. A. Forman, J. Appl. Phys. 46, 2774 (1975).
2. R. G. Munro, J. Chem. Phys. 67, 3146 (1977).
3. S. Ohnishi and S. Sugano, Japan J. Appl. Phys. 21, L309 (1982).
4. D. Curie, D. E. Berry and F. Williams, Phys. Rev. B20, 2323 (1979).

Luminescence from $LiGa_5O_8 : Co^{2+}$

J. F. Donegan, F. J. Bergin, G. F. Imbusch

Physics Department, University College, Galway, Ireland

and

J. P. Remeika

Bell Laboratories, Murray Hill, New Jersey.

Crystals of cobalt doped $LiGa_5O_8$ have a deep blue colour and the absorption spectrum is characteristic of Co^{2+} in tetrahedral sites. The cobalt ions enter tetrahedral gallium sites in this material. The strong absorption in the visible is due to the $^4A_2 \rightarrow {}^4T_1(^4P)$ transition which peaks at around 16,000 cm^{-1}. Luminescence occurs in the red and near infrared. In this material the $^4T_1(^4P)$ level lies below the $^2E(^2G)$ level and consequently the luminescence occurs from the $^4T_1$ state. These luminescence transitions are thus spin-allowed and, since the tetrahedral site lacks inversion symmetry, the transitions occur by an electric dipole process - the lifetime at 77 K is around 200 ns. At low temperatures the $^4A_2 \leftrightarrow {}^4T_2(^4P)$ luminescence and absorption transitions are characterized by a sharp strong zero-phonon line. At higher temperatures the fine structure is lost, and the luminescence shows up as a broad band.

OPTICAL PROPERTIES OF $LiGa_5O_8$:Mn

T.ABRITTA, F. DE SOUZA BARROS AND N.V.VUGMAN,
Instituto de Física-UFRJ, 21944, Rio de Janeiro, Brasil
and
N. T. MELAMED,
Westinghouse R & D Center,
Pittsburgh, Pennsylvania, 15235, USA

Luminescence and EPR measurements were done on single crystals of $LiGa_5O_8$ having nominal Mn concentrations of 0.4, 1.0, and 10wt%. These crystals were grown by the flux method and supplied by Deltronic Crystals Industries, Inc.‡ The dominant fluorescent signal is due to the B-site Mn^{4+} ions. At 10K the emission is characterized by a sharp zero-phonon line at 721.6nm due to the $^2E(G) \rightarrow {}^4A_2(F)$ transition. This fluorescence has a decay time of 450μs, and its lower-energy side bands have a very rich structure. For the more concentrated Mn samples the intensity behaviour of some of these side bands indicates the presence of pair lines. The comparison between the observed luminescence properties of Mn^{4+} with those of its isoelectronic Cr^{3+} in the same compound[1] shows that the Mn^{4+} zero-phonon line and its vibronics are shifted to lower energies, and that the $^4T_2$ excitation bands are shifted to higher energies, giving rise to a Dq value of $2000cm^{-1}$. These trends are due to the fact that both covalence and crystal field parameters must have larger values with the increase of central ionic charge. The $^4T_1$ excitation band of Mn^{4+} is hidden at the tail of a charge transfer band shifted towards longer wavelengths. Assuming the relation C=4B for these Racah parameters one has for Mn^{4+} a B value of $660cm^{-1}$ and a C value of about $2640cm^{-1}$. Similar results for Mn^{4+} and Cr^{3+} emissions were obtained in the isomorphous compound $LiAl_5O_8$[2].

For ultraviolet excitation it is observed another

emission band which remains broaden even at 10K, and with a baricenter at 605nm. This band is associated to the Mn^{2+} B-site emission resulting from some reduction of Mn^{4+} ions. The preliminary assignment of this band to Mn^{2+} B-site occupancy is due to the fact that in the literature broad luminescence bands in the red of phosphors containing manganese are ascribed to Mn^{2+} ions in an octahedral oxygen surrounding [3,4].

X-band EPR measurements at room temperature indicate unambigously the presence of Mn^{2+} ions, among other paramagnetic centers. The spin Hamiltonian parameters obtained have almost the same values as those reported by Tsintsadze et al[5] for the Mn^{2+} in B-sites of this compound, thus confirming the present optical observations concerning Mn^{2+} ions. Mn^{4+} EPR spectra lying at the intense central part of that due to Mn^{2+} i under study.

References :

‡ Dover, N.J 07801

(1) T. J. Glynn, J. P. Larkin, G. F. Imbush, D. L.Wood and J. P. Remeika, Phys. Letters 30A (1969) 189.

(2) B. D. McNicol and G. T. Pott, J. Lumin., 6 (1973) 320

(3) D. T. Palumbo and J. J. Brown Jr., J. Electro chem. Soc.118 (1971) 1159.

(4) A. L. N. Stevels, J. Lumin., 20 (1979) 99.

(5) G. A. Tsintsadze, V. A. Shapovalov, and V.N. Seleznev, Phys. Stat. Sol. (a), 22 (1974) K205.

Efficient Sensitization of Mn^{2+} emission by Sn^{2+} in Fluoroapatites.

R.G. Pappalardo and T.E. Peters
Physical Electronics Technology Center
GTE Laboratories, Waltham, MA 02254.

SUMMARY

New schemes[1] for increasing the brightness output of fluorescent lamps rely on combining a yellow emission band, as produced by Mn^{2+}, with a narrow, blue emission band, as provided by Eu^{2+}. In this connection we have observed that coactivation of Ca fluoroapatites [$Ca_5(PO_4)_3F$, or CaFAP in brief] with Sn^{2+} and Mn^{2+} can provide in the yellow spectral region a Mn^{2+} emission, with intensity exceeding by roughly 20% the highest intensity obtained from current Ca fluoroapatites coactivated with Sb and Mn.

While in the case of the latter material a sizeable Sb^{3+} emission, with peak at ≈500 nm, is still present in the phosphor emission, the absence of any significant Sn^{2+} emission in the corresponding Sn-Mn coactivated materials is strong evidence, together with the enhanced intensity of the Mn^{2+} emission, of very efficient transfer of excitation energy from Sn^{2+} to Mn^{2+}.

The excitation spectra for 575 nm emission, as measured in the long-UV and visible spectral region for direct absorption by Mn^{2+}, are similar for both Sb-Mn and Sn-Mn coactivation, the overall intensity enhancement by almost a factor of two in the Sn-Mn case being due to the higher Mn content. The only spectral difference of note occurs in the structure of the excitation triplet centered at 350 nm. The decay constants for Mn emission at 575 nm are also comparable in both materials (14ms-15ms).

Depending on the synthesis conditions, the singly activated CaFAP:Sn materials exhibit, on 254 nm excitation, either a gaussian-shaped emission band with peak at ≈350 nm, or a composite band shape, with a pronounced emission tail extending into the visible spectral region.

At room temperature, sampling of the decay kinetics along the spectral profile of the composite band emitted by Sn^{2+} reveals a dominant fast decay (shorter than the 2 μs excitation pulse) in the short-wavelength portion of the emission band, and a longer decay (20-30 μs to the first 1/e folding) for the long-wavelength emission components. The UV excitation spectra are also markedly different on monitoring the emission along the short-wavelength and long-wavelength components of the Sn^{2+} emission band, or while monitoring the Mn^{2+} emission in the yellow spectral region. Additional measurements are under way to identify the corresponding electronic levels of Sn^{2+} associated with the different decay kinetics and different excitation spectra, and to determine the actual levels of Mn^{2+} involved in the sensitization process.

It is anticipated that Sn^{2+} will act as an efficient sensitizer of Mn^{2+} emission not only in the class of apatite materials, but also in other classes of phosphors of interest to the lighting industry.

References.

1. W.W. Piper, J.S. Prener, and C.G.R. Gillooly, US Patent 4,075,532 (1978).

WD8-1

Fluorescence Characteristics of X-ray Excited CaF_2:Mn(x)

(x = 0.1%, 1.0%, 3.0%)

Joanne F. Rhodes, R. J. Abbundi, D. Wayne Cooke[†], V. K. Mathur, and M. D. Brown

Naval Surface Weapons Center, White Oak, Silver Spring, Maryland 20910

[†]Present address: Los Alamos National Laboratory, Los Alamos, New Mexico 87545

Summary

The characteristic 500 nm emission of CaF_2:Mn has been attributed to the de-excitation of Mn^{2+}. However, several mechanisms have been proposed for the formation of the excited Mn^{2+} ion. We have conducted a detailed systematic study of the emission spectra of CaF_2:Mn over the temperature range, 13 - 672 K, which covers the entire thermoluminescence glow peak region. We compared our data for samples with 0.1% and 1.0% Mn to previously reported[1] data for a sample with 3.0% Mn to determine the effects of Mn concentration on the spectra. The entire spectral region was simultaneously recorded by a microcomputer-based diode array, which allowed the accumulation of a large number of spectra with good reproducibility. The data were analyzed to quantitatively determine the centroid, full-width at half-maximum (FWHM), intensity, and skewness of the spectra.

Analyses of the data revealed a significant systematic shift in the centroid of 4-6 nm toward longer wavelengths as temperature was reduced below 250 K, with the amount of shift depending on the Mn concentration. Since the skewness is small and changes little with temperature, the centroid behaves as the emission peak. This shift has not been previously reported or

theoretically predicted. The well-known hyperbolic cotangent expression for the FWHM did not fit the experimental data well over the extended temperature range investigated. The quality of the fit decreased as Mn concentration decreased. The integrated intensity of the emission increased by a factor of 2 - 4 in the temperature range of 150 - 250 K, with a steeper increase accompanying a lower Mn concentration. The present data did not support the large amount of high-temperature thermal quenching previously reported[2].

In the temperature range below 250 K where the centroid shift and the large intensity increase is observed, several other physical phenomena are known to occur in CaF_2. There is experimental evidence supporting the formation and extinction of Mn^+, V_k and V_{ka} centers in this interval. The centroid shift is attributed to a change in the environment that the Mn^{2+} sees below 250 K. A huge thermoluminescence glow peak is observed around 200 K where the sharp increase in the integrated emission intensity is observed. Competition between trap filling and radiative recombination may account for the sharp rise in intensity. Though phenomenological explanations of the salient features of these results are possible, we emphasize the lack of a comprehensive theory to explain our data.

[1] R. J. Abbundi, D. W. Cooke, V. K. Mathur, G. A. Royce and M. D. Brown Radiation Protection Dosimetry 6, 329 (1984).

[2] S. G. Gorbics, A. E. Nash and F. H. Attix, Intl. J. of Appl. Radiation and Isotopes 20, 829 (1969).

Renewing Investigation of Luminescence Spectrum of Manganese Ion Doped in Cadmium Chloride

Hsia Shang-ta Chen Shao-jiang
Department of Physics
China University of Science and Technology
Hefei, Anhui, China

Summary

We have made a new assignment of spectrum of $CdCl_2:Mn^{++}$ which had been published by B.Ghosh et.al.[1] . The main points which are different from theirs are as following:

1).There have been some evidences of D_{3d} distortion in this spectrum.

2). The six peaks between 26660 cm^{-1} and 27390 cm^{-1} have been assigned as phonon sideband which is based on the D_{3d} and spin-orbit splitting of $^4T_2(D)$. Because of Cd^{++} and Cl^- have no magnetic momentum and the concentration of Mn^{++} is very low. They should not look as exciton-magneton-phonon sideband.

3). The sharp peaks at 23670 cm^{-1} and 23860 cm^{-1} have been regard as a result of No-phonon magnetic transition $^6A_1 \rightarrow {}^4E(G)$ and $^6A_1 \rightarrow {}^4A_1(G)$ (^4E-$^4A_1$ degeneration is removed by $H_{D_{3d}}$). Because of the diagonal martrix elements of H_{SL} in $^4E(G)$ equal zero, the previous assignment in which both of them have been due to $^4E(G)$ is unlike to us. Moreover, the peak at 23980 cm^{-1} has been identified as One-phonon sideband of the transition $^6A_1 \rightarrow {}^4A_1(G)$ [2].

4). The electrical dipole transition ought to be assisted

by phonons for the parity conservation. In our fitting computation the phonon spectra of $CdCl_2$ and $MnCl_2$ have been consulted[3][4] and included.

Using the irreducible tensor method of Tanabe-Sugano[5], at first, we have diagonalized the martrix of $H_o = H_e + H_{Trees} + H_{Ch} + H_{D_{3d}}$ in the complete configuration of $(3d)^5$ to fit all the principal No-phonon lines, and then, diagonalized the martrix of $(H_o + H_{SL})$ only in the multiplet of $^4T_2(D)$ to fit its sideband. In this way we have obtained a good result so long as the parameters take the following values:

B= 776 C=2900 α=76

D_q=642 τ=2680 σ=670 ζ=300 (cm^{-1})

where $\tau = \langle t_2 \| V(T_2) \| t_2 \rangle$

$\sigma = \langle t_2 \| V(T_2) \| e \rangle$

are parameters in $H_{D_{3d}}$.

Reference

[1]. B.Ghosh, et.al., Phys. Stat. Sol. (B) 102 k89(1980)

[2]. J.Ferguson, et.al., Mol. Phys. 27, 577(1974); 28, 879(1974)

[3]. A.Anderson, et.al., Spectroscopy Letters 14(2), 105(1981)

[4]. D.J.Lockwood, J.Opt. Soc. Amer. 63, 374(1973)

[5]. Y.Tanabe, et.al., J.Phys. Soc. Japan. 9,753(1954); 9, 766(1954); 13, 394(1958).

Unusual green emission from Mn^{2+} in $Gd(BO_2)_3$

T.E. Peters, R.G. Pappalardo and R.B. Hunt Jr.
Physical Electronics Technology Center
GTE Laboratories, Waltham, MA 02254.

SUMMARY

Recent reports[1,2] by Philips researchers on novel, efficient phosphors for lamp applications highlight the role of Gd^{3+} as sensitization intermediate in the process of cascade sensitization $S \rightarrow Gd^{3+} \rightarrow A$ (where S is a broad-band sensitizers, such as Ce^{3+} or Bi^{3+}, and A an acceptor, such as a trivalent rare-earth or Mn^{2+}). On investigating Ce,Mn-coactivated $Gd(BO_2)_3$ we observed, following excitation at 254 nm, a green emission-band, peaking at ≈530 nm, ≈60% as intense (in brightness units) as current willemite phosphors (Zn_2SiO_4:Mn) for lamp applications.

Several features of the observed green emission in $Gd(BO_2)_3$:Ce;Mn are unusual. We identify the green-emitting center as a divalent Mn ion, although no charge compensation is necessary in the formulation of the phosphor, in order to obtain the Mn^{2+} center, rather than the Mn^{3+} species anticipated from the requirement of charge neutrality.

The spectral location of the emission suggests the presence of Mn^{2+} in a four-coordinated site, as observed in oxide hosts, such as willemite (Zn_2SiO_4:Mn) or Mn-activated spinels[3] and hexa-aluminates (β-alumina and magneto-plumbite). Yet, we were unable to detect in the 330-500 nm region the typical excitation pattern for four-coordinated Mn^{2+}. In addition, the emission decay of the green emission in question is much slower (15 ms decay constant) than the ≈3 ms constant expected for four-coordinated Mn^{2+}.

Both the weak excitation pattern detected in the ≈330-500nm region, and the emission decay kinetics are reminiscent of yellow-emitting and orange-emitting Mn^{2+} centers, as found in various apatite phosphors, wherein the coordination number for Mn^{2+} is six or higher. If this is indeed the case, then the spec-

tral shift to the green in the phosphors under discussion must be associated with a unusually-low crystal field in the Tanabe-Sugano diagram[4] .

Excitation of $Gd(BO_2)_3$:Mn at 275 nm and 313 nm, in the absorption lines of trivalent Gd produced strong green emission, thereby proving that the Gd→Mn energy transfer is highly efficient. In the spectral region contiguous to the Gd^{3+} emission at ≈313 nm, we carried out detailed measurements of the excitation spectra for green emission, in order to detect the presence of Mn^{2+} absorption centers overlapping the Gd^{3+} emission, in line with Forster-Dexter energy-transfer models. No excitation regions that could be associated with Mn centers have been detected so far.

Evidence for the cascade sensitization $Ce^{3+}\rightarrow Gd^{3+}\rightarrow Mn^{2+}$ in the doubly-activated materials is provided by the risetime (≈ 600 μs) of the green emission, observed either on excitation of the Ce^{3+} centers at 254 nm, or into the Gd^{3+} centers at 275 nm and 313 nm (in the singly-activated analogs). This risetime is in fair agreement with the lifetime of the emitting Gd^{3+} level. In order to confirm this interpretation of the sensitization process, measurements of the decay kinetics of the Mn emission, following dye-laser excitation directly into the levels of Mn^{2+} , are in progress.

1. J.Th.W. de Hair, J. Luminescence, 18/19, 797 (1979)
2. J.Th.W. de Hair and W.L. Konijnendijk, J. Electrochem. Soc. *127*,161(1980).
3. D.T. Palumbo and J.J. Brown, J. Electrochem. Soc., *117*,1184(1970).
4. Y.Tanabe and S. Sugano. J. Phys. Soc. Japan *9*,766(1954).

DYNAMICAL JAHN-TELLER EFFECT ON THE TRIPLET STATES $^4T_2(D)$ OF Mn^{++} IN POLYMORPHIC ZnS

R. Parrot, C. Naud and D. Curie
Université Pierre et Marie Curie, Laboratoire de Luminescence
4, Place Jussieu, 75230 Paris Cedex 05

H.E. Gumlich, W. Busse and U. Pohl
Institut für Festkörphysik der Technischen Universtät B erlin
Str. des 17 Juni 135
D-1000 Berlin (West)

ABSTRACT

New experimental and theoretical results have been obtained for the orbital triplet states $^4T_2$ arising from the spectroscopic term ^4D of the d^5 configuration of Mn^{++} in polymorphic ZnS.

SUMMARY

The zero phonon lines (ZPL) and phonon assisted lines (PAL) appearing in the $^4T_2$ (D) band centered at 22900 cm^{-1} of Mn^{++} in cubic ZnS with stacking faults and in ZnS with the wurzite structure have been analyzed by using dye laser site selection spectroscopy. Four different excitation spectra have been unambiguously associated to the cubic sites, to two axial sites SF_1 and SF_2 due to stacking faults and to the axial sites in wurzite.

The ZPL's have been separated from the PAL's for each type of center and have been associated to the electric dipolar transitions: $^6A_1 \longrightarrow \Gamma_6$ $^6A_1 \longrightarrow \Gamma_8(3/2)$ and $^6A_1 \longrightarrow \Gamma_8(5/2)$ of the $^4T_2$ (D) multiplet, the transition $^6A_1 \rightarrow \Gamma_7$ being strictly forbidden by symmetry. The experimental spectra show that the states $\Gamma 8$ are split by the axial crystal field of axial centers.

A theoretical analysis shows that a moderate Jahn-Teller (JT) coupling to E vibrational modes corresponding to a Jahn-Teller energy of $\sim 20\ cm^{-1}$ (the energy of the effective phonon being $\hbar\omega_g = 100\ cm^{-1}$) correctly describes the observed fine structure patterns and the relative dipole strengths for Mn^{++} in the cubic sites and axial sites. In particular, this moderate JT coupling cannot strongly quench the influence of the axial crystal field in non-cubic centers so that the orbital degeneracy of the Γ_8 states of Mn^{++} in axial sites can be lifted by the axial crystal field as observed experimentally.

Finally, a careful comparison of the JT coupling in the $^4T_2$ (D) and in the $^4T_2$ (G) multiplet which has been extensively studied previously, shows that no selective energy transfer is expected for the fine structure lines of the $^4T_2$(D) multiplet.

Exciton Migration and Capture in a Linear Chain Manganese Salt. Gary L. McPherson, Roy A. Auerbach, Gary N. Kwawer and Katherine F. Talluto, Department of Chemistry, Tulane University, New Orleans, LA 70118

Like a number of AMX_3 salts, $CsMnBr_3$ adopts the lexagonal $CsNiCl_3$ structure which consists of infinite linear chains of MX_6^{4-} octahedra sharing opposite faces. The physical properties of many of the linear chain AMX_3 salts have attracted considerable attention because of the one-dimensional character of the structure. Yamamoto, McClure, Marzzacco and Walderman observed that the luminescence of $(CH_3)_4NMnCl_3$ is quenched by the presence of transition metal impurities. (Yamamoto et al., 1977). The temperature and concentration dependence of the luminescence quenching indicated that the exciton migration is thermally activated and restricted to the linear chains (one-dimensional). Subsequently it was shown that trivalent rare-earth ions such as Nd^{3+}, Er^{3+} and Tm^{3+} could be introduced into crystals of $CsMnBr_3$ and that these ions behaved as radiative traps for the manganese excitons. (McPherson and Francis, 1978, McPherson et al., 1979).

The luminescence spectra of $CsMnBr_3$ crystals containing three different classes of trapping centers have been carefully investigated in the 12K to 300K temperature range. Two of the classes consist of trivalent rare-earth ions which are incorporated into the lattice with differing modes of change compensation. The third class of trapping center is a "perturbed" Mn^{2+} ion which results when Li^+ is doped into $CsMnBr_3$. This perturbed Mn^{2+} ion has an emission maximum approximately 1000 cm^{-1} lower in energy than that from the Mn^{2+} ions of the bulk crystal. These perturbed ions behave as shallow exciton traps with thermal detrapping between 150K and 200K. The data from the doped crystals indicate that two processes with distinctly different activation

barriers contribute to the rate of exciton capture at the impurity centers. The apparent trapping rate is accurately expressed by simple expression shown below.

$$\text{rate} = A \exp(-E/KT) + B \exp(-E'/KT)$$

For $CsMnBr_3$, E and E' are 200 cm^{-1} and 500 cm^{-1}. The luminescence spectra of crystals where varying fractions of the Mn^{2+} ions of the bulk lattice are replaced by spectroscopically inert Cd^{2+} ions have also been studied. The data indicate that there is considerable excitonic motion above 200K even when the mole fraction of Mn^{2+} is as low as 0.2. This observation strongly suggests that the exciton migration in $CsMnBr_3$ is not restricted to the linear chains, in sharp contrast to the behavior of $(CH_3)_4NMnCl_3$.

References

McPherson, G. L. and Francis, A. H. Phys. Rev. Lett., 41, 1681 (1978).

McPherson, G. L.; Devaney, K. O.; Willard, S. C. and Francis, A. H. Chem. Phys. Lett., 68, 9 (1979).

Yamamoto, H.; McClure, D. S.; Marzzacco, C. and Waldman, M. Chem. Phys., 22, 78 (1977).

Luminescence Centers in Quartz

N. Kristianpoller

Department of Physics and Astronomy, Tel Aviv University,

Tel Aviv 69978, Israel.

SUMMARY

The photoluminescence (PL), radioluminescence (RL) and thermoluminescence (TL), excited in natural Norwegian quartz crystals by monochromatic uv light, beta and X-rays, were studied. Excitation and emission spectra were measured and the dependence of the intensities and the spectral composition of the emission on irradiation temperature as well as on thermal pre-treatment was investigated. The PL excitation spectra in the vacuum uv region between 115-185 nm shows a main maximum at 127 nm. A strong excitation maximum of the TL has recently been recorded at the same wavelength and the TL intensities were found to be comparable to those induced by a 10 m Ci ^{90}Sr beta source.(1) The 127 nm excitation maximum coincides with the long-wavelength tail of an exciton peak, previously recorded in the reflectance spectrum of quartz.(2) However, the PL and TL could also be excited with photons of energies lower than the absorption edge. The PL, as well as the RL and TL emissions showed a broad emission band centered at 440 nm (with a half-width of about 0.80 ev), which was dominant at 80K. Another broad main emission band appeared near 370 nm and could be resolved under certain conditions in 355 and 380 nm bands (with half-widths of 0.50 and 0.42 ev). Additional weaker bands were recorded at about 340 and 520 nm. The relative intensities of these bands depend markedly on the temperature of excitation as well as on thermal pre-treatment. The 440 nm band decreases sharply with increasing temperature near 200K, which resembles the temperature

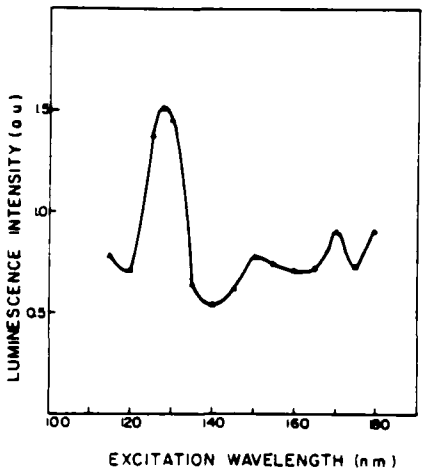

Fig.1. Excitation Spectrum of the Photoluminescence recorded at 80K.

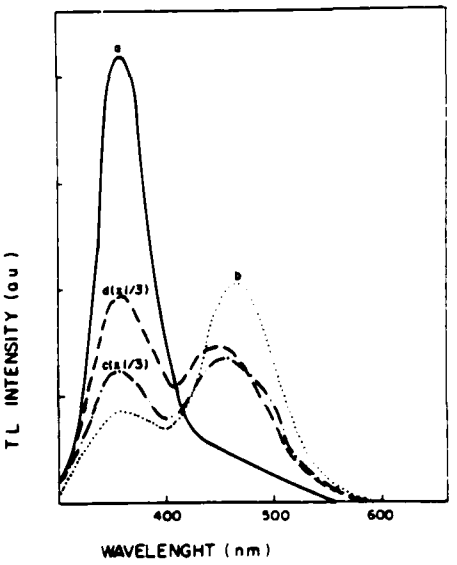

Fig.2. TL Emission Spectra recorded at: a-345K; b-410K; c-465K; d-485K.

dependence of a STE luminescence. This band may possibly be due to radiative decay of a self trapped exciton. The 355 and 380 nm bands showed a different temperature dependence. Emission bands near 380 nm have previously been reported by various authors.[e.g.3,4] Alonso et al. ascribed the broad 380 nm band, recorded in the X-luminescence, to a recombination of electrons with holes, trapped at an adjacent Al-M^+ center.[4] The fact that the same emission bands appeared in the uv excited PL as in the X and beta excited RL and TL, indicates that the emission is due to the same luminescence centers.

References

(1) N. Kristianpoller, Solid State Comm. 48, 621 (1983).

(2) E. Loh, Solid State Comm., 2, 269 (1964).

(3) A. Halperin, A. A. Braner and J. Schapira, J. Luminesc., 1, 385 (1970).

(4) P. J. Alonso, L. E. Halliburton, E. E. Kohnke R. B. Bossoli, J. Appl. Phys., 54, 5369 (1983).

The Oscillator Strength of Interstitial Fe^{4+} in α-Quartz

Alvin J. Cohen
Department of Geology and Planetary Science
321 Old Engineering Hall
University of Pittsburgh
Pittsburgh, Pa. 15260 USA

While α-quartz is trigonal, optically (+), the biaxial spectra of interstitial Fe^{4+} appears to have orthorhombic symmetry with oscillator strength, f, equal 0.011 for E in π and σ and for normal light in a wafer cut in $(1\bar{1}00)$. In a wafer cut in (0001), f is 0.011 with E ∥ a and 0.0065 with E ⊥ a. In normal light in the a-plane f is 0.0084 (while the vectorial average is 0.0087). Evidence is presented that Fe^{4+} can only be interstitial and only appear in major rhombohedral, r, growth in α-quartz, as the mechanism of its production requires the presence of potential trapped-hole centers which are quenched by the electron donor role of interstitial Fe^{3+}.

The potential trapped hole centers in the specimen studied (NMNH No. R-1454) are three Al-trapped hole centers, A_1, A_2 and A_3 (Cohen and Makar, 1982). A_2 seems to be the major center involved. These centers do appear in this specimen only in minor rhombohedral growth, z, being absent in r. The amount of substitutional Al^{3+} and interstitial Fe^{3+} involved in forming Fe^{4+} is determined by comparing the atomic absorption analyses of these impurities in r and z growth. This allows one to eliminate interstitial Al^{3+}, Fe^{2+} and substitutional Fe^{3+} from the calculations.

The mechanism in r growth in the presence of ionizing radiation is as follows:

$$Fe^{3+}(\text{Int.}) \longrightarrow Fe^{4+}(\text{Int.}) + e^-$$

$$Al^{3+}\text{——}O^- - e^- \longrightarrow Al^{3+}\text{——}O \text{ (trapped holes)}$$

$$Al^{3+}\text{——}O \text{ (trapped holes)} + e^- \longrightarrow Al^{3+}\text{——}O^-.$$

This scenario occurs because a void is present perpendicular to the r face and is absent perpendicular to the z face. Possible compression and tension due to interstitial Fe^{3+} seems to be relieved by occurrence of optical (Brazil Law) twinning in most crystals in major rhombohedral growth. These interstitial impurities such as Fe^{2+}, Fe^{3+}, etc. appear to be present as charge compensators in addition to the well studied Na^{+}, Li^{+} and H^{+}.

The role of substitutional Fe^{3+} and interstitial Fe^{2+} in quartz will be reviewed and the reason substitutional Fe^{3+} cannot be a charge compensator, and electron donor for quenching of the trapped-hole centers will be discussed.

The oscillator strength of the Fe^{4+} band indicates it has charge-transfer characteristics.

A. J. Cohen and L. N. Makar (1982) Models for Color Centers in Smoky Quartz. phys. stat. sol. (a) 73, 593-596.

The Effect of Hydrostatic Pressure on the Luminescence of $CaO:Ni^{2+}$

Andrzej P. Radlinski, Zameer U. Hasan and Neil B. Manson

Department of Solid State Physics
Research School of Physical Sciences
Australian National University
Canberra ACT 2601 Australia

Summary

In CaO, Ni^{2+} impurity ions replace Ca^{2+} ions at sites of octahedral symmetry and give rise to several crystal field bands each with considerable vibronic structure.[1,2] In this work the influence of hydrostatic pressure on the structure of two of these bands has been investigated.

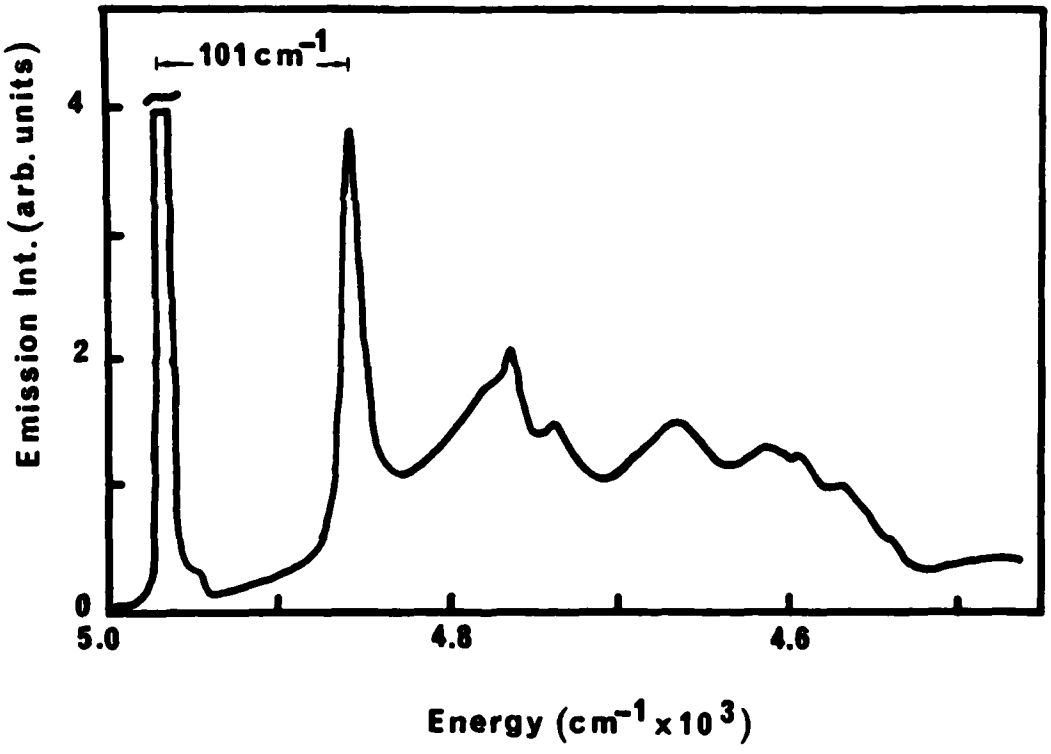

Fig. $^3T_{2g}$ (E) → $^3A_{2g}(T_2)$ emission in $CaO:Ni^{2+}$

The $^3T_{2g} \rightarrow {}^3A_{2g}$ luminescence of $CaO:Ni^{2+}$ shows a zero-phonon line at $4963cm^{-1}$ accompanied by a vibrational sideband which includes a prominent line $101cm^{-1}$ from the zero-phonon line (Fig.). The latter feature corresponds to a transition where a low energy resonance mode with a frequency $\omega = 101cm^{-1}$

couples to the electronic transition. With hydrostatic pressure up to 13k-bars the zero-phonon line and sideband are moved to higher energies at a rate of ~10cm^{-1}/kbar and the frequency of the localised mode is increased in frequency by ~2cm^{-1}/kbar.

The $^3A_{2g} \rightarrow {}^1T_{2g}$ excitation spectrum has been measured by using dye laser excitation while monitoring the infra-red luminescence at 2.'µm. The band shows structure associated with the coupling of the T_{1u} local mode to the T_{2g} electronic state.[1] The quadratic terms in the vibrational displacement cause a splitting of the T_{1u}, T_{2g} vibronic states and in particular the electron-vibration interaction $V_{T_{2g}}$ with T_{2g} symmetry causes the splitting of the $(T_{1u} + T_{2u})$ and $(E_u + A_{2u})$ vibronic levels by

$$\Delta = \langle v | V_{T_{2g}} | v \rangle \frac{\hbar}{\omega}$$

where $|v\rangle$ denotes a vibronic state. The excitation band is moved to higher energy with pressure but the splitting Δ is unchanged. There are two opposing contributions to the value of the splitting. With pressure the frequency ω of the soft localised mode is increased. This by itself would lead to a reduction of the vibronic splitting. However, in a compressed lattice the crystal field gradients will be larger and hence the matrix element $\langle v | V_{T_{2g}} | v \rangle$ can increase. At 13kbars ω has increased by 12% and consequently the latter matrix element must have increased by a similar amount for the splitting to be unchanged.

The observed shift of the bands to higher energy is a direct consequence of the increase of the crystal field strength with lattice compression.

References

1. Manson, N.B. and Wong, K.Y. J. Phys. C Solid State 8, L73-L76 (1975).

2. Wong, K.Y. and Manson, N.B. J. Phys. C Solid State 9, 611-626 (1976).

Optical Properties of Cu^+ Ions in $RbMgF_3$ Crystals

K. Tanimura and W. A. Sibley
Physics Department
Oklahoma State University
Stillwater, Oklahoma 74078

Summary

The optical properties of Cu^+ ions in $RbMgF_3$ single crystals have been investigated. In this material, two distinct sites are available for the Cu^+ ions when they replace Rb^+ host lattice ions. The symmetry of the two Rb^+ sites is C_{3v} and D_{3h} respectively. Therefore, this crystal structure provides the opportunity to study the same ion, Cu^+, in two different sites in one crystal. Two sets of optical absorption and emission bands are observed. The two sets of optical transitions are quite different in nature. In one case, the optical data suggest that there is very weak coupling between Cu^+ ions and the lattice, whereas in the other case strong coupling exists. This is evidenced also by the transition lifetimes of the luminescence associated with these centers. The off-center nature of the copper ions in one lattice position give rise to interesting low temperature optical effects. These effects can be explained in terms of weak and strong lattice coupling and can be utilized to yield an energy level diagram for Cu^+ ions in $RbMgF_3$.

Host lattice dependence of the Bi^{3+} luminescence in orthoborates $LnBO_3$

A. Wolfert, E.W.J.L. Oomen and G. Blasse,
Physical Laboratory, State University,
P.O. Box 80.000, 3508 TA Utrecht,
The Netherlands

The luminescence properties of Bi^{3+} in the orthoborates $LnBO_3$ are strikingly different and depend in a dramatical way on the choice of the host lattice cation Ln. These borates are isomorphous with the several modifications of calcium carbonate. $ScBO_3$ and a modification of $LuBO_3$ have calcite structure with Ln in six coordination. Another modification of $LuBO_3$ and also YBO_3 and $GdBO_3$ have vaterite structure with a six- and a twelve coordinated site. Finally $LaBO_3$ has aragonite structure with a nine coordinated site.

The Bi^{3+} ion shows luminescence in all these host lattices with the exception of $GdBO_3$. In this lattice the Bi^{3+} emission overlaps the Gd^{3+} $^8S \rightarrow {}^6P$ transitions. Efficient energy transfer from the Bi^{3+} ion to the Gd^{3+} sublattice occurs. The fate of the excited state depends on the temperature and on the presence of activators in the Gd^{3+} sublattice.

In the borates with calcite structure the Bi^{3+} ion emits in the ultraviolet spectral region. The spectra show considerable vibrational structure which can be assigned. Energy migration among the Bi^{3+} ions occurs at low Bi^{3+} concentrations.

In the borates with vaterite structure we observed energy transfer from the six to the twelve coordinated site. The emission shows a larger Stokes shift than in the calcite structure. In $LaBO_3$ more than one Bi^{3+} centre appears to be present. Both show a considerable Stokes shift. They are ascribed to isolated

Bi^{3+} ions and to Bi^{3+} pairs. Their decay characteristics are also different.

The results show that the relaxation of the excited state of the Bi^{3+} ion increases if the space available in the lattice for the activator is larger. These results can be related to those for Bi^{3+} compounds (like $Bi_2Ge_3O_9$, $Bi_4Ge_3O_{12}$) which are, from crystallographic data, known to have Bi^{3+} in an off-centre position (1). The large variation in the luminescence properties of Bi^{3+}-activated compounds is, therefore, related to the position of the Bi^{3+} ion in the coordination polyhedron.

References

1. C.W.M. Timmermans and G. Blasse, J. Solid State Chemistry, in press.

Tunneling Luminescence in Zinc Silicate Doped with Gallium

H. Hess, H. Kahlert and E. Krautz

Institut für Festkörperphysik, Technische Universität Graz
A-8010 Graz, Petersgasse 16, Austria.

When zinc silicate with a violet luminescence peaked at 370 nm is doped with gallium in concentrations of 1).001 2).005 3).2 4)1.0 mol % gallium oxide a new emission band with a maximum at 420 nm is established as shown in Fig.1. The separation of both superimposed emission bands is possible because of their different luminescent decay times. By such doping additional traps are introduced as could be proved by the thermal glow curves for the 1) 0 2).01 3).2 mol % gallium oxide concentrations after a 4 minute excitation with 220 nm and a heating rate of 14 K/min as shown in Fig.2. The doped samples are distinguished by an increased light sum and photoconductivity. The red shift of the time-resolved emission spectra for zinc silicate doped with .8 mol % gallium oxide at 20 K as shown in Fig.3 allows to assume that radiating donator-acceptor-pair transitions i.e. radiating tunneling processes between shallow traps and excited activator centers are involved in the charge recombination process. This is in agreement with the results shown in Fig.4a, where the time dependence of the temperature (1) and the luminescence (2) of the doped sample after excitation with 250 nm at 100 K are compared. Below 50 K a remarkable increase in luminescence intensity is observed. The number of electrons

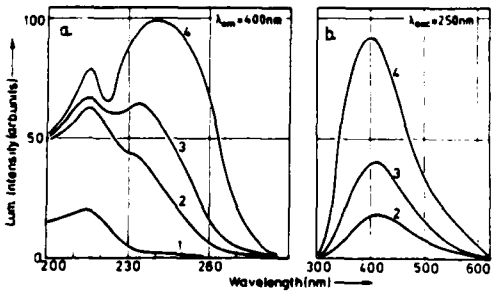

Fig.1

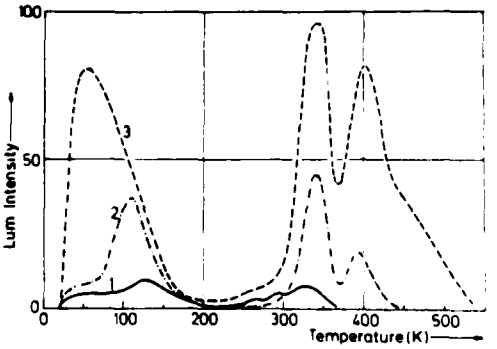

Fig.2

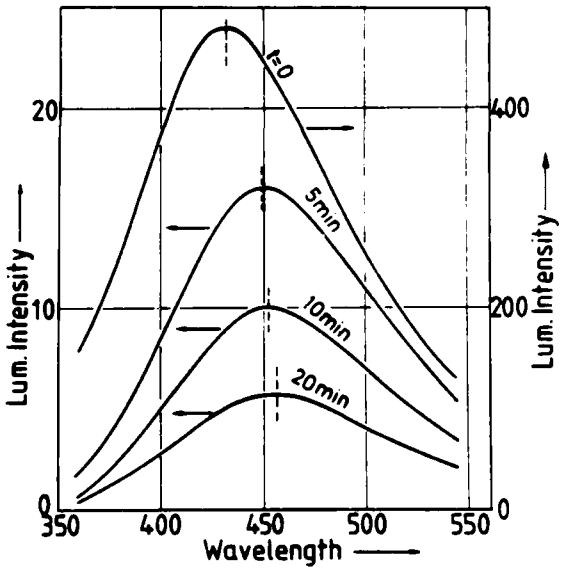

Fig.3

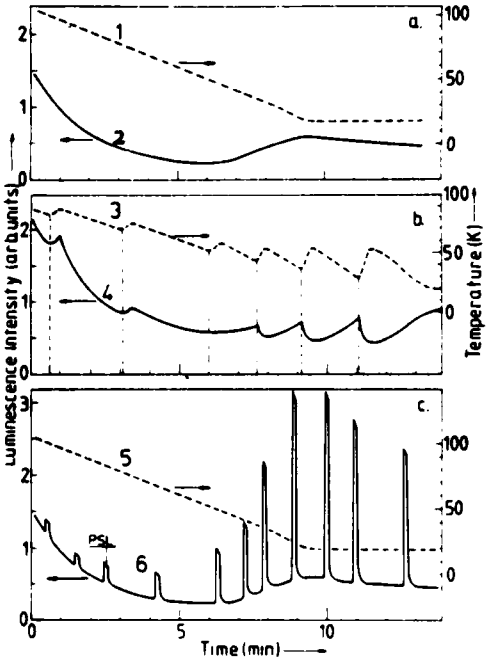

Fig.4

thermally released from the shallow traps is certainly small at these low temperatures. This behaviour is also seen in Fig.4b, where the cooling process has been interrupted by short periods of heating. In the range between 45 K and 60 K the decay of the luminescence is temperature independent, which demonstrates that no thermally stimulated recombination occurs. The additional luminescence can therefore be explained only by electron tunneling from shallow traps to excited activator centers.

Below 45 K short periods of heating cause a decrease in luminescence intensity. Here, thermal activation results in a decrease of electron density in shallow traps wherefrom preferential tunnel recombination is possible.

This fact becomes particularly evident, if short-time photostimulation (PSL) with 900 nm is applied as shown in Fig.4c. Sharp peaks in the tunneling luminescence appear in the critical low temperature region.

Luminescence in pure and Tl^+-doped Alkali Halides, excited by Synchrotron Radiation.

F. Antonangeli[(a)], F. Fermi[(b)], U.M. Grassano[(c)], M. Piacentini[(a)], A. Scacco[(d)] and N. Zema[(a)]

(a) Istituto di Struttura della Materia del C.N.R., Via E. Fermi 38, 00044 Frascati (Roma), Italy

(b) Dipartimento di Fisica, Università di Parma, Italy

(c) Dipartimento di Fisica, Seconda Università di Roma, Italy

(d) Dipartimento di Fisica, Università La Sapienza, Roma, Italy

The energy transfer between the site where the photon is absorbed and the recombination center, where the radiative emission takes place, has been investigated in pure and Tl^+-doped potassium halides.

Excitation in the vacuum-ultraviolet between 13 and 30 eV was performed with the synchrotron radiation from the ADONE storage ring of Frascati.

The main result of the primary ionizing excitation is the creation of electron-hole pairs. The fate of these carriers depends upon temperature and doping in a way analogous to that found in $NaCl:Ag^+$ (1). At low temperature the exciton or the hole are easily self-trapped in the lattice and radiative recombination produces only the intrinsic luminescence. The excitation spectra we observed are almost identical for pure and Tl^+-doped samples and the main feature of the spectra are marked dips at the position of the core excitons absorption (2). It is evident that in these conditions the excitation remains localized at the self-trapping site and no transfer to the Tl^+ ion is possible.

On the contrary, the room temperature excitation spectra are quite different for pure and doped samples. The intrinsic emission is thermally

quenched and luminescence is observed only in doped crystals where a complete energy transfer toward the activator impurity takes place. The luminescence observed in these doped samples is the ordinary Tl^+ emission (A_X and A_T bands).

No clear evidence has been found, in the low temperature excitation, of the sharp increase of the emission quantum yield at energies equal to twice or three times the band gap and explained as a "photon multiplication process". Further experiments are in progress to elucidate this point, expecially in view of the different results reported by the various authors (2)(3)(4).

1) E.A. Vasil'chenko, N.E. Lushchik and Ch.B. Lushchik, Soviet Physics - Solid State 12, 167 (1970).

2) M. Yanagihara, Y. Kondo and H. Kanzaki, SRL - ISSP Tokyo (1980) 44.

3) G. Zimmerer in Defects in insulating crystals, Eds. V.M. Tuchkevich and K.K. Shvarts (Springer, Berlin, 1981) p. 503.

4) H. Onuki and R. Onaka, J. Phys. Soc. Japan 34, 720 (1973).

RESONANT RAMAN SCATTERING OF THE LASER-ACTIVE $Tl^0(1)$ DEFECT IN KCl *

W. JOOSEN, E. GOOVAERTS and D. SCHOEMAKER
Department of Physics, University of Antwerp (U.I.A.), 2610 Wilrijk (Belgium).

The vibrational properties of the laser-active $Tl^0(1)$ center in KCl have been studied by means of resonant Raman scattering. This center consists of a substitutional Tl^0 atom with a negative ion vacancy in a nearest neighbor position and possesses C_{4v}[001] symmetry.[1] It was found to be an attractive laser-active center with output in the infrared around 1.5 μm upon optical excitation of the 1.05 μm optical absorption band.[2]

We have measured the resonant Raman scattering of the $Tl^0(1)$ defect in KCl and it was found to possess two distinct features: a localized vibration at 30 cm^{-1}, with two detectable overtones, and a broad defect-induced first-order phonon spectrum. The Raman scattering was attributed to the $Tl^0(1)$ center on the basis of its well-known production and thermal anneal properties.[1] In Raman scattering experiments with several Ar^+ and Kr^+ laserlines between 457.5 and 647.1 nm the resonant effect becomes stronger towards the $Tl^0(1)$ absorption band at 550 nm. A Behavior Type (BT) analysis[3] of the polarized Raman intensities confirms that the localized vibration belongs to an A_1 representation of the C_{4v}[001] point group. In such a mode the Tl^0 moves along the fourfold symmetry axis, the z-axis of the local reference frame. The validity of the BT method in the case of resonant scattering will be discussed.

As a result of the σ-polarization of the 550 nm absorption band and because of the resonance situation the T_{zz} component of the Raman tensor of the A_1 mode at 30 cm^{-1} is very strongly enhanced. Only in the corresponding polarization geometry is Raman scattering of the $Tl^0(1)$ center detectable. A search was performed for the resonant Raman scattering of the E mode through excitation in the π-polarized absorption band of the defect at 725 nm. This search was unsuccesfull

primarily because of the much lower optical density in this band compared to the 550 nm one, the ratio of which is quadratically reflected in the Raman scattering efficiencies.

A resonant Raman study of the $Tl^0(1)$ center in the other alkali halides is underway and promising results have been obtained for NaCl and RbCl.

References

1. E. Goovaerts, J. Andriessen, S.V. Nistor and D. Schoemaker, Phys. Rev. B 24, 29 (1981).
2. W. Gellerman, F. Lüty and R.C. Pollock, Opt. Commun. 39, 391 (1981); L.F. Mollenauer, N.D. Viera and L. Szeto, Opt. Lett. 9, 414 (1982).
3. J.-F. Zhou, E. Goovaerts and D. Schoemaker, Phys. Rev. B 29 (in press) (1984).

* Work performed under contracts with I.I.K.W. and the Geconcerteerde Acties.

Luminescence of In^+ and Tl^+ in Alkali Halides with the Caesium Chloride Structure

by

D.S. Simkin
Department of Chemistry
McGill University
Montreal, Quebec, Canada
H3A 2K6

and

V.S. Sivasankar* and P.W.M. Jacobs
Department of Chemistry
University of Western Ontario
London, Ontario, Canada
N6A 5B7

Phosphors formed from alkali halides with the CsCl structure that contain activator ions with the ground-state configuration ns^2, differ from their analogues with the NaCl structure in several respects. In addition to the usual A($^1A_{1g} \rightarrow {}^3T_{1u}$), B($^1A_{1g} \rightarrow {}^3E_u$, $^3T_{2u}$) and C($^1A_{1g} \rightarrow {}^1T_{1u}$) absorption bands, a variable number (up to three) charge-transfer bands may be distinguished and in CsI:Tl^+ these CT states actually lie between the $^3T_{1u}$ and $^1T_{1u}$ unrelaxed excited states instead of above $^1T_{1u}$ as is usually the case. In CsI:Tl^+ the CT bands lie in their usual location between the C band and the absorption edge while in CsBr:In^+ no CT bands are seen, presumably because the CT states overlap the intrinsic exciton states. The emission spectrum of CsBr:In^+ contains three bands, none of which are CT bands. Two of these are from coexistent minima of tetragonal and trigonal (or possibly orthobombic) symmetry and the third is from the relaxed B state. The CsI:In^+ emission spectrum also contains these three bands and, in addition, a fourth band

* Permanent Address: Solar Cells Division, Bharat Electronics Limited, Bangalore, India.

that is excited only in the CT absorption band. The emission spectrum of quenched CsI:Tl^+ crystals consist of three bands all of which can be excited in the A band. The coexistence of three types of minima in the adiabatic potential energy surface that represents the relaxed excited $^3T_{1u}$ state is a most unusual occurrence - indeed unique so far in these phosphors - and two possible models for the RES are formulated

In the CsCl structure a $^3T_{1u}$ state can couple with vibrational modes of α_{1g}, ε_g, $\tau_{2g}^{(1)}$ and $\tau_{2g}^{(2)}$ symmetry. This leads to the possibility of one set of minima of tetragonal symmetry and two sets of trigonal (or orthorbombic) symmetry, provided the coupling constants lie in the ranges that permit the coexistence of three sets of minima. The alternative model requires that the ground-state minimum and the $^3T_{1u}$ Jahn-Teller cross-over point in the unrelaxed excited state are not connected by a vertical transition in configuration space. No definite decision can be reached between these two models at present, although the excitation spectra favour the latter one. In all three systems the experimental evidence requires that spin-orbit coupling be a stronger perturbation that the Jahn-Teller interaction. This in turn means that the energy level structure in both the A & B RES consists of only two levels, an upper state from which transitions to the ground state are allowed through spin-orbit coupling, and a lower state from which transitions are forbidden at this level of approximation but which became partly allowed because of the defect strain field. The temperature dependence of the experimental decay times is in complete accord with the kinetic predictions deduced from this model.

IMPORTANCE OF PSEUDO-JAHN-TELLER EFFECT IN THE EXCITED STATE FOR $(TL^+)_2$-TYPE CENTERS IN ALKALI HALIDES

Yoshio Kamishina, Akira Matsushima+, and Atsuo Fukuda*

Shimane University, Faculty of Education, Matsue, Japan 690
+ Nagasaki University, Faculty of Liberal Arts, Japan 852
* Tokyo Institute of Technology, Japan 152

The excited states for (Tl^+)-type centers in alkali halides have been established to be characterized by the Jahn-Teller effect in both aspects of absorption and emission process. In the case of $(Tl^+)_2$-type centers, on the other hand, there is a general belief that the interaction between the paired ions lifts the orbital degeneracy of the active electrons and Jahn-Teller effect can not be expected any more. As a matter of fact, the absorption spectra for $(Tl^+)_2$-type centers have been successfully interpreted in terms of the interaction between the paired ions. The luminescence, however, is not so clear-cut to be understood with the same model. For the purpose of understanding the relaxed excited states (RES's) responsible for the luminescence in $(Tl^+)_2$-type centers, we have investigated their spectral and polarization characteristics and the temperature dependence of the radiative decay times in KI:$(Ga^+)_2$, KI:$(In^+)_2$, and KI:$(Tl^+)_2$, and concluded that some of the RES's are principally determined by the Jahn-Teller effect in $(Tl^+)_2$-type centers, just like in (Tl^+)-type centers. In all the investigated emission bands, the degree of polarization measured as a function of azimuthal angle in the (001) plane is zero in the <110> direction and

its absolute value is maximum in the <100> direction. Therefore, <100> is the direction connecting the paired ions. The emission band excitable by the A_Σ and A_Π absorption bands in the paired-ion center is located close to the A_T emission band in the corresponding single-ion center for KI:$(Ga^+)_2$ and KI:$(In^+)_2$, while that is close to the A_X emission band for KI:$(Tl^+)_2$. Since the interaction between the paired ions is small in the triplet excited states, the interaction can be regarded as a perturbation to the RES's responsible for A_T and A_X emission bands due to the Jahn-Teller effect. The perturbation destroys the equivalence of the three tetragonal distortions for A_T RES; one of them becoms slightly different from the other two. Thus the $A_{T\Sigma}$ and $A_{T\Pi}$ emission bands are observed separately as in KI:$(Ga^+)_2$. Although these two bands could not be separated in KI:$(In^+)_2$, the polarization characteristics observed indicate that the 2.76 eV emission band consists of at least two component bands, $A_{T\Sigma}$ and $A_{T\Pi}$.

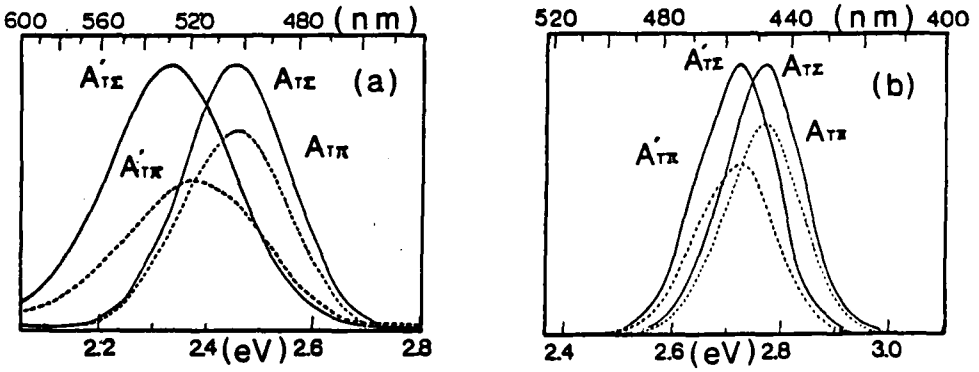

Figure 1. Polarized luminescence at 4.2 K for (a) KI:$(Ga^+)_2$, and (b) KI:$(In^+)_2$.

LUMINESCENCE BEHAVIOR OF Pb^{2+} IN NaCl: ADEQUACY OF A JAHN-TELLER APPROACH

F. Jaque, F. Cussó, F. Agulló-López, J. García Solé and J.L. Martínez
Departamento de Optica y Estructura de la Materia and Instituto de Física del Estado Sólido (C.S.I.C.-U.A.M.), Universidad Autónoma de Madrid, Madrid-34, Spain.

M. Manfredi
Istituto di Fisica dell'Università and Gruppo Nazionale di Struttura della Materia del Consiglio Nazionale delle Ricerche, Parma, Italy.

SUMMARY

It is well known that A band excitation of monovalent ns^2 ions incorporated into alkali halide lattices produces two emission bands designated as A_T and A_x [1]. This situation also appears in NaCl:Pb^{2+} with the special feature that the relative intensity of both emissions depend drastically on the aggregation state and is affected by additional doping with other divalent impurities [2].

In this work, the luminescence and decay-time scheme of A_T and A_x emission in NaCl:Pb^{2+},M^{2+} (M^{2+} = Mg, Ca, Sr, Pb) have been studied in the 11-330 K temperature range. Main results are the following:

i) The A_T emission is single and its position is independent of the M^{2+} ions. At variance, the A_x emission band presents some structure and its position is affected by the M^{2+} ions.

ii) The excitation spectra of both bands are slightly different, being the A_x emission more efficient when excited

in the high energy tail of the A absorption band.

iii) A Jahn-Teller splitting higher than that founding the A_T excitation [3], has been observed for the A_x excitation band, Fig. 1.

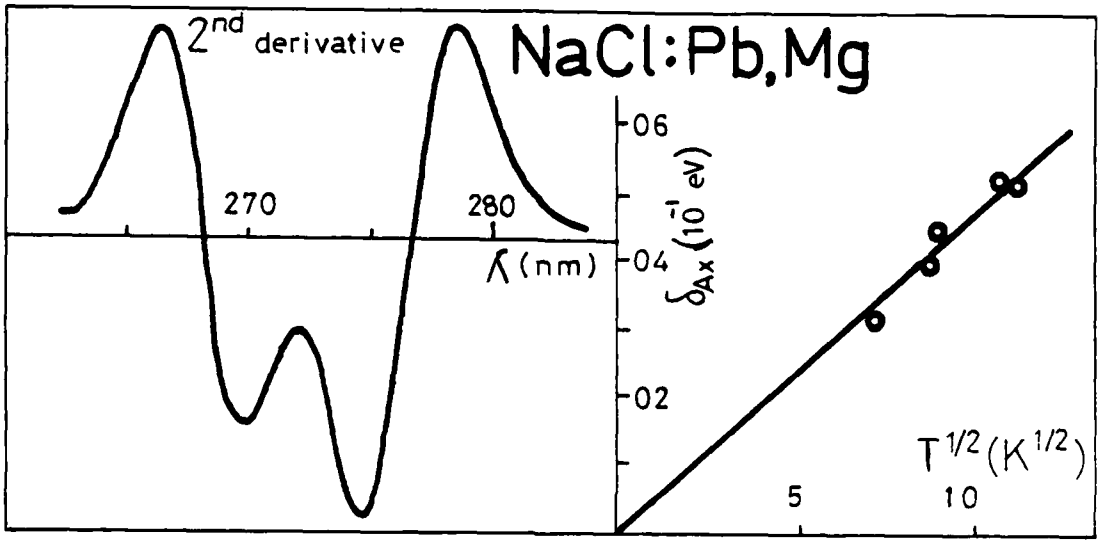

iv) The luminescence decay-time of both bands above 50 K presents a temperature dependence which is in accordance with the presence of a reservoire level. This behaviour cannot be associated to a thermal quenching effect, because the intensity of A_x and A_T bands keep constant until 220 K.

These results as well as the role of the M^{2+} ions are discussed by means of a double-well model in the APES, initially put forward by Fukuda [1].

1. A. Fukuda, Phys. Rev. B1, 4161 (1970).
2. J.L. Pascual, L. Arizmendi, F. Jaque and F. Agulló-López, J. Lumin. 17, 325 (1978) and P. Aceituno, F. Cussó, F. Jaque and F. Agulló-López, to be published.
3. F. Jaque, P. Aceituno, F. Agulló-López, J. Rubio O. y H. Murrieta S., Sol. Stat. Comm. 41, 127 (1982).

Excited State Absorption and the 4p-electron Levels of Cu^+ in Alkali Halide Hosts

Ring-Ling Chien, John Simonetti and Donald S. McClure
Department of Chemistry, Princeton University
Princeton, New Jersey 08544 USA

The Cu^+ ion in NaF, LiCl and NaCl shows weak near UV and strong vacuum UV sets of absorption bands, identifiable as 3d→4s and 3d→4p respectively.[1] The weak, temperature-dependent 4s transitions occur 1-2 eV higher in energy than in the free Cu^+ ion, while the 4p bands lie 1-2 eV lower. The simplest interpretation of these facts is that the 4s electron is more strongly antibonding toward the ligands than are the 3d electrons, while the 4p electron is partly bonding and partly spread out beyond the nearest neighbor anion shell into the next neighbor cation shell. This general description was confirmed by the calculations of Harrison and Lin.[2]

The characteristics of the 4s state have been investigated in some detail, but the more interesting 4p states are difficult to study since transitions to them from the ground state are clearly observable in only the above three cases. A study of this less localized state would be valuable as an example of a loosely bound electron at an impurity site; we would like to see how such states are related to exciton states of the host crystal as perturbed by the impurity.

We have compared the 3d→4p absorptions originating in the ground state, and appearing in the vacuum ultraviolet with the 4s→4p absorptions originating in the $^3E_g(d^9s)$ state and appearing in the visible. The absorptions from the ground $^1A_{1g}$ state terminate on $^1T_{1u}(e^3t^6p)$ and $^1T_{1u}(e^4t^5p)$, but the two corresponding bands are not clearly resolved as 10Dq(=3000 cm^{-1})is comparable to the band width even at 4.2K. The $^3T_{1u}$ states belonging to these configurations have not been seen in absorption

from the ground state.

The transition from the $^3E_g(d^9s)$ reaches the $^3T_{1u}$ and $^3T_{2u}$ states of d^9p. These are not resolved; a single broad band is observed for the $^3E_g \rightarrow {}^3T_u$ transitions. In table 1, the first column shows the experimental results of the excited state absorption of all four crystals at 300K; the triplet ^3E_g 0-0 energy is then added in the second column. Also shown is the energy region of the T_{1u} states from the vacuum UV spectra.

These results show that the $^3T_{1u}$, $^3T_{2u}$ states lie in almost the same spectral region as the $^1T_{1u}$ states. In the free atom, however, the triplet states range from 66418 to 73102 while the singlets range from 71920 to 73595, an average separation of about 3000 cm^{-1}. As this separation is absent in the crystals, we conclude that the d-hole, p-electron interaction is much weaker than in the free ion. This would be in agreement with the picture of the p-orbital presented above.

1. J. Simonetti and D. S. McClure, Phys. Rev. B16, 3887 (1977).

A. B. Goldberg, D. S. McClure and C. Pedrini, Chem. Phys. Lett, 87, 508 (1982).

2. J. G. Harrison and C. C. Lin, Phys. Rev. B23, 3894 (1981).

Table 1
The energy levels of the d^9p states

	$^3T_u - {}^3E_g$	$^3T_u - {}^1A_g$	$^1T_u - {}^1A_g$
NaCl	22472-41667 cm^{-1} (26882)*	52472-71667 (56882)	50000-70000 (58800)
KCl	20325-38462 (27397-31250)	49825-67962 (66897-60750)	
NaF	25000-41667 (30769)	54000-70667 (59769)	51000-65000 (60000)
LiCl	17391-29411 (21053-24691)	52071-64091 (55733-59371)	52000-60000 (57500)

*peak position

Spectral band assignments for Cu^+ and Ag^+ in alkali halides via two-photon spectroscopy

Donald S. McClure, Department of Chemistry, Princeton University
Princeton, New Jersey 08544 USA
Christian Pedrini, Laboratoire de Physico-Chemie
des Matériaux Luminescents, Université de Lyon, 69622
Villeurbanne, France

The absorption spectra of Cu^+ and Ag^+ in alkali halide crystals have been studied for some time by way of ordinary absorption and emission spectroscopy.[1] It has been established that the near ultraviolet transitions are due to $3d^{10} \rightarrow 3d^9 4s$ for Cu^+ and $4d^{10} \rightarrow 4d^9 5s$ for Ag^+, and that these occur at considerably higher energies (1-2 eV) in the crystal than in the free ion. A detailed understanding of the band shapes and their assignment to specified transitions had not been achieved, however.

For those host-impurity systems in which the impurity replaces an alkali metal ion and remains centered on that site, the 3d↛4s and 4d↛5s transitions are parity forbidden in one-photon spectroscopy, but parity allowed in two-photon spectroscopy. This fact enabled the discovery of the zero-phonon line of $NaF:Cu^+$.[2] Furthermore, there are two polarizations in the 2-photon spectroscopy of a cubic crystal, thus doubling the information, and permitting a separation of the overlapping bands of the $^1A_{1g} \rightarrow {}^1E_g$ and $^1A_{1g} \rightarrow {}^1T_{2g}$ transitions, for example.

Polarization information is most important for band assignments. The $A_{1g} \rightarrow E_g$ bands are polarized according to $P_E = 1 - 3/4 \sin^2 2\theta$ where θ is the angle between the 100 axis of the cubic crystal and the polarization vector when light is propogated along a 010 axis. We will call this the E-polarization in the following text. The $A_{1g} \rightarrow T_{2g}$ bands are polarized according to $3/4 \sin^2 2\theta$, and thus have maximum intensity at 45° to the cubic axis. This will be called the T_2 polarization. No other transitions are allowed in 2-photon excitation.

Figure 1 shows the superposed one- and two-photon spectra of $NaCl:Cu^+$ at 298K. In the latter, the Jahn-Teller double humped band is clearly present in the 0° or E polarization, and a single band is present in the T_2 polarization when corrected for the 1/4 factor. The one-photon spectrum shows no such detail. Its position shows that it is almost entirely the $A_{1g} \rightarrow T_{2g}$ transition, but this could not have been concluded without the two photon spectrum. The two photon spectrum shows that the Jahn-Teller energy is about 2000 cm^{-1}, and 10Dq is about 3000 cm^{-1}.[3]

Figure 2 shows the one-photon spectrum of NaCl:Ag^+ at several temperatures, and indicates the two-photon polarization (E or T_2) of the bands.[4] These enable us to make the assignments shown in the caption of fig. 2. The Jahn-Teller double peak splitting is somewhat smaller than for NaCl:Cu^+, but 10Dq is 8000 cm^{-1}, very much larger, giving the spectrum of Ag^+ quite a different appearance. Another factor contributing to the different appearance is the much larger spin-orbit coupling in Ag^+, so that the components of $^3T_2$ appear almost as strong as ^1E_g.

The new results presented here, combined with previous work have enabled us to make unambiguous assignments of the excited states of Cu^+ and Ag^+ in the alkali halides we have investigated. The same methods should lead to the assignments for other such systems.

1. W.B. Fowler, The Physics of Color Centers, Academic Press, N.Y., 1968, Ch. 2.
2. S.A. Payne, A.B. Goldberg and D.S. McClure, J. Chem. Phys. 78, 2688 (1983).
3. S.A. Payne, A.B. Goldberg and D.S. McClure, J. Chem. Phys. to be publ. (1984).
4. C. Pedrini, H. Chermette, A.B. Goldberg, D.S. McClure and B. Moine, Phys. Stat. Solidi (b) 120, 753 (1983).

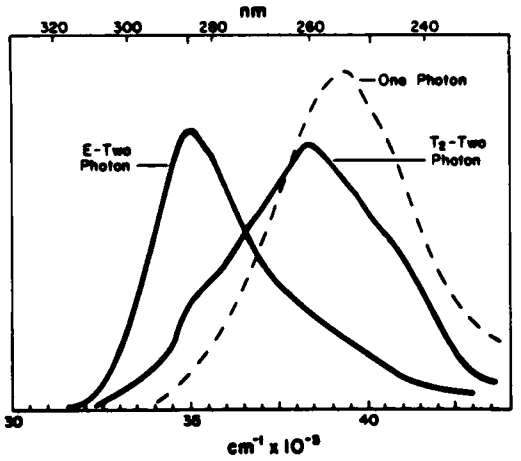

Figure 1. One- and two-photon spectra of Cu^+ in NaCl at 298K. The E polarization shown is a best line through the data points; the T_2 polarization is obtained by subtracting 1/4 XE from the data points of the 45° polarization, The one-photon spectrum has an absorbance maximum of 0.95.

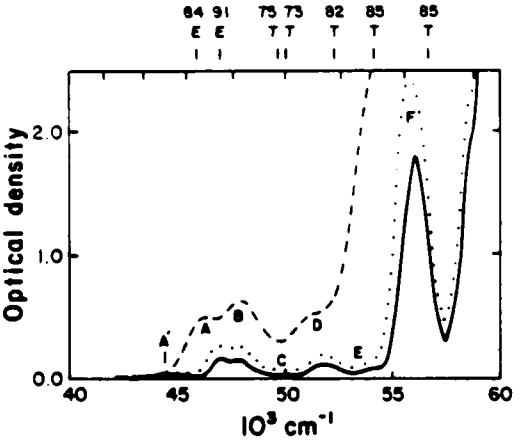

Figure 2. The one-photon spectrum of NaCl:Ag^+ showing the results of two-photon polarization measurements at selected wavelengths (above). The resulting assignments are $A' = {}^3E_g(T_1+T_2)$; $A+B = {}^1E_g$(Jahn-Teller splitting); C, D, E = $^3T_{2g}(E_1T_1)$, T_2, A_2); $F = {}^1T_{2g}$. The spectra shown were taken at temperatures 300, 77 and 12K, reading from top to bottom.

Experimental and theoretical studies of optical properties of $(Ag^+)_2$ pairs in NaCl

C. Pédrini, B. Atoussi, H. Chermette* and B. Moine
E.R.A. 1003 C.N.R.S.
Physico-Chimie des Matériaux Luminescents
Université Claude Bernard - Lyon I -
43 Bd du 11 Novembre 1918 - 69622 VILLEURBANNE CEDEX
FRANCE

* Institut de Physique Nucléaire (et IN2P3)
Université Claude Bernard - Lyon I -
43 Bd du 11 Novembre 1918 - 69622 VILLEURBANNE CEDEX
FRANCE

Summary

The study of the $(Ag^+)_2$ pairs in NaCl has been investigated on strongly doped single crystals grown in our laboratory by the Bridgman technics. Both experimental and theoretical aspects have been considered.

The experimental studies consist of spectroscopic measurements of optical properties of dimer centers. In heavily doped crystals, in addition to the absorption and emission bands assigned to the electronic transitions of isolated Ag^+ ions, new bands are observed. These new luminescent centers are identified as nearest neighbour Ag^+ ion pairs, owing to the quadratic dependence of the absorption band intensities with Ag^+ impurity concentration. The polarization of the luminescence excited by polarized light shows that the two main observed emissions are due to two types of Ag^+ dimers, the orientation of the $Ag^+ - Ag^+$ axis of which is parallel in both cases to a [100] axis of the crystal. Several possible atomic arrangments of paired-ions are proposed and discussed. The kinetics of fluorescence has been studied by an analysis of the luminescent decays. Their thermal dependence reflects a complex recombination mecanism, which can be described with a simplified model including three excited states in thermal equilibrium.

The electronic structure of dimers has been theoretically investigated by a molecular orbital calculation using the multiple scattering Xα (MSXα) method. The pair centers are described as clusters including two Ag^+ ions surrounded by the nearest Cl^- ions. Two kind of pairs are considered with D_{4h} and D_{2h} symmetries having their pair axis parallel to [100] and [110] crystal axis, respectively. In the computation, an external lattice potential is taken into account. The theoretical and experimental results are compared and discussed. They are in good agreement and lead to a good description of the systems. In particular, the chemical bondings, on the one hand between the two Ag^+ ions with either a chlorine ion between them (D_{4h} symmetry) or two non central chlorine ions bridging them (D_{2h} symmetry), and on the other hand between the Ag^+ ions with the other Cl^- ligands, are well described by wave function contours. This analysis points out the important role played by the bridging chorine ion(s) which make(s) possible to exchange electrons between silver ions.

Relaxation of Localized Excitons in KCl:I and RbCl:I

Osamu ARIMOTO, Kazuaki SASAKI, Hiroyuki NAKATANI,
Ken-ichi KAN'NO and Yoshio NAKAI
Department of Physics, Kyoto University, Kyoto 606, JAPAN

Recombination luminescence in alkali halides is originated from the relaxed exciton in the form (X_2^- + e), where X_2^- means halogen molecular ion. Similar situations have been recognized also in the cases of localized excitons in alkali halides containing heavier halogen impurities. Excitation into the absorption bands due to isolated halogen impurities gives rise to broad emission bands in the region of blue-green light (BG emission). They are attributed to the radiative decays from relaxed excited states with a configuration (XY^- + e) of two-center type, where XY^- means a heteronuclear diatomic molecule consisting of a host (X) and an impurity (Y) halogen ion.[1)]

In KCl:I, an emission band (NE emission) is observed at 5.88 eV near the absorption edge of localized excitons along with the BG emission (2.64 eV), when isolated iodine ions are excited at low temperatures below ∿15 K.[2)] It is characterized by a small half-width and a small Stokes-shift. It is found that quite similar situation is also realized in RbCl:I. In Fig. 1 is shown temperature dependence of luminescent intensities of the NE emission (closed circles) and the BG emission (open circles) of RbCl:I. At LHeT the NE emission is dominant. Its intensity falls abruptly to vanish at ∿15 K. This decrease is compensated by complementary increase of the BG emission, just as is so in the case of KCl:I.[3)] These behaviors can be understood in terms

of coexistence of two different types of relaxed states with intervening potential barrier of ΔE = 14 meV.

[Fig.1]

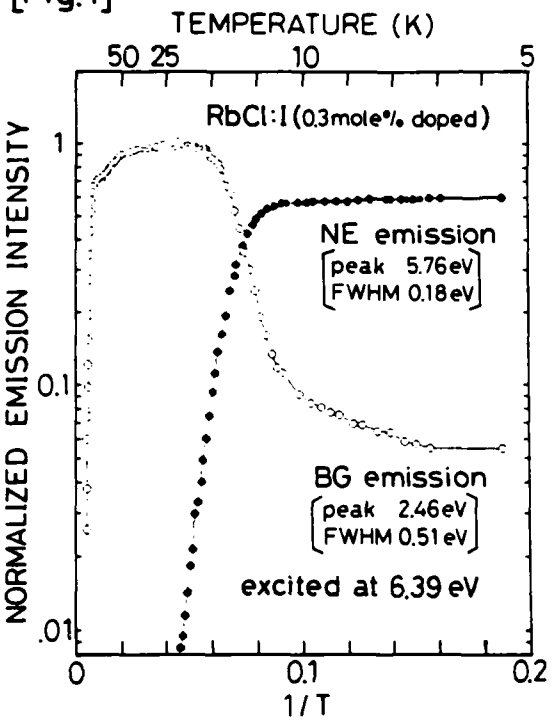

[Fig.2]

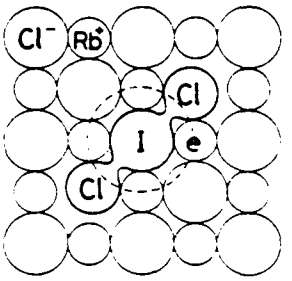

A. one-center type

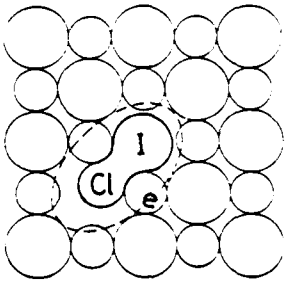

B. two-center type

Present study suggests that the initial state of NE emission is a relaxed excited state with small lattice relaxation in which an electron-hole pair is centered mainly on the site of an iodine ion (Fig. 2A), instead of forming a relaxed excited state of [ClI^- + e]-type (Fig. 2B). It is certain that two different types of relaxed excitons coexist in alkali halide systems like as those in solid rare gas.[4)]

1) L.S.Goldberg: Phys. Rev. 168 (1968), 989
2) K.Kan'no, M.Itoh and Y.Nakai: J. Phys. Soc. Jpn 47 (1979), 915
3) T.Higashimura, H.Nakatani, M.Itoh, K.Kan'no and Y.Nakai: J. Phys. Soc. Jpn 53 (1984), No.5. (in press)
4) T.Suemoto and H.Kanzaki: J. Phys. Soc. Jpn 46 (1979) 1554

IMPACT IONIZATION RATE IN CdF_2 CRYSTALS

V.Dallacasa, C.Paracchini
Dipartimento di Fisica - Università di Parma - Parma - Italy

CdF_2 crystals doped with trivalent element and heated in Cd vapour become semiconducting[1]. Electronic conduction is observed also in doped samples without any thermal treatment[2]. At higher electric fields electroluminescence is also obtained and this effect has been evidenced in CdF_2 crystals doped with Ga, Y, Sm, Eu, Gd and Tb.

In all cases the electroluminescence emission spectrum evidences a large band extending from 300 to 550 nm, with the maximum at about 380 nm, which is independent on the doping substance and is attributed to the radiative recombination of electrons and holes. The excitation energy of such luminescence is comparable with that of the gap (7.6 eV). In some cases the spectrum includes the intentional impurity emissions, which can be excited with much smaller energy. The comparison of the spectra obtained at different applied fields shows that at higher voltages the intrinsic luminescence prevails over that due to impurity, suggesting that the observed luminescence is due to impact processes[4]. A method for studying the impact probability is obtainable in these cases.

One assumes that the light output L is proportional to the current i as: $L = iwf$, where the impact rate w depends on the applied field E and on the temperature T, while the radiative recombination efficiency f is only temperature dependent.
The ratio L/if gives then a relative evaluation of the impact rate and this is examined as a function of E and T, obtaining the relation: $w = A \exp(-aT/E^{\frac{1}{2}}) + B \exp(-b/E^{\frac{1}{2}})$, which evidences two

impact rate regimes in dependence of the applied field.

1) Y.Tan, D.Kramp, J.Chem.Phys. 53, 3691 (1970).
M.Manfredi, C.Paracchini, Phys.Status Solidi (a) 21, 341 (1974).

2) J.D.Kingsley, J.S.Prener, Phys.Rev.Lett. 8, 315 (1962).

3) C.Paracchini, Solid State Commun. 38, 1263 (1981).

4) D.C.Krupka, J.Appl.Phys. 43, 476 (1972).

Study on the Energy Transfer Process of Tb^{3+}, Ce^{3+} Ions Doped Phosphate Glasses

Oi Changhong Gan Fuxi

Shanghai Institute of Optics and Fine Mechanics,

Academia Sinica, Shanghai, China

Summary

We have systematically studied the spectral properties of Ce^{3+}, Tb^{3+} ions in different glass hosts[1]. In this paper the concentration effect and energy transfer process between Tb^{3+} and Ce^{3+} ions were reported. A series of glasses with the following doping concentration were prepared. (1) Tb^{3+} — 2, 4, 8, 12, 16 wt%. (2) Ce^{3+} — 1, 3, 5 wt%, 17 mol%. (3) 8 wt% Tb, Ce^{3+} — 1, 3, 5 wt% The emission and excitation spectra of these glasses were obtained using Hitachi Model 650-60 fluorescence spectrophotometer. Decay times of the $^5D_4$ - $^7F_5$ transition (542nm, 548nm) at the different Tb^{3+} concentrations were measured using an KrF excimer laser with pulse duration 10ns as the exciting light source.

Under the excitation of 378nm, the emission intensities of transitions $^5D_4$ - $^7F_{4,5,6}$ were increased with increasing Tb^{3+} concentration up to 16%wt Tb_2O_3, but the emission intensities of the $^5D_3$ - $^7F_{5,4,3}$ transitions were decreased simultaneously. It can be considered that the resonance energy transfer may take place, because the energy gaps between ($^5D_3$ - $^7F_{0,1}$) and ($^7F_6$ - $^5D_4$) for Tb^{3+} ion are equivalent. With the increasing Tb^{3+} concentration, the excited energy of the $^5D_3$ level trasfers to the $^5D_4$, it can be noticed that the fluorescence lifetime of $^5D_4$ level is not effected by the increasing Tb^{3+} concentration, and about 2 ± 0.1ms.

The fluorescence lifetime of four Ce^{3+} - doped glasses were measured by excimer laser excitation at 248nm wavelength, and the lifetime values are 47, 43.5, 41.5 and 31ns, respectively. The both fluorescence lifetime and emission intensity were decreased with increasing Ce^{3+} concentration. It can be found that the peak positions of emission band shift to the longer wavelength. The emission band in the vicinity of 330nm of Ce^{3+} doped phosphate glass arises from $^2D(5d) - {}^2F_{7/2}, {}^2F_{5/2}(4f)$ transitions the action of the ligand field of glass host on 5d state is more sensitive, doping with large amount of Ce_2O_3, the glass structure will be something changed, as a result, the emission bonds are shifted and broadened.

The emission intensity of Tb^{3+} ($^5D_4 - {}^7F_5$, 542nm) in the (Ce + Tb) codoped glasses is much more strong than that of Tb^{3+} singly doped glass. The luminescence sensitization of Tb^{3+} by Ce^{3+} ion in phosphate glasses is remarkable. The values of luminescence lifetime of Tb^{3+} ion in (Ce^{3+} + Tb^{3+}) codoped glasses are not vary basically, but the values of lifetime of Ce^{3+} ion in (Ce^{3+} + Tb^{3+}) codoped glasses are smaller than that of Ce^{3+} singly doped glasses. This is consistent with the excitation spectra (monitored at 542nm) of Tb^{3+} ion in (Ce^{3+} + Tb^{3+}) codoped glasses, there appears a strong and broad excitation band in the region of 270-330nm, that just coincide with the absorption band of Tb^{3+} and luminescence band of Ce^{3+}. The energy transfer efficiency and probability from Ce^{3+} to Tb^{3+} were measured and calculated. A linear dependence of the transfer probabilities P_{da} with the squared sum of the concentrations $(Ce^{3+} + Tb^{3+})^2$ was found, i.e. $P_{da} \propto \frac{1}{R_{ad}^6}$, R_{ad} is the dis-

tance between the acceptor and donor ions. It may be recognized as a dipol-dipole resonant nonradiative energy transfer process.

Reference

[1] Qi Changhong, Gan Fuxi, Luminescence and Display Devices, 3, 48 (1983).

Site-Selection Spectroscopy

Of Eu^{3+} Ions In Different Types of Glasses

Xu Gang and Richard C. Powell
Department of Physics, Oklahoma State University
Stillwater, OK 74078

Laser time-resolved site-selection spectroscopy measurements were used to characterize the properties of Eu^{3+} ions in seven types of glass hosts including oxide glasses of lithium phosphate, lithium silicate, sodium silicate, potassium germanate, lithium borate, and europium pentaphosphate as well as the fluoride glass ZBLA. The $^7F_0$–$^5D_0$ transition was resonantly excited and the results were obtained by monitoring the $^5D_0$–$^7F_0$ fluorescence which has not been done in most previous work of this type because of laser scattered light. This was overcome by the use of a fast electronic shutter. Measurements were made of the spectral structure, fluorescence lifetime, inhomogeneous linewidth, fluorescence line-narrowed (FLN) width, and energy transfer rate parameter as a function of host composition, temperature, and excitation position within the inhomogeneous line.

Significant variation in spectral structure was observed for the samples investigated. The network modifier ions appear to be more important in determining the structure than the network former ions with the heavier modifiers giving more discrete peaks with larger FLN widths.

At 10 K the vlaues of the energy transfer rates were found to vary linearly with the product of the inhomogeneous linewidth

and the square of the fluorescence decay rate for the oxide glasses. This product is proportional to the ion-ion interaction rate. The results for the fluoride glass do not fit on the same curve as the oxide glasses indicating a difference the screening of the ion-ion interaction in the different types of hosts. In scanning the excitation wavelength across the inhomogeneous absorption band, the energy transfer rate is found to change by about a factor of 3 for the samples with significant spectral structure and to be approximately constant for samples with little spectral structure. The variation of the energy transfer rate with temperature is less for the samples with less spectral structure than for the samples with significant structure except for the borate glass which has a very weak temperature dependence.

The results are interpreted in terms of the effects of the local crystal field environment on the properties of Eu^{3+} ions. The descrete structure is associated with more local order and a smaller variety of types of crystal field sites. As the relative order increases, the fluorescence lifetime becomes shorter and the energy transfer rate larger.

Cr^{3+} INDUCED NUCLEATION AND LUMINESCENCE IN SILICATES GLASSES

B. Champagnon, F. Durville, E. Duval and G. Boulon
Physico-Chimie des Matériaux Luminescents - ERA 1003 CNRS
Université Lyon I - 69622 VILLEURBANNE - FRANCE

Nucleation and growth of small particles induced by Cr^{3+} ion in a magneso-alumino silicate glass so called cordierite (52 % SiO_2, 34.7 % Al_2O_3, 12.5 % MgO and 0.8 % Cr_2O_3) has been studied by Small Angle Neutron Scattering (1). The advantage of the Cr^{3+} ion is that this activator is sensitive to spectroscopic techniques such as E.P.R. and laser spectroscopy so that the different particles which develop during heat-treatment can be characterized and studied.

Microcrystallites with sizes up to 400 Å are identified from E.P.R. and luminescence as two kinds of spinels. In a first stage there is formation of $Mg(Al_{1-x}Cr_x)_2O_4$ spinel with x close to 1, then when the temperature of the heat-treatment increases the spinel with 1-x close to 1 grows. From absorption and excitation spectra evidence is shown for radiative energy transfers between chromium ions in glassy phase and microcrystallites. We further observed a wide distribution of sites both in the glassy phase and in the crystalline phase. So, for a given sample, the emitting energy level can be either ^2E level or $^4T_2$ level giving rise to a broad line and a broad band. F.L.N. of $^2E \rightarrow {}^4A_2$ emission in $MgAl_2O_4:Cr^{3+}$ allows to measure the splittings and inhomogeneous broadening in ^2E and $^4A_2$ levels. Figure shows inhomogeneous broadening and splitting for the $^4A_2$ level.

Other results as the observation of the ^2E - $^4A_2$ pair level emission in the $MgCr_2O_4$ spinel by T.R.S. are presented. Correlations with recent works on Cr^{3+} ions in other glasses (2), enhancement of luminescence

in transparent glass ceramics (3) and measurements of quantum efficiency in similar silicate glasses are suggested (4).

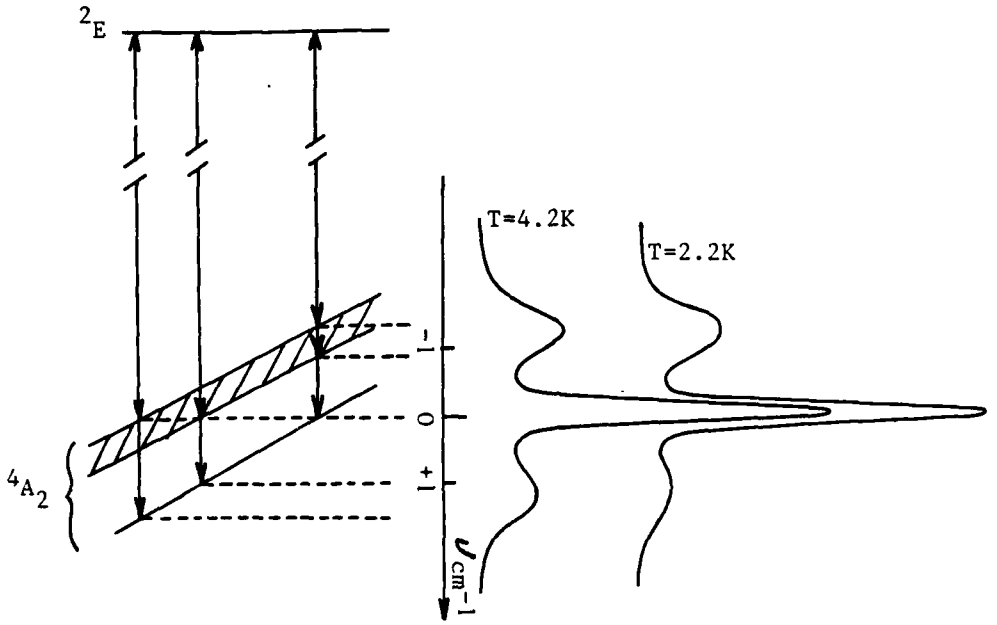

Energy levels and F.L.N. of Cr^{3+} ions in Mg Al_2O_4 spinel microcrystals.

REFERENCES

(1) F. Durville, B. Champagnon, E. Duval, G. Boulon, F. Gaume, A.F. Wright and A.N. Fitch - Physics Chem. Glasses - to be published (1984).

(2) V.P. Gapontsev, T. Glynn and Y.M. Yen (unpublished work).

(3) L.S. Andrews, B.C. Mc Collum, S.M. Stone, A. Lempicki 161th Electrochemical Society Meeting, Montreal, May (1982).

(4) R. Reisfeld, A. Kisilev, E. Greenberg, A. Buch and M. Ish-Shalom Submitted for publication to Chem. Phys. Letters (1984).

Optical Properties of Rare Earth and 3d Ions in Fluorozirconate Glass

W. A. Sibley, M. D. Shinn, K. Tanimura, L. Feurhelm
Physics Department
Oklahoma State University
Stillwater, Oklahoma 74078

Summary

Fluorozirconate and fluoroha fnate glasses have great potential in fiber optics and laser host applications. For this reason, there has been exceptional interest in the optical properties of ions in this material. In this work, the optical absorption, emission, excitation and lifetimes of the various transitions for impurities such as Ho^{3+}, Pr^{3+}, Er^{3+}, and Mn^{2+} in these glasses is presented. The measured oscillator strengths and radiative rates for several transitions are compared with calculated values based on Judd-Ofelt theory. Non-radiative transition rates for the excited states were determined by the difference between the measured rates and the calculated radiative rates. As the impurity levels approach 2% energy transfer becomes important. In almost all cases multiphonon emission and energy transfer account for the nonradiative transitions. The low temperature multi-phonon emission rates are generally in agreement with the rates predicted by the phenomological energy gap law. In addition, the crystallization of ZBLA glass was studied using Er^{3+}, Ho^{3+} and Mn^{2+} ions as probes. Isocronal heating data indicate that the glass undergoes rapid devitrification around 630K.

Luminescence of amorphous and crystalline $Ca_3Cr_2Si_3O_{12}$

H.Szymczak, A.Pajączkowska, K.Pataj

Institute of Physics, Polish Academy of Sciences,

02-668 Warszawa, al. Lotników 32/46, Poland.

Luminescence spectroscopy is essentially sensitive to local environments. Consequently, it can be one of the most useful methods for elucidation of the short-range structure of the amorphous material. The luminescence studies of amorphous materials are not very common in literature. We report here on a comparative study of the luminescence spectra in amorphous insulating $Ca_3Cr_2Si_3O_{12}$ and its corresponding crystalline counterpart. The amorphous $Ca_3Cr_2Si_3O_{12}$ compound has been obtained by a fast cooling of the liquid solution. The amorphous state was confirmed by x-ray diffraction analysis. The chemical composition of the specimens was determined by electron-probe microanalyser. In the crystalline state this compound has garnet structure and exhibits long-range antiferromagnetic order with the Neel temperature of 12 K. According to our magnetic and EPR measurements no magnetic long-range order has been found in amorphous $Ca_3Cr_2Si_3O_{12}$. Below 20 K this compound has to be considered as insulating spin glass with large antiferromagnetic interactions. The luminescence spectra of both considered compounds have been measured at 1.7 K. The emission decreases strongly with increasing temperature and disappears above 10 K. In both cases the luminescence spectra consist of the sharp lines followed by a number of broad bands. The emission which is observed in garnet crystal is not intrinsic but results from ^2E - to - $^4A_2$

transitions of impurity-perturbed Cr^{3+} ions. The bound-exciton lines are not observed in luminescence spectrum. Several very sharp lines, found at energies lower than intrinsic $^4A_2$-to-^2E absorption, are attributed to the magnon assisted transitions. The luminescence spectrum of amorphous $Ca_3Cr_2Si_3O_{12}$ is interpreted in terms of spin-wave-like excitations. The spin-wave-like excitations in spin-glass state have been predicted theoretically and confirmed experimentally in number of neutron scattering experiments. In the luminescence spectrum of amorphous $Ca_3Cr_2Si_3O_{12}$ the sharp line near 13240 cm^{-1} is interpreted as zero-phonon-zero-magnon transition and strong line near 13025cm^{-1} is attributed to magnon-assisted transition. Second broad band at 12840cm^{-1} is identified as a vibronic transition. Analysis of the magnon-assisted transition yields value of the average nearest-neighbour exchange interaction between chromium ions of about 20cm^{-1}. This result is in agreement with our EPR data. In the case of antiferromagnetic garnet the value of the exchange interaction is estimated to be equal 0.6cm^{-1}. This surprising difference can be explained by considerable change in distance between magnetic ions in garnets after amorphization. Analysis of the emission line shape leads to the conclusion that the distribution of the crystal field acting on Cr^{3+} ions in amorphous $Ca_3Cr_2Si_3O_{12}$ is narrow in contrary to that observed by Mössbauer spectroscopy in amorphous $Y_3Fe_5O_{12}$ [1].

References

[1] M.E. Lines, Phys. Rev. B20 (1979) 3729 .

Luminescence of Titanium-Containing Fluorophosphate Glass

Gan Fuxi Liu Huiming

Shanghai Institute of Optics and Fine Mechanics,

Academia Sinica, Shanghai, China

Summary

With the development of turnable solid state lasers much attention has been paid to the study on luminescence of inorganic glasses doped with transition metal ions. However, in traditional oxide glasses, even though a great deal of spectral studies had been made, luminescence due to titanium ions so far has never been reported to our knowledge.

Based upon a series of the recent studies on spectra and the dynamic luminescent process of transition metal ions in inorganic glasses[1-5], the titanium-containing fluorophosphate glass (MgF_2-CaF_2-SrF_2-BaF_2-AlF_3-$NaPO_3$) was chosen as the sample. An attempt was carried out at using excitation transfer to realize luminescence of titanium in a new kind of glass.

The absorption, ESR, excitation, fluorescence and lifetime measurements have been performed respectively. It is found that the absorption spectrum is composed of an asymmetrical absorption band at 529nm and a shoulder at 685nm. The Jahn-Teller splitting is about $4500cm^{-1}$. ESR measurement shows a subtle difference from phosphate to fluorophosphate glasses, which implies the change of chemical bonding between activated titanium ion and ligand with the replacement of oxygen by fluorine ligands. Hence, combined with the ESR spectra the absorption spectrum shows that Ti^{3+} ions are located at disordered octahedral sites with axial symmetry.

The absorption bands can be assigned to $^2B_{2g}$ -- $^2B_{1g}$ and $^2B_{2g}$-- $^2A_{1g}$ transitions, respectively.

In comparison with phosphate glass having almost the same midifier ions composition as fluorophosphate glass, the former can hardly show fluorescence, and the latter has a fluorescence with the peak position at 550nm as well as the band-width of 180nm. The fluorescence is then to be assigned to the $^2B_{1g}$ -- $^2B_{2g}$ transition of Ti^{3+} ions. Its lifetime is about 2 μs.

The excitation spectrum shows that with the excitation around 300nm which corresponds to the Ti^{4+} CT band, the intenser fluorescence can be obtained. However, with the excitation around 240nm which corresponds to the Ti^{3+} CT band, no fluorescence could then be obtained.

In addition, the discussion is also given in the paper that as an emitting species, Ti^{3+} could not be excited in isolation to realize luminescence. It must be proceeded by means of the excitation of Ti^{4+} at its UV charge transfer band which corresponds to $2t_{1u}$ -- $2e_g$ transition with different parity, then the activated Ti^{4+} ions are converted into the activated Ti^{3+} ions, accompaning the charge transfer in the form of Ti^{4+} - F - Ti^{3+} and the energy transfer by ion - phonon coupling. Finally, those Ti^{3+} ions through the radiative transition emit from the excited state to the ground.

References

[1] Gan Fuxi and Liu Huiming, Jour. Non-Cryst. Solids, 52(1982), 135.

[2] Gan Fuxi and Liu Huiming, Jour. de Physique, 43(1982) C9-303.

[3] Gan Fuxi and Liu Huiming, Jour. Chinese Silic. Soc., 11(1983),49.

[4] Gan Fuxi and Liu Huiming, Dig. 83' Intern. Conf. Laser (China, Canton), p.373.

[5] Gan Fuxi and Liu Huiming, KEXUE TONGBAO (A Monthly Journal of Science, Academia Sinica, in English), 29(1984), 133.

Photoluminescence in obliquely deposited a-$GeSe_2$ films

M. Koós and I. Kósa Somogyi

Central Research Institute for Physics

H-1525 Budapest 114, P.O.B.49, Hungary

Obliquely deposited thin films of the a-Ge_xSe_{1-x} system have gained widespread interest as high resolution photoresists [1]. This paper reports the results of our photoluminescence (PL) studies of a-$GeSe_2$ thin films deposited simultaneously at 0, 10, 30, 50 and 70° angles of incidence. Examination of the PL characteristics were carried out to throw light on changes in the electronic structure and the distribution of the radiative recombination centres induced by the columnar structure of these films and their gradual disappearance upon prolonged illumination.

We have shown that the peak energy and the half width of the PL spectra does not change with obliqueness. This observation indicates that the band gap and the energetic distribution of PL centres remain unchanged in the 0°-70° films inspite the ~15% density difference between the normally and 70° deposited films. The initial PL intensity I_o is practically the same for the 0, 10 and 30° specimens but decreases somewhat in the films deposited beyond 50°. The intensity of PL during prolonged exposure to exciting light increases in the films deposited above 30° angle of incidence.

The fatigue of PL (i.e. the decrease of its intensity during measurement) is observed in all samples: after one hour exposure the intensity decreases to one third of its initial value in the 0^{o} films while the decrease is twentyfold for the 70^{o} films. The PL intensity of fatigued samples kept in dark for one minute at low temperatures increases; on subsequent excitation regaining 13-40% of the initial value I_{o}. This regeneration is the smallest for the 70^{o} films.

Oblique deposition increases the density of both volume and surface dangling bonds resulting in the formation of more D^{+} and D^{-} charged states. During excitation of $> 30^{o}$ films excess D^{o} centres are created which enhance the fatique of PL. In 0^{o} deposited films illumination leads to bleaching i.e. removal of voids and some of the defects. consequently weaker fatigue is expected as observed.

Our PL measurements which were accompanied by FIR and Raman structural studies corraborate earlier observations [2] but are in part at variance with predictions of the Mott-David-Street model used extensively for the interpretation of recombination processes in amorphous semiconductors.

[1] K. Balasubramanyam, L. Karapiperis, C.A. Lee and A.L. Ruoff: J. Vac. Sci. Technol. 19, 18 (1981)

[2] K.L. Chopra, K. Solomon Harshvardhan, S. Rajagopalan and L.K. Malhotra: Solid State Comm. 40, 387 (1981)

Photoluminescence in Amorphous Alloys: a-SiO_x:H, a-SiN_x:H, a-Si_xC_{1-x}:H

R. Carius, K. Jahn, W. Siebert, W. Fuhs

Fachbereich Physik, University of Marburg, F.R. Germany

D-3550 Marburg, Renthof 5

We report on the photoluminescence (PL) in the amorphous alloys: a-SiO_x:H, a-SiN_x:H, a-Si_xC_{1-x}:H over a wide range of x. The films were prepared by glow discharge decomposition of suitable mixtures of SiH_4 with N_2O, NH_3, and CH_4 (C_2H_4), respectively.

All photoluminescence spectra exhibit a one band structure. The PL-peak energy (E_{PL}) shifts continuously to higher energy with increasing concentration of the alloying constituents and the bands broaden considerably. Similarly the absorption edges shift to higher energy and flatten. The data are discussed by considering the average number of Si-Si bonds (Z) at a given x of the compound. We find that the full width at half maximum of the spectrum (E_{FWHM}) at a given Z decreases with increasing chemical valency of the alloying atoms, e.g. in the sequence O, N, C. With decreasing Z the difference between the width of the gap, measured by E_{04}, and the photoluminescence peak energy E_{PL}, increases enormously. Most remarkably we find that E_{04}-E_{PL}/E_{FWHM} = const. for all films irrespective of their composition down to Z ≈ 1.5. The electronic structure of the alloy systems is discussed on basis of a simple tight binding model. It is shown that the states near the band edges (optical gap E_{04}) and in the bandtails originate predominantly from Si-Si bonding and antibonding states. The disorder in the films increases with decreasing Z and at a given Z decreases in the sequence O, N, C.

Information about the role of network relaxation is obtained from excitation spectroscopy using also subbandgap light. We find that E_{PL} remains essentially unchanged, but the bands become unsymmetric, the high energy part beeing diminished with decreasing energy of the exciting photons. This behaviour is thus different from that of a-Si:H films [1]. These results strongly suggest that network relaxation plays a minor role in these alloys and that the carriers thermalize in the bandtails until they recombine by radiative tunneling. It is remarkable that in time resolved measurements the spectra do not shift with increasing delay time in the range 10^{-8}-10^{-3}s. This decoupling of PL-energy and decay time points against a strong Coulomb interaction of the recombining carriers [2]. The flatter the bandtails, the deeper states are attained by thermalization, hence E_{04}-E_{PL} increases with decreasing Z in all alloy systems. This is consistent with the observed temperature dependence of the photoluminescence efficiency, which is supposed to arise from thermal detrapping and diffusion to non-radiative recombination centers. With increasing E_{04}-E_{PL} the temperature dependence becomes less pronounced and in alloys with low Z, photoluminescence in the visible range can be observed even at 300 K.

[1] J. Shah, A. Pinczuk, F.B. Alexander, B.G. Bagley, Solid State Comm. 42, 717 (1982)

[2] B.A. Wilson, T.P. Kervin, Phys.Rev. B 25, 5276 (1982)

Thermal Zero-phonon Line Widths of Impurities in Crystals: Theory and Experiment

D. Hsu and J. L. Skinner, Department of Chemistry, Columbia University, New York, NY 10027

Summary

We examine the problem of the absorption zero-phonon line shape for dilute impurities in crystals. We consider the usual two-level electronic model, where both the ground and excited state Born-Oppenheimer surfaces are harmonic in the phonon coordinates. The difference between the two surfaces (the electron-phonon interaction) has terms which are both linear and quadratic in the phonon coordinates. In contrast to the usual perturbative theories,[1] we calculate the zero-phonon line width to all orders in the electron-phonon interaction. We find that only the quadratic term is responsible for line broadening, and that at $T=0^{\circ}K$ this contribution vanishes. Our results are presented as integrals, which can be performed analytically or numerically, involving the weighted phonon density of states. We also show that within the model, the zero-phonon lines in the absorption and fluorescence spectra coincide exactly for all temperatures. Our results resolve the theoretical controversy produced by the two previous attempts to solve the line shape problem for strongly coupled electron-phonon systems. The work by Osad'ko[2] is shown to be correct.

We evaluate our results for two model densities of states. The first model involves the usual Debye approximation. We find that at low temperatures, the line width is proportional to T^7, in agreement with weak coupling theory.[1] At higher temperatures the nonperturbative and weak coupling theories can differ substantially. The second model density of

states is sharply peaked at a nonzero phonon frequency. This is appropriate if the impurity strongly perturbs the crystal lattice and creates a pseudo-local mode. This model leads to an exponentially activated (Arrhenius) temperature dependence of the line width.

At high temperatures, the homogeneous line width can be obtained directly by absorption or fluorescence spectroscopy. For example, McCumber and Sturge[1] measured the width of the R lines in ruby from 77° to 350°K. Although the data can be fit by the weak coupling theory with the Debye approximation, the resulting Debye temperature is 20% smaller than that found from specific heat measurements. However, with the nonperturbative theory, we obtain excellent agreement with these experiments using the independently measured Debye temperature. We are in the process of analyzing similar absorption line width data of Burke and Small[3] for organic impurities in naphthalene.

At low temperatures, one must use nonlinear techniques such as the photon echo to obtain the homogeneous line width. An Arrhenius temperature dependence of the line width is usually found in these experiments. This is in agreement with our results for the sharply peaked density of states. We have analyzed several different low temperature experiments,[4] and conclude that most systems are not in the weak coupling limit.

In summary, this work shows that absorption, fluorescence and photon echo experiments over a wide range of temperatures can be explained with a harmonic, but nonperturbative theory.

1. D. E. McCumber and Sturge, J. Appl. Phys. 34, 1682 (1963).

2. I. S. Osad'ko, Fiz. Tverd. Tela 17, 3180 (1975) [Sov. Phys. - Solid State 17, 2098 (1976)].

3. F. P. Burke and G. J. Small, J. Chem. Phys. 61, 4588 (1974); Chem. Phys. 5, 198 (1974).

4. See, for example: D. A. Wiersma, Adv. Chem. Phys. 47 part 2, 421 (1981).

Excimer Migration in Crystals: Analysis of Experiments in Pyrene and Dichloroanthracene

D. H. Dunlap and V. M. Kenkre
Department of Physics and Astronomy
University of Rochester, Rochester, NY 14627

Excimers in molecular crystals constitute an intriguing object of study in luminescence investigations. Basic questions have remained unanswered about their formation and about their migration. The latter presents particularly interesting challenges. The necessity of large distortions and considerable activation energies for their motion leads one to expect excimers to be relatively immobile. However, experimental evidence for their motion has been presented several times in the literature. Such evidence has been gathered both indirectly from the supposed mutual annihilation of excimers as in recent experiments on dichloroanthracene,[1] and more directly from their trapping by dopants as in earlier experiments on pyrene.[2] The two kinds of systems involved are representative of two different physical situations; stacks are involved in the former and preformed dimers in the latter. We have analyzed the motion observations from a general theoretical framework and found that considerable latitude exists in the interpretation of the reported observations. We examine the applicability of polaron transport concepts to excimer motion and comments on what further experiments are necessary to remove the considerable uncertainties that exist in our present understanding of excimers.

(1) U. Mayer, H. Auweter, A. Braun, H. C. Wolf, and D. Schmid; Chem. Phys. 59. 449 (1981).

(2) W. Kloepffer, H. Bauser, F. Dolezalek, and G. Naundorf; Molecular Crystals and Liquid Crystals 16, 229 (1972).

Effects of Energy Trapping on Time-Resolved Degenerate Four-Wave-Mixing

G. P. Morgan, S. Z. Chen and W. M. Yen

Physics Department, University of Wisconsin, Madison, WI 53706

Time resolved four-wave-mixing has proven to be a useful tool for studying the spatial transfer of energy in optically active materials. When spatial migration of energy occurs, it is found that the transient grating decays with a lifetime which is less than half the fluorescence lifetime of the excited species. By studying the dependence of the decay rate on the grating periodicity, a diffusion constant for the energy transfer can be obtained.

This technique has been used to study energy transfer in $Nd_xLa_{(1-x)}P_5O_{14}$ which has a high quantum efficiency even when doped up to the stoichiometric limit with Nd^{3+} ions. An energy diffusion constant which varies with Nd^{3+} concentration has been reported.[1] We have observed that at small crossing angles of the writing beams the grating decays with a component which is slower than half the fluorescent lifetime. We believe that this behaviour is due to cross-relaxation of the Nd^{3+} ions.

MnF_2 is also a good candidate for observing the effects of energy trapping. The visible fluorescence observed from MnF_2 at low temperatures originates mainly from Zn and Mg impurity induced trapping sites. These traps are fed efficiently by the intrinsic excitons. The transfer rate to the traps is on the order of microseconds at liquid helium temperatures and this has been explained as due to a small dispersion of the lowest E1 exciton state.[2] In this material we expect that the decay of a transient grating is characterized by multiexponential behaviour. One component is due to the migration of excitons to trapping sites and so will be dependent

on the grating periodicity. The other component is due to the radiative decay of the excited traps. Since no spatial transfer of energy is involved in this process it will not be dependent on the grating periodicity.

We will present the results of experiments that investigate the transfer of energy to traps in these materials.

1. C. M. Lawson, R. C. Powell and W. K. Zwicker, Phys. Rev. B 26, 4836 (1982).

2. B. A. Wilson, W. M. Yen, J. Hegarty and G. F. Imbusch, Phys. Rev. B 19, 4238 (1979).

The Optically Detected Stimulated Spin Echo as a Probe of Triplet Energy Migration in Mixed Molecular Crystals

Henry C. Brenner and Stephen M. Janes
Department of Chemistry, New York University, New York, NY 10003 USA

We report the first application of optically detected stimulated echoes to the measurement of trap to trap migration rates in mixed molecular crystals. The stimulated echo (1) can be thought of as a 2-pulse echo in which the 180^{o} refocussing pulse is split into two 90^{o} pulses. This has the effect of storing local field information along the longitudinal or population difference axis in the rotating frame. This information is then "read-out" in the form of an echo by the third 90^{o} pulse. Since the ability to recall or "stimulate" the echo at the later time depends on how well the local field alignment is preserved during the long waiting time T, the stimulated echo intensity reflects changes in local fields and can be used to probe trap to trap energy migration.

We studied isotopic mixed (h_2 in d_2) 1,2,4,5-tetrachlorobenzene (TCB) at 1.7 K at h_2 concentrations of 1.5, 4.5, 7.5 and 9.5 mole percent. The echoes appeared to decay biexponentially as T was varied. The short component of about 1 msec is attributed mainly to nuclear spin flipping processes (1,2). The long lifetime shortens markedly with increasing h_2 concentration; the values of the long lifetime for the concentrations given above are (in msec) 19, 10.4, 7.6, and 6.1. We attribute this long component to a mixture of energy migration and triplet state decay. If one defines a migration rate constant k_m, and assumes that the local fields which give rise to inhomogeneous broadening vary randomly from trap to trap, then one expects the stimulated echo to decay as

$$I \alpha \exp\{-(k_m + k_x)T\} + \exp\{-(k_m + k_y)T\}$$

where k_x and k_y are the sublevel decay constants (measured previously for TCB in durene). A fit of this equation to the tail of the stimulated echo decays gives the following k_m values (in sec^{-1}) for the concentrations given above: 40.8, 83, 118 and 149.

At least two types of triplet energy migration are important in this crystal system at 1.7 K: (a) trap to band promotion, with subsequent band migration and retrapping, and (b) trap to trap superexchange. Previous temperature dependent spin locking experiments with the h_2 trap (3) give evidence for thermally induced detrapping. The marked dependence of k_m on h_2 concentration in our experiments suggests that trap to trap superexchange, which varies strongly with trap separation, is also important. Using the previously measured (4) nearest neighbor exchange interaction (0.34 cm^{-1}), we estimated that the stimulated echo decay is monitoring the increase in the number of h_2 trap pairs separated by four or five intervening host molecules as the h_2 concentration is increased.

References

1. H. B. Levinsky and H. C. Brenner, Chem. Phys. Letters 78 (1981) 177.

2. S. M. Janes and H. C. Brenner, Chem. Phys. Letters 95 (1983) 23.

3. M. T. Lewellyn, A. H. Zewail and C. B. Harris, J. Chem. Phys. 63 (1975) 3687.

4. D. D. Dlott and M. D. Fayer, Chem. Phys. Letters 41 (1976) 305.

SPECTRAL NARROWING OF EXCITATION SPECTRA IN N-PHOTONS UP-CONVERSION PROCESSES BY ENERGY TRANSFERS

F. AUZEL

Laboratoire de Bagneux, C.N.E.T.

196 rue de Paris - 92220 Bagneux - FRANCE

By using a CW tunable F-center laser emitting between 1.4 and 1.6$_{\mu}$, room temperature excitations for 1 to 5 photons APTE effect (Addition de photon par transfert d'énergie [1]) are obtained for Er^{3+} doped vitroceramics. Theses materials, higly doped with R.E (1 to 15 %), have been shown to be very efficient medium for such up-conversion process because though in a glassy form they behave as doped microcrystals [2].

The progressive narrowing of the spectra is found with the increase in n as shown on Fig 1. The obtained spectra are found to be essentially the n^{th} power of the line shape of the first excited state transition $^4I_{15/2} \rightarrow {}^4I_{13/2}$ of Er^{3+} and found to loose memory of the other excited states transitions involved in the process.

These results stress the role of energy diffusion between the first excited state ($^4I_{13/2}$) of Er^{3+} acting as sensitizer for other excited states and rule out successive absorptions between either single ions or pair states [3].

This last process, a cooperative process, is known to be less efficient than successive transfer summation [1] and can be seen only when the much more probable APTE effects are forbidden by lack of "real" levels (single states ions) to promote energy transfers or when due to low concentration, energy diffusion is precluded [4].

Rate equation based upon energy scheme of Fig 2, in which Er^{3+} acts either as a sensitizer or as an activator according to [1] describes the essential features of the experimental results provided the energy transfer probabilities are assumed to be frequency independant on the bandwidth range of the initial transition.

References

[1] F. AUZEL, Proc. IEEE 61, 758 (1973)

[2] F. AUZEL, D. PECILE and D. MORIN, J. Electrochem. Soc. 122,101 (1975)

[3] M.R. BROWN, H. THOMAS, J.M. WILLIAMS and R.J. WOODWARDS, J. Chem. Phys. 51, 3321 (1969)

[4] J.C. VIAL, R. BUISSON, F. MADEORE, M. POIRIER, J. Physique 40, 913 (1979)

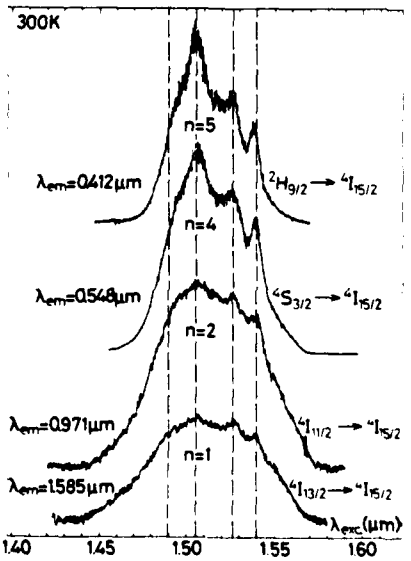

Fig. 1

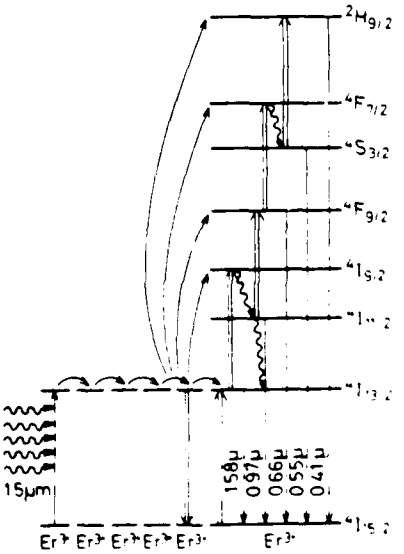

Fig. 2

AD-A148 470 INTERNATIONAL CONFERENCE ON LUMINESCENCE HELD AT MADISON WISCONSIN ON 13-17 AUGUST 1984(U) WISCONSIN UNIV-MADISON W M YEN OCT 84 N00014-84-G-0053 5/7

UNCLASSIFIED F/G 20/6 NL

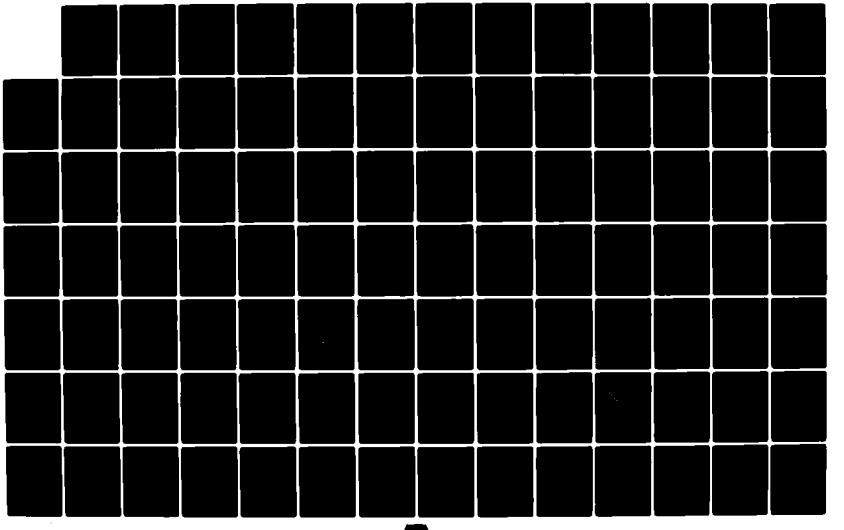

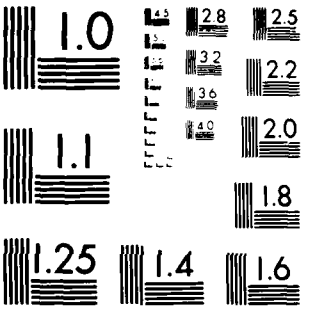

MICROCOPY RESOLUTION TEST CHART

A Direct Observation of Excitation Energy Transfer in Ruby Induced by the Resonant 29 cm^{-1} Phonons

A.A.Kaplyanskii, S.A.Basoon, and S.P.Feofilov

A.F.Ioffe Physicotechnical Institute, Academy of Sciences of the USSR, Leningrad 194021, USSR

Participation of the 29 cm^{-1} phonons resonant with the $2\bar{A}$-$\bar{E}$ interval in the Cr^{3+} metastable ^2E-state in the excitation energy transfer between the Cr^{3+} ions in ruby has been discussed repeatedly in the literature [1,2]. The present experiments have been carried out at 1.8 K on Al_2O_3:0.02% Cr crystals under stationary laser pumping. The inhomogeneously broadened R_1 luminescence line reveals weak extended structured wings associated with $\bar{E}$-$^4A_2$ transitions in the strongly perturbed Cr^{3+} ions (Fig.1). Injection into the sample of heat pulses from a heater film deposited on its surface has been found to generate positive luminescence pulses I(t) on the short wavelength wing of the R_1 line. These pulses originate from the phonon induced $\bar{E}$-excitation energy transfer from the main distribution ions (line center) to the perturbed ions.

The frequency of the transfer inducing phonons was derived by studying the dependence of the I(t) amplitude I_0 on heater power W determining the heat pulse phonon spectrum. Fig.2 displays a $\ln I_0(W^{-1/4})$ plot for the pulses measured at distances 6.4 cm^{-1} and 4.8 cm^{-1} from R_1 line center. Shown for comparison is a power dependence of the R_2 ($2\bar{A}$-$^4A_2$) fluorescence pulses associated with the 29 cm^{-1} phonons inducing

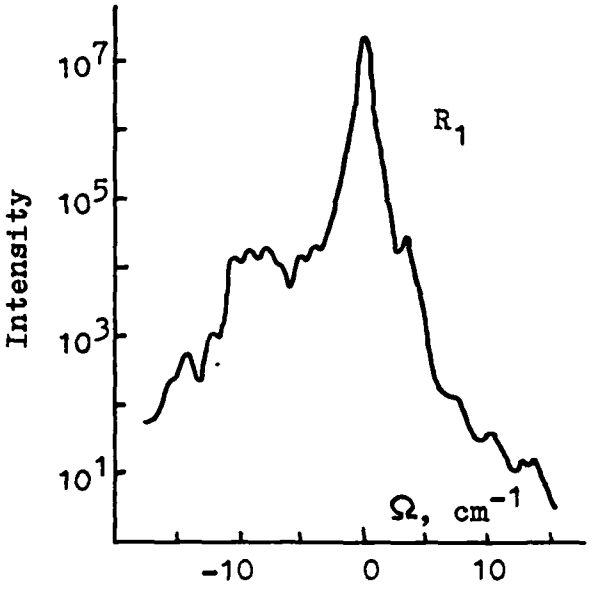

Fig.1

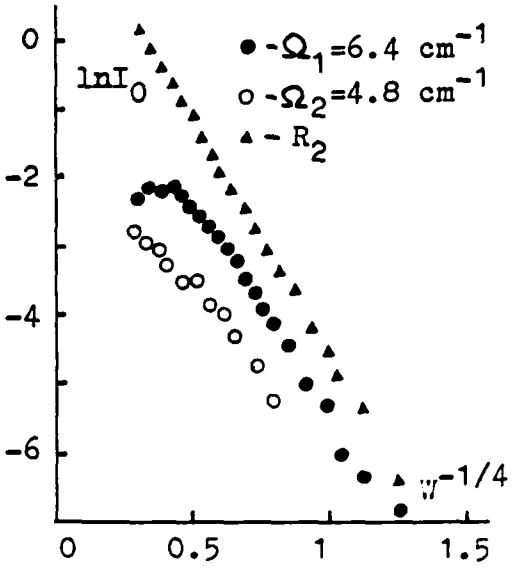

Fig.2

the $\bar{E}$-$2\bar{A}$ transitions [3]. One readily sees that the amplitudes of pulses in the wings vary similar to those of the pulses in the R_2 line over a broad heater power range.

Hence the transfer of $\bar{E}$-excitation to the high energy R_1 line wing initiated by heat pulse injection involves predominantly the nonequilibrium resonant 29 cm^{-1} phonons. Thus the present experiment provides a direct support to the theoretical idea [1] on the existence of resonant two-phonon-assisted transfer of the $\bar{E}$-excitation in ruby.

[1]- T.Holstein, S.K.Lyo, and R.Orbach. Phys. Rev. Lett. 36, 891, 1976. [2]- R.S.Meltzer, J.E.Rives, and W.C.Egbert. Phys. Rev. B 25, 3026, 1982. [3]- K.F.Renk, and J.Deisenhofer. Phys. Rev. Lett. 26, 764, 1971.

Optical Generation and Detection of Near-Zone-Boundary Phonons in Ruby

R.J.G. Goossens, J.I. Dijkhuis, and H.W. de Wijn
Fysisch Laboratorium Rijksuniversiteit
P.O. Box 80.000, 3508 TA Utrecht, The Netherlands

Optically pumped luminescent centers are now widely used as generators and detectors of high-frequency phonons in crystals. Monochromatic phonon generation and detection with such centers have for the first time been demonstrated in ruby by observing the R_1 and R_2 fluorescent intensities as a function of the pumping power and a magnetic field.[1] The optical techniques have made high-frequency phonons accessible to experiment, thus allowing important new information to be obtained. Here we present a new scheme of optical phonon spectroscopy which is inherently selective for near-zone-boundary phonons. As for the detection, the scheme employs, instead of a direct phonon-associated transition, second-order Raman transitions connecting two luminescent states. As an example we consider the case of ruby.

In the process of optical pumping of the luminescent states $\overline{2A}(^2E)$ and $\overline{E}(^2E)$ via the broad bands, acoustic phonons are preferentially generated near the zone boundary by virtue of their high density of states. These phonons, when sufficiently long-lived, induce Raman transitions populating $\overline{2A}$ out of $\overline{E}$. According to simple rate-equation considerations, the resultant enhancement of the $\overline{2A}$ fluorescent intensity, ΔR_2, is a direct gauge for the average occupation number of near-zone-boundary phonons, p_{ZB}, through

$$\Delta R_2 = \alpha(p_{ZB}/T_{Ram})T_{eff}R_1.$$

Here, p_{ZB}/T_{Ram} is the effective Raman rate connecting $\overline{E}$ and $\overline{2A}$, T_{eff} is the effective relaxation time of $\overline{2A}$, R_1 is the fluorescent intensity of $\overline{E}$, and α is a known constant of order unity. For ruby T_{Ram} is calculated to be of order 10^{-11} s,[2] while T_{eff}, depending on the bottlenecking, typically is of order 1 μs. The key to p_{ZB} therefore is to arrange the experiment such that ΔR_2, R_1, and T_{eff} are determined in a single measurement. This is feasible with modulated pumping.

In the experiments, optical generation and detection of near-zone-boundary phonons in ruby (130, 700, and 2500 ppm) was achieved upon pumping with a 3W argon laser. The p_{ZB} reached is of order 10^{-8}. The dependence of p_{ZB} on power, corrected for saturation, was found to be linear at 514 nm, and quadratic at 457 nm. Also observed was a roughly linear dependence on the excited-zone diameter (50-500 μm). These results suggest for zone boundary phonons (i) efficient production by optical pumping of the broad bands, (ii) slow thermalization, and (iii) ballistic motion over the excited zone.

References

1. J.I. Dijkhuis, A. van der Pol, and H.W. de Wijn, Phys. Rev. Lett. 37, 1554 (1976).
2. J.G.M. van Miltenburg, J.I. Dijkhuis, and H.W. de Wijn, to be published.

Nature of Phonons Assisting Spectral Transfer in Ruby

A.Monteil, E.Duval, A.Attar, G.Viliani
Groupe de Spectroscopie des Solides, ERA 1003, Université Claude Bernard, 69622 Villeurbanne, France

The observation of one-phonon assisted non-radiative spectral transfer[1] is one of the several not well understood features of ruby. Actually, due to the small energy mismatch between Cr^{3+} sites (<1 cm^{-1}), the density of phonon states is low and, more important, destructive interference was expected[2] because of long wavelength. On such grounds, a two-phonon process should dominate even at low temperature (T<50 K).[2]

However, the interference effect is not operative in ruby due to the symmetry of the crystal, which causes special strains to have opposite effects on Cr^{3+} ions at different sites. As shown in the figure, a σ_{xy} or σ_{xz} uniaxial stress of 10^9 N/m^2, which is neither parallel nor perpendicular to the C_3 axis of a 0.05 at % ruby, induces a splitting of 0.17 cm^{-1} of the R_1 line. The stress separates the Cr^{3+} sites into two sublattices which are different from those originating from the application of an electric field. It is possible to show that Cr^{3+} ions separated by one oxygen plane are inequivalent with respect to stress, while Cr^{3+} ions situated between two oxygen planes are equivalent. All strains which are neither parallel/perpendicular to C_3 nor contained in the plane of the C_3 and C_2 axes, are effective for this separation.

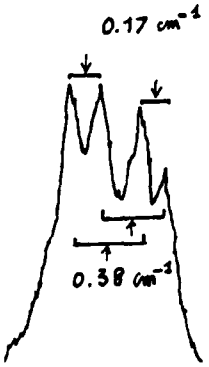

We have measured the spectral transfer rate both with and without $\sigma_{xy}(\sigma_{xz})$ stress and observed that at 30K with a 0.2 at % ruby sample the rate with stress is higher by about a factor 2. This result is interpreted by assuming that the transfer is assisted by phonons which induce strains of the same symmetry as those induced by $\sigma_{xy}(\sigma_{xz})$ stress.

There are two reasons why the transfer rate should increase: (1) The non-resonance between Cr^{3+} ions in different sublattices is increased when the stress is applied and there are more ions available for rapid spectral transfer; (2) Without stress, the interaction with transfer-assisting phonons can be quenched by internal strains or electric fields of different symmetry; such quenching effect is decreased by the stress which induces strains of the same symmetry as the phonons.

The same experiments have been carried out under electric field, and the results are completely different: no increase of the transfer rate is observed. This means that optical phonons are not effective for the one-phonon spectral transfer, which is not surprising.

1- P.M.Selzer, D.S.Hamilton, W.M.Yen, Phys. Rev. Lett. 38, 858 (1977).

2- T.Holstein, S.K.Lyo, R.Orbach, in Laser Spectroscopy of Solids, edited by W.M.Yen and P.M.Selzer, Springer 1981.

Magnetic Field Effect on Ion-Pair Transfer in Ruby

M. Montagna, L. Gonzo, O. Pilla, G. Viliani
Dipartimento di Fisica, Università di Trento, 38050 Povo, Trento, Italy
and Gruppo Nazionale di Struttura della Materia, Trento, Italy

E. Duval, A. Monteil
Spéctroscopie des Solides (ER10), Université Claude Bernard - Lyon I - 69622 Villeurbanne Cédex, France

The portion of pair emission in ruby which is due to energy transfer from single ions has been continously recorded as a function of an external magnetic field (in the range 0 - 100 kg) at various temperatures (2-77 K). 3rd and 4th neighbours pairs have been investigated (N1 and N2 emission lines respectively).

The two kind of pairs are found to behave quite differently. The N1 intensity at low temperature shows a nearly flat behaviour upon which rather intense resonances at ~25 and ~55 KG are superimposed. At higher temperatures the resonances smooth out and the flat background increases. As regards N2 intensity, at low temperature the resonances (the most intenses of which are found at 40 and 65 KG) appear on a slowly descending background whose descent is accomplished between 0 and ~35 KG. At higher temperatures the resonances tend to smooth out while the slow descent persists at least up to 77 K.

In both cases, the resonances are interpreted as level crossings between single ions and pairs, which is confirmed by excitation spectra of pairs under magnetic field. The origin of the slow descent in N2 is not clear. One spurious cause for this effect might be the field - induced decrease of the lifetime of the R-line, due to decreased reabsorption. In our samples this effect has been evaluated not to be strong enough to account for the observed decrease (of roughly a factor 2, or more) in the N2 intensity. Moreover, we recall that no or very little slow descent is observed in N1.

Possible models and their implications for the problem of energy transfer in ruby will be discussed.

Phonon Assisted Energy Transfer in $SrF_2:Er^{3+}$ [1]

John Wietfeldt, David Moore[2], and John C. Wright
Department of Chemistry, University of Wisconsin
Madison, Wisconsin 53706

Er^{3+} doped SrF_2 has been investigated using site selective laser spectroscopy.[3] Several distinct crystallographic sites have been observed, including clusters, where 2 or more charge compensated Er^{3+} ions are associated with a unique separation between Er^{3+} ions are associated with a unique separation between Er^{3+} ions. It has been shown that in one particular dimer, where the two ions are not in identical environments, energy transfer from one ion to the other can occur.

Many excitation transfer investigations have been performed on rare earth ions in crystalline environments.[4] The theoretical basis for phonon assisted excitation transfer has been well described,[5] and the dependence of the rate on temperature and energy gap can be used to explain microscopic mechanisms. Single phonon assisted transfer is observed in some cases and follows a Bose-Einstein distribution temperature dependence. Higher order phonon assisted transfer can be important. Two phonon non-resonant or two phonon Raman assisted transfer exhibit a T^N (where N = 3 to 7) temperature dependence. The resonant two phonon (Orbach) process can be important when another real electronic level in the system is resonant with one of the phonon interactions, and gives rise to the negative exponential inverse temperature dependence.

We have spectroscopically measured the excitation transfer rate in the dimer site in $SrF_2:Er^{3+}$, in the temperature range 2° to 40°K. There is a

21.3 cm^{-1} difference in the $^4S_{3/2}$ excitation lines for the two ions. The excitation transfer rate was obtained from the measured ratio of excitation peaks and the fluorescence lifetime. The unique separation of the two ions permits the extraction of the transfer rate without an ensemble average over all possible separations of the two ions. Our measurements for this system are consistent with a single phonon process at low temperatures, but require the addition of an Orbach process to explain the rapid rise in the excitation transfer rate at higher temperatures.

1) This work was supported by the National Science Foundation under grant DMR8205145.

2) Present address: Los Alamos National Laboratory, Los Alamos, New Mexico 87545.

3) M. D. Kurz and J. C. Wright, J. of Luminescence 15 (1977) 169.

4) W. M. Yen and P. M. Selzer: Laser Spectroscopy of Solids (Springer-Verlag, Berlin 1981), Chap. 5.

5) T. Holstein, S. K. Lyo, R. Orbach: Laser Spectroscopy of Solids, ed. by W. M. Yen and P. M. Selzer (Springer-Verlag, Berlin 1981), Chap. 2.

Optical Spectral Diffusion Processes in Organic Glasses on a Logarithmic Time Scale

J. Friedrich, W. Breinl, D. Haarer

(Physikalisches Institut, Universität Bayreuth, Postfach 3008, 8580 Bayreuth, W-Germany)

A photochemical hole, burnt into the lowest absorption band of quinizarin in an alcohol glass, was used as an optical detector for structural relaxation processes of the glass. The hole burning photochemistry is due to a light induced breakage of an intramolecular hydrogen bond between the dye molecule and the solvent (1). The stability of the photoproduct is determined by the local conformation of the solvent cage. Hence, one expects a wide distribution of back transfer rates R from the product to the reactant state. As a probe for the number of relaxed molecules we use the area of the photochemical hole. Fig.1 shows the normalized hole area as a function of probing time. The recovery dynamics of the hole occurs on a logarithmic time scale and is subject to a remarkable deuteration effect. In a similar way, the width of the optical transition increases on a logarithmic time scale. To find a quantitative interpretation of the measured logarithmic slopes we introduced the concept of photochemically induced tunnel systems. We consider the product and the educt state as a special two level system, with a distribution of tunneling rates R given by the well known distribution of the TLS states of glasses (2,3). We can calculate the normalized hole area A/A_1 at time t by integrating the glass distribu-

tion function between the limits $R=1/t$ and $R_1=1/t_1$. t_1 is the time of the first measurement of the hole after burning. We get a logarithmic decay law:

$$A/A_1 = 1-(\ln R_1/R_{min})^{-1} \ln t/t_1$$

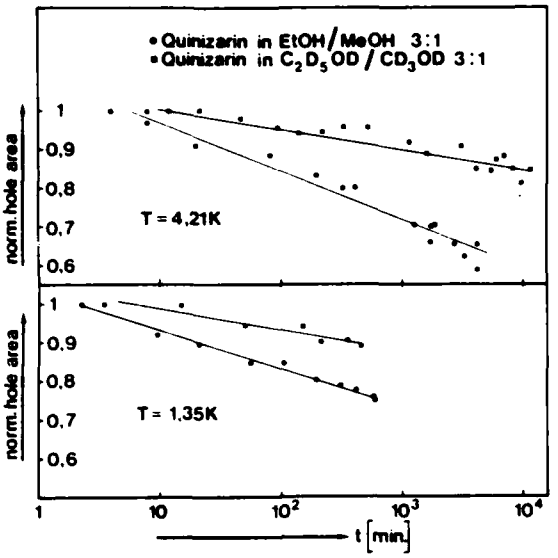

Fig. 1

From the measured slopes we find that the rates vary over more than 10 orders of magnitude for the protonated and 19 orders of magnitude for the deuterated glass. (An estimation of the maximum barrier heights show, that they are far above the glass transition temperature.)

Since the slopes of the logarithmic decay of the hole and the logarithmic increase of its width are roughly the same and show the same deuteration effect, we believe that the spectral diffusion has the same origin as the hole recovery, and, hence, is mainly due to the decay of the product state: Relaxation of the photoproduct may create strain fields which lead to the observed spectral diffusion of the optical energy characterized by a logarithmic increase of the optical width.

(1) J. Friedrich, D. Haarer, Ang.Chemie, Int.Engl.Edition, Feb. 1984

(2) J. Jäckle, Z. Physik 257, 212 (1972)

(3) "Amorphous Solids", ed. by W.A. Philips, Springer (1981)

Phonon Processes in Disordered Systems, Probed by Spectral Hole Burning and Refilling of Dyes

U. Bogner, G. Röska and P. Schätz

Naturwissenschaftliche Fakultät II-Physik,

Universität Regensburg, 8400 Regensburg, Fed.Rep.Germany

With heat pulse technique (pulse duration $\Delta t \geq 20$ ns) we measured the effects of phonons on the persistent spectral holes of dye molecules in thin organic films, e.g. Langmuir-Blodgett films, or of dye molecules adsorbed at the surface of crystals. The measurements include phonon memory[1] and real time effects of phonons, i.e., the irreversible and the reversible phonon-induced filling in the center of the spectral hole. In particular we measured the dependence on the duration and on the power density or calculated temperature T_H of the heat pulses. The dependence of the fluorescence intensity I_o of the first vibronic zero phonon line on the number N of the irradiated heat pulses (or to be precise on the time $t = N \cdot \Delta t$) in the case of the phonon memory is demonstrated in Fig. 1. The observed logarithmic time dependence is explained by a theory based on thermally activated processes in double well potentials[2] with constant density of states concerning their barrier heights.

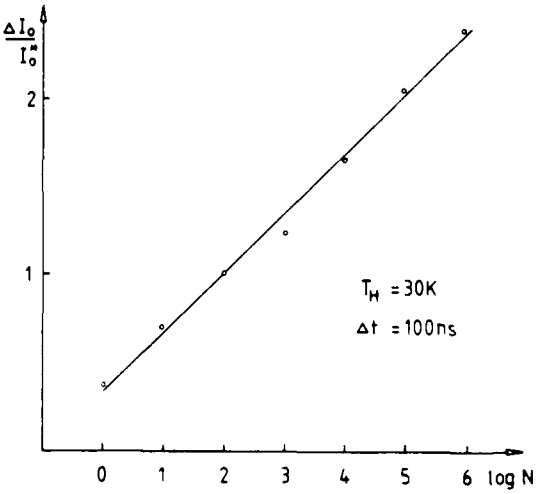

Fig. 2 shows the fluorescence intensity at the surface opposite that containing the heater in dependence of the time of flight of the transverse (T) and longitudinal (L) acoustical phonons, propagating ballistically in a sapphire single crystal. This demonstrates a real-time effect of the phonons; the fluorescence increase is due to reversible filling in the center of the spectral hole by the phonon pulses and is explained by the model also. The results and the investigation of phonon scattering in quartz crystals and in addition the observed fluorescence in the anti-Stokes region of the zero-phonon lines demonstrate that the system can be used for phonon detection.[3] Furthermore we present experimental results providing information about the number of double-well potentials coupled to a dye molecule and we suggest a microscopic model in which double-well potentials are formed by adsorbed molecules.

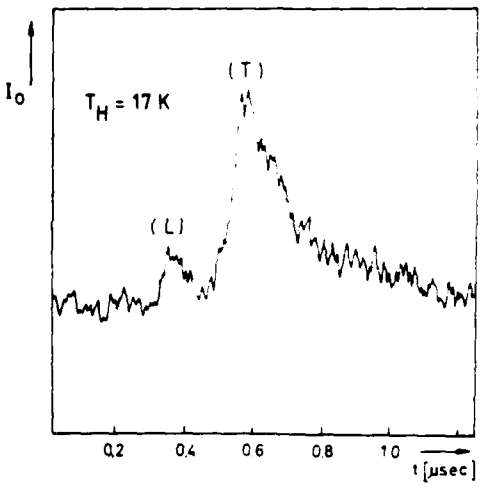

References

[1] U. Bogner, Phys. Rev. Lett. 37, 909 (1976).

[2] P. W. Anderson, B. I. Halperin, and C. M. Varma: Philos. Mag. 25, 1 (1972); W. A. Philips, J. Low. Temp. Phys. 7, 351 (1972).

[3] U. Bogner and G. Röska, in *"Phonon Scattering in Condensed Matter"*, ed. W. Eisenmenger (Springer, Berlin 1984).

Electric-Field-Induced Changes of Persistent Spectral Holes in Amorphous Solids and their Applications

U. Bogner, P. Schätz, K. Beck and Max Maier
Naturwissenschaftliche Fakultät II - Physik,
Universität Regensburg, 8400 Regensburg, Fed.Rep.Germany

The effect of an external electric field on spectral holes of dye molecules in disordered systems, e.g. polymer films and Langmuir-Blodgett films, [1,2] and its applications are studied. We observed a filling in the center of the persistent spectral hole, which is caused by electric-field-induced shifts of the electronic levels of the dye molecules. The experimental results for perylene in polyvinylbutyral (PVB) are explained by a linear electric field dependence of the level shifts which is ascribed to the interaction of the dye molecules with the amorphous matrix. The magnitude of the level shifts is determined by comparing the experimental results with the calculations [2]. Experiments are reported which provide information about phonon-induced transitions in the double well potentials which are characteristic of amorphous solids.

We apply the electric-field-induced filling in the center of the spectral hole to determine characteristics of the linear electron-phonon interaction for strongly inhomogeneously broadened optical transitions. A method is presented which allows the determination of the spectral shape of the true phonon sideband and the Debye-Waller factor. It is based on

the fact, that the electric-field-induced change of the number of resonantly excited dye molecules is large compared to the change of the number of molecules excited via their phonon sidebands. Experimental results for the first vibronic (0'→1) fluorescence transition of perylene in PVB are presented. The electric-field method is compared with other methods [3,4].

We present also experimental results on holes burned at various voltages, which are of possible interest for voltage-tunable optical data storage and switching of the optical properties of materials. The figure shows stable multiple holes in the fluorescence intensity versus voltage diagram for 9-aminoacridine in PVB. The suitability of various dyes and matrices for applications is discussed.

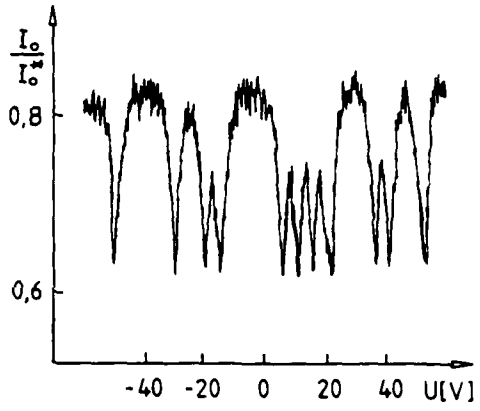

References

[1] U. Bogner, R. Seel and F. Graf, Appl. Phys. B29 (1982)152.

[2] U. Bogner, P. Schätz, R. Seel and Max Maier, Chem. Phys. Lett. 102 (1983) 267.

[3] R. Personov in "Spectroscopy and Excitation Dynamics of Condensed Molecular Systems" ed. V. Agranovich and R. Hochstrasser (Springer, 1983).

[4] U. Bogner and R. Schwarz, Phys. Rev. B24 (1981) 2846.

Optical Dephasing of Impurities in Amorphous Organic Solids down to 0.3 K.

Silvia Völker, H.P.H. Thijssen and R. van den Berg
Huygens Laboratory, University of Leiden,
P.O. Box 9504, 2300 RA Leiden, The Netherlands

Photochemical hole-burning has been used to measure the temperature dependence (between 0.3 and 20 K) of homogeneous linewidths (Γ_{hom}) of 0-0 $S_1 \leftarrow S_0$ transitions of a variety of organic molecules in alcoholic glasses and polymers [1]. It was found that Γ_{hom} obeys a $T^{1.3\pm0.1}$ law independent of the system studied. The results suggest that the guest only acts as a sensor to probe low-temperature relaxation processes in the amorphous state. Furthermore, it was observed for the first time that some of the organic glassy systems reach the lifetime-limited value of a few MHz at $T > 0.3$ K, which implies a very weak coupling between impurity and amorphous host. In all systems Γ_{hom} extrapolates to the T_1-limited value for $T \rightarrow 0$. In addition, a cross-over from a $T^{1.3}$ to a linear power-law occurs in systems where $\Gamma_{hom} \lesssim 60$ MHz, at a temperature which depends on the structure of the glass. This structure also determines the magnitude of Γ_{hom} : stiff alcoholic networks with a high degree of hydrogen bonding or linear polymer chains with no side chain groups (and, presumably, a high degree of short range order) yield very narrow linewidths of the same magnitude as in crystalline solids. This is in contrast to previous results in organic and inorganic glasses where differences of two to three orders of magnitude have been reported between amorphous and crystalline solids. From these results it appears that hole-burning can be used as a sensitive technique to study slow motions of polymer side chain groups at low temperatures.

It has been postulated that glasses have a broad distribution of two level tunneling systems (TLS) by means of which physical properties of glasses at low temperatures can be understood. Recently, theoretical explanations for the present $T^{1.3}$ - results based on this TLS-model have been developed. In one of the models the TLS-interaction is combined with librational modes localized on the impurity [2]. In an other, the

phonons coupled to the TLS of the glass are replaced by "fractons", assuming that polymers are percolating networks[3]. A third model, based on "spectral diffusion" of the electronic transition due elastic dipolar coupling to "flipping" TLS [4], yields not only a $T^{1.3}$-temperature dependence of Γ_{hom}, but also a logarithmic dependence on time. All three models, however, are only partly consistent with the experimental results, and they differ significantly in their predictions for $T \to 0$, $T < 20$ K and in the mechanism for the cross-over from $T^{1.3}$ to T. Experiments are currently in progress to check which, if any, of the above models do in fact explain the measurements.

Very recent photon echo results in an inorganic glass between 0.1 and 1 K also show a $T^{1.3}$ - dependence but, in contrast to organic glasses [1], Γ_{hom} at 0.1 K is still orders of magnitude larger than the T_1-limited value [5]. This indicates that amorphous solids at low temperatures, whether organic or inorganic, probably undergo similar dephasing processes, but in different temperature regimes.

References

[1] H.P.H. Thijssen, R. van den Berg and S. Völker, Chem. Phys. Lett. 103, 23 (1983) and references therein.

[2] B. Jackson and R. Silbey, Chem. Phys. Lett. 99, 331 (1983).

[3] S.K. Lyo and R. Orbach, Phys. Rev. B. 29, 2300 (1984).

[4] S. Hunklinger and M. Schmidt, Z.f. Physik B (submitted)

[5] J. Hegarty, M. Broer, B. Golding, G. Simpson and J. MacChesnev, Phys. Rev. Lett. 51, 2033 (1983).

Coherent Singlet Polariton to Trap Energy Transfer in Naphthalene Crystals

Gerald J. Small, Sylvia H. Stevenson and Maureen A. Connolly

Ames Laboratory-USDOE and Department of Chemistry

Iowa State University, Ames, Iowa 50011

One-photon studies of coherent energy transfer are hampered by the fact that excitons of well-defined and different wavevectors ($\underline{k}$) cannot be prepared in the bulk. In addition, the group velocities of the excitons in molecular crystals and semiconductors are typically low so that even momentary exciton self-trapping can lead to coherence loss over short distances.

Recent studies from this laboratory have shown that coherent polariton fusion in naphthalene crystals can be used to study the dependence of polariton-phonon scattering on temperature and wavevector $\underline{k}$[1]. Specifically, $\underline{k}$-selected polaritons associated with the upper and lower branches from the singlet $\underline{a}$-exciton were utilized with wave packet velocities (v_p) in the range $10^6 \lesssim v_p \lesssim 10^9$ cm s^{-1}. The polariton-phonon scattering for these velocities was shown to be markedly weaker than normal exciton-phonon scattering; the difference being attributed to motional narrowing due to fast polariton motion. At temperatures near 4K, the polariton coherence lengths are several tens of microns for sufficiently high v_p.

These large coherence lengths and polariton velocities have prompted us to study polariton to trap electronic energy transfer in naphthalene crystals containing anthracene as the fluorescent trap. At concentration levels of $\lesssim 10^{-5}$ mole/mole, fluorescence from both the naphthalene host (h) and trap (t) are observed over the T-range of interest, ~ 2-20K. The T-dependence of the fluorescence intensity ratio I_h/I_t for coherent excitation of the polari-

ton is expected to be different and markedly stronger than for incoherent excitation of the exciton. The reason is that for coherent excitation, two processes compete in trap population: direct unidirectional polariton to trap transfer; and indirect polariton to trap transfer via excitons produced by polariton-phonon scattering. Their relative importance depends critically on the temperature through this scattering. Data supporting this view are presented. The ratio I_h/I_t for coherent excitation increases rapidly with T until it plateaus at a $T = T_p$. The obvious explanation for plateauing is that $\ell_{coh} < R$ for $T \gtrsim T_p$, where ℓ_{coh} is the polariton coherence length due to polariton-phonon scattering ($\gamma(T)$) and R is the average host-trap separation. Since $\ell_{coh} = v_p/\gamma(T)$, the T-dependence of I_h/I_t should depend on the polariton $\underline{k}$, e.g. $T_p = T_p(\underline{k})$. Data confirming this are presented. A theoretical model for explaining the data is presented.

References

1. S. H. Stevenson and G. J. Small, Chem. Phys. Lett. 100, 334 (1983); ibid 95, 18 (1983).

Scattering and trapping of photo-excited triplet excitons in one-dimensional molecular crystals.

J. Schmidt
Huygens Laboratory, University of Leiden, P.O. Box 9504,
2300 RA LEIDEN, The Netherlands.

In the last few years it has been possible to obtain detailed information about scattering and trapping of photo-excited triplet excitons in the molecular crystal of 1, 2, 4, 5 - tetrachlorobenzene (TCB). The attraction of TCB is that the intermolecular interaction in good approximation is one-dimensional which makes it a prototype for investigating the properties of tightly bound excitons [1].

At liquid helium temperatures the "coherent" description of the triplet excitons in TCB applies i.e. the excitations of the linear chain are characterized by a wave vector k and a well defined band structure exists. By pulsed laser excitation it is possible to prepare the triplet excitons in a non-equilibrium situation where only exciton states with a very small k value are populated. The subsequent evolution is observed via pulsed Electron Spin Echo (ESE) methods. These experiments show that no restriction exists in the scattering probability and that theoretical models about exciton-phonon interaction, which predict conservation of energy and quasi-momentum [2] do not apply. It appears that in the TCB system at temperatures where kT is small compared with the bandwidth of the exciton band the k to k' scattering is an "impurity assisted" process [3]. We have been able to prove that chemical impurities do not play an important role. Hence we believe that the scattering is caused either by structural defects, related to shallow X-traps, or by isotopic impurities (^{13}C or ^{2}H). At higher temperatures the results can be explained nicely by two-phonon Raman-type processes. Here however it is not necessary to invoke impurities to explain the results.

To obtain more detailed information about the type of impurity responsible for the observed k-k' scattering we have compared our results with computer simulations of the scattering pattern. For these simulations we have used scattering probability functions derived by Benk and Silbey [4] for various types of impurity induced exciton-phonon interactions. It appears that all models which assume a change in site energy fail to reproduce the observed scattering pattern but that a very nice fit is obtained when it is assumed

that the translational symmetry of the exciton-phonon interaction is disturbed.

In addition to the scattering experiments we have also been able to derive a value for the width Δk of the triplet exciton wave packets. From the observed sinusoidal variation of the phase memory time T_M of the triplet spins over the zero-field lineshape we conclude that Δk corresponds with about 0,5% of the first Brillouin zone, indicating that the triplet exciton extends over about 200 molecules [5].

References.

1. A.H. Francis and C.B. Harris, Chem. Phys. Lett. 9, 181; 188 (1971).
2. A.S. Davydov, "Theory of Molecular Excitons" (McGraw Hill, New York 1962).
3. A.J. van Strien, J. Schmidt and R.J. Silbey, Mol. Phys. 49, 151 (1982).
4. H. Benk, and R.J. Silbey, J. Chem. Phys. 79, 3487 (1983).
5. J.F.C. van Kooten, A.J. van Strien and J. Schmidt, Chem. Phys. Lett. 90, 337 (1982).

Time-resolved Excimer Dynamics in Perylene Crystals

H.Port, B.Walker and H.C.Wolf

Physikalisches Institut, Teil 3, Universität
Pfaffenwaldring 57, D-7000 Stuttgart 80

Perylene crystals of the α-phase are prototypes for excimer formation, since the molecules are arranged in sandwich configuration. The prominent feature of the perylene fluorescence spectrum is the appearance of two spectral contributions, an actual excimer-type emission and the Y-emission, which has been attributed to a partially relaxed excimer.

We have investigated the dynamics of the excimer formation in perylene measuring rise and decay of both Y- and excimer-fluorescence as a function of temperature (4 K ÷ 300 K) using picosecond time resolution. The experiments have been performed applying a modelocked Nd-glass laser at low excitation densities and a streak camera.

Examples for the fluorescence transients at 80 K are given in fig.1. The experimental rise- and decay-times are plotted as a function of temperature in fig.2.

For a broad temperature range it is demonstrated, that the risetime of the excimer fluorescence corresponds to the decaytime of the Y-fluorescence. It is confirmed, that the formation of the excimer in perylene is a two-step process. The excimer excited state is not formed directly from the absorbing state, but via the Y-state as a precursor. A complete analysis of the kinetics is provided.

Furthermore it is shown, that the risetime of the Y-fluorescence actually is measurable. The time constant of the Y-state formation is 150 ps and does not depend on temperature.

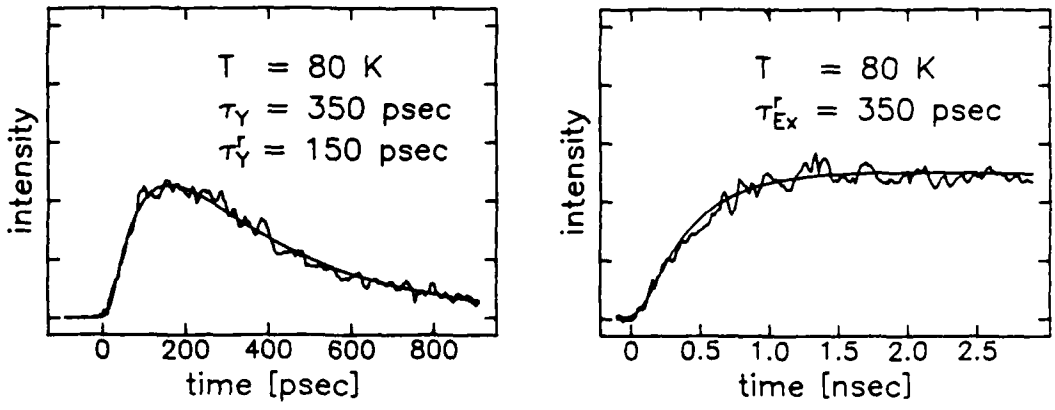

Fig.1: Time-resolved fluorescence after ps-pulse excitation at 80 K, (a) Y-state and (b) excimer.

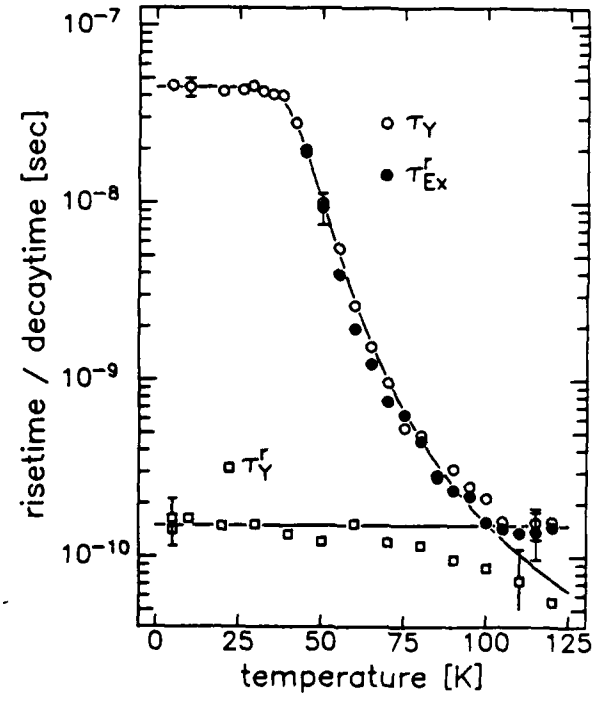

Fig.2: Decay time of the Y-fluorescence (τ_Y) and rise times of both Y- and excimer fluorecence (τ_Y^r and τ_{Ex}^r) as a function of temperature.

Singlet Exciton Annihilation in the Picosecond Fluorescence Decay of 1,1'-Diethyl-2,2'-Cyanine Chloride Dye J-Aggregate

Donald V. Brumbaugh and Annabel A. Muenter
Research Laboratories, Eastman Kodak Company, Rochester, NY 14650
and
Wayne H. Knox, Bruce Wittmershaus, and Gerard Mourou
the University of Rochester, Rochester, NY 14623

We present a new study which reveals a strong dependence on excitation intensity in the time-resolved fluorescence decay of the J-aggregate of the title dye. Strong intermolecular interaction in the J-aggregate is indicated by the large red shift (1700 cm^{-1}) and band narrowing (1475 to 125 cm^{-1}) in the absorption spectrum compared with unassociated dye molecules in solution. Exciton dynamics in the J-aggregate are interesting because of the lower dimensionality and stronger intermolecular interaction compared to other molecular crystals and because of the photographic spectral sensitization properties of the J-aggregate.

In these experiments, J-aggregation was induced at 293 K by squeezing a drop of 10^{-2} M aqueous dye solution between two glass slips. Fluorescence decay of the J-aggregate was observed by two techniques: time-correlated single-photon counting (TCSPC) and a streak camera with jitter-free signal averaging.[1] The excitation power in TCSPC was 3×10^{17} photons absorbed cm^{-2} s^{-1}. Over the range from 0 to 6 ns, TCSPC detected two lifetime components, 138 and 659 ps. In the 0.4-ns time window of the streak camera, the 138-ps component was confirmed at an excitation energy of 2×10^{22} photons absorbed cm^{-2} s^{-1}. With the streak camera, fluorescence decay was investigated at excitation intensities greater than 10^{22} photons absorbed cm^{-2} s^{-1} (30-ps laser pulse). A very short new decay component appeared and increased in relative intensity with increasing excitation intensity, as shown in the figure. This observation is attributed to singlet-singlet exciton annihilation in the J-aggregate. (The rise in the curves at 0.3 ns is an artifact resulting from a weak delayed excitation.) The simulated curves in the figure were obtained by the equation

$$dn/dt = AI(t) - Kn(t) - \gamma n^2(t)$$

where A is the percent absorption, I(t) is the excitation function, K is the excited-state decay rate (5×10^9 s^{-1}), and γ is the exciton annihilation

constant (7.7×10^{15} cm^2 s^{-1}). At the highest excitation intensity 2×10^{24} photons absorbed cm^{-2} s^{-1}, the initial portion of the curve is strongly influenced by exciton annihilation and can be fit with a 42-ps single exponential function. This explains four literature values[2] for the excited-state lifetime ranging from 15 to 35 ps, which were obtained with excitation powers of 5×10^{24} to 10^{27} photons cm^{-2} s^{-1}.

Fifty percent fluorescence quenching is reached when the fraction of molecules excited in one pulse is 1/240. In photographic supersensitization experiments,[3] 50% quenching was observed with a ratio of supersensitizer to cyanine dye of 1/210. These two experiments indicate a lower limit to the exciton mobility in the J-aggregated dye.

References

1. W. Knox and G. Mourou, Opt. Commun. 37, 203 (1981).
2. Z. X. Yu, P. Y. Lu, and R. R. Alfano, Chem. Phys. 79, 289 (1983), and references therin.
3. A. A. Muenter and W. Cooper, Photogr. Sci. Eng. 20, 121 (1976).

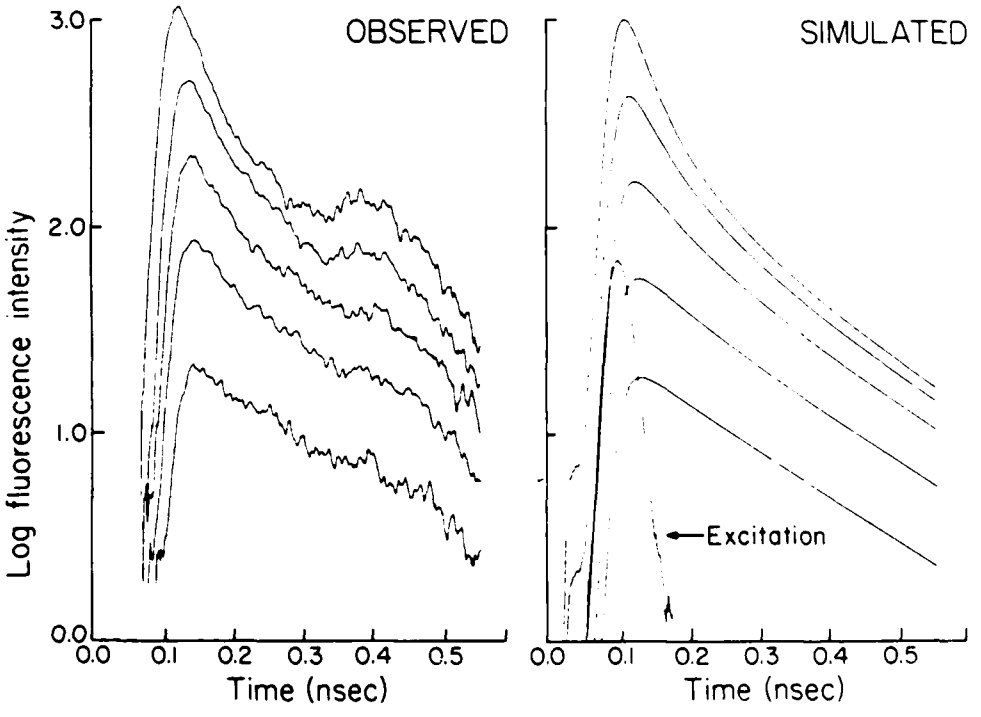

Luminescence Associated with Free and Bistable Self-Trapped Excitons in β-Perylene

H. Nishimura
Department of Appl. Phys., Osaka City Univ.,
Sumiyoshi-ku, Osaka, JAPAN 558

K. Mizuno and A. Matsui
Department of Phys. Konan Univ.
Okamoto, Kobe JAPAN 658

The luminescence spectra in β-perylene crystals reveal a strange temperature dependence[1] (Figure 1). Analysis of the spectra provides clear evidence that at high temperatures the free exciton luminescence and the deeper self-trapped exciton luminescence dominate, while at low temperatures the shallower self-trapped exciton luminescence dominates.

The intensity of the free exciton luminescence decreased quickly with decreasing temperature but very gradually below 100 K. The luminescence decaytime (13 ns at room temperature) decreased gradually upon reducing temperature but below about 80 K it increased quickly. Those complicated phenomena are interpreted by taking account of coexistence of deeper and shallower self-trapped exciton states and they are compared with those in α-perylene in which only two-center type self-trapped excitons (excimers) are stable.

It is suggested that one of the two self-trapped states is of one-center type and the other two-center type (Figure 2). We would like to emphasize that bistable self-trapped exciton states must be recognized in many organic solids in which the exciton-

phonon coupling is strong, because β-perylene crystal has an ordinary monoclinic structure as in many organic solids whose unit cell contains two translationally inequivalent molecules.

Discussion will be also extended over sharp luminescence lines which are observed below 30 K (Fig. 1) and involve precise information such as self-trap depths and the configuration of molecular aggregates at the self-trapped lattice sites[2].

1) A. Matsui and H. Nishimura: J. Phys. Soc. Jpn **51** (1982) 1711.

2) A. Matsui, K. Mizuno and H. Nishimura: will be submitted to J. Phys. Soc. Jpn.

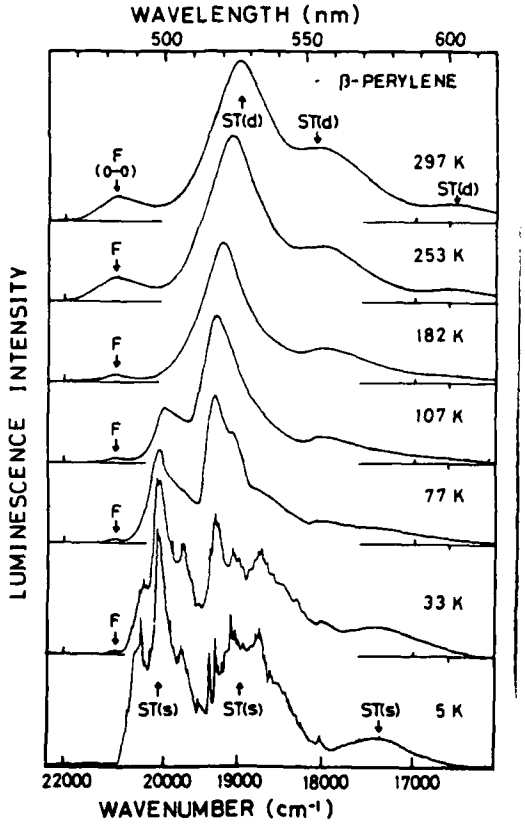

Fig. 1

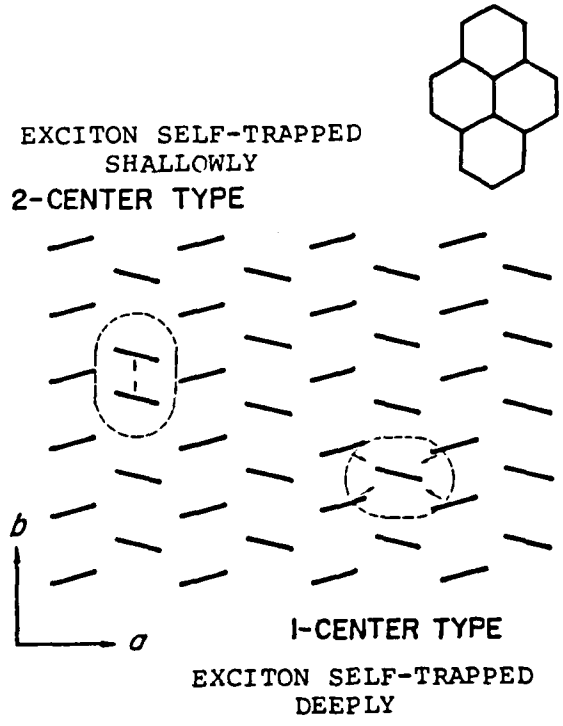

Fig. 2

Mobility and Conformation of Side Chains in Copolymers of the Methacryl Amide Type. Study of Depolarization of Fluorescence and Nonradiative Energy Transfer

František Mikeš, Drahomír Vyprachtický, Jaroslav Králíček, Department of Polymers, Prague Institute of Chemical Technology Suchbátarova 1905, 166 28 Prague, Czechoslovakia and Jiří Labský, Institute of Macromolecular Chemistry, Czechoslovak Academy of Sciences, Heyrovského nám. 2, 162 06 Prague, Czechoslovakia.

The authors studied the mobility and conformation of side chains of different lengths in the copolymers of the N-alkyl acryl amide and methacryl amide types from the depolarization of fluorescence and from the efficiency of the nonradiative energy transfer between tryptophane fluorochrome bonded in the immediate vicinity of the polymer backbone and 1-dimethyl amino-5-naphthalene sulphonamide fluorochrome at the end of the side chain.

František Mikeš, Drahomír Vyprachtický, Jaroslav Králíček, Department of Polymers, Prague Institute of Chemical Technology, Suchbátarova 1905, 166 28 Prague, Czechoslovakia

Jiří Labský, Institue of Macromolecular Chemistry, Czechoslovak Academy of Sciences, Heyrovského nám.2, 162 05 Prague, Czechoslovakia

By means of a polymeranalogous reaction of polymeric 4-nitrophenol esters with 1-dimethyl amino-5-/β-aminoethyl/ sulphonamidonaphtalene /DNS fluorochrome/ /Type I/, and by a reaction of polymeric tryptophane /TRY fluorochrome/phthalimide esters with 1-dimethyl amino-5-/ω-aminoalkyl/ sulphoamidonaphthalenes soluble polymers /Type II/ were obtained.

From the temperature dependence of the change in the polarization of fluorescence of DNS fluorochrome bonded to the polymer /Type I/ in water and in methanol the relaxation times /τ/ of the fluorochrome were calculated.

With the increasing lenght of the side chain the reciprocal value of the relaxation time increaces linearly with the number of atoms /d/ constituting the side chain /polymer in methanol/. In an aqueous medium the reciprocal value of the relaxation time of the DNS fluorobrome attains the maximum value when the number of atoms constituting the side

chain d = 12, and further prolongation of the chain results in its lower mobility. The increasing length of the side chain results in a growth of its hydrophobic character, and water, contrary to methanol, becomes a poor solvent for it. As a result of this there can occur an intramolecular interaction, the collapse of the aliphatic hydrophobic side chain. The collapse of the side chain is linked with an expansion of its hydrodynamic volume, and consequently leads to the prolongation of the relaxation time of the DNS fluorochrome.

From the efficiency of the intramolecular energy transfer between the TRY and the DNS fluorochromes, using the Förster theory of longe-range excitation energy transfer, the distance of these two fluorochromes in the side chain was estimated. The orientation effects for the calculation of the orientation factor for a given donor-acceptor pair were analyzed from the depolarization measurements.

The results obtained show that in the long side chains in the copolymers of TypeII the distance of the TRY and the DNS fluorochrome in the aqueous medium is smaller than that in the corresponding polymers in methanol or ethanol. These measurements indicate a collapse of the long side chains in the aqueous medium. /In this connection the influence of the character of alkyl R_1 and R_2 on the distance of the ends of the side chains is discussed; R_1, R_2 are backbone and N-substituents, respectively/

Nonlinear Optical Properties of Fluorescein in Glass

M. A. Kramer, J. Krasinski, and R. W. Boyd

The Institute of Optics

University of Rochester

Rochester, New York 14627

Summary

There is much interest in materials displaying a small saturation intensity for use in four-wave mixing and optical bistability. In this paper we report on one such material comprised of fluorescein dye molecules imbedded in a matrix of boric acid glass. This material shows a luminescence decay time of about 2 sec and hence an extremely small saturation intensity which we have measured to be about 10 mW/cm^2. We have found that four-wave mixing can easily be observed at intensities of 10 mW/cm^2.

The origin of the long luminescent decay time in the fluorescein-doped boric acid glass is due primarily to delayed fluorescence. Decay out of the triplet state can be due either to thermal activation[1] or triplet-triplet annihilation[2]. We believe triplet-triplet annihilation plays some role in our experiment since the observed decay rate is intensity dependent. Since the decay rate of this process is concentration dependent, nonexponential decay of the excited state results. Although the nonlorentzian lineshape resulting from this nonexponential decay is masked in spontaneous emission, these nonlorentzian features do appear in the nonlinear response of the system. Through use of amplitude modulation spectroscopy[3] we have observed such nonlorentzian features in the probe-beam absorption lineshape. In fluorescein-doped glass, a dip of width approximately 750 milliherz which is markedly nonlorentzian in

shape was observed.

The probe-beam absorption lineshape of fluorescein in glass measured using amplitude modulation spectroscopy is shown in figure 1. The data are well fit by the lower solid curve showing nonexponential decay due to triplet-triplet annihilation. Also shown is the upper solid curve which is a lorentzian constrained to fit our data in the wings. The experimental lineshape shows a pronounced cusp at line center.

In conclusion, we have demonstrated four-wave mixing and observed nonlorentzian features in the probe-beam absorption lineshape of fluorescein in glass. The saturation intensity of this system has also been measured and is foun to be approximately 10 mW/cm^2. This remarkably low value suggests that this system will prove useful as a new nonlinear material.

References

1) G. N. Lewis, D. Lipkin, and T.T. Magle, J. Amer. Chem. Soc. 63, 3005 (1941)

2) S. Czarnecki, Bull. Acad. Polon. Sci. 9, 561 (1961)

3) L.W. Hillman, R.W. Boyd, J. Krasinski, and C. R. Stroud,Jr., Opt. Commun., 45, 416 (1983)

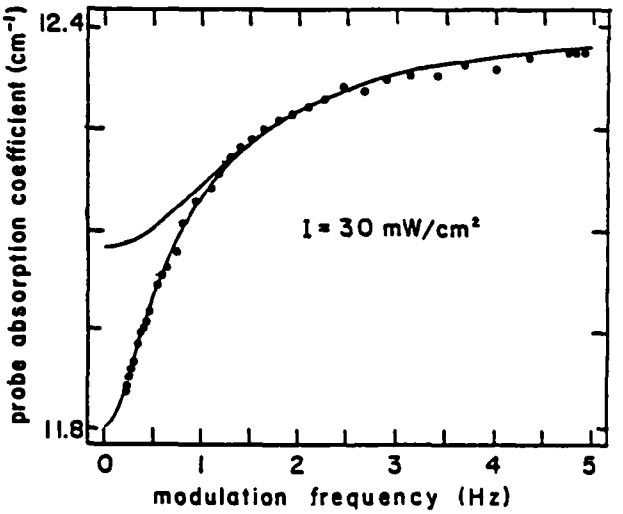

Figure 1. Measured propbe-absorption lineshape for a 1.4-mm thick sample of fluorescein-doped glass.

Facile Nonphotochemical Hole Burning and Filling of Laser Dyes and Rare Earth Ions in Deuteroxy and Hydroxy Polymers

Bryan L. Fearey, Thomas P. Carter and Gerald J. Small
Ames Laboratory-USDOE and Department of Chemistry
Iowa State University, Ames, Iowa 50011

Nonphotochemical hole burning (NPHB) has been well established as a method of investigating the microscopic properties of doped amorphous solids, typically molecular impurities in organic glasses and polymers or rare earth ions in hard inorganic glasses[1]. The NPHB of ionic dye molecules in hydroxylated polymer films recently has been shown to be significantly more efficient than many other systems[2] and the temperature dependence of the optical dephasing of one such system has been reported[3].

Whereas previous holeburning studies on rare earth ions have been performed exclusively in hard inorganic glasses[4] where dephasing times are relatively slow, recent experiments have shown that, for several rare earth ion-polymer systems (Pr^{3+}, Nd^{3+}, Ho^{3+} in poly(vinyl alcohol) (PVOH), efficient hole burning is observed with considerably faster dephasing times. The temperature dependence of the optical dephasing for Pr^{3+} in PVOH over the range 1.6K to 20K has been measured and is compared to other sytems incorporating rare earth ions which show a T^n temperature dependence with n = 1, 1.3 or 2 at low temperatures.

The optical dephasing and quantum efficiency have also been measured over the same temperature range for cresyl violet (CV) perchlorate in hydroxyl-deuterated poly(vinyl alcohol) (PVOD). These results, along with those from earlier reports for CV in PVOH,[2,3,5] are used to infer the importance of

hydrogen bonding in the NPHB process and to test theoretical models which depend on the two-level system model[1].

In these polymer systems, it is possible to significantly reduce the depth of an existing hole by burning at the same spatial position with a frequency removed from the initial burn. By varying the frequency difference between the two burns and the position of the initial burn in the inhomogeneous absorption profile, the mechanism of the hole filling process can be investigated. This method has been used to study the system rhodamine 640 (R640) perchlorate in PVOH which has yielded useful information about two-level system connectivity and other mechanisms important in hole filling.

References

1. G. J. Small, in Modern Problems in Solid State Physics. Molecular Spectroscopy, Eds. V. M. Agranovich and R. M. Hochstrasser (North Holland, Amsterdam 1983).
2. B. L. Fearey, T. P. Carter and G. J. Small, J. Phys. Chem. 87, 3590 (1983).
3. T. P. Carter, B. L. Fearey, J. M. Hayes and G. J. Small, Chem. Phys. Lett., 102, 272 (1983).
4. R. M. MacFarlane and R. M. Shelby, Opt. Commun. 45, 46 (1983) and references therein.
5. B. L. Fearey, R. P. Stout, J. M. Hayes and G. J. Small, J. Chem. Phys. 78, 7013 (1983).

Low Temperature Optical Dephasing of Rare Earth Ions by Tunneling Systems in Glass

M.M. Broer
AT&T Bell Laboratories
Murray Hill, N.J. 07974

Optical dephasing of paramagnetic ions and molecules in organic and inorganic amorphous solids at low temperatures ($\lesssim$100K) is characterized by unusual temperature dependences and enhanced relaxation rates compared to crystalline systems[1]. For a large variety of impurity-host combinations the dephasing rate has been found to follow a T^m temperature dependence with m approximately 2. Several theories have attempted to explain this behavior by assuming interactions between the optical center, phonons, and atomic tunneling systems. However, the role of the intrinsic disorder in optical dephasing in these systems is not clearly understood.

We have studied[2] the dephasing of the $^4F_{3/2}(1) \rightarrow {}^4I_{9/2}(1)$ transition of Nd^{3+} doped SiO_2 glass between 0.05 and 1K. The dephasing rate T_2^{-1} is measured with two-pulse photon echoes in a novel geometry. The Nd^{3+} ions are imbedded in the SiO_2 core of a single mode optical fiber. This method has the intrinsic advantages of long interaction lengths, phase-matching and efficient heatsinking. The echo decays exponentially with a characteristic time constant related to T_2. The rate T_2^{-1} obeys a $T^{1.3}$ dependence between 0.1 and 1K. Earlier homogeneous linewidth measurements[3] of the same transition in Nd^{3+} doped glasses showed the typical T^2 dependence above $\simeq$20K. The echo results indicate that this T^2 dependence does not persist to low temperatures and constitute the first evidence for a different temperature dependence of the dephasing rate other than that at higher temperatures. This indicates the existence of a crossover in the temperature dependence above 1K.

The photon echo results show a striking similarity to the homogeneous linewidths of tunneling systems, as studied earlier with microwave acoustic methods[4] in silica based glasses. Both the magnitude and the temperature dependence of the optical and acoustic dephasing rates are comparable below 1K. A low temperature model (<10K) of dephasing has been developed[5] based on these similarities, which invokes elastic coupling between the ion and the tunneling systems. This model assumes spectral diffusion among the tunneling systems to play a key role in the optical dephasing at these temperatures. A quantitative analysis of the echo decay for arbitrary multipolar interactions indicates that an elastic dipole-dipole coupling is consistent with the observed exponential decay and $T^{1.3}$ dependence in the long-time regime[5]. Although this theory can explain the anomalous T^2 behavior at higher temperatures if higher order interactions are invoked, the contribution of tunneling systems to the linewidth in this regime is too weak to account for the observed linewidths. This is consistent with the suggested crossover and implicates other dephasing processes[6] as the dominant contributor to T^2 linewidths.

With these very low temperature photon echo results and the resemblance between the optical and acoustic dephasing rates we have provided the first quantitative evaluation of the role of tunneling systems in optical dephasing in an inorganic glass at low temperatures.

1. P.M. Selzer, D.L. Huber, D.S. Hamilton, W.M. Yen, and M.J. Weber, Phys. Rev. Lett. 36, 813(1976)

2. J. Hegarty, M.M. Broer, B. Golding, J.R. Simpson, and J.B. MacChesney, Phys. Rev. Lett. *51*, 2033(1983)

3. J.M. Pellegrino, W.M. Yen, and M.J. Weber, J. Appl. Phys. *51*, 6332(1980)

4. B. Golding and J.E. Graebner, Phys. Rev. Lett. *37*, 852(1976), and in *Amorphous Solids*, edited by W.A. Phillips (Springer-Verlag, Berlin, 1981), Chap. 7

5. D.L. Huber, M.M. Broer, B. Golding, (to be published).

6. D.L. Huber, J. Non-Cryst. Solids, *51*, 241(1982).

WF2, WF3, WF4 and WF5

WF2 Optical Dephasing of Impurities in Amorphous Organic Solids down to 0.3 K, Silvia Volker, H. P. H. Thijssen, and R. van den Berg, University of Leiden, The Netherlands. See WE14 for summary.

WF3 Facile Nonphotochemical Hole Burning and Filling of Laser Dyes and Rare-Earth Ions in Deuteroxy and Hydroxy Polymers, Bryan L. Fearey, Thomas P. Carter, and Gerald J. Small, Ames Laboratory-U.S. DOE and Iowa State University. See WE22 for summary.

WF4 Thermal Zero-Phonon Line Widths of Impurities in Crystals: Theory and Experiment, D. Hsu and J. L. Skinner, Columbia University. See WE1 for summary.

WF5 Phonon Processes in Disordered Systems Probed by Spectral Hole Burning and Refilling of Dyes, U. Bogner, G. Roska, and P. Schatz, Universitat Regensburg, FRG, and Electric-Field-Induced Changes of Persistent Spectral Holes in Amorphous Solids and Their Applications, U. Bogner, P. Schatz, K. Beck, and Max Maier, Universitat Regensburg, FRG. See WE12 and WE13 for summaries.

WG1, WG2, WG3 and WG4

WG1 Cr^{3+}-Induced Nucleation and Luminescence in Silicate Glasses, B.Champagnon, F. Durville, E. Duval, and J. Loulon, Universite Lyon I, France. See WD31 for summary.

WG2 Photoluminescence in Amorphous Alloys: a-SiO_x:H, a-SiN_x:H, a-Si_xC_{1-x}:H, R. Carius, K. Jahn, W. Siebert, and H. Fuhs, University of Marburg, FRG. See WD36 for summary.

WG3 Measurement of Exciton Absorption Spectrum in KI Using New Method, H. Nishimura, Osaka City University, Japan. See MB10 for summary.

WG4 Resonant Light Scattering and Hot Luminescence at the Indirect Gap in SiI_3, T. Karasawa, T. Komatsu, and Y. Kaifu, Osaka City University, Japan, and Spectral Structure of Secondary Emission in Indirect Exciton-Phonon System, T. Iida and M. Sakai, Osaka City University, Japan. See MB43 and MB44 for summaries.

Theory of the Nonlinear Optical Properties of Semiconductors

Hartmut Haug
Institut f. Theoret. Physik, Universität
Robert-Mayer Str 8, D-6000 Frankfurt, F.R. Germany

The optical spectra of laser-excited semiconductors change with varying laser intensity. Close to exciton or biexciton resonances these optical nonlinearities are, e.g., large enough to obtain optical bistability. The cause for these large nonlinearities are many-body effects in the system of the electron-hole pair excitation. The use of nonequilibrium Green's functions, or if a quasi-equilibrium exists of thermal Green's functions, makes it possible to take radiative and Coulomb interactions consistently into account.

The screening of the Coulomb forces by the many excited electron-hole pairs is the most important physical process in highly excited semiconductors. We will discuss why the screening due to excitons is less efficient than that of free carriers. Taking into account only the latter contribution, we calculate how the spectra change with increasing laser intensity from a series of sharp excitonic resonances to the relatively broad bands of an electron-hole plasma. These results are obtained by solving the integral equation for the electron-hole polarization function numerically by matrix inversion. Results will be presented and compared with corresponding experiments for Ge, GaAs and InSb.

Triplet Exciton Recombination in Amorphous and Crystalline Semiconductors

B. C. Cavenett

Department of Physics, University of Hull, Hull, U.K.

The occurrence of the excited triplet state in crystalline materials has long been associated with molecular and related crystals which have been investigated by a variety of techniques for ~20 years (e.g. see articles in Clarke (1)) whereas in semiconducting crystalline materials the excited or exciton state has generally been associated with electron-hole pairs where the orbital character of the holes (J = 3/2) is reflected in the electronic structure. However, in recent years a combination of detailed luminescence spectroscopy combined with optically detected magnetic resonance (ODMR) studies have demonstrated that in the case of defect complexes which place the host lattice into compression, the orbital angular momentum of a bound hole is quenched; bound exciton formation is then between two $S = {}^{1}/_{2}$ particles. The resulting singlet and triplet spectra observed in many materials, but particularly GaP, show that donor and acceptors aggregate to give a wide variety of isoelectronic or isovalent centres and recombination via these centres is the dominant radiative process. (2)

In the case of the amorphous semiconductors the situation is remarkably similar, particularly in the cases of the group V and chalogenide glasses. Although it was generally thought that exciton recombination in these materials would be non-radiative, optically detected magnetic resonance measurements have shown conclusively the existence of radiative singlet and triplet excitons bound at axial isoelectronic centres which have been assumed to be intrinsic structural defects (3). These results have been shown to be consistent with lifetime and time resolved luminescence measurements.

In crystalline semiconductors detailed symmetry information of the defects can be determined because angular dependence measurements of the magnetic resonance spectra is possible, but in the amorphous semiconductors the magnetic resonance spectra of these triplets are very broad, because of the random orientation of the defect axes with respect to the direction of the applied magnetic field. However, the application of zero-field optically detected magnetic resonance (ZF-ODMR) techniques enables the energy splittings in zero magnetic field to be determined irrespective of whether the material is crystalline or amorphous.

This paper will review the origins of the triplet state in semiconductors and give examples of defect spectra in both crystalline and amorphous materials. The first zero-field optically detected resonance measurements in semiconductors will be discussed.(4)

References

1. Clarke, R.H. Ed. "Triplet State ODMR Spectroscopy", Wiley, New York, 1982

2. Gislason, H.P., Monemar, B., Dean, P.J., Herbert, D.C., Depinna, S.P., Cavenett, B.C. and Killoran, N. Phys. Rev. B26, 827 (1982)

3. Cavenett, B.C., J. Non-Cryst. Solids 59/60, 125 (1983)

4. Salib, E.H. and Cavenett, B.C., J. Phys. C. 17, L251 (1984).

Statistical Distribution of Phonons Emitted in Multiphonon Transitions

Kun Huang
Institute of Semiconductors, Academia Sinica
Beijing, China

The multiphonon transition theory as formulated by Kubo and Toyozawa provides a general framework for dealing with arbitrary phonon spectra. However, in dealing with concrete problems, single frequency models are widely used. To overcome the inadequacy of over-simplified models and to make theoretical calculations practically feasible, the concept of multi-frequency models is developed. The theoretical basis for the use of the method of steepest descent with multi-frequency models is discussed. It is shown that the use of the contribution of the principal saddle point alone just serves to smooth out artificial singular structures introduced by the model.

Traditionally, the theory of multiphonon transitions has focussed on the calculation of the transition probability. Through the use of the multi-frequency models, it has been found that the phonons emitted in a multiphonon transition obey a simple statistical distribution law with respect to phonon energy. Moreover, the principal saddle point in the steepest descent method corresponds directly to the statistical phonon distribution.

By theoretical arguments and direct computation,

it has been shown that the phonon distribution shifts systematically with various physical parameters, such as electronic transition energy, electron-lattice coupling etc. This has a profound effect on the multiphonon transition behaviours and serves to show up the inadequacy of single frequency models in an illuminating way.

Laser Study of No-phonon Lines in the Inhomogeneously Broadened Spectra via Photochemical Hole Burning.

Karl K. Rebane

Institute of Physics, Estonian SSR Academy of Sciences,

2o24oo Tartu, Riia Str. 142, USSR

1. When the inhomogeneous broadening (IHB) is eliminated, the no-phonon lines (NPL) in optical spectra (absorption, luminescence, hot luminescence, light-scattering, excitation of luminescence) actually become the optical analogues of the Mössbauer γ -resonance lines. The basic reason of this analogue lies in the symmetry of the Hamiltonian of the harmonic oscillator in coordinates and momenta [1,2].

2. NPL-s, especially the purely electronic line (PEL), of a wide variety on molecular and atomic impurities in different matrices are at low temperatures of very high peak intensity. In time-dependent spectra it is possible to get the NPL-s narrower than the corresponding life-time determined natural linewidths in conventional spectra.

3. The photochemical hole burning (PHB) [3,4] is not only a method of high-resolution spectroscopy of matrice-isolated molecules but an effective way to perform frequency-selective photochemistry as well.

4. An inhomogeneously broadened band of a purely electronic transition actually is a quasicontinuum of very narrow and intense resonances - the PEL's. These unique properties of the PEL media (inhomogeneous spectral bandwidth - 1oo - 1ooo cm^{-1}; linewidth of PEL - $1o^{-3}$ - $1o^{-4}$ cm^{-1} (and less for forbidden transitions); the transition frequency to linewidth relation of PEL - $1o^{7}$ - $1o^{9}$) [2] can be utilized via PHB in two complementary ways.

5. It is possible to burn in a IHB band up to 1ooo-1oooo holes at different frequencies using narrow lines of continuous-wave lasers and create so frequency selective optical memories of high capacity. Some principal and practical limitations of those possible memories are discussed.

6. Excitation of the PEL medium by a picosecond pulse creates a broad (2-5 cm^{-1}) hole whose frequency distribution represents the intensities of the harmonics in the pulse. The information about the phases of the Fourier-components of the pulse spectrum is lost. In the case of two consequent pulses separated be time interval shorter than the phase relaxation time of the excited electronic state of the impurity system, the phase relations between the pulses will be fixed as well by the burnt in picture of the spectral hole. Very high relative intensity ($\geq$ 3o%) coherent optical free-decay signals can be stimulated by weak picosecond excitation of these persistent spectral holograms [5]. Some other experiments related to photochemical time-domain holography of weak picosecond pulses via PEL media are discussed.

1. J.D.Trifonov, Dokladi Akademii nauk SSSR, 147, 826, 1962 (in Russian).

2. K.K.Rebane, Impurity Spectra of Solids, Plenum Press, New York, 197o.

3. A.A.Gorokhovskij,R.K.Kaarli,L.A.Rebane, JETP Letters,2o, 474, 1974.

4. B.M.Kharlamov,R.I.Personov,L.A.Bykovskaya, Opt. Commun., 12, 191, 1974.

5. A.Rebane, R.Kaarli, P.Saari, A.Anijalg, K.Timpmann, Opt. Commun.,47, 73, 1983; A.Rebane, R.Kaarli, Chem.Phys.Letters 1o1, 317, 1983.

The Role of Nonequilibrium Relaxation Phonons in the Luminescence of Activated Crystals

A.A.Kaplyanskii

A.F.Ioffe Physicotechnical Institute, Academy of Sciences of the USSR, Leningrad 194021, USSR

Optical excitation of activated crystals is usually accompanied by the creation of "relaxation" phonons in the lattice (the "Stokes losses"). At low temperatures when the equilibrium phonon occupancies are small the nonequilibrium phonons thus formed may affect markedly the processes involving excited impurity ions and their luminescence characteristics. Investigation of luminescence effects associated with the nonequilibrium phonons provides valuable information on the dynamic processes in the excited state, on the various mechanisms of phonon interaction with impurity ions, as well as on the characteristics of the phonons proper, primarily of the terahertz range acoustic phonons.

The present paper reviews the following topics:

1. The relaxation phonon frequency spectrum and various mechanisms of phonon scattering resulting in a temporal phonon imprisonment in the optically pumped volume of the crystal.

2. The enhancement of luminescence from the upper excited electron states as a major effect of the presence of nonequilibrium phonons in the pumped volume (the phonon bottleneck effect). The relation of the luminescence intensity and kine-

tics with the particular mechanisms of phonon imprisonment, with the characteristics of the electron-phonon interaction and with the actual experimental conditions (optical pumping level, pumplight wavelength and polarization, dimension and shape of the pumped volume, the concentration of the luminescence centers and of other impurities and defects in the lattice, the presence of external fields).

3. Specific features of the luminescence from the upper states in the case of resonant interaction of nonequilibrium phonons with a Stark-splitted electronic excited state (as examplified by multiple resonant scattering of the 29 cm^{-1} phonons in excited ruby). The nonlinear dependence of luminescence on the pumping level, manifestation of the various mechanisms of elastic and inelastic phonon scattering from the electronic states of impurity ions.

4. Observation of an efficient conversion of the Stokes energy losses into a monochromatic phonon resonant mode through successive nonresonant Raman scattering of the high frequency relaxation phonons from a system of Stark-splitted electronic states of impurity ions [1].

5. The effect of nonequilibrium phonons on the energy transfer and the inhomogeneously broadened luminescence spectra.

6. Determination of the anharmonic lifetime of the terahertz acoustic phonons from luminescence studies.

---

[1] S.A.Basoon, A.A.Kaplyanskii, and V.L.Shekhtman. Fiz. Tverd. Tela 24, 1913, 1982.

ThA4 and ThA5

ThA4 Spectral Narrowing of Excitation Spectra in n-Photon Upconversion Processes by Energy Transfers, F. Auzel, CNET, France. See WE5 for summary.

ThA5 Optically Detected Stimulated Spin Echo as a Probe of Triplet Energy Migration in Mixed Molecular Crystals, Henry C. Brenner and Stephen A. Janes, New York University. See WE4 for summary.

ThB1, ThB2 and ThB3

ThB1 Picosecond Luminescence Spectroscopy of Electron-Hole Plasma in GaAs/AlAs Quantum-Well Structure, S. Tanaka, M. Kumo, A. Yamamoto, A. Watanabe, and H. Kobayashi, Tottori University, Japan; S. Mizuta and H. Mukimoto, Tokyo Institute of Technology, Japan, and T. Saito, Okayama College of Science, Japan. See FE19 for summary.

ThB2 Photoluminescence Studies of Ga(As,P) Strained-Layer Superlattices, P. L. Gourley, Sandia National Laboratories. See FE18 for summary.

ThB3 Reabsorption Kinetics of Free- and Bound-Exciton Luminescence in High-Purity n-GaAs, K. Aoki and K. Yamamoto, Kobe University, Japan. See FE6 for summary.

Suppression of the Free-to-Bound Luminescence by EL2

W.Ossau, Phys. Inst. der Univ. Würzburg, D-8700 Würzburg, Rontgenring 8.

High purity nominally undoped and Sn-doped liquid phase epitaxial layers irradiated with 2 MeV electrons have been characterized by low temperature photoluminescence measurements. Analysis of the line-shape and the peak shift of the free-to-bound transition in magnetic fields up to 10 T allows an unambiguous identification of the impurities involved /1/. Care was taken to use identical excitation conditions for the measurements of unirradiated and irradiated samples during the annealing stages.

In undoped, unirradiated samples Si is the major residual acceptor. Small amounts of Mg and C (based on the relative peak heights) can be observed too. The conduction band to acceptor luminescence of the irradiated and annealed samples has changed completely. At annealing temperatures less than 400 ^{o}C carbon is the major acceptor. With further increase of annealing temperature the (e,C^{o})-transition becomes undetectible and the Mg acceptor dominates the free-to-bound luminescence.

After electron irradiation and annealing it is evident from the experimental results that acceptors substitute for arsen sites (C,Si,Ge,Sn) are suppressed compared to those occupying gallium sites as Mg or Be.

The change from dominating group IV to group II-impurities acting as acceptors can't be explained by outdiffusion, because the luminescence of the unirradiated samples does not change, applying the same heat treatment.

It is supposed that during annealing acceptors on arsen sites capture antisite As_{Ga} defects (known as EL2) or vice versa. This arsen antisite is a double donor and therefore passivates the nearest-neighbour acceptor. Passivation of two donor levels is observed in GaAs by interaction of hydrogen with the unsaturated bonds of the As_{Ga} defect /2/. In this work

the formation of a complex As_{Ga}-IV_{As} would passivate the acceptor, that means removing the electronic level and forming a "single donor".

It is easy to see that this nearest-neighbour passivation is much more effective for group IV than for second-nearest-neighbour group II-elements beeing responsible for acceptors in III/V compounds.

The postulated mechanism will also explain recent measurements on molecular beam epitaxial GaAs /3/. The authors found a strong dependence of the carbon contamination on the arsen sources applied during crystal growth. It seems that the activation or incorporation of carbon is reduced by the use of monomeric arsen as well as by increasing the As/Ga ratio. Both conditions will advance the formation As_{Ga} and therefore result in an enhanced passivation of native acceptors.

In this study no luminescence line correlated to the complex As_{Ga}-IV_{As} has been found up to now. However, a double donor-acceptor complex is used to explain sharp line luminescence /4/. Additional superhyperfine structure EPR-measurements on GaAs indicates that this kind of complex exists frequently/5/.

1.D.J.Ashen, P.J.Dean, D.T.J.Hurle, J.B.Mullin, A.M.White and P.D.Greene, Phys.Chem.Solids,**36**,1041 (1975)

2.J.Lagowski, M.Kaminska, J.M.Parsey,JR, H.C.Gatos and M.Lichtensteiger, Appl.Phys.Lett.**41**,1079 (1982)

3.B.J.Skromme, G.E.Stillman,A.R.Calawa and G.M. Metze, Appl.Phys.Lett. **44**, 240 (1984)

4.D.C.Reynolds,R.J.Almassy, C.W.Litton, S.B.Nam and G.L.McCoy, J.Appl.Phys. **49**,5336 (1978)

5.N.K.Goswani,R.C.Newmanand J.E.Whitehouse, Solid State Commun.**40**,473 (1981)

Mechanism of Photoluminescence in Hydrogenated and Chlorinated Amorphous Silicon Prepared by Glow Discharge

Shawqi Al - Dallal

University College of Bahrain - Bahrain/

Centre National de Recherche Scientifique - France

Summary:

Chlorinated and hydrogenated amorphous silicon films have been prepared by glow discharge at various R. F. power. Chlorine content in our samples are measured by electron microprobe analysis. Typical concentration of chlorine is 6%. The hydrogen content is 5 to 10% as calculated by integrating the $640cm^{-1}$ wagging band. At low powers (5 watts), the infra-red vibrational spectra show the appearance of a chlorine induced band at $545cm^{-1}$ and several hydrogen induced bands at $640cm^{-1}$, $740cm^{-1}$, $840cm^{-1}$, $890cm^{-1}$, $2000cm^{-1}$ and $2100cm^{-1}$.

We have measured the photoluminescence spectra as a function of temperature and plasma power. The main photoluminescence band is situated at 1.3 eV and shifts toward low energies as the temperature is increased from 10 to 130°K. The integrated intensity of the photoluminescence band shows a saturation for temperatures lower than 50°K. Above 50°K, unlike a-SiH[1], our material exhibits a first quenching region in the 65-72° range followed by a sharp rise. Above 80°K the integrated intensity decreases with an activation energy of 100meV. As the plasma power increases the first quenching region disappears progressively. On the other hand, when the sample is annealed, the I = f(T) anomaly becomes more pronounced. From these observations we attributed the existance of this anomaly in a-Si H Cl to a chlorine induced density of states in the band gap. Other proof on the origin of this anomaly comes from the correlation between the electrical and vibrational

properties of a-Si H Cl. Using this approach, we have shown that, as the plasma power increases, the reduction of $SiCl_2$ species ($545cm^{-1}$ band) is accompanied by a change in the transport mechanism, from hopping in localized band gap states, to conduction in the extended states[2] . We have measured the position of the maximum of the photoluminescence band, E_{max}, and the width at half height as a function of temperature. In our samples, E_{max}, shifts toward low energies as the temperature increases from 10 to 130°K. Above 130°K, the position of E_{max} remains constant. The width at half height decreases from 250 to 200meV as the temperature increases from 10 to 150°K.

To account for these observations we proposed a model based on band gap fluctuations [3]. According to this model, geminated carriers can first thermalize and then diffuse to lower energy states and this process is temperature dependent. The geminated pair can then recombine by tunneling. At relatively high temperatures (above 130°K), the diffusion of pairs will result in their disassociation which explains the E_{max} = f(T) behaviour above this temperature. We have shown also that the band fluctuation model can account for the difference in energy between the emission and absorption bands.

References:

[1] M. A. Paesler and W. Paul, Phil. Mag. B, 41, 393(1980)

[2] S. Al-Dallal, J. Chevallier, S. Kalem and J. Bourneix, J. de Phys. Col. C9, 43, 323(1982)

[3] D. J. Dunstan and F. Boulitrop, J. de Phys. Col. C4, 42, 331(1981)

LUMINESCENCE RECOMBINATION IN MAGNETRON SPUTTERED a-Si:H

A J Rhodes, P K Bhat, T M Searle and I G Austin

Department of Physics, University of Sheffield, Sheffield S3 7RH, UK

Recent work has shown that a-Si:H films prepared by magnetron sputtering (MSP) have a defect density much lower than that produced by Rf sputtering, because of the decrease in damage from electron bombardment. Photoluminescence (PL) studies on a-Si:H show a broad peak near 1.3 - 1.5 eV due to tail state recombination and a peak near 0.9 eV which is generally ascribed to a dangling bond defect. The 0.9 eV band has been observed in a wide range of a-Si films when excited with subgap light, but comparatively little has been reported on MSP films, especially the effects of doping.

We report here a detailed study of the 0.9 eV luminescence band and its temperature dependence, intensity and excitation energy dependence in doped and undoped MSP a-Si:H. Measurements of the temperature dependence of the 0.9 eV PL decay are presented for the first time. The broad distribution of lifetimes indicates recombination between distant pairs.

We have also investigated the effects of doping and oxygen incorporation in MSP films. Low concentrations of phosphorous are found to enhance the 0.9 eV band as with glow discharge a-Si:H. Small quantities of oxygen have no effect on PL excited with a photon energy > 1.8 eV, but as the excitation energy is reduced below 1.65 eV, a new emission band at 1.1 eV is observed. This is the first report of selective excitation of an oxygen impurity-related transition in a-Si:H. Since the 0.9 eV emission can be selectively excited by subgap photons, like the oxygen defect emission, we suggest that the 0.9 eV band may also be related to an extrinsic impurity.

Photoluminescence Study of Nitrogen Implanted Silicon

H. Ch. Alt, L. Tapfer, Max-Planck-Institut für Festkörperforschung, Heisenbergstraße 1, D-7000 Stuttgart 80, F.R.G.

Up to now the properties of nitrogen as an impurity in silicon, e.g. the low electrical activity and the strong interaction with dislocations, are hardly understood. Recently Tajima et al. (1) reported a luminescence line at 1.1223 eV which appears only in nitrogen doped samples. Sauer et al. (2) showed that this line is identical to the A transition of the A, B, C system. This system is due to an exciton localized at an isoelectronic defect of axial symmetry around <111> (C_{3v}) the chemical nature of which is still unknown.

We systematically investigated the photoluminescence from silicon implanted with 100 keV N^+ ions at doses of 10^{10} to 10^{16} cm^{-2}. After thermal annealing (30 min at 700 °C) we observed for the first time A line emission in N implanted silicon (Fig. 1). The maximum intensity appears after implantation at a dose of $5 \cdot 10^{14}$ cm^{-2} (Fig. 2). Below this value the intensity increases with the dose but data show a scatter too large to establish a definite power law. The drastic decrease at doses $>5 \cdot 10^{14}$ cm^{-2} is attributed to precipitation of nitrogen in non-radiative nitrogen-silicon-complexes which is substantiated by the analysis of x-ray rocking curves. Spreading resistance measurements give a linear increase of the average carrier density of the implanted layer with the dose. From that we conclude that the A line is not correlated with electrically active nitrogen.

The dependence on annealing time and temperature was studied in detail at a fixed implantation dose of $5 \cdot 10^{14}$ cm^{-2} (Fig. 3). At 600 °C the A line appears only after long annealing times ($>2^h$). The maximum is found after 10 min at 700 °C followed by a slow

decay. At $T \gtrsim 800$ °C the center decays rapidly. We compare this behaviour with measurements of Astakhov et al. (3). They determined the lifetime τ of minority carriers in diodes produced by nitrogen implantation of p-type silicon dependent on the annealing conditions. At 700 °C an abrupt decrease of τ and a strong increase of the reverse current are found. They conclude that effective generation-recombination centers are formed by the ejection of nitrogen from substitutional positions and by the formation of vacancy-interstitial nitrogen complexes. The energy of the ejected nitrogen atoms is not sufficient for the complete break down of the bond with the remaining vacancy. At $T \gtrsim 800$ °C the nitrogen gets completely loose and forms N_2 molecules or precipitates as Si_3N_4 complexes together with other nitrogen atoms. This model is a first indication of a correlation of the A, B, C exciton with vacancy-interstitial nitrogen complexes in silicon.

1 M. Tajima, T. Masui, T. Abe and T. Nozaki, Jpn. J. Appl. Phys. 20, L 423 (1981)

2 R. Sauer, J. Weber and W. Zulehner, Appl. Phys. Lett. 44,440(1984)

3 V. P. Astakhov, T. B. Karashev, L. Ya. Konyushenko and R. M. Aranovich, in: Physical Foundations of the Ion-Beam Doping, Ed. P. V. Pavlov, Gorkii State Univ., Gorkii 1972

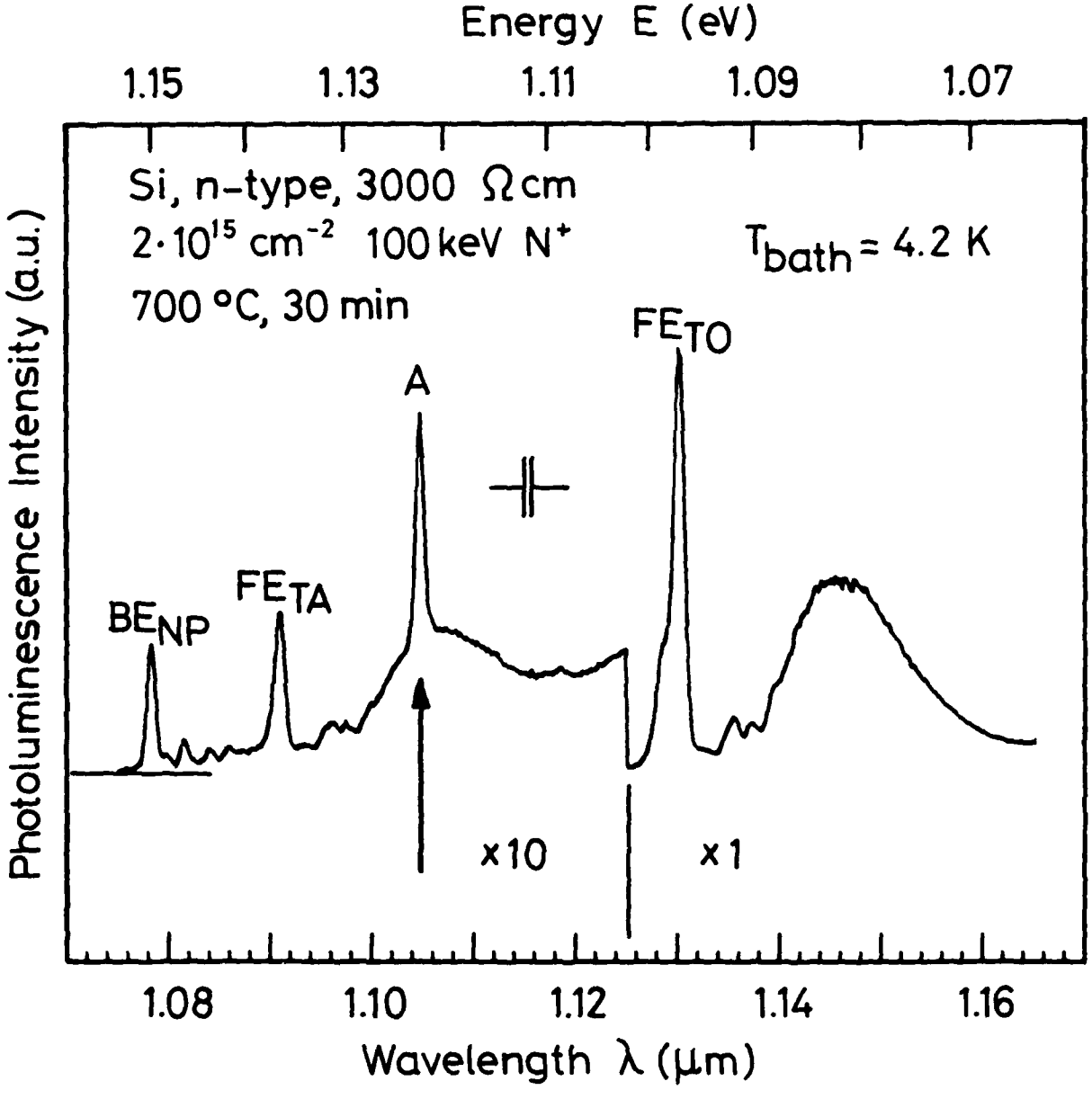

Fig. 1. Near band-edge photoluminescence spectrum of nitrogen implanted silicon.

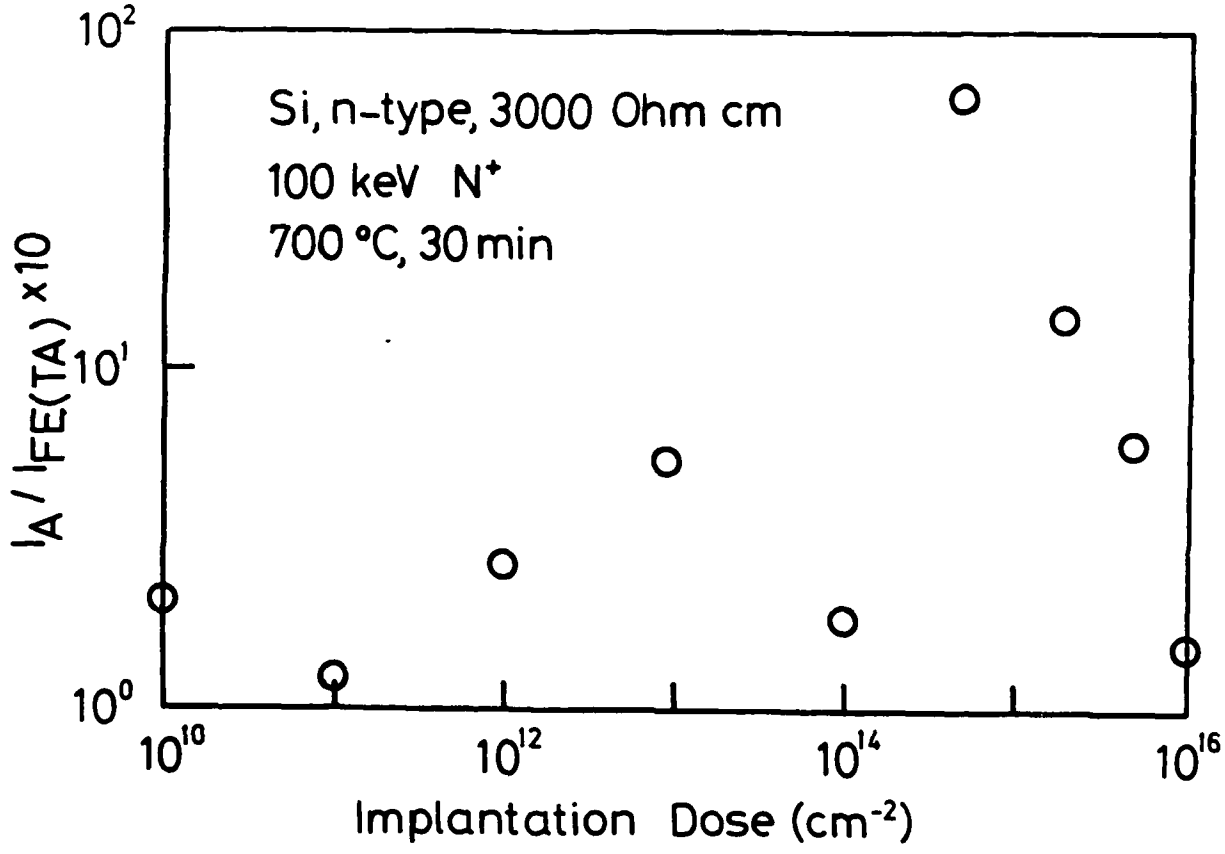

Fig. 2. Dependence of the intensity ratio $I_A/I_{FE(TA)}$ on the implantation dose.

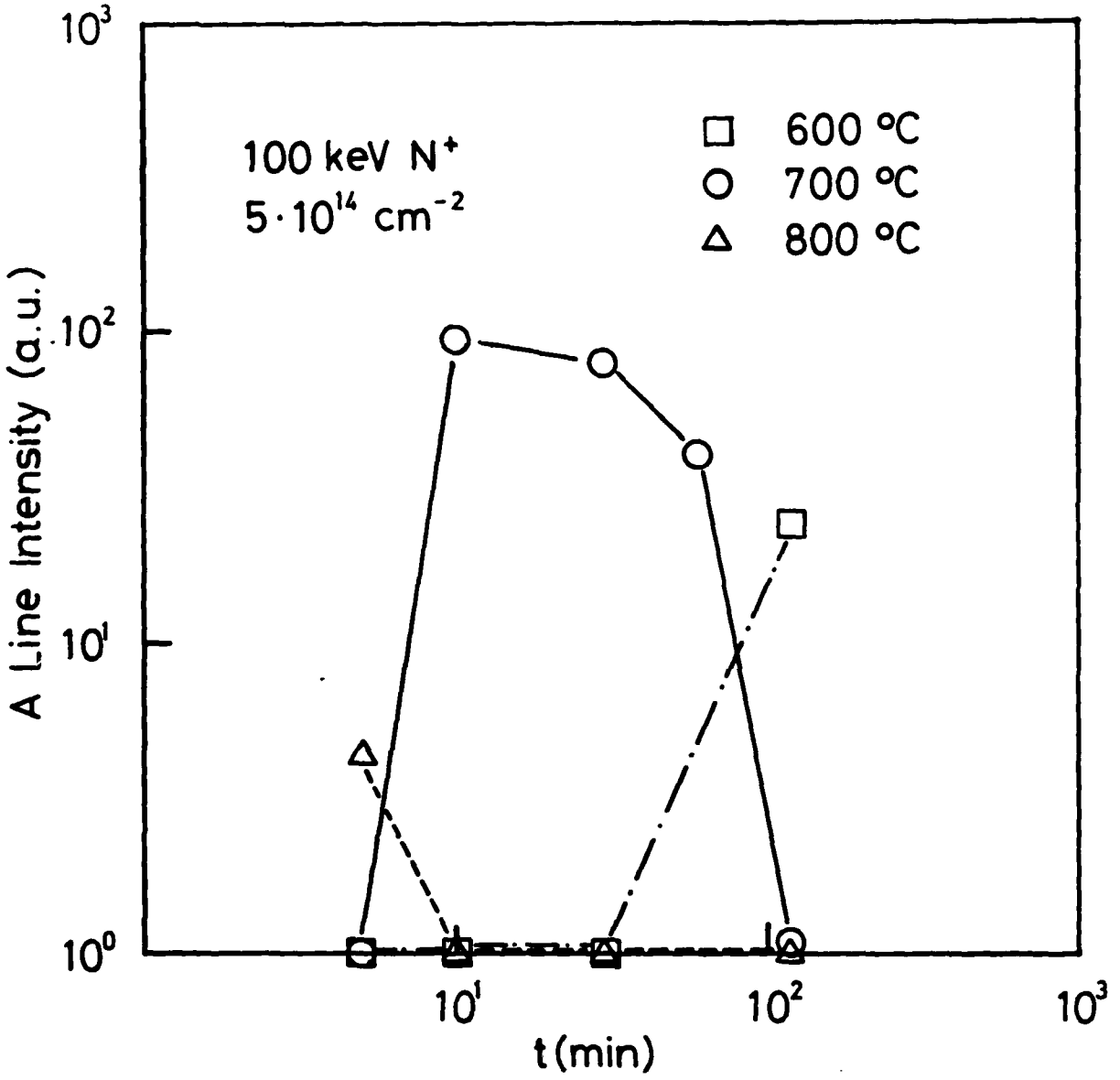

Fig. 3. A line intensity as a function of annealing time and temperature.

Luminescence and Related Optical Properties
of Iron Ions in II-VI Compounds

G. Roussos, H.-J. Schulz, M. Thiede

Fritz-Haber-Institut der Max-Planck-Gesellschaft
Faradayweg 4-6, D-1000 Berlin 33

Optical absorption and emission spectra of Fe centers have been studied at low temperatures in chalcogenides of Zn and Cd. For comparison, emission spectra have been recorded with semi-insulating in InP:Fe substrate material.

The internal transitions $^5T_2(D) \rightleftarrows {}^5E(D)$ of Fe^{2+} are now well established for cubic ZnS. High-resolution emission spectra are obtained which are free from self-absorption (Fig.). In transmission spectra of ZnS and ZnSe, "hot" transitions from the spin-orbit components of ^5E are studied for different doping levels in the temperature range up to 20K and are proved to coincide with the no-phonon lines in emission at 4K. In stacking-faulted ZnS, three types of axially distorted centers with main transitions at 2830,2945, and 2947 cm^{-1} are discerned in addition to the cubic center ($\bar{\nu}$ = 2950 cm^{-1}).

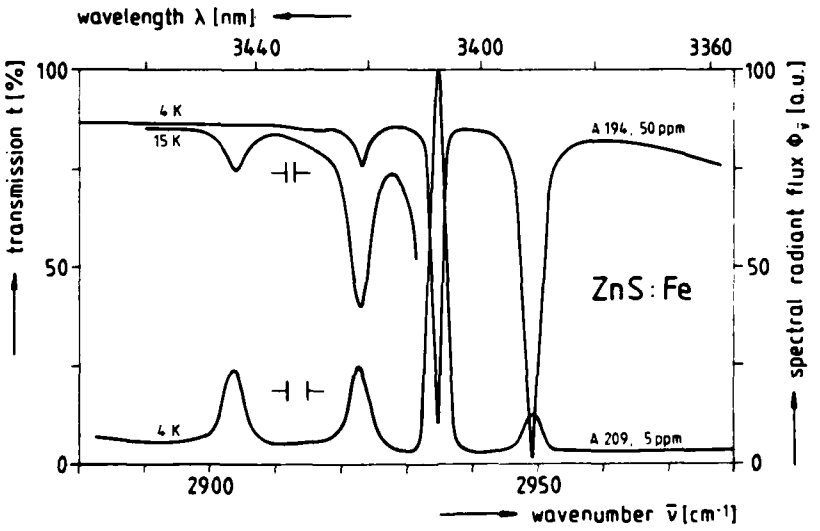

The four no-phonon transitions $^5T_2(D) \rightleftarrows {}^5E(D)$ of cubic $ZnS:Fe^{2+}$ in transmission and emission. Excitation: $16500 \leq \bar{\nu} \leq 28500$ cm^{-1}

For CdS:Fe, the absorption is dominated by a doublet at $\bar{\nu}$ = 2558/2564 cm^{-1} which represents the C_{3v} splitting of the excited state in the

Γ_5-$^5T_2(d) \rightarrow \Gamma_1$-$^5E(D)$ transition. The $^5T_2(D) \rightarrow {}^5E(D)$ emission had not been reported with CdS before. High-resolution emission spectra exhibit transitions to the Γ_5, Γ_3, Γ_4, and Γ_1 2nd-order spin-orbit components of the ^5E ground state. Moreover, the trigonal splitting $\Delta\bar{\nu} \approx 4$ cm^{-1} of the Γ_5 and Γ_4 ground state components is resolved. The resulting sublevels are identified by polarization studies and consideration of the electric-dipole selection rules for the irreducible representations of C_{3v}. The internal transitions of CdSe:Fe [1] do not form the quartet pattern familiar from other hosts. Resonant phonon interaction could account for an apparent quenching of one of the expected dipole-allowed transitions.

A luminescence of ZnSe:Fe in the 11000 cm^{-1} range had been attributed [2] to the $^3T_1(H) \rightarrow {}^5E(D)$ transitions of Fe^{2+}, based on analogy to ZnS [3]. The separation of the zero-phonon lines at 11128 and 11154 cm^{-1} had been related to that of the Γ_5 and Γ_4 components in the ground state, as determined from previous absorption data [4]. Since the $^5T_2(D) \rightleftarrows {}^5E(D)$ spectra now yield 31 cm^{-1} for this difference, the former interpretation [2,3] needs to be reconsidered although the conclusions of [2] have recently been confirmed in an interpretation of ODMR data [5]. With ZnS:Fe, however, the respective separations agree well. A comparison of the vibronic satellites in the $^5T_2(D) \rightarrow {}^5E(D)$ and the $^3T_1(H) \rightarrow {}^5E(D)$ emissions indicates the concurrent coupling of an optical mode while acoustic modes interact additionally in $^3T_1(H) \rightarrow {}^5E(D)$.

[1] D. Buhmann, H.-J. Schulz, M. Thiede: Phys. Rev. B24, 6221 (1981)

[2] A. Karipidou, H. Nelkowski, G. Roussos: J. Crystal Growth 59, 307 (1982)

[3] M. Skowronski, Z. Liro: J. Lumin. 24/25, 253 (1981)

[4] J.M. Baranowski, J.W. Allen, G.L. Pearson: Phys. Rev. 160, 627 (1967)

[5] K.P. O'Donnell, K.M. Lee, G.D. Watkins: J. Phys. C: 16 L723 (1983)

On the Nature of the CdS: In,Cd Film Edge Emission Bands

N.A.Vlasenko and Z.L.Denisova

Institute of Semiconductors, Academy of Sciences of the Ukrainian SSR, Kiev, U.S.S.R.

Edge emission is known to be observed in donor-doped CdS /1-3/. The question that remains is the nature of its individual bands, especially in emission spectra of films. In this paper the edge photoluminescence (PL) and electroluminescence (EL) of vacuum-deposited low-resistivity (10-10^{-1} Ohm·cm) CdS:In, Cd films have been studied over the range 4.2 to 300 K. The films, 1-3μthick, were deposited onto glass, mica or molibdenum substrates by the methods described in /3/. The MISM structures of Au-In_2O_3-CdS-In_2O_3(Mo) were used in EL experiments.

At T < 77 K the well-known 514 nm emission band dominates in spectra of undoped films. Doping with In results in enhancing of its long-wavelength series mainly. New bands appear in the range of 485-520 nm when the CdS:In films were doped with Cd (Fig.a,b). The activation energy E_T of temperature quenching for these bands and the energy separation Δ between their maxima and the free exciton emission band A at 4.2 K are listed in the Table (here and below the $h\nu_A$ values were taken from the absorbtion spectra of the films and from /4/. As the temperature is inc-

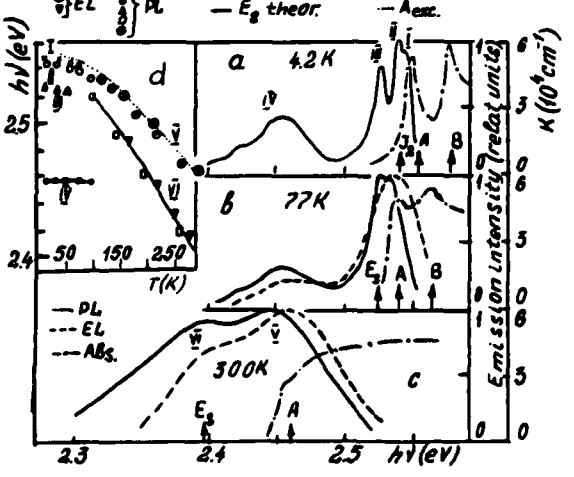

reased the bands 1-III shift just like the A band, but the position of the band IV together with its first and second LO phonon replicas does not shift (see Fig.d). The bands I and III are quenched at T<50 K whereas the IV one is observed up to 130 K. The temperature quenching of the band II is followed by the appearence of knees on its sides at 70-100 K, i.e. by the onset of two new bands. These bands become predominant at temperatures between 100 and 300 K. The maximum of one of them (the band V on Fig.c) is close to the A band. Its high energy side at $h\nu \geq E_g$ becomes more prominent with the temperature. The peak of the low-energy band VI coinsides in the whole temperature range with the calculated maximum of E_s band associated with exciton-electron interaction (Fig.d).

Table

Band	Δ, meV	E_r, meV
I	5	5
II	10	10
III	25	4
IV	500	50

The PL and EL spectra are identical at T=77-300 K (see Fig.).

The following conclusionswere made on the models of the observed emission bands. The bands I-III are attributed to excitons bound to neutral In donors, to neutral and ionized Cd_i donores, respectively. The band IV results from bound-to-bound transition in the D-A complex, where D is the Cd_i donor but the nature of acceptor is not yet established. The band $\bar{V}$ is due to the decay of free excitons and to band-to-band recombination at $h\nu \geq E_g$. . Finally, the band $\bar{V}\bar{I}$ may be associated with the exciton-electron interaction.

1. X.W.Fan. J.Woods, phys.stat.sol.(a) 70, 325 (1982).
2. W.P.Bleha, R.N.Peacock. J.Appl.Phys.41, 4992 (1970).
3. N.A.Vlasenko et al., Ukr.Fiz.Zh.20, 1492 (1975).
4. J.Voigt, F.Spiegelberg, phys.stat.sol. 30, 659(1968).

LUMINESCENCE EXCITATION MECHANISMS IN CdS FROM DEPENDENCE OF PHOTOLUMINESCENCE AND THERMOLUMINESCENCE ON PERSISTENT CONDUCTIVITY STORED CHARGE STATE

M. A. Reed[a] and A. Honig

Syracuse University, Syracuse, NY 13210

The details of the mechanisms for energizing donor-acceptor (D,A) pairs which result in recombination luminescence are still not completely understood. Recent work[1] on CdS has indicated that polaritons generated directly or as a consequence of incident photon excitation processes play the principal role in the D^+,A^- to D^o,A^o charging process, and that the luminescence emanates from the near-surface (~1 μm) regions. Experiments we report here indicate that polaritons also generate the stored charge associated with persistent conductivity phenomena[2] observed in high resistivity CdS. We show that generation of stored charge in the near-surface region (~1 μm), from which edge luminescence may be emitted[1], is a precondition for polariton-energized edge emission actually to occur. This requirement, taken together with the results of more detailed studies of the correlation between persistent conductivity and edge luminescence, supports the reported restriction of edge emission to near-surface regions[1] and also establishes the spatial extent of the stored charge region at saturation of persistent conductivity as a few hundred microns into the interior. It is further shown that the stored charge associated with persistent conductivity is the source of thermoluminescence, with the glow curves associated with the free-to-bound high energy series (HES) and with the bound-to-bound low energy series (LES) peaking respectively at

temperatures of 22K and 27K for a 10K/min temperature scan rate. These results, as well as those from isothermal thermoluminescence experiments, establish a low activation energy electron localized state as the source of persistent conductivity stored charge. We have associated this state with a large-lattice-relaxation[3] D^- center, based on the luminescence as well as other experiments. Edge luminescence produced by thermal release of these charges, residing at known spatial location (depending on the accumulated fraction of saturated stored charge), complements time-resolved excitation spectroscopic photoluminescence experiments in elucidating the impurity pair charging mechanisms. Luminescence spectral response to near infrared stimulation as a function of stored charge state is also presented and discussed.

(a) Permanent address: Central Research Laboratories, Texas Instruments, P.O. Box 225936, Dallas, TX 75265

1. A. Honig and M. Moroz, Solid St. Comm. 44, 148 (1982).

2. See, for example, M. K. Sheinkman and A. Ya. Shik, Fiz. Tekh. Poluprovodn. 10, 209 (1976) [Sov. Phys. Semicond. 10, 128 (1976)].

3. D. V. Lang, R. A. Logan and M. Jaros, Phys. Rev. B19, 1015 (1979).

Electron-Beam Annealing of Green Luminescence of Undoped and In-Doped CdS Crystals: S. Fujieda and R. Takahashi Department of Applied Physics, Faculty of Engineering, University of Tokyo, Bunkyo-ku, Tokyo 113, Japan.

It is well known that semi-insulating undoped CdS crystals often show green cathodoluminescence at room temperature. As reported previously, In-doped CdS layer and whisker prepared by vapor reaction show green photo- and cathodo-luminescence[1] which does not degrade for being left in air for many years. On one hand, In-doped CdS crystals prepared by Piper-Polich method also show the same luminescence[2] at room temperature, but the photoluminescence is lost in several months. These empirical facts on the degradation of luminescence of CdS were verified by an experiment of electron-beam annealing as follows.

The experiment was performed under a scanning electron microscope by means of cathodoluminescence mode. At first, the as-grown or the cleavage surface of the crystal parallel to the c-axis was imaged to get good focusing of the beam on the surface, and next the beam was stopped on any favorable point and held for a desired time with an increased current. After irradiation, the change in the luminescence at the irradiated point was pictured, and the quantity was measured by line mode for various accelerating voltages. Usually, the imaging current was 1×10^{-10}A, the irradiation voltage, current and time were 15kV, 1×10^{-9}A and 120s respectively. As a result of irradiation, a dark elliptic spot with a diffused margin appeared in the picture of the surface. The size of the spot strongly depended on the crystal: In-doped layer and whisker showed null, In-doped Piper-Polich-method crystals showed slight, and undoped crystals showed a remarkable change. This fact is attributed to Cd vacancies: In-doped whisker and layer are free from Cd vacancy[1], so Cd vacancy cannot move and hence cannot be newly produced during the irradiation, however, un-doped crystals include much Cd vacancies which facilitate the diffusion and the succeeding creation of Cd vacancies during the irradiation.

References 1) R. Takahashi: J. of Luminescence. 24/24 Part I (1981)67.

2) R. Takahashi: Jpn. J. Appl. Phys. 20(1981)L67.

Time Dependent Luminescence Spectroscopy of highly doped $Zn_{1-x}Mn_xS$ and $Cd_{1-x}Mn_xTe$

W. Busse, H.-E. Gumlich, M. Krause, H.-J. Moros, J. Schliwinski and D. Tschierse
Institut für Festkörperphysik (III) der Technischen Universität Berlin
Jebensstraße 1, D 1000 Berlin 12

The present interest in the luminescence of II-VI compounds doped by high amounts of Mn is due to the role which the Mn plays in thin film electroluminescence of ZnS:Mn and in the field of semimagnetic semiconductors such as $Cd_{1-x}Mn_xTe$. In both cases more than one emission band are observed when the amount of Mn passes a lower limit. For $Zn_{1-x}Mn_xS$ this limit is x=0.01 (1). Above this limit emission bands peaking at 1.97, 1.66 and 1.3 eV are registered in addition to the wellknown band peaking at 2.1 eV ($^4T_1(G) \rightarrow {}^6A_1(S)$). Recently Goede et al. tried to explain parts of these bands by octahedraly coordinated Mn^{2+} within local α-MnS domains (2).

In $Cd_{1-x}Mn_xTe$ the lower limit at x=0.3 of the appearance of a second emission band peaking at 2.0 in addition to the band at 1.2 eV is obviously determind by the opening of the forbidden gap with increasing x. Becker et al. and Vecchi et al. suggested models having luminescence centres which emit both bands (3).

From our measurements however we conclude that in both cases, in $Zn_{1-x}Mn_xS$ and in $Cd_{1-x}Mn_xTe$ different emission bands are due to different centers, but these centers are coupled by energy transfer.

One of the most important features in considering any possible model is the difference of the excitation spectra of both emission bands of $Cd_{1-x}Mn_xTe$. There is only a restricted spectral range of excitation near 2.3 eV where both bands can be excited by the same excitation wavelength. The width of this restricted range depends strongly on temperature. The time dependence of the 1.2 eV emission band is considerably influenced by the excitation wavelength. When the 1.2 eV emission band is excited within the restricted range near 2.3 eV, a built-up period was observed: The infrared emission

does not reach immediately its highest value after the laser pulse (10 ns) starts, but increases during about 10 µs. The built-up phenomenon depends on temperature: It can be registered at 80 K, it disappears at temperatures above 120 K.

Corresponding observations can be made with regard to the decay time of the infrared emission band. When the infrared emission band is excited within the intermediate range (near 2.3 eV) the decay time depends on temperature whereas by excitation within the maximum of the excitation band we obtain a temperature independend exponential decay (τ = 18 µs).

It should be noted that the maxima of the infrared emission band is slightly shifting when the excitation wavelength and temperature are varied.

Corresponding experiments have been made with $Zn_{1-x}Mn_xS(x>0.01)$. Built-up phenomena could be observed by registering the emission band peaking at 1.66 eV. Also in this case the built-up period depends on temperature.

For the three new emission bands of $Zn_{1-x}Mn_xS$ due to high concentrations the decay-time is different as it was recently observed in electroluminescence by Benoit et al. (4). The decay even within these bands depends on emission energy, too.

Our results are discussed within the framework of energy transfer between locally separated luminescence centers by hopping process as it was suggested by Gebhardt et al. (5).

1. H.-E. Gumlich, R. Moser, E. Neumann, phys.stat.sol. 24, K 13 (1967)
2. Dang Dinh Thong and O. Goede, phys.stat.sol(b) 120, K 145 (1983)
3. M.M. Moriwaki, R.Y. Tao, R.R. Galazka, W.M. Becker, physica 117B,467(1983)
   M.P. Vecchi, W. Giriat, L. Videla, Appl.Phys.Lett., 38, 99 (1981)
4. J. Benoit, P. Benalloul, A. Geoffroy, N. Balbo, C. Barthou, J.P. Denis, B. Blanzat, phys.stat.sol. (to be published)
5. E. Müller, W. Gebhardt, V. Gerhardt, phys.stat.sol. (b), 113, 209 (1982)

High Resolution Spectroscopy of Ni^{2+}- and M-centers in Polytypic ZnS Crystals

I. Broser, R. Broser, E. Birkicht

Fritz-Haber-Institut der Max-Planck-Gesellschaft

Faradayweg 4-6, D-1000 Berlin 33, Germany

A. Hoffmann

Institut für Festkörperphysik II, Technische Universität Berlin,

Straße des 17. Juni 112, D-1000 Berlin 12, Germany

Investigations of polytypic crystals have the advantage to allow a comparison of optical transitions in a center, which is situated in different symmetric environments. Cubic ZnS crystals, containing around 10^{-8} cm^{-3} nickel atoms, exhibit in the spectral region of about 810 nm several very narrow absorption lines, which can be attributed to crystal field transitions between the $^3T_1(F)$ and the $^3T_1(P)$ term of Ni^{2+} ions.[1] ZnS crystals (with stacking faults), consisting of a great number of polytypic regions, show besides the cubic lines additional structure. Unexpectedly, the linewidth is as narrow as in the crystallographic homogenious case.

In the figure the highly resolved absorption spectra of two crystals containing the nickel isotopes 62 and 58/64, respectively, are reproduced. Each spectrum consists of four zero phonon lines, three of them showing distinct polarization effects; their origin can thus be attributed to nickel atoms in an axial symmetric surrounding. Isotope splittings are clearly resolved, the energy difference being δ = 18 μeV per neutron. Magneto-optical and stress experiments give evidence that the different lines belong to the same kind of transitions, but the $^3T_1(P)$ term is split by axial fields of different strengths. As in other II-VI compounds [1] the energy structure of Ni^{2+} levels is strongly influenced by a dynamical Jahn-

Teller interaction and will be discussed using a theory developed for the interpretation of corresponding spectra in CdS[2].

For the first time luminescence transitions which coinside with the absorption lines could be observed. Their intensity ratios are, however, markedly different from that of the absorption lines. Very intense satellite lines could be detected shifted 22,1 meV to longer wavelengths. They can be explained by transitions to the first excited spin-orbit split level of the $^3T_1(F)$ term.

At longer wavelengths a series of luminescence lines has been found, which is explained as phonon satellites of the described zero-phonon Ni^{2+} lines. As their positions are identical to some lines not yet understood in the short wavelength part of the multi-line spectrum of the M-center[3], an up to now open problem could be solved. The rest of the M-center spectrum behaves quite differently: here, in polytypic crystals a new additional series of lines exists, which is in contrast to the pure cubic case, strongly polarized. They are interpreted as M-center transitions in a surrounding with axial symmetry.

1.) I. Broser, R. Germer et al. J. Lumin. 24/25, 225 (1981)

2.) B. Nestler, U. Scherz, J. Lumin 24/25, 229 (1981)

3.) I. Broser, R. Germer et al.; J. Phys. Chem. Solids 41, 101 (1980)

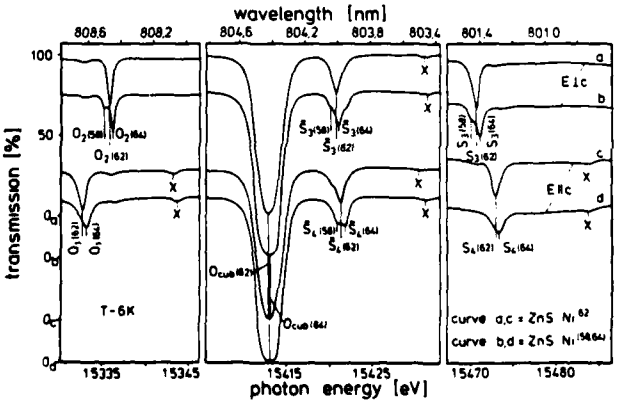

The $^3T_1(P) \rightarrow {}^3T_1(F)$ luminescence of ZnS:Ni^{2+} and other internal transitions of the $Ni^{2+}(3d^8)$ configuration

G. Roussos and H.-J. Schulz

Fritz-Haber-Institut der Max-Planck-Gesellschaft
Faradayweg 4-6, D-1000 Berlin 33

ZnS:Ni crystals exhibit at low temperatures a new emission [1] which is assigned to the transition $^3T_1(P) \rightarrow {}^3T_1(F)$ of the $Ni^{2+}_{Zn}(3d^8)$ ion, based on absorption data [2,3] and on preparation evidence. The structured emission spectrum observed in Ni-doped cubic crystals is superimposed on the tail of a broad Ni-related recombination band peaking at higher energy. A dip (c_1) coincides with the most prominent absorption line at $\bar{\nu}$ = 12438 cm^{-1} thus indicating self-absorption. The luminescence is dominated by a sharp peak C_4 at $\bar{\nu}$ = 12259 cm^{-1}. By shifting the emission spectrum along the $\bar{\nu}$ abscissa such that C_4 coincides with the main emission line A_4 at $\bar{\nu}$ = 4200 cm^{-1} representing the $^3T_2(F) \rightarrow {}^3T_1(F)$ Ni^{2+} transition [3], a striking similarity of these structures is revealed (Fig.). They are coined by vibronic interactions

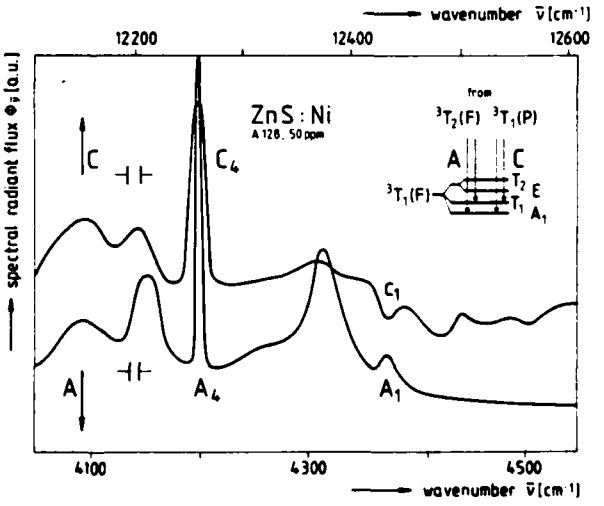

Comparison of the $^3T_2(F) \rightarrow {}^3T_1(F)$, i.e. "A", and the $^3T_1(P) \rightarrow {}^3T_1(F)$, i.e. "C", emission bands of ZnS:Ni^{2+} at T = 2K. Range of excitation: 16500 $cm^{-1} \leq \bar{\nu} \leq$ 28500 cm^{-1}

in the common ground state of both transitions. Considering the selection rules for electric-dipole transitions in various splitting models [1,2,4], the prominent A_4 and C_4 lines are understood as transitions terminating in T_1-$^3T_1(F)$. The position of this T_1 sublevel is in agreement with an earlier estimation based on susceptibility studies. These findings imply a quenching of spin-orbit interaction in the $^3T_1(F)$ ground state sublevels. Both a tetragonal and a trigonal pseudo Jahn-Teller distortion of the Ni^{2+} ground state result in a reduced T_1/A_1 accompanied by an increased $E,T_2/A$ splitting. The E,T_2 sublevels could not be ascertained with ZnS, they give however rise to satellites in the corresponding $^3T_1(P) \rightarrow {}^3T_1(F)$ and $^3T_2(F) \rightarrow {}^3T_1(F)$ emissions of ZnSe.

Finally, a high-resolution experiment with a low-doped ZnS:Ni specimen reveals that the emission line A_1 at $\bar{\nu}$ = 4377 cm^{-1} coincides with an absorption line a_1' but not with the smaller absorption line a_1 near $\bar{\nu}$ = 4375 cm^{-1} which had earlier been taken for the inverse transition [3]. Hence, the T_2 sublevel of $^3T_2(F)$ is situated 1.8 cm^{-1} above T_1 -- in agreement with the T-dependence of the A_4 emission sub-lines and with recent theoretical reasoning [4]. Implementing this description by transmission details which include Fano-type anti-resonances in the $^1T_1(G)$ and $^1T_2(G)$ transitions, a unified description of the Ni^{2+} level fine-structure for both ZnS and ZnSe [5] comes into sight.

[1] G. Roussos: Dissertation Technische Universität Berlin D83 (1983)

[2] U.G. Kaufmann, P. Koidl: J. Phys. C: 7, 791 (1974)

[3] G. Roussos, H.-J. Schulz: phys. stat. sol. (b) 100, 577 (1980)

[4] A.G. O'Neill: Ph.D. Thesis, St. Andrews Univ., Scotland (1983)

[5] A. Karipidou, H. Nelkowski, G. Roussos: J. Crystal Growth 59, 307 (1982)

VARIATIONS IN EMISSION PROPERTIES OF ZnSe CRYSTALS UNDER HIGH EXCITATION

S. Colak, R.N. Bhargava, B.J. Fitzpatrick, A. Sicignano

Philips Laboratories, Briarcliff Manor, New York 10510

There has been a resurgence of studies in wide band gap II-VI semiconductors for applications such as electron beam pumped visible lasers.[1,2] For this purpose we have studied the luminescence properties of a variety of ZnSe crystals with various impurities under e-beam excitation densities up to several MW/cm^2 for temperatures above 100°K.

The initial studies done by observing the cathodoluminescence at 300°K from the excitation side (up to $10KW/cm^2$ in figure) revealed a large variation of band edge emission intensities for differently grown ZnSe. In general it was found that samples with higher ratio of donor-acceptor pair band (DAP) to bound exciton (BE) line observed in photoluminescence at 5°K yielded a stronger cathodoluminescence band edge emission at room temperature. This result indicates that the presence of donors and acceptors enhances the band edge emission at 300°K and this emission may be associated with a free electron to bound hole transition.

Higher excitation experiments (up to $2MW/cm^2$) done by observing luminescence in the transmission mode through the sample also resulted in varying intensities for different materials but with smaller variations (dashed lines in figure). The band edge emission in these experiments showed features different from the bands described earlier for high optical excitation[3,4] where the origin of the recombination was explained by exciton-free carrier scattering.[4] The difference is expected to be due to

the geometry of the experiments, and a different recombination mechanism based on e-h plasmas generated by e-beam excitation.[5]

The experiments on some samples resulted in lasing with emission at about 2.615 eV with 6 to 20 meV width at 300°K, and at 2.754 eV with 6 to 15 meV width at around 100°K. Variations were due to different levels of excitation and to differences in laser samples.

1. N.G. Basov, J. Luminescence, 24/25, p.11, (1981).
2. I.V. Akimova, et al, Sov. J. Quantum Electron., 12, 1366 (1982).
3. K. Era, D.W. Langer, J. Luminescence, 1/2, 514 (1970).
4. W. Maier, C. Klingshirn, Solid State Commun., 2, 13 (1978).
5. V.I. Kozlovskii et al, Sov. J. Quantum Electron., 9, 104 (1979).

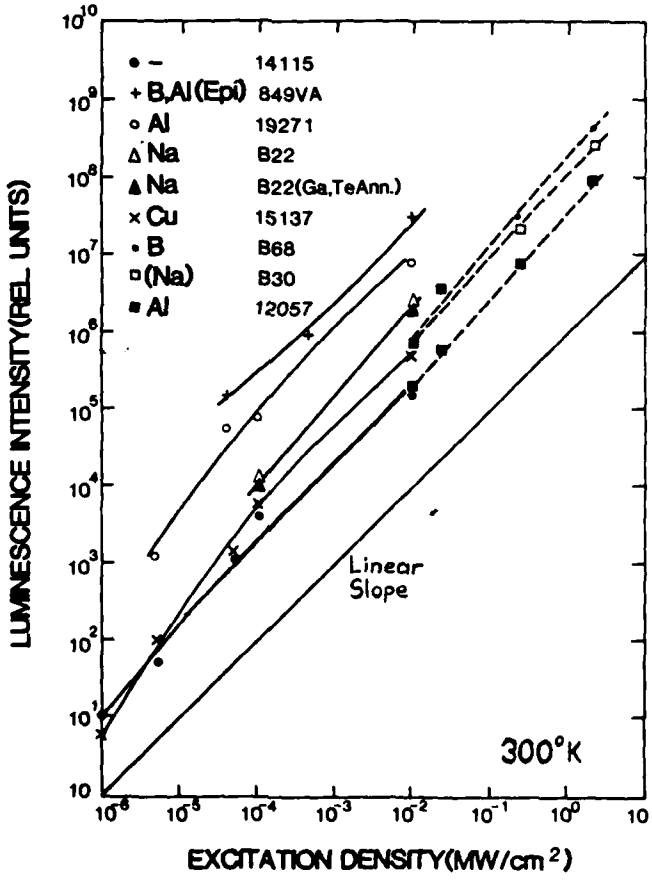

Identification of Deep Radiative Levels in VPE ZnSe

K. A. Christianson and B. W. Wessels

Department of Materials Science and Engineering and
Materials Research Center, Northwestern University,
Evanston, Illinois 60201

The defect centers responsible for the deep level emission commonly seen in the photoluminescence (PL) spectra of high purity VPE ZnSe have been studied. The ZnSe layers examined were heteroepitaxially deposited on GaAs by chemical vapor deposition, with palladium diffused hydrogen as the carrier gas. Under low excitation conditions, the 1.94, 2.2 and 2.7 eV emissions are usually observed at 77 K. A large dependence of the relative magnitudes of the observed PL bands upon crystal growth conditions was noted. For example, the free to bound emission at 2.7 eV was found to peak in intensity at a substrate growth temperature of 730 ^{o}C. For those samples whose free to bound emission at 2.7 eV predominates, hole traps at E_v+0.09 and E_v+0.13 eV have been observed by optical deep level transient spectroscopy (ODLTS). For these centers, concentrations as high as $2x10^{15}$ cm^{-3} have been measured. The origin of the two deeper emissions is not as clear, since the defect center responsible has not been detected by ODLTS. However, a potentially responsible defect level (at E_v+ 0.5 eV) has been observed by steady state photocapacitance at 77 K.

To aid in the identification of defect centers, electron irradiations have been used to modify the defect structure. Irradiation with 1.5 MeV electrons at room temperature at doses to 10^{17} e/cm^2 have given increased

1.94 and 2.2 emission relative to an nonirradiated sample. Corresponding increases in the concentration determined by steady state photocapacitance for the E_v+ 0.5 eV level have been noted upon irradiation. The annealing behavior of the induced centers will be discussed with respect to their identification.

Laser Spectroscopy Studies of Recombination at Isoelectronic Oxygen Centers in ZnTe:O*

E. D. Jones, Harold P. Hjalmarson and C. B. Norris
Sandia National Laboratories
Albuquerque, NM 87185

Using pulsed laser techniques, we have performed high-resolution excitation spectroscopy experiments on the luminescence of the oxygen center in ZnTe. These experiments were initiated to investigate the conjecture that free excitions are directly captured at oxygen impurities[1]. The luminescence measurements were made for laser wavelengths varying from the bound-exciton zero-phonon absorption line to well above the band gap of ZnTe. A typical luminescence spectrum obtained at 10k with the pump laser tuned to the one phonon absorption peak is shown in the accompanying figure. When the laser was tuned to the free-exciton band, we found that the oxygen luminescence was enhanced. This result confirms the earlier conjecture of free exciton capture.

In addition to these excitation studies, the oxygen luminescence linewidth and lifetime were measured as a function of time delay, laser power and laser wavelength. The oxygen-bound-exciton lifetimes, for laser energies below the free-exciton energy, are found to be in good agreement with those obtained from cathodoluminescence measurements[2], e.g., τ is approximately 90 ns at 10K, decreasing to about 45 ns at 27K and rising to 430 ns at 250K. At a temperature of 10K, the zero-phonon FWHM linewidth was measured to be 0.86 meV.

(1) Harold P. Hjalmarson and C. B. Norris (to be published).

(2) J. D. Cuthbert and D. G. Thomas, Phys. Rev. 154, 763 (1967).

*This work performed at Sandia National Laboratories supported by the U.S. Department of Energy under contract number De-AC04-76DP00789.

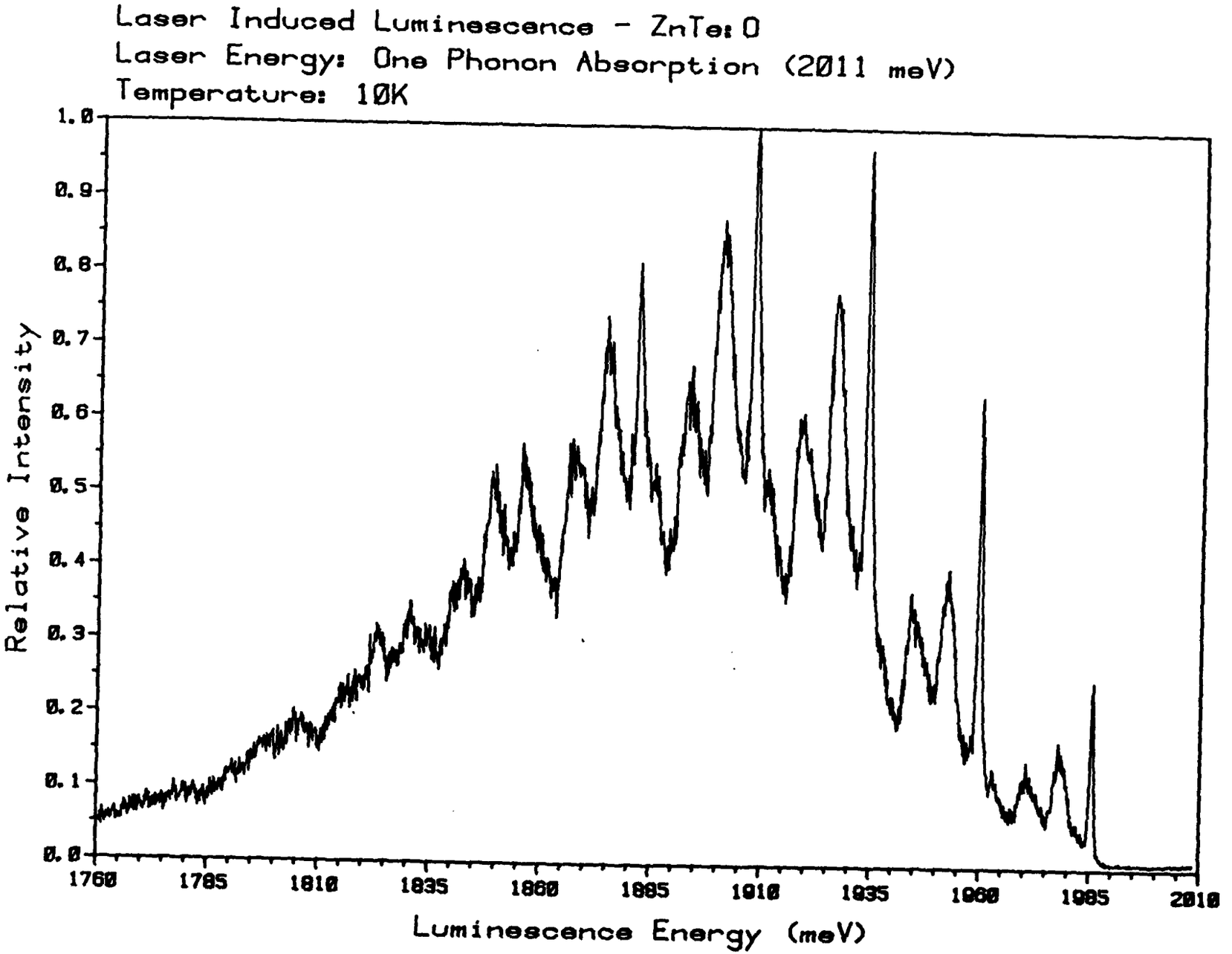
Laser Induced Luminescence - ZnTe:O
Laser Energy: One Phonon Absorption (2011 meV)
Temperature: 10K
Relative Intensity
1.0
0.9
0.8
0.7
0.6
0.5
0.4
0.3
0.2
0.1
0.0
1760
1785
1810
1835
1860
1885
1910
1935
1960
1985
2010
Luminescence Energy (meV)

DECAY OF 3d ELEMENT INTERNAL PHOTOLUMINESCENCE TRANSITION IN III-V SEMICONDUCTORS

G. GUILLOT, C. BENJEDDOU, P. LEYRAL, A. NOUAILHAT
Laboratoire de Physique de la Matière (LA 358)
Institut National des Sciences Appliquées de Lyon
20, Avenue Albert Einstein 69621 VILLEURBANNE CEDEX (France)

The decay processes of infrared emissions due to internal transitions after laser excitation have been studied systematically for the first time for several III-V semiconductors (GaAs, InP, GaP) doped with 3d ions (V, Cr, Fe and Co).

The decay curves recorded at low temperatures, where no non radiative transitions occur, are always exponential. They can be divided into two main classes depending their order of magnitude.

a) The microseconde range for Cr and Fe, as already published for this last ion (1)

b) The milliseconde range for V and Co emissions and for a luminescence band peaked at 0.5 eV found systematically in Fe doped InP.

The microseconde decay time seems typical of parity forbidden d-d internal transitions for the 3d ion impurities in semiconductors, which are observable because of an add parity mixing mechanism (2).

The milliseconde range found for V and Co is explained by other transition interdiction rules between states (spin selection and symetry rules). For V, this result is coherent with a new model of spectroscopic properties of V in GaAs (3) which attributes the internal photoluminescence emission to the transition :

$$^1E\ (^1D) \rightarrow {}^3A_2\ (^3F) \quad \text{of } V_{Ga}^{+3}$$

The decay time of 1.5 msec concerning the 0.5 eV band typical of InP:Fe indicates also strong interdiction rules for the transition. This band is tentatively attributed to the internal transition $^4T_1(^4G) \rightarrow {}^6A_1(^6S)$ of a Fe^{+3}_{In} ion formed by a hole capture at a Fe^{+2} center (4).

REFERENCES

(1) P.B. KLEIN, J.E. FURNEAUX, R.L. HENRY : Phys.Rev.B, 29, 1947 (1984)

(2) R. RENZ, H.J. SCHULZ : J.Phys.C 16, 4917 (1983)

(3) B. CLERJAUD, C. NAUD, C. BENJEDDOU, G. GUILLOT, P. LEYRAL, B. DEVEAUD, B. LAMBERT : accepted at Third Int. Conf. on SI III-V Materials USA, April 1984

(4) B. DEVEAUD, G. GUILLOT, P. LEYRAL, C. BENJEDDOU, A. NOUAILHAT, B. LAMBERT : accepted at Third Int. Conf. on SI III-V Materials USA, April 1984

PHOTOLUMINESCENCE PROPERTIES OF DISORDERED GaAs HEAVILY DOPED WITH Si

H. Takano, T. Kamijoh and M. Sakuta

Research Laboratory, OKI Electric Industry Co., Ltd.

Higashi-Asakawa, Hachioji, Tokyo 193, Japan

The GaAs heavily doped with Si is one of prototypes of disorder-semiconductor with high concentration of charged impurities.[1] Si impurities show the amphoteric behavior in the GaAs, namely Si on Ga- and As-sites act as donor and acceptor, respectively. In LPE grown GaAs, the distribution of Si impurities on each site is mainly due to the growth temperature.[2] The coexistence of both positive(donor) and negative(acceptor) ions cause the large potential fluctuations mixing with conduction and valence band states[1], and luminescence properties of this system are very interesting because of heavy-doping and compensation effects in the radiative recombination processes. In this report, we show photoluminescence properties of the GaAs heavily doped with Si which is highly compensated. Aspects of radiative recombination process in this system are proposed.

Samples, the GaAs crystals which were both heavily Si-doped and highly compensated were grown by liquid phase epitaxy at the growth temperatures of 800 - 880 ^{o}C. Si concentration in the epitaxial layers is 1.1 - 1.4 x 10^{19} cm^{-3} which was estimated from SIMS data. All epitaxial layers were p-type with carrier concentration of 3 x 10^{16} - 5 x 10^{18} cm^{-3} at the room temperature. The compensation ratios, (N_D/ N_A), were estimated from the carrier and Si concentrations. Photoluminescence spectra were obtained with samples immersed in liquid helium or nitrogen using an Ar^{+} laser operating at 514.5 nm. Photoluminescence spectra consisting of a broad-band emission peaking at 1.28 - 1.36 eV were observed. The peak shifs to higher energy

with decrese of N_D/N_A. This result indicates the growth of conduction band tail with increase of N_D/N_A. A considerable feature of the broad-band emission is a shift of emission peak to higher energy as the excitation intensity is increased as shown in Fig. 1. From this result, it is expected that there is Coulombic interactions between the recombination centers as in the case of donor-acceptor pair recombination process, and moreover the centers are associated by the Si-related defects which are donors and acceptors. The heavily doped semiconductors have the deformable lattice and the recombination centers are dressed with phonon cloud.[3] In this point of view, the recombination process of observed broad-band emission is interpreted as the localized donor-acceptor pair recombination, in which the donor and the acceptor are associated by the Si-related defects. In this process, we interpreted that the excited electrons are cascaded down to the localized states in the band-tail, and transited to the localized Si_{As}-related states with Coulomb interactions. This cascade process was supported by our Raman data. In conclusion, we observed photoluminescence spectra of both heavily Si-doped and highly compensated p-GaAs, and propose radiative recombination process of donor-acceptor pair dressed with phonon cloud.

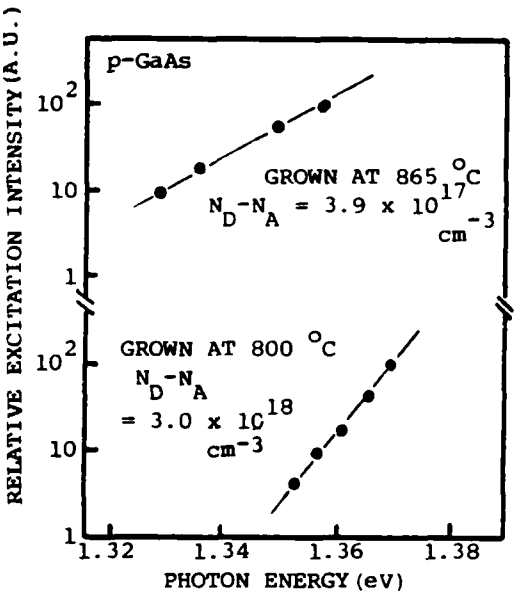

Fig. 1 Variation in peak energy of the broad-band emission VS. excitation intensity.

References: 1. D.Redfield et al., Phys. Rev. B2 1830 (1970). 2. D.J.Ashen et al., J. Phys. & Chem. Solids 36 1014 (1975). 3. Y. Toyozawa, Physica 117B, 23 (1983).

Luminescence in Annealed Electron-Irradiated High-Purity GaAs

P.L. Liu, G. Schmieder and W. Ossau, Physikalisches Institut der Universität Würzburg, D-8700 Würzburg, Röntgenring 8.

The samples studied are non-intentional doped and iron-doped high-purity GaAs liquid phase epitaxial layers irradiated with 2 MeV-electrons at room temperature. After annealing at 550 ^{o}C a new line appears at 1.5015 eV. The spectral position does not shift with the excitation intensity.We observe a fast decrease of the integrated luminescence intensity with increasing sample temperature. This points out to a particle (electron) loosely bound to the complex. No change in the energy position is observed in this temperature range.

At zero magnetic field the new line has a symmetrical shape with 0.2 eV half-width. In an applied external magnetic field the line splits into four components. Rotation of the field direction in a (100) plane shows no directional dependence of the Zeeman spectrum at 12 T and also no polarisation is observed. The diamagnetic shift of the spectral center of mass ($a= 5.6\ \ 10^{-2}$ mev/T^2) agrees with that of the exciton bound to a tin, cobalt and copper acceptor in GaAs ($a= 6.2\ 10^{-2}$ meV/T^2), as well as with that of the effective mass donor. This suggests that the electron is bound to the center only by the Coulomb potential, and therefore the emission is not due to an intracenter transition. Furthermore, the symmetric line shape and the narrow half-width less than k·T confirms that the line is caused by a recombination of bound excitons.

The photon energy deviation from the spectral center of mass as a function of magnetic field strength shows a large and linear splitting. The observed four-line isotropic, unpolarized Zeeman spectra can be explained by a strong axial field of C_{2v} symmetry. The binding energy of the center can be

calculated to 13.7 meV. This is about four times the binding energy of excitons bound to effective mass acceptors. This means, the holes are tightly bound to the center which results in a strong localization of the wave functions in real space. In a field with symmetry C_{2v} the acceptor ground state split into two Γ_5 levels /1/. One of these states is split off into the valence band. Therefore the acceptor bound exciton transition ($\Gamma_6-\Gamma_8$) is reduced by the axial field to a ($\Gamma_5-\Gamma_5$) recombination in zero magnetic fied.

An external magnetic field splits the two Γ_5 states into four Γ_2 levels resulting in four dipole allowed transitions. From this transition scheme we obtain effective g-values g_{eff} = -0.465 (electron) and k_{eff} = 1.626 (hole). g_{eff} is in good agreement with the conduction band electron g-factor. The value for the hole is large compared to k = 1.0 obtained from studies of the free exciton as well as k = 0.8 for bound exciton complexes. The observed k-factor only differs little from k = 2.01 reported of a double acceptor-neutral donor complex/2/.

It is noted that some behaviours of the new line, for instance no clear dependence on the magnetic-field direction and no polarization of the emitted radiation, are similiar to those of the F_0-line (1.4832 eV) arised for the exciton bound to a copper complex/1/. The chemical origin of the binding center of our new line studied here hasn't been known yet.

1. F.Willmann, D. Bimberg and M.Blättle,
Phys.Rev. **B7**,2473 (1973)

2. D.C.Reynolds, R.J.Almassy, C.W.Litton, S.B.Nam and G.L.McCoy,
J.Appl.Phys.**49**, 5336 (1978)

A Comparison Of Calculated Impurity Wavefunctions With GaP:N Luminescence

Paul G. Snyder, Department of Electrical Engineering, University of Southern California; Charles W. Myles, Departments of Physics and Engineering Physics, Texas Tech University; and Martin A. Gundersen, Departments of Electrical Engineering and Physics, University of Southern California.

Martin A. Gundersen
SSC-420
Department of Electrical Engineering
University of Southern California
Los Angeles, CA 90089-0484

Luminescence spectra due to impurities in a semiconductor contain contributions from both direct and indirect electronic transitions. In the indirect transition, a momentum conserving phonon is emitted or absorbed simultaneously with the emission of a photon. Because such transitions occur in all parts of the rillouin zone where the impurity wavefunction is non-vanishing, ch information about the wavefunction (in k-space) can, in inciple, be obtained from the phonon sidebands of the minescence spectrum. In this paper, we derive an expression or the luminescence intensity due to indirect transitions, as a unction of energy, and relate it to the k-space charge density, $|\psi(k)|^2$, of the impurity level. This expression can then be used to test the accuracy of particular theoretical models of localized wavefunctions and energy levels. A charge density in k-space is calculated by the use of a theoretical model, and the corresponding spectrum is then calculated according to our expression. We compare this with the measured luminescence spectrum, which has first been treated to remove configuration coordinate electron-phonon interactions.[1]

While the above method is generally applicable to either shallow or deep levels in any semiconductor which has a known energy band structure, the method is probably most useful for the study of deep levels in indirect gap materials. As a test case, we follow the procedure for an exciton bound to nitrogen in GaP. Although the energy level is shallow in this case, the electron wavefunction is strongly localized, just as for a deep level wavefunction. Furthermore, the low temperature luminescence spectrum is well resolved and the momentum conserving and configuration coordinate phonons are distinguishable from one another. An extended Koster-Slater model[2] is used to calculate the trial electronic wavefunction. A comparison of the calculated and measured luminescence spectra, as well as details about the sensitivity of the method to the choice of the theoretical model, and extension to true deep levels, will be presented.

1. B. Monemar and L. Samuelson, Phys. Rev. B **18**, 809 (1978).

2. W.Y. Hsu, J.D. Dow, D.J. Wolford, and B.G. Streetman, Phys. Rev. B **16**, 1597 (1977).

The 0.839 eV Cr-related luminescence center in GaAs:Cr

Y. Fujiwara, A. Kojima, T. Nishino and Y. Hamakawa
Faculty of Engineering Science, Osaka University
Machikaneyama 1-1, Toyonaka, Osaka 560, Japan

We have found that an arsenic vacancy contributes to the 0.839 eV Cr-related luminescence line in GaAs:Cr and the luminescence center is a complex involving a Cr at a Ga site and an arsenic vacancy in its nearest neighbor, based on systematic studies on high temperature thermal annealing of GaAs:Cr under excess arsenic pressure. This Cr-related deep center luminescence line was assigned as due to intra d-shell transitions in a Cr impurity in GaAs. Recent Zeeman data[1] on this 0.839 eV line have shown that the luminescence center has <111> C_{3v} axial symmetry rather than T_d symmetry of an isolated Cr at the Ga site in GaAs crystal. This suggests that the contribution of another impurity or defect to the Cr-related center. The chemical identification of this partner of the Cr impurity in GaAs has not definitely been done, though the symmetry of the Cr-related center was confirmed by these Zeeman experiments. We have investigated this Cr-related deep center luminescence with samples prepared by different diffusion conditions of Cr into GaAs. As a result, we have found that the intensity of the 0.839 eV Cr-related luminescence line decreases with increasing the arsenic pressure in a sealed quartz ampoules for Cr diffusion in GaAs. Based on these results we have proposed that an arsenic vacancy is a probable candidate as the partner of the Cr in the complex.[2,3]

In this work we have measured systematically the in-depth profiles

of the 0.839 eV Cr-related luminescence intensity in GaAs crystals grown-in doped with Cr annealed at temperatures around 900 °C under various excess arsenic pressure. The 0.839 eV luminescence intensity is normalized by the well-known 1.49 eV C-related donor-acceptor pair luminescence intensity. We have found that in the region of several microns from the surface the intensity of the 0.839 eV Cr-related luminescence in annealed GaAs:Cr is nearly constant against the distance from the front surface and proportional to $P_{As}^{1/4}$, where P_{As} is the pressure of excess As_4. We have analyzed this result based on mass-action equations for reactions involving several point defects in GaAs, the result revealing the fact that the concentration of the partner of the Cr impurity in the complex is proportional to $P_{As}^{-1/4}$, where we considered the excess arsenic pressure dependence of the concentration of various types point defects in GaAs. As a result of this analysis, we have obtained the conclusion that an arsenic vacancy contributes to the 0.839 eV Cr-related luminescence center in GaAs:Cr and the luminescence is due to a complex involving a Cr impurity and an arsenic vacancy in its nearest neighbor, in agreement with our previously proposed model. This complex, of course, satisfies the C_{3v} symmetry of the center responsible for the 0.839 eV Cr-related luminescence line in GaAs:Cr.

References

1) Ch. Uihlein and L. Eaves; Phys. Rev. B26 (1982) 4473.

2) Y. Fujiwara, T. Nishino and Y. Hamakawa; Jpn. J. Appl. Phys. 21 (1982) L727.

3) T. Nishino, Y. Fujiwara and Y. Hamakawa; Proc. Intern. Symposium GaAs & Related Compounds, New Mexico, 1982 (Inst. Phys., Bristol & London, 1982) p. 71.

COMPUTER SIMULATION OF ENERGY TRANSFER: APPLICATION TO THE PHOTOLUMINESCENCE IN CdMnTe

H. Kett, W. Gebhardt
University of Regensburg, Dpt. of Physics
84 Regensburg, F.R. Germany

We report on a computer simulation of the radiationless energy transfer[1] between Mn^{2+}-ions in $Cd_{1-x}Mn_xTe$. The model was applied to explain the photoluminescence properties in this material and in other II-VI-semiconductors with high manganese concentration. An fcc-lattice with 4096 lattice points and periodic boundary conditions is randomly occupied with "active" ions corresponding to a molar concentration x. The active ions are given 2 electronic states with energies E_g and $E_e = E_g + E_o + N \cdot \Delta E$, where N is the number of "active" neighbors. The expression for E_e simulates the

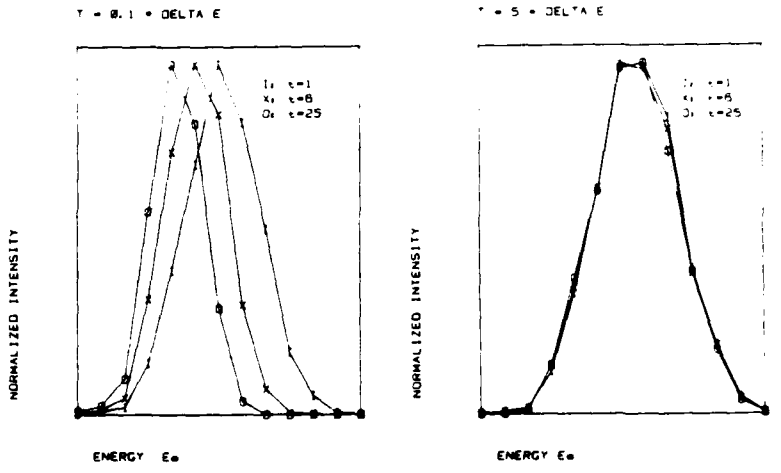

Fig. 1

random crystal field seen by one active ion. The simulation starts with the excitation of a random active lattice point x. After an internal time interval Δt the excitation either decays with a certain probability W by photon emission or is transfered to a random neighboring active lattice

point x'. If it has to step up in energy, the transition probability is equal to exp $\frac{(E_e(x)-E_e(x'))}{k_B T}$, if it steps down, the transition probability is one. This procedure is repeated until the excitation decays radiatively with energy E(x') after n time intervals Δt. After 500 000 excitations the time resolved spectrum is determined from E(x') and n, which is equivalent to the delay time in the time resolved luminescence experiment. The spectra depend on temperature and delay time.

Fig. 1 shows two spectra plotted as a function of spectral energy and delay time. At low temperatures $T \ll \Delta E$ the redshift and band narrowing increases with delay time as was observed in the experiment.[2] At high temperatures $T \gg \Delta E$, redshift and narrowing vanish.

In Fig. 2 the emission intensity is plotted as a function of time after excitation for low temperatures $T = 0.1\ \Delta E$. The low energy emission shows

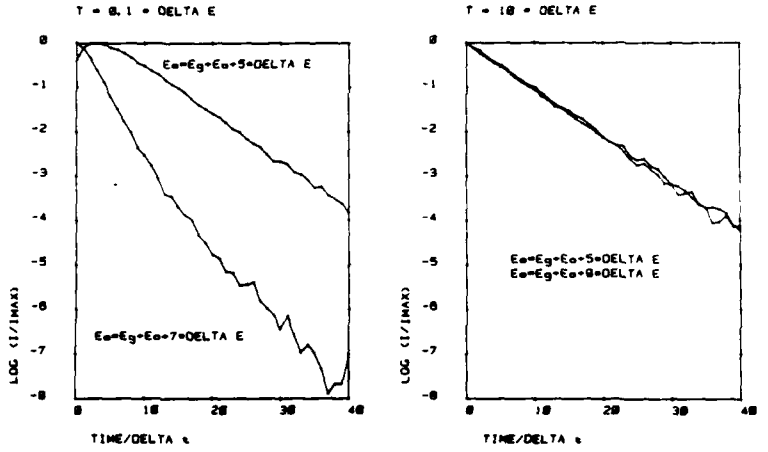

Fig. 2

an exponential decay for $n > 5\Delta t$, while the high energy emission does not. For $T = 10\Delta E$ the low and high energy emission can be fitted by a single exponential. The results of the simulation agree qualitatively well with the experimental data obtained with $Cd_{0.5}Mn_{0.5}Te$.

1) A. Blumen, G. Zumofen
Chem. Phys. Lett. 70 (1980) 387

2) E. Müller, W. Gebhardt, V. Gerhardt
phys. stat. sol. (b) 113 (1982) 209

A NOVEL MECHANISM FOR ENERGY TRANSFER BETWEEN RARE EARTH IONS

W. Stręk

Institute for Low Temperature and Structure Research,
Polish Academy of Sciences, P.O.Box 937, 50-950 Wrocław, Poland

The theoretical understanding of resonant energy transfer between a pair of spatially localized lanthanide ions has been developed by Kushida [1]. His model was based on a simple application of Förster-Dexter theory [2,3] in which the transition rate of dipole-dipole energy transfer from the initial state $|D_\alpha A_\beta>$ to the final state $|D_\alpha A_{\beta'}>$ is proportional to the square of of modulus of

$$<D_\alpha | D_q^1 | D_{\alpha'}><A_\beta | D_q^1 | A_{\beta'}> R^{-3} \qquad (1)$$

where R is the separation between the donor - D and the acceptor - A ions. Because the electric dipole transitions are forbidden between the metal states of the same parity Kushida [1] has invoked in his model the explicite expressions for the electric dipole moment in rare earth ions taken from the model of Judd [4] and Ofelt [5]. Such an approach is not general and does not take into account the specific properties of hypersensitive transitions associated with the polarizability of environment.

In this paper we present a general model of energy transfer between rare earth ions.

Let the zeroth order basis states of the system will be expressed as a product of metal (donor and acceptor) ions and ligands wavefunctions - $|D_\alpha A_\beta L_o>$ and $|D_{\alpha'} A_{\beta'} L_o>$ for the initial and final states, respectively. The perturbation operator leading to the energy transfer process in the composite system which may be written as

$$V = V_{DA} + V_{DL} + V_{AL} \qquad (2)$$

where V_{DA}, V_{DL} and V_{AL} are the donor-acceptor, donor-ligand and acceptor--ligand interaction potentials, respectively. Since the first-order contribu-

tion to the matrix element $(D_\alpha A_\beta L_o|V|D_{\alpha'} A_{\beta'} L_o)$ being in general of the form (1) vanishes, the non-zeroth contributions to the dipole-dipole energy transfer arises from the admixture of odd parity states into the f^n states through crystal field perturbation or the admixture of the excited ligand states perturbed by the metal ion (dynamic coupling).

A typical term for the second- and third-order contributions to $(D_\alpha A_\beta L_o | V | D_{\alpha'} A_{\beta'} L_o)$ are proportional to

$$<D_\alpha A_\beta|V_{DA}|D_{\alpha''} A_{\beta''}><D_{\alpha''} A_{\beta''}|V_{DA}|D_{\alpha'} A_{\beta'}> \quad (3)$$

and

$$<D_\alpha L_o|V_{DL}|D_{\alpha''} L_o><D_{\alpha''} A_\beta|V_{DA}|D_{\alpha'} A_{\beta''}><A_{\beta''} L_o|V_{DL}|A_{\beta'} L_o> \quad (4)$$

$$<D_\alpha L_o|V_{DL}|D_{\alpha''} L_\gamma><D_{\alpha''} A_\gamma|V_{DA}|D_{\alpha'} A_{\beta''}><A_{\beta''} L_\gamma|V_{DL}|A_{\beta'} L_o> \quad (5)$$

respectively. The term (4) associated with the static crystal field is specific for the Kushida's treatment of pairwise dipole-dipole energy transfer between rare earth ions. The term (5) associated with the dynamic coupling is appropriate for treating the energy transfer involving the hypersensitive transitions. Similarly the role of the second-order terms is also limited to the energy transfer involving the hypersensitive transitions.

REFERENCES

1. T. Kushida, J. Phys. Soc. Jap. 34, 1318, 1973.

2. T. Forster, Ann. Phys. (Leipzig) 2, 55, 1948.

3. D.L. Dexter, J. Chem. Phys. 21, 836, 1953.

4. B.R. Judd, Phys. Rev. 127, 750, 1962.

5. G.S. Ofelt, J. Chem. Phys. 37, 511, 1962.

STUDIES OF ION PAIR INTERACTION IN $KNd_xGd_{1-x}P_4O_{12}$ CRYSTALS USING SITE SELECTION TIME RESOLVED SPECTROSCOPY

M. Malinowski and W. Woliński

Institute of Electron Technology, Warsaw Technical University, ul. Koszykowa 75, 00-662 Warsaw, Poland.

$KNdP_4O_{12}$ crystals belong to the group of so called stoichiometric laser compounds characterized by a very weak concentration dependent fluorescence quenching.
Although the most important spectroscopic and laser parameters of $KNdP_4O_{12}$ have been determined [1,2] the precise nature of the ion-ion interaction has not been established. In an earlier paper [3] we presented results of spectroscopic investigations of the mixed $KNd_xRE_{1-x}P_4O_{12}$ system, where RE = Y, La and Pr. The satellite structure of the excitation spectra and the fluorescence spectra dependence on excitation wavelength have been examined and related to the existence of Nd^{3+} clusters.
In this paper we report the results of an investigation of the $KNd_xGd_{1-x}P_4O_{12}$ crystals. In order to study the microscopic interaction between the Nd^{3+} ions a technique of selective excitation by a short pulses of a tunable dye laser at liquid helium temperature was employed. The satellite structure of the excitation and absorption spectra was examined. It was possible to distinguish between the satellites resulting from the pairs of Nd^{3+} ions and the single neodymium ions in different crystal field sites. The decay of the $^4F_{3/2}$ state after selective excitation was measured and the values of quenching rates for different Nd^{3+} pairs were calculated.
The fluorescence lifetimes of $KNd_xGd_{1-x}P_4O_{12}$ in the whole concentration region were calculated using the microscopic interaction parameters measured in the low concentrated samples. The calculations were performed in the framework of the discrete host structure model developed by Huber [4]. A very good consistency between the measured and calculated lifetimes was found, for pure $KNdP_4O_{12}$ we obtained $\tau_{exp} = 95\ \mu s$, $\tau_{calc} = 111\ \mu s$, for $KNd_{0.5}Gd_{0.5}P_4O_{12}$ $\tau_{exp} = 153\ \mu s$, $\tau_{calc} = 158\ \mu s$ and for $KNd_{0.2}Gd_{0.8}P_4O_{12}$ the values of $\tau_{exp} = 207\ \mu s$ and $\tau_{calc} = 210\ \mu s$ were obtained.

This clearly indicates that the cross relaxation between the nearest neighbours is responsible for the quenching of the $^4F_{3/2}$ fluorescence.

From the energy level diagram of Nd^{3+} in $KNdP_4O_{12}$ it was shown that the probable process of cross relaxation is the nonresonant energy transfer via $^4I_{13/2}$ and $^4I_{15/2}$ levels [2]. At low temperature the process assisted by the emission of 1064 cm^{-1} phonon has to be considered.

$$^4F_{3/2}(1) \rightarrow {}^4I_{13/2}(7) - 1064\ cm^{-1} = {}^4I_{9/2}(1) \rightarrow {}^4I_{15/2}(8)$$

Assuming the one phonon assisted process and the electric dipole interaction between the ions of the pairs the probability of the energy transfer was eveluated. The electrostatic interaction hamiltonian in the form giver by Kushida [4] was used in the calculations. The overlap integral of the line shape functions including the phonon side bands in the approximation of the exponential dependence on the energy gap was evaluated according to Miyakawa and Dexter theory [5].

The good agreement between the calculated and experimentally determined values confirms that some pairs are coupled by the electric dipole interaction. For strongly coupled pairs the exchange interaction must be taken into account and in highly concentrated crystals processes involving more than two ions are probably essential.

References

1 C. Gueugnon, J.P. Budin, IEEE J. Quantum Electron. QE-16 (1980) 94.
2 M. Malinowski, W. Woliński, Acta Phys. Polon. A 65/3 (1984)
3 M. Malinowski, W. Woliński, accepted for publication in the Journal of Luminescence.
4 T. Kushida, J. Phys. Soc. Jap. 34 (1973) 1318.
5 T. Miyakawa, D.L. Dexter, Phys. Rev. B1 (1970) 2961.

MODERN STATUS OF ENERGY TRANSFER PROBLEM IN SOLIDS ACTIVATED BY RARE-EARTH SYSTEMS

V.P.Gapontsev, N.S.Platonov

Institute of Radioengineering & Electronics AS USSR,
103907, Moscow, Marx 18

We fulfilled systematic investigations of energy transfer(ET) processes for more than 60 donor(d)-acceptor(a) systems of RE^{3+} in wide line of phosphate, silicate, borate, germanate, and tellurite glass hosts, also as in crystals of pentaphosphates, tetraphosphates, double potassium molibdates, and so on, with using the arsenal of modern precise experimental methods, in particular, the selective laser excitation method, or the method of luminescence decay kinetic in the intensity range of 4-5 orders of value. New significant results were obtained which allowed us to form the clear viewpoint on the regularities and mechanisms of different ET processes, the dependences of their constants from composition and micriscopic structure of host, the activator concentrations, the temperature, the energy mis-match, and the other factors, also as on the principal changes of ET regularities when crossing from crystalline to amorphous state.

It is fixed, in particular,next: (i) The dipole-dipole interaction of RE^{3+} is decisive for ET processes in the whole range of interionic distances of $R \geq 3{,}5$ Å practically for all d-a pairs, independently from the relative contribution of higher order termes of electric multipole interaction in strength of individual transitions coupled with ET process; (ii) the ET efficiency feebly depends on the energy mis-match in the limits of $\tilde{\nu} \leq \tilde{\nu}_{max}$, where $\tilde{\nu}_{max}$ - the highest frequency of harmonic host vibrations. Moreover, for nonresonant pairs this efficiency exceeds essentially

AD-A148 470 INTERNATIONAL CONFERENCE ON LUMINESCENCE HELD AT MADISON WISCONSIN ON 13-17 AUGUST 1984(U) WISCONSIN UNIV-MADISON W M YEN OCT 84 N00014-84-G-0053 6/7

UNCLASSIFIED F/G 20/6 NL

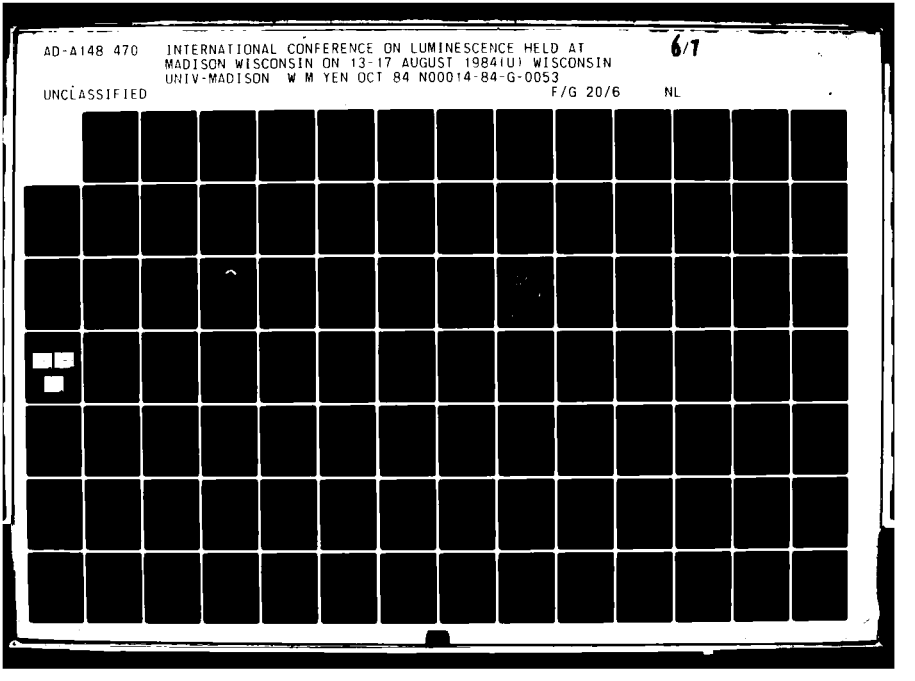

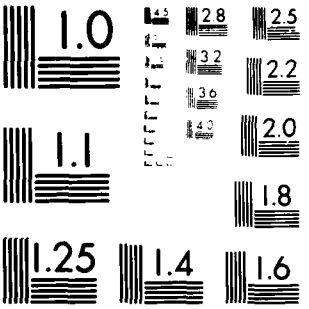

MICROCOPY RESOLUTION TEST CHART

the values calculated using the approach of dipole-dipole resonance of the electronic transitions with the electron-vibrational side-bands of partners.

On the other hand, we haven't found the significant dependence of ET elementary act efficiency on host composition and the crystal -glass crossing, or the spectral disordering degree of active media The 4,2 - 500 K temperature dependences of those efficiencies are proved to be also very week for the most d - a systems, excepting the Yb-Er pair and some others.

It is reliably shown that energy migration processes in the systems of Yb, Nd, Eu, Tb, and other ions possesses the dipole-dipole character, and the elementary act mechanism of those process es is defined more precisely. On examples of Yb-Dy, Yb-Tm, Yb-Ho, Yb-Er, Nd-Yb, Er-Nd, Eu-Tm, and other double systems of activators, it is shown, that regularities of migration-accelerated quenching (MAQ) of fluorescence in glass hosts are unlike qualitatively from those in crystal hosts. The sharp increasing of the macro-scopic ET rate $\overline{W}$ at the crystal-glass transition in systems with high activator's concentrations results of this situation. The relation of $\overline{W}$ with the elementary act parameters of d - d and d - a interactions, also as the minimum possible spacing between RE^{3+} is revealed both for migration- controlled and kinetic stages of process. The pecularities of MAQ process for the systems with essential contribution of back transfer, in particular, Yb-Er and Nd-Yb systems, which are important for applications.

The received data give us the possibility to calculate a priory the quantitative characteristics of ET processes between RE^{3+} in new hosts using minimum number of accessible spectroscopic data.

Nonradiative Energy Transfer Without Quenching of Donor Lifetime in Mn-Based Crystals

B. Di Bartolo (*)
Department of Chemistry
Massachusetts Institute of Technology
Cambridge, Massachusetts 02139, U.S.A.

and

J. Danko and D. Pacheco
Department of Physics
Boston College
Chestnut Hill, Massachusetts 02167, U.S.A.

Nonradiative energy transfer between donor and acceptor ions in solids takes place by various processes, i.e. dipole-dipole, exchange, etc. Also, before transfer, migration of excitation energy among donors may occur and may influence the time evolution of the donor and acceptor luminescence. It is well known that, regardless of the process present, the decay pattern of the donor ions is affected by the presence of the acceptor ions.

We have found that stoichiometric Mn-based crystals, such as MnF_2 and $RbMnF_3$, doped with rare earth ions present an interesting exception to this rule. The luminescence of the undoped samples is associated mostly with localized impurity-induced traps which are present in concentrations on the order of only ten parts per million. Energy transfer among unperturbed Mn^{2+} ions assures the prompt filling of these traps and their efficient emission.

When these systems are doped with rare earth ions (REI) Mn → REI energy transfer takes place. We have observed that in such processes the decay pattern of the donor (Mn) luminescence is not affected by the presence of the acceptor

---

* Permanent address: Department of Physics, Boston College, Chestnut Hill, Massachusetts 02167

ions. The crystals examined were: $RbMnF_3$, MnF_2, $RbMnF_3:Nd^{3+}$, $MnF_2:Er^{3+}$ and $RbMn_xMg_{1-x}F_3$ (x = 0.4, 0.8). The following was found:

1) The excitation spectra of Nd^{3+} in $RbMnF_3$ and Er^{3+} in MnF_2 provide the evidence that Mn → REI energy transfer takes place, even at room temperature, where no Mn^{2+} luminescence is observed. Even when this luminescence is present there is no evidence of any reabsorption by the REI sharp energy levels. The points above imply that the Mn^{2+} → REI energy transfer mechanism is of the nonradiative type.

2) The luminescence emission of Mn^{2+} is mainly concentrated in two bands. Only the high-energy band excitation becomes available for transfer to the rare earth ions, or energy sinks.

3) The luminescence of Mn is mainly due to localized centers, but the absorption levels preserve their delocalized exciton-like character. In particular the lowest absorption level, called A level, is the communication channel between the donor Mn traps and the acceptors. No energy is transferred <u>directly</u> from the Mn traps to the acceptors. Correspondingly the time evolution of the (donor) trap population is not affected by the presence of the acceptors.

ThD6-1

L.V.KIRILUK

(USSR, Kiev State University)

SENSITIZED LUMINISCENCE AND ENERGY TRANSFER IN CaF_2-Ho^{3+},Eu^{2+} SYSTEM.

The Spectra of luminiscence and the absorption of concentration series of monocrystals CaF_2-Ho^{3+} and CaF_2-Ho^{3+},Eu^{2+} synthesized in a fluorined medium under 300 and 77°K (Stockbarger method) have been investigated on the difraction spectrometer with the riverse linear dispersion of 5 Å/mm and monocrystals CaF_2-Eu^{2+} have been investigated on the spectrophotometer (SF-4A).

The Comparison of the spectra made it possible to construct the empirical scheme of Eu^{2+} and Ho^{3+} levels in CaF_2. The Interception of the spectral radiation of Eu^{2+} (max.~426 nm) with the spectral absorption of Ho^{3+} (max.~415 and 450 nm) testifies to the presence of a resonance non-radiative transfer of energy from Eu^{2+} to Ho^{3+}; this fact is also proved by the adrupt decrease ($9,2-1,8.10^{-7}$ s) in the Eu^{2+} luminiscence time of decay in a set of samples with a stable (0,08%mol.) presence of Eu^{2+} and a variable concentration of Ho^{3+}. It has been shown that the probability of energy transfer biactivated system increases monotonicali alongside with the increase in Holmium concentration.

Conditions of an effective migration of energy through the Europium radiation levels have been cleared up. This migration encreases the probability of "convergence" of excited ions with quiet ions of Eu^{2+} and it leads to the concentration extinquishing on one hand and increases the probability of convergence of excited ions of Eu^{2+} with quiet ions of Ho^{3+}, on the other hand. It results in a rather intensive (more than in 22 times) sensitized luminiscence of Ho^{3+} on λ =551,2 nm under an optimal concentration of activators (0,04% mol. Ho^{3+} and 0,08 % mol.Eu^{2+}).

The investigation has shown that under the condition ofalow excitement (mercury lamp ДРШ-1000) the non-radiative resonance transfer of energy occurs during a lifetime of an excited state of sensitizer and it is independent on the temperature under the condition of its low concentration.

Single- and multi-step energy transfer from Mn^{2+} to Sm^{3+} in ZnS:Mn,Sm

XU Wu, ZHANG Xin-yi and XU Xu-rong

Changchun Institute of Physics
Chinese Academy of Sciences
Changchun, China

We found that the excitation energy can be transfered from Mn^{2+} to Sm^{3+} in ZnS:Mn,Sm.[1] For a given concentration of $Mn^{2+}(C_{Mn})$, the energy transfer rate (P) varies with the concentration of $Sm^{3+}(C_{Sm})$, as shown in Fig.1. But, when C_{Mn} increases from lower than 10^{-4} mol. to 10^{-3}mol., the corresponding dependence of P upon C_{Sm} changes from $P \propto C_{Sm}^2$ to $P \propto C_{Sm}$. This result can be explained by the different paths of energy transfer : a single-step direct transfer from Mn^{2+} to Sm^{3+} for small C_{Mn} and a multi-step diffusion limited transfer, $Mn^{2+} \rightarrow Mn^{2+} \rightarrow \cdots\cdots \rightarrow Sm^{3}$ for large

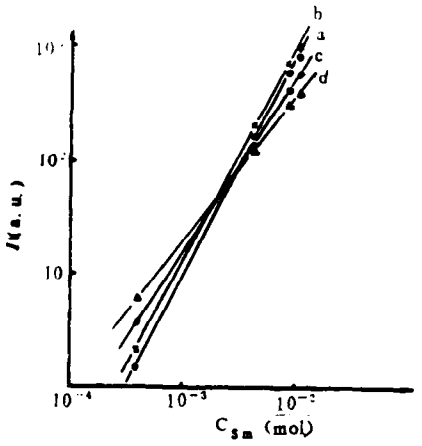

Fig.1 Variation of P as a function of C_{Sm} for different C_{Mn}: (a) 10^{-5} mol. (b) $5X10^{-5}$ mol. (c) 10^{-4} mol. and (d) $2X10^{-3}$mol.

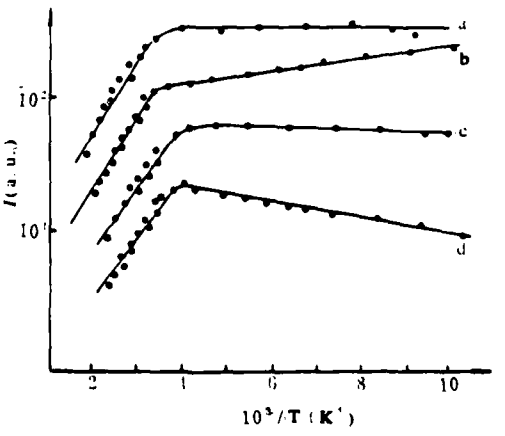

Fig.2 Temperature dependence of emission intensity of Mn and Sm : I_{Mn}(o), I_{Sm}(•) in (a) ZnS:Mn, (c) ZnS:Sm, (b) and (d) ZnS:Mn,Sm

C_{Mn}. According to the energy transfer theory of dipole-dipole interaction, for diffusion limited transfer[2], $P = 4\pi\alpha^{1/4}D^{3/4}C_{Sm}$, where D is the diffusion coefficient, α is a constant. On the other hand, P is proportional to C_{Sm}^2 for direct transfer[3].

In Fig.2 are shown the temperature dependences of the intensity of luminescence of Mn^{2+} and Sm^{3+} in ZnS:Mn, ZnS:Sm or in ZnS:Mn,Sm. The quenching temperature of luminescence is approximately 340K for both Mn^{2+} and Sm^{3+}. In the temperature range 77-340K, in ZnS:Mn,Sm the increases of the luminescence due to Sm^{3+} and the decrease of that due to Mn^{2+} are attributed to the increase of the energy transfer rate with the rising of temperature.

Due to the mismatch of the excitation levels of Mn^{2+} and Sm^{3+}, the energy transfer between them is considered as phonon assisted. Taking this situation into account, we have from the rate equations derived the theoretical formulas which describe very well the experimental temperature dependence of luminescence intensity due to Mn^{2+} and Sm^{3+} in ZnS:Mn,Sm respectively. On fitting the theoretical calculations to experimental results, it is found that the mean number of phonons participated in the energy transfer process is about 2-3.

It is interesting to mention that if Mn^{2+} is excited to an higher state by two-photon absorption method, one can observe an enhanced luminescence of Sm^{3+}. Perhaps, this is connected to the processes in which the higher excited states are involved. The mechanism of these processes is under studying.

References

(1) XU Wu, ZHANG Xin-yi (H. Chang), XU Xu-rong Luminescence and Display Devices, 1983, NO.2,1; 1983, NO.4,14.

(2) M. Yokota and O. Tanimoto, J. Phys. Soc. Japan, 22(1967),779.

(3) Inokuti and F. Hirayama, J. Chem. Phys. 43(1965), 1978.

Up-converted ultraviolet emission in Pr^{3+}:LaF_3; Arturo Lezama, Anderson S.L. Gomes, Cid B. de Araujo and J.R. Rios Leite; Departamento de Física, Universidade Federal de Pernambuco, 50000 Recife, Brasil.

Ultraviolet (U.V.) pair emission in PrF_3 has been reported recently (1). We show here that it can take place even at very low Pr^{3+} concentration in LaF_3 via an up-conversion energy transfer.

Pr^{3+}:LaF_3 is well known (2-4) for presenting blue fluorescence associated with the emission from the ^3P_o level of Pr^{3+}, when iluminated by a resonant laser around the $^4H_4(1) \rightarrow {}^1D_2(2)$ (~16900 cm^{-1}) transition. Impurity pairs, absorbing and interchanging energy, are responsible for this up-converted emission. We report here, for the same excitation conditions the first observation of U.V. generation in this material.

Experiments were carried out on 0.1% and 0.5% Pr^{3+} concentration crystals (Optovac) at 20K. Excitation were 0.4 cm^{-1} linewidth pulses from a NdYAG pumped dye laser. The linearly polarised laser beam propagates parallel to the c-axis. Fluorescence was collected sideways and analysed by a double monochromator or directly detected through broad band filters. Boxcars integrators were used allowing simultaneous observation of time resolved excitation spectra of the U.V. and blue fluorescences.

The table below shows the observed U.V. wavelengths, the corresponding pair transitions and relative intensity to the blue fluorescence. Observing only such lines is in reasonable agreement with a transition probability calculation assuming dipole-dipole ion interaction. Notice that stronger allowed dipole-quadrupole transition at 3964 and 4336 Å were not observed.

Wavelength (Å)	Pair transitions	I(U.V.)/I(blue)
3527 ± 1	$^3P_0 + {}^1G_4(1) \rightarrow {}^3H_5(2) + {}^3H_4(2)$	7×10^{-6}
3533 ± 1	$^3P_0 + {}^1G_4(1) \rightarrow {}^3H_5(3) + {}^3H_4(2)$	
3801 ± 1	$^3P_0 + {}^1G_4(1) \rightarrow {}^3H_6(2) + {}^3H_4(2)$	3×10^{-6}
3805 ± 1	$^3P_0 + {}^1G_4(1) \rightarrow {}^3H_6(3) + {}^3H_4(2)$	

The intensity dependence is quadratic for both fluorescences. As shown in the figure the U.V. excitation spectrum around the $^3H_4(1)$ to $^1D_2(2)$ transition have a satellite structure similar to the blue one (5) indicating that the two emissions arise from two photon absorption by impurity pairs. For most of the satelite lines the U.V. time evolution is faster than the blue one. For the 0.1% sample, the contribution from the isolated ions frequency to the U.V. excitation spectrum is large and dominates the spectrum even at short delay times (~1μs).

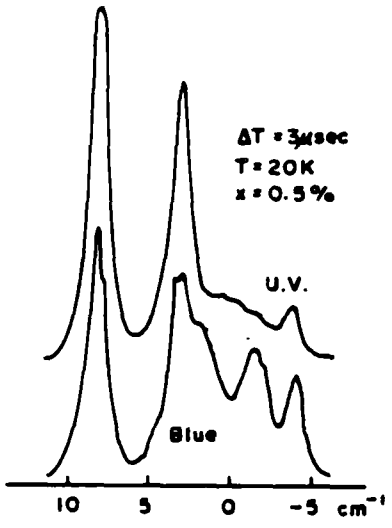

Our observation of U.V. emission is in agreement with the up-conversion mechanism proposed in Ref.(3) to explain the blue emission. However differences in the concentration and time evolution between both lights require further investigation currently under way.

References:

(1) S.C. Rand, L.S. Lee, A.L. Schawlow. Optics Commum 42, 179 (1982).

(2) D.J. Zalucha, J.C. Wright, F.K. Fong. J. Chem. Phys. 59, 997 (1973).

(3) J.C. Vial, R. Buisson, F. Madeore, M. Poirier. J. Physique 40, 913 (1979).

(4) S.T. Lai, Shihua Huang, W.M. Yen. Phys. Rev. B 26, 2349 (1982).

(5) R. Buisson, J.C. Vial. J. Physique Lett. 42, L-115 (1981).

Energy Upconversion and Energy Transfer Processes in $LaF_3:Nd^{3+}$

by

Putcha Venkateswarlu
Department of Physics, Alabama A&M University
Normal, Alabama 35762

and

B. R. Reddy
Department of Physics, Indian Institute of Technology,
Kanpur 208016, India and National Research Council.
Ottawa, Canada KIA OR6

On resonant excitation of the D levels of $LaF_3:Nd^{3+}$ with a tunable dye laser, fluorescence is observed from the R, S, A, D, E, K and L levels of which the last three levels are higher than the D levels. It has been reported by the authors[1] recently that both sequential two photon excitation process (STEP) and energy upconversion process (ETU) are responsible for the population drain mechanism from the lower D levels to the higher L level. In the present paper, the fluorescence from the R, S, and E levels and the processes through which they are populated will be discussed. Excitation spectra of the fluorescence from the R, S, and E levels have been recorded using the tunable laser excited by N_2 laser. The decay times for the D, R and S levels for three different concentrations 0.5, 2.0 and 5.0 percent by weight of Nd^{3+} have been determined. The decay times for R and S come out to be equal and they are 600, 400 and 150μs respectively for the three concentrations respectively. The fluorescence spectrum from the R level has been studied for concentrations of Nd^{3+} (0.1, 0.5, 2.0 and 5.0 percent by weight). The intensity increases as the concentration increases from 0.1 to 2.0 percent and then it decreases when the concentration becomes 5.0 percent. These studies indicate that the R level gets populated and depopulated through ion pair relaxations. The S levels are found to be populated due to thermal contribution from R levels. The two processes STEP and ETU are possibly responsible for the population of E level in the same manner as for the L level.

---

1. B. R. Reddy and P. Venkateswarlu, J. Chem. Phys. 79,5845 (1983).

FLUORESCENCE LINEWIDTHS AND EXCITATION TRANSFER IN $Eu_{0.2}Tb_{0.8}P_5O_{14}$ CRYSTALS

I. Laulicht, S. Meirman and B. Ehrenberg
Department of Physics, Bar-Ilan University,
Ramat-Gan

Laser induced fluorescence spectra of $Eu_{0.2}Tb_{0.8}P_5O_{14}$ crystals is studied at various temperatures in the 40-550°K range:

a) Linewidth (steady state) experiments

Fluorescence linewidth experiments show that the linewidths of the $^5D_0 \rightarrow {}^7F_1$ triplet of Eu^{3+} change linearly with temperature in the 300-500°K range and do not demonstrate critical behaviour near the ferroelastic phase transition which is expected to occur at about 440 K in this crystal. Such a phase transition is accompanied by a strong reduction of the sound velocity, v, of some of the low $\vec{q}$ acoustic modes[1], and an enormous increase of the linewidths $\Delta\nu$ is expected, at first sight, near T_c on account of $\Delta\nu \propto v^{-5}$ dependence[2]. A possible explanation for this discrepancy is that the effective sound velocity which governs $\Delta\nu$ is governed by the sound velocities of the high q modes which are very similar to those of the low q modes only in the temperature range where the Debye approximation is valid[3].. In the present crystal the high q modes are hardly affected by the phase transition. Moreover, the contribution of the soft mode velocity to the directional average of v is quite small in low symmetry crystals[3].

b) Energy transfer (pulsed) experiments

The $^5D_4$ manifold of Tb^{3+} is excited selectively by a dye laser and the energy transfer from this manifold to the $^5D_0$ level of Eu^{3+} is studied by the time resolved spectroscopy technique. The rise time of the emission from the $^5D_0$ level and the decay time of the $^5D_4$ manifold are very similar. A large change of these times with temperature (2.5 msec at 50K and 0.6 msec at room temperature) is observed. The time development of the excitation transfer is studied in detail and compared with recent theoretical models[4].

It is of interest to note that at room temperature there is a spectral overlap between the $^5D_4 \rightarrow {}^7F_4$ emission lines of Tb^{3+} and the $^7F_1 \rightarrow {}^5D_0$ absorption lines of Eu^{3+} and the transfer is certainly via the thermally populated $^7F_1$ level. At low temperature the excitation transfer is phonon assisted. No emission from the $^5D_1$ level of Eu^{3+} could be observed in the

present work. Neither has such an emission been reported by other workers[5] who studied the $^5D_4(Tb) \rightarrow {}^5D_0(Eu)$ transfer via the $^5D_4$ manifold in other systems. Emission from the $^5D_1$ manifold of Eu is observed however, very clearly in the present system when the Eu ions are excited directly. We can therefore exclude the possibility of a Tb → Eu transfer through this manifold since if this would be the case one would expect that the $^5D_1$ emission would have been observed. It seems therefore that the transfer is via the (a) $^5D_4(Tb) + {}^7F_0(Eu) \rightarrow {}^7F_4(Tb) + {}^5D_0(Eu) + 120 cm^{-1}$ interaction and not via the (b) $^5D_4(Tb) + {}^7F_0(Eu) \rightarrow {}^7F_5(Tb) + {}^5D_1(Eu) + 600\ cm^{-1}$ interaction.

This conclusion is interesting since the oscillator strengths of the transitions which are involved in (b) are larger by a factor of ten than the corresponding ones in (a), and the electron phonon couplings are also expected to be much larger. On the other hand the energy gap in (a) is smaller by a factor of five. It is consistent with the empirical rule[6] by which the dominant factor in phonon assisted excitation transfer between rare-earth ions is the energy mismatch between the participating levels and not the strengths of the specific transitions or the specific electron phonon coupling.

1) G. Errandonea, Phys. Rev. B21 5221 (1980)
2) J. Pellegrino and W.M. Yen, Phys. Rev. B24 6719 (1981)
3) I. Laulicht and D.L. Huber, Ferroelectrics (in press)
4) a. D.L. Huber in Laser Spectroscopy of Solids Ed. W.M. Yen and P.M. Selzer (Springer Verlag Berlin 1981) p. 83
   b. D.L. Huber, J. of Luminescence 28 475 (1983)
5) a. L.G. Van Uitert, Proc. Int. Conf. Luminescence (Budapest) p. 1588 (1966)
   b. J. Chrsochoos, J. of Luminescence 9 79 (1974)
6) N. Yamada, S. Shionoya and T. Kushida, J. Phys. Soc. Japan 32 1577 (1972)

Energy Transfer Phenomena in Lanthanide Metaborates (LnB_3O_6)

Hao Zhiran and G. Blasse,
Physical Laboratory, State University,
P.O. Box 80.000, 3508 TA Utrecht,
The Netherlands

The lanthanide metaborates LnB_3O_6 contain chains of composition $[B_6O_{12}]^{6-}_{\infty}$ which are linked together by the lanthanide ions. These ions are situated in a distorted ten-cornered polyhedron. These polyhedra, linked together by their common oxygen edges, form infinite layers (1). The shortest Ln-Ln distance is about 4 Å. Here we wish to report that these compounds are excellent host lattices for efficient luminescent materials.

The key position is for GdB_3O_6, because the Gd^{3+} ions form a sublattice in which excitation energy can easily migrate (via the $^6P_{7/2}$ level). The transfer rate exceeds the radiative rate by a factor of about 10^4. Because the absorption transitions of the Gd^{3+} are strongly forbidden, it is necessary to find a suitable sensitizer for the Gd^{3+} ions. We have found that Bi^{3+} and Ce^{3+} are very effective for this purpose. Their emission overlaps favourably with the Gd^{3+} $^8S \rightarrow {}^6P$ transitions. In fact these ions do not emit in GdB_3O_6, but they can be studied in LaB_3O_6.

The sensitized GdB_3O_6 samples can now be excited effectively. The fate of the migrating excitation energy depends on the impurities in the host lattice. For ultrapure GdB_3O_6, Gd^{3+} emission is observed. Small amounts of Eu^{3+} and Tb^{3+}, however, can trap very easily the migrating energy. Only at very low temperatures the migration is hampered due to the inhomogeneous broadening of the Gd^{3+} levels. At the sensitizer and activator concentrations applied, the energy transfer

between these two in the lanthanum compound is far from complete, which illustrates the intermediary role of the Gd^{3+} ions.

The several transfer rates and their mechanisms will be evaluated and discussed. Some results on Sb^{3+} activation will be given. Finally we note that the Bi^{3+} ions in these lattices can form pairs with a different emission. This excludes their role as a sensitizer.

References

1. G.K. Abdullaev, Kh. S. Mamedov and G.G. Dzhafarov, Sov. Physics Crystallography 20, 161 (1975); 26, 473 (1981).

Energy transfer studies of Nd^{3+} doped borate glass

S.C. SEN
Department of Physics
Indian Institute of Technology, Kanpur-208016, India

The results of X-ray diffraction and energy transfer studies of glass with composition $14K_2O$, 2KCl, $85B_2O_3$ with Tl^+, Mn^{2+} and Nd^{3+} have been reported. In absorption studies, an absorption edge at 280 nm and bands with peaks at (310 and 355 nm) are obtained for 0.25%, Tl^+ in the glass. These bands (310, 355 nm) are quenched by the addition of Mn^{2+} (1.25%). Addition of Nd^{3+} (1%) with Tl^+ and Mn^{2+} introduces new bands which grow in intensity very rapidly and for Nd^{3+} (5%) the bands with peaks at 570,600 and 750 nm are found to saturate in intensity. The band responsible for laser action at 870 nm ($^4I_{9/2} - {}^4F_{3/2}$) is found to split in two sublevels with a difference of 140 cm^{-1}. The emission spectra when excited with 265 nm shows four bands with peaks at (330, 365, 420, 600 nm) for Tl^+ (0.25%) and Mn^{2+} (0.25%) in the glass. Introduction of Nd^{3+} (5%) enhances the growth of long wave length bands at the cost of 330 nm. No emission in the visible region could be recorded when excited by Neodymium absorption bands even with the laser source. The ordered region of alkali borate glass is found to be (15-20 $\overset{o}{A}$).

Concentration Quenching in Nd-Doped Glasses

S. E. Stokowski
Lawrence Livermore National Laboratory

L. Cook, H. Mueller
Schott Glass Technologies, Inc.

M. J. Weber
Office of Basic Energy Sciences
Department of Energy

Summary

We have measured Nd fluorescence lifetimes versus Nd concentration (ρ_{Nd}) in a large variety of pure, water-free glasses. The Nd self-quenching rate varies as ρ_{Nd}^n where $1<n<3.3$, its value depending on glass structure.

We are investigating concentration quenching in Nd-doped laser glasses with hopes of finding glasses with long fluorescent lifetimes at high Nd concentrations. Our purpose in this work is to elucidate the physical mechanisms for concentration quenching and how they are controlled by the Nd spectroscopic properties and glass structure.

We measured Nd fluorescent lifetimes as a function of Nd concentration in several silicate glasses and many phosphates. The glasses were almost water-free and low in transition-metal impurities which strongly quench the Nd fluorescence. We also took care to eliminate the effects of radiation trapping by fabricating a special sample, which consisted of cylinders of less than 1 mm^3 volume and radiatively isolated from each other by absorbing optical cement.

We find that the magnitude of concentration quenching in silicate glasses is proportional to the strength of the $^4F_{3/2}$ to ^4I transitions. In most cases the self-quenching rate (W) is proportional to a power law in the Nd density, $W = a\rho^n$. The power n is commonly 2, as predicted by the dipole-dipole interaction theory at low concentrations. (See Table.) However, we observe n = 3.3 for LG-650 silicate glass.

Phosphate glasses, in contrast to silicates, have $1<n<2$. Some ultraphosphates have Nd self-quenching rates that are only slightly higher than linear in the Nd concentration. These glasses have lifetimes greater than 200 μs at 10^{21} Nd ions/cm^3.

We studied the compositional variations of UP16 and UP91. Most substitutions resulted in an increase in the quenching rate; however, adding B_2O_3 is effective in decreasing this rate.

The lower self-quenching rate in phosphates is due to the local structure, which maintains a large distance between Nd ions. This large Nd-Nd distance in ultraphosphate glasses is suggested by the measured Nd-Nd distances in their crystalline analogues. Our measurements show that the quenching rates in glasses and crystals of the same composition are nearly the same indicating that the local structures of the ordered and amorphous materials are similar.

Table

Concentration Quenching of Nd Fluorescence in Glasses

Glass	Lifetimes (μs) at Nd Concentrations ($10^{20}cm^{-3}$) <0.5	10	Quenching Rate ($W = \rho^n$) exponent, n
Silicates			
LG-670	360	55	2
LG-660	560	70	2
LG-650	850	400	3.3
Phosphates			
LG-750	390	140	2
$65P_2O_5$-$23K_2O$-$12La_2O_3$ (UP16)	390	210	1.1
$68P_2O_5$-$12Al_2O_3$-$14K_2O$-$6La_2O_3$ (UP91)	380	188	1.6
$69P_2O_5$-$12.5B_2O_3$-$12.5K_2O$-$6La_2O_3$ (UP 99)	380	214	

Energy Transfer in Ytterbium Doped Inorganic Glasses

R. T. Brundage and W. M. Yen

Dept. of Physics, Univ. of Wisconsin-Madison, Madison, WI 53706

Energy transfer in glasses has been a topic of interest for some time,[1] but due to experimental and theoretical difficulties there has not yet been a satisfactory description of the processes involved. We have carried out time-resolved fluorescence line narrowing (TRFLN) experiments over a range of temperatures in Yb^{3+} doped inorganic glasses in an attempt to help resolve this problem.

Yb^{3+} ions have several properties which make them attractive for use in energy transfer studies. As the heaviest of the lanthanides, ytterbium has a simple spectrum consisting of two crystal field multiplets separated by about 10,000 cm^{-1}. The crystal field splittings within the multiplets are large enough that the levels are well separated in glass hosts despite the large inhomogeneous broadening due to the random nature of the local fields. The lifetime of the excited state is relatively long (>1 ms), so that time resolved measurements are not difficult.

The wavelength of the Yb^{3+} fluorescence transition at around 1μm is in an experimentally difficult region both for excitation and detection, so that to date there have been few studies conducted on Yb^{3+} doped systems.[2] We have developed a high peak power (15kw), narrow band (<1Å) pulsed color center laser to carry out TRFLN experiments on Yb^{3+} in glasses. Using a LiF crystal containing F_2^+ centers, tunable laser emission has been obtained from .88μm to 1.0μm, covering the transitions of interest. A Varian VPM 159 photomultiplier with an InGaAsP photocathode was used to detect the

fluorescence. Examples of TRFLN spectra obtained with this system are shown in Fig. 1.

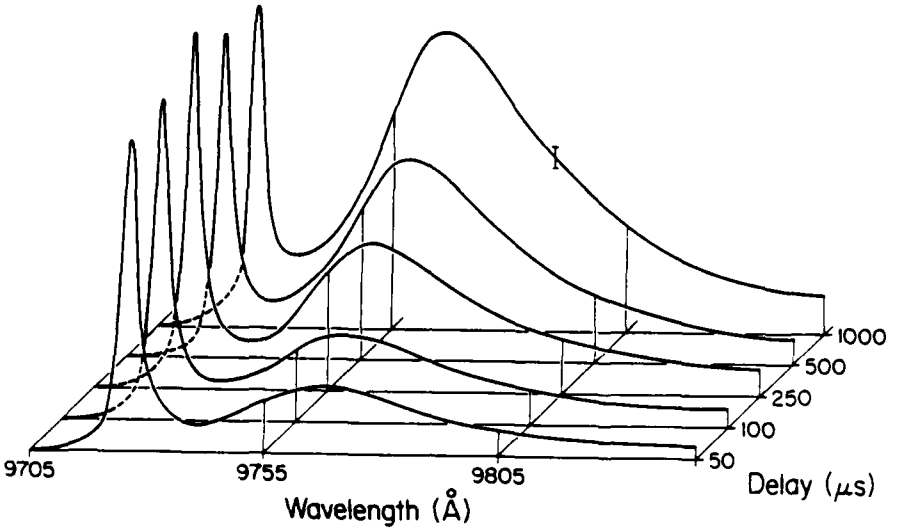

Fig. 1 Fluorescence intensity in number of photons vs. wavelength for increasing delay after laser excitation at 9728Å, for 1.0 molar % Yb_2O_3 in silicate glass at 15K. Intensity scale is arbitrary and compensates for the overall decrease in intensity with delay.

The TRFLN spectra along with data on the inhomogeneous profile and the lifetime of the excited state can be used to test models of energy transfer. We will discuss the ability of current energy transfer theories to explain the observed behavior of the Yb^{3+} glass system.

References

1. M. J. Weber, "Laser Excited Fluorescence Spectroscopy in Glass" in Laser Spectroscopy in Solids, eds. W. M. Yen and P. M. Selzer (Springer, Berlin, 1981).

2. M. J. Weber, J. A. Paisner, S. S. Sussman, W. M. Yen, L. A. Riseberg and C. Brecher, J. Lumin. 12/13, 729 (1976).

Energy Transfer and Concentration Quenching for Cr^{3+}- and Yb^{3+}-doped Lithium Lanthanum Phosphate Glass

W.J. Miniscalco

GTE Laboratories Incorporated, 40 Sylvan Road, Waltham, MA 02254

The quantum yield of Cr^{3+} is low in all glasses for which it has been determined, but rare earth ions in glasses typically have high quantum yields. Thus, co-doping Cr^{3+} with a rare earth is an attractive approach to improving the overall efficiency of glass lasers and flat panel luminescent solar concentrators. To be effective, the Cr^{3+} → rare earth energy transfer must be rapid compared to the Cr^{3+} decay rate. We have investigated Cr^{3+} → Yb^{3+} energy transfer and concentration quenching for singly and doubly doped lithium lanthanum phosphate glass. This glass composition was chosen because it has been found to be a suitable host for increasing the overall efficiency of Nd^{3+} when co-doped with Cr^{3+}.[1] Our results indicate that rapid Cr^{3+} → Yb^{3+} energy transfer occurs in this glass. However, for dopant levels at which energy transfer dominates the Cr^{3+} relaxation, significant Yb^{3+} concentration quenching is found.

Because the only *f*-shell excited state of Yb^{3+} is the relatively low-lying $^2F_{5/2}$ manifold, the spectral overlap between Cr^{3+} emission and Yb^{3+} absorption is relatively poor and one expects energy transfer to be less effective than in the Cr^{3+} - Nd^{3+} system. The extremely low-ligand-field sites present in phosphate glasses, however, offset this mismatch and lead to significant Cr^{3+} - Yb^{3+} coupling. The Cr^{3+} decay is nonexponential for all concentrations and an effective lifetime τ^* was calculated for purposes of analysis. For

a fixed Cr^{3+} concentration, varying the Yb^{3+} concentration changes τ^* by more than an order of magnitude. At the highest Yb^{3+} concentrations investigated (3 mole %), however, concentration quenching also reduced the Yb^{3+} lifetime by as much as a factor of 5.

For the lower Cr^{3+} concentration samples (0.05 mole %), energy transfer was only significant within the first decade of decrease in Cr^{3+} luminescence intensity. The higher Cr^{3+} concentration samples (0.3 mole %) were quenched by Yb^{3+} uniformly over three decades of luminescence intensity. We attribute this difference in behavior to fast $Cr^{3+} \rightarrow Cr^{3+}$ energy transfer between high- and low-ligand-field sites in the more concentrated samples. This effectively couples the entire Cr^{3+} population to Yb^{3+} through the low-field sites. In the less concentrated samples only the short-lived, low-field sites which are directly coupled to Yb^{3+} are quenched. This leaves unaffected the longer-lived, shorter-wavelength sites which dominate the luminescence after the first decade of decrease. Since the low-field sites which are directly coupled to Yb^{3+} also have the lowest quantum yield, proper selection of concentrations may produce a co-doped system with higher efficiency than a singly doped system.

No direct evidence of $Cr^{3+} \leftarrow Yb^{3+}$ back-transfer was found. Exciting the $^2F_{5/2}$ manifold of Yb^{3+} directly did not produce Cr^{3+} luminescence. Nevertheless, a shortened Yb^{3+} lifetime was observed for a sample with a high Cr^{3+} concentration.

1. T. Harig, G. Huber, I.A. Shcherbakov, J. Appl. Phys. 52, 4450 (1981).

THE ENERGY TRANSFER IN MULTI-COMPONENT PLASTIC SCINTILLATORS

Yuan Huijun Wang Xiangtuo Ji Yuying Zhang Yuanli
Beijing Nuclear Instrument Factory, Nuclear Industry Ministry P. O. Box 8800 Beijing China

Summary. In the present work the energy transfer in four-dimensional polystryrene scintillators containing solute B-PBD, POPOP, Sg5 and RhB has been investigated. The scintillation procees in plastic scintillators containing primary and secondary solute has also been investigated by Birks (1.2). Here, more attention is point to the discussion of the energy transfer from secondary to fourth solute.

The absorption peak, the emission peak and the decay time excited by 300 nm violet ray of polystryrene scintillators containing single solute are listed in table 1.

Table 1

scintillators composition		absorp. peak	emis. peak	decay time
matrix	solute (mol/L)	(nm)	(nm)	(ns)
polystryrene	B-PBD (5.8×10^{-2})	300	385	1.50
"	POPOP (2.0×10^{-3})	360	420	1.56
"	Sg5 (4.4×10^{-4})	460	520	6.76
"	RhB (4.2×10^{-4})	550	595	5.94

The curve 1 in fig. 1 shows the emission spectrum of ternary scintillators. The curve 2 shows the emission spectrum of four-dimensional scintillators. The time resolved emission spectrum of four-dimensional scintillators are shown in fig. 2.

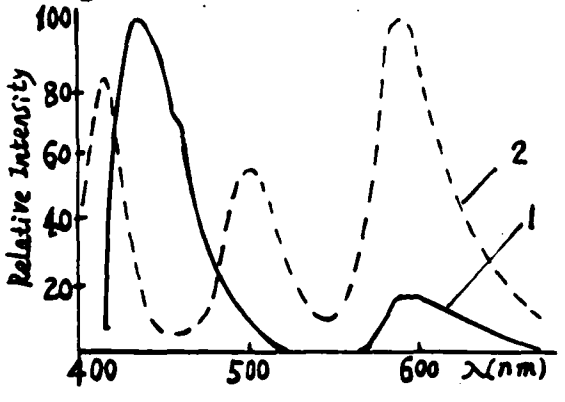

Fig. 1 The emission spectrum of the ternary scintillators (B-PBD 5.8 x 10^{-2} POPOP 2.0 x 10^{-3} and RhB 4.2 x 10^{-4} mol/L) and the four-dimensional scintillators (B-PBD 5.8 x 10^{-2}, POPOP 1.6 x 10^{-4}, Sg5 2.6 x 10^{-5} and RhB 6.7 x 10^{-5} mol/L).

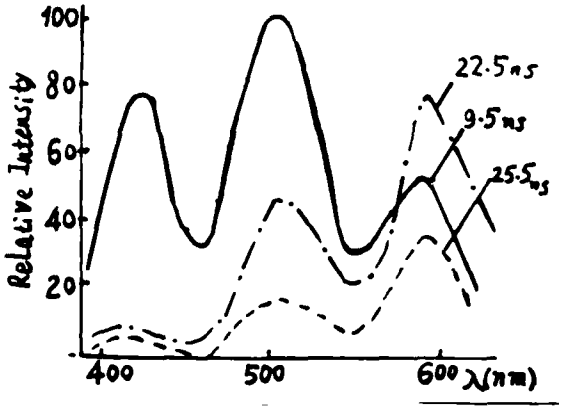

Fig. 2 The time resolved emission spectrum of four-dimensional scintillators (delay time 9.5 - 25.5ns excited by 300nm violet ray).

The relative luminescence intensity of red band in unitary, ternary and four-dimensional scintillators excited by γ ray and the various wavelength decay time excited by 300nm violet ray are listed in table 2.

Table 2

scintillators composition					decay time (ns)					rel.inten.of red band exci. by γ ray
matrix	solute (mol/L)				420(nm)	520(nm)		595(nm)		
	B-PBD	POPOP	Sg5	RhB	τ	τ_1	τ_2	τ_1	τ_2	
ps	—	—	—	4.2×10^{-4}	—	—	—	—	5.94	1.0
ps	5.8×10^{-2}	2.0×10^{-3}	—	4.2×10^{-4}	non-exponential decay				8.94	11.3
ps	5.8×10^{-2}	4.6×10^{-3}	4.4×10^{-4}	4.2×10^{-4}	1.9	3.02	4.54	4.95	5.97	23.6

ps - polystryrene

(1) By the comparison of curve 1 and curve 2 in fig. 1 it can be seen that the red emission band is greatly intensifed because of adding solute Sg5 to ternary scintillators. From fig. 2 we can see that the blue emission band is rapidly decreased, contrarily the red emission band is increased with the time delay. It is obvious that energy transfer occurs from polystryrene to solute B-PBD, POPOP, Sg5 and RhB in series.
(2) By the comparison curve 2 in fig. 1 and table 1 it is obvious that the blue emission peak (410nm) and the green emission peak (500nm) of four-dimensional scintllators are shifted to shorter waveleagth than those of the scintillators containing gingle solute POPOP or Sg5. It can be seen that the radiative transfer is dominant in four-dimensional scintillators containing little solute Sg5 and RhB.
(3) As indicated in table 1 and table 2, the decay time of the green emission band in four-dimensional scintillators is shorter than that of the scintillators containing single solute Sg5. It is proven that the long-range resonance transfer has occurred between the solute Sg5 and RhB.
(4) The fact that the solute RhB emission band is nonexponential decay shows diffusion transfer occur in ternary scintillators.

Reference

(1) J. B. Birks The Thory and Practice of Scintillation Counting Pergamon London 1964

(2) A. Hallam and J. B. Birks J. Phys.B: Atom Molec.Phys. vol. 11 (1978) 3273

Raman Scattering Resonant With Two Dimensional Excitons In Semiconductor Heterostructures

J. E. Zucker
Crawfords Corner Road - Room 4D-409
AT&T Bell Laboratories, Holmdel, N.J. 07733

There is much current interest in GaAs-(AlGa)As heterojunctions as model semiconductor systems of reduced dimensionality. One of the striking features of GaAs-(AlGa)As quantum well heterostructures is the strong enhancement of exciton properties. We have recently discovered that the resonant Raman scattering (RRS) method has novel applications in the study of quasi-two dimensional excitons in GaAs quantum wells. The resonantly enchanced Raman signal can be observed even in the presence of a large luminescence background. RRS also shows extremely high contrast as a spectroscopic tool for higher-lying exciton states where absorption and excitation spectroscopy are less effective. In addition, RRS provides new insight into the electron-phonon interactions and vibrational properties unique to this layered system. The Raman spectra show direct evidence of the degree of exciton localization within the quantum wells. Also, the shape of the resonant Raman profile can be used to determine exciton-phonon scattering channels. Polarization selection rules for the scattered light have established the effects of reduced dimensionality on the optical lattice vibrations and allow comparison between deformation potential and Frohlich exciton-phonon interactions.

SECONDARY EMISSION SPECTRA AND ENERGY RELAXATION OF POLARITONS IN LAYER POLAR SEMICONDUCTORS

Prof. M.S.Brodin, dr. I.V.Blonskii
Institute of Physics of the Akademy of Sciences of the Ukrainian SSR, Prospect Nauki 144, Kiev, USSR 252028

Our previous studies of integral characteristics of excitonic absorption bands in a number of typical layer semiconductors led us to some conclusions on the pecularities of relaxation mechanisms responsible for excitonic absorption. In particular, the nonlinear exciton-phonon interaction, indirect phototransitions and phonon anharmonism are all important (1). They are related to the pecularities in vibrational spectrum of layer crystals: the existence of bending waves in acoustic phonon spectrum and low-energy optical phonons (LOP) with $\hbar\omega = 1 \div 3$ meV due to extrinsic inter-layer vibrations.

We'll show in this report that LOP play a decisive role in formation of polariton emission spectra as well. These spectra were studied in typical ionic layer semiconductors, namely, 2H-polytype of PbI_2 and red modification of HgI_2. The strong interaction of light with excitons is their common property while LOP exist in HgI_2 only.

We've studied the polariton emission spectra at various $h\nu_{exc}$ and temperatures as well as the excitation spectra for various polariton bands. It was shown that in PbI_2 at $T < 55$ K and in HgI_2 at $T < 12$ K polariton emission developes at the early stage of relaxation when quasiequilibrium between polaritons and phonons is not achieved. The relaxation of high-energy polaritons $E_p > E_1$ is mainly due to dipole-active LO-phonons - 12 meV in PbI_2 and 3 meV in HgI_2. The relaxation path is the same for both compounds: upper branch - lower branch with subsequent relaxation along the lower branch for which the epectral density of states is higher.

Above the transition temperature T_t (12 K for HgI_2 and 55 K for PbI_2) polariton emission turns into thermalized luminescence. Aiming to better understanding of scattering processes

responsible for termalization of polaritons and the reasons for T_t to be didderent in two compounds, we've studied the spectra of resonant Brillouin scattering (RBS) when the sam - ples were excited into the region of mixed exciton-photon states. The measurements were performed at different T and energy detunings $E_p - E_t$. The most striking feature observed was the appearance of sharp anti-Stokes lines $L + E_{g3}$ (5318,7 Å) and $L + 2E_{g3}$ (5316,4 Å) - only in case of HgI_2 at $T \geqslant 12$ K. They are due to first and second-order scattering on LOP of E_{g3} symmetry and $\hbar\omega$ = 1 meV. Their presence in anti-Stokes region only exhibits the higher value of the density of final states for anti-Stokes processes as compared with Stokes ones. This is the first experimental proof of "thermal barrier" effect (2). Its contribution into polariton relaxation causes the effec-increase of lifetimes of polaritons prior to emission, so that the equilibrium of their temperature with lattice temperature is favored.

In 2H-polytype of PbI_2 the LOP are absent and the necessary "thermal barrier" is made by anti-Stokes scattering processes of polaritons from bottle-neck region which involves ordinary intra-layer optical phonons with $\hbar\omega$ = 6,8 meV.

Method of reversible spectral task used to calculate the frequency dependence of exciton-phonon coupling efficiency for several values of T. The qualitative difference on the final stage of polariton relaxation between PbI_2 and HgI_2 was demonstrated.

1. M.S.Brodin, I.V.Blonskii, B.M.Nitsovitch, Sol.St.Cem V 44, № 2, 1982
2. M.S.Brodin, S.V.Marisova, E.N.Miasnikov -Ukr.fiz.zhurnal, V.27, № 6, 1982

Time Resolved Spectroscopy of Excitons in Indirect Band Gap Superlattice Materials

B. A. Wilson and R. A. Logan
AT&T Bell Laboratories - 1D-465
600 Mountain Avenue, Murray Hill, N. J. 07974

and

G. E. Derkits and J. P. Harbison
Bell Communications Research, Inc.
Murray Hill, N. J. 07974

There is currently a great deal of interest in exciton states in semiconductor superlattice materials. Since these studies are driven primarily by possible applications in laser diode technology, this work has been restricted to direct band gap crystalline semiconductors, where large radiative matrix elements support laser action. It is likely, however, that materials with weaker radiative transitions provide a different, but equally interesting arena for study. Longer-lived excitons undergo more complete thermalization allowing studies of relaxation processes and ground state interactions. For example, in bulk materials it is in indirect band gap semiconductors where the condensation of electron-hole droplets has provided extensive information on exciton-exciton interactions. In this paper we shall discuss recent experiments in which we use time-resolved spectroscopy to probe the dynamics of exciton states in superlattice materials with long exciton lifetimes.

One of the systems commonly studied in the direct gap region is $Al_xGa_{1-x}As$ and the associated superlattice structures $GaAs/Al_xGa_{1-x}As$. Taking advantage of the extensive efforts to optimize these materials, we have studied the optical properties of $Al_xGa_{1-x}As$ in the indirect region above the $x \sim 0.45$ crossover point. Even at $x = 0.9$ we find exciton lifetimes in the bulk material $\sim$ 100 ns, indicating relatively few nonradiative recombination channels. The cw luminescence spectrum is dominated by a donor-acceptor pair

band, and trapping at these sites appears to be the primary mechanism for exciton decay. After pulsed excitation, time-resolved spectra of the bulk material reveal complex dynamics that depend on excitation density and temperature. Using two alloys above the crossover point, indirect band gap superlattice structures may be constructed from MBE grown layers of these materials. We shall discuss the effects of the two-dimensional quantization on the exciton dynamics.

Long lifetimes and efficient luminescence are also observed in superlattices constructed of a-Si:H/a-Si:N:H layers. We find no sharp structure associated with quantized two-dimensional states, but the broad spectrum is shifted uniformly to higner energy. Superlattice structures of $Si/Si_{1-x}Ge_x$ have also been studied. In a certain range of growth conditions the alloy layers grow lattice-matched to the Si creating a strained superlattice. Although these are indirect band gap materials with slow radiative recombination rates, the exciton lifetimes are limited by the presence of nonradiative channels that reduce the quantum efficiency by $\sim 10^4$ in the best materials available to date.

Quantum Size Effects and the Surface Photochemistry of Small Semiconductor Crystallites

L. E. Brus, AT&T Bell Laboratories, Murray Hill, NJ

Time resolved Raman scattering studies of the surface reactions of organic molecules adsorbed on colloidal semiconductor (TiO_2 and CdS) crystallites, following optical excitation of the crystallite, show that single electron redox reactions occur.[1] The vibrational structures of the initial transient species show negligible distortion due to adsorption on the crystallite surface. TEM micrographs of the CdS crystallites (zinc blende cubic) directly image the crystallite internal lattice. The crystallites are essentially excised fragments of the corresponding bulk lattices. As diameter decreases in the range 50 to 20Å, CdS and ZnS crystallites show an increasing blue shift of the optical absorption edge (exciton peak), by as much as 0.8 eV.[2,3] The exciton peak intensity also increases relative to the above gap absorption, as it shifts to higher energy. CdS crystallites of $\approx$ 45Å average dimeter show corresponding exciton shifts in the LO phonon Raman excitation spectra, and the relaxed fluorescence spectra. We interpret these observations as quantum size effects. That is, these crystallites are too small for the bulk band gap to completely form. The size dependence of the crystallite lowest excited state is modelled, without adjustible parameters, at the same level of approximation as in the Wannier bulk exciton Hamiltonian.[4] The exact Coulomb interaction between an electron and hole in a polarizable small crystallite is derived. The size dependences of the ionization potential and chemical redox potentials are also modelled.[5] Materials with strong chemical bonds involving the valence electrons, and hence small effective masses for holes and electrons at the band edges, should show significant quantum size effects.

References:

1) R. Rossetti, S. M. Beck, and L. E. Brus, J. Am. Chem. Soc. *106*, 980 (1984).

2) R. Rossetti, S. Nakahara, and L. E. Brus, J. Chem. Phys. *79*, 1086 (1983).

3) R. Rossetti, J. L. Ellison, J. M. Gibson, and L. E. Brus, J. Chem. Phy. *80*, (May 1984).

4) L. E. Brus, J. Chem. Phy. *80* (May 1984).

5) L. E. Brus, J. Chem. Phys. *79*, 5566 (1983).

Picosecond Studies on Phase and Energy Relaxation of Excitons in Semiconductors

Yasuaki Masumoto

The Institute for Solid State Physics, The University of Tokyo

Roppongi 7-22-1, Minato-ku, Tokyo 106, Japan

Picosecond relaxation processes of excitons are extensively studied in CuCl, CdSe and GaAs-AlAs MQW (multi-quantum well structures) by means of time-resolved induced absorption, luminescence and non-degenerate four-wave mixing. We have applied the picosecond time-resolved induced absorption and luminescence measurements to excitons in CuCl, CdSe and GaAs-AlAs MQW (Fig.1).[1-3] Aside from the typical nature of Wannier excitons in CuCl, excitons in CdSe and GaAs-AlAs MQW have distinct characters, such as strong piezoelctricity and two-dimensional disorder. The analysis of the experiments derives the distribution of excitons in the two-dimensional energy-time coordinates. Thus, energy relaxation processes of excitons in a variety of semiconductors are clearly visualized. Prior to energy relaxation, coherently generated excitons are considered to be dephased. Phase relaxation of excitons in CuCl is directly measured for the first time in the picosecond time domain by means of time-resolved non-degenerate four-wave mixing (Fig.2).[4] These new techniques will be demonstrated and the dephasing as well as energy relaxation mechanism of excitons and excitonic polaritons will be discussed.

References

1) Y.Masumoto & S.Shionoya: J. Phys. Soc. Jpn. 51, 181 (1982).

2) Y.Masumoto & S.Shionoya: Submitted to Phys. Rev. B.

3) Y.Masumoto, S.Shionoya & H.Kawaguchi: Phys. Rev. B 29, 2324 (1984).

4) Y.Masumoto, S.Shionoya & T.Takagahara: Phys. Rev. Letters 51, 923 (1983).

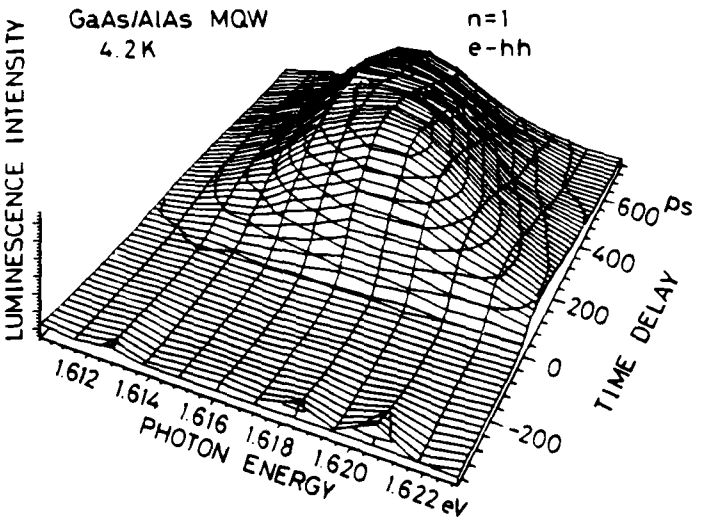

Fig.1. A bird's-eye view of energy- and time-resolved luminescence intensity of the excitons (n=1, e-hh) in GaAs-AlAs MQW (75 Å GaAs well, 33 Å AlAs barrier, 2.98 μm) at 4.2 K.

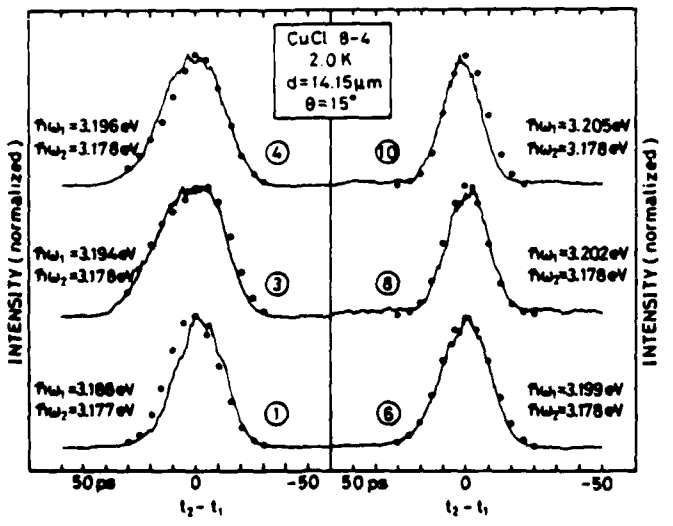

Fig.2. Intensity of the four-wave mixing ($2\omega_2-\omega_1$) beam emitted from a CuCl crystal as a function of the relative time delay between the ω_2 and ω_1 pulses, t_2-t_1.

FA4 Luminescence Recombination in Magnetron Sputtered a-Si:H, A. J. Rhodes, P. A. Shah, J. T. Searle, and R. H. Austin, University of Sheffield, United Kingdom. See FA3 for summary.

FA5 Exciton Hole Burning in GaAs/GaAlAs Multiquantum Wells, J. Hegarty, AT&T Bell Laboratories, and M. D. Sturge, Bell Communications Research Inc. See FE17 for summary.

THE EXCITATION DEPENDENCE OF THE PHOSPHORESCENCE OF PHENAZINE IN ETHANOL AT 77K

A.J.Kallir, G.W.Suter and U.P.Wild, Physical Chemistry Laboratory
Swiss Federal Institute of Technology, CH-8092 Zurich, Switzerland

The phosphorescence spectrum of phenazine in ethanol at 77K is strongly excitation dependent. In the spectra shown in fig. 1b three components may be recognized:

1. A very weak component A may be observed at about 15600cm^{-1}, i.e. at the blue edge of the phosphorescence spectrum. Its excitation spectrum is significantly different from that observed at 15370cm^{-1}, i.e. that of the main component (see fig. 1a).
2. The main component B with its 0-0 band at 15370cm^{-1}.
3. A weaker component C whose 0-0 phosphorescence band shifts to the red (down to about 15100cm^{-1}) upon excitation into the red edge of the absorption spectrum.

The phosphorescence spectra in different solvents revealed the following:

1. In 3-methylpentane (3MP) the phosphorescence exhibits the same features as observed for component A in ethanol: The 0-0 band (at 15680cm^{-1}) is blue-shifted relative to the main peak in ethanol and the excitation spectrum shows an energetically high position (25950cm^{-1}) of the first peak and a broad wing down to 24000cm^{-1}.
2. The spectrum in water-free ethanol clearly shows a dual structure and may be understood as a superposition of components A and B only.
3. In mixtures of ethanol with water, the contribution of component B increases with increasing water-content at the cost of component A. Above 5% water component A practically disappears, whereas the relative intensity of component C increases drastically.
4. In 2-methytetrahydrofuran (2MTHF) the phosphorescence spectrum is identical to that of component A in ethanol except for a small red-shift of about 40cm^{-1}.
5. None of the components results from protonated phenazine.

The phosphorescence decays obtained at excitation/emission wavelength pairs

which allowed a selective monitoring of the individual forms were strictly monoexponential. The lifetime of component A was nearly as long as that observed in nonprotic solvents (3MP: 12.6ms; 2MTHF: 12.2ms). On the other hand, the lifetimes of B and C show a significantly larger D-effect than that of A:

Lifetimes:	τ_A (ms)	τ_B (ms)	τ_C (ms)
in EtOH/H_2O	11.0 ± 0.1	9.1 ± 0.1	8.1 ± 0.1
in EtOD/D_2O	11.6 ± 0.1	10.5 ± 0.1	9.2 ± 0.1

This suggests the following assignments:

Component A: "free" phenazine molecules, i.e. molecules with no specific interaction to the solvent.

Component B: phenazine molecules forming one H-bond to ethanol (or to water, if present)

Component C: H-bond-complexes of phenazine with two solvent molecules, at least one of them being water.

Hence, several species, differing in their interaction to the protic surrounding may be found in the phosphorescence of phenazine in ethanol. Even in solutions containing 3% water, non-H-bonded species can still be observed.

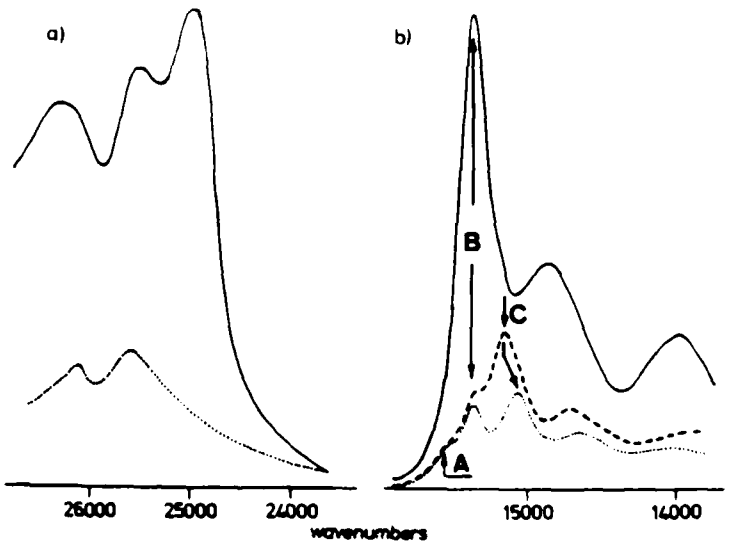

Fig.1: Phosphorescence of phenazine in ethanol (97%) at 77K:
a) excitation for
$\tilde{\nu}_{em}$= 15370cm^{-1} ——
$\tilde{\nu}_{em}$= 15600cm^{-1} .....
b) emission for
$\tilde{\nu}_{ex}$= 25000cm^{-1} ——
$\tilde{\nu}_{ex}$= 24370cm^{-1} - - - -
$\tilde{\nu}_{ex}$= 24210cm^{-1} .....
All spectra are normalized relative to the main band of component B.

THE ANALYSIS OF EXCITATION DEPENDENT LUMINESCENCE SPECTRA BY TOTAL LUMINESCENCE SPECTROSCOPY

G.W.Suter, A.J.Kallir and U.P.Wild, Physical Chemistry Laboratory
Swiss Federal Institute of Technology, CH-8092 Zurich, Switzerland

In Total Luminescence Spectroscopy (TLS) the luminescence intensity is recorded as a function of both the excitation and the emission frequency, yielding a two-dimensional spectrum (TDS) $I_{lum}(\tilde{\nu}_{ex},\tilde{\nu}_{em})$.

Most of the TLS literature deals with the quantitative analysis of multicomponent mixtures. However, excitation dependent emission spectra have been observed for many chemically pure compounds. In these cases a TDS provides all the information on the interdependence of emission and excitation simulaneously and greatly aids the analysis of the spectra.

Energy-selection effects are a well known origin of excitation dependent emission spectra at low temperatures. The TDS of pyrene in ethanol at 6K shows the typical features of E-selection spectra, i.e. a shift of the emission spectrum parallel to the excitation frequency. From fig.1 it is apparent, that the rather complicated spectrum obtained by exciting at 27380cm^{-1} consists of four subspectra originating from molecules being excited into different excited state vibronic levels.

Excitation dependent emission spectra due to interactions of the chromophor with the solvent are very common. Using TLS the edge excitation red shifts observed in the phosphorescence spectra of several N-heterocycles in alcohol were found to be due to H-bond formation (fig.2).

The site-pattern in Shpolskii-matrices depend on the electronic transition considered. The correlation between the individual lines in e.g. the S_{10}-S_{00}- and the T_{10}-S_{00}-multiplet may be easily visualized in a TDS, as is shown in the two-dimensional phosphorescence spectrum of benzophenazine in n-hexane at 4K (fig.3).

Furthermore, the case of different excitation spectra for fluorescence and phosphorescence as it is observed for N,N'-dimethylnitroaniline and the selective population of two different emitting triplet states in indanones have been characterized by TLS.

To summarize, TLS allows the representation of complex luminescence pro-

perties of a sample in a concentrated and easily interpretable form.

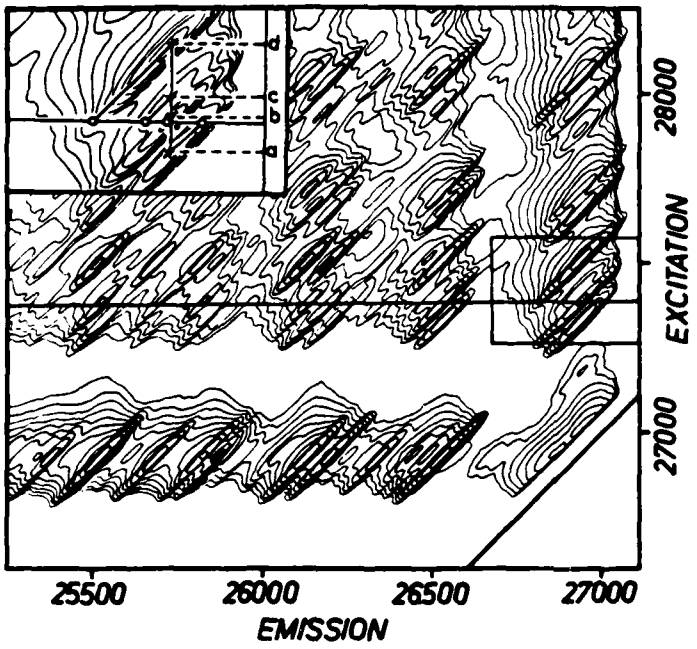

Fig.1:(left) E-selection spectrum of pyrene in ethanol at 6K. Inserted: Graphical assignment of the 0-0 bands in the emission spectrum obtained upon excitation at 27380cm^{-1} to various subspectra.

Fig.2:(right) Edge-excitation red shift of the phosphorescence spectrum of benzoquinoxaline in ethanol at 77K.

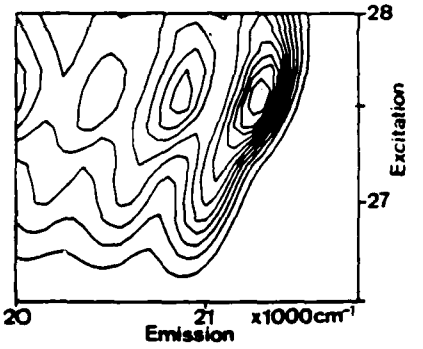

Fig.3:(below) Two-dimensional representation of the quasilinear phosphorescence spectrum of benzophenazine in n-hexane at 4K.

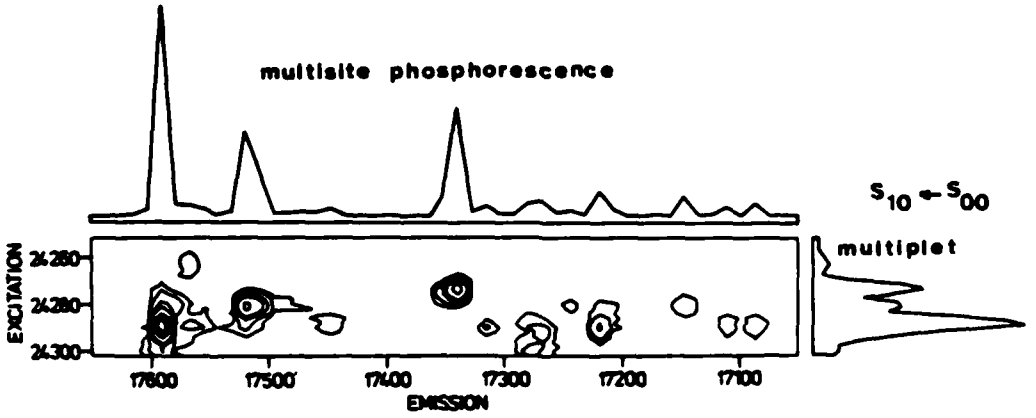

Investigations of the luminescence of N-alkenylcarbazoles and their charge-transfer complexes with 2,4,7-trinitro-9--fluorenone and 7,7,8,8-tetracyanoquinodimethane

Andrzej Janowski, Jadwiga Rzeszotarska, Włodzimierz Makulski Department of Chemistry, University of Warsaw, 02-093 Warsaw Pasteur Street 1, Poland, and Jerzy Ranachowski, Institute of Fundamental Technological Research, Polish Academy of Sciences, 00-049 Warsaw Świętokrzyska Street 21, Poland.

The effect of the quencher and length of the carbon chain on fluorescence quenching of N-alkenylcarbazoles with 7,7,8,8-tetracyanoquinodimethane (TCNQ) and 2,4,7-trinitro--9-fluorenone (TNF) was investigated. During quenching the maxima of fluorescence for N-vinyl-, N-allyl-, N-pentenyl-, and N-hexenylcarbazole, similar to each other, are slightly shifted towards higher wavenumbers. Qeunching of the carbazoles is also similar. However, it differs considerably for TNF and TCNQ, the differences having both qualitative and quantitative character. The fluorescence intensity of the carbazoles is almost equal to zero at the carbazole:TCNQ concentration ratio 1:1 whereas in the case of TNF a large excess of the quencher is needed. The quenching factor, both for TCNQ and TNF, increases with increasing carbon chain length. The quenching factor for TCNQ is almost of an order of magnitude higher than for TNF. This is due to higher electron-acceptor properties of TCNQ, compared with TNF, since the quenching is associated with formation of charge--transfer complexes. The qualitative differences in fluorescence quenching (Fig. 1) consist in changes of the shape of the fluorescence band on addition of TCNQ (appearance of a second maximum). On the contrary, this phenomenon is not

observed for TNF. In this case a decrease in the intensity of fluorescence is observed only. The formation of a second maximum in the fluorescence spectra indicates that during quenching with TCNQ the intensity of monomer fluorescence decreases more rapidly than that of excimer fluorescence. On the other hand, in the case of TNF the quenching constants of the two fluorescences are similar. Excitation in the charge-transfer band gives rise to the fluorescence spectrum of a composite character consisting of two subbands. The spectra are dependent on the wavelength of excitation. This indicates the formation of two different orien - tational isomers of the complex. The existence of such isomers in solution at room temperature reveals a fairly high potential barrier of rotation between them.

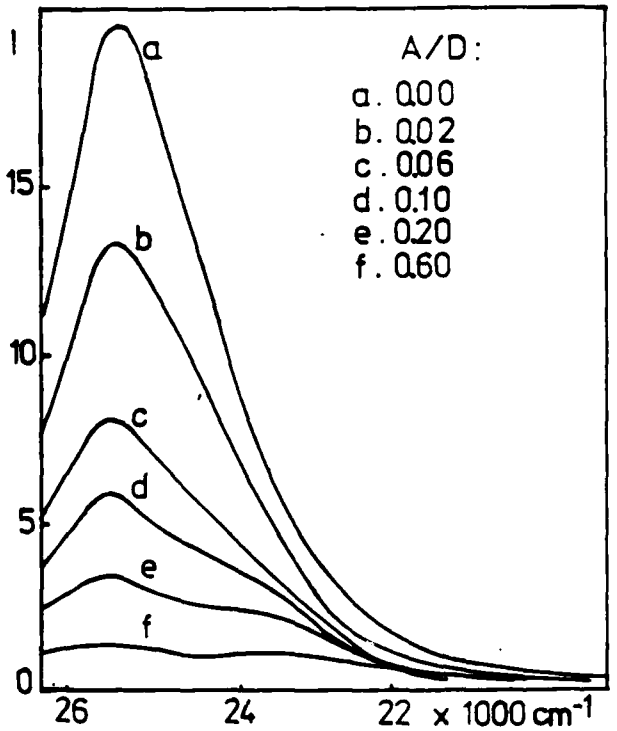

Fig. 1. Fluorescence spectra of allyl-carbazole (D) + TCNQ (A) in 1,2-dichloroethane

MULTIPLE FLUORESCENCE IN 1,8-DIHYDROXY, 6-METHOXY, 3-METHYL, ANTHROQUINONE AND 8-HYDROXY, 1,6-DIMETHOXY, 3-METHYL ANTHROQUINONE.

ASHUTOSH SHARMA
WELL-LOGGING (INTERPRETATION) SECTION
OIL AND NATURAL GAS COMMISSION
EASTERN REGION, NAZIRA,
ASSAM-785685, INDIA

SUMMARY

Environment dependent fluorescence spectroscopy has proved to be a valuable tool in studying primary photochemical processes. It is well established that excited state properties of a molecule may differ drastically from the corresponding ground state properties, due to the difference in charge distribution in the two combining states.

An intersting phenomenon is phototautomerism: as a result of charge transfer excitation, a molecule is protonated at one site and deprotonated at another site to form a tautomer. This often results in an anomalous large red shift of the fluorescence band. The importance of such phenomenon lies in the fact that the variety of simultaneous prototropic processes present, give rise to several fluorescencence bands, covering a broad region in the uv and visible spectrum. This in turn may provide the possibilities for broad band laser tuning.

Chromones, flavones etc. has been discovered capable of undergoing phototautomerism[1-3]. No studies for such type of process in anthroquinones has been reported sofar.

This paper presents the results obtained on naturaly occuring, 1,8-Dihydroxy, 6-Methoxy, 3-Methyl Anthroquenone (I),8-Hydroxy, 1,6-Dimethoxy, 3-Methyl Anthroquinone (II) and its methalated product 1,6,8-Trimethoxy, 3-Methyl Anthroquinone (III)

Fluorescence excitation and emmission spectra were recorded on Aminco-Bowman Spectrophotofluorometer. Compounds I-III were purified by preprative TLC and recrystallized from absolute ethanol. All the spectra were recorded at room temperature 20^{0}C. Absolute ethanol and analytical grade sulphuric acid were used.

All the title compounds are fluorescent in nutral solution On acidification, anthroquinones begins to fluoresce intensely. Compound(I) exhibits two excitation bands: at 290 nm and 450 nm, fluorescence bands at 350nm and 520 nm were observed (exci 290nm). For compound (II) three excitation bands, one each at 250 nm, 296 nm and 450 nm, were observed. Fluorescence bands at 350 nm and 580 nm (with shoulder at 520 nm),were observed for compound (II). For methelated product (i.e. III) only one fluorescence band at 350 nm (excitation 290 nm.) was observed.

Red shifted fluorescence bands (i.e. 520 nm and 580 nm bands, of I and II respectively) can not be from a normal molecule and were contributed to excited state exciplex or photo tautomer. Observ ations on compound (III) give strength to the inference drawn above.

REFERENCES

1. P. K. Sengupta and M.Kasha; Chem. Phy. Lett., 68, 382,(1979)
2. O. S. Wolfbeis and R.Schipfer; Photochem. Photobio.,34,567,(1981)
3. O.S.Wolfbeis and A.Knierzinger; Z. Naturforsch, 34a,51..,(1979)

Emission from Photoproducts of Benzene

A. N. Dharamsi and V. Shahmirian
Department of Electrical Engineering
Old Dominion University
Norfolk, VA 23508

In our investigation of charge-transfer complexes, we have observed emission from the photoproducts of benzene in the gaseous phase. KrF 248 nm radiation from an excimer laser was incident upon the experimental gases contained in a glass vessel with suprasil windows. Emission was detected in the orthogonal direction by a photomultiplier tube mounted at the exit slit of a monochromator. The incident energy at the input window at 248 nm was ~400 mJ (beam area ~2 cm^2, FWHM Δt~20 ns, FWHM $\Delta\nu$~5 nm). Benzene (Fisher, 99.95% pure, Thiophene $\lesssim$0.5 ppm) and O_2 (99.996% pure) were used without further purification. The cell was evacuated to pressures ~10^{-7} mbar and flushed out at least twice before experiments were performed.

In addition to the fluorescence expected from the benzene S_1 state at 263 nm and shorter wavelengths [1], we found emission at all wavelengths between 263-409 nm, peaking around 274 nm. The long wavelength cutoff of this radiation indicates that it is from a photoproduct of benzene since the latter has a T_1 state at 339 nm [1]. The lifetime of the observed emission is approximately 1.5 times that of the benzene S_1 state indicating further that the emitter is probably a singlet species.

Figure 1 shows the emission measured at 274 nm with 10 mbar benzene in the cell. The introduction of 2 mbar of O_2 substantially quenches the signal. The latter approaches the 248 nm pump profile as the partial pressure of O_2 is increased. Figure 2 shows the signal at 274 nm with 10 mbar benzene and 40 mbar O_2. Comparison with Figure 3, which shows the pump signal at 248 nm with the cell evacuated, shows that the signal at 274 nm follows the pump very closely. This indicates that the emitting species produced as a result of the 248 nm pump is quenched rapidly in the presence of excess O_2.

Photodissociation and photochemical rearrangement of benzene has been recorded by many researchers previously [2-5]. However, to our knowledge the emission noted above has not been reported. Further experimental and analytical work is required before the emitting species, which could be a photodissociative product or one of the products formed upon photochemical rearrangement of benzene [2,5] can be identified positively.

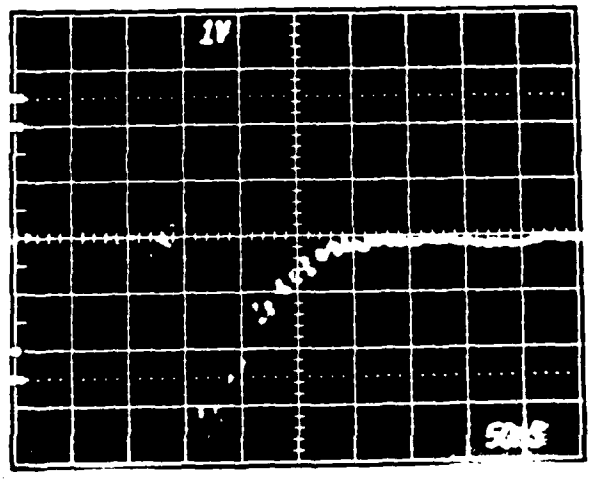

Fig. 1. Emission at 274 nm.

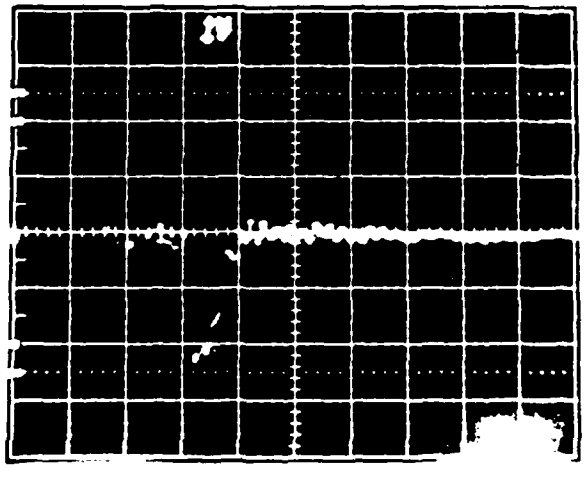

Fig. 2. Emission at 274 nm with 40 mbar O_2 Added.

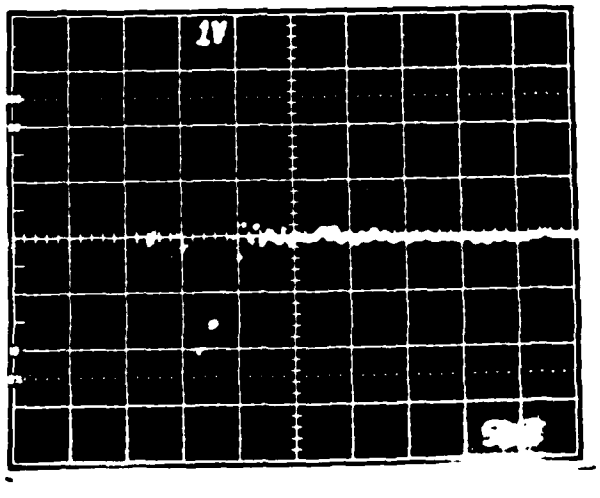

Fig. 3. KrF Pump Signal at 248 nm.

References

[1] N. Nakashima and H. Inoue, J. Chem. Phys., 73, 5976 (1980).

[2] J. E. Wilson and W. A. Noyes, J. Am. Chem. Soc., 63, 3025 (1941).

[3] J. K. Foote, M. H. Mallon and J. N. Pitts, Jr., J. Am. Chem. Soc., 88, 3698 (1966).

[4] H. R. Ward, J. S. Wishnok, P. Dwight Sherman Jr., J. Am. Chem. Soc., 89, 162 (1967).

[5] K. E. Wilzbach, A. L. Harkness and L. Kaplan, J. Am. Chem. Soc., 90, 1116 (1968).

The Dual Fluorescence of 9,9'-Bianthryl - A Study on Excited State Dipole Moments

Wolfram Baumann, Eckhard Spohr, Hilmar Bischof
Institute of Physical Chemistry, University of Mainz
Jakob-Welder-Weg 26
D 6500 Mainz, FRG

The influence of an external electric field on the intensity and spectral position of the fluorescence of solute bianthryl has been studied in various solvents of different polarity. Two different interpretations of the experimental results are given.

First it is assumed that bianthryl fluoresces from a single fluorescent state only. A consistent set of molecular data can be derived from the measurements, the most important result of which is

$\mu_a = 6 \cdot 10^{-30}$ Cm $\approx -\mu_g^{FC}$.

The Franck-Condon (FC) ground state dipole moment μ_g^{FC} has about the same small value as the excited state dipole moment μ_a, but shows opposite direction. Although exactly derived from the measurements, this result cannot be understood. Hence it must be assumed that the standard initial assumption that there is only one single state emitting is wrong. Strong support towards two emitting states comes from Grabowski et al [1], who already argued that there is an emission from a twisted internal charge transfer (TICT) state, rivaling with an anthracene - like local fluorescent transition, dependent on the solvent used. Rettig [2] showed that with some assumption and approximation two spectra can be deconvoluted. From the electrooptical emission measurements presented here it can be shown without any assumption that the fluorescence

of bianthryl consists of two superimposed fluorescence bands, even in non-polar and medium polar solvents. Full evaluation of the experimental material then shows that the results are consistent with the assumption of a non-polar anthracene-like fluorescing local excited state and a polar fluorescing (TICT) state, the dipole moment of which has been determined to be about $40 - 60 \cdot 10^{-30}$ Cm. This latter fluorescence process ends up with a FC-ground state with vanishing dipole moment, just as molecular symmetry claims for. Also, from these investigations, the energy difference of the two emitting states of an isolated bianthryl molecule is derived to be about 500 cm^{-1}. This is in agreement with the experimental fact that the fluorescence decay is merely single exponential, which means that the two emitting states are in thermal equilibrium.

An additional result of this paper: a formal interpretation of the solvent dependence of the primarily measured data as due to polarizabilities of one single fluorescent species generally might be wrong with molecules with near-by electronic states, where careful analysis of spectroscopic evidence for dual fluorescence is necessary.

References:

[1] Z.R. Grabowski, K. Rotkiewicz, A. Siemiarczuk, D.J. Cowley, W. Baumann, Nouveau J. Chim. 3, 443 (1979)

[2] W. Rettig, M. Zander, Ber. Bunsenges. Phys. Chem. 87, 1143 (1983)

Thermally Stimulated Luminescence of Irradiated Caffeine

M.S.Jahan, Physics Department, Memphis State University, Memphis, TN 38152
and D.W.Cooke, Los Alamos National Laboratory, Los Alamos, NM 87545

Summary

This study is part of a continuing investigation of the factors which affect radiation damage in methylxanthines, which are of immense biomedical importance. In order to gain knowledge regarding charge trapping mechanisms in caffeine (1,3,7-trimethylxanthine) we employed the well-known technique of thermally stimulated luminescence (TSL) and investigated the system in the temperature interval 77 - 300 K.

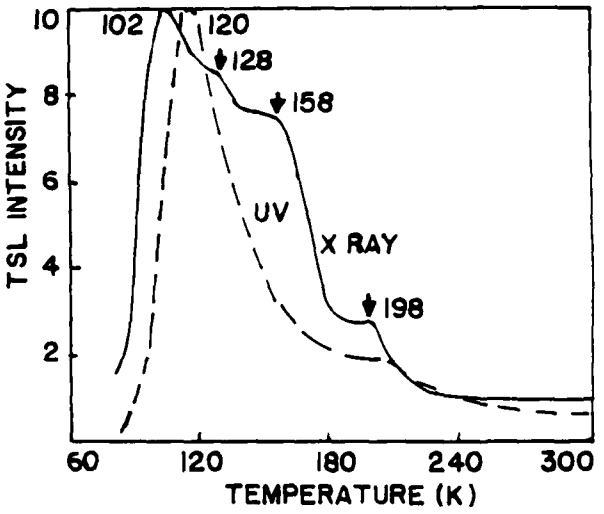

Figure 1. Typical glow curve of caffeine, x-irradiated (——) and uv-irradiated (----) at 77 K.

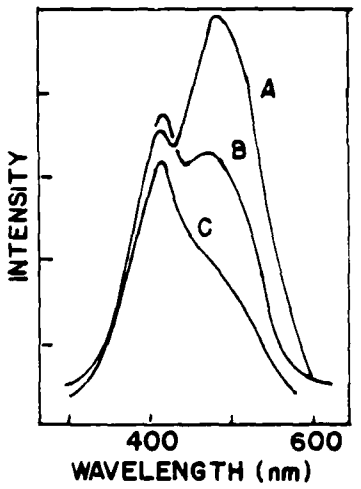

Figure 2. Characteristic emission spectra of caffeine at 110 K(A), 140 K(B) and 150 K(C)

Shown in Fig. 1 (solid line) is a typical glow curve of caffeine, x-irradiated (2.22×10^3Gy) at 77 K and subsequently heated to 300 K. A broad glow curve with peaks at 102, 128, 158 and 198 K was observed. The glow

peak parameters, such as activation energy (E), frequency factor (s) and heating rate (β), that describe each peak are as follows: 102 K (E = 90 meV, $s = 1.18 \times 10^2 sec^{-1}$ and $\beta = 0.042$ K sec^{-1}); 128 K (E = 126 meV, $s = 4.73 \times 10^2 sec^{-1}$ and $\beta = 0.058$ K sec^{-1}); 158 K (E = 165 meV, $s = 4.73 \times 10^2 sec^{-1}$ and $\beta = 0.050$ K sec^{-1}) and 198 K (E = 450 meV, $s = 8.50 \times 10^8 sec^{-1}$ and $\beta = 0.040$ K sec^{-1}). Also shown in Fig. 1 (dashed line) is a broad glow curve with a maximum at 120 K observed after uv-irradiation (λ = 254 nm) at 77 K. Identical emissions, centered near 405 and 470 nm, observed from x-ray- and uv-induced glow peaks, suggest that the final recombination mechanisms of trapped charges are the same in each case regardless of the thermal activation energies. The thermally released charges reside in metastable states (first excited singlet, S_1, and the first excited triplet, T_1) and subsequently decay to the ground state (S_0) giving rise to 405 and 470 nm emissions. The 405 nm emission is assigned to the $S_1 \rightarrow S_0$ transition, and the 470 nm emission to the $T_1 \rightarrow S_0$ transition. In the temperature regime below 158 K, the thermal process follows a first-order kinetics, whereas at or above 158 K, the probability of intersystem crossing for the charges residing in state T_1 increases and the decay process follows a mixed-order kinetics, viz., 1.3 for the 158 K peak and 1.8 for the 198 K peak. We believe that the decay of the 470 nm emission (see Fig. 2) is due to the intersystem crossing of charges from T_1 to S_1. Similar observation was made by Cooke, et al.[1] in the TSL study of L-histidine.

1. D. W. Cooke, S. L. Fortner and M. S. Jahan, J. Lumin., 26, 319 (1982).

LUMINESCENCE PROPERTIES OF ULTRA-PURE PYRIDINE

By

S. K. Ghoshal, A. K. Maiti and G. S. Kastha

Optics Department,

Indian Association for the Cultivation of Science

Jadavpur, Calcutta - 700 032,

India.

We report here for the first time the observation of both fluorescence and phosphorescence emissions from extensively purified samples of pyridine. An ultra-pure sample of pyridine was obtained through the following purification steps. E. Merck spectrograde pyridine was first treated with hydrochloric acid (GR grade) and the pyridine hydrochloride thus formed was subjected to repeated fractional distillation. The final middle fraction pyridine hydrochloride was then treated with sodium hydroxide. The pyridine liberated was fractionally distilled several times, dried over anhydrous sodium hydroxide, and finally fractionated before use. Pyridine when freed of impurities (viz., pyrazine) has been found to exhibit weak but readily observable fluorescence as well as phosphorescence emissions, both of π,π^* character, in its pure crystalline state and in a variety of glassy and crystalline matrices (e.g., benzene, cyclohexane, methylcyclohexane, ethanol and water) at 77 K. Phosphorescence of pyridine is characterized by a long phosphorescence lifetime ($\tau_p \sim 2$s) and a broad and structureless spectrum with $\lambda_{max} \sim 420$ nm. The fluorescence spectrum ($\lambda_{max} \sim 290$ nm) shows some vibrational structure in crystalline media. In addition to these S_2 (π,π^*) $\longrightarrow S_o$ and T_1 (π,π^*) $\longrightarrow S_o$ emissions, a very weak emission attributable to S_1 (n,π^*) $\longrightarrow S_o$ fluorescence (stretching a spectral region 310 - 350 nm) has also been observed in the emission spectrum of pyridine in rigid matrices. No fluorescence emission could be dected either in the vapor or in solution phase at room temperature.

The luminescence quantum yields and the phosphorescence lifetime of pyridine have been found to be sensitively dependent on the impurity content in the sample and on the rigidity and crystalline structure of the host medium. In glassy and relaxed hydrocarbon matrices (e.g., n-hexane, methylcyclohexane and 3-methylpentane) the luminescence intensity of pyridine is much weaker and its τ_p- value much shorter in comparison to those

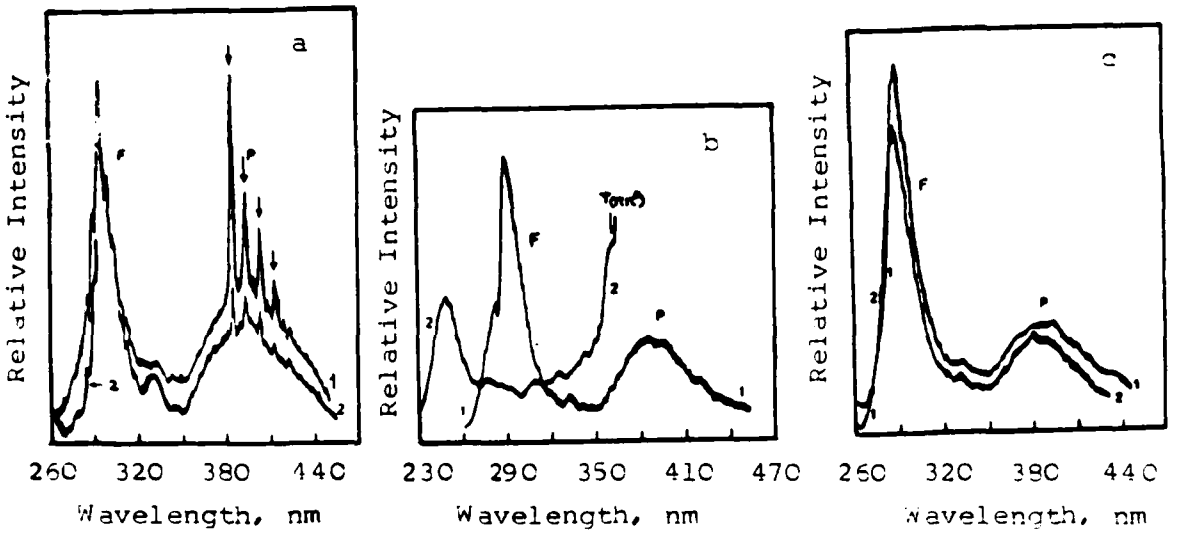

Fig. 1 Fluorescence (F) and phosphorescence (P) spectra of pyridine in various rigid matrices at 77 K: (a) in benzene, pyridine containing traces of pyrazine impurity (1), a more purified sample of pyridine (2), the sharp bands indicated by (↓) are the phosphorescence bands of pyrazine; (b) total emission (1) and phosphorescence excitation (2) spectrum of pure crystalline pyridine; (c) total emission spectrum of pyridine in water (1), in ethanol (2). The spectra were recorded on a Perkin Elmer MPF 44A Fluorescence Spectrophotometer, $\lambda_{excit.} \sim$ 250 nm.

observed in rigid polar media. The conditions under which emission from pyridine could be observed are : Both the solvent and solute should be completely freed of impurities and a more concentrated solution ($\geqslant 10^{-3}$M) should be used in rigid matrices at low temperatures.

PHOTOPROPERTIES OF DCM
(4-dicyanomethlene-2-methyl-6-p-dimethyl amino styrl-4H-pyran)

Michael Lesiecki, Federico Asmar
and Michael Drake
Chemistry Department
University of Puerto Rico
Río Piedras, PR 00931

The dye DCM(4-dicyanomethlene-2-methyl-6-p-dimethyl amino styrl-4H-pyran) is well known as a broadly tunable efficient laser dye and as an active element in luminescent solar concentrators[1,2]. Our interest has been to study the primary photochemical and photophysical process that are operative in this system.

We have identified the *cis/trans* isomers of DCM by magnetic resonance and liquid chromatographic techniques. We find that the *cis/trans* ratio is solvent and concentration dependant. A dark preparation of DCM yields only *trans* whereas ambient lights induce the primary step of photoisomerization to the *cis*. Using detector wavelength dependant ratios of the two isomers in HPLC we have deduced the absorption spectrum of each isomer as shown below.

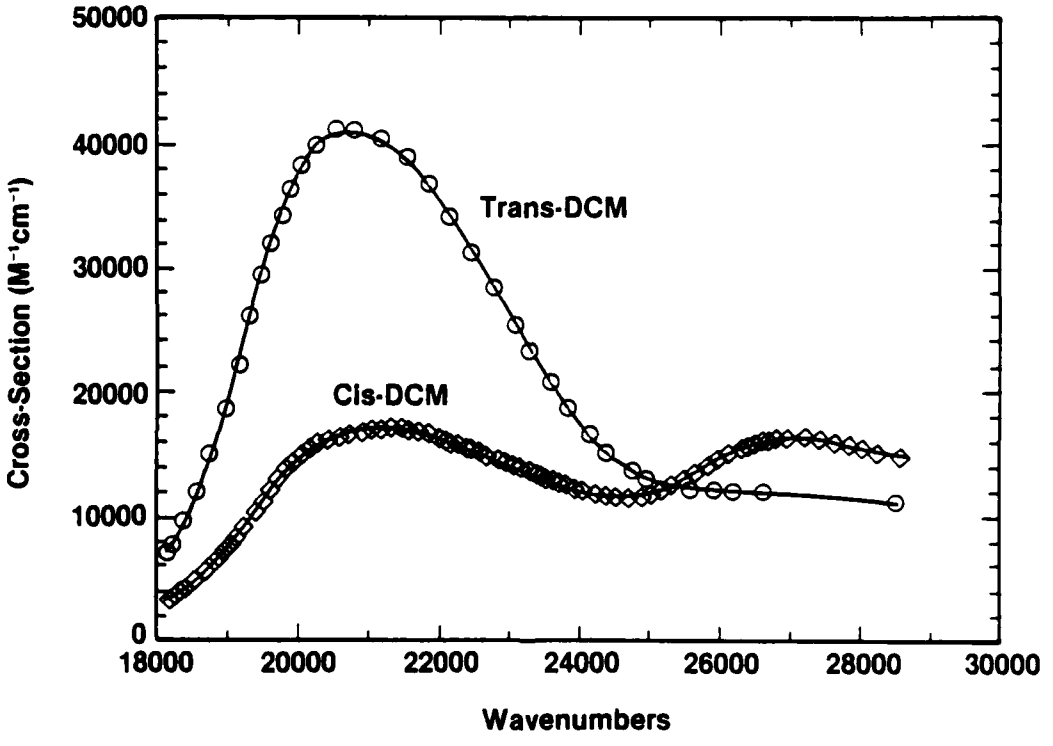

This quantitative demonstration of the *cis-trans* photoisomerization process is the main impact of this study.

Preliminary results on secondary photochemical branching are based on HPLC evidence following laser photolysis. We also find a dark reaction of *cis*-DCM to *trans*-DCM and *cis*-monomethyl-DCM. Our studies of the fluorescent quantum yield show a strong solvent dependance as the value of the yield ranges from 0.80 in DMSO to 0.35 in $CHCl_3$ at 10^{-4}M.

---

[1] E.G. Marason, Opt. Commun. 37, 56 (1981)

[2] J. Sansregret, J.M. Drake, W.R.L. Thomas and M.L. Lesiecki, Appl. Opt. 22, 573 (1983)

SITE SELECTION SPECTROSCOPY OF o- AND m-XYLYLENES AND THEIR METHYLATED DERIVATIVES IN SHPOLSKII MATRICES

V. LEJEUNE, A. DESPRES and E. MIGIRDICYAN

Laboratoire de Photophysique Moléculaire du CNRS
Bâtiment 213, Université Paris-Sud
91405 - ORSAY Cedex, FRANCE

The highly reactive o- and m-xylylenes and their methylated derivatives are biradicaloid species which exist as transient intermediates in chemical reactions. They result from the photodissociation of CH bonds on two different methyl groups of methylbenzenes. Many years ago, we have reported the first direct characterization, by electronic spectroscopy, of these fragments photolytically generated "in situ" from the corresponding methylbenzenes in organic glasses[1] and then in polycrystals[2]. Here we present the laser induced fluorescence and excitation spectra of o- and m-xylylenes and their methylated derivatives trapped in well defined lattice sites of Shpolskii matrices at 5-10 K.

Theory[2] predicts that m-xylylene (C_{2v}) biradical has a triplet ground state of B_2 symmetry (this has recently been confirmed by ESR experiments[3]) and two close-lying triplet excited states having A_1 and B_2 symmetries. O-xylylene (C_{2v}) has a singlet ground state[2] and two close-lying excited singlet states having A_1 and B_1 symmetries. Both species are therefore good candidates for studies of interelectronic state vibronic coupling.

The site selected fluorescence spectra in the visible of methylated m-xylylene biradicals can be analyzed using the vibrational modes and ground state frequencies of the parent molecules, but the activity of these modes depends on the number and the position of methyl groups on the aromatic rings. The emissions of biradicals produced from m-xylene, durene-h_{14} and -d_{14} contain only the totally symmetric modes 1 and 6a forming progressions, as expected for allowed transitions. In contrast, the fluorescence spectra of biradicals produced from mesitylene, isodurene and pseudo-cumene show activity in both the totally symmetric modes 6a and 1, and the non-totally symmetric in-plane mode 6b having b_2 symmetry. This corresponds to

a partially (accidental) forbidden transition.

The laser induced fluorescence excitation spectra of methylated m-xylylene biradicals do not present mirror image symmetry with the corresponding fluorescence spectra. In particular, neither progressions of fundamentals nor combinations between two frequencies can be found. This unusual behaviour is expected for species having two close-lying electronic states of different symmetry which can interact vibronically.

O-durylene (3,4-dimethyl-o-xylylene) is the only o-isomer which shows well resolved electronic spectra in Shpolskii matrices[4]. The fluorescence spectra of o-durylene-h_{12} and -d_{12} in n-hexane at 5-10 K are dominated by progressions of the CH_2 substituents in-plane bending modes around 350-400 cm^{-1}, and of the C=C stretching mode around 1530 cm^{-1}. Such spectral features are consistent with the polyenic rather than the aromatic character of the species. The laser induced fluorescence excitation spectra of o-durylenes are composed of two systems separated by 225 and 232 cm^{-1} in the perprotonated and perdeuterated species. Each system present mirror image symmetry with the corresponding fluorescence spectra. In contrast with the case of m-xylylene biradicals, no indication of vibronic coupling can be found in excitation spectra of o-durylenes.

REFERENCES

1 - E. MIGIRDICYAN, C.R. Hebd. Seances Acad. Sci. 266, 756 (1968)

2 - E. MIGIRDICYAN and J. BAUDET, JACS 97, 7400 (1975)

3 - B. WRIGHT and M.S. PLATZ, JACS 105, 628 (1983)

4 - W.P. COFINO, G. Ph. HOORNWEG, C. GOOIJER, C. MacLEAN and N.H. VELTHORST Chem. Phys. 72, 73 (1982)

Luminescent Properties of Lamellar Solids Derived from Hydrogen Uranyl Phosphate and Cr(III) Werner Complexes

Michael M. Olken, Carla M. Verschoor, and Arthur B. Ellis
Department of Chemistry, University of Wisconsin-Madison
Madison, Wisconsin 53706

The emissive layered solid $HUO_2PO_4 \cdot 4H_2O$ (HUP) readily undergoes intercalative ion exchange reactions with a variety of cationic species, leading, in many cases, to substituted lamellar materials which retain the luminescence characteristic of UO_2^{2+}.[1] We have recently carried out such substitution reactions using the following Cr(III) Werner complexes: $Cr(NH_3)_6^{3+}$; $Cr(NH_3)_5(H_2O)^{3+}$; Cr(ethylenediamine)$_3^{3+}$ ($Cr(en)_3^{3+}$); Cr(2,2'-bipyridine)$_3^{3+}$($Cr(bpy)_3^{3+}$); and $Cr(urea)_6^{3+}$.

Partial substitution typically obtains in the aqueous co-precipitation reaction which produces the solids, leading to general formulations of the compounds as $H_x[CrL_6]_{1/3(1-x)}UO_2PO_4 \cdot yH_2O$ (HCrUP). The lamellar structure is retained in samples of HCrUP, with expansion of the interlamellar spacing from 8.69 Å (HUP) to ~9-12 Å accompanying introduction of the Cr(III) complex.

To a first approximation, the electronic structures of host and guest are not perturbed when juxtaposed. Thus, absorption and emission spectra of HCrUP appear to be a superposition of bands observed for HUP (characteristic of the UO_2^{2+} chromophore) and the Cr(III) complex ($^2E \rightarrow {}^4A_2$); in fact, spectra of physical mixtures of HCrUP and salts of the Cr(III) complexes strongly mimic the HCrUP spectra.

That the host and guest do influence the excited-state properties of one another is, however, apparent from measurements of emissive efficiency and lifetime. For the $Cr(NH_3)_6^{3+}$ derivative, for example, excitation spectra reveal efficient host-to-guest, excited-state energy transfer. Moreover, emission from the UO_2^{2+} moiety is substantially quenched by the Cr(III) complex, and its lifetime correspondingly reduced.

The $Cr(bpy)_3^{3+}$ and $Cr(urea)_6^{3+}$ derivatives of HUP provide other interesting emissive properties. In the former case, the Cr(III) emissive quantum yield and lifetime increase by a factor of $\sim$30 over solution values; this result is qualitatively similar to the observed luminescent behavior of $Cr(bpy)_3^{3+}$ when intercalated into a dehydrated layered silicate[2] and highlights the ability of environment to influence excited-state properties. For the $Cr(urea)_6^{3+}$ derivative of HUP, both fluorescence and phosphorescence are observed in the solid, but the efficient photoaquation observed in solution[3] is not found in the solid, despite the presence of interlamellar water. The ratio of fluorescence to phosphorescence intensity indicates that the intercalated complex is trigonally distorted from octahedral symmetry.[4] These results typify interactions occurring in the solid and will be discussed for the full range of HCrUP solids prepared.

References

1. M. M. Olken, R. N. Biagioni, and A. B. Ellis, Inorg. Chem., 22, 4128 (1983).
2. D. Krenske, S. Abdo, H. VanDamme, M. Cruz, and J. J. Fripiat, J. Phys. Chem. 84, 2447 (1980).
3. E. E. Wegner and A. W. Adamson, J. Am. Chem. Soc. 88, 394 (1966).
4. J. L. Laver and P. W. Smith, Aust. J. Chem. 24, 1807 (1971).

Luminescence Studies of Interacting Metal Complexes in Two Dimensions

Howard H. Patterson[1], Gerald Roper[1], Andreas Ludi[3] and Nils Blom[2], University of Maine, Orono, Maine 04469, USA[1] and University Bern, Switzerland[3].

Salts of $AAu(CN)_2$ (A = K^+, Rb^+, Cs^+, Tetrabutylammonium) in the solid state have an interesting two-dimensional layered structure for the gold atoms. For example, for $KAu(CN)_2$ individual layers of gold atoms at room temperature are separated by 9.2 Å while the nearest neighbor gold distance in a layer is 3.36 Å. When the cation is changed, or the temperature is changed, the Au-Au nearest neighbor separation varies.

We have temperature dependent luminescence and absorption experiments on selected dicyanogold (I) salts to probe how the photophysical properties of these systems are dependent on the interactions between Au atoms in two dimensions. Laser excited emission studies and lifetime measurements have been made on the pure solids as a function of cation and temperature. Both room temperature and temperature dependent x-ray crystallographic measurements have been made to correlate the observed emission with changes in the nearest neighbor Au-Au distances. Also, emission studies have been made of $Au(CN)_2^-$ in mixed crystals of alkali halides and in frozen aqueous solutions of varying concentrations to probe the mechanism of energy transport.

The dependence of the emission energies, and energy transfer rates, on the choice of cation and temperature has been correlated with an excitonic model and with a tight binding band theory model.

The emission and absorption results for the two-dimensional layered gold (I) salts may be compared with our previous studies (1, 2, 3) for quasi-one dimensional tetracyanoplatinate (II) type systems.

(1) A. Kasi Viswanath, J. Vetuskey, R. Leighton, M.B. Krogh-Jesperson and H.H. Patterson, Molec. Phys. 48,567 (1983).

(2) A. Kasi Viswanath and H.H. Patterson, Chem. Phys. Lett 82, 25 (1981).

(3) A. Kasi Viswanath, M.B. Krogh-Jesperson, C. Baker, W.D. Ellenson, Molec. Phys. 42, 1431 (1981).

CIRCULARLY POLARIZED LUMINESCENCE OF $(-)_D$-$[Cr(R\text{-}pn)_3]^{3+}$ AND RELATED CHIRAL CHROMIUM(III) COMPLEXES USING A MICROCOMPUTER-BASED DIGITAL SPECTROPHOTOMETER SYSTEM

M.Morita,K.Eguchi,M.Shishikura,H.Nishikawa and M.Inoue

Department of Industrial Chemistry, College of Technology
Seikei University,Kichijoji,Musashino,Tokyo 180,Japan

Circularly polarized luminescence (C.P.L.) spectroscopy has been recently accepted as a unique technique which detects a difference in intensities between left- and right-circularly polarized emission and thereby elucidates chirality of optical active molecules in the emitting state[1].This spectroscopic means is complementary to circular dichroism(CD) spectroscopy in which information in the ground state is obtained.We have been interested in studying vicinal effects of chiral rare earth cmoplexes by CPL spectroscopy[2].In order to investigate conformational and configurational effects,we have extended our work to tris chelate chromium (III) complexes of D_3 symmetry.Since chiral fluorescent molecules are easily damaged by photolysis,we have also constructed a very sensitive and stable digital instrument based on an Apple II microcomputer for the measurements of CPL spectra.

In our new CPL spectrophotometer system,frequency-modulated photocurrents are monitored by two digital lock-in amplifiers connected with a microcomputer.This computer gives digital pulses to control a modified Spex 1401 spectrophotometer and a quarter-wave

modulator as well. A general purpose program for accurate data acquisition and display,written in a maschine language,enhances utility of the system for a variety of luminescence measurements.

Measurements of luminescence (I) and circularly polarized luminescence (ΔI) were made at temperatures between 300K and 12K of four tris chelate chromium(III) complexes: $(\pm)_D$-$[Cr(en)_3]^{3+}$(en= ethylenediamine), $(\pm)_D$-$[Cr(R\text{-}pn)_3]^{3+}$(pn=propylenediamine).The CPL spectrum of (-)$Cr(R\text{-}pn)_3$ originates from the $^2E \rightarrow {}^4A_2$ transition and spectral features are similar to $(\pm)Cr(en)_3$[3,4].The electroinc origin centered at 14900 cm^{-1} gives the luminescence dissymmetry factor $g_{lum}(2\Delta I/I)$ of -0.0682 in solution which is comparable to the CD dissymmetry factor $g_{abs}(\Delta\varepsilon/\varepsilon)$ of -0.0687.The g_{lum} of $(\pm)Cr(R\text{-}pn)_3$ is almost two times larger than that of $(\pm)Cr(en)_3$.These results indicate that the stereochemical electronic structure in the ground state does hold in the excited state.

We have observed no vibronic bands in the CPL spectra of four compounds while they are characteristic in the luminescence. The theoretical reason is not clarified as yet.However,the totally symmetric Cr-N stretching mode of about 500 cm^{-1},responsible for vibronic emissions, is mixed strongly with the $^2T_1$ state and this quenches presumably the vibronic optical activity in the ^2E state.

REFERENCES

[1] M.Morita,Bunko Kenkyu 29(1980)357.

[2] K.Murata and M.Morita,J.Luminescence 24/25(1981)747.

[3] G.L.Hilmes,H.G.Brittain, and F.S.Richardson,Inorg.Chem.16(1977)528

[4] R.D.Peacock and B.Stewart,J.Chem.Soc.Commun.1982,295.

Time-Resolved Study of Resonant Secondary Emission in $NaNO_2$ Crystal

Hiroshi Murata, Toshihiro Kobayashi and Riso Kato
Department of Physics, Faculty of Science, Kyoto University
Sakyo, Kyoto 606, Japan

$NaNO_2$ crystal shows multiple order Raman scattering due to ν_2-vibration of NO_2^- when excited near the zero-phonon line at ν_{00}(3848.9A) of the singlet absorption ($^1A_1 \rightarrow {}^1B_1$).[1] We have studied the resonant secondary emission in highly purified $NaNO_2$ crystal by nanosecond time-resolved measurements.

The behavior of the time-integrated emission spectrum for the change of exciting photon energy ν_i is shown in Fig.1. A Raman-like component(|) shifts with increase in ν_i and is enhanced resonantly at $\nu_i=\nu_{00}$, while a luminescence-like component(*) becomes appreciable separately from the former and grows up rapidly for $\nu_i>\nu_{00}$.

Figure 2 shows a typical time-resolved spectra of the secondary emission under the excitation at 3848.2A ($\nu_i=\nu_{00}+5$ cm^{-1}). The origin of the time (t=0) is determined by the peak of exciting laser pulse. The Raman-like component shows the similar time response as the exciting light, while the luminescence-like component shows a delay from the former. Since the life time of the ordinary luminescence is about 6 nsec, the observed delay of the luminescence-like component is consistent with the life time within the experimental error.

Under $\nu_i = \nu_{00}$, the time response of the emission line is likely decomposed into those of Raman and luminescence components by assuming that the Raman component has the same time response as the exciting light. The dependence of the intensity ratio of decomposed components on ν_i and temperature are also reported.

1) M.Hangyo, H.Yamanaka and R.Kato: J.Phys.Soc.Jpn 52 1064 (1984).

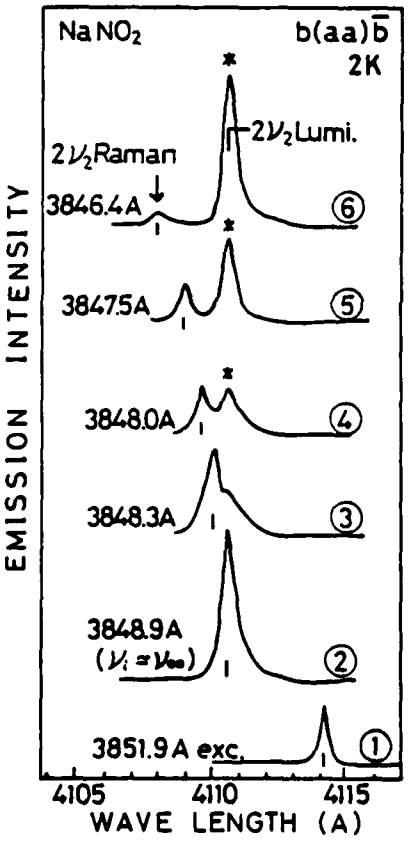

Fig.1 Time-integrated spectra of secondary emission at 2K.

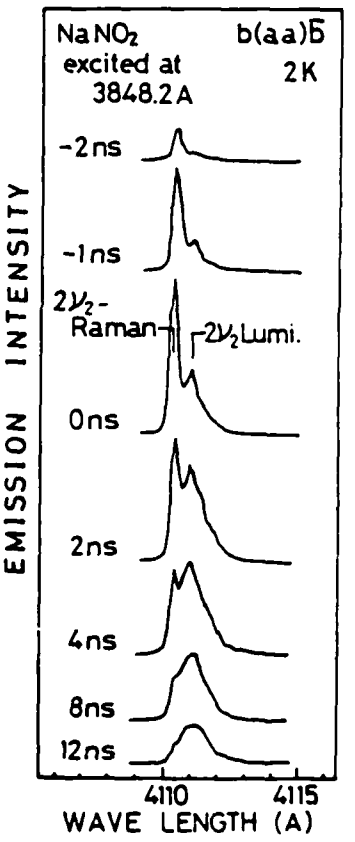

Fig.2 Time-resolved spectra excited at 3848.2A.

Luminescent Properties of Bis(η^5-pentamethylcyclopentadienyl)ytterbium Derivatives

Alan C. Thomas and Arthur B. Ellis*
Department of Chemistry, University of Wisconsin-Madison
Madison, Wisconsin 53706

Several adducts of $(\eta^5\text{-}Me_5C_5)_2Yb(II)$ (1) and $(\eta^5\text{-}Me_5C_5)_2YbCl(III)$ (2) have been found to exhibit photoluminescence (PL) at 295K. The mono-THF adducts of 1 and 2 have served as the parent complexes for this study;[1,2,3] they are orange-red (λ_{max} ~ 445, 505 and 790 nm)[4] and purple (λ_{max} ~ 520 nm), respectively. Electronic spectra of the adducts are sensitive to the Lewis base coordinated to the Yb(II) or Yb(III) center. Excitation into any of the visible absorption bands of 1 at 295K in toluene yields a broad (FWHM ~100 nm) PL band with uncorrected λ_{max} ~935 nm. Solutions of 1 in THF, compositionally dominated by the bis-THF adduct, exhibit a band of similar character, but possessing, in addition, a shoulder at ~900 nm. Solid-state PL spectra of the mono- and bis-THF adducts of 1 display band maxima at ~960 and 910 nm, suggesting that the shoulder observed in THF solution is due to the bis-THF adduct. The THF data suggest that excited-state adduct dissociation competes favorably with other decay routes of the bis-THF adduct. Other adducts studied by dissolving 1·THF in the corresponding solvent include Et_2O, for which PL at 875 nm is found, and CH_3CN and pyridine, for which no PL between ~700-1000 nm is observed. In THF, 2 exhibits the sharp PL bands characteristic of f-f transitions between ~950-1000 nm; spectra are compared to those previously observed for adducts of $(\eta^5\text{-}C_5H_5)_3Yb(III)$.[5]

Reaction of 1 with O_2 in THF produces chemiluminescence (CL) characteristic of an excited Yb(III) species. The CL signal (λ_{max} ~990 nm) is also found using O_2^- as the oxidant. In both cases the metal is oxidized, but the two experiments differ in that O_2 addition also causes ligand oxidation to Me_5C_5OOH, isolated by post-hydrolysis VPC analysis. Another CL-producing reaction is that of O_2 and 2 in THF. Again, Yb(III) emission and the hydroperoxide are found, but CL differs from that produced with 1 in that λ_{max} occurs at ~980 nm. In all of these reactions, the PL spectrum of the reaction mixture is similar to that of the CL spectrum. Mechanistic aspects of these reactions will be discussed.

References

1. P. L. Watson, J. C. S. Chem. Commun. 1980, 652.
2. T. D. Tilley, R. A. Andersen, B. Spencer, H. Rubin, A. Zalkin, and D. H. Templeton, Inorg. Chem. 19, 2999 (1980).
3. T. D. Tilley and R. A. Andersen, Inorg. Chem., 20, 3267 (1981).
4. A. B. Ellis, A. C. Thomas, and C. J. Schlesener, Inorg. Chimica. Acta, 94, 20 (1983).
5. C. J. Schlesener and A. B. Ellis, Organometallics, 2, 529 (1983).

SCINTILLATION YIELD OF THIN POLYSTYRENE FILMS

A. M. Botelho do Rego, M. I. Morais and J. Lopes da Silva
Centro de Química Física Molecular, Complexo I (INIC)
Instituto Superior Técnico, Lisboa, Portugal

The effects of quenching on the value of the scintillation (prompt plus delayed component) induced by a heavy ionizing particle of energy E and specific energy loss dE/dx are analysed measuring the specific luminescence dS/dx of polystyrene films dopped with different concentrations of DPA. In a previous work[1] we deduced the following expression for the delayed specific luminescence

$$\frac{dL'}{dx} = \frac{\eta\alpha}{W_T}\{(1-\phi_1)\frac{dE}{dx}(1-\exp(-(1-\phi_1)\frac{dE}{dx}B_T))\exp(-(1-\phi_1)\frac{dE}{dx}B_T) + \phi_2\frac{dE}{dx}(1-\exp(-\phi_2\frac{dE}{dx}B_T))\exp(-\phi_2\frac{dE}{dx}B_T) + (\phi_1-\phi_2)\frac{dE}{dx}(1-\exp(-(\phi_1-\phi_2)\frac{dE}{dx}B_T))\} \quad (2)$$

Quantities $(1-\phi_1)$, ϕ_2 and $(\phi_1-\phi_2)$ are the fractions of energy transferred by the incident particle to the track, blobs and spurs respectively. These ones represent the three distinct regions considered in the track model proposed before[2]. $B_T = 2R_{ST}/W_T \approx 2R_{TT}/W_T$ define the quencher parameter concerning the degradation of triplet excitons, where R_{ST} and R_{TT} are the critical distances for singlet-triplet and singlet-singlet interactions respectively and W_T is the mean energy required to produce a T_1 state. Similarly, we have deduced in this work the following expression for the prompt luminescence

$$\frac{dL}{dx} = \frac{\eta}{W_S}\{(1-\phi_1)\frac{dE}{dx}\exp(-(1-\phi_1)\frac{dE}{dx}B_S) + \phi_2\frac{dE}{dx}(-\phi_2\frac{dE}{dx}B_S) + (\phi_1-\phi_2)\frac{dE}{dx}\} \quad (2)$$

Where B_S is the quencher parameter defining the degradation of singlet excitons. Assuming that this degradation can take place through interactions such as[3]

$$S_1 + S_1 \rightarrow S_n + S_0 \rightarrow S_1 + S_0$$

$$S_1 + T_1 \rightarrow T_n + S_0 \rightarrow T_1 + S_0$$

we can write $B_S = 2R_{SS}/W_T + 2R_{ST}/W_T$. Adding (1) and (2) we obtain dS/dx. Theoretical values proportional to dS/dx defined by

$$\frac{W_T}{\eta\alpha}\ \frac{dS}{dx} = A + W\,B \qquad (3)$$

(where A and B are the quantities within bracketts in (1) and (2) respectively and $W = W_T/\alpha W_S$), are fitted to experimental values, measured by single photoelectron technique with films containing 0%, 1% and 2% of DPA. A good agreement between theoretical curves and experimental points is verified. Similarly to what is observed with B_T[1], B_S values are higher for increasing values of DPA concentration. Nevertheless, a more pronounced increasing of B_S is remarked here, which means that the mean energy W_S decreases more swiftly than W_T with increasing solute concentration. This agrees with the idea that the energy transfer between singlet states of solvents and solute is favoured.

References

(1) A. M. Botelho do Rego and J. Lopes da Silva, Chem.Phys.Lett. (in Press)

(2) A. M. Botelho do Rego and J. Lopes da Silva, Proc. I. Simp. Ibérico Física Matéria Condensada, Lisboa (1983), 163

(3) C. Fuchs, F. Heisel and R. Voltz, J.Phys.Chem. 76 (1972), 3867

OPTICALLY DETECTED MAGNETIC RESONANCE STUDIES OF TRIPLET CYCLOPENTANONE*

W. B. Lynch and D. W. Pratt, Department of Chemistry, University of Pittsburgh, Pittsburgh, PA 15260

Neat cyclopentanone (CYP), when cooled to $\leq$4.2 K and irradiated with ultraviolet light, exhibits a sharp zero-field optically detected magnetic resonance (zf-ODMR) spectrum. Three transitions were initially found [1,2]; however, Shain and Sharnoff [3] subsequently detected six additional resonances (two "satellite" triads) of much lower intensity separated from the "normal" triad by 9-214 MHz. A double resonance experiment using two microwave fields to excite transitions in different triads seemed to indicate some communication between them. For this reason, it was suggested that different electronic and/or nuclear configurations of the isolated molecule are responsible for the different triads, and that these communicate via a rapid exchange process, perhaps enhanced by tunneling. But later CW and pulsed ODMR experiments [4] failed to reveal the existence of such a process, thus casting doubt on this interpretation.

We have performed a number of additional zf-ODMR experiments on CYP, CYP-d_4, and CYP-d_8 in an attempt to determine the origin of these triads and their dynamic behavior. These include studies of the pure compounds, isotopic mixtures, and solutions in hydrocarbon glasses at different temperatures. Our principal findings are that (1) the triads are observed in all environments, (2) the decay constants of the satellite triad sublevels are much larger than those of the normal sublevels, (3) deuteration affects both the sublevel lifetimes and the frequencies of all transitions, unequally, (4) isotopically mixed samples exhibit spectra which show lines at the expected positions but which have anomalous relative intensities, and

(5) the spectra in dilute matrices are extremely sensitive to both the concentration of the guest and the rate of cooling. In particular, we find that the FWHM linewidths increase dramatically with decreasing concentration and/or increasing cooling rate.

All of these observations, plus those of earlier workers, may be explained if one assumes a strong propensity for molecular aggregation of cyclopentanone in even the most dilute matrices on cooling, and that small, weakly interacting aggregates (e.g., trimers) are the species responsible for the observed ODMR spectra. Both the frequencies and relative intensities of all nine lines in the spectrum of triplet CYP may be interpreted on the basis of such a structure in which the excitation is shared, unequally, between the different "monomer" units with differently oriented fine-structure tensors. Solutions of the resulting spin Hamiltonian, in the weak-coupling limit appropriate to this problem [5], will be described. The importance of "exchange-narrowing" effects which result from this coupling and produce sharp lines in the zf-ODMR spectra of randomly oriented samples will also be discussed.

References

* To be presented at the International Conference on Luminescence, Aug. 13-17, 1984 at Madison, WI. This work has been supported by NSF (CHE-8021082).

[1] A. L. Shain, W. T. Chiang, and M. Sharnoff, Chem. Phys. Letters 16, 206 (1972).

[2] A. L. Shain and M. Sharnoff, Chem. Phys. Letters 16, 503 (1972).

[3] A. L. Shain and M. Sharnoff, Chem. Phys. Letters 22, 56 (1973).

[4] M. E. Tarrasch, C. R. Chen, and C. B. Harris, Chem. Phys. Letters 48, 579 (1977).

[5] Solutions in the strong coupling limit have been described by several workers. See, for example, J. P. Lemaistre and A. H. Zewail, J. Chem. Phys. 72, 1055 (1980) and references contained therein.

Optically Detected Chlorine Nuclear Quadrupole Resonance in Organic Molecular Crystals

C. v. Borczyskowski

FU Berlin, Dept. of Physics, Arnimallee 14, D-1000 Berlin 33, FRG

Some years ago an optical pumping cycle has been designed to transfer via the solid state effect electron spin alignment to nuclei such as bromine and chlorine /1/. The obtained nuclear spin alignment can be destroyed by nuclear quadrupole resonance (NQR) transitions in the ground state of the molecule resulting in phosphorescence intensity changes. By this method the sensitivity of optical detection of magnetic resonance (ODMR) is obtained and NQR on quadrupole nuclei with concentrations as low as 10^{-5} molar is feasible.

This improved sensitivity has been used to perform NQR on organic molecules highly diluted (10^{-5} molar) in molecular crystals. By this chlorine NQR transitions in the excited triplet state have been compared with those in the singlet ground state of a series of chlorine substituted benzenes. This group of molecules is of special interest for the basic understanding of the distortion of the symmetry (known as pseudo-Jahn-Teller instability) in the excited triplet state of benzene itself /2/. A direct comparison of NQR transitions in different electronic states in one and the same host crystal is crucial in experiments, where crystal fields are non-negligible concerning the observed symmetry distortion.

Moreover, the orientation of the electric field gradient tensor of the ground state serves a probe to investigate the incorporation of the diluted molecules in the host material relative to crystallographic axes, which is

not possible e.g. with X-ray methods.

Combining these advantages of optically detected NQR, a distortion of the D_{2h} symmetry in the excited triplet state of para-dichlorobenzene and tetra-chloropyrazine but not of tetra-chlorobenzene has been observed. The distortion mainly results in an in-plane rotation of the fine structure axes in the excited triplet state versus the symmetry axes of the ground state molecule. This is shown in Fig. 1 for tetra-chloropyrazine. The different behavior of the molecules can be interpreted by assuming an inherent antiquinoid structure of benzene itself /2/. Additionally, it could be shown, that tetra-chloropyrazine is not substitutionally incorporated in a durene crystal, but exhibits a rotation in the molecular plane by 4°.

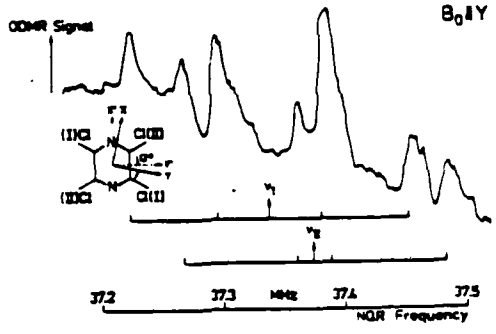

Fig. 1: Optically detected NQR in the ground state for tetra-chloropyrazine in durene. An external magnetic of 14 mT has been applied to obtain tensor orientations relative to this field

An additional feature of the improvement of the sensitivity of optically detected NQR is, that it is possible to study the influence of the electric field of the crystal on electric field gradient tensors at the position of the chlorine nuclei. It has been found for chlorobenzene compounds, that halogen free matrices result in coupling constants similar to gas phase data. This can be explained in terms of an electrostatic interaction between electric dipole moments located on the C-Cl bonds.

/1/ C.v. Borczyskowski and E. Boroske, Chem. Phys. 35, 367 (1978)
/2/ C.v. Borczyskowski and E. Fallmer, Chem. Phys. Lett. 102, 433 (1983)

Photoluminescent Properties of the Conducting Polymer Poly-(Para-Phenylene)

A. Heim, G. Leising, and H. Kahlert
Institut für Festkörperphysik, Technische Universität Graz
A-8010 Graz, Petersgasse 16, Austria.

Recently a whole class of conjugated organic polymers has been discovered, the members of which undergo a transition to a conductive state on doping with electron acceptors or donors. One of the most prominent members of this class is poly-(para-phenylene) (PPP), which exhibits a conductivity increase as high as 18 orders of magnitude on appropriate doping [1]. The basic chemical unit of PPP is shown in Fig. 1. Doped PPP and similar polymers in many respects show transport and optical properties reminiscent of those of conventional semiconductors like silicon. Undoped PPP-type polymers composed of coupled aromatic rings are very heat resistant and have already been used as materials which must stand against high temperatures. We have performed measurements of the excitation and emission spectra of the photoluminescence of PPP in the wavelength region between 200 nm and 800 nm. Samples have been prepared by two different methods, the one designed by Kovacic et al. [2], which is known to yield material with a higher degree of polymerization, and by the Yamamoto [3] method. Both synthetical routes not only result in high-molecular weight insoluble PPP, but also in products which are soluble in toluene and exhibit a much lower molecular weight. The emission spectra for the Kovacic-product show a series of three bands in the blue region of the spectrum and a broad maximum around 625 nm, whereas the Yamamoto-samples show similar bands in the blue region and an additional band around 505 nm. A comparison of these spectra with photoluminescence spectra of the commercially available oligomer p-terphenyl is shown in Fig. 2 together with the excitation spectra for p-terphenyl (dashed curve a) and for

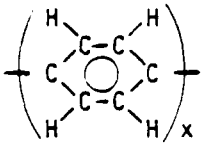

Fig. 1

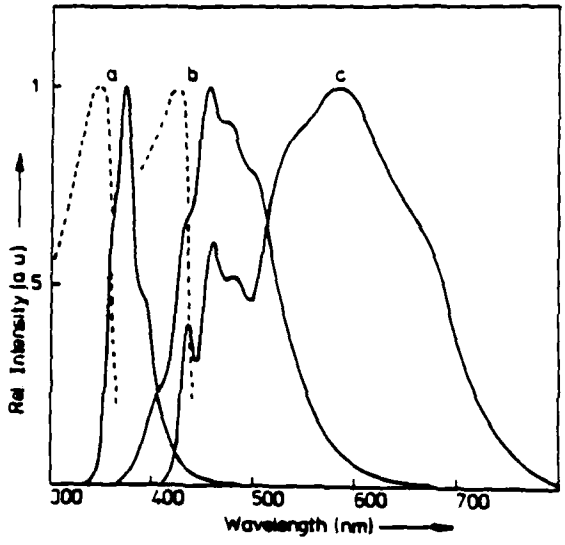

Fig. 2: Excitation (---) emission (——) spectra of
a): p-terphenyl
b): Yamamoto - PPP
c): Kovacic - PPP

PPP (dashed curve b), which coincide for both types of samples. These measurements on two differently produced kinds of PPP allow a critical discussion of the role of impurities for the strong photostimulated luminescence of PPP.

References:

1 R. R. CHANCE, R. H. BAUGHMAN, J. L. BREDAS, H. ECKHARDT, R. L. ELSENBAUMER, J. E. FROMMER, and L. W. SHACKLETTE, Mol. Cryst. Liq. Cryst. 83, 217 (1982)

2 P. KOVACIC and A. KYRIAKIS, J. Am. Chem. Soc. 85,454(1963)

3 T. YAMAMOTO and A. YAMAMOTO, Chemistry Lett. 353, (1977)

FC1 and FC2

FC1 Usefulness of Sensitized Luminescence as a Probe for Exciton Motion in Molecular Crystals, V. M. Kenkre and R. S. Parris, University of Rochester, and Proposal for New Experiments for the Investigation of Transport Coherence of Excitons in Molecular Crystals, V. M. Kenkre and C. P. Tsironis, University of Rochester. See FD13 and FD14 for summaries.

FC2 Mobility and Conformation of Side Chains in Copolymers of the Methacryl Amide Type: Study of Depolarization of Fluorescence and Nonradiative Energy Transfer, František Mikeš, Branomír Vyprachtický, and Jaroslav Kralíček, Prague Institute of Chemical Technology, Czechoslovakia, and Jiří Labský, Institute of Macromolecular Chemistry, Czechoslovak Academy of Sciences, Czechoslovakia. See ME20 for summary.

Luminescence Spectra and Kinetics of various Radical Pair Products following Photochemical Hydrogen Transfer in Doped Fluorene Single Crystals

C. v. Borczyskowski, P. Steidl, D. Stehlik

FU Berlin, Dept. of Physics, WE 1, Arnimallee 14, D-1000 Berlin 33, FRG

We have shown previously that photoexcited phenazine doped as acceptor in a fluorene single crystal is able to abstract a hydrogen atom from the methylen group of a specific neighbor host molecule. Reaction product is a radical pair (RP) triplet state the molecular structure of which is known in detail /1/. Precursor is the photoexcited triplet state of the phenazine acceptor. The H-transfer is fully reversible. At room temperature the RP product has a lifetime of only ~ 0.2 µs.

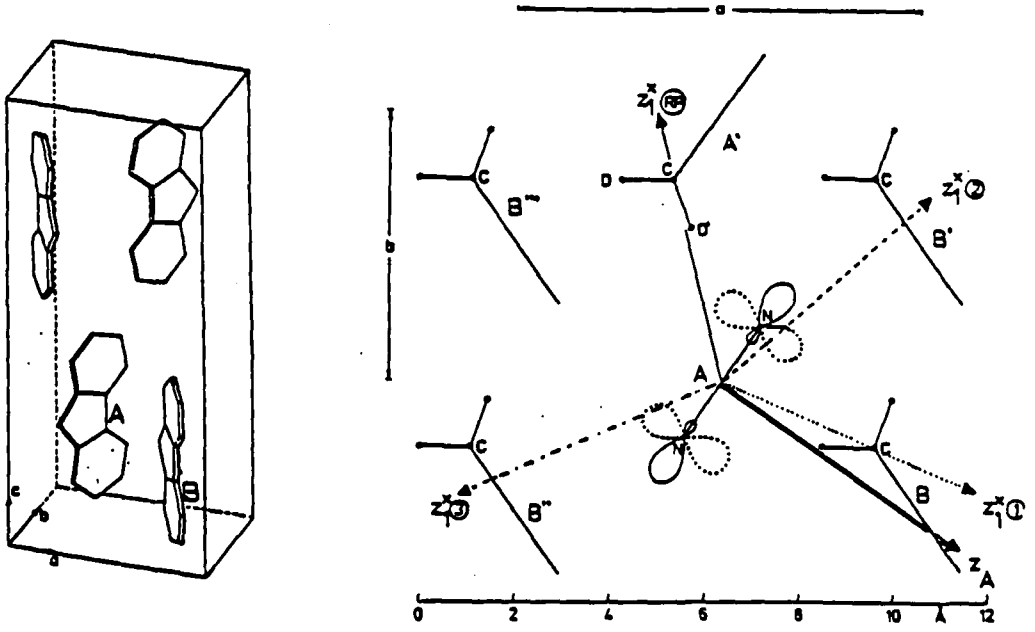

Fig. 1 Unit cell of fluorene (left) and ab-reaction plane (right) with an acceptor molecule phenazine doped substitutionally in site A. The fluorene methylen group is deuterated.

Crystal structure and reaction plane are shown in Fig. 1. The latter contains the molecular centers and the plane of the donor methylen group. From the crystal structure it is not obvious why a chosen acceptor (drawn for site A) should react only with the specific neighbor A' as found for the RP product /1/ observed so far.

We have now been able to observe other photochemical products, in luminescence and in triplet state ESR. Deuteration of the fluorene methylen group lengthens the product lifetime such that products become stable under certain irradiation and temperature conditions. The ESR results allow the identification of three main products (termed ①, ②, ③) as radical pairs formed from the same acceptor and a specific fluorene neighbor as indicated by principal fine structure axes z* in Fig. 1, connecting the centers of electron spin density of the free electron spins on the radical molecules after deuterium transfer. With reference to the same acceptor site A the molecular sites AA' form the short-lived previous product (RP) /1/, AB form the new product ①, AB' form ② and AB" form ③.

The optical spectra can be assigned in part to the above mentioned products identified in ESR by using the specific formation and decay characteristics as a function of duration of the exciting light and sample temperature and appropriate warming up procedures. Thus optical observables are available to determine the full photochemical kinetics and sequential reaction processes forming all possible products, as will be documented in detail. Important aspects in the discussion are the role of symmetry considerations for the various reaction pathways /2/ and the range in which formation and decay rates of reversible photoreactions can be varied at will.

/1/ D. Stehlik, R. Furrer, V. Macho; J. Phys. Chem. 83 (1979) 3440
/2/ J.P. Colpa, D. Stehlik; Chem. Phys. 81 (1983) 175

ROLE OF VISCOSITY EFFECT ON PHOTOISOMERIZATION

A.A. Villaeys and A. Boeglin

Centre de Recherches Nucléaires et
Université Louis Pasteur
Laboratoire de Physique des Rayonnements et
d'Electronique Nucléaire
67037 STRASBOURG CEDEX France

S.H. Lin

Department of Chemistry
Arizona state University
TEMPE Arizona 85287° U.S.A.

Many rate processes like diffusion, dielectric relaxation, electron transfer reactions, nonradiative decay etc..., in dense media can be treated from a unified quantum statistical mechanical viewpoint [1]. In these unimolecular rate processes, one can regard that two potential surfaces, say a and b, are involved. It is assumed that when the two potential surfaces cross, the resonance interaction is small. A general theoretical approach has been developed that will treat these rate processes by properly choosing the perturbation associated with each rate process.

We consider a rate process for which the rate constant for a → b can be described by the golden rule expression

$$W_{a\to b} = \frac{2\pi}{\hbar} \sum_{v} P_{av} |\langle bv'|H'|av\rangle|^2 \, \delta(E_{av} - E_{bv'}) \qquad (1)$$

where (v,v') represent the quantum states of nuclear motion and (a,b) denote the two potential surfaces involved in the rate process. Eq. (1) can be written as

$$W_{a\to b} = \frac{1}{\hbar^2} \int_{-\infty}^{\infty} dt \sum_{v} P_{av} \langle av|H'(t)H'(o)|av\rangle$$

$$= \int_{-\infty}^{\infty} dt \, C_{ab}(t) \qquad (2)$$

where

$$H'(t) = \exp\left(\frac{it}{\hbar} H_o\right) H' \exp\left(-\frac{it}{\hbar} H_o\right) \qquad (3)$$

and C_{ab} represents the time correlation function.

Two cases need to be considered separately [2]. Case I refers to the case in which H'_{ab} is independent of nuclear coordinates Q, while Case II refers to electronic relaxation (i.e., radiationless transitions). For example, for Case I by using the cumulant expansion to the second order approximation, we obtain

$$C_{ab}(t) = \frac{1}{\hbar^2} |H'_{ab}|^2 \exp[it\,\omega_{ab} + \gamma_{ab}(t)] \tag{4}$$

where $\hbar\omega_{ab}$ represents the energy difference between the two surfaces and $\gamma_{ab}(t)$ is given by

$$\gamma_{ab}(t) = -\sum_j \frac{\omega_j^4 d_j^2}{\hbar^2} \int_0^t dt_1 \int_0^{t_1} dt_2 \langle Q_j(t_1) Q_j(t_2) \rangle \tag{5}$$

where d_j denotes the normal coordinate displacement and $\langle Q_j(t_1)Q_j(t_2)\rangle$ represents the coordinate correlation function for the Q_j oscillator.

Case II can be treated similarly and the rate constant can be expressed as

$$W_{a\to b} = \frac{1}{\hbar^2} |P_i(ab)|^2 \int_{-\infty}^{\infty} dt\, \langle P_i(t)P_i(o)\rangle \exp[it\omega_{ab} + \gamma_{ab}(t)] \tag{6}$$

where the electronic matrix element $P_i(ab)$ is defined by $P_i(ab) = \langle \Phi_a | P_i | \Phi_b \rangle$ in terms of electronic wavefunctions Φ_a and Φ_b and $\langle P_i(t)P_i(o)\rangle$ represents the momentum correlation function for the Q_i oscillator (i.e., the promoting mode). In other words we have first expressed the rate constant for a process under consideration $W_{a\to b}$ in terms of the correlation functions $\langle Q_j(t)Q_j(o)\rangle$ and/or $\langle P_i(t)P_i(o)\rangle$. To study the viscosity effect on $W_{a\to b}$, it is then necessary to calculate these correlation functions by solving the Langevin equation (i.e., assuming classical oscillators). For example, the generalized Langevin equation for a damped oscillator can be used which is expressed as

$$\frac{d^2x}{dt^2} + \int_0^t \beta(t-t')\, u(t')\, dt' + \omega^2 x = A(t) \tag{7}$$

where $u(t) = \frac{dx}{dt}$. $A(t)$ is the fluctuation force, the second term on the left-hand side of Eq. (7) represents the frequency-dependent friction

and ω is the vibrational frequency of the oscillator. In order to discuss the viscosity effect we must solve Eq. (7). We consider the case in which the frequency dependence of friction is ignored, i.e., $\beta(t) = \beta\delta(t)$; the Langevin equation in this case has been solved.

In our preliminary work, we have expressed the rate constant for isomerization in liquids (case I) as a product of the viscosity-independent rate constant $W_{a\to b}(\beta=0)$ and the correction term, i.e.,

$$W_{a\to b} = W_{a\to b}(\beta=0)\ \mathrm{Re}\left[e^{-\frac{\omega^4 d^2}{\hbar^2} F(\beta,t^*)}\right] \qquad (8)$$

where t^* denotes the saddle-point value of t in $W_{a\to b}(\ =0)$ and Re means the real portion should be taken. The quantity $F(\beta,t)$ originates from the friction and fluctuation force in evaluating the correlation function $\langle x(t_1)x(t_2)\rangle$. The experimental results of Velsko et al [3] have been quite well fitted by our viscosity dependent rate constant.

[1] H.A. Kramers, Physica 7 284 (1940)

[2] H. Eyring, S.H. Lin and S.M. Lin, "Basic Chemical Kinetics" (Wiley Interscience, 1980)

[3] S.P. Velsko, D.H. Woldeck and G.R. Fleming, J. Chem. Phys. 78 249 (1983).

Photo-Oxidation of Tetracyanoplatinate Single Crystals

W.A.Pfab and V.Gerhardt

Institut Physik II - Festkörperphysik, Universität Regensburg

8400 Regensburg, Universitätsstr. 31, West Germany

$Me_x\left[Pt(CN)_4\right]_y \cdot nH_2O$ (Me = Sr, Ca, Ba, Mg, Lu, ...)-type crystals show highly anisotropic properties. The strong binding between the CN-ligands and the Pt^{2+}-ion of the $\left[Pt(CN)_4\right]^{2-}$-complex-molecule is well preserved in the crystal (1). This is the reason for the demixing of Pt-d^8-electrons (Ham-effect) and, additionally, there is formed a nearly one-dimensional dz^2-valence-band for the Pt-Pt-binding within the crystal.

Absorption of photons mainly will create Wannier-type excitons, if the polarization is parallel to the c-axis of the crystal, and mainly Frenkel-type excitons, if the polarization is perpendicular to the c-axis, respectively. Fig. 1 shows the energy-levels of the $\left[Pt(CN)_4\right]^{2-}$-complex-molecule and the corresponding bands of the crystal.

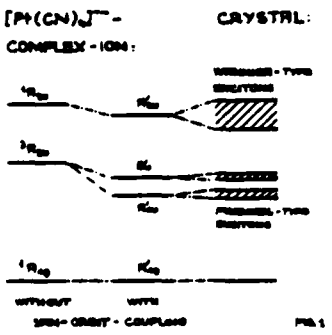

At 2 K the $A_{1u}' \rightarrow A_{1g}'$-emission has a long lifetime because of the spin-forbidden transition. At high pump-rates we observe an exciton-exciton-interaction within the A_{1u}'-state. This interaction is connected with the creation of a new absorption-band (see Fig. 2). Comparing the position and the halfwidth of this absorption-band with the $A_{1g}' \rightarrow A_{2u}'$-absorption in crystals with shorter Pt-Pt-intrachain-distance leads to the conclusion that

the exciton-exciton-interaction removes electrons from antibonding orbitals of the Pt-chain. From crystals of the type $K_2[Pt(CN)_4] \cdot Br_{0.3} \cdot 3H_2O$ ("Krogmann-salt") it is well-known that the oxidation of the Pt-chain by the Br-ion reduces the Pt-Pt-distance (2).

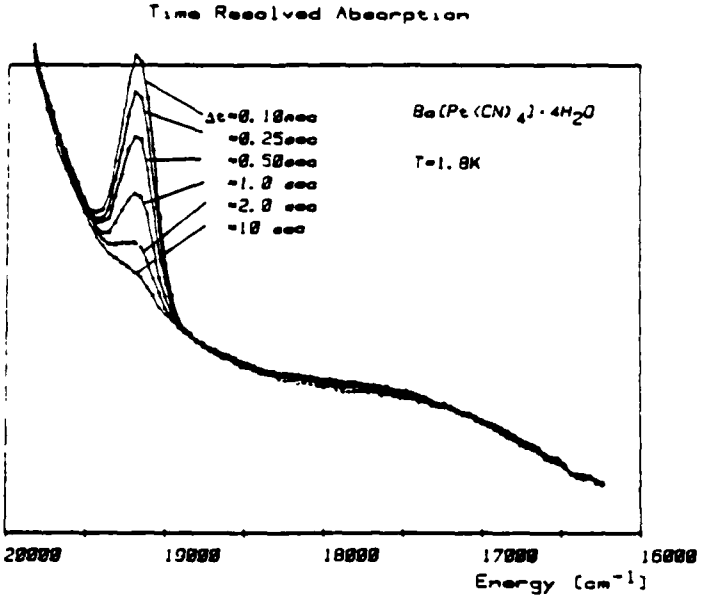

As indicated in Fig. 2 the new absorption-band can be bleached by irradiating the crystal with white light. Besides, this absorption-band will disappear, if the crystal is heated. During this heating, a thermoluminescence in the spectral range of the $A_{1u}^1 \rightarrow A_{1g}^1$-transition is observed. We propose that these effects are due to the flow-back of electrons from their interchain traps to the oxidized Pt-chains.

(1) HIDVEGI, I., AMMON, W.v., and GLIEMANN, G.: J.Chem.Phys. 76, 4361 (1982)
MARKERT, J.T. et al.: Chem.Phys. Letters 97, 175 (1983)

(2) KROGMANN, K.: Angew.Chemie 81, 10 (1969)

Deactivation of Excited States of Liquid Alkyl Benzenes at the Entrance Window

R. Sasson and A. Weinreb

The Racah Institute of Physics
The Hebrew University of Jerusalem, Jerusalem, Israel.

In a series of early investigations[1] a marked decrease of the fluorescence quantum yield of liquid alkyl benzenes(e.g.toluene,mesitylene)was found when the wavelength of the exciting radiation was decreased from those for excitation of S_1(the first excited singlet level)to those for excitation of S_2 and S_3(the second and third excited singlet levels).Further decrease of the excitation wavelength is accompanied by an increase in the fluorescence quantum yield.These results for toluene are reproduced in Fig.1,curve(a),where Φ_λ represents the fluorescence intensity for excitation at wavelength λ. The low value of Φ_λ for excitation of S_3 may be caused either by a quenching mechanism which acts on the molecule in this state,or by a non-efficient transition from this state to the emitting state S_1,or by some quenching mechanism which acts on the molecule in S_1 but which is absent when S_1 is directly excited from the ground state.(A combination of all three mechanisms or any two of them is,of course not excluded).

It was found from quenching and energy transfer measurements[2] that the conversion from S_3 to S_1 takes place with an efficiency less than unity.Several mechanisms have been proposed to explain this result[3].Among those it was suggested that excited molecules diffusing to the entrance window of the exciting radiation,or excitons migrating to the window, may be quenched there.This is suggested by the anticorrelation between the excitation and the absorption spectra. The absorption spectrum of toluene is shown in curve (e) of Fig.1.Because of the high absorption coefficient at S_3(5.5×10^4 $M^{-1}cm^{-1}$),diffusing excited molecules or migrating excitons can readily reach the entrance window.With the construction of a windowless liquid cell[4] this quenching effect can be demonstrated by measuring Φ_λ

with and without the presence of an entrance window.The results are shown in Fig.1,curves (b)-(d),which have been normalized at 2575 $\mathring{A}$(S_1).It is seen that with decreasing temperature, Φ_λ for excitation at S_3 increases markedly. (With decreasing temperature the emitted fluorescence becomes increasingly that of toluene excimer; of this effect,however, account is taken by the normalization procedure).A decrease in temperature causes a decrease in the diffusion coefficient and hence reduces the probability for an excited molecule to reach the entrance window.The quenching effect at the entrance window seems thus rather established.It is,however seen that even at the lowest temperature, Φ_λ for the enclosed liquid is still lower than that for the open liquid.At this temperature (-90°C),no material diffusion to the window is possible. We tend therefore to conclude that at this temperature,and hence also at higher temperatures, part of the observed quenching at the entrance window is due to the migration of the S_3 exciton to the entrance window at which it is quenched either in the S_3 state or after transition to the S_1 state.This window quenching effect should be taken in account in any deduction of the various transition rates from measured fluorescence intensities of liquids in a standard windowed cell.

REFERENCES:

(1)C.L.Braun,S.Kato and S.Lipsky, J.Chem.Phys.,39,1645,(1963).

(2)U.Laor and A.Weinreb,J.Chem. Phys.,50,94(1969); C.Lawson, F.Hirayama and S.Lipsky, in "Molecular Luminescence"E.C.Lim, Ed.,Benjamin,N.Y.(1969),p.837.

(3)J.B.Birks,"Photophysics of Aromatic Molecules",Wiley-Interscience,N.Y.(1970),p.171.

(4)S.Sasson and A.Weinreb,Applied Optics, 21, 2520, (1982).

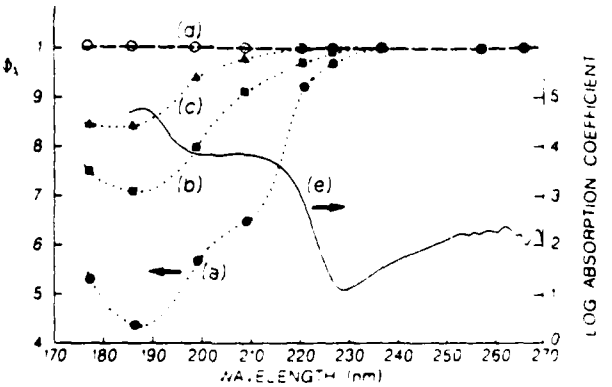

Fig.1 Curves (a)-(d):Relative fluorescence quantum yield of toluene as function of excitation wavelength. Standard cell:(a) room temperature; (b) -50°C; (c) -90°C. Open liquid:(d) -90°C. Curve (e):Absorption spectrum of toluene in n-hexane.

IS THE $S_2 \rightsquigarrow S_0$ INTERNAL CONVERSION AN IMPORTANT PATHWAY FOR RADIATIONLESS DECAY OF THE S_2 STATE OF AZULENE ?

A.L. Sobolewski and J. Prochorow

Institute of Physics, Polish Academy of Sciences

Al. Lotników 32/46, 02-668 Warsaw, Poland

The rates of the $S_1 \rightsquigarrow S_0$ and the $S_2 \rightsquigarrow S_0$ internal conversions in azulene were both estimated to be almost of three orders of magnitude greather than expected for internal conversion in aromatic hydrocarbons with equivalent energy gaps (see [1] and references therein). According to Hirata and Lim [1] the $S_2 \rightsquigarrow S_0$ internal conversion is already competitive with the $S_2 \rightsquigarrow S_1$ internal conversion in radiationless decay of S_2 of azulene. This picture is in accordance with the experimental results of Griesser and Wild [2] who didn't find a simple correlation between energy gaps of S_2, S_1 and S_0 states and the rate constants of radiationless transitions from S_2 state in azulene and its derivatives. It must be emphasized, however, that up to now all correlations and interpretations of radiationless transitions from S_2 state in azulene were based on two-electronic-state model, which seems to be particularly inadequate in this case. We may expect that besides a direct couplings $S_2 \rightsquigarrow S_0$ and $S_2 \rightsquigarrow S_1$ also coupling between S_1 and S_0 is of importance in the kinetic of deactivation of S_2 state.

In this work we are developing a model of sequential coupling of S_2, S_1 and S_0 states. With an assumption of random approximation for the matrix coupling elements [3], we are able to calculate the rate constants for $S_2 \rightsquigarrow S_1$ internal

conversion in azulene and in a series of its derivatives (details of the model and numerical calculations are given in [4]). The results are plotted in Fig. 1., where nonradiative rate constants of the deactivation of the S_2 state, k_{nr}, of azulene compounds are given versus the $S_2 - S_1$ energy gap.

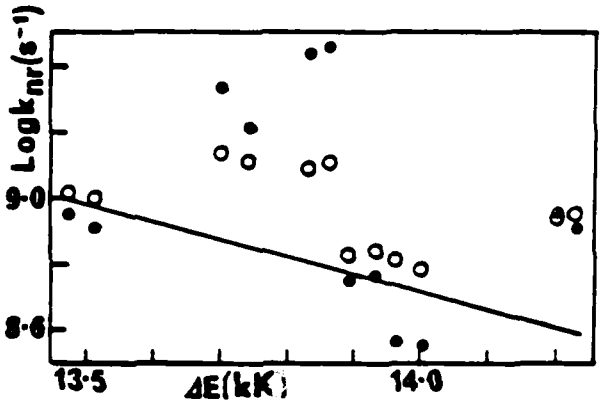

Fig. 1. Experimental results of Ref. [2] - dotts. Theoretical calculations of this work: within sequential coupling model (circles) and within two-state model (solid line).

It is concluded that a complicated dependence of k_{nr} of S_2 state in azulene compounds on the energy gap can be quite well reflected by the variation of the $S_2 \rightsquigarrow S_1$ internal conversion rate constant calculated for these molecules within the model of sequential coupling, thus indicating that the $S_2 \rightsquigarrow S_0$ internal conversion is of minor importance in deactivation of S_2 state in azulene.

1. Y. Hirata and E.C. Lim, J. Chem. Phys. 69 (1978) 3292
2. H.J. Griesser and U.P. Wild, Chem. Phys. 52 (1980) 117
3. M. Muthukumar and S.A. Rice, J. Chem. Phys. 69 (1978) 1619
4. A.L. Sobolewski, to be published

Metastable Nitrogen Energy Transfer Emission Spectroscopy: Recent Advances and Applications

J. W. Mitchell
P. K. Wittman
AT&T Bell Laboratories
Room 1D-239
Murray Hill, New Jersey 07974

Summary

Ultrasensitive operationally easy, on-line analytical techniques are required to monitor the fabrication and processing of ultrahigh purity electronic materials. Where inert atmospheres free of oxygen and carbon contamination are required, metastable transfer emission spectroscopy (MTES) is suited ideally for continuous monitoring of gas purity.

In the microwave discharge molecular specie containing oxygen and/or carbon (O_2,H_2O, CO_2, CO, oxides of nitrogen, and hydrocarbons) are fragmented. The metastable nitrogen formed simultaneously can then react with the oxygen or carbon to form NO or CN in an excited state. These chemiluminescent reactions provide a means of monitoring total oxygen and carbon levels.

Most previous investigators of the MTES technique have primarily demonstrated the potential of the method for ultratrace detection of metals. Evidently, background emissions from atmospheric contaminants of nitrogen did not

interfere spectrally with the detection of metals. In the current investigation an ultrapurified nitrogen supply to the discharge was essential to the successful detection of trace atmospheric contaminants in a high purity analyte nitrogen sample. The effectiveness of known methods most often used by experimentalists to purify nitrogen in the laboratory are compared quantitatively by MTES.

Complete removal of total oxygen impurities has been accomplished with an oxygen scavenging reactive resin. Less than 63 ppb of oxygen is present in the T-resin purified product. Other more conventional laboratory purification methods, molecular sieves-liquid nitrogen trap, copper turnings ($400^{o}C$), liquid nitrogen cold trap, and 2-propanol, dry ice cold trap reduce, but do not completely eliminate total oxygen contamination. Total carbon contamination from hydrocarbons (CH species), CO, and CO_2 is marginally reduce by a liquid nitrogen cold trap. The system consisting of a T-resin reservoir followed by a liquid nitrogen cold trap provides the most convenient and effective ultrapurification scheme for simultaneous reduction of oxygen and carbon impurities.

The quantitative determination of total oxygen impurities in nitrogen is investigated in detail. Meaningful standards and reliable techniques for calibrating the instrumental system are discussed.

Nd:YAG Laser-Induced Visible Fluorescence from Singlet Molecular Oxygen Generated in $NaOCl-H_2O_2$ Chemical Reaction System

Humio Inaba and Akio Yamagishi*

Research Institute of Electrical Communication, Tohoku University

Katahira 2-1-1, Sendai 980, Japan

*High Magnetic Field Laboratory, Faculty of Science, Osaka University

Toyonaka, Osaka 560, Japan

The oxygen molecule is known to absorb and emit photons by single-molecule transitions as well as cooperatively by pair-molecule transitions or transitions involving O_4 complexes[1,2]. From the excited singlet states $^1\Delta_g(0)$ and $^1\Delta_g(1)$, near infrared emissions at 1.06 μm and 1.27 μm take place as showin in Fig. 1, although they are generally weak due to the forbidden nature of the transitions. Also it is to be noted that the excited-state oxygen pair molecules O_2-O_2 produce fluorescence spectra in the visible region as indicated in Fig. 1. Since the metastable $^1\Delta_g(0)$ state is the first excited one, the fluorescence lines from the $^1\Delta_g(0)\cdot{}^1\Delta_g(0)$ state at 630 nm and 700 nm exhibit rather stronger intensities than those for other transition lines. However, the transition from the ground $^3\Sigma_g^-(0)$ state to the excited $^1\Delta_g(1)$ state is almost on resonance with the Nd:YAG laser output at 1.06 μm. Hence strong absorption of this radiation provides large concentrations of singlet oxygen molecules in this state from which various excited states are induced by energy transfer processes[2].

This paper reports newly measured results and discusses various interesting characteristics of visible fluorescence from singlet oxygen molecules generated in a chemical reaction system incorporated with the Nd:YAG laser excitation for the first time. The aqueous system involving $NaOCl-H_2O_2$ chemical reaction[1,3], which produces faint red-chemiluminescence easily observed by the naked eye,

was used for the experiment. This reaction is supposed to occur in biological systems such as in the antimicrobial activity of the polymorphonuclear leukocyte.

The visible fluorescence induced by the Q-switched Nd:YAG laser output was measured by an extra-high sensitive pulse-gated photon counting method. We should mention that with neither the laser excitation nor the chemical reaction, very weak or no emission was observed. When both the excitation and reaction take place simultaneously, enhanced visible emission was detected as illustrated in Fig. 2. These measured spectra well correspond to the simultaneous transitions in pairs of the excited singlet molecular oxygen as indicated in the figure. Intensity of the laser-induced fluorescence was about 10^4 times larger than that from the liquid oxygen excited by a Q-switched Nd:YAG laser[2]. It was also found experimentally that each spectral line has different laser-power dependence as well as different behavior of fluorescence decay with time. These anomalous features are explained by the interaction of oxygen molecules excited by the Nd:YAG laser pulse with those excited steadily by the chemical reaction, based on the quantitative analysis.

This method described above should offer a novel way to detect singlet molecular oxygen in various situations such as in chemical reaction and biological systems. The main advantage of this method is that the excitation wavelength is in the infrared region, while observation is performed in the visible range, and their characteristic wavelengths allow one to distinguish oxygen molecules from other various light emitting species in complex systems accompanying chemical and biomedical processes.

References

1. E.g., H. H. Wasserman and R. W. Murray, eds., Singlet Oxygen (Academic Press, New York, 1979).
2. A. Yamagishi, T. Ohta, J. Konno, and H. Inaba, J. Opt. Soc. Am. 71, 1197 (1981).
3. M. Nakano, T. Noguchi, K. Sugioka, H. Fukuyama, M. Sato, Y. Shimizu, Y. Tsuji, and H. Inaba, J. Biol. Chem. 250, 2404 (1975).

Fig. 1

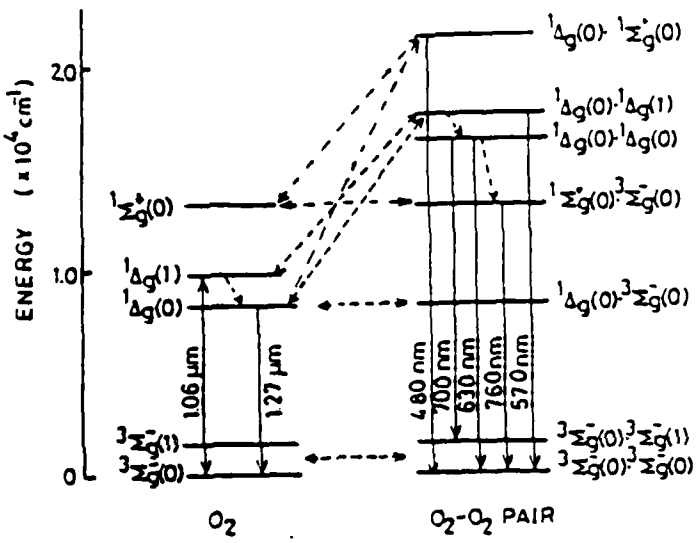

Fig. 1 Energy level diagram of the oxygen molecule and the oxygen pair-molecule. Solid arrow lines show radiative transitions, and dashed arrow lines indicate nonradiative transitions.

Fig. 2

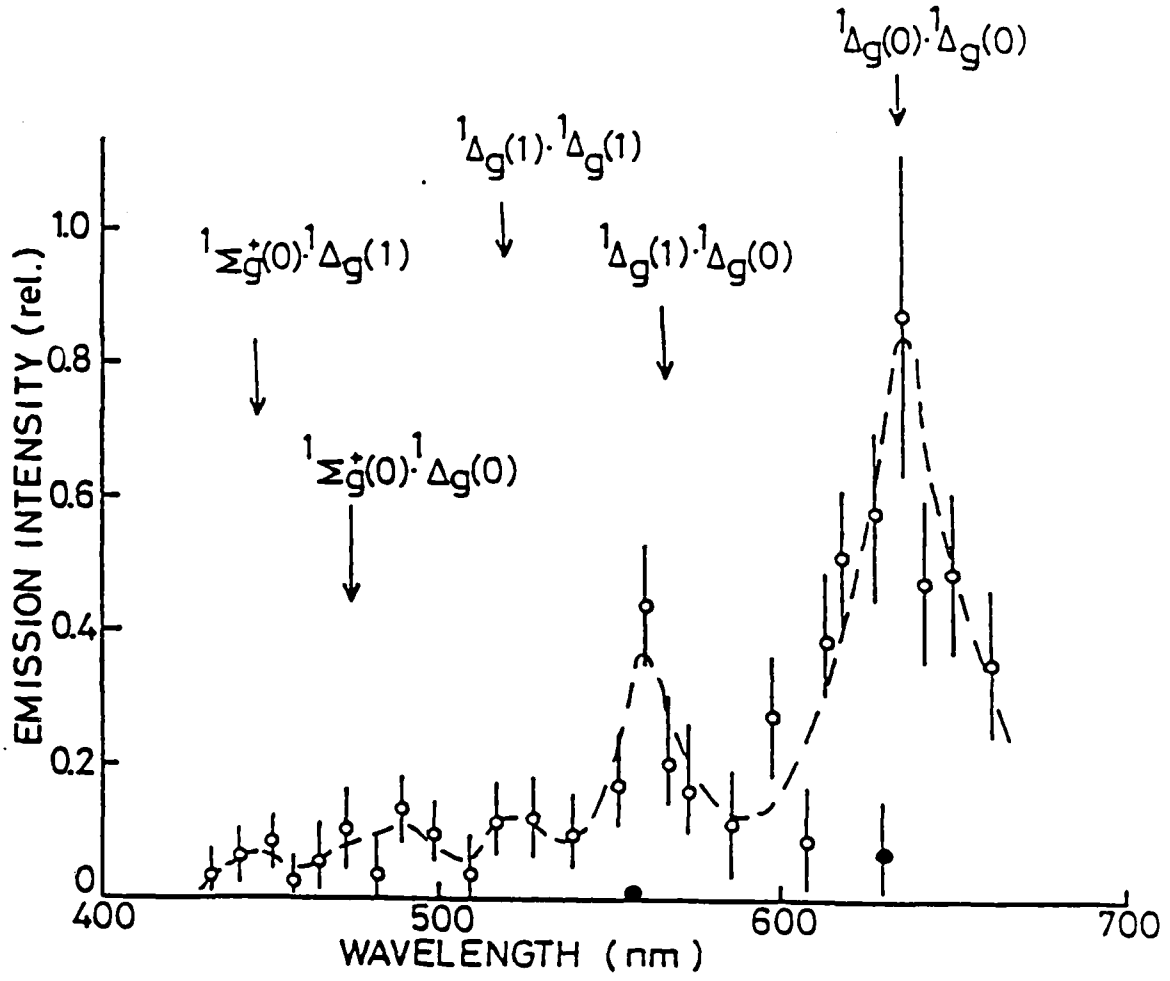

Fig. 2 Measured spectra of Q-switched Nd:YAG laser-induced fluorescence in the visible region due to the simultaneous transitions in pairs of the excited singlet molecular oxygen in NaOCl-H_2O_2 chemical reaction system. Open circles indicate fluorescence spectra enhanced by the laser radiation, and closed circles represent the background chemiluminescence level without laser radiation.

HOW ISOLATED IS NITROGEN IN A MATRIX?

M. Creuzburg, Fakultät für Physik, Universität
84 Regensburg, F.R.G.

The doubly forbidden $A^3\Sigma_u^+ \rightarrow X^1\Sigma_g^+$ (Vegard-Kaplan,V-K) emission of the N_2 molecule can serve as a probe for its interaction with the neighborhood. While the radiative lifetime in noble-gas matrices is affected only by the host, the vibrational relaxation rates in the A state depend strongly on the proximity of other imperfections.

In the X-ray luminescence from bulk samples of N_2-doped Ne, we observe: (1) The V-K bands show a red shift from the thin-film value[1] of up to 200 cm^{-1} with increasing N_2 concentrations and an apparently inhomogeneous broadening, see Fig. 1. (2) The intensity is less than proportional to the concentration; the relation is even reversed above 2000 ppm N_2. (3) Fig. 1 refers to samples grown from the stated gas mixtures by puls-deposition of 2 µm/puls at 4 K. Changes of temperature and pressure during growth, or of deposition rate influence the intensities and red shifts very

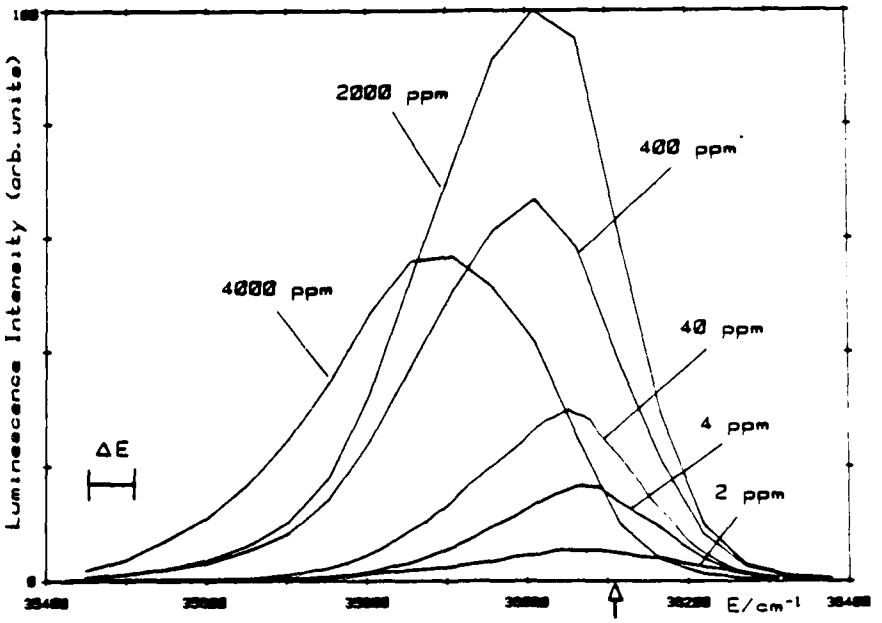

Fig. 1 X-ray luminescence spectra of the v'=0 → v"=6 V-K band of N_2 in solid Ne as a function of N_2 concentration. The arrow marks the corresponding band maximum in Ref. 1.

strongly. N_2 behaves similarly in Ar matrices. (4) A change of envelopes of the V-K bands can be explained by modified Franck-Condon factors, indicating a reduced equilibrium N-N separation in the A state.

When the radiative lifetime competes with the vibronic relaxation from the A(v'=6) state, as is the case in Ar matrices, additional effects concern the then observable hot luminescence[1)2)]: (5) Its relative intensity is reduced with increasing concentration in favor of the v'=0 bands, indicating an efficient vibrational energy transfer to imperfections. (6) A temperature increase from 4 K to 25 K can inverse the predominance of hot (v'=6) to "cold" (v'=0) luminescence.

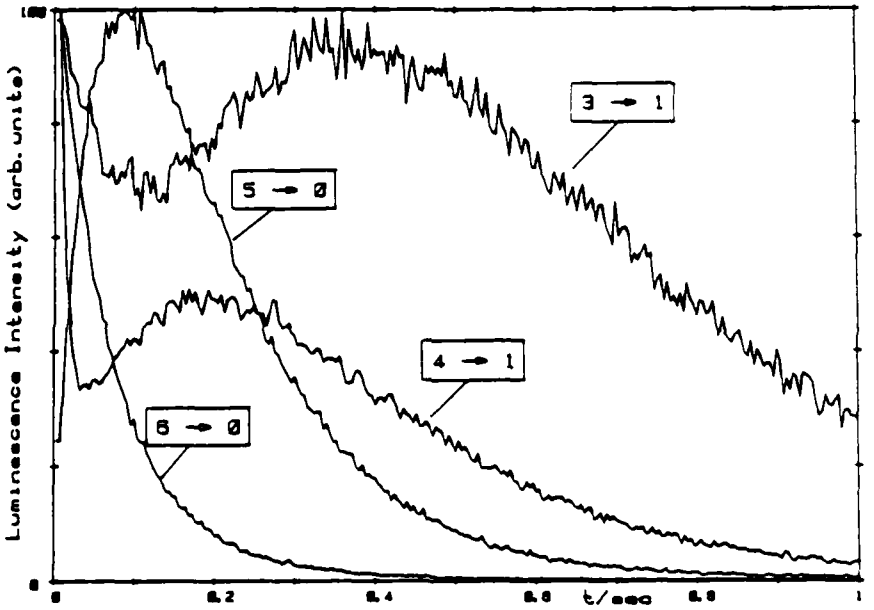

Fig. 2 Decay and swell curves of the v'→v" hot luminescence V-K bands of N_2 in an Ar matrix. The intensities are arbitrarily normalized for each curve.

The N_2 molecule relaxes vibrationally by cascading, as is evidenced by pulsed X-ray luminescence, Fig. 2. The observed decay and swell curves give the rates of the step-by-step energy relaxation and their dependences on concentration and temperature.

References

1) Tinti, D.S., and G.W. Robinson, J.Chem.Phys.49,3229 (1968)
2) Wilcke, H., Thesis, University of Kiel, F.R.G., 1983

Vibrational Relaxation Of N_2 Aggregates In Rare Gas Matrices

J. Bahrdt, H. Kühle, N. Schwentner, H. Wilcke
Institut für Atom- und Festkörperphysik, Freie Universität Berlin, Arnimallee 14, 1000 Berlin 33, Fed. Rep. Germany

In an experimental investigation of the conversion of electronic energy into vibrational degrees of freedom of a cluster followed by dissipation into matrix phonons it is essential that all intermediate steps of the energy flow can be monitored. For this purpose each vibrational level v'=1 up to v'=6 of the lowest excited electronic state A $^3\Sigma_u^+$ of N_2 in a solid Xe matrix has been excited selectively by monochromatized synchrotron radiation. The stepwise relaxation to lower A $^3\Sigma_u^+$ vibrational levels has been derived from luminescence spectra. The large vibrational energy of 174 meV corresponding to 35 matrix phonons inhibits vibrational relaxation in completely isolated N_2 molecules within the radiative lifetime of $\gtrsim 10^{-3}$s. For N_2 pairs and larger clusters a complex relaxation cascade is observed which leads to different steady state distributions for each initial level. The first relaxation steps involve only changes of v' by two quanta. For excitation of $v' \geq 4$ states also intermediate vibrational levels are populated in the end of the cascade. The experimental results indicate the following two basic processes: Radiationless electronic energy transfer between two N_2 molecules based on exchange interaction leads to a deexcitation of molecule I from the initially (v')A $^3\Sigma_u^+$ state to the groundstate (v"=1)X $^1\Sigma_g^+$ and the neighbouring molecule II is excited from (v"=0)X $^1\Sigma_g^+$ to (v'-2)A $^3\Sigma_u^+$ corresponding to a

reduction of v' by two quanta. The efficiency of this process follows from the small excess energy (∿50 meV) of 2 v' quanta (2x 174 meV) compared to one ground state vibrational quant v" (290 meV). The excess energy is dissipated into about 10 matrix phonons. Two successive down conversions result in (v'-4)A $^3\Sigma_u^+$ at molecule I and (v"=2)X $^1\Sigma_g^+$ at molecule II. Now an additional energy transfer leads to (v"=0)X $^1\Sigma_g$ and (v'-1)A $^3\Sigma_u$ which is an up conversion that increases v' by 3 quanta. The efficiency of this conversion of two ground state quanta into 3 quanta of the excited electronic state is again due to the small excess energy (50 meV). A quantitative description of the observed cascades by this energy transfer model is presented.

RELAXATION AND PREDISSOCIATION OF EXCIPLEX IN A SUPERSONIC JET

by J.Prochorow (Institute of Physics PAN, Al.Lotników 32/46, 02-668 Warsaw, Poland), M.Castella (DPC CEN-Saclay, France) and A.Tramer (Laboratoire de photophysique Moleculaire, Univ. Paris-Sud 91405 Orsay, France)

An exciplex system of perylene with N,N-dimethylaniline (DMA) with strong exciplex fluorescence in liquid solution and no indication of complex formation in the ground state is studied in this work in a supersonic jet. The aim is to get insight into the dynamics of vibrational energy redistribution in extremly large excited complex characterized by a number of low-frequency vibrations. Furthermore, a problem of a non-bonding (or repulsive) ground state of exciplex vs. van der Waals complex formation is examined.

The excitation spectrum of the overall fluorescence (FES) of perylene-DMA complex is composed of a quasi-continous background extending through the whole spectrum, with a flat maximum at $\sim 23400\ cm^{-1}$. The groups of bands corresponding to all strong vibronic transitions of free perylene ($0_o^o = 24064\ cm^{-1}$) but red shifted by $\sim 355\ cm^{-1}$ are superimposed on this background. The 0_o^o transition of the complex ($23710\ cm^{-1}$) is composed of broad incompletely resolved bands. Higher vibronic transitions of perylene ($0_o^o + 350$, $+ 2\cdot350$, $+ 1300$, $+1376$ and $+ 1603\ cm^{-1}$) although easily recognizable are almost completely diffused.

Excitations at $23400\ cm^{-1}$ (background) and in the 0_o^o and $0_o^o + 350\ cm^{-1}$ give rise to the broad, structureless fluorescence band with maximum at ca. $21200\ cm^{-1}$. For all practical purposes this fluorescence is identical with the fluorescence of perylene-DMA exciplex in liquid solution, but is shifted to higher energies (by ca. $2000\ cm^{-1}$ as compared to a non-polar liquid

solution [1]). Under excitation to higher vibronic levels fluorescence of exciplex remains unchanged but weak, narrow bands of free perylene are also appearing in the spectrum.

These results indicate that there are two closely lying excited states of the complex corresponding to its van der Waals ground state. The lowest one is a charge-transfer A^-D^+ state - transitions to and from which give rise to diffuse absorption and emission spectra (with a large Stokes shift). Somewhat above this state, a locally excited A^*D state is located. For a low excess of excitation energy in A^*D state ($E_{vib} = 0 - 700\ cm^{-1}$), a rapid (about 1 ps) electronic relaxation leads to the A^-D^+ state initial for exciplex emission. Excitations to higher vibronic levels of A^*D ($E_{vib} > 700 - 1600\ cm^{-1}$) give origin to structured perylene-like emission. A comparison of FES of the complex and of free perylene shows that perylene-like emission of the complex is due to the vibrational predissociation of A^*D state. However, vibrational predissociation is slow as compared to vibrational redistribution, as we observe both, the emission of undissociated complex and of the dissociation product (perylene). This may be due to the very high level density of low-frequency modes high in the intermolecular potential well.

It has to be noticed also that for the first time a diffuse absorption, different from absorption of exciplex' componenets, has been observed, thus indicating an existance of bonding ground-state interaction in an exciplex.

Finally, let us mention that preliminary results for an anthracene-DMA exciplex lead in general to similar conclusions.

[1] H.Leonhardt and A.Weller, Ber.Bunsenges.Phys.Chem. 67 (1963) 791 .

On the Dynamics of Excitons in Molecular Crystals.

Emilio Cortes
Universidad Autonoma Metropolitana.-Dept. of Physics, Apartado Postal 55-534
Mexico 12 D.F. MEXICO.

Return address: Dept. of Chemistry, B-014, La Jolla, Ca 92093.

SUMMARY:

The description of exciton dynamics in molecular aggregates at finite temperatures has recently been shown to require the inclusion of dissipative contributions that have heretofore not been taken into account[1,2]. The specific model considered so far has been the usual one of an exciton coupled to a bath of harmonic oscillators as described by the Hamiltonian

$$H = \sum_k E_k a_k^+ a_k + \sum_{q,\alpha} \omega_{q\alpha} b_{q\alpha}^+ b_{q\alpha} + \sum_{k,q,\alpha} \Gamma_{kq\alpha} (b_{q\alpha}^+ + b_{-q\alpha}) a_k^+ a_{k+q} \qquad (1)$$

Here $a_k^+(a_k)$ creates (destroys) an exciton of wave vector k and energy E_k, $b_{q\alpha}^+(b_{q\alpha})$ creates (destroys) a phonon in branch α of wave vector q and energy $\hbar\omega_{q\alpha}$, and $\Gamma_{kq\alpha}$ is a coupling constant. The dynamics of the excitons is then desceibed by the exact equation of motion[1,2]

$$\dot{a}_k(t) = -i E_k a_k - i \sum_{k'} f_{kk'}(t) a_{k'}(t) - \sum_{k_1,k_2,k_3} \int_0^t d\tau\, K_{k_2k_3}^{k k_1}(t-\tau) \frac{d}{d\tau} [a_{k_2}^+(\tau) a_{k_3}(\tau)] a_{k_1}(t) \qquad (2)$$

Here $f_{kk'}(t)$ depends on initial values of the phonon operators and is given explicitly in the theory. If the phonon initial conditions are assumed to be described by a distribution, then $f_{kk'}(t)$ can be interpreted as fluctuations. $K(t-\tau)$ is a dissipative kernel related to $f_{kk'}(t)$ by a (quantum mechanical) - fluctuation - dissipation relation which is again given explicitly by the theory. The last term in (2) is thus the dissipation. Previous theories differ from the present one in at least one of two respects: the evolution is usually described perturbatively (whereas Eq.(2) is exact), and/or dissipative effects are usually omitted (i.e. $K(t-\tau)$ is absent, which implies an infinite temperature). We have shown that Eq.(2) leads to the correct thermal properties of the system as $t\to\infty$ [3].

The excitons created by a_k^+ are those that would occur in a rigid lattice and are called "naked". Since the exciton - phonon coupling represented by the last term in (1) is generally not weak, the actual excitations in the system are "clothed", i.e. they are accompanied by a lattice distortion.[4] These clothed excitons interact with the lattice more weakly than do the original naked excitations. It has been customary to therefore describe the evolution of the clothed excitons perturbatively in the exciton - phonon interaction parameters. In this description(as in that of naked excitations) the dissipative effects have heretofore been omitted or at least included in a phenomenological ad hoc fashion, i.e. the description of clothed excitons has also been limited to high temperatures.

We will present results on our analysis of the evolution equations for clothed excitons. These equations contain important improvements over those previously obtained and we are thus in principle able to analyse spectra and transport coefficients for these excitons over the full parameter and temperature range.

References:

1. Stochastic Model for Exciton Lineshapes at Finite Temperature, Bruce J. West and Katja Lindenberg, Random Walks and Their Application to Physical and Biological Sciences (American Institute of Physics, New York, 1984), ed. by M. Shlesinger and B. J. West.

2. Exciton Lineshapes at Finite Temperatures, Katja Lindenberg and B. J. West, Phys. Rev. Lett., 51, 1370, (1983).

3. E. Cortes, K. Lindenberg, R. Pearlstein and B.J. West, in preparation.

4. e.g. M. Grover & R. Silbey, J. Chem. Phys. 54, 4843 (1971).

AD-A148 470 INTERNATIONAL CONFERENCE ON LUMINESCENCE HELD AT MADISON WISCONSIN ON 13-17 AUGUST 1984(U) WISCONSIN UNIV-MADISON W M YEN OCT 84 N00014-84-G-0053 1/1

UNCLASSIFIED F/G 20/6 NL

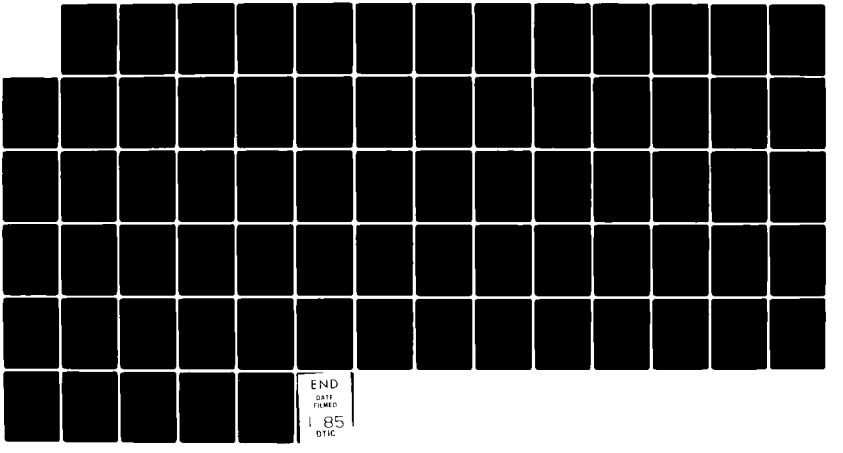

END
DATE FILMED
1 85
DTIC

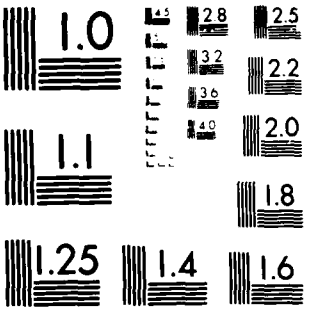

DETERMINATION METHOD OF THE CHARACTERISTIC PARAMETERS OF DIFFERENT INTERACTION POTENTIALS FROM ENERGY TRANSFER MEASUREMENTS

Bernard SIPP and René VOLTZ

Centre de Recherches Nucléaires
Physique des Rayonnements et Electronique Nucléaire
67037 STRASBOURG CEDEX (France)

In many cases, the characteristic parameters of the microscopic distance dependent transfer rate between an excited donor and an acceptor molecule are unknown. Quite generally, the transfer rate expression can be expressed as $\frac{1}{\tau} f(\frac{r}{r_o})$ where r_o is the interaction range and $1/\tau$ a frequency factor.

In a fluid solution it has been shown recently [1] that the transfer rate coefficient at long times is of the form

$$k = 4 \pi D b$$

where D is the effective diffusivity and b the reaction length whose expression has been calculated when the interaction is of multipolar or exponential type. In many situations of practical interest, excitation transfer takes place by a short- and a long range interaction. When the interaction is the sum of the contributions of exchange and dipole-dipole coupling (resonant Coulomb interaction)

$$\lambda(r) = \frac{1}{\tau_e} \exp(-\frac{r}{r_e}) + \frac{1}{\tau_d} [\frac{r_d}{r}]^6$$

calculation show that in the weak diffusion limit, the total transfer length is given by

$$b = \frac{\Gamma(3/4)}{\Gamma(5/4)} \frac{r_d^2}{2(D\tau_d)^{1/2}} \frac{I_{-1/4}(x_e)}{I_{1/4}(x_e)} \qquad (1)$$

where $I_{-1/4}(x_e)$ and $I_{1/4}(x_e)$ are modified Bessel functions and

$$x_e = \frac{r_d}{2(D\tau_d)^{1/2}} \left\{ \frac{r_d}{2r_e\left[C + \text{Log} \frac{r_e}{(D\tau_e)^{1/2}}\right]} \right\}^2$$

(C, Euler constant).

In relation (1), τ_d and r_d are supposed to be known as they can generally be deduced from auxiliary measurements (r_d is related to the spectral overlap of the donors and acceptors).

It may be remarked that the total transfer length depends on the diffusion coefficient (as it is the case for single interactions) which is of particular interest in an experimental method to estimate separately r_o and τ. The procedure is the following :

i) from measurements for small and high values of acceptor concentration corresponding respectively to exponential and non exponential donor decays, it is possible to infer the experimental values of D and b in a given solvent.

ii) from the same measurements but made now in a solvent of different viscosity one gets another numerical relation between b, r_o and τ.

Combining the information deduced from the two measurements leads then to the values of r_o and τ.

As an illustration of this method, we performed measurements of fluorescence decay of naphthalene (donor) with molecules of anthracene (acceptor). For this couple of molecules, the Förster radius r_d is well known but no quantitative information is available about the radius r_e and the frequency factor $1/\tau_e$ of the exchange interaction. The transfer rate coefficient was measured to be $25 \times 10^{-12} cm^3 s^{-1}$ in methylcyclohexane and $1.4 \times 10^{-12} cm^3 s^{-1}$ in paraffin oil. From the extension of the transfer

length in the two solvents we got for the exchange interaction parameters :

$$r_e = 0.21 \pm 0.04 \text{ nm}$$

$$\tau_e = 1.9 \times 10^{-12} \begin{matrix} + 2 \times 10^{-12} \\ - 0.5 \times 10^{-12} \end{matrix} \text{s}.$$

[1] B. Sipp and R. Voltz, J. Chem. Phys. 79 (1983) 434.

The Usefulness of Sensitized Luminescence as a Probe for Exciton Motion in Molecular Crystals

V. M. Kenkre and P. E. Parris
Department of Physics and Astronomy
University of Rochester, Rochester, NY 14627

Despite considerable work done in the field of energy transfer via sensitized luminescence,[1-3] serious questions[4] remain concerning the relationship between the primary experimental observable and microscopic parameters which govern exciton transport. We present a quantitative analysis of these questions as they pertain to several specific exciton-trap systems, particularly tetrachlorobenzene, naphthalene and anthracene. On the basis of a general theory[5] which treats the capture process on an equal footing with motion, we address quantitatively the concept of time-dependent energy transfer rates. We find that the time dependence depends strongly on the effective dimensionality, becoming more pronounced as the dimensionality decreases and that for fixed dimensionality the time dependence becomes less marked as the capture process is slowed down.

Specifically, in 1,2,4,5-TCB we find that a coherent, capture-limited picture of energy transfer consistent with spin-echo work[3] leads to as good an agreement with data as a picture[2] based on macroscopically diffusive motion and infinite capture rate. On the other hand, our analysis results in an <u>independent</u> estimate of the average scattering rate among band states ($\sim 10^9$/s) which is considerably larger than that deduced from spin-echo work.[3]

For singlet excitons in naphthalene and anthracene we find that, due to the dimensionality effect in these systems (≥ 2) any deviation from time-independent rates would be subtle and quite possibly masked by the limits of experimental error. Therefore useful information from such experiments is greatly reduced. The most that can be obtained is a lower bound for

the exciton diffusion constant and capture parameters since the observed quantity is a single rate constant determined by both motion and capture.

1. H. Auweter, A. Braun, U. Mayer, and D. Schmid, Z. Naturforsch. 34a, 761 (1979); A. Braun, U. Mayer, H. Auweter, H. C. Wolf, and D. Schmid, Z. Naturforsch. 37a, 1013 (1982).
2. D. D. Dlott, M. D. Fayer, and R. D. Wieting, J. Chem. Phys. 67, 3808 (1977); 69, 2752 (1978).
3. A. J. Van Strien, J. F. C. van Kooten, and J. Schmidt, Chem. Phys. Lett. 76, 7 (1980); A. J. Van Strien, J. Schmidt, and R. Silbey, Mol. Phys. 46, 151 (1982).
4. V. M. Kenkre and D. Schmid, Chem. Phys. Lett. 94, 603 (1983).
5. V. M. Kenkre and P. E. Parris, Phys. Rev. B27, 3221 (1983).

Proposal for New Experiments for the Investigation of Transport Coherence of Excitons in Molecular Crystals

V. M. Kenkre and G. P. Tsironis
Department of Physics and Astronomy
University of Rochester, Rochester, NY 14627

A central open fundamental question in exciton dynamics in molecular crystals concerns transport coherence of excitons, particularly at low temperatures. A large amount of effort has been spent over many years on this issue but clear answers have not emerged. Old suggestions that the temperature dependence of energy transfer rates is indicative of transport coherence have been shown to be untenable, or at least inconclusive, since a variety of alternate factors having little to do with coherence can be shown to lead quite reasonably to explanations of those observations. Careful reanalysis[1,2] of sensitized luminescence experiments is making clear that the role that capture plays in them (relative to exciton motion) can be considerable and that that category of observations is not well suited to investigations of coherence. We have recently found[3,4] that Ronchi grating experiments constitute an ideal candidate for definitive coherence studies. The observable is the time-dependent delayed fluorescence arising from mutual annihilation of triplet excitons. The parameter under experimental control is the extent of the spatial inhomogeneity of the triplets manipulated through the ruling period of the Ronchi grating covering the crystal during illumination.[5] We present a detailed analysis of the suggested experiment and describe the expected effect of two separate factors on the outcome of the experiments: (i) finite degree of coherence and (ii) finite rate of vibrational relaxation.

1. V. M. Kenkre and D. Schmid, Chem. Phys. Lett. 94, 603 (1983);
D. Schmid, in Electronic Excitations in Organic Solids, ed.

P. Reineker, H. C. Wolf and H. Haken (Springer 1983); V. M. Kenkre, ibid.

2. P. E. Parris and V. M. Kenkre, Chem. Phys. Lett. in press.
3. V. M. Kenkre, V. Ern and A. Fort, Phys. Rev. B 28, 598 (1983); Chem. Phys. Lett. 96, 658 (1983).
4. A. Fort, V. Ern and V. M. Kenkre, Chem. Phys. 80, 205 (1983).
5. V. Ern, P. Avakian, and R. E. Merrifield, Phys. Rev. 148, 862 (1966).

VIBRONIC EXCITONS IN CRYSTALLINE ANTHRACENE

Roberto E. Lagos and Richard A. Friesner
Department of Chemistry
University of Texas, Austin, Texas 78712

In a recent paper[1] we presented a cluster generalization of the Dynamical Coherent Potential Approximation (DCPA). When applied to exciton-phonon interactions in molecular crystals the theory represents a distinct improvement over perturbative and single site DCPA calculations. We also extended our formalism to the case of several molecules per unit cell. Our model assumed throughout one harmonic vibrational mode per molecule.

In the present paper we explicitly calculate the optical spectrum of crystalline anthracene (2 molecules per unit cell). We compare our results with both experiments and other non perturbative calculations (i.e., single site, one molecule per unit cell DCPA) and obtain a definite improvement over the latter, one improvement being the clear exhibition of a Davydov splitting. Furthermore, we achieve quantitative agreement with experiment by introducing in a semi-phenomenological fashion the effects of a finite phonon bandwidth, which renormalizes the width of each of the vibronic peaks of the spectrum. Finally we discuss some temperature effects.

[1] Roberto E. Lagos, Richard A. Friesner, Phys. Rev. B15, March 1984.

LUMINESCENCE of TETRACENE CRYSTALS

M.V.Kurik,Yu.P.Piryatinskii

Institute of Physics, Academy of Sciences of the Ukrainien SSR, Kiev (Prospect Nauki 144,252650,Kiev 28,USSR)

Electron spectra of molecular crystals are quite sensitive to the structural changes of a lattice. It allowed to establish by spectrum that at cooling of tetracene crystals lower than 160K it was observed that phase transition of the first kind occurs [1-2]. It is assumed that at the phase transition a weak triclinic lattice transits into a monoclinic one. Increased concentration of structural defects is observed in tetracene crystals subjected to the phase transition. These defects in tetracene lattice are the places of localization of singlet and triplet excitons and they make an essential influence on the energy transfer and luminescence spectra. We carried out investigations of luminescence by spectroscopy method with the time resolution that allowed at low tempered spectra to observe bands responsible for luminescence of free excitons and excitons localized on defects [3]. It has been determined that values of free excitons lifetime in tetracene crystals at 4,2K lies in the range from 1 to 2,5 nanoseconds.

The presence of prompt fluorescence of the band 570 nm in the spectra is characteristic for the crystals containing the increased structural defects concentration. The dependence of intensity of the band 570 nm on temperature is characteristic for the excimer luminescence. The maximum intensity of this band is at 180K. The kinetic measurements showed that at fluorescence registration by the wave length of 570 nm the components with decay time from 1 to 7mSare observed at 4,2K.

It was pointed out [4] possibility of formation of slow component and its presence is related with annihilation of triplet correlative pair. The rise of such a pair is quite probable energetically because a crystal was excitated by nitrogen laser (337,1 nm), whereas the energy of pair formation is about 20200 cm^{-1}.

The investigations of spectra of prompt flurescence with different delay times showed the following.
Bands with considerable stocks shift are observed for freely fixed crystals in which considerable concentration of structural defets are formed after frequent coolings in consequence of the phase transition. These bands are nonstructural, their depths are in the limits from 700 to 3000 cm^{-1} from the bottom of the exciton zone. The father the band is from the bottom, the more delay times are observed in. It is natural to relate the formation of such deep centres of luminescence with excitation of predimer states, that appear in places of defects
The higher energetic bands in the spectrum in this case are responsable for excimer luminescence of molecules with unfull cover of bensol rings.

Besides investigations of prompt fluorescence we have observed delay fluorescence related with annihilation of triplet excitons. As much is the lifetime of triplet excitons, delay fluorescence is the most sensitive to the presence of defects in tetracene crystals. The measurements of kinetics of the delay fluorescence decay at 4,2K showed that the decay curve composes of two plots. Starting prompt component is conditioned by annihilation of free excitons. The calculated lifetime of free triplet excitons is in the limits of 150 mcsec. The lifetime of excitons localized on defects is in region of 240-360 mcsec for different crystals and temperatures. It is obtained that for thin tetracene crystals that are on optical contact with the layer, the formation of defects with depth 223,475 and 1630 cm^{-1} and with lifetime of about 600. Obtained investigations of slow fluorescence at different temperatures allowed to suppose about the mechanism of motion of the triplet excitons in tetracene crystals at low temperatures.

REFERENCES

1 A.F.Prichotko,A.F.Skorobogatko.Optics and Spectroscopy. 20,65, 1966.
2 D.D.Kolendritskii,M.V.Kurik,Yu.P.Piryatinskii.Phys.Stat.Sol.(b). 91, 741, 1979.
3 Yu.P.Piryatinskii,M.V.Kurik,V.D.Zukov.FTT, 25, 3577, 1983.
4 G.K.Klein. Chem. Phys. Lett. 57, 202, 1978.

Is the Barrier Height of Exciton Self-Trapping Evaluated So Far Correct ?

H. Sumi

Institute of Materials Science, University of Tsukuba

Sakura-mura, Ibaraki, 305 Japan

It has theoretically been shown that in the course of self-trapping exciton surmounts a potential barrier made by lattice distortion (or penetrates it by quantum-mechanical tunneling at low temperatures). Then, how high the potential barrier is has been investigated so far by analyzing the temperature dependence of the quantum yield η (or simply, the indensity) of free-exciton luminescence in many crystals. Three examples of it for RbI measured by Nishimura *et al.*[1] are shown in the figure of the next page. η decreases with increasing temperature T. This is regarded as originating from the increase of the self-trapping rate W of a free exciton with increasing temperature. Then, assuming that the temperature dependence of W was determined by a factor $\exp(-E_B/k_BT)$ describing the classical behavior of surmounting the potential barrier with height E_B, and moreover that other nonradiative and radiative decay processes had a rate independent of temperature, many people have analyzed η by a formula proportional to $1/[C+\exp(-E_B/k_BT)]$ with a constant C. For example, this analysis gives E_B=17 $\sim$ 18 meV for RbI.[1] However, the temperature region (15 $\sim$ 30K in RbI) where η most decreases is considerably lower than the Debye temperature ($\sim$100K). In such low temperatures, lattice distortion making up the potential barrier cannot be regarded as classical, and the self-trapping process must be intermediate between the classical surmounting and the quantum-mechanical tunneling with rate almost independent of temperature. Therefore the E_B value evaluated so far must be reconsidered: It has been evaluated small.

A transition of an exciton from a free state without lattice distortion to

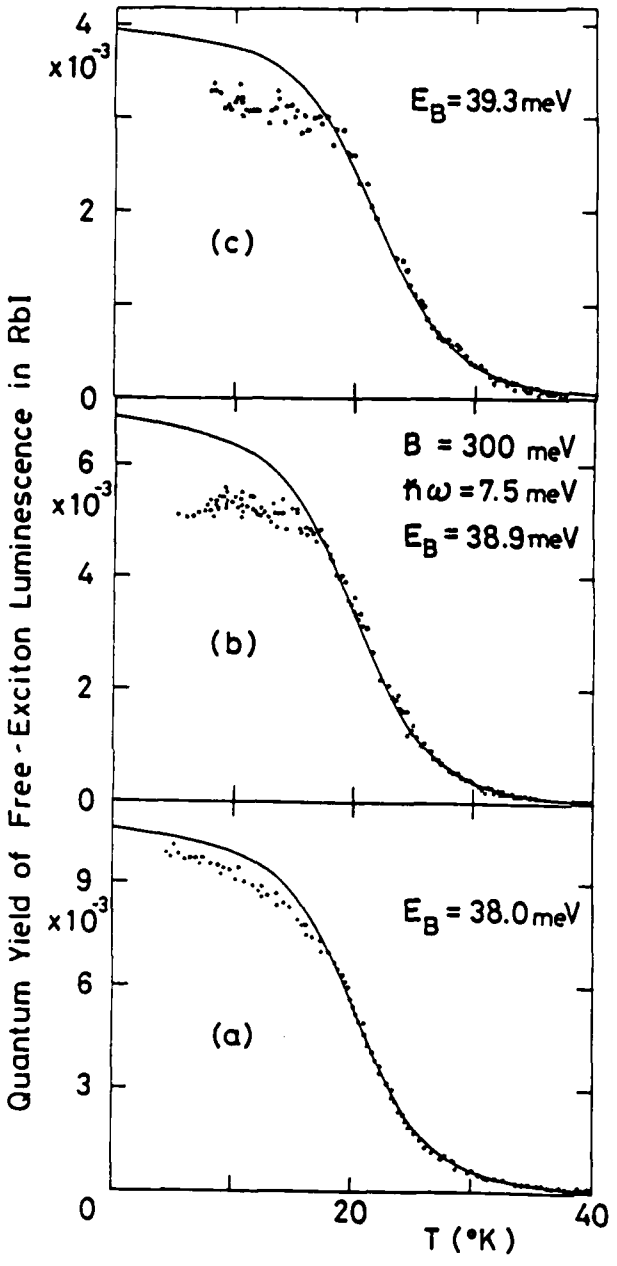

a self-trapped state with appreciable lattice distortion is a typical example of multiphonon processes. The present work gives a full quantum-mechanical expression of the self-trapping rate covering the intermediate region, and analyzes η with it. For example, observed η's of RbI shown in the figure are best fitted by a solid curve in the region above 15K below which observed η's scatter from sample to sample. This fitting gives E_B=38 ∿ 39 meV which is more than twice as large as E_B evaluated so far. In this analysis, the half width B of the exciton band was set at 300 meV of half the valence-band width, and the phonon energy $\hbar\omega$ at 7.5 meV where the density of acoustic modes becomes maximum. The obtained E_B value is also consistent with the self-trapping rate[2] measured directly at 4.2K.

1) H. Nishimura and T. Yamano: J. Phys. Soc. Jpn. 51 (1982) 2947.

2) Y. Umuma *et al.*: J. Phys. Soc. Jpn. 52 (1983) 4277.

TEMPERATURE DEPENDENCE AND ASYMMETRY OF EXCITON-LINESHAPES

K.W. Becker, H. Grötsch, U. Rössler (Inst. für Theoretische Physik, Universität Regensburg, D-8400 Regensburg, FRG)

Exciton-phonon coupling and electronic overlap (excitation transfer) are known as the competing mechanisms in the exciton-phonon problem, which become apparent in the optical lineshape of excitons. A phenomenological treatment of this problem yields a Lorentzian lineshape for weak exciton-phonon coupling and a Gaussian for strong coupling.[1] We have studied the lineshape of excitons by evaluating Kubo's expression for the optical susceptibility using the projection-operator formalism. In general, this theory yields asymmetric lineshapes due to a frequency-dependent memory function.

In the weak coupling case the lineshape becomes close to a Lorentzian in the high-temperature limit, but shows increasing asymmetry for decreasing temperature with different temperature dependences of the low and high energy half-width. This asymmetry is caused by the fact, that for low temperatures phonon assisted processes die out at the low energy side of the exciton resonance.

In the strong coupling limit the exciton-phonon problem reduces to the single-site problem, if the electronic overlap is neglected. This problem can be solved exactly. The resulting

lineshape, which contains the exciton-phonon coupling to all orders and is determined by Franck-London factors, approaches a Gaussian in the high-temperature limit with a line width proportional to $T^{1/2}$. With decreasing temperatures the line becomes again increasingly asymmetric and the temperature dependence of the line width deviates from the $T^{1/2}$-law.

The intermediate coupling region is approached from the strong coupling side by taking into account the electronic overlap in the memory function and from the weak coupling case by considering higher order corrections due to the exciton-phonon coupling.

We consider the influence of the dimensionality on the temperature dependence and asymmetry of the lineshape and compare our results with those of numerical experiments.[2] The advantage of our theoretical concept is its analytical form, which makes the physical mechanisms of temperature dependence and asymmetry of the exciton lineshapes more transparent.

[1] Y. Toyozawa, in Relaxation of Elementary Excitations, ed. by R. Kubo and E. Hanamura (Springer 1980) p. 3

[2] M. Schreiber, Y. Toyozawa, J. Phys. Soc. Japan 51, 1528 (1982)

LUMINESCENCE OF SELECTIVE OPTICAL PUMPING OF EXCITONS IN GaSe

V. Capozzi, S. Caneppele and M. Montagna
Dipartimento di Fisica, University of Trento, 38050 Povo, Italy
and Gruppo Nazionale Struttura della Materia del CNR, Trento, Italy

The conduction band of the layer semiconductor Gallium Selenide has an indirect minimum at the M point of the Brillouin zone which is very closed (25 meV) to the higher direct conduction edge. The coexistance of these two minima largely influences the features of the photoluminescence spectra in the range from 580 to 800 nm. At low temperatures the emission spectra show intrinsic lines due to free -as well bound- direct and indirect excitonic recombinations and extrinsic bands at lower energy /1/. We measured spontaneous luminescence of GaSe Bridgmann grown crystls at He and N_2 temperatures, exiting selectively (with a dye laser) a wide region of wavelengths on the excitonic absorption structures. In the same energy range we also recorded the excitation spectra of the prominent features appearing in the luminescence spectrum. Flourescence line narrowing effect on the direct free excitonic emission is observed even up to 80 K where localization of excitons, due to random microscopic lattice disorder, is not espected to occur /2/. This anomalous behaviour is interpreted in terms of macroscopic strains in our crystals, probably due to stacking faults which easily form in growing semiconductor layered compound.

The excitation spectra of the above different intrinsic and

extrinsic luminescent features have unlike shapes. We observe that the recomoination channels, trough which the carriers relaxe, is depending on the excitation energy and direct luminescence processes are in competition with the indirect excitonic re-combinations. It seems that nonradiative transitions between energy states associated to the direct and indirect minima are not very efficient to perform a complete thermalization of excitonic states. The extrinsic emission bands of localized levels in the forbidden energy gap are efficiently excited in the low energy absorption tail. Further, the excitation spectra of these extrinsic structures show a deep minimum at the energies where the direct free exciton absorption is prominent.
On the basis of our experimental results we discuss a recombination model for the different relaxation channels.

REFERENCES

/1/ V. Capozzi, Phys. Rev. B23 (1981) 836.

/2/ E. Cohen and M. D. Sturge, Phys. Rev. B25 (1982) 3828.

Emission properties of quantized excitonic polaritons in a thin GaAs layer

L. Schultheis* and K. Ploog,
Max-Planck-Institut für Festkörperforschung, Heisenbergstr. 1, D-7000 Stuttgart 80

Excitonic polaritons in a thin semiconductor layer have discrete wave vectors perpendicular to the layer. The eigenstates are standing polarization waves (Fabry-Perot modes). Previous investigators /1/ have reported interference structure from these modes in the reflectance spectra of thin II-VI semiconductors platelets.

We have investigated excitonic polaritons in a GaAs layer by means of reflectance, excitation and luminescence spectroscopy. We used a high-quality GaAs/AlGaAs double heterostructure with a central GaAs layer 500 nm thick. The observed reflectance structure in the energy range of the 1s exciton in GaAs shows three minima and two sharp maxima and is much more complicated than in bulk GaAs. The reflectance data are analyzed by using a dielectric model. The line shape analysis yields the excitonic eigenenergies and the effective layer width. Comparison with the dispersion curve shows that the reflectance maxima coincide with the energy levels of the discrete polariton states.

Excitation spectra detected at the energy position of the 'defect-induced' bound exciton are dominated by the 1s exciton and the excitonic continuum states. The observed structure shows peaks coinciding with the reflectance spectra. Using the parameters from the reflectance data we can fit the structure to the excitation of Fabry-Perot modes.

The luminescence spectrum obtained at a low excitation intensity exhibits a new emission peak at the energy position of the lowest Fabry-Perot mode as deduced from the reflectance data.

Since the wave vector parallel to the surface is conserved only those small fraction of polariton states can radiate which have a wave vector component parallel to the layer lower than the total wave vector of the emitted light. Since this is small relative to the polariton k vector the emission from the polariton states in thin layers reveals the properties of nearly discrete energy levels. Varying the excitation intensities does not change the peak position of the excitonic emission band, confirming the discrete nature of the polariton luminescence in thin layers. In addition, we observe a symmetrical broadening of the excitonic emission line indicating a reduced excitonic lifetime. Exciton-exciton and exciton-free-carrier scattering due to the high concentration of photogenerated excitons and free carriers in the confinement geometry has to be considered.

/1/ See for instance: V.A.Kiselev, Solid State Commun.43,471

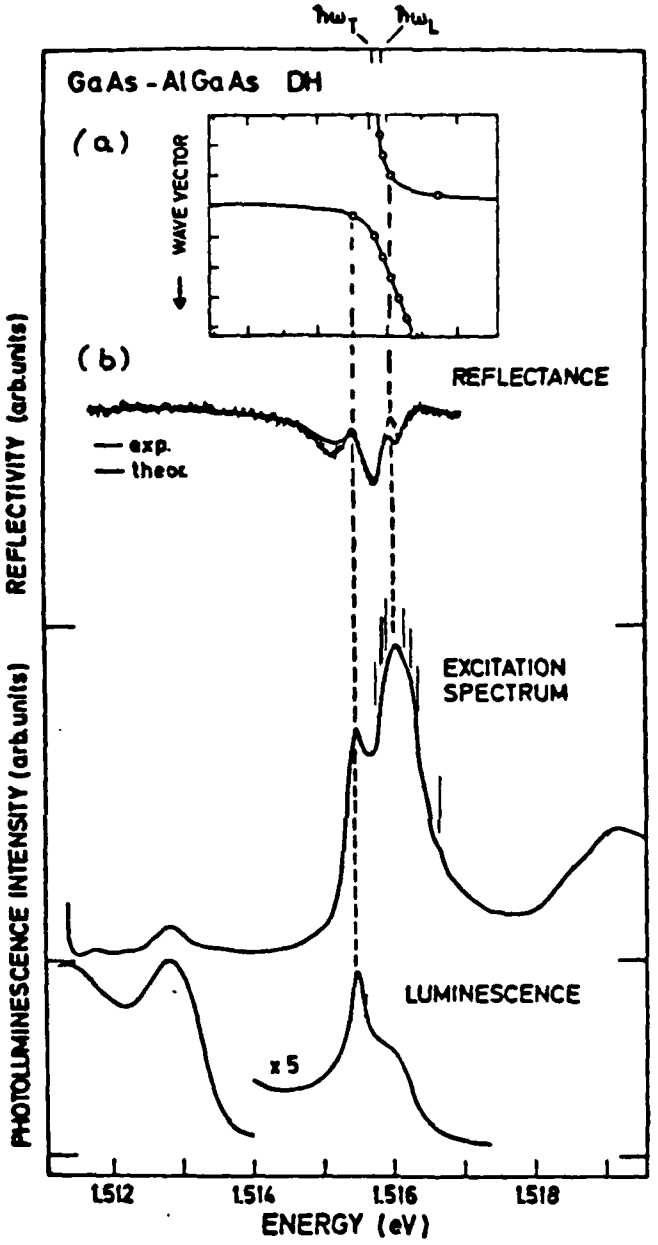

a: Energy versus wave-vector dispersion relation of excitonic polaritons in an infinite GaAs crystal. The open circles denote the polariton states with wave-vectors $k_{\perp} = N \cdot \frac{\pi}{L}$, where L=470 nm.

b: Normal incidence reflectance, excitation and luminescence spectra of the GaAs-AlGaAs DH.

FE5-1

High Luminescence due to Exciton Complex with Closed Hole Shell around Zinc in Germanium

H. Nakata and E. Otsuka

Department of Physics, College of General Education,

Osaka University, Toyonaka, Osaka 560, Japan.

A new complex, two excitons bound to a neutral double acceptor, was first observed in photoluminescence (PL) measurement of Zn doped Ge samples with extremely low concentration of other impurities. The complex, which we call a bound-double exciton complex (BDEC), has a novel feature of the closed hole shell structure and provides an extraordinarily strong PL intensity. Such a complex has been neither proposed nor observed in semiconductors. The PL spectra from our least doped sample ($N_A = 1.2 \times 10^{14}$ cm^{-3}), denoted Ge/Zn-1, are shown in Fig. 1. The peaks α are unambiguously assigned to radiative recombination of BDEC by strong dependence of their PL intensity on excitation intensity. The spectra also contain another kind of luminescence arising from a single exciton bound to the double acceptor, that we will denote $(BE)_{da}$. Existence of $(BE)_{da}$ was originally predicted by Hopfield and first detected for unidentified double acceptor in GaSb.[1] To our knowledge, there are no reports on $(BE)_{da}$ in Si or Ge. The broad peaks γ were assigned to

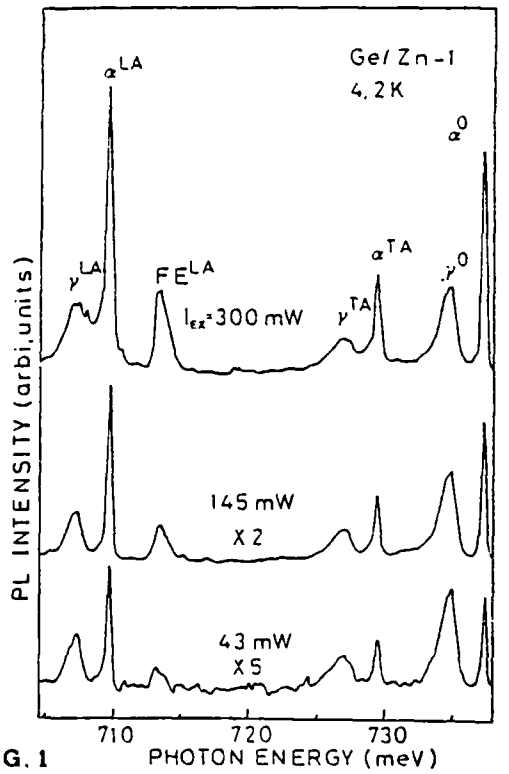

FIG. 1

$(BE)_{da}$ by their weak dependence on excitation intensity.

The dissociation energies of BDEC and $(BE)_{da}$ are found to be 3.2 and 5.7 meV, respectively. It is of interest to note that the so-called Haynes rule applies to our case of the double acceptor if we take the dissociation energy of an exciton from BDEC in place of that from $(BE)_{da}$ as the first ionization energy of zinc is 33 meV.

Figure 2 shows PL spectra of Ge/Zn-1 at 7 and 4.2 K and those of Ge/Zn-2 ($N_A = 2.1 \times 10^{15}$ cm^{-3}) at 4.2 K. Dependence of PL intensity on temperature and impurity concentration also supports our assignment of peaks α and γ.

To enrich the information, we further made far-infrared magneto-absorption measurement of $(BE)_{da}$. The observed absorption peaks correspond to excitation of electrons from 1s ground state to $2p_{\pm}$ odd parity excited states. Time-resolved magneto-absorption measurement yields the $(BE)_{da}$ lifetime of 0.75 μs and the exciton capture cross-section of 1.2×10^{-15} cm^2 at 4.2 K.

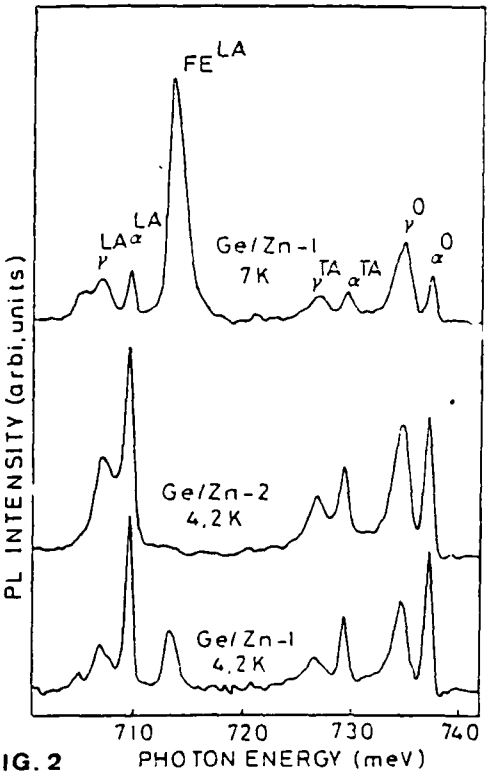

FIG. 2

1. R.A. Noack and W. Rühle, Phys. Rev. B18, 6944 (1978).

Reabsorption Kinetics of Free- and Bound-Exciton Luminescence in High-Purity n-GaAs

K. Aoki and K. Yamamoto

Department of Electrical and Electronic Engineering, Faculty of Engineering, Kobe University, Rokkodai, Nada, Kobe 657, Japan

We have investigated the reabsorption kinetics of free- and bound-exciton luminescence near the surface in high-purity n-GaAs ($n=2\times10^{14}/cm^3$) at 4.2 K, with using a sensitive detection technique which measures precisely the reabsorption quantities of the crystal-bulk luminescence excited by the dual laser beams. As well as the large reabsorption effects of the donor bound exciton (D^o,X), we have found for the first time the reabsorption anomaly of the exciton-polariton luminescence just above the bottleneck region.

The reabsorbed luminescence spectra $S(\omega)$ was detected by modulating the probe beam (a 20 mW He-Ne laser) at 800 Hz under the d.c. pump beam (a 10 mW Ar ion laser). Based on a simple model of carrier diffusion and surface recombination, the spectrum $S(\omega)$ is expressed as,

$$[S(\omega) - S_o(\omega)]/S_o(\omega) \sim -(1 + J_o/J_1)[\beta(\omega) - \beta_o(\omega)]\ell \quad , \qquad (1)$$

where $S_o(\omega)$ is the spectrum obtained by the probe beam only, J_o and J_1 are the photoexcitation densities of the pump beam and the probe beam, respectively, and $\beta(\omega)$ and $\beta_o(\omega)$ are the absorption spectra of the surface region with depth ℓ and of the crystal-bulk, respectively. Eq.(1) tells us that the reabsorbed quantities $(-\Delta S/S_o)$ are directly proportional to the increase of the absorption spectrum $\Delta\beta(\omega)$.

The (D^o,X) line shows a significant decrease in intensity as well as the appearance of the doublet structure (a typical example in Fig.1-a, with $J_o \sim 2$ W/cm^2 and $J_1 \sim 200$ mW/cm^2). The large intensity decrease and the doublet structure can be demonstrated in eq.(1) , by assuming the same Lorentzian line shapes of $\beta_o(\omega)$ and $\beta(\omega)$ with $\ell=1$ μm. The intensity reversal model by Reynolds et al.[1] shows more remarkable effects when the broadened spectrum $S_o(\omega)$ is used in eq.(1).

Exciton-polariton luminescence also exhibits the large absorption properties. The reabsorption anomaly appears as a dip structure of $\Delta\beta(\omega)$ at 818 nm (Fig.1-b), just above the longitudinal exciton energy E_L, which is never explained by the ordinary absorption spectrum[2]. The dip structure can only be explained by the emission of cold luminescence near the surface region. As a function of the pump power, the absorption coefficients considerably increase, but the dip structure remains to be unchanged. From the observations, it is concluded that there exists some particular region very close to the dead layer with depth smaller than ℓ, in which low density transverse exciton does not fully thermalize via various types of scatterings, while the emitted quanta from the crystal-bulk originate in the thermalized hot excitons. The reabsorption properties largely depend on the sample treatments. A chemically etched sample shows the increase in emission intensity ($S(\omega)>S_o(\omega)$), and exhibits the surface luminescence structure at 818 nm. The surface exciton-polariton component should be seriously considered for the origin of the reabsorption anomaly.

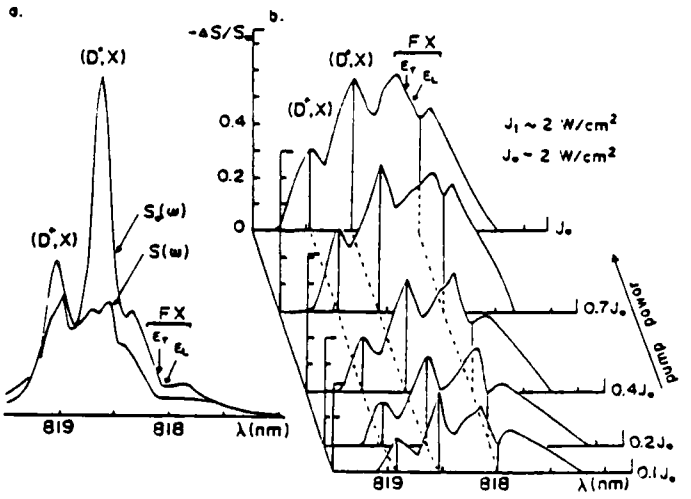

Fig.1-a,b.

REFERENCES

1) D.C. Reynolds, D.W. Langer, C.W. Litton, G.L. McCoy and K.K. Bajaj ; Solid State Commun. 46 (1983) 473.

2) Dale E. Hill ; Solid State Commun. 11 (1972) 1187

EMISSION OF FREE AND BOUND EXCITONS IN GaSe AND InSe CRYSTALS IN THE DIRECT AND INDIRECT TRANSITIONS REGION

Yu.P.Gnatenko, P.A.Skubenko, Yu.I.Zhirko, O.V.Fialkovskaya
Institute of Physics, Academy of Science of the Ukrainian SSR, Kiev (Prospect Nauki 144, 252650, Kiev 28, USSR)

The layered GaSe and InSe crystals are characterized by the presence of a great number of intensive emission lines, located near the emission line of a free exciton. The presence of various crystalline modifications notably complicates their interpretation.

Perfect samples of ε-modifications are investigated in this work, in which the number of structural defects of the crystal lattice is significantly reduced by doping them with definite concentrations ($\leq 0.1\%$) of impurity atoms of the Fe group, as well as by annealing them in inert atmosphere Ar.

It has been determined that the observed structure of the line in the region of the free exciton emission is conditioned by the splitting of the valence band by the inter-layer and spin-orbital interactions. The measurements of the GaSe emission lines in the energy region 2.07-2.10 eV at various temperatures and in polarized light, carried out in this work, made it possible to determine that their appearance is connected with the radiative decay of the direct bound excitons with different binding energy. Series have been picked out among these lines, which consist of zero-phonon lines and their phonon satellites.

As a result of the investigation of the form of the GaSe absorption edges in polarized light spread along the layers, the energy of the exciton absorption for indirect transitions has been determined -2.069 eV. This results, as well as the analysis of the emission spectrum in a more low energy region, made it possible to interpret two wide emission bands with 2.039 and 2.009 eV as being conditioned by the recombination of indirect free excitons with the emission of one and two TO-phonons. The energy position of these lines is different: it depends on the

geometry of measurement. This is caused by the dependence of the TO-phonons on the direction of their wave vector. It is shown that with the radiative decay of indirect excitons, they interact with TO-phonons, whose vector is directed along the excited layer plane.

It has been discovered that the increase in the intensity of the free excitons emission for the InSe crystals is due to the raise in temperature caused by the growth in the number of free excitons resulting from the decrease in the number of bound excitons.

The analysis of the dependence of the energy position and broadening of the emission and absorption lines of the GaSe and InSe crystals on temperature, made it possible to obtain data on the peculiarities of the exciton-phonon interaction at low temperatures. The evaluation of the sign of the exciton-phonon interaction function, square-law as to phonons $V_2(\vec{q},-\vec{q})$ coincides with the observed direction of the exciton lines shift, which is conditioned by the interaction of excitons with bending vibrations at low temperatures. It has been determined that for the direct transitions function $V_2(\vec{q},-\vec{q})$ and the force constant of phonon anharmonicity $V_a(\vec{q},-\vec{q}) < 0$, and for the indirect transitions their values > 0. It has been shown that at low temperatures ($T < 50^{\circ}K$) in the process of the exciton-phonon interaction, both low-frequency acoustic vibrations and low-frequency optic vibrations play an important role, which represent by themselves relative vibrations of separate layers of a crystal.

The doping of the GaSe crystals with the rare earth elements does not affect the emission of direct free excitons, but leads to the disappearance of the emission lines of indirect free excitons. This process is accompained by the appearance of the emission lines of the bound indirect excitons, which occurs as a result of localization of indirect excitons near the impurities because the great difference of the value of the ionic radii of the replaced ions causes local deformation of the crystal lattice.

EVIDENCE FOR A DOUBLE ACCEPTOR BOUND EXCITON IN A II-VI COMPOUND

P.J. DEAN, M. KANE, M. SKOLNICK

RSRE Malvern Worc. WR14 3PS (G.B.)

F. DE MAIGRET, LE SI DANG, A. NAHMANI, R. ROMESTAIN

Laboratoire de Spectrométrie Physique, Université Grenoble 1, B.P. 68, 38402 Saint Martin d'Hères-cédex (France)

N. MAGNEA

D.R.F., Centre d'Etudes Nucléaires de Grenoble, B.P. 68 X, 38041 Grenoble-cédex (France)

Annealing of II-VI compounds like ZnSe in contact with molten In is known to convert them to n-type. In ZnTe this procedure although increasing the donor concentration has the major effect of introducing a hole level 170-190 meV above the valence band and keeps it p-type. It also introduces an intense emission line labelled A_1^X at 2.361 eV. We will show that this line is due to the recombination of an exciton bound to a double acceptor with the same first ionization energy.

The ground states of a neutral double acceptor consist of two spin 3/2 holes. They exhibit a "hydrogenic" series (1s,ns) which can be seen on the two hole recombination lines and leads to an ionization energy equal to 180 meV. The exciton state consists of three holes and a spin 1/2 electron.

Zeeman experiments performed on the main A_1^X line do not show any anisotropy indicating that the impurity is not a complex. The measured g values are those of three holes and one electron in the exciton state whereas no magnetic splitting is detected in the ground state. This is due to the fact that in the ground $(1s)^2$ configuration the two holes couple to

form a J = 0 or J = 2 further split into a E and a T_2 component by the cubic field, the lowest being either the J = 0 or E component.

Stress experiments along the three mains directions 111, 110 and 100 also show that the excited state is made up from three holes which fill a 4 fold degenerate level S = 3/2 and thus display a level scheme inverted from the single hole. The ground state can be split by strain along 100 but not along 111 so the ground state is the E component of the J = 2 multiplet. Analysis of the selection rules under strain also shows that the broader lines observed at lower energy correspond to the J = 0 and T_2 levels respectively 2 and 5 meV above the ground E state.

We have thus been able to identify the double acceptor nature of this impurity which could be due to a Si substitutional to a Te ion. The electrostatic interaction between the two holes in the ground state is found to be very large, the most surprising result being the magnitude of the cubic E - T_2 splitting.

Radiative Recombination of Bound Excitons with Site Transfer Final State Excitations in Cu-Doped ZnTe

B. Monemar[o], P.O. Holtz[o], H.P. Gislason[o], N. Magnea[+], Ch. Uihlein[x], P.L. Liu[x]

o) University of Linköping, 581 83 Linköping, Sweden

+) DRF-PHS, CENG, 85X, 38041 Grenoble Cedex, France

x) Max Planck Hochfeld Magnetlabor, 38042 Grenoble Cedex, France

Summary

Novel recombination lines are observed as electronic satellites to bound excitons (BE:s) in photoluminescence (PL) spectra of Cu-doped ZnTe, when the doping is sufficiently strong (10^{17} - 10^{18} cm^{-3}) that complex Cu-related defects dominate the BE spectra. These replica are observed at discrete energies in the range 90-170 meV below the PL lines caused by the direct recombination of the BE state. The strength of these satellites is typically 5-10% of the parent BE line, and has a similar width (~0,2 - 0,4 meV). Such satellites occur with BE recombination for acceptor BE:s (ABE:s) as well as isoelectronic complex BE:s (IBE:s). They also occur in a similar way in resonant Raman scattering (RRS). Magnetooptical data at 10T reveal an extremely complicated Zeeman splitting pattern of these satellites. The collected experimental data from selective dyelaser

excited luminescence (SPL) spectra and excitation spectra (PLE) together with RRS and Zeeman results, suggest a recombination model where the BE state is interacting with a neutral acceptor state on a different site. In the recombination process final state electronic shake up excitations of the type 1s-2s are observed on acceptors which are interacting with the defect site carrying the initial state BE excitation.

High-density excitation and Raman Spectroscopy of the Bound-Exciton Complex (A^o,X) in CdS

I. Broser and J. Gutowski

Institut für Festkörperphysik II der Technischen Universität Berlin, Straße des 17. Juni 112, D-1000 Berlin 12, Germany

Luminescence and Raman spectroscopy using high-density tunable laser sources in the bound exciton region of CdS yield new informations about excitation channels and excited states of the four-particle (A^o,X) complex. Excitation spectroscopy of the I_1 luminescence due to the recombination of the (A^o,X) complex with two A-valence-band holes in its electronic ground state led to the identification of four fine structure levels of the (A^o,X_B) complex with one hole from the second B valence band. Excitation with light of polarization $\vec{E} \| \vec{c}$ and of an energy which coincides with one of these four levels, split off by hole-hole and electron-hole exchange interaction, is followed by a B-A hole conversion and subsequent I_1 recombination of the complex. The sharp and strong excitation resonances due to the (A^o,X_B) levels allow measurements in a magnetic field giving detailed informations about the nature of these states and the interaction mechanisms involved. Investigations of a resonant electronic Raman effect due to hole scattering from the B to the A valence band within the (A^o,X) complex supported these results. Four Raman lines showing resonance behaviour successively at the four (A^o,X_B) levels with distinctly different properties from known low-density Raman spectroscopy[1] could be observed. Polarization and magnetic field dependent measurements were

used to identify the Raman mechanism to be a one-photon resonant electronic scattering process within the (A^o,X) levels while gain measurements and the observation of a mode structure in the high-density excitation spectra supported the excistance of stimulated Raman transitions. High-density excitation spectra of the I_1 bound exciton with polarization $\vec{E} \perp \vec{c}$ showed resonances due to first order forbidden electronic excited states[2] of the (A^o,X_A) complex. Extremely high excitation intensities led to the observation of vibration like resonances of the I_1 luminescence. Intensity, temperature and magnetic field dependent measurements enabled us to develop a theoretical model to explain these resonances to be vibrations of the particles within the (A^o,X) complex analogous to the case of a diatomic molecule.

In conclusion high-density spectroscopy of the bound exciton (A^o,X) in CdS yields a lot of information about new excited states and excitation mechanisms which could not be obtained under low intensity conditions.

References:

1. D. Munz and M.H. Pilkuhn, Solid State Commun. 36,205 (1980)

2. R. Baumert, I.Broser, J. Gutowski, and A. Hoffmann, Phys.Rev. B 27, 6263 (1983)

EXCHANGE INTERACTION AND OSCILLATOR STRENGTH IN NEUTRAL BOUND EXCITON

G. Staszewska[+], M. Suffczyński[‡], W. Ungier[‡], L. Wolniewicz[+]

[+]Institute of Physics, Nicholas Copernicus University, 87-100 Toruń, Poland

[‡]Institute of Physics, Polish Academy of Sciences, 02-668 Warsaw, Poland

In an exciton bound to a neutral donor the electron-hole exchange interaction mixes states of opposite symmetry with respect to the interchange of two electrons[1]. We take a perturbation parameter proportional to the electron-hole exchange integral and use a variational-perturbation method to compute wave function in the first order and the ground state energy in the second order. The basis functions of Page and Fraser with nonlinear parameters of Stebe and Munschy [2] and reoptimized scale parameter for each electron-to-hole mass ratio, practically reproduce the best ground state energy, and are used to compute the linear combinations for the envelope function corrections symmetric and antisymmetric with respect to interchange of two electrons. The electric dipole moment of the exciton radiative recombination is proportional to overlap integral of the envelope and the donor ground state wave function. Squared overlap integral gives the ratio of the bound exciton to the conduction-band-to-valence-band transition. The Page-Fraser 70-term envelope function and the correction due to electron-hole exchange interaction with the exchange integral taken from the free exciton singlet-triplet splitting [3],

lead to agreement of the calculated oscillator strength for bound exciton recombination with the measured radiative lifetime of bound excitons in wurtzite type semiconductors CdS [4] and CdSe.

1 W. Ungier and M. Suffczyński, Phys. Rev. B 27, 3656 (1983)

2 B. Stebe and G. Munschy, Solid State Commun. 35, 557 (1980)

3 M. Suffczyński, L. Swierkowski and W. Wardzyński, J. Phys. C 8, L 52 (1975)

4 C. H. Henry and K. Nassau, Phys. Rev. B 1, 1628 (1970)

SATURATION EFFECTS OF THE 2 eV-PHOTOLUMINESCENCE IN CdMnTe

E. Müller, W. Gebhardt
University of Regensburg, Dpt. of Physics
84 Regensburg, F.R. Germany

The luminescence in the random system $Cd_{0.45}Mn_{0.55}Te$ which is due to a $^4T_1 \rightarrow {}^6A_1$ transition within the Mn^{2+}-ions covers a phonon-broadened distribution of $^4T_1$-states.[1] The data of fig. 1 are obtained from a cw-experiment using a focussed Ar-laser beam at 514 nm. The luminescence was recorded at the short- and longwavelength side of the band at 580 and 680 nm respectively. Both intensities show a nonlinear increase with laser power, but only that from the 580 nm side saturates.

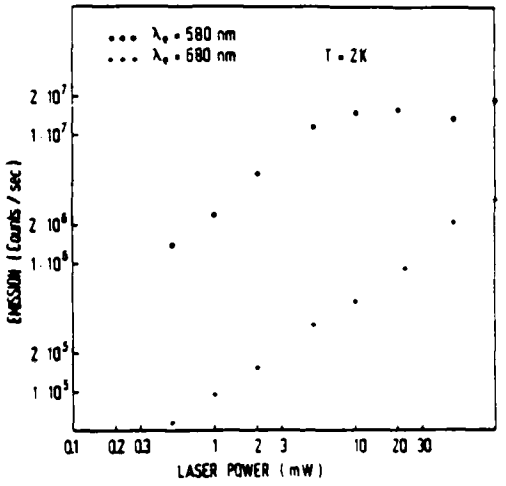

Fig. 1

In fig. 2 the kinetics of the shortwavelength intensity are shown, recorded during and after the exciting pulse. The rise becomes steeper with increasing power. The 50- and 100 mW-curves reach even a maximum at about 16 µs before the intensity falls off to the cw-level. All curves are normalised to equal intensity at 96 µs.

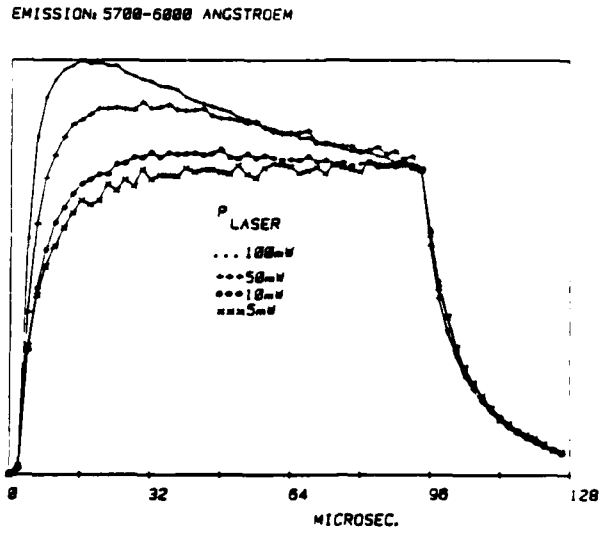

Fig. 2

The kinetics at 680 nm is not shown here, since the rise is monotonous even at highest laser power.

An interpretation consistent with previous results[2] can be given as follows:

1. Radiationless energy transfer at LHeT is only possible at the short-wavelength side of the band ($^4T_1(2)$-states). Localised states contribute to the longwavelength side ($^4T_1(1)$-states). They show only radiative decay.
2. The lifetime of $^4T_1(2)$-states at LHeT is controlled by radiative decay, energy transfer and biexcitonic decay via two channels:
   $2\ ^4T_1(2) \rightarrow {}^4T_1(1)$ and $^4T_1(2) + {}^4T_1(1) \rightarrow {}^4T_1(1)$
3. The latter process contributes with a term $\beta_{12}N_1N_2$ to the rate equations. As shown by computer simulations this process is essential to explain the peculiar kinetics in fig. 2.

1) M.M. Moriwaki, W.M. Becker, W. Gebhardt and R.R. Galazka
Sol. State Comm. 39, 367 (1981)

2) E. Müller, W. Gebhardt, V. Gerhardt
phys. stat. sol. (b) 113 (1982)

Study of M_0^X Band in Indirect-Gap $GaAs_{1-x}P_x$ by Resonant Excitation

Shui T. Lai

Materials Research Laboratory

Allied Corporation, Morristown, NJ 07960

M.V. Klein

Physics Department

University of Illinois, Urbana, IL 61801

Two basic characteristics of localized excitons in $GaAs_{1-x}P_x$ are depicted in this study. They are: (1) the density of state extends into the band gap, and (2) the effective range of the wavefunction is a sensitive function of its binding energy.[1] The photoluminescence (PL) properties of the M_0^X band in indirect gap $GaAs_{1-x}P_x$ has been reported.[2,3] The origin of the M_0^X band has been attributed to the exciton localized by the potential fluctuation in the GaAs-GaP solid solution. In n-type $GaAs_{1-x}P_x$, the excitons bound at the donor centers (D_0^X) are located at a lower energy (8~13 meV) than those at the M_0^X (Fig. 1, top trace). Inelastic tunneling to the short-lived D_0^X centers is the dominant quenching process for

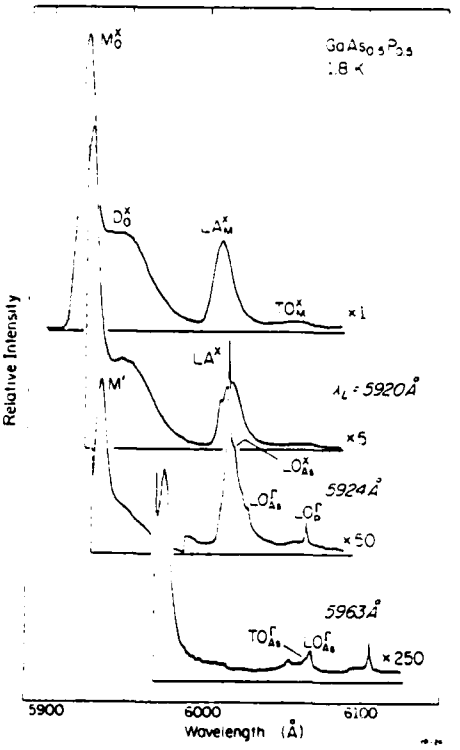

Fig. 1 Fluorescence spectra by resonant excitation onto the M_0^X band of a $GaAs_{0.5}P_{0.5}$ sample at 1.8K. The laser wavelength (λ_L) for each scan is shown. The dashed line indicates where the scan starts.

the localized excitons. Since the probability of the tunneling is related to the spatial extent of the wavefunction, the exciton wavefunction can be studied through the tunneling processes. Sharp phonon structures appear as the excitation energy is in resonance with the M_0^X band excitons (Fig. 1, λ_L>5920Å). The most prominent feature, labelled LA^X, is the LA phonon side-band of the localized excitons at the laser energy. It's narrow linewidth derives from a small energy portion of the localized exciton population which is selectively and resonantly excited by the narrow-width laser. A PL peak M' (Fig. 1, λ_L = 5924Å) occurs at ~3 meV below the laser energy. This "Raman-like" peak persists even at excitation energy well below the M_0^X band (λ_L = 5963Å). The M' band results from excitons created at the laser energy, tunneling to more deeply localized states. The fact that it has a peak rather than a portion of the M_0^X lineshape indicates that the effect of tunneling processes has a dominant role in the exciton luminescence lineshape. Localized exciton at higher energy has a lower fluorescence quantum efficiency due to its more spatially extended wavefunction. Rapid variation of the fluorescence lifetime across the M_0^X band lineshape has also been observed.[2] The ratio of M' peak intensity to that of the LA^X increases as the laser energy is tuned below the D_0^X peak. This increase is consistant with our model that D_0^X center is the energy sink for the localized exciton

1. P.W. Anderson, Proc. Nat. Acad. Sci. USA 69, 1907 (1972).

2. Shui Lai and M.V. Klein, Phys. Rev. Lett. 44, 1087 (1980).

3. Shui T. Lai and M.V. Klein, Phys. Rev. B29, March 15, 1984.

Photoluminescence in Liquid Phase Epitaxially grown $Hg_{0.3}Cd_{0.7}Te$ and its CdTe Substrate at 4.2 and 77K

Bernard J. Feldman
Department of Physics
University of Missouri-St. Louis
St. Louis, Missouri 63121

J. Bajaj and S. H. Shin
Rockwell International Science Center
Thousand Oaks, California 91360

Summary

The photoluminescence spectra of liquid phase epitaxially (LPE) grown $Hg_{0.3}Cd_{0.7}Te$ and its CdTe substrate have been measured. The CdTe spectra at 4.2 K consist of two band edge sets of lines, B and C, while the $Hg_{0.3}Cd_{0.7}Te$ spectra consist of one set of lines, A. From the temperature dependence of both the integrated intensity and peak position, we determined that the A line is unrelated to the C line but is very possibly related to the B line. The B line in CdTe is due to recombination of electrons and holes bound to a neutral donor or acceptor. This suggests that the same neutral donor or acceptor may be present in both materials, whereas the impurity or defect responsible for the C line in CdTe is undetectable in LPE grown $Hg_{0.3}Cd_{0.7}Te$. In contrast the photoluminescence spectra of both $Hg_{0.3}Cd_{0.7}Te$ and CdTe at 77 K consist of a single narrow, high energy line with a free exciton lineshape and a broad, low energy line due to a deep level. From binding energy considerations, the origin of the observed deep level in $Hg_{0.3}Cd_{0.7}Te$ is unrelated to that in CdTe.

References

B. J. Feldman, J. Bajaj and S. H. Shin, Journal of Applied Physics, in press.

A. T. Hunter and T. C. McGill, Journal of Applied Physics, 52, 5779 (1981).

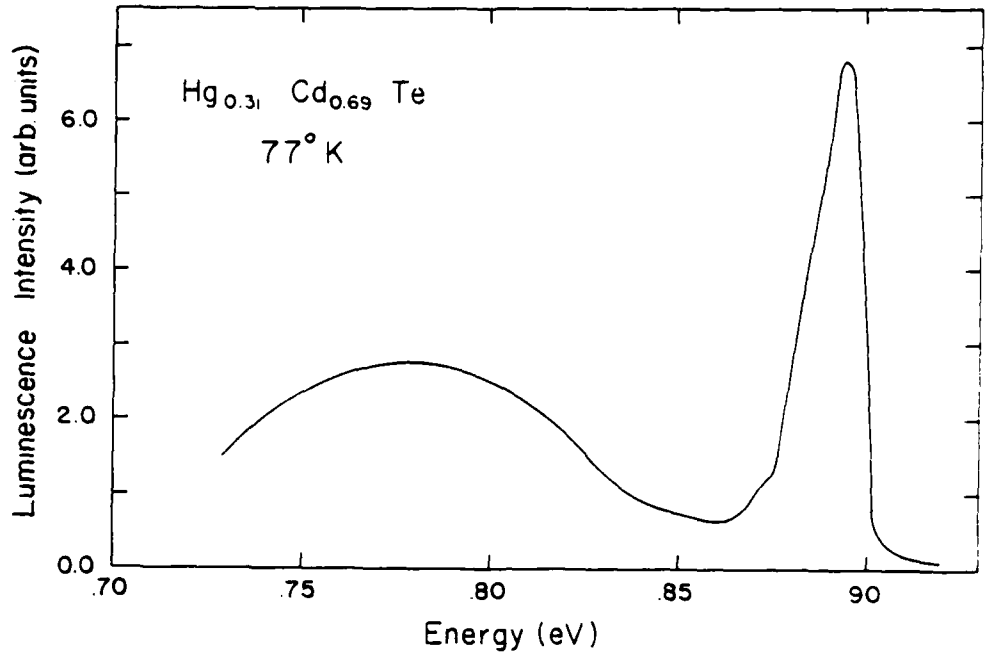
Hg0.31 Cd0.69 Te
77° K
Luminescence Intensity (arb. units)
6.0
4.0
2.0
0.0
.70
.75
.80
.85
.90
Energy (eV)

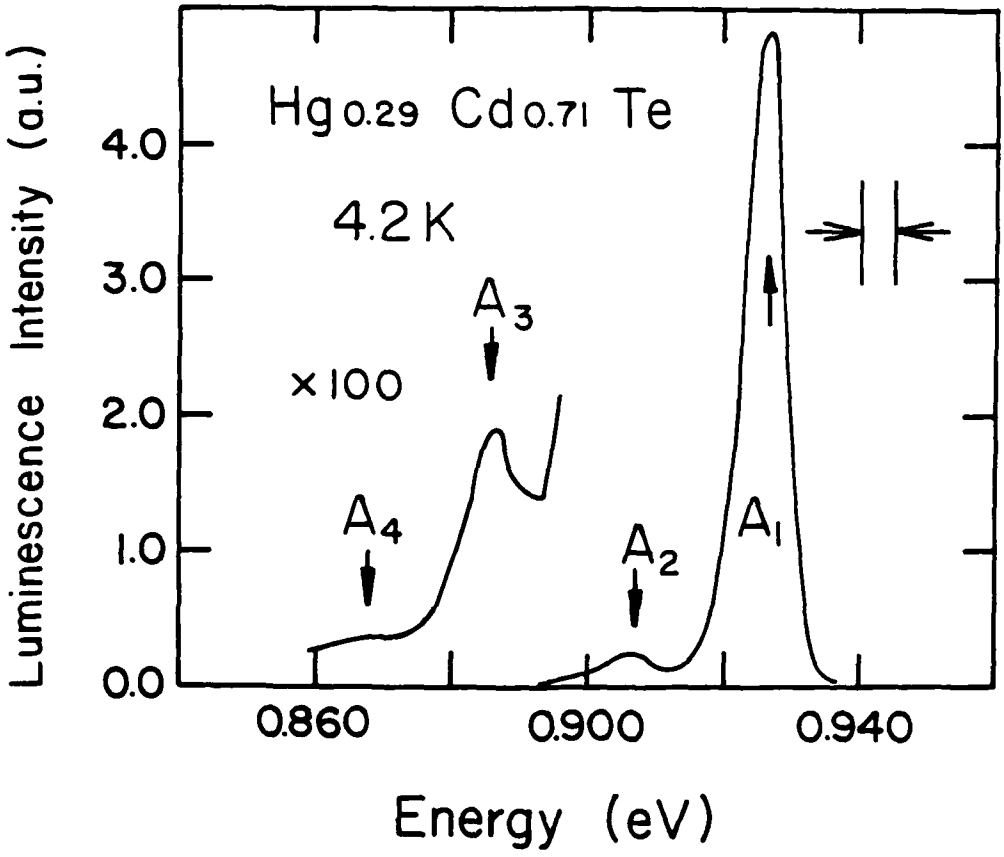
Hg0.29 Cd0.71 Te
4.2 K
×100
A3
A4
A2
A1
Luminescence Intensity (a.u.)
4.0
3.0
2.0
1.0
0.0
0.860
0.900
0.940
Energy (eV)

Multiple LO phonon scattering in indium bromide

Masashi Yoshida, Hideo Watanabe, Nobuhito Ohno, Kaizo Nakamura
and Yoshio Nakai
Department of Physics, Kyoto University
Kitashirakawa Oiwake-cho, Sakyo-ku, Kyoto 606, Japan

Multiple scattering lines of Raman forbidden LO phonon ($\hbar\omega_{LO}$=16meV) have been observed in orthorhombic InBr by the excitation above the direct exciton energy (Ex=2.331 eV).[1] Scattering spectra are characterized by the intensity alternation that even numbered lines are stronger than odd numbered lines. In the present study incident photon energy dependence and temperature dependence of multiple LO phonon lines are investigated to clarify exciton relaxation mechanism in polar semiconductor with inversion symmetry and the origin of intensity alternation.

Figure 1 shows intensity of scattering lines as a function of incident photon energy measured at 2K. The shapes of all curves are similar to one another, with clear alternation of scattering intensity. Large enhancement occurs when scattered photon energy is resonant with 1s exciton indicating the importance of 1s exciton in light scattering. However, in

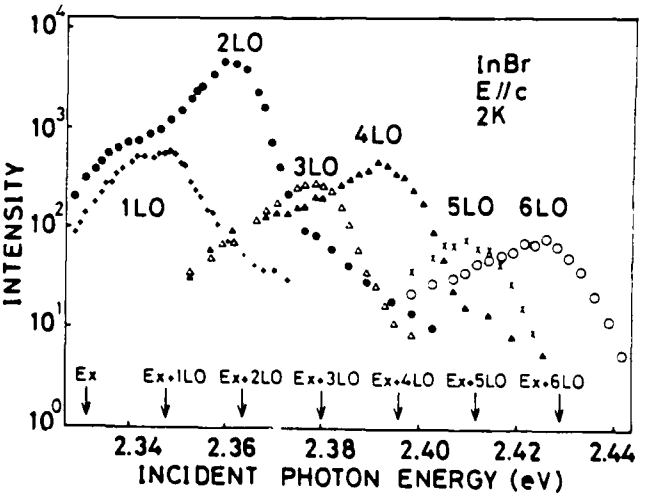

Fig. 1

order to explain the intensity alternation the contribution from interband Fröhlich scattering between states of different parity should be taken into account as well as intraband scattering.

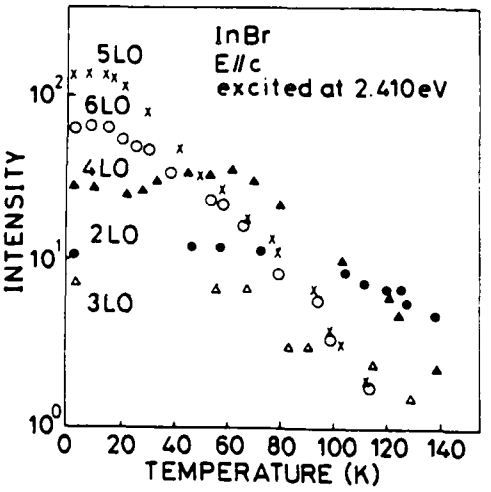

Fig. 2

In Fig. 2 is shown temperature dependence of lines excited at 2.410 eV by Ar laser which corresponds to $Ex+5\hbar\omega_{LO}$ at 2K. Intensity of both 5LO and 6LO lines begins to decrease above 20K, which can be attributed to blue shift of 1s exciton energy with increasing temperature.[2] Intensity of 2, 3 and 4LO lines does not change below 60K. Decrease of intensity of 2, 3 and 4LO lines above 60K is caused by the increasing probability of nonradiative decay, which becomes comparable with the LO phonon scattering rate above this temperature. The fact that higher order lines decrease more rapidly implies that exciton relaxes with cascade LO phonon emission above Ex in competition with nonradiative process, probably scattering into indirect exciton valley. On the other hand, thermal quenching of 5LO and 6LO lines is similar to each other above 60K, which suggests that simultaneous multi-phonon emission process is effective for scattering lines located below Ex.

1) K. Nakamura et al: Solid State Commun. 36 (1980) 211.

2) M. Yoshida et al: Phys. Status Solidi b109 (1982) 503.

Photoluminescence from Two-Dimensional Electrons in a Magnetic Field.

C.H. Perry, A. Petrou & M.C. Smith, Northeastern University Boston, MA 02115

J.M. Worlock, Bell Communications Research Inc., Holmdel, NJ 07733

R.L. Aggarwal, National Magnet Laboratory, M.I.T., Cambridge, MA 02139

A.C. Gossard & W. Wiegmann, A.T.&T. Bell Laboratories, Murray Hill, NJ 07974

We have studied photoluminescence from modulation-doped GaAs/AlGaAs multiple quantum well (MQW) structures, grown by molecular beam epitaxy, in the presence of high magnetic fields. Experiments were performed using a variety of lasers as excitation sources. In zero field, electrons in the valence band (VB) are photo-excited by the incident laser light to conduction band (CB) states, creating VB holes. They radiatively recombine with the holes, producing the infrared luminescence observed in our experiments which is, in general, rather broad and extends from about 12100-12400cm^{-1}.

When subjected to magnetic fields in the range 0-20T, the main luminescence peak breaks into discrete components attributed to radiative transitions between CB and VB Landau levels of equal quantum number ℓ, as shown for example in Fig. 1. Here, the spectra were recorded with 4880A excitation, which promotes a high electron temperature and accounts for the relatively intense high energy tail. Six distinct Landau levels are clearly visible even in fields as low as 2T.

Using 6328A excitation, only the lower two Landau levels are observed at 70K for sample 2-11-80. Fig. 2(a) shows the linear behaviour that occurs over the entire range of fields investigated. The lines follow the relation: $E = \hbar (\omega_{CB} + \omega_{VB})(\ell + 1/2)$, where $\ell = 0,1,2,\ldots$; $\omega_{CB} = eH/m^*_{CB}c$ and $\omega_{VB} = eH/m^*_{VB}c$. Fig. 2(b) contrasts similar studies taken at 2K. In these studies a swept field technique was also used as it enhanced the high Landau transitions. The same linear behaviour is

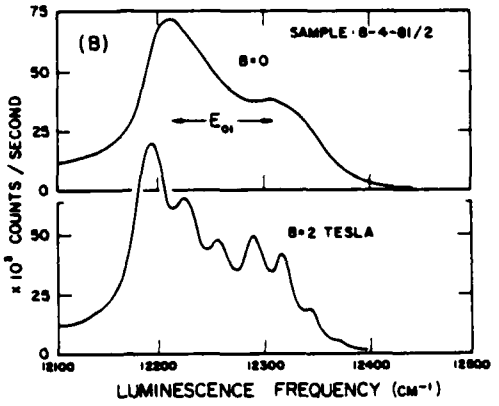

Fig. 1 Landau luminescence

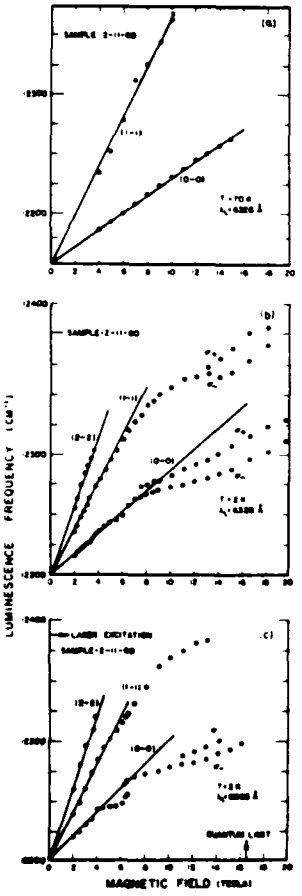

Fig. 2. Landau transitions as a function of temperature and incident laser energy

observed at low fields and high $l \to l$ transitions. Numerical fitting of the Landau luminescence data to the equation above yielded a heavy hole mass of $m=0.5m_e$. However, in high fields at 2K, the $0 \to 0$ and $1 \to 1$ transitions shown in Fig. 2(b) indicate significant deviations from linear behaviour and they split into two circularly polarized components, σ_+ and σ_-. This doublet is associated with an enhanced spin splitting of the two spin states in each Landau level.

By further decreasing the laser excitation energy to just above the Fermi level (~8060A) at 2K, Fig. 2(c), it is possible to achieve the quantum limit where all the electrons are in the lowest Landau spin state. At this point the σ_+ transition disappears and only the σ_- is observed. Under these conditions a more enhanced step-like discontinuity occurs between one quarter and one third the quantum limit. These effects are probably a result of the electron-electron exchange interaction.

Exciton Holeburning in GaAs/GaAlAs Multiquantum Wells

J. Hegarty, AT&T Bell Laboratories, 600 Mountain Avenue, Murray Hill, NJ 07974

M. D. Sturge, Bell Communications Research Inc., 600 Mountain Avenue, Murray Hill, NJ 07974

The lowest energy two-dimensional exciton in GaAs/GaAlAs multiquantum wells (MQW) is inhomogeneously broadened at low temperature by fluctuations in the layer width. The broadening permits probing of the excitons as a function of position within the inhomogeneous line[1]. At high densities interaction between the excitons becomes important and leads to saturation and to an increase of the homogeneous linewidth[2]. Using the picosecond pump/probe technique we have measured the saturation behavior as a function of exciton energy within the inhomogeneously broadened line. Figure 1 shows the transmission spectrum T of a weak narrowband probe (dotted) and the change in transmission ΔT of the probe induced by the presence of a pump for two different pump wavelengths for 102 Å thick layers of GaAs separated by 200 Å layers of AlGaAs. An increase in transmission (holeburning) at the pump wavelength is observed showing that the interaction between resonant excitons is much stronger than between nonresonant excitons. The strength of the hole decreases rapidly on passing through the center of the line towards the high energy side.

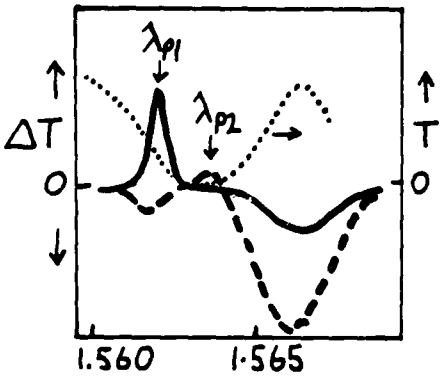

Figure 1

This is consistent with an increase in the homogeneous linewidth of the higher energy excitons[1,3]. By delaying the probe we measured the rate of decay of the hole which was found to depend strongly on pump intensity. At low intensity the hole lifetime approaches the luminescent lifetime but becomes shorter at exciton densities greater than $\sim 10^9$ excitons/cm^2/layer. We attribute this to exciton-exciton scattering leading to spectral diffusion. The behavior was similar in 51 Å and 102 Å layers. In addition to holeburning, Figure 1 shows an increased absorption in the wings of the line whose shape is almost independent of pump wavelength and which is similar to that observed in bulk GaAs[2].

[1] J. Hegarty, M. D. Sturge, C. Weisbuch, A. C. Gossard, and W. Wiegmann, Phys. Rev. Letts. 49, 930 (1982).

[2] C. W. Fehrenbach, W. Schafer, J. Treusch, and R. G. Ulbrich, Phys. Rev. Letts. 49, 1281 (1982).

[3] J. Hegarty, Phys. Rev. B25, 4324 (1982).

Photoluminescence Studies of Ga(As,P) Strained-Layer Superlattices†

P. L. Gourley
Sandia National Laboratories
Albuquerque, New Mexico 87185

Semiconductor Strained-Layer Superlattices (SLS's) are composed of thin (few hundred A) alternating layers of lattice-mismatched materials that grow in a coherently strained condition which avoids the formation of misfit dislocations.[1] The growth of SLS's permits the freedom to combine lattice-mismatched semiconducting materials in a superlattice structure. These SLS's form a new class of semiconductors with useful and tailorable electronic properties.[2]

We have studied two different kinds of MOCVD grown SLS's composed of alternating layers of 1) GaAs and $GaAs_xP_{1-x}$ and 2) GaP and $GaAs_xP_{1-x}$ using photoluminescence with spectral, spatial and temporal resolution and photoluminescence excitation spectroscopy. Using these techniques in several different studies, we have been able to elucidate a wide range of the electronic properties of SLS's. The following survey of important results drawn from these photoluminescence studies will be presented.

In studies of the SLS band structure we have measured the energy bandgap and higher lying optical transitions as a function of the

---

†This work was performed at Sandia National Laboratories and supported by the U.S. Department of Energy under contract number DE-AC04-76DP00789.

compositional parameter x from 0 to 1. These measurements demonstrate that the SLS has an energy gap that can be varied independently of its lattice constant. We have observed quantum size effects in the near-gap optical transitions of type 1 SLS's. These transitions are associated with electrons and holes localized in quantum wells induced by the superlattice layering. With regard to the transport properties of SLS's, we have measured the electron and diffusion lengths in the directions parallel and perpendicular to the interfaces. The perpendicular diffusion is largely inhibited by potential barriers in both the conduction and valence bands. These results are confirmed by separate measurements of the minority carrier lifetimes which reveal that SLS surface recombination is greatly decreased. This explains why the SLS photoluminescence efficiency is much higher than epitaxial layers of GaAs grown by the same MOCVD process. Finally, using microimaging of luminescence, we have detected a class of dark line defects that are probably associated with misfit dislocations in the buffer layer which is grown on the substrate before the deposition of SLS layers. These defects do not appear to propagate into the SLS.

References

1. J. W. Matthews and A. E. Blakeslee, J. Cryst. Growth 27, 118 (1974).

2. G. C. Osbourn, Phys. Rev. B27, 5126 (1983).

Picosecond Luminescence Spectroscopy of Electron-Hole Plasma in GaAs/AlAs Quantum Well Structure

S. Tanaka, M. Kuno, A. Yamamoto, A. Watanabe, H. Kobayashi, M. Mizuta,† H. Kukimoto† and H. Saito††

Department of Electronics, Tottori University
Koyama, Tottori 680, Japan

†Image Science and Engineering Laboratory,
Tokyo Institute of Technology
Nagatsuda-cho, Midori-ku, Yokohama 227, Japan

††Okayama College of Science, Ridaicho, Okayama 700, Japan

We report the picosecond temporal character of high-density electron-hole plasma (EHP), such as carrier trapping and radiative recombination process, in highly excited GaAs/AlAs multiple quantum well (MQW) structures.

The MQW sample, which consists of four undoped 140 Å (L_z) thick GaAs wells between the 200 Å thick AlAs barriers, was grown by metal-organic chemical vapor deposition. Figure 1 shows the typical time-resolved spectra of EHP luminescence in the MQW, measured at 15 K under 532 nm picosecond pulse excitation. Each luminescence spectrum has a peak at photon energy of 1.53-1.54 eV, which is lower than n=1 electron to heavy-hole

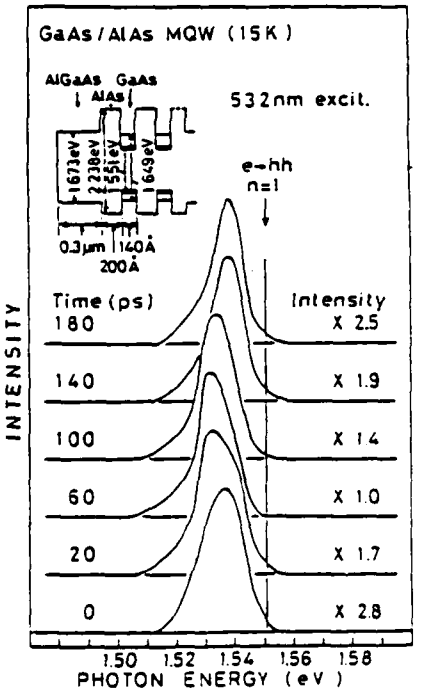

Fig. 1

transition energy. This result indicates a band gap shrinkage of about 20 meV due to Coulomb interaction in the EHP.

The high density EHP in the MQW is characterized by its carrier density N_{QW}. The time variation of N_{QW} results from carrier trapping and radiative recombination of electrons and holes. Here, one may assume that the recombination process obeys the bimolecular kinetics. The temporal variation of N_{QW} and also luminescence intensity I_{QW} after picosecond pulse excitation are analyzed by using simple rate equations. Calculated variations of I_{QW} and N_{QW} are shown in Fig. 2(a) and (b), respectively. The calculated curve with trapping time of 65 ps and bimolecular recombination coefficient of 3.5×10^{-8} $cm^{-3}s^{-1}$ gives a best fit to the experimental time response of I_{QW} shown by open circles in Fig. 2(a). The decay time of the EHP is estimated to be about 80 ps.

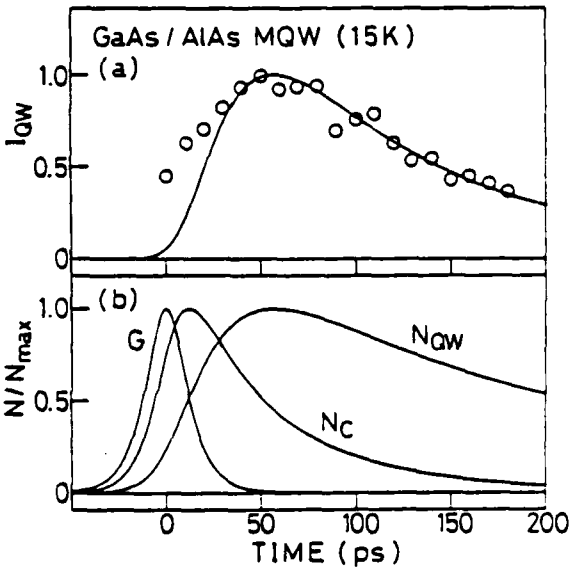

Fig. 2

Intraband relaxation of the EHP is also discussed.

SUBNANOSECOND CARRIERS LIFETIME MEASUREMENT IN 1.3μ InGaAsP

B.SERMAGE and J.L.BENCHIMOL

Laboratoire de Bagneux, C.N.E.T.

196 rue de Paris - 92220 - FRANCE

and J.P.HERITAGE

Bell Laboratoire, Crawford Corner Road, Holmdel,

New Jersey 07733 - USA

Luminescence decay time has been measured in pure InGaAsP layers (Nd-Na- 10^{16} cm^{-3}) whose composition corresponds to a band gap of 1.3μ [1]. The sample was excited by a 1.06μ mode locked yag laser giving 100ps long pulses separated by 10ns. An accoustooptic cristal select one impulsion every 200ns to avoid heating of the sample and allow measurement of long decays. The carrier density is calculated by the knowledge of the excitation spot size and of the absorbed power. We make sure that the layer is situated at the beam waist by taking profit of the saturation of the absorption. The carriers density is varied between 4.10^{16} and 2.10^{19} cm^{-3} by changing the excitation intensity. The radiative recombination life time τ_r has been calculated with the Fermi golden rule, using the Kane model for the description of the lower conduction band and the three upper valence bands near the center of the Brillouin zone. The value of the matrix element is obtained by taking into account the measured absorption coefficient (α = 1.6 10^4 cm^{-1}) at 1.06μ. The carriers life time τ is deduced from the luminescence decay time τ_L by taking into account

the theoretical variation of the luminescence intensity as a function of the carriers density.

At low carriers density (n 10^{18} cm^{-3}), the lifetime follows the variation with excitation of the theoretical radiative lifetime. At high carriers density, the lifetime decreases more rapidly with carriers density than the radiative one. We make sure by varying the spot size between 8 and 16μ and by varying the layer thickness between 0.6μ and 1.6μ that the stimulated recombination is negligible. Thus the fast decrease of the lifetime with carriers density is interpreted as due to an additionnal recombination mechanism of lifetime τ_a :

$$\frac{1}{\tau} = \frac{1}{\tau_r} + \frac{1}{\tau_a}$$

Since $1/\tau_a$ varies like the square of the carriers density, we interpret this additionnal recombination as due to an Auger process. The Auger coefficient has been determined by this way at 281K and 346K and found in both cases to be equal to 2.6 10^{-29} cm^6 s^{-1}. This shows that the Auger coefficient is larger by two orders of magnitude in these materials than in Gallium Arsenide which is probably due to the small value of the band gap compared to the valence band spin-orbit splitting. However, it is smaller than previously calculated values [2]. On an other part it shows that the Auger coefficient apparently does not increase with temperature which is controversial [2,3].

References

(1) B.SERMAGE, H.J.EICHER, J.P.HERITAGE, R.J.NELSON, and N.K.DUTTA, Appl. Phys. Lett. 42, 259 (1983)

(2) N.K.DUTTA, and R.J.NELSON, J. Appl. phys. 53, 74 (1982)

(3) A.SUGIMURA, Appl. Phys. Lett. 39, 21 (1981)

Fast Carrier Expansion Effects in the Optical Spectra of CdTe

H. Schweizer, E. Zielinski, and A. Forchel
Physikalisches Institut, Teil 4
G. Mahler
Institut für Theoretische Physik, Teil 1
Universität Stuttgart, D-7000 Stuttgart-80, Germany

We have investigated the spectra of the spontaneous and stimulated emission and transmission of CdTe at temperatures below 50K using a N_2-laser pumped dye laser for the plasma excitation. Fig. 1 depicts the spatially resolved results of luminescence measurements in a back-scattering geometry. In going from the edge to the centre of the excitation spot of approximately 40 μm diameter we observe a strong line width narrowing. At intermediate positions even two distinct emissions are observed. We attribute this to a fast carrier drift from the surface into the bulk of the sample, resulting in a spatial carrier distribution which - particularly at the center of the excitation - extends deep into the sample. The spatial variation of the luminescence is explained straightforwardly, if the two bands in Fig. 1 are attributed to the spontaneous and stimulated emission of the plasma: The stimulated emission is observed mainly at the center of the excitation since the optical amplification is strongly enhanced by the wide spatial range over which the carriers are distributed. If the plasma were limited to the absorption length of the laser, the optical path would be too short for a significant amplification.

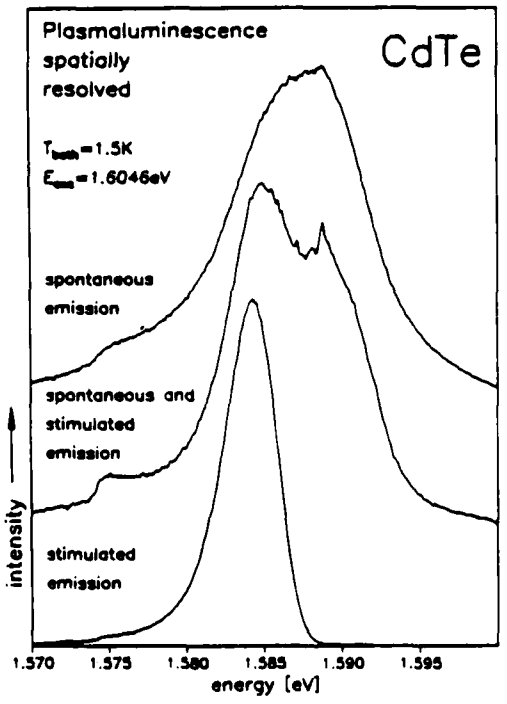

Fig. 1 Spatially resolved luminescence of highly excited CdTe.

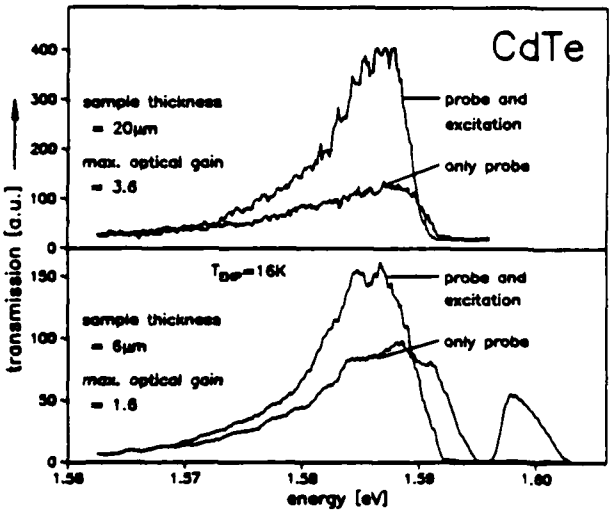

Fig. 2 Plasma transmission in samples of different thickness (see text).

We provide direct evidence for the plasma expansion in CdTe from the investigation of the optical gain as a function of the sample thickness. As displayed in Fig. 2 the optical amplification increases proportional to the sample thickness d, even if d is much larger than the absorption length. This implies that even the 20 µm thick sample is completely filled with carriers and due to the short lifetime of ≈ 300ps requires a fast EHP expansion ($v \approx 7 \cdot 10^6$ cm/s). Plasma velocities in the high 10^6 cm/s range are also obtained from our detailed lineshape fits to emission and transmission of the EHP. Fig. 3 shows e.g a measured spectrum of the stimulated emission (dots) and calculated curves which include or neglect the carrier drift, respectively. For the model curve obtained using the simple single particle picture including momentum conservation we observe a remarkable agreement with the measured data. If drift effects are neglected, experiment and theory disagree strongly, implying again the inclusion of plasma transport in the evaluation of the spectra.

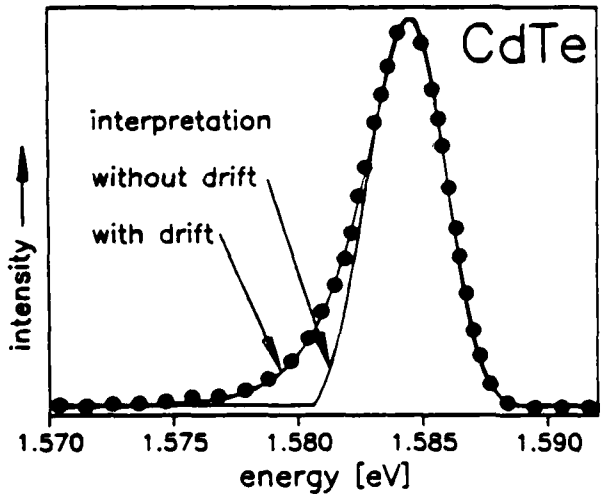

Nonequilibrium Steady States of Electrons and Holes in Semiconductors

K.N. Shrivastava and G.S. Tripathy
School of Physics, University of Hyderabad
Hyderabad 500134, India

We report an interesting instability in the excitation of pairs of electrons and holes in semiconductors by light absorption. The distribution of electrons and holes is bistable as a function of input power. As the nonequilibrium electrons and holes emit light, the total light intensity is a multivalued function of input power. This effect is of interest to study the electron-hole drops.[1]

We describe the electromagnetic field by a vector potential as,

$$A(x) = \left(\frac{2\pi\hbar c^2}{\Omega n^2}\right)^{1/2} \vec{e}(B+B^\dagger), \tag{1}$$

where

$$B = \alpha_0+\beta_0\, e^{-i\Omega t}, \quad B^\dagger = \alpha_0^\dagger+\beta_0^\dagger\, e^{i\Omega t}, \tag{2}$$

$\vec{e}$ is the polarization vector, Ω the photon frequency, n the index of refraction, and α_0, $\alpha_0^\dagger$ and β_0, $\beta_0^\dagger$ are the annihilation and creation operators of the stationary cavity and incident photons respectively. The electron-hole pair creation is described by

$$H_I = \sum_k G_k(c_k^\dagger b_{-k}^\dagger B+c_k b_{-k} B^\dagger), \tag{3}$$

where

$$G_k = -\frac{e}{m_0 n}\left(\frac{2\pi\hbar}{\Omega}\right)^{\frac{1}{2}} < ck|e.p|vk > , \tag{4}$$

$c_k^\dagger, c_k$ and $b_k^\dagger, b_k$ being the creation and annihilation operators for electrons and holes respectively. The cavity photon field is represented by $\alpha_0^\dagger\alpha_0$. We take the time dependence as

$$\tilde{\alpha}_0 = \alpha_0\, e^{i\Omega t}; \quad \tilde{B} = B\, e^{i\Omega t}; \quad \text{and} \quad A = (c_k b_{-k}+c_{-k} b_k)\, e^{i\Omega t}. \tag{5}$$

The rate equations in Bloembergen's[2] approach are calculated to be,

$$\frac{d}{dt}A^{\dagger} = \frac{i}{\hbar}(\varepsilon_k^e+\varepsilon_k^h)A^{\dagger} - \frac{i}{\hbar}G_k(c_k^{\dagger}c_k+c_{-k}^{\dagger}c_{-k}+b_k^{\dagger}b_k+b_{-k}^{\dagger}b_{-k}-2)\tilde{B}^{\dagger}+\gamma_2 A^{\dagger}-i\Omega A^{\dagger}, \tag{6}$$

$$\frac{d}{dt}\tilde{\alpha}_o = -\frac{i}{2\hbar}G_k A + \gamma_3\tilde{\alpha}_o \tag{7}$$

and

$$\frac{d}{dt}(c_k^{\dagger}c_k+b_k^{\dagger}b_k) = -\frac{i}{\hbar}G_k(A^{\dagger}\tilde{B}-A\tilde{B}^{\dagger})+\gamma_1(c_k^{\dagger}c_k+b_k^{\dagger}b_k). \tag{8}$$

which are solved to give

$$\langle\tilde{B}^{+}\rangle\langle\tilde{B}\rangle = \frac{\hbar^2\gamma_1\gamma_2 f_k\left[1+\left(\frac{\varepsilon_k^e+\varepsilon_k^h-\hbar\Omega}{\hbar\gamma_2}\right)^2\right]}{4G_k^2(1-f_k)} \tag{9}$$

$$\langle\beta_o^{\dagger}\rangle\langle\beta_o\rangle = \frac{\hbar^2\gamma_1\gamma_2 f_k}{4G_k^2(1-f_k)}\left[\left(\frac{\varepsilon_k^e+\varepsilon_k^h-\hbar\Omega}{\hbar\gamma_2}\right)^2+\left\{1+\frac{G_k^2}{\hbar^2\gamma_2\gamma_3}(1-f_k)\right\}^2\right] \tag{10}$$

We define the total field intensity as x and incident field as y, then

$$y = \frac{x}{(1+c_1^2+x)^2}[(1+c_1^2+x)^2 + 2c_2(1+c_1^2+x) + c_2^2(1+c_1^2)]. \tag{11}$$

where

$$c_1 = (\hbar\Omega-\varepsilon_k^e-\varepsilon_k^h)/\hbar\gamma_2 \quad \text{and} \quad c_2 = G_k^2/(\hbar^2\gamma_2\gamma_3)$$

There are three real solutions. This means that as the luminescence intensity is traced as a function of increasing and reducing input power, there is the phenomenon of hysteresis. Our predictions are in accord with the experiments.

References

1. A. Suguna and K.N. Shrivastava, Phys. Rev. B22, (1980) 2343.

2. N. Bloembergen, Nonlinear Optics, Benjamin, New York 1965; N. Bloembergen and Y.R. Shen, Phys. Rev. 133 (1964) A37.

Vacancy-Vacancy Interaction in the Excitation Spectra of Lattice Perturbation Bands in Cu_2O

R. G. Kaufman and R. T. Hawkins
Amoco Research Center
Standard Oil Company (Indiana)
P. O. Box 400, Naperville, Illinois 60566

We have recently found techniques for easily changing the density of copper vacancies in 30 μm films of Cu_2O on copper. A high density of copper vacancies is produced at 1000°C in a thin layer near the surface of the Cu_2O film, subsequent heat treatment in argon at lower temperatures lowers the vacancy density by diffusion throughout the film. Water quenching quickly stops diffusion and prevents further oxidation. New excitation spectra using a double monochromator have been measured at twenty five degree intervals between room and liquid nitrogen temperature for oxygen vacancy emissions at 740 nm, 840 nm, and the copper vacancy emission at 940 nm for heat treatment temperatures of 300°C, 400°C, 500°C, 600°C, and 700°C.

Three strong excitation bands, at 590 nm, 530 nm, and 450 nm, were observed. The 590 nm excitation band has a sharp rise at 610 nm and tails off into the blue. It produces all three defect emissions and begins to anneal out at temperatures above 500°C. The relative intensity of each emission, surprisingly, depends on the heat treatment temperature as well as the temperature of measurement. The 530 nm excitation band, an interesting new feature, is strongly dependent on heat treatment temperature. It is not present with heat treatment at 300°C and 700°C, but is a maximum and becomes the dominant band at 500°C. This can only occur if the formation and destruction of the band is non-linear in defect density. Only the 940 nm

emission is excited in this band and in the 450 nm band. The 450 nm excitation band has a gradual monotonic decrease with increasing heat treatment temperature and is at sufficient energy to give electron hole pairs. There are significant changes in the relative intensity of the three excitation bands between 77 K and 175 K which appear to be related and, therefore, suggestive of some form of energy transfer. Above 175 K there is a marked decrease in the intensity of all three defect emissions.

These unexpected new results can be understood when consideration is given to how the defect excitation bands arise. The 590 nm excitation band comes and goes with the defects, and is not intrinsic to the perfect crystal, so that the defects are the cause of the band. Since the vacancy itself doesn't absorb light, the excitation must be in the crystal lattice around a defect, a perturbation on the intrinsic absorption edge, and yet not an exciton since the luminescence has a broad excitation and emission spectrum at all low temperatures. The 300°C heat treatment makes little change in the as-grown condition. Most of the vacancies are in a very thin layer and are probably aggregated near the surface. Higher temperatures tend to break up the aggregates and diffuse vacancies into the film and also to surfaces where they are destroyed. In some intermediate conditions, the lower aggregates such as vacancy pairs will maximize. It is proposed that the 530 nm excitation band arises from copper vacancy-vacancy interaction since it anneals in and out non-linearly and gives only 940 nm copper vacancy emission. An analogous interaction between copper and oxygen vacancies appears to be responsible for the related shifts of emission intensity between 940 nm, 840 nm, and 740 nm with temperature.

Donor-Acceptor Pair Line Luminescence in ZnSe Re-Visited

G.F. Neumark

Division of Metallurgy and Materials Science
Columbia University, New York, N.Y. 10027 and
Philips Laboratories, Briarcliff Manor, N.Y. 10510

Donor-acceptor (DA) pair line luminescence in semiconductors[1] is both useful as a materials probe, and, in view of the analogy of the pairs to diatomic molecules, it is also of interest as a quantum chemical system. In the present paper we consider, for ZnSe, both aspects: using an improved value of the dielectric constant obtained from a re-analysis of literature data, we check agreement with quantum models.

As a materials probe, the luminescence can for instance give both the sum of the DA energies ($E_D + E_A$) and the dielectric constant (ε_o), in principle from the approximate relation[1] for the energy $h\nu(R)$ emitted by a pair at separation R:

$$h\nu(R) = h\nu^{\infty} + e^2/\varepsilon_o R, \qquad (1)$$

where e is the electron charge, and $h\nu^{\infty} = E_g - (E_D + E_A)$, with E_g the band-gap. In practice this relation is adequate only at large R, where accurate values of $h\nu(R)$ are not usually available (the lines are generally too close together and too broad). At smaller R, accurate $h\nu(R)$ have been tabulated, e.g. by Merz[2] for ZnSe. However, here corrections (ΔE) are required due to quantum interactions, i.e., one must use

$$h\nu(R) = h\nu^{\infty} + e^2/\varepsilon_o R - \Delta E(R). \qquad (2)$$

Using values of ΔE calculated by Kartheuser, Evrard, and Williams[3], and intermediate values of R (R = 30 Å to 45 Å), we have re-analyzed[4] Merz's data[2] for ZnSe (In-Li); we obtained $h\nu^{\infty} = 2.680$ eV, and $\varepsilon_o = 8.84$, both in excellent agreement with various literature values.[4]

It remains to be checked how well quantum calculations fit the data at small values of R ($R < 30$ Å), since it is the close pairs which are most sensitive to the quantum effects. To evaluate this, we follow the quantum treatment of Kartheuser et al[3], but with $\varepsilon_o = 8.84$ rather than the excessively high value of $\varepsilon_o = 9.42$ used there. Here, since the hole effective mass (m_h^*) is poorly known (literature values[5] range from 0.21 to 0.75), we adjusted this value to give agreement with $h\nu^\infty$, resulting in $m_h^* = 0.47$. The results are shown in Fig. 1, which compares our fit and the one of Ref. 3 with Merz's data[2]. (The "experimental" ΔE is given by Eq. 2, and the theoretical ΔE is given by $[E_p(R) - (E_D + E_A)]$, where $E_p(R)$ is the theoretical pair energy.) The fit to the data is very good, appreciably better than that of Ref. 3, showing the importance of a proper value of the dielectric constant. Despite the agreement we will also discuss corrections, such as valance band degeneracy and central cell effects, required in an improved quantum treatment.

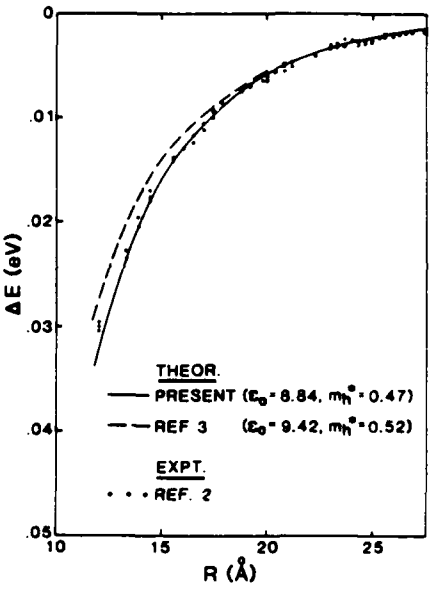

Support from NSF Grant PRM-82-12024 is gratefully acknowledged.

References

1. For reviews see, for ex., P.J. Dean, "Prog. in Sol. St. Chem." 8, 1 (1973) or F. Williams, Phys. Stat. Sol. 25, 493 (1968).
2. J.L. Merz, Phys. Rev. B9, 4593 (1974).
3. E. Kartheuser, R. Evrard and F. Williams, Phys. Rev. B21, 648 (1980).
4. G.F. Neumark, Phys. Rev. B29, 1050 (1984).
5. H. Venghaus, Phys. Rev. B19, 3071 (1979) and G.E. Hite, D.T.F. Marple, M. Aven, and B. Segall, Phys. Rev. 156, 850 (1967).

Picosecond Time-Resolved Spectroscopic Study

of

Vibrational Relaxation Processes in Alkali Halides

W. H. Knox+

Institute of Optics
Laboratory for Laser Energetics
University of Rochester
Rochester, NY 14623

The vibrational dynamics of fluorescent defects in alkali halides are interesting for a number of reasons. Information on electron-phonon interactions, relaxation of localized excitations and energy transfer phenomena may be obtained from a detailed study of the fluorescence properties at short times after optical excitation. In particular, the vibrational state, or states, of an impurity center may be directly determined from the time-resolved fluorescence spectrum under certain conditions, revealing details about internal energy relaxation processes. Recent advances such as the modelocked color center laser [1] and the demonstration of vibrational fluorescence [2] have provided increased interest in the vibrational properties of defects and defect systems in alkali halides.

The principal difficulty in studying the vibrational dynamics of impurity centers by fluorescence detection is the large disparity between the vibrational relaxation (VR) rate and the fluorescence decay rate. Typically, the VR rate is 10^3 - 10^5 times larger than the fluorescence decay rate, thus there is very little fluorescence emission during the period of the VR.

The streak camera provides detection of fluorescence signals in generality, with time resolution in the single picosecond range and detection sensitivity from UV to near IR, however the synchronization problem (jitter)

+ Present Address: AT&T Bell Laboratories, Holmdel, NJ 07733

typically encountered with commercial streak cameras precludes their use in extensive signal averaging operations which are necessary for the detection of extremely weak signals. Using a solid-state deflection driver to generate a synchronized sweep ramp pulse, streak camera operation with 2 ps jitter has been demonstrated [3]. Since this jitter is significantly less than the pulse width in use (25 ps), a direct-accumulation signal averaging mode is implemented which results in enhanced signal-to-noise ratio [4], enabling the study of fluorescence transients with greater sensitivity and precision than possible with single-shot systems which are common. A new technique of time-resolved spectroscopy is demonstrated which relies upon the absolute timing capability of this streak camera system.

Results will be presented on two classes of impurity-lattice systems: strongly coupled (such as M centers in NaF and LiF and Tl^+ in KBr), and weakly coupled (such as O_2^- in KBr). For strongly coupled systems, VR times of less than 1 ps are indicated. For O_2^- in alkali halides, VR times of 20 to 80 ps are measured. In the case of O_2^- in KBr, measurement of the time-resolved fluorescence spectrum reveals hot luminescence lines which can be clearly assigned to vibrational levels in the excited electronic state. This represents the first reported direct measurement of hot luminescence of a defect in alkali halides.

References

[1] L. F. Mollenauer and D. M. Bloom, Opt. Lett. 4, 247 (1979).

[2] Y. Yang and F. Lüty, Phys. Rev. Lett. 51, 419 (1983).

[3] W. Knox and G. Mourou, Opt. Comm. 37, 203 (1981).

[4] W. Knox and L. Forsley, ACS Symposium Series, 236, 221 (1983).

ACKNOWLEDGEMENTS

This work was partially supported by the following sponsors: General Electric Company, Northeast Utilities, New York State Energy Research and Development Authority, The Standard Oil Company (SOHIO), The University of Rochester, Empire State Energy Research Corporation, and NSF Grant #PCM-80-18488. Such support does not imply endorsement of the content by any of the above parties.

Two-Center Optical Transitions in Condensed Matter

Michael Stavola
AT&T Bell Laboratories
Murray Hill, New Jersey 07974

The absorption of a single photon by the simultaneous excitation of two rare-earth ions was first reported by Varsanyi and Dieke in 1961.[1] D. L. Dexter explained this unusual observation by including the electron-electron interactions (that also give rise to energy transfer) between the rare earth ions with perturbation theory.[2] In the 70's Dexter became interested in electronic-vibrational coupling. A theory of two-center optical transitions was developed for a rare-earth ion weakly coupled to a high energy, internal vibrational mode of a near-lying ion.[3] Using theoretical techniques that had been developed for rare-earth ion pairs, intensities and selection rules could be determined.

Vibronic transitions that involve the O-H stretching motion of a water molecule have been observed in aqueous solutions of rare earth salts and in hydrated crystals such as $GdCl_3.6H_2O$.[4] The observed intensities and selection rules were in agreement with the theory. Such a vibronic band is shown in the figure for an aqueous solution of $GdCl_3$. The fluorescence originating from the $^6P_{7/2}$ level of Gd^{3+} includes a vibronic sideband at ~ 28400 cm^{-1} (shifted from its electronic origin by the OH stretching frequency). The observation of vibronic spectra provides the

opportunity to examine the local environment of the rare-earth ion. From the vibronic spectrum it is possible to deduce the vibrational lineshapes for water molecules in the solvation spheres of the ion and to learn about the nature of the hydrogen bonding in solvation shells.

1. F. Varsanyi and G. H. Dieke, Phys. Rev. Lett. 7, 442 (1961).
2. D. L. Dexter, Phys. Rev. 126, 1962 (1962).
3. M. Stavola and D. L. Dexter, Phys. Rev. B20, 1867 (1979).
4. M. Stavola, L. Isganitis, and M. G. Sceats, J. Chem. 74, 4228 (1981).

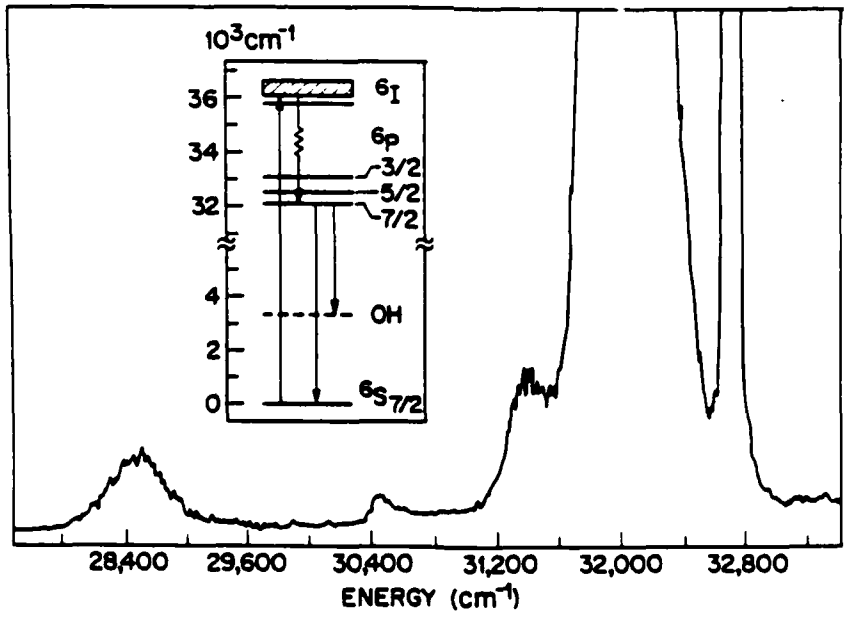

FF3-1

Optical Spectra of Excitons in Photon Fields

Y. Toyozawa

University of Tokyo

Tokyo, Japan

Dynamics of excitons in the phonon field and its reflection in the absorption, resonance Raman, and luminescence spectra are studied with particular attention to localization versus the delocalization.

FF4-1

Triplet Excimers in Hexachlorobenzene Crystals

H. C. Wolf

Universitat Stuttgart

Stuttgart, Federal Republic of Germany

From ENDOR measurements on tiplet excimers in single crystals of hexachlorobenzene doped with trichlorobenzene, one can derive for the first time the detailed electronic and geometric structure of an excimer.

KEY TO AUTHORS AND PAPERS

KEY TO AUTHORS AND PAPERS—Continued

UNCLASSIFIED

SECURITY CLASSIFICATION OF THIS PAGE (When Data Entered)

REPORT DOCUMENTATION PAGE		READ INSTRUCTIONS BEFORE COMPLETING FORM
1. REPORT NUMBER	2. GOVT ACCESSION NO.	3. RECIPIENT'S CATALOG NUMBER
4. TITLE (and Subtitle) International Conference on Luminescence - 1984 (ICL'84)		5. TYPE OF REPORT & PERIOD COVERED Technical Digest, Final Report - August, 1984 6. PERFORMING ORG. REPORT NUMBER
7. AUTHOR(s) W. M. Yen, Principal Investigator Chairman ICL'84		8. CONTRACT OR GRANT NUMBER(s) N00014-84-G-0053
9. PERFORMING ORGANIZATION NAME AND ADDRESS University of Wisconsin-Madison 750 University Ave. Madison, WI 53706		10. PROGRAM ELEMENT, PROJECT, TASK AREA & WORK UNIT NUMBERS
11. CONTROLLING OFFICE NAME AND ADDRESS Office of Naval Research, Code 410 800 North Quincy Street Arlington, VA 22217		12. REPORT DATE October, 1984 13. NUMBER OF PAGES 750 pages
14. MONITORING AGENCY NAME & ADDRESS(if different from Controlling Office)		15. SECURITY CLASS. (of this report) Unclassified 15a. DECLASSIFICATION/DOWNGRADING SCHEDULE

16. DISTRIBUTION STATEMENT (of this Report)

Approved for public release; distribution unlimited.

17. DISTRIBUTION STATEMENT (of the abstract entered in Block 20, if different from Report)

NA

18. SUPPLEMENTARY NOTES

The view, opinions, and/or findings contained in this report are those of the author(s) and should not be construed as an official Department of the Army position, policy, or decision, unless so designated by other documentation.

19. KEY WORDS (Continue on reverse side if necessary and identify by block number)

Luminescence; Optical Properties; Relaxation; Energy Transfer; Electroluminescence; Fractals

20. ABSTRACT (Continue on reverse side if necessary and identify by block number)

This report presents the extended abstracts of papers presented at the International Conference on Luminescence-1984 held at the University of Wisconsin-Madison, August 13-17, 1984.

DD FORM 1 JAN 73 1473 EDITION OF 1 NOV 65 IS OBSOLETE

UNCLASSIFIED

SECURITY CLASSIFICATION OF THIS PAGE (When Data Entered)